INSIGHTS IN ETHNOPHARMACOLOGY: 2021

EDITED BY: Michael Heinrich, Valentina Echeverria Moran, Judit Hohmann, Javier Echeverria, Hung-Rong Yen, Cheorl-Ho Kim and Aiping Lu

PUBLISHED IN: Frontiers in Pharmacology

frontiers Research Topics

frontiers

ISSN 1664-8714
ISBN 978-2-83250-392-8
DOI 10.3389/978-2-83250-392-8

About Frontiers

Frontiers is more than just an open-access publisher of scholarly articles: it is a pioneering approach to the world of academia, radically improving the way scholarly research is managed. The grand vision of Frontiers is a world where all people have an equal opportunity to seek, share and generate knowledge. Frontiers provides immediate and permanent online open access to all its publications, but this alone is not enough to realize our grand goals.

Frontiers Journal Series

The Frontiers Journal Series is a multi-tier and interdisciplinary set of open-access, online journals, promising a paradigm shift from the current review, selection and dissemination processes in academic publishing. All Frontiers journals are driven by researchers for researchers; therefore, they constitute a service to the scholarly community. At the same time, the Frontiers Journal Series operates on a revolutionary invention, the tiered publishing system, initially addressing specific communities of scholars, and gradually climbing up to broader public understanding, thus serving the interests of the lay society, too.

Dedication to Quality

Each Frontiers article is a landmark of the highest quality, thanks to genuinely collaborative interactions between authors and review editors, who include some of the world's best academicians. Research must be certified by peers before entering a stream of knowledge that may eventually reach the public - and shape society; therefore, Frontiers only applies the most rigorous and unbiased reviews.
Frontiers revolutionizes research publishing by freely delivering the most outstanding research, evaluated with no bias from both the academic and social point of view. By applying the most advanced information technologies, Frontiers is catapulting scholarly publishing into a new generation.

What are Frontiers Research Topics?

Frontiers Research Topics are very popular trademarks of the Frontiers Journals Series: they are collections of at least ten articles, all centered on a particular subject. With their unique mix of varied contributions from Original Research to Review Articles, Frontiers Research Topics unify the most influential researchers, the latest key findings and historical advances in a hot research area! Find out more on how to host your own Frontiers Research Topic or contribute to one as an author by contacting the Frontiers Editorial Office: frontiersin.org/about/contact

INSIGHTS IN ETHNOPHARMACOLOGY: 2021

Topic Editors:
Michael Heinrich, University College London, United Kingdom
Valentina Echeverria Moran, Bay Pines VA Healthcare System, Veterans Health Administration, United States Department of Veterans Affairs Bay Pines, United States
Judit Hohmann, University of Szeged, Hungary
Javier Echeverria, University of Santiago, Chile
Hung-Rong Yen, China Medical University (Taiwan), Taiwan
Cheorl-Ho Kim, Sungkyunkwan University, South Korea
Aiping Lu, Hong Kong Baptist University, Hong Kong, SAR China

Citation: Heinrich, M., Moran, V. E., Hohmann, J., Echeverria, J., Yen, H.-R., Kim, C.-H., Lu, A., eds. (2022). Insights in Ethnopharmacology: 2021. Lausanne: Frontiers Media SA. doi: 10.3389/978-2-83250-392-8

Table of Contents

frontiers | Frontiers in Pharmacology

TYPE Editorial
PUBLISHED 20 September 2022
DOI 10.3389/fphar.2022.997577

OPEN ACCESS

EDITED AND REVIEWED BY
Marco Leonti,
University of Cagliari, Italy

*CORRESPONDENCE
Cheorl-Ho Kim,
chkimbio@skku.edu
Michael Heinrich,
m.heinrich@ucl.ac.uk

SPECIALTY SECTION
This article was submitted to Ethnopharmacology, a section of the journal Frontiers in Pharmacology

RECEIVED 19 July 2022
ACCEPTED 16 August 2022
PUBLISHED 20 September 2022

CITATION
Kim C-H, Echeverria Moran V, Hohmann J, Echeverria J, Yen H-R, Lu A and Heinrich M (2022), Editorial: Insights in ethnopharmacology: 2021. *Front. Pharmacol.* 13:997577. doi: 10.3389/fphar.2022.997577

Editorial: Insights in ethnopharmacology: 2021

Cheorl-Ho Kim[1]*, Valentina Echeverria Moran[2,3], Judit Hohmann[4], Javier Echeverria[5], Hung-Rong Yen[6], Aiping Lu[7] and Michael Heinrich[8]*

[1]Department of Biological Science, College of Science, Sungkyunkwan University, Samsung Advances Institute of Health Science and Technology (SAIHST), Suwon, South Korea, [2]Facultad de Medicina, Universidad San Sebastián, Concepción, Chile, [3]Research and Development Service, Bay Pines VA Healthcare System, Bay Pines, FL, United States, [4]Department of Pharmacognosy, University of Szeged, Szeged, Hungary, [5]Departamento de Ciencias del Ambiente, Facultad de Química y Biología, Universidad de Santiago de Chile, Santiago, Chile, [6]Research Center for Traditional Chinese Medicine, China Medical University, Taichung, Taiwan, [7]School of Chinese Medicine, Hong Kong Baptist University, Kowloon, Hong Kong SAR, China, [8]Research Group "Pharmacognosy and Phytotherapy", UCL School of Pharmacy, Univ.London, London, United Kingdom

KEYWORDS

insights in ethnopharmacology: 2021, ethnomedicine, future perspectives, phytochemicals, therapeutic strategies

Editorial on the Research Topic
Insights in ethnopharmacology: 2021

Over 20 years after the start of the new millennium, ethnopharmacology clearly is making essential contribution to understanding medicines and their pharmacology, but at the same time science in general faces new and crucial challenges, not the least with regards to climate change and the need to treat existing and emerging major diseases. Human beings have always been faced with the unexpected. As humans we have always lacked experience, have been doubtful or hopeful, disappointed or forward looking. These developments have accelerated since the modernization, "Westernization" or globalisation of societies. We, today, all accept a historic milestone dividing the developments–in philosophical and scientific terms–into pre-modern and modern times, considering René Descartes (1596–1650) as the father of modern philosophy (Rodis-Lewis, 1998) and Galileo Galilei (1564–1642), as the father of science (Brodrick, 1965). Since Charles Darwin's (1809–1882) revolutionary conceptualisation of biological evolution current biological thinking and practice including pharmacology has made tremendous contributions to our understanding of the natural world and humans' place in it (Browne, 1995). Methods and technologies relevant for the pharmacological approaches are now stepping up to new levels of complexity focusing on evidence-based approaches in many areas including in understanding the metabolism, structure, interaction and combinational action of human cells, tissues and organisms and how this can be used to treat and prevent diseases.

Ethnopharmacology has gained a global reputation most notably in Asian countries as an approach which can contribute to such developments. Evidence

for the efficacy, pharmacological effects and relative safety of traditional herbal medicine has resulted in advantages in treating human diseases even for indications, we had not considered some decades ago. To meet the challenges of globalising such local or traditional uses, ethnopharmacology has to embrace the standards of pharmacological research practice. If pharmacokinetic safety and pharmacodynamic effects are guaranteed, a wider therapeutic use can be endorsed and this will most likely depend on the competent regulatory agencies of the nearly 200 countries globally. Various phytotherapeutic preparations have been known to treat many human diseases in the forms of decoction, extracts, or powder (Heinrich et al., 2023). Its future direction therefore includes field, pharmacological, clinical and case studies of local and traditional medicines in clearly defining and quantifying metabolites relevant for the activity (both directly and indirectly).

The present topic highlights integrative approaches using different both classical and modern pharmaceutical preparations (including decoctions, pills, powders, and supercritical fluid extracts) targeting migraine, cholestatic hepatic injury, rheumatoid arthritis and lipid malfunction. Intractable diseases including ischemic stroke, hyperglycaemia, skin photo-ageing, gastrointestinal and respiratory tract infections have been highlighted by reviews. This Research Topic includes eleven independent publications of seven reviews and four original research papers, as below:

1) Crocins for ischemic stroke: a review of current evidence by Shahbaz et al. Crocins (CRs) and other metabolites from *Crocus sativus* L. (Saffron) are clinically effective for ischemic stroke and cerebral ischemia. Saffron and CR are effective in metabolic syndrome, depression, Alzheimer's disease, neuro- and cardiovascular diseases by multiple mechanisms with mitochondrial apoptosis, NF-κB, S100 calcium-binding protein B, IL-6 and VEGF-A. Pharmacokinetically, CR is poorly bioavailable and conversion to crocetin allows translocation of the blood-brain barrier. While this certainly is a very interesting botanical drug, further research will need to focus on a larger scale sustainable production of the source material
2) Role of phytochemicals in skin photoprotection *via* regulation of Nrf2 by Chaiprasongsuk and Panich. The review highlights photoprotecting phytochemicals for skin *via* Nrf2. It focuses on natural products exerting skin protective and photoprotective effects mitigating ultraviolet radiation (UVR)-caused skin damage *via* nuclear factor erythroid 2-related factor 2 (Nrf2) including potential effect against photoaging and hyperpigmentation. The review highlighted phytochemicals-targeted Nrf2 in photoprotection of skin.
3) Phytochemistry in the Ethnopharmacology of North and Central America by Arnason et al. (review). This paper highlights phytochemicals of plants in North and Central America. New integrated approaches have been applied for metabolomic biomakers and synergist effects on phytochemicals, plant species and cultivars. Taking a geographical approach, this paper highlights the contribution of ethnopharmacological research in the context of a continent where more research on the local resources seems essential.
4) Approaches to decrease hyperglycemia by targeting impaired hepatic glucose homeostasis using medicinal plants by Mata-Torres et al. (review). It highlights pharmacological strategies using medicinal plants for preventing and treating hyperglycemia caused by hepatic insulin resistance. *Coreopsis tinctoria* Nutt., *Lithocarpus polystachyus* (Wall. ex A.DC.) Rehder and *Panax ginseng* C.A.Mey have been reviewed for effective glucose metabolism. Phenolic compounds and terpenoids are involved in the gluconeogenic pathway.
5) Bupleuri radix for acute uncomplicated respiratory tract infection: a systematic review of randomized controlled trials by Yan et al. (review). This highlights efficacy, clinical effectiveness, and safety issues of the *Bupleuri radix* (Bupleurum spp.) on acute uncomplicated respiratory tract infections (ARTIs) covering literature indexed in English and Chinese databases since 2021. The authors have used the Cochrane Risk of Bias Tool 2.0. RevMan 5.4 software. Injection solutions, pills, and decoctions similarly exhibit effects on AURTI symptoms such as nasal discharge and cough, calling for antipyretic effect.
6) P*lectranthus ecklonii* Benth: a comprehensive review into its phytochemistry and exerted biological activities by Antão et al. This review highlights genus *Plectranthus* (Lamiaceae), which has anti-inflammatory and anti-microbial activities in gastrointestinal and respiratory-related diseases. Diterpenes, triterpenes, flavonoids, and hydroxycinnamic acids of *P. ecklonii* are discussed.
7) *Reynoutria japonica* Houtt. for acute respiratory tract infections in adults and children: a systematic review by Wang et al. *Reynoutria japonica* Houtt. [alsoknown as *Fallopia japonica* (Houtt.) Ronse Decr.)] has been highlighted due to heat clearing, blood and qi circulating, phlegm elimination, and cough relieving activities with resveratrol and glycosides. From databases obtained from randomized trials, the respiratory tract infections-effective agents have been searched.
8) Study on the chemical constituents and anti-migraine activity of supercritical CO_2 extracts of *Zanthoxylum schinifolium* by Yuan et al. (original research). Supercritical CO_2 extraction technology has been highlighted in phytochemical research, as applied to *Zanthoxylum schinifolium* Siebold & Zucc. (CO_2-ZSE) as a condiment known to relieve migraine. CO_2-ZSE decreased

the levels of serum nitric oxide (NO), endothelin-1 (ET-1), calcitonin gene–related peptide (CGRP), IL-1β, NF-κB, p65, and IκBα, and increased 5-hydroxytryptamine (5-HT) level in migraine animals. Linalool reduces the frequency of scratching the head and the NO, ET-1, and CGRP levels with effective migraine therapy observed by vasomotor factors and the inflammatory pathway.

9) Integrating network analysis and metabolomics to reveal mechanism of Huaganjian decoction in treatment of cholestatic hepatic injury by Dong et al. (original research). Bioactive constituents with pharmacological mechanism have been approached, integrating networking and metabolomics in high cholestatic hepatic injury associated with PI3K/Akt/Nrf2 signaling/GSH synthesis. Huaganjian decoction (HGJD) was known for 300 years for liver diseases.
10) An integrative pharmacology model for decoding the underlying therapeutic mechanisms of Ermiao powder for rheumatoid arthritis by Wu et al. (original research). Erimiao powder composed of *Phellodendron amurense* Rupr. and *Atractylodes lancea* (Thunb.) DC. shows anti-rheumatoid arthritis effect through coordinated molecular mechanism,
11) Lipid metabolism and its mechanism triggered by supercritical CO_2 extract of Adlay [*Coix lacryma-jobi* var. *ma-yuen* (Rom. Caill.) Stapf] bran in high-fat diet induced hyperlipidemic hamsters by Huang et al. (original research). This novel approach to extraction of job's tears seeds highlights how improved technologies, as in this case supercritical fluid extraction form the basis for new economically relevant extracts. Adlay bran (AB-SCF) extracts improves lipid metabolism in high fat-diet-induced hyperglycemic animals. AB-SCF extract prevents body weight gains and improves serum TG, TC, LDL-C and HDL-C levels as well as cardiovascular risk, lipid peroxidation, cholesterol metabolism and bile acid excretion via action on lipoprotein lipase, AMPK, p-AMPK and fatty acid synthase. Lipids (linoleic acid and oleic acid) and non-lipid components of 3-O-(trans-4-feruloyl)-β-sitostanol, 3-O-(*cis*-4-feruloyl)-β-sitostanol, and β-sitosterol are synergistically active.

Ethnopharmacological research has become increasingly valuable in the development of botanical products and their bioactive phytochemicals as novel and effective preventive and therapeutic strategies for various diseases including genetic intractable diseases and environmental intractable diseases as well cosmetic products preventing photo-caused skin damage and photoaging-based dermal problems including pathological or non-pathological hyperpigmentation.

Similarly, many efforts focus on preventive interventions including the use of food supplements. All this offers insights into medicinal and ethnopharmacological potential for developing novel and effective therapeutic agents. Outputs from ethnopharmacological research have become much more widely recognised as source candidates of active phytochemicals preventive and therapeutic strategies. The biological activity of isolated metabolites also justifies the increased interest in multiple herbal species, keeps the spotlight on individual metabolites or combinatory drug therapy. The widespread analyses need to be assessed scientifically to better understand the individual metabolites and safeties of local and traditional medicines (Silveira et al., 2020; Kim, 2021; Park et al., 2021). Indeed, complementary and alternative medicine has been highlighted to prevent and treat intractable diseases. These are considered as a complementary supplement for functional foods or combined botanical drugs in the near future, although these discoveries remain to be confirmed and applicable by reasonable clinical trials. In future perspective, systemic evaluation of the effectiveness and safety of local and traditional medicines are important. Using eleven case studies, this Research Topic highlights the current state-of-the-art in ethnopharmacology. We as editors also want to encourage researchers to more systematically embrace the huge challenges in the field of medicinal plant research and their application. Sustainable sourcing (including the dramatic challenges of climate change), equitable benefits of the primary producers, a better understanding of the clinical efficacy of chemically well-defined extracts, the safety of these preparations and last but not least the need for truly transdisciplinary approaches in ethnopharmacology all are themes we as scholars need to tackle and contribute to their solution.

Author contributions

C-HK wrote the draft manuscript and MH edited the manuscript. VE, JH, JE, H-RY, and AL read the manuscript and revised.

Funding

This study has in part been supported by the National Research Foundation of Korea (NRF) grant funded by the Korean government (the Jungjum yonguso Program funded by the NRF-2019R1A6A1A1007307921). VE was funded by an ANID-FONDECYT (1190264).

Conflict of interest

The authors declare that the research was conducted in the absence of any commercial or financial relationships that could be construed as a potential conflict of interest.

Publisher's note

References

Brodrick, J. (1965). *Galileo: The man, his work, his misfortunes*. London: G. Chapman.

Browne, E. J. (1995). *Charles Darwin*. London: Jonathan Cape. ISBN 978-1-84413-314-7.

Heinrich, M., Barnes, J., Prieto-Garcia, J. M., Gibbons, S., and Williamson, E. M. (2023). *Fundamentals of pharmacognosy and phytotheraphy*. 4th ed. Edinburgh, GBPaperback: Churchill Livingstone Elsevier. ISBN: 9780702070082. eBook ISBN: 9780702070068.

Kim, C. H. (2021). Anti-SARS-CoV-2 natural products as potentially therapeutic agents. *Front. Pharmacol.* 12, 590509. doi:10.3389/fphar.2021.590509

Park, J., Choi, H., Abekura, F., Lim, H. S., Im, J. H., Yang, W. S., et al. (2021). Avenanthramide C suppresses matrix metalloproteinase-9 expression and migration through the MAPK/NF- κB signaling pathway in TNF-α-Activated HASMC cells. *Front. Pharmacol.* 12, 621854. doi:10.3389/fphar.2021.621854

Rodis-Lewis, G. (1998). *Descartes: His life and thought, trans*. Ithaca and London: Jane Marie ToddCornell University Press.

Silveira, D., Prieto-Garcia, J. M., Boylan, F., Estrada, O., Fonseca-Bazzo, Y. M., Jamal, C. M., et al. (2020). COVID-19: Is there evidence for the use of herbal medicines as adjuvant symptomatic therapy? *Front. Pharmacol.* 11, 581840. doi:10.3389/fphar.2020.581840

frontiers in Pharmacology

ORIGINAL RESEARCH
published: 17 November 2021
doi: 10.3389/fphar.2021.785944

Lipid Metabolism and its Mechanism Triggered by Supercritical CO_2 Extract of Adlay (*Coix lacryma-jobi var. ma-yuen* (Rom. Caill.) Stapf) Bran in High-Fat Diet Induced Hyperlipidemic Hamsters

Chiao-Chih Huang[1], *Tzu-Ching Lin*[1], *Chiung-Hui Liu*[1], *Hao-Chun Hu*[1], *Szu-Yin Yu*[1], *Shu-Jing Wu*[2], *Ming-Hong Yen*[1], *Yi-Hong Tsai*[1,3]* and *Fang-Rong Chang*[1,4,5,6]*

[1]Graduate Institute of Natural Products, College of Pharmacy, Kaohsiung Medical University, Kaohsiung, Taiwan, [2]Department of Nutritional Health, Chia-Nan University of Pharmacy and Science, Tainan, Taiwan, [3]Department of Pharmacy and Master Program, Collage of Pharmacy and Health Care, Tajen University, Pingtung County, Taiwan, [4]Drug Development and Value Creation Research Center, Kaohsiung Medical University, Kaohsiung, Taiwan, [5]Department of Medical Research, Kaohsiung Medical University Hospital, Kaohsiung Medical University, Kaohsiung, Taiwan, [6]Department of Marine Biotechnology and Resources, National Sun Yat-sen University, Kaohsiung, Taiwan

OPEN ACCESS

Edited by:
Cheorl-Ho Kim,
Sungkyunkwan University, South Korea

Reviewed by:
Ningyang Li,
Shandong Agricultural University, China
Jung Chao,
China Medical University, Taiwan

***Correspondence:**
Yi-Hong Tsai
lyph0719@hotmail.com
Fang-Rong Chang
aaronfrc@kmu.edu.tw

Specialty section:
This article was submitted to Ethnopharmacology, a section of the journal Frontiers in Pharmacology

Received: 29 September 2021
Accepted: 01 November 2021
Published: 17 November 2021

Citation:
Huang C-C, Lin T-C, Liu C-H, Hu H-C, Yu S-Y, Wu S-J, Yen M-H, Tsai Y-H and Chang F-R (2021) Lipid Metabolism and its Mechanism Triggered by Supercritical CO_2 Extract of Adlay (Coix lacryma-jobi var. ma-yuen (Rom. Caill.) Stapf) Bran in High-Fat Diet Induced Hyperlipidemic Hamsters. Front. Pharmacol. 12:785944. doi: 10.3389/fphar.2021.785944

Adlay (*Coix lacryma-jobi var. ma-yuen* (Rom. Caill.) Stapf) seeds are edible crop classified as Traditional Chinese Medicine (TCM). Adlay bran (AB) is one of the wastes generated during adlay refining processes. In this work, supercritical fluid extract of AB (AB-SCF) was investigated to reveal its lipid regulating potential and decode its bifunctional ingredients. AB-SCF×0.5 (30.84 mg/kg/body weight), AB-SCF×1 (61.67 mg/kg/BW), AB-SCF×5 (308.35 mg/kg/BW) and AB-SCF×10 (616.70 mg/kg/BW) were administrated to high fat-diet (HFD) induced hyperglycemic hamsters for 8 weeks. The results indicates that AB-SCF displays a prevention of dramatic body weight gains, lower levels of serum TG, TC, LDL-C and higher in HDL-C, amelioration of cardiovascular risk, alleviation of hepatic TG, TC and lipid peroxidation, and enhancement on cholesterol metabolism with higher bile acid excretion. Investigations on energy metabolic mechanism demonstrates that the hyperlipidemia mitigating capacities of AB-SCF are up-regulated on lipoprotein lipase, AMPK, p-AMPK and down-regulated at fatty acid synthase. Major bio-functional lipid compositions are identified as linoleic acid (28.59%) and oleic acid (56.95%). Non-lipid chemical and active markers are confirmed as 3-*O*-(*trans*-4-feruloyl)-*β*-sitostanol (1463.42 ppm), 3-*O*-(*cis*-4-feruloyl)-*β*-sitostanol (162.60 ppm), and *β*-sitosterol (4117.72 ppm). These compositions might synergistically responsible for the mentioned activities and can be regarded as analytical targets in quality control. AB-SCF may be considered as a promising complementary supplement, and developed as a functional food or new botanical drug in the future.

Keywords: adlay bran, supercritical fluid extract, hypolipidemic capacity, unsaturated fatty acids (UFAs), ferulate phytostanol esters

INTRODUCTION

Adlay (*Coix lacryma-jobi var. ma-yuen* (Rom. Caill.) Stapf), an annual crop, distributed and had been widely cultivated around Asian centuries. Adlay seeds, the dehulled and polished endosperm, have long been used as edible crop with both medicinal and nutritious properties for thousands of decades, even classified as a Traditional Chinese Medicine, TCM. It was applied to relieve edema, warts, chapped skin, beriberi, neuralgia, edema, dysuria, hypertension, rheumatism, damp arthralgia and contracture of tendons and vessels, diarrhea due to spleen deficiency (Kuo et al., 2012; Wang et al., 2016; Li et al., 2017; Xu et al., 2017). Adlay seeds has also been processed as gluten-free products which were popularly available nowadays in the nutritious supplement market (Comino et al., 2013).

However, the procedures of manufacturing "polished adlay" are relatively a high-cost matter with causing large amounts of wastes. Since the concept of circular bioeconomy (CBE) is increasingly noticed and becomes a prominence trend (Stegmann et al., 2020). Adlay bran (AB) is one of those byproducts of "polished adlay" refining processes worthy to be salvaged and developed. In the recent decade, more and more researches had indicated that AB might be an important resource apart from the polished adlay used traditionally. It may be developed as health-promoting products, along with additional benefits to reduce production waste and increase the economic value during adlay processing (Chang et al., 2020). For example, lactams, spiroenones, ferulic acid and flavonoids from EtOAc soluble fractions of AB alcoholic extracts showed *in vitro* and *in vivo* capacities against the formation and proliferation of breast, lung and colon cancers. The probable mechanism might work through the delay of carcinogenesis by suppressing chronic inflammation (Lee et al., 2008; Chung et al., 2010; Chung et al., 2011a; Chen et al., 2011; Li et al., 2011; Huang et al., 2014). Caffeic and chlorogenic acids were the other major compounds identified in the same fraction with the suppressive effects on the growth of human gastric adenocarcinoma cell-line (AGS) and ulcer index (UI) (Chung et al., 2011b). Furthermore, luteolin as well as phenolic acids of the fraction were proven to exert allergic immune-regulatory effects and can probably be used to treat rheumatism (Chen et al., 2012a; Chen et al., 2012b). Sinapic acid, a special phenolic acid identified in AB methanol extract, majorly possessed the strong xanthine oxidase inhibitory activity to prevent the incidence of hyperuricemia (Zhao et al., 2014; Lin et al., 2018). In dermatological utilizations, the pressed AB oil was reported to be used against hyperpigmentation through the reductions of tyrosinase activity and melanin synthesis (Ting et al., 2019). Moreover, a clinical investigation demonstrated that orally administrated AB ethanol extract may prevent breast cancer patients suffered from severe acute radiation dermatitis after radiotherapy (Huang et al., 2015).

In a small scale of screen aiming at discovering new entities with bioactive potential, we prelimilarily found that supercritical fluid extracted aldlay bran (AB-SCF) showed blood-lipid regulating effect in hyperlipidemic hamsters (n = 3, data not shown). The use of supercritical carbon dioxide (SC-CO_2) is an attractive alternative for organic solvents as "green" chemistry and classified as GRAS (Generally Recognized as Safe) by the Food and Drug Administration of the United States (US-FDA, 2008; Ramsey et al., 2009; Hsieh et al., 2012).

According to the literature survey, there was still no report focused on AB-SCF in revealing its anti-dyslipidemic/hypercholesterolemic capacities and the bioactive-responsible ingredients. The specific aims of this work were included as: *1*) to evaluate the serum and hepatic lipid regulating potential of AB-SCF on high-fat diet (HFD) induced hyperlipidemic hamsters, *2*) to clarify the lipid and energy metabolic mechanism triggered by AB-SCF, and *3*) to identify the nutritional and chemical compositions of AB-SCF.

In order to clarify the relationship between *in vivo* blood-lipid regulating effects and major compounds of AB-SCF, we hereby conducted evidence-guided column chromatography to isolate and identify its substances. Lipid compositions and its analytical fingerprint were further established by gas chromatography (GC) system. A comprehensive study, including bio-functional evidences and analytical properties of AB-SCF, were carried out in this work.

MATERIALS AND METHODS

Plant Materials and Reagents

Adlay seeds (*Coix lacryma-jobi var. ma-yuen* (Rom. Caill.) Stapf) were purchased in 2016 from the Daya District Farmers' Association, which is directed by Taichung District Agricultural Research and Extension Station, Council of Agriculture, Taiwan. The raw plant material (batch number: 3A0015) was identified by Dr. Ming-Hong Yen. A voucher specimen (code no. KMU-Coix 001) was stored in the Graduate Institute of Natural Products, College of Pharmacy, Kaohsiung Medical University and Joben Bio-Medical Co., Ltd., Taiwan. The exact name of plant material has been checked on the authoritative website in Taxonomy: http://www.worldfloraonline.org. *Coix lacryma-jobi var. ma-yuen* (Rom. Caill.) Stapf was indicated as an accepted name in genus *Coix* (family Poaceae). The seeds were dried at room temperature by an air circulator and dehulled with a grinding mill. The grinded particles of adlay were then separated with an industrial-designed AB collector to obtain the AB. It was further grinded into powder and sieved through 20-mesh (aperture = 0.84 mm) for supercritical fluid extraction. The recovery of AB from whole adlay seeds (including hull, testa, bran and endosperm) was 9.8–10.8% (**Figure 1**).

Hepatic TG and TC were measured by ELISA kits, No. 10010303 and No. 10007640 purchased from Cayman Chemical Company (Ann Arbor, MI, United States), respectively. Fecal bile acid was analyzed with the Bile Acids kit (Product No. 450) obtained from Trinity Biotech Plc. (Wicklow, Leinster, Ireland). The anti-AMPK, anti-p-AMPK, anti-rabbit IgG, and mouse IgG bodies were purchased from Cell Signaling Technology Inc. (Danvers, MA, United States). Anti-FAS, anti-LPL, and anti-β-actin bodies were obtained from Abcam Inc. (Cambridge, MA, United States). Standard laboratory

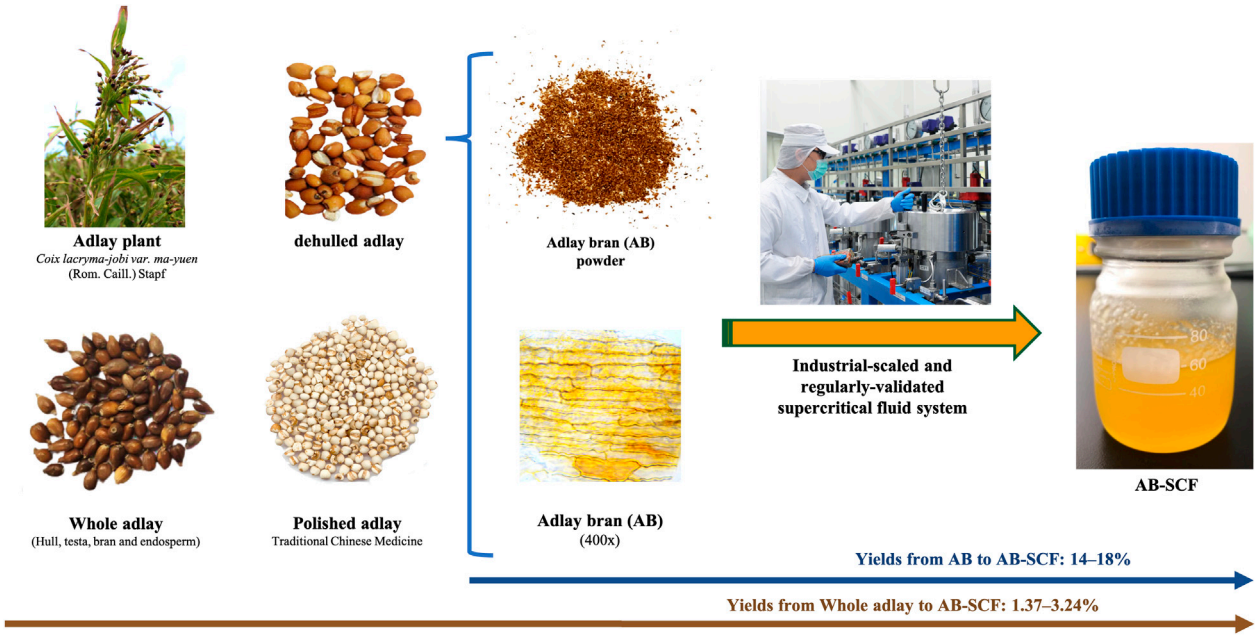

FIGURE 1 | Adlay, adlay bran and the AB-SCF manufacturing processes. The yields of AB-SCF from AB were averagely 14–18%. The recovery of AB-SCF from whole adlay seeds was 1.37–3.24%. AB-SCF was extracted by an industrial-scaled and regularly-validated supercritical fluid system (NATEX Process Technology GmbH, Ternitz, Austria) settled in the Joben Bio-Medical Co., Ltd. (Pingtung, Taiwan).

chow diet (No. 5001) was purchased from PMI® Nutrition International (Brentwood, MO, United States). Standard mixtures for qualitative and quantitative analysis, F.A.M.E (Fatty acid methyl esters) Mix RM-4 (methyl linoleate, methyl oleate, methyl palmitate, methyl stearate), were purchased from Supelco® (Sigma-Aldrich, St. Louis, MO, United States). Experimental animals in this work were fed either the standard chow diet or the HFD adapted from previous study (Yu et al., 2011). The nutrition facts of the standard chow diet were 3.36 kcal/g, containing 58.0% carbohydrates, 28.5% proteins and 13.5% fats. The HFD was 3.93 kcal/g, containing 44.53% carbohydrates, 21.88% proteins and 33.59% fats in one portion of 89.8% (wt/wt). 10% (wt/wt) of lard and 0.2% (wt/wt) of cholesterol were the rest of ingredients added, respectively (Sigma-Aldrich, St. Louis, MO, United States).

Supercritical Fluid Extraction of AB-SCF

AB-SCF was extracted by an industrial-scaled and regularly-validated supercritical fluid system (NATEX Process Technology GmbH, Ternitz, Austria) settled in the Joben Bio-Medical Co., Ltd. (Pingtung, Taiwan). 2–3 kg AB for each batch was weighed accurately and supplied into the instrumental vessel to process the extraction. Detail parameters for the SCF solvent, SC-CO_2, were optimized as 30–35 MPa and 40–60°C at a flow rate of 30–35 kg CO_2 per hour, along with 60–75 min period for the balance between the recovery and production capacity. Every extraction was terminated depending on whether the yield was less than 0.1%. The yields of AB-SCF from AB were averagely 14–18%. The recovery of AB-SCF from whole adlay seeds was 1.37–3.24% (**Figure 1**).

Animals and the *In Vivo* Experimental Design

Lipid metabolism of hamsters have been reported that closely resemble to human beings. Thus, hamsters were usually considered as the first and appropriate animal model for estimating hypolipidemic effects (Suica et al., 2016). Male Golden Syrian hamsters (6 weeks old) were purchased from the National Laboratory Animal Center (NLAC), Taipei City, Taiwan. All of them were housed under standard temperature (25 ± 1°C) and 50–60% relative humidity of conditions with a 12 h/12 h light-dark cycle. Standard chow diet and distilled water were provided *ad libitum*. Before the initiation of experiments, the hamsters were accommodated for 1 week to be stabilized and familiarize to the environment. All animal experimental protocols were supervised by the institutional animal care and use committee (IACUC) of Chia-Nan university (Tainan, Taiwan). The study conformed to the guidelines of the protocol CN-IACUC-105008R approved by the IACUC ethics committee.

The human equivalent dose (HED) of AB-SCF for hamsters were converted from the recommended daily dose for an adult human (assumed as 60 kg) which is 500 mg per day (one capsule/serving/day). HED between human and hamsters were calculated with a conversion coefficient, i.e., 7.4, based on body surface area (issued by the US Food and Drug Administration: http://www.fda.gov/

downloads/Drugs/GuidanceComplianceRegulatoryInformation/Guidances/ucm078932.pdf). The formula would be as follows:

HED of hamsters = (Recommended daily dose of human/kg) × 7.4 (coefficient) = [500 (mg)/60 (kg)] × 7.4 = 61.67 mg/kg (designed as 1×)

After 1-week acclimatization, 70 hamsters were randomly divided into seven groups (n = 10/each group): C, a blank control group fed with standard chow diet and water; HFD, an HFD induced hyperlipidemic group fed with water; EM, a reference group for the vehicle (solubilizer) of AB-SCF fed with HFD and emulsifier (prepared with Tween 80/Span 80 in the ratio of 5:1 v/v, then diluted with sterilized RO water to 5%). Experimental groups were induced with HFD and administrated AB-SCF/emulsifier with a dose-ascending manner, i.e., AB-SCF×0.5, 30.84 mg/kg/BW (body weight); AB-SCF×1, 61.67 mg/kg/BW; AB-SCF×5, 308.35 mg/kg/BW; AB-SCF×10, 616.70 mg/kg/BW. The food intakes and water consumptions were daily monitored. The body weights were recorded weekly. All hamsters were fast for 16 h and sacrificed with 95% CO_2 asphyxiation after the complete experimental period of 8 weeks. Serum, hepatic and fecal biochemical data, along with the energy metabolic mechanism(s) from proteins of liver tissues were further investigated.

Quantitation of Lipid and Lipoprotein Levels in Serum and Feces

Biochemical data related to serum lipid and lipoprotein levels, such as triglyceride (TG), total cholesterol (TC), low density lipoprotein cholesterol (LDL-C), high density lipoprotein cholesterol (HDL-C), LDL-C/HDL-C ratio (a predictor of cardiovascular risk, Jukema et al., 2005). Blood samples were collected with cardiac puncture and immediately centrifugated at 1500 × g (4°C) for 15 min in anticoagulant-treated tubes (Greiner Bio-One GmbH, Frickenhausen, Germany) to obtain the serum samples. Fecal samples were gathered within 2 days (48 h) before the termination. The feces were dried, powdered, weighted and extracted with Folch Solution (chloroform/methanol 2:1, vol/vol). An aliquot of the organic phase was then dried and resuspended in isopropyl alcohol (Mera et al., 2015). Lipid and lipoprotein profiles including TG, TC, HDL-C, LDL-C were measured by the use of an automated clinical chemistry analyzer, Fuji Dry-Chem 4000i, and its dedicated biochemical slides (Fujifilm, Tokyo, Japan).

Measurement of Fecal Bile Acid

Fecal lipid and bile acid were assessed. The feces were dried, weight and then grounded as fine powder in a mechanical blender. Aliquots of ground feces were well-mixed with sodium borohydride and then subjected to strong alkaline hydrolysis at 120–130°C for 12 h. The extracted fecal bile acid was measured enzymatically measured with a commercial bile acids kit (Product No. 450-A from Trinity Biotech Plc., Wicklow, Leinster, Ireland).

Analysis of Hepatic Triglyceride, Total Cholesterol Levels and the Oxidative Stress Markers

Hepatic lipid profiles (TC and TG) and oxidative stress markers i.e., MDA (malondialdehyde) and GSH (glutathione) were evaluated. All liver tissues were carefully collected, washed three times in ice cold saline, blotted individually on ash-free filter paper, weighted and aliquoted into few parts and frozen stored at −80°C. Before further analysis of hepatic TG and TC, each piece was homogenized with Tris-buffer (Sigma-Aldrich, St. Louis, MO, United States). The centrifuged supernatants were extracted by chloroform-isopropanol-NP40 (7:11:0.1, v/v) with a bullet blender (Lee et al., 2015). After the centrifugation again at 12,000 × g (4°C) for 10 min, hepatic TG and TC levels of the supernatants were measured in triplicate by using commercial enzymatic kits for TG (No. 10010303) and for TC (No. 10007640) from Cayman Chemical Company (Ann Arbor, MI, United States).

For the estimations of GSH and MDA, liver tissues were homogenized in phosphate buffer saline (PBS) 50 mM pH (7.4) and potassium phosphate buffer 10 mM pH (7.4), respectively. GSH levels were carried out with a commercial glutathione assay kit (product CS0260 from Sigma-Aldrich, St. Louis, MO, United States). This principle of MDA assessment depends on its formation as an end product of lipid peroxidation which reacts with thiobarbituric acid to produce thiobarbituric acid reactive substance (TBARS). TBARS, a pink chromogen, would be detected at 532 nm in a Spectrophotometry. A TEP (1,1,3,3-tetraethoxypropane) standard (Sigma-Aldrich, St. Louis, MO, United States) was used to build a standard curve against which readings of the samples were plotted (Noeman et al., 2011).

Extraction of Liver Tissue Protein and Western Blot Analysis

Bio-markers related to energy-balance, lipoprotein metabolism and oxidative-stress in liver, e.g., AMPK (adenosine-monophosphate-activated protein kinase), p-AMPK (phosphorylated-AMPK), FAS (fatty acid synthase) and LPL (hepatic lipoprotein lipase) were investigated to elaborate the energy metabolic mechanism. Protein extraction was conducted by homogenizing each liver sample in 1 ml lysis buffer (containing 10 mM-HEPES, pH 7.8), 10 mM KCl, 2 mM $MgCl_2$, 1 mM dithiothreitol (DTT), 0.1 mM EDTA, and 0.1 mM phenylmethylsulfonyl fluoride) at 4°C. Meanwhile, 80 µl of 10% NP-40 solution used for breaking the nuclear membrane within a cell was added as well. After the homogenization, the lysates were centrifuged for 2 min at 14,000 × g. Equal amounts of lysed protein (30 µg/lane) were loaded onto SDS-polyacrylamide gels, and electrophoretically transferred to a PVDF membrane (Bio-Rad Laboratories, Hercules, CA, United States). After blocking with 5% (w/v) skim milk in 0.1% (v/v) Tween 20-containing PBS (PBST) for 1 h at room temperature, the membrane was incubated with the following specific primary antibodies for 1 h at room temperature: anti-AMPK (1:1000), anti-phospho-AMPK (1:1000), anti-FAS (1:1000), anti-LPL (1:1000), and anti-β-actin (1:25000) antibodies (in 5% w/v skim milk with PBST). Antibody recognition was detected with the respective secondary antibody, either anti-mouse IgG or anti-rabbit IgG antibodies linked to horseradish peroxidase. Antibody-bound proteins were detected with the ECL western blotting analysis

TABLE 1 | Body weight (BW) gains and daily food intake (DFI) among normal and hyperlipidemic hamsters administrated with AB-SCF.

Body weight (BW)							
week	**C (g)**	**HFD (g)**	**HFD (g)**				
			EM	**AB-SCF×0.5**	**AB-SCF×1**	**AB-SCF×5**	**AB-SCF×10**
0	100.00 ± 4.88^{ab}	104.40 ± 7.47^{a}	97.50 ± 5.44^{b}	99.30 ± 6.53^{ab}	99.00 ± 4.81^{ab}	98.90 ± 7.20^{ab}	98.30 ± 2.06^{ab}
1	115.80 ± 2.35^{a}	110.90 ± 1.29^{b}	108.00 ± 1.05^{c}	105.20 ± 1.03^{d}	101.70 ± 1.16^{e}	100.40 ± 2.27^{e}	101.00 ± 3.06^{e}
2	119.40 ± 2.55^{ab}	121.40 ± 4.97^{a}	115.60 ± 9.91^{bc}	116.10 ± 2.47^{bc}	111.40 ± 2.41^{cd}	107.90 ± 4.28^{d}	108.50 ± 4.97^{d}
3	122.30 ± 3.16^{bc}	130.40 ± 8.37^{a}	125.30 ± 8.62^{ab}	122.90 ± 5.95^{bc}	118.80 ± 2.49^{c}	118.10 ± 6.26^{c}	118.30 ± 5.74^{c}
4	126.50 ± 4.17^{b}	138.10 ± 9.05^{a}	136.70 ± 9.43^{a}	131.80 ± 6.65^{ab}	127.30 ± 4.19^{b}	129.60 ± 6.54^{b}	127.00 ± 7.83^{b}
5	130.90 ± 6.52^{d}	147.60 ± 8.75^{ab}	150.20 ± 9.27^{a}	139.20 ± 7.21^{bc}	139.20 ± 8.72^{bc}	136.40 ± 7.49^{cd}	133.00 ± 8.43^{cd}
6	134.10 ± 5.70^{c}	153.30 ± 10.09^{a}	152.50 ± 7.59^{a}	145.40 ± 8.40^{ab}	142.80 ± 9.68^{b}	143.20 ± 7.91^{b}	135.20 ± 7.55^{c}
7	138.50 ± 6.33^{b}	159.50 ± 11.22^{a}	164.10 ± 12.24^{a}	156.20 ± 9.83^{a}	146.30 ± 10.67^{b}	145.40 ± 7.53^{b}	142.50 ± 9.91^{b}
8	141.10 ± 6.97^{f}	164.60 ± 11.06^{ab}	167.10 ± 11.37^{a}	158.40 ± 8.46^{bc}	152.90 ± 5.36^{cd}	149.40 ± 10.59^{de}	143.80 ± 7.21^{ef}
Daily food intake (DFI)							
week	**C (g/day)**	**HFD (g/day)**	**HFD (g/day)**				
			EM	**AB-SCF×0.5**	**AB-SCF×1**	**AB-SCF×5**	**AB-SCF×10**
0	9.10 ± 0.57^{a}	9.00 ± 0.67^{a}	9.30 ± 1.25^{a}	9.40 ± 0.97^{a}	9.00 ± 0.47^{a}	9.20 ± 0.79^{a}	9.20 ± 1.14^{a}
1	9.20 ± 1.32^{a}	9.90 ± 2.64^{a}	9.90 ± 1.85^{a}	9.90 ± 1.29^{a}	9.20 ± 1.03^{a}	9.30 ± 1.57^{a}	9.50 ± 0.85^{a}
2	10.60 ± 2.17^{a}	10.40 ± 1.26^{a}	10.40 ± 2.59^{a}	10.80 ± 1.93^{a}	10.40 ± 2.17^{a}	10.10 ± 1.10^{a}	10.40 ± 1.84^{a}
3	11.80 ± 1.87^{a}	11.80 ± 1.99^{a}	11.30 ± 1.64^{a}	11.20 ± 1.32^{a}	11.70 ± 1.34^{a}	11.70 ± 0.95^{a}	11.80 ± 1.40^{a}
4	11.90 ± 1.29^{a}	11.90 ± 1.37^{a}	11.60 ± 1.65^{a}	11.50 ± 1.78^{a}	11.80 ± 2.25^{a}	11.90 ± 1.20^{a}	11.80 ± 1.62^{a}
5	11.90 ± 1.20^{a}	11.90 ± 1.20^{a}	12.00 ± 1.49^{a}	11.70 ± 1.64^{a}	11.90 ± 1.52^{a}	11.80 ± 0.92^{a}	11.90 ± 1.37^{a}
6	12.00 ± 0.82^{a}	11.80 ± 0.92^{a}	12.00 ± 0.67^{a}	11.80 ± 1.03^{a}	12.00 ± 0.82^{a}	12.00 ± 1.05^{a}	12.10 ± 1.10^{a}
7	12.00 ± 0.67^{a}	11.90 ± 0.74^{a}	12.10 ± 1.66^{a}	11.90 ± 0.99^{a}	11.80 ± 1.87^{a}	12.00 ± 0.82^{a}	12.40 ± 1.35^{a}
8	12.10 ± 1.66^{a}	12.30 ± 2.31^{a}	12.40 ± 3.27^{a}	12.00 ± 2.98^{a}	12.00 ± 2.31^{a}	12.30 ± 2.00^{a}	12.40 ± 1.07^{a}

HFD, high-fat diet; EM, Tween 80/Span 80 = 5:1 v/v, diluted water to 5%; AB-SCF, supercritical fluid extracted aldlay bran. C, a blank control group fed with standard chow diet and water; HFD, a high fat diet induced hyperlipidemic group fed with water; EM, a high fat diet induced fed with the emulsifier of AB-SCF; Experimental groups were induced with HFD and administrated AB-SCF/emulsifier with a dose-ascending manner, i.e., AB-SCF×0.5, 30.84 mg/kg/BW; AB-SCF×1, 61.67 mg/kg/BW; AB-SCF×5, 308.35 mg/kg/BW; AB-SCF×10, 616.70 mg/kg/BW. Data are mean ± SD, n = *10 hamsters in each group. Means with different letters in the same column were significantly different at* $p < 0.05$ *as statistically analyzed by Duncan's multiple range tests.*

system (Amersham, Aylesbury, UK). The expression of β-actin was used as loading control. Relative protein expressions were quantified densitometrically with an AlphaImager 2200 (Alpha Innotech Corp., San Leandro, CA, United States), and processed using AlphaEaseFC software in referring to the β-actin reference bands in triplicate (Wei et al., 2017).

Preparation of Fatty Acid Methyl Esters of AB-SCF for GC Analysis

An aqueous concentrated HCl (conc. HCl; 35%, w/w) catalyzation was conducted to prepare the fatty acid methyl esters (FAMEs) of AB-SCF for GC analysis (Ichihara and Fukubayashi, 2010). Briefly, an 8% (w/v) HCl prepared in methanol/water (85:15, v/v) was diluted in 9.7 ml of concentrated HCl with 41.5 ml of methanol. Toluene (0.2 ml), methanol (1.5 ml), and the 8% HCl solution (0.3 ml) were added sequentially to the AB-SCF. The final HCl concentration was 1.2% (w/v). This solution (2 ml) was incubated at 45°C overnight or heated at 100°C for 1.5 h. The catalyzed AB-SCF was dried, then dissolved in EtOAc, filtered through 0.22 μm filter and subjected to GC analysis.

GC Analysis

The analysis of major compositions and the establishment of AB-SCF fingerprint were carried out with a gas chromatography system (Trace GC Ulture/ITQ 900, Thermo fisher Scientific, United States) with a flame ionization detector (FID). The capillary column was RT®-2560 (100 m × 250 μm × 0.2 μm) coated with biscyanopropyl polisiloxane as stationary phase (Restek Corporation, Bellefonte, PA, United States). The column oven temperature was programmed 150°C (held for 2 min), increased to 220°C at a rate of 35°C/min (held for 1 min), then raised to 225°C a rate of 0.5°C/min (maintained for 1 min). The other parameters were as follows: injection temperature, 225°C; detector temperature, 250°C; carrier gas, Helium at 1 ml/min; injection volume, 1 μl. The relative percentage of each major component in AB-SCF was quantified based on the peak area integrated by Thermo Xcalibur™ data analysis program (Thermo fisher Scientific, United States). Qualitative and quantitative analysis of AB-SCF (C16:0 Palmitate, C18:0 Stearate, C18:1 Oleate, C18:2 Linoleate) was carried out in comparing with the F.A.M.E Mix RM-4 standards.

Separation, Isolation and Purification of Chemical Substances of AB-SCF

10.0614g (density = 0.922 g/ml) of AB-SCF was firstly subjected into a Sephadex® LH-20 column in an environment of Dichloromethane (DCM):Methanol = 1:1 for gel filtration (Fine Chemicals AB, Uppsala, Pharmacia). Sephadex® LH-20 is

TABLE 2 | Serum and fecal lipid and lipoprotein profiles among normal and hyperlipidemic hamsters administrated with AB-SCF.

Serum							
	C	**HFD**	**HFD**				
			EM	**AB-SCF×0.5**	**AB-SCF×1**	**AB-SCF×5**	**AB-SCF×10**
TG (mg/dl)	47.30 ± 9.59^{f}	328.50 ± 30.15^{a}	286.20 ± 21.37^{b}	216.60 ± 36.61^{c}	153.90 ± 24.26^{d}	142.90 ± 32.37^{de}	135.40 ± 29.76^{e}
TC (mg/dl)	53.60 ± 3.44^{d}	360.90 ± 30.22^{a}	372.90 ± 46.24^{a}	236.30 ± 36.21^{b}	214.50 ± 20.90^{b}	148.30 ± 13.97^{c}	143.20 ± 26.98^{c}
HDL-C (mg/dl)	39.30 ± 2.54^{d}	52.20 ± 4.73^{c}	52.90 ± 4.28^{c}	55.20 ± 7.45^{c}	70.80 ± 8.74^{b}	83.00 ± 9.24^{a}	85.90 ± 9.06^{a}
LDL-C (mg/dl)	4.10 ± 1.37^{e}	242.90 ± 33.89^{a}	225.60 ± 39.85^{a}	140.70 ± 28.81^{b}	116.20 ± 0.09^{c}	40.60 ± 6.45^{d}	40.20 ± 18.37^{d}
LDL-C/HDL-C	0.11 ± 0.04^{e}	4.73 ± 1.04^{a}	4.30 ± 0.90^{a}	2.60 ± 0.66^{b}	1.69 ± 0.50^{c}	0.49 ± 0.10^{d}	0.48 ± 0.26^{d}
Feces							
Every 100 mg feces	**C**	**HFD**	**HFD**				
			EM	**AB-SCF×0.5**	**AB-SCF×1**	**AB-SCF×5**	**AB-SCF×10**
TG (mg)	6.50 ± 1.29^{c}	14.00 ± 1.41^{b}	18.00 ± 1.25^{a}	17.00 ± 1.4^{a}	17.00 ± 1.41^{a}	17.5 ± 2.12^{a}	19.00 ± 1.41^{a}
TC (mg)	11.00 ± 0.82^{c}	35.00 ± 4.08^{a}	34.00 ± 0.83^{a}	39.00 ± 1.41^{a}	27.00 ± 1.41^{b}	26.5 ± 0.71^{b}	26.00 ± 2.83^{b}
LDL-C (mg)	0.18 ± 0.05^{b}	0.35 ± 0.06^{a}	0.33 ± 0.12^{a}	0.35 ± 0.07^{a}	0.30 ± 0.02^{a}	0.35 ± 0.07^{a}	0.35 ± 0.07^{a}
HDL-C (mg)	0.55 ± 0.10^{c}	1.25 ± 0.1^{a}	1.05 ± 0.07^{ab}	1.05 ± 0.06^{ab}	1.05 ± 0.07^{ab}	1.05 ± 0.05^{ab}	1.05 ± 0.03^{ab}
Bile Acids (μmol)	17.37 ± 1.46^{e}	116.08 ± 9.73^{c}	113.28 ± 3.10^{c}	126.28 ± 7.10^{cd}	167.42 ± 14.03^{c}	236.91 ± 19.85^{ab}	256.62 ± 11.45^{a}

TG, triglyceride; TC, total cholesterol; LDL-C, low-density lipoprotein cholesterol; HDL-C, high-density lipoprotein cholesterol; HFD, high-fat diet; EM, Tween 80/Span 80 = 5:1 v/v, diluted water to 5%; AB-SCF, supercritical fluid extracted aldlay bran. C, a blank control group fed with standard chow diet and water; HFD, a high fat diet induced hyperlipidemic group fed with water; EM, a high fat diet induced fed with the emulsifier of AB-SCF; Experimental groups were induced with HFD and administrated AB-SCF/emulsifier with a dose-ascending manner, i.e., AB-SCF×0.5, 30.84 mg/kg/BW; AB-SCF×1, 61.67 mg/kg/BW; AB-SCF×5, 308.35 mg/kg/BW; AB-SCF×10, 616.70 mg/kg/BW. Data are mean ± SD, n *= 10 hamsters in each group. Means with different letters in the same column were significantly different at* p *< 0.05 as statistically analyzed by Duncan's multiple range tests.*

TABLE 3 | Hepatic triglyceride, total cholesterol, GSH and MDA among hyperlipidemic hamsters administrated with AB-SCF.

	Hepatic TG (mg/dl)	**Hepatic TC (mg/dl)**	**Hepatic MDA (μM/g liver tissue)**	**Hepatic GSH (nmole/mg protein)**
C	189.90 ± 11.80^{bc}	13.80 ± 1.91^{d}	179.10 ± 11.30^{d}	15.90 ± 0.60^{a}
HFD	239.00 ± 8.01^{a}	30.40 ± 2.47^{a}	362.10 ± 16.4^{a}	13.70 ± 0.40^{bc}
EM	243.00 ± 7.30^{a}	29.80 ± 1.23^{a}	359.50 ± 8.30^{a}	13.60 ± 0.30^{bc}
AB-SCF×0.5	205.00 ± 6.20^{b}	22.00 ± 1.03^{b}	215.70 ± 7.80^{b}	13.65 ± 0.60^{bc}
AB-SCF×1	193.10 ± 12.39^{bc}	18.30 ± 1.61^{c}	203.20 ± 9.40^{bc}	13.60 ± 0.50^{bc}
AB-SCF×5	193.30 ± 8.93^{bc}	18.63 ± 1.37^{c}	190.50 ± 9.40^{cd}	14.70 ± 0.30^{ab}
AB-SCF×10	173.70 ± 9.65^{d}	14.43 ± 1.16^{d}	177.80 ± 5.80^{d}	14.90 ± 0.50^{a}

TG, triglyceride; TC, total cholesterol; MDA, malondialdehyde; GSH, glutathione; HFD, high-fat diet; EM, Tween 80/Span 80 = 5:1 v/v, diluted water to 5%; AB-SCF, supercritical fluid extracted aldlay bran. C, a blank control group fed with standard chow diet and water; HFD, a high fat diet induced hyperlipidemic group fed with water; EM, a high fat diet induced fed with the emulsifier of AB-SCF; Experimental groups were induced with HFD and administrated AB-SCF/emulsifier with a dose-ascending manner, i.e., AB-SCF×0.5, 30.84 mg/kg/BW; AB-SCF×1, 61.67 mg/kg/BW; AB-SCF×5, 308.35 mg/kg/BW; AB-SCF×10, 616.70 mg/kg/BW. Data are mean ± SD, n *= 10 hamsters in each group. Means with different letters in the same column were significantly different at* p *< 0.05 as statistically analyzed by Duncan's multiple range tests.*

composed by cross-linked dextran for molecular sizing natural products in accordance to molecular weight. The purpose would be to divide the nonlipid substances from apolar/lipid mixtures (Wells and Dittmer, 1963). Seven fractions, AB-SCF-S1 to S8, were yielded after passing AB-SCF through the Sephadex® LH-20 column. Thin-layer chromatography was monitored with silica gel 60 F_{254} and RP-18 F_{254S} TLC plates (Merck, Darmstadt, Germany) with substance visualized by 10% (v/v) H_2SO_4/ethanol spray (**Supplementary Figure S1**). After brief screen of ^{1}H NMR (Nuclear Magnetic Resonance) spectroscopy on every AB-SCF-Sn fraction, AB-SCF-S1 was the main ingredient composed of 78.92% triglyceride, along with AB-SCF-S4 and S5 were detected 8.39% for mostly fatty acids. AB-SCF-S2 (192.50 mg, 1.91%) and S3 (282.27 mg, 2.86%) were observed with interesting minor signals different but still mixed with triglyceride and fatty acids. Meanwhile, the last three fractions, AB-SCF-S6 to S8, occupied only 0.58% (58.36 mg) in AB-SCF with signals of oil and complicate mixtures (**Supplementary Figure S2**).

AB-SCF-S3 was combined into AB-SCF-S2 as S2' (totally 479.77 mg, 4.77% weight/total weight of eluents) and fractioned with silica gel (230–400 mesh, Merck, Darmstadt, Germany) open column and stepwise eluted with *n*-hexane:EtOAc from 80:1–100% into 17 subfractions (S2′-1–17). With the continuous monitor of ^{1}H NMR, S2′-7 which was different from oil constituents were separated with another silica gel open column from the solvent system of *n*-hexane:EtOAc from 80:1–100%. S2′-7-1 to 5 were obtained. S2′-7-5-1 to 9 were further got carried out by silica preparative TLC *n*-Hexane:DCM (1:1). However, the amounts of these fractions

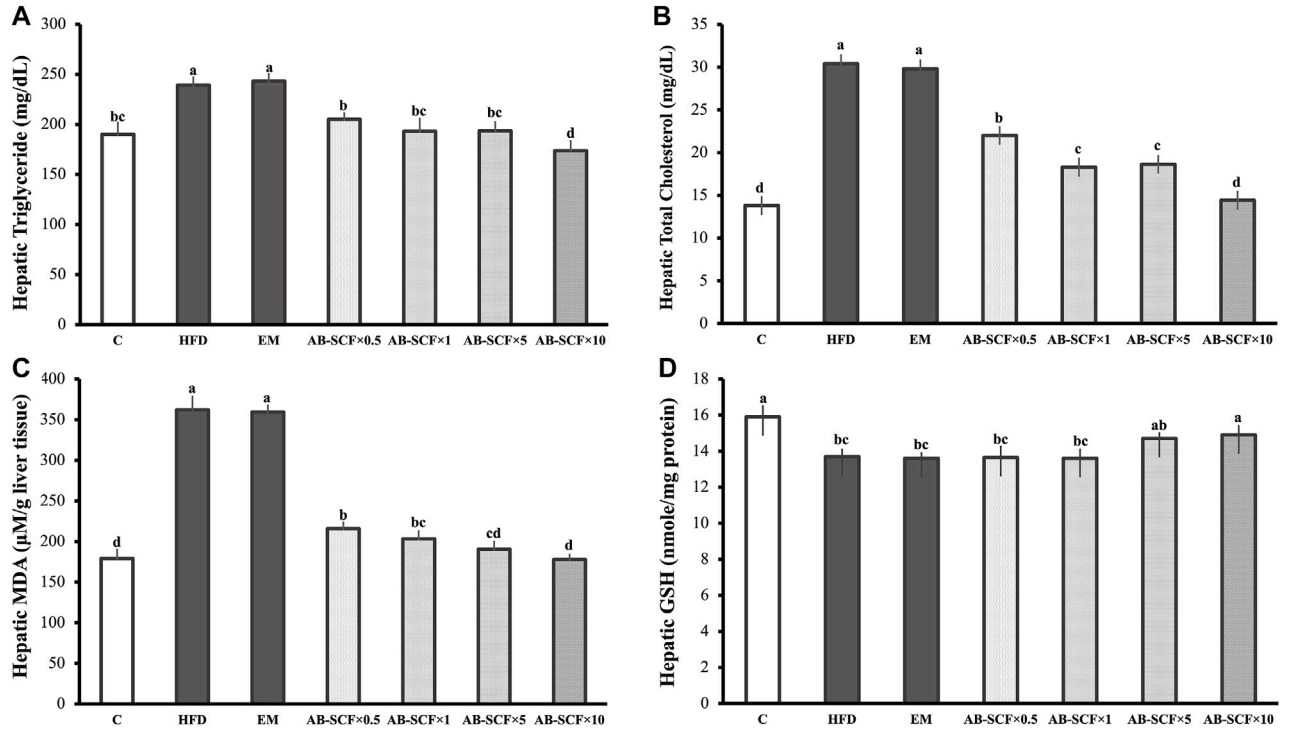

FIGURE 2 | Effects of AB-SCF on the lipid accumulation and oxidative stresses in liver. **(A)** Levels of hepatic triglyceride; **(B)** Levels of hepatic total cholesterol; **(C)** Levels of hepatic MDA (malondialdehyde); **(D)** Levels of hepatic GSH (glutathione) in normal, HFD induced and AB-SCF administrated hyperlipidemia hamsters. HFD, high-fat diet; EM, Tween 80/Span 80 = 5:1 v/v, diluted water to 5%; AB-SCF, supercritical fluid extracted aldlay bran. C, a blank control group fed with standard chow diet and water; HFD, a high fat diet induced hyperlipidemic group fed with water; EM, a high fat diet induced fed with the emulsifier of AB-SCF; Experimental groups were induced with HFD and administrated AB-SCF/emulsifier with a dose-ascending manner, i.e., AB-SCF×0.5, 30.84 mg/kg/BW; AB-SCF×1, 61.67 mg/kg/BW; AB-SCF×5, 308.35 mg/kg/BW; AB-SCF×10, 616.70 mg/kg/BW. Data are mean ± SD, $n = 10$ hamsters in each group. Means with different letters in the same column were significantly different at $p < 0.05$ as statistically analyzed by Duncan's multiple range tests.

were too low (all less than 2 mg) to be re-measured by ^{1}H NMR. The other fraction considered not being fatty acids from S2′, the S2′-11, was directly processed by silica preparative TLC *n*-hexane: DCM (1:2) to yield two mixed geometric isomers, (**1**) (*Rf* = 0.58) and (**2**) (*Rf* = 0.58). (**3**) was filtered out from S2′-11-6 by using DCM and Methanol (*Rf* = 0.38) (**Supplementary Figures S3, S4**).

Statistical Analysis

Data were presented as mean ± standard deviation (SD) from different and independent experiments. Values were evaluated by one-way ANOVA, followed by Duncan's multiple range test using the 9.0 Statistical Analysis System (SAS Institute, Cary, NC, United States). Difference was considered significant when *p*-value was <0.05.

RESULTS

Effects of AB-SCF on Body Weight and Daily Food Intake in Hyperlipidemic Hamsters

The effects of AB-SCF×0.5, AB-SCF×1, AB-SCF×5, AB-SCF×10 on the changes of body weight (BW) and daily food intake (DFI) were recorded in the model of high-fat diet induced hyperlipidemic male hamsters (**Table 1**). After an 8-week administration, the external appearances and health conditions of all hamsters were remained ordinarily with no adverse effects observed. BWs were stable and steadily increased in each group. High fat diet induced groups were generally heavier than C with significance ($p < 0.05$). Meanwhile, AB-SCF×10 displayed significantly lower BW than EM, AB-SCF×5, AB-SCF×1 and AB-SCF×0.5 ($p < 0.05$), and close to C at the 6th to 8th week. The daily food intake (DFI) data showed no difference among all groups.

Effects of AB-SCF on Lipid and Lipoprotein Levels in Serum and Feces of Hyperlipidemic Hamsters

After the 8 weeks administrations, effects of AB-SCF×0.5, AB-SCF×1, AB-SCF×5, and AB-SCF×10 groups on the changes of serum and fecal lipid and lipoprotein profiles were examined after the termination (**Table 2**). TG and TC levels of the C group were 47.30 ± 9.59 and 53.60 ± 3.44 mg/dl, respectively. However, HFD and EM had been increased significantly to 328.50 ± 30.15 and 360.90 ± 30.22 mg/dl ($p < 0.05$). All AB-SCF administrated groups, compared to the HFD and EM, exhibited markedly lower data in not only TG and TC, but also in LDL-C ($p < 0.05$). In addition, HDL-C levels were significantly higher ($p < 0.05$) in all AB-SCF groups than in HFD and EM. The ratios of LDL-C/HDL-C, a predictor of cardiovascular risk, were dose-

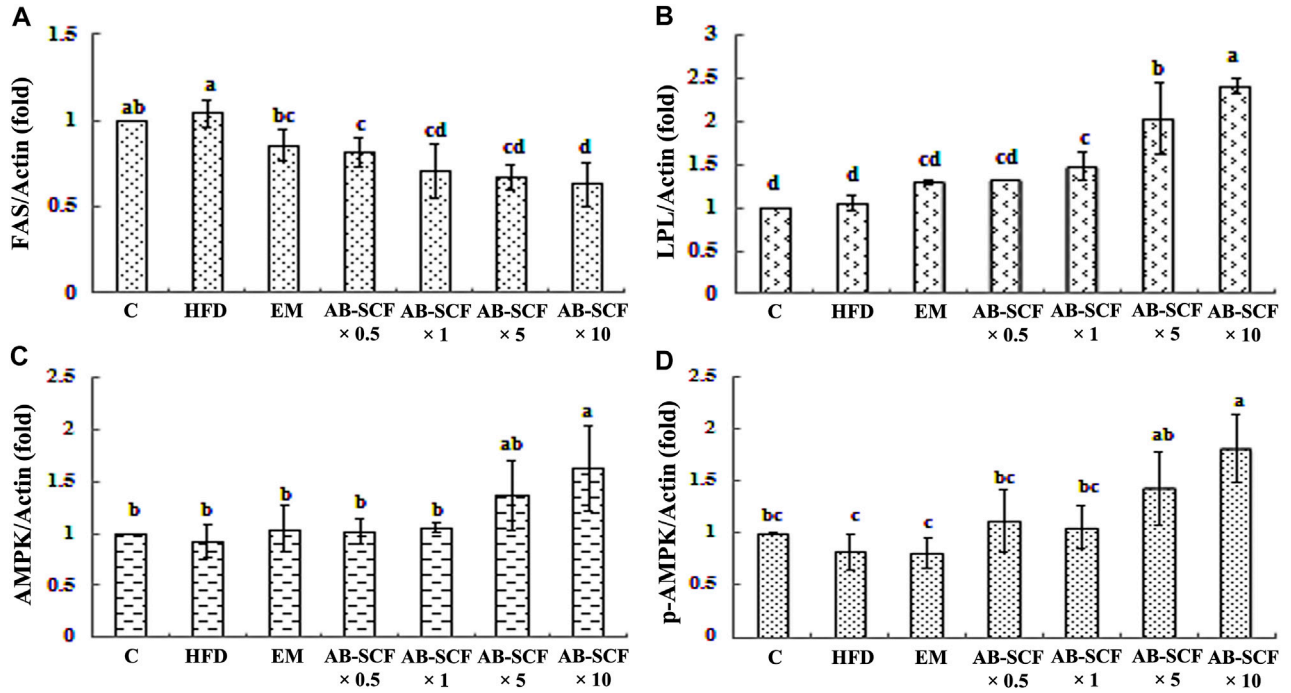

FIGURE 3 | Effects of AB-SCF on the expression of FAS, LPL, AMPK, and p-AMPK in the liver tissues. **(A)** FAS, Fatty acid synthase; **(B)** LPL, Lipoprotein lipase; **(C)** AMPK, Adenosine-monophosphate-activated protein kinases; **(D)** p-AMPK, phosphorylated-AMPK. The expression of β-actin was used as loading control. Relative protein expressions were quantified densitometrically with an AlphaImager 2200, and processed using AlphaEaseFC software in referring to the β-actin. HFD, high-fat diet; EM, Tween 80/Span 80 = 5:1 v/v, diluted water to 5%; AB-SCF, supercritical fluid extracted aldlay bran. C, a blank control group fed with standard chow diet and water; HFD, a high fat diet induced hyperlipidemic group fed with water; EM, a high fat diet induced fed with the emulsifier of AB-SCF; Experimental groups were induced with HFD and administrated AB-SCF/emulsifier with a dose-ascending manner, i.e., AB-SCF×0.5, 30.84 mg/kg/BW; AB-SCF×1, 61.67 mg/kg/BW; AB-SCF×5, 308.35 mg/kg/BW; AB-SCF×10, 616.70 mg/kg/BW. Data are mean ± SD, $n = 10$ hamsters in each group. Means with different letters in the same column were significantly different at $p < 0.05$ as statistically analyzed by Duncan's multiple range tests.

TABLE 4 | Nutrition facts in AB-SCF (per 100 g).

AB-SCF	Ingredients
Gross energy	793.57 ± 1.88 Kcal
Lipid	81.13 ± 0.25%
Trans fats	0% (ND)
Proteins	15.85 ± 0.15%
H_2O	2.30 ± 0.32%
Ash	0.72 ± 0.17%
Na	30.79 ± 1.07 mg
Carbohydrates, CHO	0% (N.D.)
Sugar	0% (N.D.)

AB-SCF, supercritical fluid extracted aldlay bran; N.D., not detected. The data shown are means ± SD of triplicated experiments. Analytical data was provided by the Joben Bio-Medical Co., Ltd., (Pingtung, Taiwan).

dependently and meaningfully decreased ($p < 0.05$) in AB-SCF administrated hyperlipidemic hamsters as 2.60 ± 0.66, 1.69 ± 0.50, 0.49 ± 0.10, 0.48 ± 0.26, respectively (with 0.11 ± 0.04 in C, 4.73 ± 1.04 in HFD, and 4.30 ± 0.90 in EM).

In feces, the lipid and lipoprotein profiles were generally higher in high fat diet induced hyperlipidemic hamsters. Only TC were expressively alleviated ($p < 0.05$) by AB-SCF×1, AB-SCF×5, AB-SCF×10 with 27.00 ± 1.41 mg, 26.00 ± 2.83 mg, 26.5 ± 0.71 mg in every 100 mg feces (11.00 ± 0.82 from C, 35.00 ± 4.08 from HFD, 34.00 ± 0.83 from EM and 39.00 ± 1.41 from AB-SCF×0.5). Bile acids (μmol/100 mg feces) in HFD (116.08 ± 9.73) and EM (113.28 ± 3.10) was obviously elevated ($p < 0.05$) than in C (17.37 ± 1.46). AB-SCF groups would improve the excretions of bile acids with significances in dose-dependent manner.

Effects of AB-SCF on Hepatic Triglyceride, Total Cholesterol Levels and the Oxidative Stress Markers of Hyperlipidemic Hamsters

Hepatic TG and TC were both aggravatedly higher in HFD and EM groups than the other ones (**Table 3** and **Figure 2**). In contrast, AB-SCF had significantly ameliorated the levels of hepatic TG and TC ($p < 0.05$). Especially in the AB-SCF×10 group, hepatic TG and TC of hyperlipidemic hamsters were almost retrieved back to levels of the standard chow diet ones.

As compared to the C in the measurement of MDA and GSH (179.10 ± 11.30; 15.90 ± 0.60), HFD (362.10 ± 16.4; 13.70 ± 0.40) and EM (359.50 ± 8.30; 13.60 ± 0.30) showed significant increases and depletions, respectively. In lipid peroxidation of hyperlipidemic hamster livers, AB-SCF groups exhibited promising protective affections with dose-dependent manner (MDA: AB-SCF×0.5, 215.70 ± 7.80; AB-

TABLE 5 | Major lipid compositions of AB-SCF.

Retention time (min)	Referenced methyl esters	Ratio (%)	Identified compounds	Molecular formula	C:D*
6.66	Methyl palmitate	13.07	Palmitic acid	$C_{16}H_{32}O_2$	C16:0
8.64	Methyl linoleate	28.59	Linoleic acid	$C_{18}H_{32}O_2$	C18:2
8.74	Methyl oleate	56.95	Oleic acid	$C_{18}H_{34}O_2$	C18:1
9.11	Methyl stearate	1.39	Stearic acid	$C_{18}H_{36}O_2$	C18:0

*The analysis of Major compositions and the establishment of AB-SCF fingerprint were carried out with a gas chromatography system (Trace GC Ulture/ITQ 900, Thermo fisher Scientific, United States) with a flame ionization detector (FID). The capillary column was RT®-2560 (100 m × 250 μm × 0.2 μm) coated with biscyanopropyl polisiloxane as stationary phase (Restek Corporation, Bellefonte, PA, United States). The column oven temperature was programmed 150°C (held for 2 min), increased to 220°C at a rate of 35°C/min (held for 1 min), then raised to 225°C a rate of 0.5°C/min (maintained for 1 min). The other parameters were as follows: injection temperature, 225°C; detector temperature, 250°C; carrier gas, Helium at 1 ml/min; injection volume, 1 μl. The relative percentage of each major component in AB-SCF was quantified based on the peak area integrated by Thermo Xcalibur™ data analysis program (Thermo fisher Scientific, United States). Qualitative and quantitative analysis of AB-SCF (C16:0 Palmitate, C18:0 Stearate, C18:1 Oleate, C18:2 Linoleate) was carried out in comparing with the F.A.M.E Mix RM-4 standards. *C:D is the numerical symbol: total amount of (C)arbon atoms of the fatty acid, and the number of (D)ouble (unsaturated) bonds in it; if D > 1 it is assumed that the double bonds are separated by one or more methylene bridge(s).*

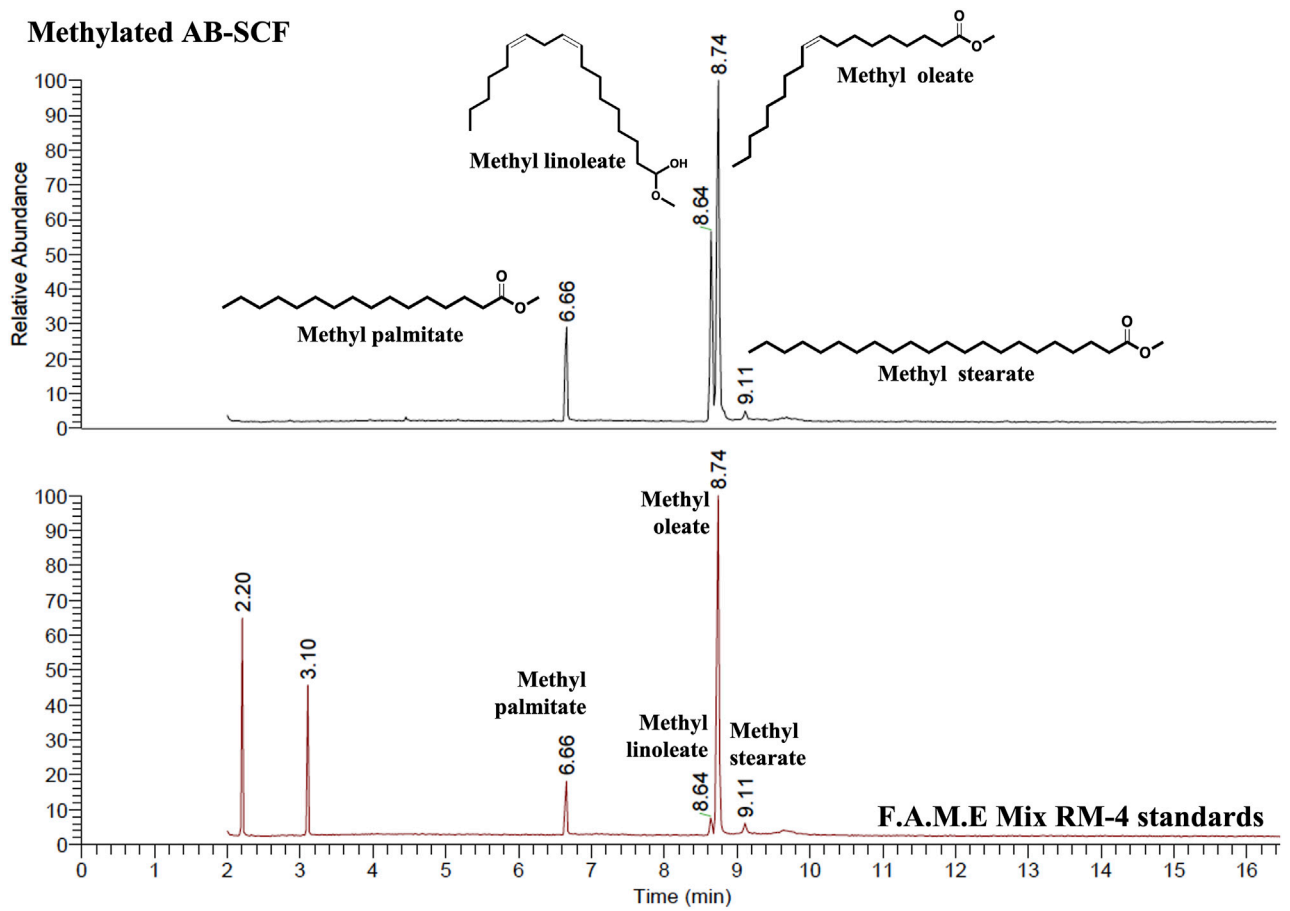

FIGURE 4 | The analytical fingerprint of AB-SCF methyl esters. The analysis of Major compositions and the establishment of AB-SCF fingerprint were carried out with a gas chromatography system (Trace GC Ulture/ITQ 900, Thermo fisher Scientific, United States) with a flame ionization detector (FID). The capillary column was RT®-2560 (100 m × 250 μm × 0.2 μm) coated with biscyanopropyl polisiloxane as stationary phase (Restek Corporation, Bellefonte, PA, United States). The column oven temperature was programmed 150°C (held for 2 min), increased to 220°C at a rate of 35°C/min (held for 1 min), then raised to 225°C a rate of 0.5°C/min (maintained for 1 min). The other parameters were as follows: injection temperature, 225°C; detector temperature, 250°C; carrier gas, Helium at 1 ml/min; injection volume, 1 μl. The relative percentage of each major component in AB-SCF was quantified based on the peak area integrated by Thermo Xcalibur™ data analysis program (Thermo fisher Scientific, United States). Qualitative and quantitative analysis of AB-SCF (C16:0 Palmitate, C18:0 Stearate, C18:1 Oleate, C18:2 Linoleate) was carried out in comparing with the F.A.M.E Mix RM-4 standards.

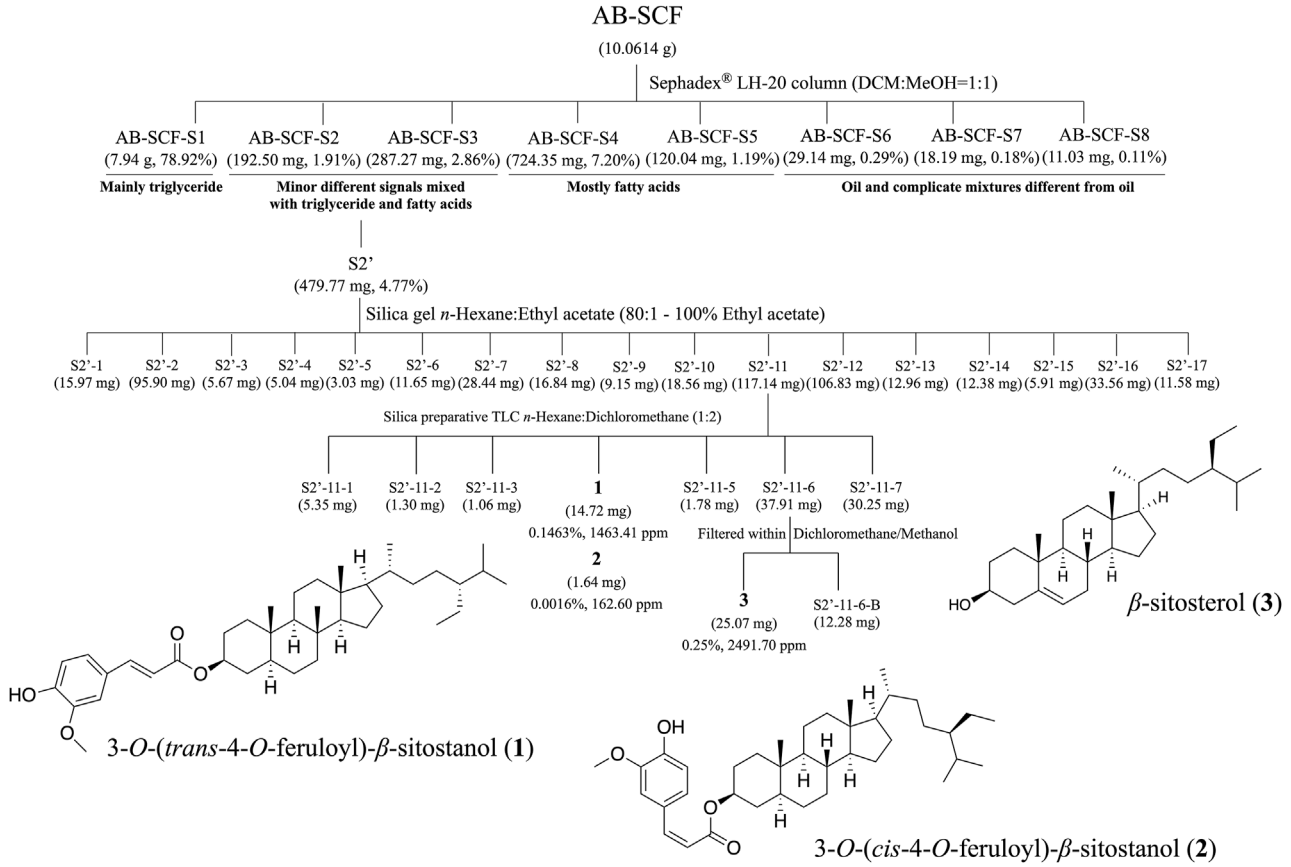

FIGURE 5 | The separation processes and isolated compounds of non-lipid constituents from AB-SCF. AB-SCF was first size-meshed through Sephadex® LH-20 to be pre-divided from fatty acids. AB-SCF-S2 and S3 were detected with minor signals different from lipid in ^{1}H NMR screens, and combined as S2′ for further SiO_2 column chromatography and preparative TLC separations and purifications. Three non-lipid pure compounds, 3-*O*-(*trans*-4-feruloyl)-*β*-sitostanol (**1**), 3-*O*-(*cis*-4-feruloyl)-*β*-sitostanol (**2**) and *β*-sitosterol (**3**), were obtained, and identified based on MS, ^{1}H NMR, ^{13}C NMR and comparison with authentic samples or with published data.

SCF×1, 203.20 ± 9.40; AB-SCF×5, 190.50 ± 9.40; AB-SCF×10, 177.80 ± 5.80. $p < 0.05$). Meanwhile, the GSH results were positively regulated in the relatively higher doses of AB-SCF×5 and AB-SCF×10 which were indicated as 14.70 ± 0.30 and 14.90 ± 0.50, respectively. Thus, AB-SCF might be able to be considered as an alleviating agent against the accumulation and lipid peroxidation in liver.

Effects of AB-SCF Triggered Expressions of Hepatic Energy Metabolic Mechanism Through FAS, LPL, AMPK and p-AMPK Proteins in Hyperlipidemic Hamsters

To reveal the molecular-biochemical mechanism of energy metabolism exerted by AB-SCF, actions targeted on hepatic proteins from hyperlipidemic and normal hamsters, such as fatty acid synthase (FAS), lipoprotein lipase (LPL), AMPK and p-AMPK, were investigated. As results presented in the **Figure 3** and **Supplementary Figure S5**, the expression of FAS was elevated in HFD, along with AMPK, p-AMPK were down-regulated. It is noteworthy that, just in opposite, the expression of hepatic FAS was decreased in the AB-SCF administrated hamsters with a dose-depend manner. Meanwhile, hepatic LPL, AMPK and p-AMPK had improved significantly in the both of AB-SCF×5 and AB-SCF×10 groups. These evidences suggested that the consumption of AB-SCF may exhibit the capacities in mitigating hyperlipidemia through the modulation of hepatic fat metabolism.

Nutrition Facts in AB-SCF (per 100 g)

In **Table 4**, a nutrition fact list was offered. The gross energy of every 100 g AB-SCF is 793.57 ± 1.88 Kcal. Lipids (81.13 ± 0.25%) was the most abundant ingredient with no trans fats was found comprising. Proteins constituted 15.85 ± 0.15%, meanwhile, no carbohydrates, including sugar, were found in AB-SCF.

Major Lipid Compositions and the Analytical Fingerprint of AB-SCF

Supercritical fluid extraction with the solvent, SC-CO_2, was characterized by its apolar property, and known as an effective

approach to obtain the oil/apolar substances. The analysis focused on the lipid compositions of AB-SCF with anti-dyslipidemic/hypercholesterolemic capacities is a considerable issue to be investigated as well. As the results presented in the **Table 5**, four major fatty acids, palmitic acid (C16:0; 13.07%), linoleic acid (C18:2; 28.59%), oleic acid (C18:1; 56.95%) and stearic acid (C18:0; 1.39%) were identified. Unsaturated fats majorly occupied up to 85.18% (linoleic acid + oleic acid) along with 14.16% saturated fats (palmitic acid + stearic acid) were detected. Fingerprint of AB-SCF lipids was established as shown in the **Figure 4**. Optimized and detailed analytic parameters for quality control using gas chromatography system were established in this work (**section 2.8** and **2.9**).

General Separation Processes and Identification of the Isolated Compounds From AB-SCF

The complete flow chart for separation and isolated pure compounds from AB-SCF were presented in the **Figure 5**. Detailed chromatographic works were recorded in **Supplementary Figures S1–S4** as described in the **section 2.9**. Three compounds, 3-*O*-(*trans*-4-feruloyl)-*β*-sitostanol (**1**) (Condo et al., 2001), 3-*O*-(*cis*-4-feruloyl)-*β*-sitostanol (**2**) (Akihisa et al., 2000) and *β*-sitosterol (**3**) (Chaturvedula and Prakash., 2012), were the obtained with the yields of 14.724 mg (0.1463%, 1463.41 ppm), 1.636 mg (0.0016%, 162.60 ppm) and 25.07 mg (0.2491%, 2491.70 ppm), respectively. Each compound was identified by MS, ^{1}H NMR, ^{13}C NMR and comparison with authentic samples or with published data.

3-*O*-(trans-4 feruloyl)-*β*-sitostanol (**1**): EISMS *m/z* 591.71 $[M\text{-}H]^-$. ^{1}H NMR ($CDCl_3$): δ_H 0.6–2.0 (*β*-sitostanol moiety, ~50H), 3.91 (s, 3H), 4.82 (tt, *J* = 11.0, 4.8 Hz, 1H), 5.88 (s, 1H), 6.27 (d, *J* = 15.9 Hz, 1H), 6.91 (d, *J* = 8.1 Hz, 1H), 7.03 (d, J = 1.7, 1H), 7.06 (dd, 8.2, 1.8, 1H), 7.59 (d, *J* = 15.9 Hz, 1H). ^{13}C NMR: 11.96, 12.05, 12.24, 18.71, 19.01, 19.80, 21.29, 23.04, 24.20, 26.05, 27.62, 28.25, 28.62, 29.12, 31.99, 33.90, 34.16, 35.48, 35.48, 36.16, 36.78, 39.96, 42.57, 44.67, 45.81, 54.22, 55.89, 56.15, 56.40, 73.71, 109.22, 114.66, 116.18, 122.98, 127.11, 144.36, 146.71, 147.79, 166.81 (**Supplementary Figure S6**).

The ^{1}H NMR ($CDCl_3$) data of 3-*O*-(*cis*-4-feruloyl)-*β*-sitostanol (**2**), a rotated geometric isomer minorly mixed in (**1**) were listed as follows (**Supplementary Figure S7**): δ 7.11 (d, *J* = 8.2 Hz, 3H), 6.87 (d, *J* = 8.2 Hz, 2H), 6.76 (d, *J* = 13.0 Hz, 2H), 6.47 (d, *J* = 15.9 Hz, 1H), 6.06 (d, *J* = 15.9 Hz, 0H), 5.80 (d, *J* = 4.0 Hz, 1H), 5.77 (d, *J* = 4.2 Hz, 1H), 5.39 (s, 1H), 4.37 (q, *J* = 7.2 Hz, 1H), 3.65 (s, 3H). (**1**) and (**2**) would interconvert to be each other, and steadily exist with a ratio of 9:1 observed according to the integral quantities of ^{1}H signals.

β-sitosterol (**3**): EIMS m/z 414.72 $[M^+]$. ^{1}H NMR ($CDCl_3$): H-3 (δ_H 3.55, dtt, *J* = 27.0, 10.9, 4.6 Hz, 1H), H-5 (δ_H 5.34, m, 1H), H-19 (δ_H 0.91, d, *J* = 6.6 Hz, 3H), H-24 (δ_H 0.85, d, *J* = 7.6 Hz, 3H), H-26 (δ_H 0.82, s, 3H), H-27 (δ_H 0.80, s, 3H), H-28 (δ_H 0.67, s, 3H), H-29 (δ_H 1.00, s, 3H). ^{13}C NMR: 11.99, 12.21, 18.91, 19.16, 19.53, 19.95, 21.21, 23.19, 24.43, 28.38, 29.28, 31.78, 32.04, 36.64, 37.39, 39.91, 40.63, 42.42, 42.45, 45.96, 50.26, 56.19, 56.90, 71.92, 77.00, 121.84, 129.41, 138.46, 140.91 (**Supplementary Figure S8**).

^{1}H NMR and ^{13}C NMR spectra were performed on JEOL JNM-ECS 400 MHz NMR Spectrometer (^{1}H, F400 MHz; ^{13}C, 100 MHz) and Varian Mercury Plus 400 MHz FT-NMR (^{1}H, 400 MHz; ^{13}C, 100 MHz) in $CDCl_3$. Mass spectra were obtained from Waters 2695 Separations Module (ESI-MS).

DISCUSSION

In this work, high-fat diet severely induced hyperlipidemia-related syndromes on hamsters, i.e., higher BW, serum TG, TC, LDL-C, lowered HDL-C; and hepatic lipid accumulation (TG and TC) in hamsters, which situations were consistent with similar models of previous investigations (Rideout et al., 2014; Wang et al., 2011). EM, an HFD group administrated with the emulsifier prepared as vehicle (Tween 80/Span 80 in the ratio of 5:1 v/v, then diluted with sterilized RO water to 5%) for AB-SCF did not influent the induction of HFD on hamsters.

After 8 weeks of administration of AB-SCF×0.5, AB-SCF×1, AB-SCF×5 and AB-SCF×10 to hyperglycemic hamsters, AB-SCF×10 displayed a significant prevention of dramatic body weight gains, and stably remain it close to the normal group. Higher dose of AB-SCF may exert anti-obesity properties. All AB-SCF groups exhibited markedly lower data than HFD-induced group in not only serum TG and TC, but also in LDL-C. Since HDL-C levels were ascendingly improved, LDL-C/HDL-C ratios, the predictor of cardiovascular risk (Jukema et al., 2005), were meaningfully ameliorated by AB-SCF as well. In feces, no obvious difference in lipid and lipoprotein profiles were detected. However, AB-SCF groups would improve the excretions of bile acids with significances. These positive responses of serum biochemical data and fecal bile acids were all occurred in a dose-dependent manner. To the assessments of hepatic TG, TC, AB-SCF had significantly ameliorated the levels of hepatic TG and TC. Especially in the AB-SCF×10 group, these two indicators were almost retrieved back to the levels of the standard chow diet hamsters. AB-SCF may also be considered as an alleviating agent against lipid peroxidation in liver due to the proper regulation of tissue MDA and GSH.

According to the results of chemical constituent analysis in this work, lipid related components in AB-SCF, e.g., triglyceride, fatty acids (saturated fat and unsaturated fat) were occupied at least 80% in the investigations of nutrition facts (**Table 4**) and the separation processes (**Figure 5**). Although there was no direct report focused on the ingredients of AB-SCF, adlay was once indicated containing a significantly abundant amount of lipids than most of the common cereals (Xi et al., 2016). Unsaturated fatty acids, composed by linoleic acid and oleic acid, were totally detected up to 85.54% in the major lipid compositions of AB-SCF. Previous studies have revealed that linoleic acid would reduce the level of LDL-C and enhance the level of HDL-C in hamsters (Valeille et al., 2004; Lock et al., 2005). Furthermore, linoleic acid was descripted to exhibit health effects against obesity and other diseases of lipid metabolism (Shen and McIntosh, 2016). Linoleic acid which exists 28.59% in the AB-SCF may be suggested as being responsible for the beneficial effects of lipid metabolism disorders carried out in this study. Oleic acid, 56.95% comprised in the AB-SCF, would improve lipid profile. The supplementation with oleic acid showed a beneficial effect on antioxidant capacity related to components of metabolic syndrome (Pastor et al., 2021). It was also proved against hepatic ischemia and reperfusion injury in mice and would able to reduce the amount of

intracellular ROS due to the enhancement of intracellular GSH production and the limit of intracellular lipid peroxidation levels induced by H_2O_2 (Guo et al., 2019). Meanwhile, linoleic acid may also enhance GSH content through an induction of gamma-glutamylcysteine ligase (Arab et al., 2006). Linoleic acid and oleic acid can be considered as the key for alleviating lipid peroxidation in liver due to the positive responses in tissue MDA and GSH assessments.

3-*O*-(*trans*-4-feruloyl)-*β*-sitostanol (**1**) and 3-*O*-(*cis*-4-feruloyl)-*β*-sitostanol (**2**) were isolated compounds from non-lipid partitioned fraction of AB-SCF are ferulate phytostanol esters (phytostanols). They were known to lower LDL-C levels in humans by up to 15% by inhibiting the absorption of cholesterol from the intestine. USFDA has permitted a rare health claim for their use in low-fat diets (Condo et al., 2001). On the other hand, the structure of *β*-sitostanol (**3**) was similar to that of cholesterol. It was even long known about its hypocholesterolemia capacity (Zák et al., 1990). Phytosterol and phytostanols were reported to increase bile acid excretion (Becker et al., 1993; Normén et al., 2000). Since bile acid was a metabolite from cholesterol, it would be secreted to intestine from liver to assist in the digestion of intake fat. The increase of bile acid expend would lead to more cholesterol metabolized in liver for filling up the spent bile acid. 3-*O*-(*trans*-4-feruloyl)-*β*-sitostanol, 3-*O*-(*cis*-4-feruloyl)-*β*-sitostanol and *β*-sitostanol summed as 0.41% (4117.72 ppm), along with linoleic acid and oleic acid (85.54%) in the AB-SCF may play an important role in the enhancement of cholesterol metabolism and bile acid excretion. These compositions may synergistically trigger the mentioned anti-dyslipidemic/hypercholesterolemic capacities of AB-SCF.

To the bio-molecular mechanism of hepatic energy metabolism, AB-SCF which exhibited the capacities in activating AMPK and p-AMPK may not only suppress the syntheses of fatty acids and cholesterol, but also reduce the hepatic gluconeogenesis and insulin resistance (Viollet et al., 2009; Liu et al., 2017). Through AMPK pathway, AB-SCF would also regulate lipid oxidation and hepatic lipid accumulation in liver (Long and Zierath, 2006). AB-SCF which also increase the hepatic LPL would impact on the hydrolysis of circulating TG, chylomicrons and VLDL (very low-density lipoprotein). AB-SCF may play a role in lipoprotein metabolism activated to launch hypolipidemic effect and prevention of atherogenesis (Santamarina-Fojo et al., 2004; Wang and Eckel, 2009). FAS which down-regulated by AB-SCF is a key enzyme in lipogenesis. The suppression of hepatic FAS would inhibit the fatty acid and TG synthesis in HFD-induced hamster owing to the catalysis of acetyl-CoA and malonyl-CoA (Engin, 2017; Rideout et al., 2014).

CONCLUSION

In the current study, AB-SCF exhibited a lipid-regulating potential on hyperlipidemic hamsters by preventing the body weight gain, ameliorating the elevation of serum TG, TC and LDL-C levels, as well as improving the rises of hepatic TG and TC levels. HDL-C was enhanced, along with the attenuation on the crucial predictor of cardiovascular risk, the LDL-C/HDL-C ratios. The energy metabolic mechanisms were clarified with the down-regulation of FAS, along with the up-regulations of LPL, AMPK and p-AMPK proteins in liver tissues. These results were exhibited with a dose-dependent manner. The active ingredients of AB-SCF were indicated and composed by linoleic acid, oleic acid, 3-*O*-(*trans*-4-feruloyl)-*β*-sitostanol, 3-*O*-(*cis*-4-feruloyl)-*β*-sitostanol and *β*-sitostanol. These compositions may be synergistically responsible for the anti-dyslipidemic/hypercholesterolemic capacities of AB-SCF. They can also be monitored as crucial standards in quality control.

The evidences carried out in this work brought out a hint for further utilization aiming at the byproduct generated during the refining processes of polished adlay. AB-SCF may be considered as a promising complementary supplement, and developed as a functional food or new botanical drug in the future.

DATA AVAILABILITY STATEMENT

The raw data supporting the conclusions of this article will be made available by the authors, without undue reservation.

ETHICS STATEMENT

The animal study was reviewed and approved by The institutional animal care and use committee (IACUC) of Chia-Nan university: CN-IACUC-105008R. Written informed consent was obtained from the owners for the participation of their animals in this study.

AUTHOR CONTRIBUTIONS

C-CH and C-HL contributed conception and design of the study; C-HL, Y-HT, S-JW, and F-RC designed the experiments and the utilized methodologies; Investigation was implemented by C-CH, T-CL, C-HL, S-JW, and Y-HT; data analysis was conducted by T-CL, H-CH, S-YY, C-HL, Y-HT, S-JW, and F-RC; original draft was prepared by C-CH, Y-HT, and S-JW; Y-HT and F-RC processed the writing-review and editing; project administration was supervised by C-HL, S-JW, and F-RC. All authors contributed to manuscript revision, read and approved the submitted version.

FUNDING

This research was funded by the Ministry of Science and Technology, Taiwan awarded to F-RC, grant number: MOST 108-2320-B-037-022-MY3, 109-2927-I-037-502, 106-2811-B-037-025, 110-2811-B-037-518. In addition, this research was

partially funded by the Drug Development and Value Creation Research Center of Kaohsiung Medical University; Department of Medical Research of Kaohsiung Medical University Hospital awarded to F-RC (grant number: KMU-TC108A03-11 and KMU-TC108A03-4).

ACKNOWLEDGMENTS

We would like to specially thank Joben Bio-Medical Co., Ltd. (Pingtung, Taiwan) for extracting AB-SCF with their the industrial-scaled supercritical fluid system. The Center for Research Resources and Development (CRRD) of Kaohsiung Medical University for providing the assistance in NMR, LC-MS and GC-MS are sincerely appreciated as well.

SUPPLEMENTARY MATERIAL

The Supplementary Material for this article can be found online at: https://www.frontiersin.org/articles/10.3389/fphar.2021.785944/full#supplementary-material

REFERENCES

Akihisa, T., Yasukawa, K., Yamaura, M., Ukiya, M., Kimura, Y., Shimizu, N., et al. (2000). Triterpene Alcohol and Sterol Ferulates from Rice Bran and Their Anti-inflammatory Effects. *J. Agric. Food Chem.* 48 (6), 2313–2319. doi:10.1021/jf000135o

Arab, K., Rossary, A., Soulère, L., and Steghens, J. P. (2006). Conjugated Linoleic Acid, Unlike Other Unsaturated Fatty Acids, Strongly Induces Glutathione Synthesis Without Any Lipoperoxidation. *Br. J. Nutr.* 96 (5), 811–819. doi:10.1017/BJN20061910

Becker, M., Staab, D., and Von Bergmann, K. (1993). Treatment of Severe Familial Hypercholesterolemia in Childhood with Sitosterol and Sitostanol. *J. Pediatr.* 122 (2), 292–296. doi:10.1016/S0022-3476(06)80136-8

Chang, W.-C., Hu, Y.-T., Huang, Q., Hsieh, S.-C., and Ting, Y. (2020). Development of a Topical Applied Functional Food Formulation: Adlay Bran Oil Nanoemulgel. *LWT* 117, 108619. doi:10.1016/j.lwt.2019.108619

Chaturvedula, V. S. P., and Prakash, I. (2012). Isolation of Stigmasterol and? Sitosterol from the Dichloromethane Extract of Rubus Suavissimus. *Int. Curr. Pharm. J.* 1 (9), 239–242. doi:10.3329/icpj.v1i9.11613

Chen, H. J., Chung, C. P., Chiang, W., and Lin, Y. L. (2011). Anti-inflammatory Effects and Chemical Study of a Flavonoid-Enriched Fraction from Adlay Bran. *Food Chem.* 126, 1741–1748. doi:10.1016/j.foodchem.2010.12.074

Chen, H. J., Hsu, H. Y., and Chiang, W. (2012a). Allergic Immune-Regulatory Effects of Adlay Bran on an OVA-Immunized Mice Allergic Model. *Food Chem. Toxicol.* 50, 3808–3813. doi:10.1016/j.fct.2012.07.011

Chen, H. J., Lo, Y. C., and Chiang, W. (2012b). Inhibitory Effects of Adlay Bran (*Coix Lachryma-jobi* L. Var. Ma-Yuen Stapf) on Chemical Mediator Release and Cytokine Production in Rat Basophilic Leukemia Cells. *J. Ethnopharmacol.* 141 (1), 119–127. doi:10.1016/j.jep.2012.02.009

Chung, C. P., Hsia, S. M., Lee, M. Y., Chen, H. J., Cheng, F., Chan, L. C., et al. (2011a). Gastroprotective Activities of Adlay (*Coix Lachryma-jobi* L. Var. *Ma-Yuen* Stapf) on the Growth of the Stomach Cancer AGS Cell Line and Indomethacin-Induced Gastric Ulcers. *J. Agric. Food Chem.* 59, 6025–6033. doi:10.1021/jf2009556

Chung, C. P., Hsu, C. Y., Lin, J. H., Kuo, Y. H., Chiang, W., and Lin, Y. L. (2011b). Antiproliferative Lactams and Spiroenone from Adlay Bran in Human Breast Cancer Cell Lines. *J. Agric. Food Chem.* 59, 1185–1194. doi:10.1021/jf104088x

Chung, C. P., Hsu, H. Y., Huang, D. W., Hsu, H. H., Lin, J. T., Shih, C. K., et al. (2010). Ethyl Acetate Fraction of Adlay Bran Ethanolic Extract Inhibits Oncogene Expression and Suppresses DMH-Induced Preneoplastic Lesions of the Colon in F344 Rats through an Anti-inflammatory Pathway. *J. Agric. Food Chem.* 58, 7616–7623. doi:10.1021/jf101084e

Comino, I., Moreno, Mde. L., Real, A., Rodríguez-Herrera, A., Barro, F., and Sousa, C. (2013). The Gluten-free Diet: Testing Alternative Cereals Tolerated by Celiac Patients. *Nutrients* 5, 4250–4268. doi:10.3390/nu5104250

Condo, A. M., Baker, D. C., Moreau, R. A., and Hicks, K. B. (2001). Improved Method for the Synthesis of Trans-feruloyl-beta-sitostanol. *J. Agric. Food Chem.* 49 (10), 4961–4964. doi:10.1021/jf010703f

Engin, A. (2017). Non-alcoholic Fatty Liver Disease. *Adv. Exp. Med. Biol.* 960, 443–467. doi:10.1007/978-3-319-48382-5_19

Guo, J., Zhang, T., Gu, J., Cai, K., Deng, X., Chen, K., et al. (2019). Oleic Acid Protects Against Hepatic Ischemia and Reperfusion Injury in Mice by Inhibiting AKT/mTOR Pathways. *Oxid. Med. Cel Longev.* 2019, 4842592. doi:10.1155/2019/4842592

Hsieh, T. J., Tsai, Y. H., Liao, Y. C., Lien, P. J., Sun, C. C., et al. (2012). Anti-diabetic Properties of Non-polar Toona Sinensis Roem Extract Prepared by Supercritical-CO2 Fluid. *Food Chem. Toxicol.* 50, 779–789. doi:10.1016/j.fct.2011.12.023

Huang, C. J., Hou, M. F., Kan, J. Y., Juan, C. H., Yuan, S. S., Luo, K. H., et al. (20152015). Prophylactic Treatment with Adlay Bran Extract Reduces the Risk of Severe Acute Radiation Dermatitis: A Prospective, Randomized, Double-Blind Study. *Evid. Based Complement. Alternat Med.* 2015, 312072. doi:10.1155/2015/312072

Huang, D. W., Wu, C. H., Shih, C. K., Liu, C. Y., Shih, P. H., Shieh, T. M., et al. (2014). Application of the Solvent Extraction Technique to Investigation of the Anti-inflammatory Activity of Adlay Bran. *Food Chem.* 145, 445–453. doi:10.1016/j.foodchem.2013.08.071

Ichihara, K., and Fukubayashi, Y. (2010). Preparation of Fatty Acid Methyl Esters for Gas-Liquid Chromatography. *J. Lipid Res.* 51 (3), 635–640. doi:10.1194/jlr.D001065

Jukema, J. W., Liem, A. H., Dunselman, P. H., van der Sloot, J. A., Lok, D. J., and Zwinderman, A. H. (2005). LDL-C/HDL-C Ratio in Subjects with Cardiovascular Disease and a Low HDL-C: Results of the RADAR (Rosuvastatin and Atorvastatin in Different Dosages and Reverse Cholesterol Transport) Study. *Curr. Med. Res. Opin.* 21 (11), 1865–1874. doi:10.1185/030079905X74952

Kuo, C.-C., Chen, H.-H., and Chiang, W. (2012). Adlay (薏苡 Yì Yǐ; "Soft-Shelled Job's Tears"; the Seeds of Coix Lachryma-Jobi L. Var. Ma-Yuen Stapf) Is a Potential Cancer Chemopreventive Agent toward Multistage Carcinogenesis Processes. *J. Traditional Complement. Med.* 2, 267–275. doi:10.1016/S2225-4110(16)30112-2

Lee, L. C., Wei, L., Huang, W. C., Hsu, Y. J., Chen, Y. M., and Huang, C. C. (2015). Hypolipidemic Effect of Tomato Juice in Hamsters in High Cholesterol Diet-Induced Hyperlipidemia. *Nutrients* 7 (12), 10525–10537. doi:10.3390/nu7125552

Lee, M. Y., Lin, H. Y., Cheng, F., Chiang, W., and Kuo, Y. H. (2008). Isolation and Characterization of New Lactam Compounds that Inhibit Lung and Colon Cancer Cells from Adlay (*Coix Lachryma-jobi* L. Var. Ma-Yuen Stapf) Bran. *Food Chem. Toxicol.* 46 (6), 1933–1939. doi:10.1016/j.fct.2008.01.033

Li, B., Qiao, L., Li, L., Zhang, Y., Li, K., Wang, L., et al. (2017). A Novel Antihypertensive Derived from Adlay (Coix Larchryma-Jobi L. Var. Ma-Yuen Stapf) Glutelin. *Molecules* 22 (4), 534. doi:10.3390/molecules2204053410.3390/molecules22010123

Li, S. C., Chen, C. M., Lin, S. H., Chiang, W., and Shih, C. K. (2011). Effects of Adlay Bran and its Ethanolic Extract and Residue on Preneoplastic Lesions of the colon in Rats. *J. Sci. Food Agric.* 91, 547–552. doi:10.1002/jsfa.4219

Lin, L., Yang, Q., Zhao, K., and Zhao, M. (2018). Identification of the Free Phenolic Profile of Adlay Bran by UPLC-QTOF-MS/MS and Inhibitory Mechanisms of Phenolic Acids Against Xanthine Oxidase. *Food Chem.* 253, 108–118. doi:10.1016/j.foodchem.2018.01.139

Liu, C., Ma, J., Sun, J., Cheng, C., Feng, Z., Jiang, H., et al. (2017). Flavonoid-rich Extract of *Paulownia Fortunei* Flowers Attenuates Diet-Induced Hyperlipidemia, Hepatic Steatosis and Insulin Resistance in Obesity Mice by AMPK Pathway. *Nutrients* 9 (9), 959. doi:10.3390/nu9090959

Lock, A. L., Horne, C. A., Bauman, D. E., and Salter, A. M. (2005). Butter Naturally Enriched in Conjugated Linoleic Acid and Vaccenic Acid Alters Tissue Fatty

Acids and Improves the Plasma Lipoprotein Profile in Cholesterol-Fed Hamsters. *J. Nutr.* 135, 1934–1939. doi:10.1093/jn/135.8.1934

Long, Y. C., and Zierath, J. R. (2006). AMP-activated Protein Kinase Signaling in Metabolic Regulation. *J. Clin. Invest.* 116, 1776–1783. doi:10.1172/JCI29044

Mera, Y., Kawai, T., Ogawa, N., Odani, N., Sasase, T., Miyajima, K., et al. (2015). JTT-130, a Novel Intestine-specific Inhibitor of Microsomal Triglyceride Transfer Protein, Ameliorates Lipid Metabolism and Attenuates Atherosclerosis in Hyperlipidemic Animal Models. *J. Pharmacol. Sci.* 129 (3), 169–176. doi:10.1016/j.jphs.2015.10.004

Noeman, S. A., Hamooda, H. E., and Baalash, A. A. (2011). Biochemical Study of Oxidative Stress Markers in the Liver, Kidney and Heart of High Fat Diet Induced Obesity in Rats. *Diabetol. Metab. Syndr.* 3, 17. doi:10.1186/1758-5996-3-17

Normén, L., Dutta, P., Lia, A., and Andersson, H. (2000). Soy Sterol Esters and Beta-Sitostanol Ester as Inhibitors of Cholesterol Absorption in Human Small Bowel. *Am. J. Clin. Nutr.* 71 (4), 908–913. doi:10.1093/ajcn/71.4.908

Ramsey, E., Sun, Q., Zhang, Z., Zhang, C., and Gou, W. (2009). Mini-review: Green Sustainable Processes Using Supercritical Fluid Carbon Dioxide. *J. Environ. Sci. (China)* 21, 720–726. doi:10.1016/S1001-0742(08)62330-X

Santamarina-Fojo, S., González-Navarro, H., Freeman, L., Wagner, E., and Nong, Z. (2004). Hepatic Lipase, Lipoprotein Metabolism, and Atherogenesis. *Arterioscler. Thromb. Vasc. Biol.* 24, 1750–1754. doi:10.1161/01.ATV.0000140818.00570.2d

Shen, W., and McIntosh, M. K. (2016). Nutrient Regulation: Conjugated Linoleic Acid's Inflammatory and browning Properties in Adipose Tissue. *Annu. Rev. Nutr.* 36, 183–210. doi:10.1146/annurev-nutr-071715-050924

Stegmann, P., Londo, M., and Junginger, M. (2020). The Circular Bioeconomy: Its Elements and Role in European Bioeconomy Clusters. *Resour. Conservation Recycling: X* 6, 100029. doi:10.1016/j.rcrx.2019.100029

Suica, V. I., Uyy, E., Boteanu, R. M., Ivan, L., and Antohe, F. (2016). Comparative Proteomic Analysis of Membrane Microdomains Isolated from Two Hyperlipidemic Animal Models. *Biochim. Biophys. Acta* 1864 (9), 1061–1071. doi:10.1016/j.bbapap.2016.05.009

Ting, Y., Hu, Y. T., Hu, J. Y., Chang, W. C., Huang, Q., and Hsieh, S. C. (2019). Nanoemulsified Adlay Bran Oil Reduces Tyrosinase Activity and Melanin Synthesis in B16F10 Cells and Zebrafish. *Food Sci. Nutr.* 7 (10), 3216–3223. doi:10.1002/fsn3.1176

Us-Fda (2008). United States – Food and Drug Administration. Available at: http://www.accessdata.fda.gov/scripts/cdrh/cfdocs/cfcfr/CFRSearch.cfm?fr=184.1240/.

Valeille, K., Gripois, D., Blouquit, M. F., Souidi, M., Riottot, M., Bouthegourd, J. C., et al. (2004). Lipid Atherogenic Risk Markers Can Be More Favourably Influenced by the *Cis*-9,*trans*-11-Octadecadienoate Isomer Than a Conjugated Linoleic Acid Mixture or Fish Oil in Hamsters. *Br. J. Nutr.* 91, 191–199. doi:10.1079/BJN20031057

Viollet, B., Lantier, L., Devin-Leclerc, J., Hebrard, S., Amouyal, C., Mounier, R., et al. (2009). Targeting the AMPK Pathway for the Treatment of Type 2 Diabetes. *Front. Biosci. (Landmark Ed.* 14, 3380–3400. doi:10.2741/3460

Wang, C. Y., Lin, H. T., and Wu, S. C. (2011). Influence of Dietary Supplementation with Bacillus-Fermented Adlay on Lipid Metabolism, Antioxidant Status and Intestinal Microflora in Hamsters. *J. Sci. Food Agric.* 91, 2271–2276. doi:10.1002/jsfa.4450

Wang, H., and Eckel, R. H. (2009). Lipoprotein Lipase: from Gene to Obesity. *Am. J. Physiol. Endocrinol. Metab.* 297, E271–E288. doi:10.1152/ajpendo.90920.2008

Wang, L., Chen, C., Su, A., Zhang, Y., Yuan, J., and Ju, X. (2016). Structural Characterization of Phenolic Compounds and Antioxidant Activity of the Phenolic-Rich Fraction from Defatted Adlay (*Coix Lachryma-jobi* L. Var. *Ma-Yuen* Stapf) Seed Meal. *Food Chem.* 196, 509–517. doi:10.1016/j.foodchem.2015.09.083

Wei, C. K., Tsai, Y. H., Korinek, M., HungEl-Shazly, P. H. M., El-Shazly, M., Cheng, Y. B., et al. (2017). 6-Paradol and 6-shogaol, the Pungent Compounds of Ginger, Promote Glucose Utilization in Adipocytes and Myotubes, and 6-paradol Reduces Blood Glucose in High-Fat Diet-Fed Mice. *Int. J. Mol. Sci.* 18 (1), 168. doi:10.3390/ijms18010168

Wells, M. A., and Dittmer, J. C. (1963). The Use of Sephadex for the Removal of Nonlipid Contaminants from Lipid Extracts. *Biochemistry* 2 (6), 1259–1263. doi:10.1021/bi00906a015

Xi, X. J., Zhu, Y. G., Tong, Y. P., Yang, X. L., Tang, N. N., Ma, S. M., et al. (2016). Assessment of the Genetic Diversity of Different Job's Tears (*Coix Lacryma-jobi* L.) Accessions and the Active Composition and Anticancer Effect of its Seed Oil. *PLoS One* 11, e0153269. doi:10.1371/journal.pone.0153269

Xu, L., Chen, L., Ali, B., Yang, N., Chen, Y., Wu, F., et al. (2017). Impact of Germination on Nutritional and Physicochemical Properties of Adlay Seed (*Coixlachryma-Jobi* L.). *Food Chem.* 229, 312–318. doi:10.1016/j.foodchem.2017.02.096

Yu, F., Gao, J., Zeng, Y., and Liu, C. X. (2011). Effects of Adlay Seed Oil on Blood Lipids and Antioxidant Capacity in Hyperlipidemic Rats. *J. Sci. Food Agric.* 91, 1843–1848. doi:10.1002/jsfa.4393

Zák, A., Zeman, M., Vítková, D., Hrabák, P., and Tvrzická, E. (1990). [Beta-sitosterol in the Treatment of Hypercholesterolemia]. *Cas Lek Cesk* 1292 (42), 1320267–1323275. doi:10.1016/S2225-4110(16)30112-2

Zhao, M., Zhu, D., Sun-Waterhouse, D., Su, G., Lin, L., Wang, X., et al. (2014). In Vitro and In Vivo Studies on Adlay-Derived Seed Extracts: Phenolic Profiles, Antioxidant Activities, Serum Uric Acid Suppression, and Xanthine Oxidase Inhibitory Effects. *J. Agric. Food Chem.* 62 (31), 7771–7778. doi:10.1021/jf501952e

Conflict of Interest: The authors declare that the research was conducted in the absence of any commercial or financial relationships that could be construed as a potential conflict of interest.

Publisher's Note: All claims expressed in this article are solely those of the authors and do not necessarily represent those of their affiliated organizations, or those of the publisher, the editors and the reviewers. Any product that may be evaluated in this article, or claim that may be made by its manufacturer, is not guaranteed or endorsed by the publisher.

frontiers in Pharmacology

ORIGINAL RESEARCH
published: 30 November 2021
doi: 10.3389/fphar.2021.744035

Study on the Chemical Constituents and Anti-Migraine Activity of Supercritical CO_2 Extracts of *Zanthoxylum schinifolium*

Ruifang Yuan[1†], Yunzhen Shi[2†], Jinming Zhang[1], Qi Hu[1], Xichuan Wei[1], Chuanhong Luo[1], Yi Wu[4], Jinhui Yang[3], Ming Yang[4], Fang Wang[4], Chuan Zheng[5]* and Dingkun Zhang[1]**

[1]Pharmacy School, State Key Laboratory of Southwestern Chinese Medicine Resources, Chengdu University of Traditional Chinese Medicine, Chengdu, China, [2]Institute of Chinese Medical Sciences, State Key Laboratory Chuan of Quality Research in Chinese Medicine, University of Macau, Macau, China, [3]Sichuan Baicao Jinggong Biotechnology Co., Ltd., Chengdu, China, [4]Key Laboratory of Modern Preparation of Traditional Chinese Medicine Under Ministry of Education, Jiangxi University of Traditional Chinese Medicine, Nanchang, China, [5]Hospital of Chengdu University of Traditional Chinese Medicine, Chengdu, China

OPEN ACCESS

Edited by:
Judit Hohmann,
University of Szeged, Hungary

Reviewed by:
Marco Biagi,
University of Siena, Italy
Pengfei Tu,
Beijing University of Chinese Medicine, China

***Correspondence:**
Fang Wang
cat689apple@163.com
Chuan Zheng
zhengchuan@cdutcm. edu.cn
Dingkun Zhang
465790643@qq.com

[†]These authors have contributed equally to this work

Specialty section:
This article was submitted to Ethnopharmacology, a section of the journal Frontiers in Pharmacology

Received: 19 July 2021
Accepted: 05 November 2021
Published: 30 November 2021

Citation:
Yuan R, Shi Y, Zhang J, Hu Q, Wei X, Luo C, Wu Y, Yang J, Yang M, Wang F, Zheng C and Zhang D (2021) Study on the Chemical Constituents and Anti-Migraine Activity of Supercritical CO_2 Extracts of Zanthoxylum schinifolium. Front. Pharmacol. 12:744035. doi: 10.3389/fphar.2021.744035

Background: *Zanthoxylum schinifolium* is a common herbal medicine in Southwest China. It is also a condiment commonly used in many families. In Chinese folk medicine, *Z. schinifolium* is considered to have the effect of relieving migraine, but there is no modern evidence on its anti-migraine mechanism.

Objective: The aim of this study was to investigate the chemical constituents of the supercritical carbon dioxide extracts of *Z. schinifolium* (CO_2-ZSE) and its effects on migraine animals.

Materials and Methods: Supercritical CO_2 extraction technology was applied to extract the dried fruit of *Z. schinifolium*, and the chemical components were determined by gas chromatography–mass spectrometry (GC-MS). Two migraine animal models were established by subcutaneous injection of nitroglycerin (NTG) and reserpine, respectively, to further evaluate the therapeutic effect of CO_2-ZSE and explore its mechanism. On the basis of the experimental results, the therapeutic effects of linalool in different dosages and different ways of administration on NTG-induced migraine rats have been further investigated.

Results: About 125 peaks were detected in CO_2-ZSE, and the relative content of linalool was 74.16%. CO_2-ZSE decreased the number of head-scratching significantly and the levels of serum nitric oxide (NO), endothelin-1 (ET-1), calcitonin gene–related peptide (CGRP), interleukin-1β (IL-1β), nuclear factor kappa B (NF-κB) p65, and inhibitor of kappa B alpha (IκBα), and increased the level of 5-hydroxytryptamine (5-HT). Linalool has the

Abbreviations: CO_2-ZSE, supercritical CO_2 extraction of *Zanthoxylum schinifolium*; CGRP, calcitonin gene–related peptide; ET-1, endothelin-1GC-MS, gas chromatography-mass spectrometry; 5-HT, 5-hydroxytryptamine; NTG, nitroglycerin; IL-1β, interleukin-1β; NF-κB, nuclear factor kappa B; IκBα, inhibitor of kappa B alpha; NIST, National Institute of Standards and Technology; NO, nitric oxide; PGs, prostaglandins; SD, standard deviation.

potential to reduce the frequency of scratching the head and the expressions of NO, ET-1, and CGRP in NTG-induced migraine rats.

Conclusion: CO_2-ZSE has a definite therapeutic effect on migraine by affecting the expression of vasomotor factors and the inflammatory pathway. Linalool has been proven to be the main effective substance against migraine. These findings provide scientific basis for the development of effective and simple migraine therapy.

Keywords: *Zanthoxylum schinifolium*, supercritical CO_2 extracts, migraine, nitroglycerin, reserpine, linalool

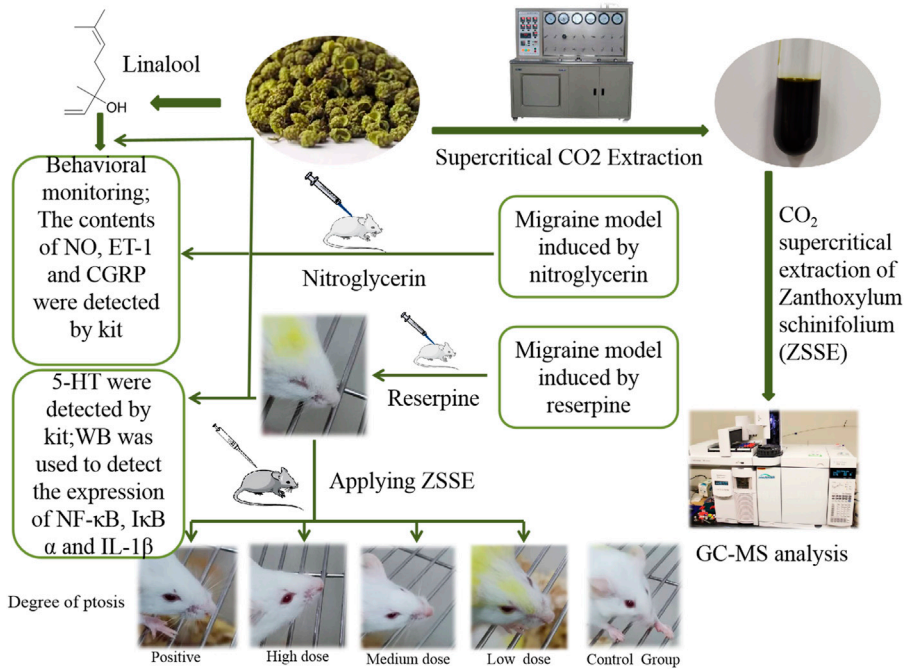

Graphical Abstract |

INTRODUCTION

Migraine is a common primary headache disease, characterized by unilateral or bilateral pulsatile pain, accompanied by photophobia, voice fear, nausea, vomiting, and other symptoms (Yuan et al., 2021). Many epidemiological studies have demonstrated its high prevalence and impact on social economy and individuals (Vos et al., 2017). The prevalence of migraine in China had reached 9.3% by 2012 (Sirri et al., 2018). Due to the recurrent attacks and difficulty in curing, it not only leads to serious physiological and psychological problems in patients but also places a huge economic burden on the family.

At present, there is no final consensus on the pathogenesis of migraine. More and more studies have shown that the migraine phase involves the activation of the trigeminocervical complex (TCC) (Goadsby, 2005), which triggers the inflammatory cascade and affects vasomotor function (Martins et al., 2017). In this pathophysiological process, some factors such as 5-HT (Deen et al., 2019), nitric oxide (NO), calcitonin gene–related peptide (CGRP), and endothelin-1 (ET-1) that affect vasomotor and the nuclear factor kappa B (NF-κB) inflammatory pathway play an important role (Iljazi et al., 2018). Triptan 5-hydroxytryptamine (5-HT) receptor agonists have been used in clinics as a migraine treatment drug, such as triptan drugs, but the safety of its long-term use remains to be investigated (de Vries et al., 2020). It is thus urgent to find a safe and effective anti-migraine drug.

Zanthoxylum schinifolium, with strong aroma and hemp flavor, is the dry mature pericarp of *Zanthoxylum schinifolium* Sieb. et Zucc. (Meng et al., 2020). It is also a well-known condiment worldwide, especially in southern and northwestern China. The chemical constituents mainly include volatile oils, alkaloids, amides, coumarin, and lignin (Chen et al., 2016). Among them, amides are the main numb-taste components in *Z. schinifolium*, and volatile oil is the main aroma component. The pharmacological effects of *Z. schinifolium* are mainly focused on analgesic, anti-inflammatory, antibacterial, anticancer,

antiviral properties, and so on (Tong and Wang, 1995; Cao et al., 2009). It was recorded in the book "*Properties Theory of Materia Medica* (yao xing lun)" in the Tang Dynasty that *Z. schinifolium* has the effect of treating migraine, and it is also used in the folk medicine. However, there is no evidence of classical model experiments on the treatment of migraine. Existing studies have shown that the volatile oil of *Z. schinifolium* has obvious analgesic effect, and the analgesic effect and duration of *Z. schinifolium* are stronger than those of *Zanthoxylum bungeanum* (Wu and Wu, 2014; Song and Liu, 2009). Therefore, the anti-migraine effect of *Z. schinifolium* was investigated *in vivo* in this study. The NTG and reserpine migraine models are recognized as reliable and practical and are widely used to study the mechanism of migraine. Accordingly, we studied the anti-migraine effect of the supercritical CO_2 extracts of *Z. schinifolium* (CO_2-ZSE), and explored the material basis of CO_2-ZSE anti-migraine by discussing the dosage and different administration methods of linalool, the main component of CO_2-ZSE. We believe that this research will provide a quick, simple, and effective relief method for migraine patients worldwide, and will attract more doctors and pharmaceutical workers to pay attention to the anti-migraine effect of *Z. schinifolium*.

MATERIALS AND METHODS

Plant Material

The peel of dried *Z. schinifolium* was purchased from Sichuan Neautus Traditional Chinese Medicine Co., Ltd. (Chengdu, China) and authenticated by Xu Runchun (Associate Professor of Chengdu University of Traditional Chinese Medicine). A voucher specimen (ID 20191006) has been preserved in the School of Pharmacy, Chengdu University of Traditional Chinese Medicine.

Equipment and Regents

The supercritical CO_2 extraction device used to extract the volatile oil of *Z. schinifolium* was produced in Haian Huada Petroleum Instrument Co., Ltd. (Jiangsu, China). Nitroglycerin (NTG) injection was purchased from Beijing Yimin Pharmaceutical Co., Ltd. (Beijing, China). Reserpine was purchased from Chengdu Must Bio-technology Co., Ltd. (Chengdu, China). Zolmitriptan tablets were purchased from Venturepharm Pharmaceutical (Hainan) Co., Ltd. (Hainan, China). The commercial enzyme-linked immunosorbent assay (ELISA) kits for NO, 5-HT, CGRP, and ET-1 were purchased from Elabscience Biotechnology Co., Ltd. (Wuhan, China). IL-1β was purchased from Abcam (United Kingdom). NF-κB p65 was purchased from Immunoway (United States). GAPDH, BCA Protein Quantitative Detection Kit, HRP-labeled goat anti-rabbit, HRP-labeled goat anti-mouse, and HRP-labeled goat anti-rat were purchased from Multisciences (Lianke) Biotech Co., Ltd. (Hangzhou, China). IκBα, SDS-PAGE gel preparation kit, and phosphorylated protease inhibitor were purchased from Wuhan Servicebio Technology Co., Ltd. (Wuhan, China).

Animals and Ethics Statements

Sprague–Dawley rats and Kunming mice used in this study were obtained from the Chengdu Dossy Experimental Animals Co., Ltd., and the animal license number was SCXK (Chuan) 2020-030. They were maintained at room temperature (25 ± 1°C) and humidity (60 ± 5%) with a 12-h light/dark cycle and free access to chow and water. This study was conducted in strict accordance with the recommendations of the Guidelines for the Care and Use of Laboratory Animals of the Ministry of Science and Technology of China. The protocol and experimental designs were approved by the Ethical Committee of Hospital of Chengdu University of Traditional Chinese Medicine (Approval ID: 2019KY-082).

Preparation of CO_2-ZSE

Two kilograms of *Z. schinifolium* was crushed by a pulverizer and separated by No. 10 screen, and the passing part was used to extract ZSE. The extraction pressure of the supercritical CO_2 extraction device was 26 MPa, the temperature was 60°C, the analytical pressure was 7 MPa, the temperature was 55°C, the CO_2 flow rate was 3 $L{\cdot}h^{-1}$, and the extraction time was 6 h. The calculation formula of the CO_2-ZSE yield is given as follows:

$$CO_2 - \text{ZSE yield}/\% = \frac{M1/g}{M2/g} \times 100. \quad (1)$$

M1 represents the weight of CO_2-ZSE and M2 represents the weight of *Z. schinifolium*.

Gas Chromatography Mass Spectrometry Analysis of CO_2-ZSE

1 ml of CO_2-ZSE was put into a 10-ml volumetric flask, fixed with ethyl acetate, and then ultrasonically mixed. After 1 ml of the solution was taken out of the volumetric flask, it was filtered with a 0.45 μm microporous filter membrane, and the filtrate was used for GC-MS analysis.

The samples (1 μL each) were injected into the gas chromatograph system with a split inlet equipped with an HP-5 capillary column (30 m × 250 μm inner diameter and 0.25 μm film thickness) under the following conditions: initial oven temperature was set at 60 °C for 2 min, increased to 200°C at a rate of 5°C min^{-1} for 5 min, and then increased to 260°C at a rate of 10°C·min^{-1}. Helium was applied as the carrier gas at a constant flow rate of 1 ml min^{-1}, the injector temperature was set at 280°C, and the split ratio was 100:1.

The mass spectrometry conditions included a standard electron ionization (IE) source (70eV), an ion source temperature of 230°C, and an interface temperature of 150°C. The quadrupole mass analyzer had a scan range of 35–550 amu.

The components of CO_2-ZSE were positively identified using the National Institute of Standards and Technology (NIST) 14.0 Mass Spectral Database. The semi-quantitative analysis of CO_2-ZSE was performed by comparing their peak areas in the GC-MS total ion chromatogram. The percentage compositions of the compounds were calculated using the area normalization method.

NTG-Induced Migraine Rats

Sixty adult Sprague–Dawley rats weighing 220–250 g, half male and half female, were randomly divided into six groups according to the weight, including control, model, positive zolmitriptan (0.25 mg·kg^{-1}), high dose (250 mg·kg^{-1}), medium dose (125 mg·kg^{-1}), and low dose (62.5 mg·kg^{-1}) of CO_2-ZSE, respectively. On the day before the experiment, all the rats were depilated 2 cm × 3 cm on the back. The dosages of CO_2-ZSE were determined according to the results of the preliminary experiments. Normal saline was applied on the back of the rats in the control group. NTG was injected subcutaneously into the rats (10 mg·kg^{-1}) in other groups to copy the migraine models (Ni et al., 2019). CO_2-ZSE was applied on the back of rats at 30 and 120 min after modeling. The positive group was administered zolmitriptan solution orally. The occurrence time of head scratching was recorded within 3 h after modeling, and the number of head scratching was recorded every 30 min. The occurrence time of head scratching was marked by more than five consecutive scratches. Four hours after the establishment of the migraine model, the rats in all groups were anesthetized by an intraperitoneal injection of 0.2 g·ml^{-1} urethane (1.5 g·kg^{-1}). Subsequently, blood was taken from the abdominal aorta, and the brain tissue was rapidly excised to separate the TCC and then stored at −80°C until further processing.

Reserpine-Induced Migraine Mice

Sixty Kunming mice weighing 18–22 g, half male and half female, were randomly divided into six groups according to body weight, which were control, model, positive zolmitriptan (0.36 mg·kg^{-1}), high dose (360 mg·kg^{-1}), medium dose (180 mg·kg^{-1}), and low dose (90 mg·kg^{-1}) of CO_2-ZSE. On the day before the experiment, all the mice were depilated 2 cm × 3 cm on the back. Except the control group, the mice were injected subcutaneously with reserpine at a dose of 1.0 mg·kg^{-1} once a day for 10 days, with the mice in the control group receiving injections of isovolumic saline (Pu et al., 2019). After the establishment of the migraine model, RCXTA(in the CO2-ZSE groups), zolmitriptan (in the positive group), or tap water (in the control and model groups) were applied on the back of the mice for 5 days, One hour after the last administration, the eyeballs of the mice were taken and blood samples were collected. Then, the mice were euthanized, and the brain tissues were placed on ice and rapidly dissected while the isolated midbrain was immediately frozen and thereafter stored at −80°C until homogenization.

Intervention Effect of Different Doses of Linalool on Nitroglycerin-Induced Migraine Rats

Thirty adult Sprague–Dawley rats weighing 220–250 g, half male and half female, were randomly divided into five groups according to body weight, including control, model, high dose (185 mg·kg^{-1}), medium dose (92.5 mg·kg^{-1}), and low dose (46.5 mg·kg^{-1}) of linalool. The dosage of linalool was based on the amount of CO_2-ZSE multiplied by the percentage of linalool. On the day before the experiment, all the rats were depilated 2 cm × 3 cm on the back. Except for the control group, NTG was injected subcutaneously into the rats (10 mg·kg^{-1}) in each group to copy migraine models. Linalool was applied on the back of rats at 30 and 120 min after modeling, and normal saline was applied on the back of rats in the control group. The occurrence time of head scratching was recorded within 3 h after modeling, and the number of head scratching was recorded every 30 min. The occurrence time of head scratching was marked by more than five consecutive scratches.

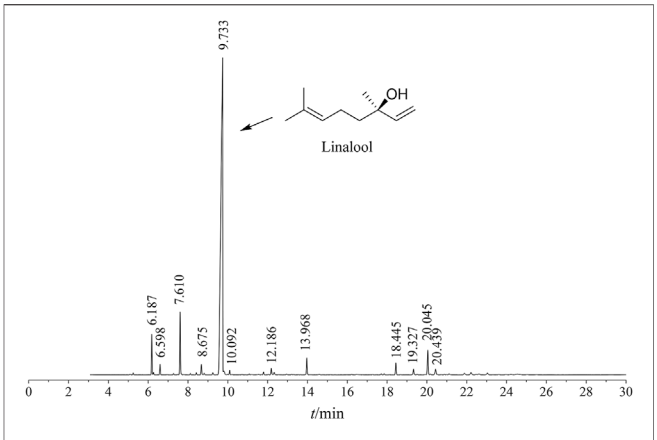

FIGURE 1 | Total ion flow map of ZSSE

Intervention Effects of Different Administration Methods of Linalool on Nitroglycerin-Induced Migraine in Rats

Sixty adult Sprague–Dawley rats weighting 220–250 g, half male and half female, were randomly divided into six groups according to body weight, which were the normal, model, positive, linalool oral administration, linalool transdermal administration, and linalool inhalation groups. On the day before the experiment, all the rats were depilated 2 cm × 3 cm on the back. The migraine model was copied by subcutaneous injection of 10 mg·kg^{-1} NTG into the back of the neck of each group. The positive group was given 0.25 mg·kg^{-1} zolmitriptan, the control group was given the same amount of normal saline, and the linalool oral administration group was given linalool by gavage at 30 and 120 min. Linalool was applied on the back of the rats in the linalool transdermal administration group at the same time, and the rats in the linalool inhalation group were placed in the sniffing device; the dosage of linalool was 185 mg·kg^{-1}. The occurrence time of head scratching was recorded within 3 h after modeling, and the number of head scratching was recorded every 30 min. The occurrence time of head scratching was marked by more than five consecutive scratches. Four hours after the establishment of the migraine model, the rats in all groups were anesthetized by an intraperitoneal injection of 0.2 g·ml^{-1} urethane (1.5 g·kg^{-1}). Subsequently, blood was taken from the abdominal aorta until further processing.

Enzyme-Linked Immunosorbent Assay

The levels of 5-HT in the brainstem tissue and NO, CGRP, and ET-1 in serum were determined by ELISA. The tissue was mixed with nine times the homogenate medium and ground. Then the ground

TABLE 1 | Composition and relative content of ZSSE.

Peak number	Retention time/min	Chemical compound	Molecular formula	CAS number	Relative content/%
1	5.087	Alpha-thujene	$C_{10}H_{16}$	002867-05-2	0.06
2	5.251	Alpha-pinene	$C_{10}H_{16}$	000080-56-8	0.14
3	6.187	Sabinene	$C_{10}H_{16}$	003387-41-5	3.19
4	6.269	Beta-pinene	$C_{10}H_{16}$	000127-91-3	0.2
5	6.598	Beta-myrcene	$C_{10}H_{16}$	000123-35-3	0.82
6	6.957	Alpha-phellandrene	$C_{10}H_{16}$	000099-83-2	0.03
7	7.281	2-carene	$C_{10}H_{16}$	1000149-94-6	0.11
8	7.498	*p*-cymene	$C_{10}H_{14}$	000099-87-6	0.04
9	7.610	D-limonene	$C_{10}H_{16}$	005989-27-5	5.45
10	8.122	Beta-ocimene	$C_{10}H_{16}$	013877-91-3	0.11
11	8.422	Gamma-terpinene	$C_{10}H_{16}$	000099-85-4	0.18
12	8.675	*cis*-beta-terpineol	$C_{10}H_{18}O$	007299-40-3	1.04
13	8.816	*cis*-alpha,alpha,5-trimethyl-5-vinyltetrahydrofuran-2-methanol	$C_{10}H_{18}O_2$	005989-33-3	0.15
14	9.733	Linalool	$C_{10}H_{18}O$	000078-70-6	74.16
15	9.998	Phenylethyl alcohol	$C_8H_{10}O$	000060-12-8	0.07
16	10.092	Thujone	$C_{10}H_{16}O$	000546-80-5	0.4
17	11.075	(+)-Citronellal	$C_{10}H_{18}O$	002385-77-5	0.11
18	11.798	(-)-4-terpineneol	$C_{10}H_{18}O$	020126-76-5	0.27
19	12.945	Gamma-terpinene	$C_{10}H_{16}$	000099-85-4	0.11
20	13.545	Cuminaldehyde	$C_{10}H_{12}O$	000122-03-2	0.03
21	13.663	(-)-carvone	$C_{10}H_{14}O$	006485-40-1	0.02
22	13.904	Cyclofeuchene	$C_{10}H_{16}$	000488-97-1	0.02
23	13.968	Linalyl acetate	$C_{12}H_{20}O_2$	000115-95-7	1.54
24	16.227	5,9,9-trimethyl-spiro[3.5]non-5-en-1-one	$C_{12}H_{18}O$	1000185-13-4	0.06
25	17.856	Tetradecane	$C_{14}H_{30}$	000629-59-4	0.12
26	18.445	Caryophyllene	$C_{15}H_{24}$	000087-44-5	1.21
27	18.686	Cubebene	$C_{15}H_{24}$	013744-15-5	0.03
28	19.327	Humulene	$C_{15}H_{24}$	006753-98-6	0.66
29	20.045	Germacrene D	$C_{15}H_{24}$	023986-74-5	2.71
30	20.18	γ-Selinene	$C_{15}H_{24}$	000515-17-3	0.11
31	20.439	Bicyclogermacrene	$C_{15}H_{24}$	067650-90-2	0.85
32	20.88	Calarene	$C_{15}H_{24}$	017334-55-3	0.08
33	21.115	Delta-cadinene	$C_{15}H_{24}$	000483-76-1	0.17
34	21.886	Elemol	$C_{15}H_{26}O$	000639-99-6	0.27
35	22.215	Nerolidol	$C_{15}H_{26}O$	040716-66-3	0.42
36	22.474	(Z)-3-hexadecene	$C_{16}H_{32}$	034303-81-6	0.1
37	23.038	Hexadecane	$C_{16}H_{34}$	000544-76-3	0.31
		Total percentage of identified compounds			95.35

solution was centrifuged at 3,000–4,000 r·min^{-1} for 10 min. The supernatant was prepared into 10% tissue homogenate and used immediately or directly frozen, and stored at −80 C. The serum was separated by centrifugation at 3,000 r·min^{-1} for 10 min at 4°C. Each multiplex assay was performed in accordance with the manufacturer's instructions. The absorbance was measured in the microplate spectrophotometer.

Western Blotting Analysis

The tissue was thoroughly homogenized with 10 times the tissue volume of the RIPA lysate on ice and centrifuged at 4°C at 12000 r·min^{-1} for 10 min, and the supernatant was separated and collected. The total protein was extracted according to the manufacturer's instructions, and the protein concentration was determined by the BCA method. The protein was separated by SDS-PAGE and transferred onto the PVDF membrane, and the transformed membrane was placed on a decolorizing shaker at room temperature and sealed with 5% skimmed milk (0.5% TBST) for 1 h. The diluted primary antibody (5% skim milk dissolved by TBST, phosphorylated protein using 5% BSA dissolved by TBST) was incubated overnight at 4°C, and then incubated with the secondary antibody at room temperature for 30 min. ChemiScope Capture software filmed and quantified the samples. The intensity of the GAPDH protein band was used as the internal control.

Statistical Analysis

The experimental data were expressed as mean ± standard error of the mean (SEM) ($\bar{x} \pm s$). The experimental data were statistically analyzed and plotted with SPSS 21.0. One-way analysis of variance (ANOVA) was used for comparison between groups. A p value < 0.05 indicates a significant difference, and a p value < 0.01 indicates a very significant difference.

RESULTS

CO_2-ZSE Yield

The results showed that the extraction rate of ZSE by supercritical CO_2 extraction was 12.3%.

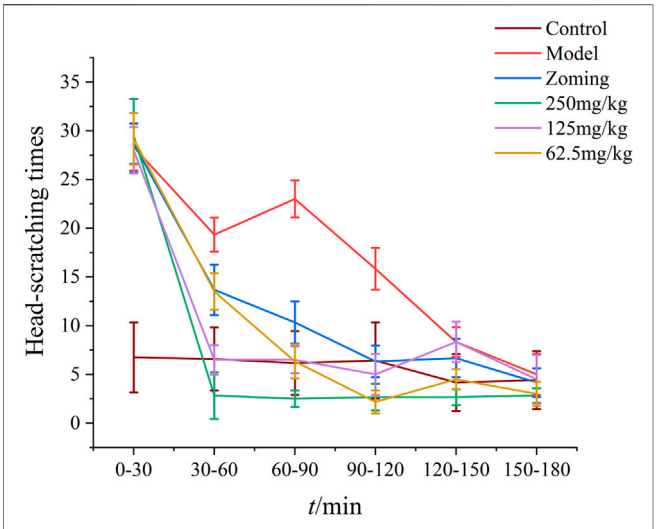

FIGURE 2 | Effect of ZSSE on scratching times of migraine rats induced by NTG ($\bar{x}$±SD, n = 10)

GC-MS Analysis of CO_2-ZSE

The ZSE extracted by supercritical CO_2 extraction showed a total of 125 peaks by GC-MS analysis. Thirty-seven chemical constituents were identified. As shown in **Figure 1** and **Table 1**, the main component of CO_2-ZSE is linalool, accounting for 74.16% of the total volatile oil, followed by D-limonene and sabinene, with contents of 5.45 and 3.19%, respectively.

Effect of CO_2-ZSE on Nitroglycerin-Induced Migraine Rats

Behavioral Investigation

After subcutaneous injection of NTG for 3–5 min, red ears, frequent head scratching, cage climbing, and photophobia began to appear in rats, which lasted for at least 3 h and then gradually disappeared, and the rats entered a quiet state. As shown in **Figure 2**, the control rats occasionally scratched their heads and climbed into the cage within 3 h of behavioral monitoring. After treatment with the drugs, the number of head scratching was reduced in different degrees in the zolmitriptan group, and all doses of CO_2-ZSE groups (p-*value* < 0.05, p-*value* < 0.01). The effect of high dose and low dose in the CO_2-ZSE groups lasted for at least 150 min.

Determination of NO, CGRP, and ET-1 in Serum

The contents of NO, CGRP, and ET-1 in rat serum are shown in **Figure 3**. Compared with the control group, subcutaneous injection of NTG significantly increased the contents of NO, CGRP, and ET-1 in the serum of the model group (p-*value* < 0.01). Zolmitriptan decreased the expression of these three factors to some extent. High dose of CO_2-ZSE significantly decreased the

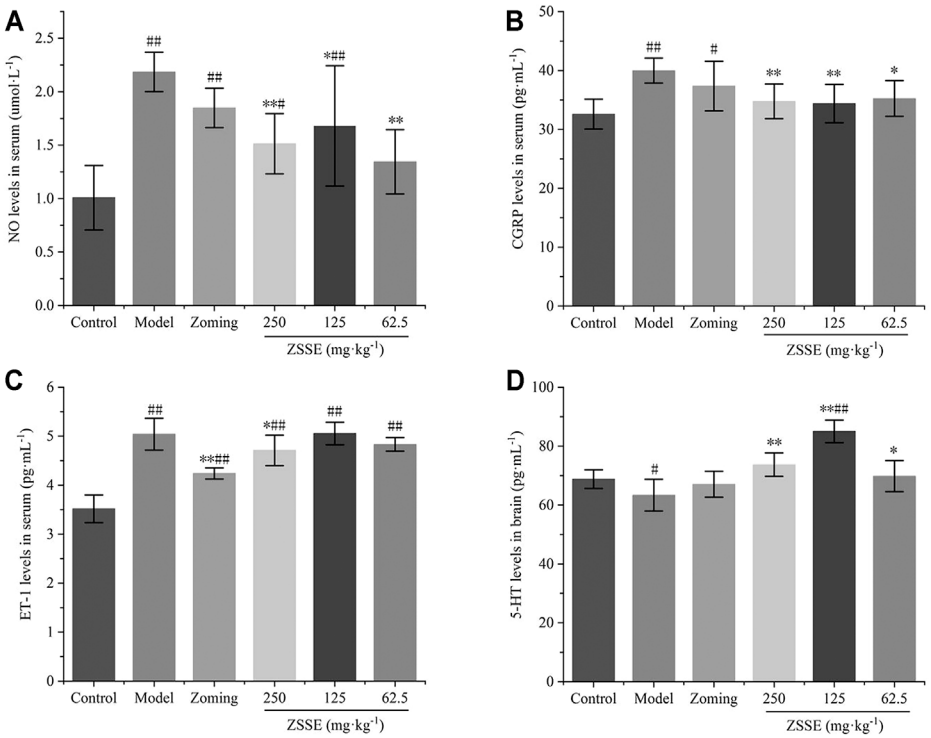

FIGURE 3 | Effect of ZSSE on serum NO, CGRP, and ET-1 levels and TCC 5-HT levels in NTG-induced migraine rats ($\bar{x}$±SD, n = 10). **(A)** NO levels in serum; **(B)** CGRP levels in serum; **(C)** ET-1 levels in serum; **(D)** 5-HT levels in the TCC. $^{\#}p < 0.05$, $^{\#\#}p < 0.01$ vs the control group, $^{*}p < 0.05$, $^{**}p < 0.01$ vs the model group.

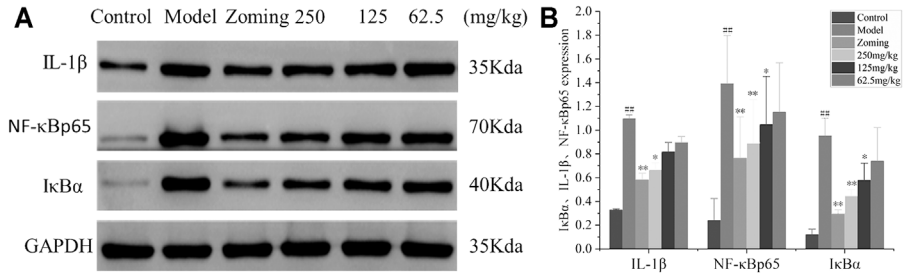

FIGURE 4 | Western blotting analysis of IκBα, IL-1β, and NF-κBp65 expressions in the TCC of NTG-induced migraine rats ($\bar{x}$±SD, n = 4). **(A)** WB strips; **(B)** Grayscale scan results of IL-1β, NF-κBp65, and IκBα. $^{\#}p < 0.05$, $^{\#\#}p < 0.01$ vs the control group, $^{*}p < 0.05$, $^{**}p < 0.01$ vs the model group.

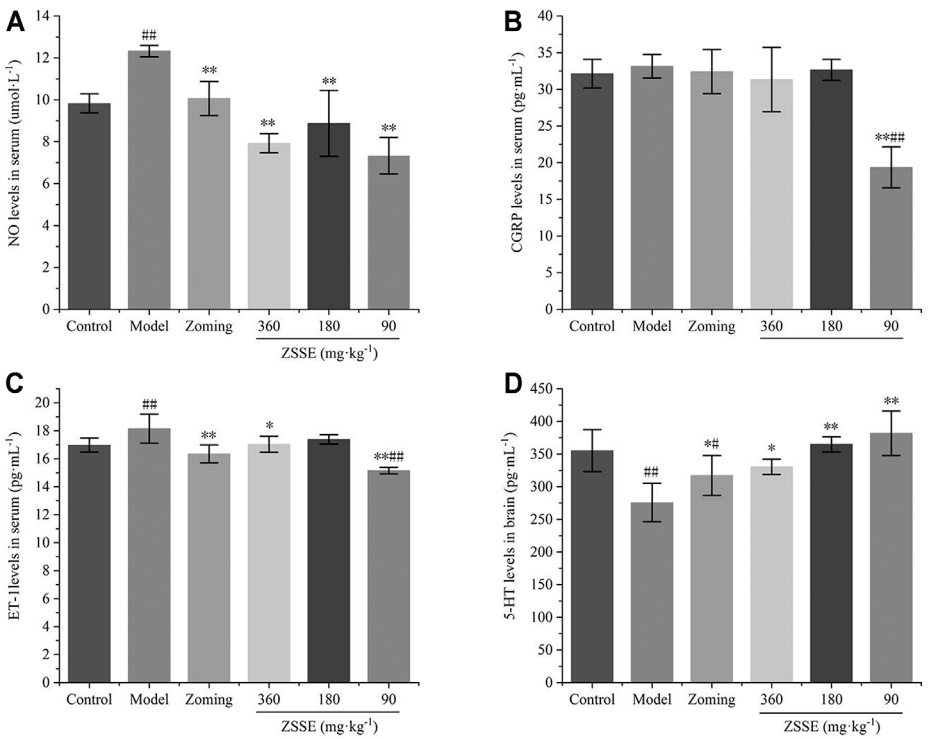

FIGURE 5 | Effects of ZSSE on the levels of NO, CGRP, and ET-1 in serum and 5-HT in the brain tissue of migraine rats with reserpine ($\bar{x}$±SD, n = 10). **(A)** NO levels in serum; **(B)** CGRP levels in serum; **(C)** ET-1 levels in serum; **(D)** 5-HT levels in the TCC. $^{\#}p < 0.05$, $^{\#\#}p < 0.01$ vs the control group, $^{*}p < 0.05$, $^{**}p < 0.01$ vs the model group.

expression of NO, CGRP, and ET-1, while medium dose of CO_2-ZSE significantly downregulated the expression of NO and CGRP, but had no significant effect on the content of ET-1. Low dose of CO_2-ZSE significantly decreased the expression of NO and CGRP ($p < 0.05$, $p < 0.01$), and inhibited the expression of ET-1 with no significance.

Determination of the 5-HT Level in the Trigemino-Cervical Complex

The results of **Figure 3** showed that NTG could significantly reduce the expression of 5-HT in the TCC of rats, zolmitriptan could upregulate the expression of 5-HT, 250 mg·kg^{-1} and 62.5 mg·kg^{-1} of CO_2-ZSE could significantly increase the expression of 5-HT, and the upregulation effect of 125 mg·kg^{-1} of CO_2-ZSE on 5-HT was the most obvious, which was significantly higher than that in the TCC of control rats.

Determination of Interleukin-1β, NF-κBp65, and Inhibitor of kappa B Alpha in the TCC

The expressions of IL-1β, NF-κBp65, and IκBα in the TCC are shown in **Figure 4**. Compared with the expressions of IL-1β, NF-κBp65, and IκBα in the TCC site of the control group, the levels of

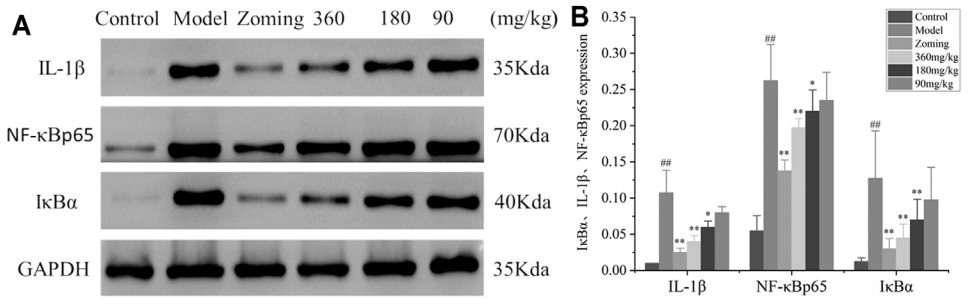

FIGURE 6 | Western blot analysis of I κ B α, IL-1β, and NF-κbp65 expressions in the brain tissue of reserpine-type migraine rats ($\bar{x}$±SD, $n = 4$). **(A)** WB strips; **(B)** Grayscale scan results of IL-1β, NF-κBp65, and IκBα. $^{\#}p < 0.05$, $^{\#\#}p < 0.01$ vs the control group, $^{*}p < 0.05$, $^{**}p < 0.01$ vs the model group.

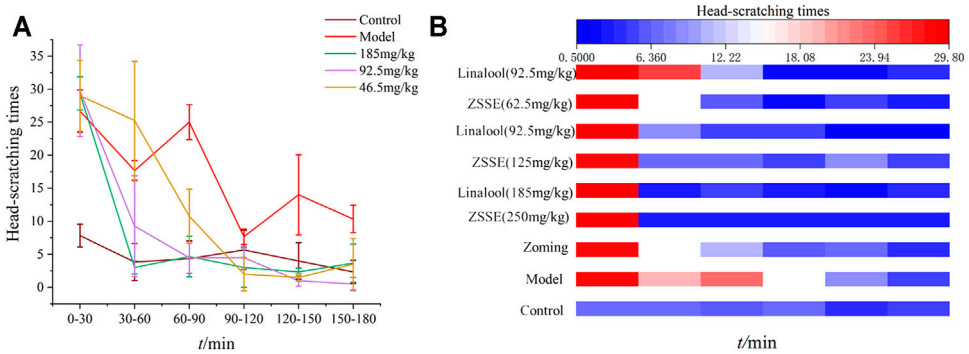

FIGURE 7 | Number of head scratching in rats ($\bar{x}$±SD, $n = 6$). **(A)** Effect of linalool intervention on scratching times of migraine rats induced by NTG; **(B)** comparison of the effects of ZSSE and linalool on the number of head scratching in rats.

IL-1β, NF-κBp65, and IκBα in the model group treated with subcutaneous injection of NTG were significantly increased ($p < 0.01$). The rats injected with NTG were treated with zolmitriptan and CO_2-ZSE. It was found that zolmitriptan and a high dose of ZSE could significantly reverse the upregulation of IL-1β, NF-κBp65, and IκBα induced by NTG (*p-value* < 0.05). The medium dose of CO_2-ZSE could significantly reduce the expression of NF-κBp65 and IκBα, and also inhibit the expression of IL-1β, but not significantly. Low dose of CO_2-ZSE could reduce the expression of these three factors. However, there was no significant difference compared with the model group.

Effect of CO_2-ZSE on Reserpine Migraine Model Mice

Behavioral Investigation

Three days after subcutaneous injection of reserpine, the mice showed lethargy, the eyes narrowed slightly, curled up and showed little activities, and body temperature decreased. With the increase of modeling time, to the 10th day of modeling, the eyes of mice had narrowed into a linear shape, and the body temperature was significantly lower than that of the normal group. The phenomenon of limb tremor occurred occasionally, which was consistent with the description in the literature (Lou et al., 2012).

Determination of NO, CGRP, and ET-1 Levels in Serum

The determination of NO, CGRP, and ET-1 levels is shown in **Figure 5**. Compared with the control group, reserpine could significantly increase the contents of NO and ET-1 in the serum of the model group, and had an increasing trend on the content of CGRP, but it was not significant. Zolmitriptan and high and low dose of CO_2-ZSE could significantly reduce the expression of NO and ET-1 ($p < 0.05$, $p < 0.01$). Zolmitriptan and high and low dose of CO_2-ZSE could significantly reduce the expression of NO and ET-1 ($p < 0.05$, $p < 0.01$), Medium dose of CO_2-ZSE could significantly reduce the expression of NO. It is worth mentioning that zolmitriptan and high and medium doses of CO_2-ZSE can downregulate the expression of CGRP, but not significantly. Low doses of CO_2-ZSE can significantly downregulate the expression of CGRP and ET-1, which is significantly lower than that of the control group.

Determination of 5-HT Level in Brain

The 5-HT level in the brain is shown in **Figure 5**. Reserpine significantly decreased the expression of 5-HT in the brain,

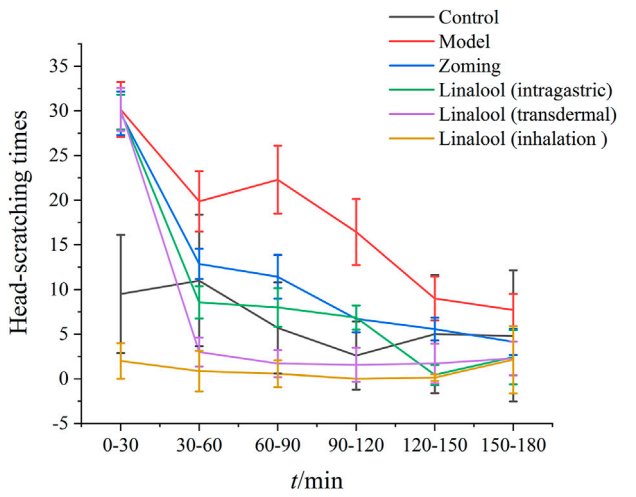

FIGURE 8 | Number of head scratching in rats (x̄±SD, n = 10)

zolmitriptan could upregulate the expression of 5-HT, and high, medium, and low dose of CO_2-ZSE could significantly increase the expression of 5-HT ($p < 0.05$, $p < 0.01$). The upregulation effect of low dose of CO_2-ZSE on 5-HT was the most obvious, which was higher than that in the brain of control rats, but there was no significant difference.

Determination of IL-1β, NF-κBp65, and I κ B α Levels in the Brain

The determination of IL-1β, NF-κBp65, and IκBα levels is shown in **Figure 6**. Compared with the expressions of IL-1β, NF-κBp65, and IκBα in the brain of the control group, the expressions of IL-1β, NF-κBp65, and IκBα were significantly increased in the model group treated with subcutaneous injection of NTG. The rats injected with NTG were treated with zolmitriptan and CO_2-ZSE. It was found that zolmitriptan and high and medium doses of CO_2-ZSE could significantly reverse the upregulation of IL-1β, NF-κBp65, and IκBα induced by nitroglycerin ($p < 0.05$, $p < 0.05$). Low dose of CO_2-ZSE could significantly reduce the expression of IL-1β, NF-κBp65, and IκBα, but the effect is not obvious.

Intervention Effect of Different Doses of Linalool on Nitroglycerin Migraine Rats

After the rats were injected with NTG, the behavioral characteristics were consistent with those described in "3.3.1 behavioral investment." The rats in the normal group had no red ear symptoms and occasionally scratched their heads to climb the cage within 3 h of behavioral monitoring. As shown in **Figure 7**, after the intervention of linalool, the high and medium doses of linalool could significantly reduce the number of head scratching in rats within 30 min, and this effect lasted at least 150 min, especially in the high-dose group. The number of head scratching in the low-dose linalool group suddenly increased 30 min after administration, even higher than that in the model group, and decreased slowly after 60 min of administration, indicating that different doses of linalool may have different regulatory effects on NTG-induced migraine rats. Low dose of linalool aggravates migraine symptoms, while high dose of linalool can relieve migraine symptoms. In addition, the effects of linalool and CO_2-ZSE with the same amount of linalool on the number of head scratching in migraine rat models induced by NTG were basically the same, indicating that linalool is, indeed, the main active component of CO_2-ZSE against migraine.

Intervention Effects of Different Administration Methods of Linalool on Nitroglycerin-Induced Migraine in Rats

Behavioral Investigation

According to the therapeutic effect, the dosage of linalool 185 mg·kg^{-1} each time was selected in this experiment. As shown in **Figure 8**, there were significant differences in the effects of different administration methods of linalool on the number of head scratching in rats with NTG-induced migraine. Within 0–30 min, compared with the normal group, NTG significantly increased the number of head scratching in the other five groups, indicating that the model was successfully established. After 30 min of linalool administration, the number of head scratching decreased significantly in the oral administration and transdermal administration groups, especially in the transdermal

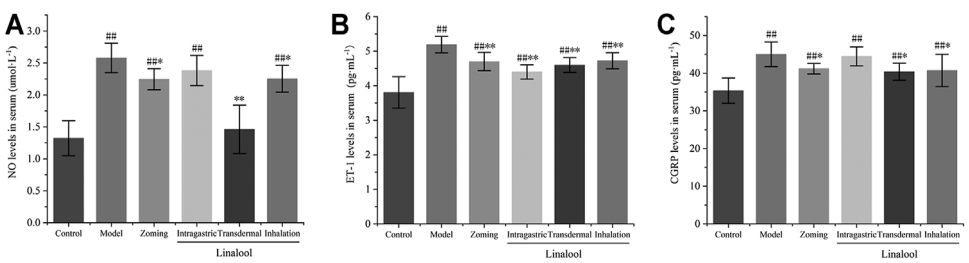

FIGURE 9 | Effects of different administration methods of linalool on serum NO, ET-1, and CGRP levels in migraine rats (x̄±SD, n = 10). **(A)** NO levels in serum; **(B)** ET-1 levels in serum; **(C)** CGRP levels in serum. $^{\#}p < 0.05$, $^{\#\#}p < 0.01$ vs the control group, $^{*}p < 0.05$, $^{**}p < 0.01$ vs the model group.

administration group, and the effect lasted at least 150 min. The head scratching behavior of the rats in the olfactory administration group was always in a state of little activity, and there were significant differences among the rats. In the course of the experiment, the rats were basically in a state of eye-closing and motionless. It may be mainly because the relatively airtight space of the sniffing device affects the behavior of the rats, so the behavioral characteristics of the rats in this group cannot be used as a standard to evaluate the therapeutic effect, and the best mode of administration can be determined by further examination of rat serum factors.

Determination of NO, CGRP, and ET-1 in Serum

As shown in **Figure 9**, compared with the control group, NTG could significantly increase the contents of NO, ET-1, and CGRP in the serum of the model group. Zolmitriptan can reduce the expression of these three factors to some extent. Oral administration of linalool significantly decreased the expression of ET-1, but had no significant effect on the contents of NO and CGRP. Transdermal administration of linalool could significantly downregulate the expressions of NO, ET-1, and CGRP ($p < 0.05$). Inhaling linalool could also significantly reduce the expressions of NO, ET-1, and CGRP ($p < 0.05$, $p < 0.01$), but the inhibitory effect on the expression of NO was not as significant as that of transdermal administration. The aforementioned results show that among the three modes of linalool administration, the effect of transdermal administration is the most significant, sniffing administration is the second, and oral administration is the worst. The shortcomings of oral administration, such as first-pass effect and slow absorption, may be the main reasons for the insignificant effect of linalool.

DISCUSSION

Migraine, as the second leading cause of disability in the world (Vos et al., 2017), is related to the health and quality of life of most people around the world. Current research shows that NO, 5-HT, CGRP, and NF-κB pathways play an important role in the pathophysiology of migraine. NO is a key molecule in the pathogenesis of migraine (Olesen, 2008). Excessive production of NO in the vascular smooth muscle cells will lead to excessive vasodilation, which, in turn, activates the nociceptive nerve fibers in the vascular wall and mediates the release of vasoactive substances such as CGRP, which further triggers perivascular neurogenic inflammation to participate in the occurrence of migraine (Yao et al., 2020). The pathophysiological changes of migraine rats induced by this model are also similar to those of human migraine. Reserpine is a monoamine neurotransmitter depletion agent that can reduce 5-HT in the body and cause migraine (Pu et al., 2019).

5-HT is recognized as a neurotransmitter closely related to migraine (Vila-Pueyo, 2018). During the aura of migraine attack, the increase of the 5-HT level causes vasoconstriction, which is then metabolized into 5-HIAA excreted in urine. Low concentration of 5-HT stimulates perivascular pain fibers, and local release of NO, prostaglandins (PGs), and neuropeptides cause vasodilation and enter the migraine attack.

CGRP is a kind of vasoactive neuropeptide composed of amino acids, which has the same vasodilative capacity as that of NO (Sohn et al., 2020). ET-1 is an endogenous vasoconstrictor released by the vascular endothelium (Hougaard et al., 2020), and it is also the strongest vasoconstrictor known at present.

The NF-κB pathway plays an important role in neurogenic inflammation of migraine (Antonova et al., 2013). Under normal physiological conditions, the phosphorylation site of NF-κB is blocked by IκB. After inflammatory injury, IKK kinase degrades IκB, exposing the nuclear localization signal of p50 and rapidly transferring p65 to the nucleus. p65 can bind to the κ B sites of some inflammatory factor gene promoters or enhancers by identifying specific DNA sequences, which starts the transcription of related genes and induces the overexpression of a variety of cytokines to cause inflammation (Reuter et al., 2002). Previous studies have shown that inflammatory factors such as TNF-α, IL-1β, and IL-6 can be induced by NF-κB (Li et al., 2019).

In this experiment, the rat model of NTG-induced migraine and the mouse model of reserpine migraine with good repeatability, economy, and simplicity were selected to explore the therapeutic effect of CO_2-ZSE on migraine. NTG and reserpine can regulate vascular tension and neurotransmitter balance by regulating vasomotor factors such as NO, CGRP, and ET-1 and neurotransmitters such as 5-HT, resulting in the activation and accumulation of proinflammatory mediators, finally leading to migraine (Sun et al., 2017; Wang et al., 2019). We found that CO_2-ZSE decreased the number of head scratching significantly; the levels of NO, ET-1, and CGRP; and the levels of IL-1β, NF-κB p65, and inhibitor of IκBα, and increased the level of 5-HT in NTG-induced rats or reserpine-induced mice. This indicates that CO_2-ZSE reverted both migraine models, and it mainly regulated the upstream inflammatory pathway by affecting vasomotor and neurotransmitter levels to achieve therapeutic effect.

The content of linalool in CO_2-ZSE is 74.16%. It is doubtful whether linalool can play an anti-migraine effect. At present, studies have shown that linalool has significant neurointervention and anti-inflammatory and analgesic effects, and can relieve anxiety (Harada et al., 2018) and depression (Goadsby, 2005) and cause a certain neuroprotective effect. This antidepressant effect is reflected by the interaction with the monoaminergic pathway. Linalool can also block the phosphorylation of the IkBa protein in raw 264.7 cells stimulated by lipopolysaccharide (LPS) and inhibit the NF-κB pathway (Huo et al., 2013), and the expression of inflammatory factors such as IL-1β, NO, and TNF-α, which reflects the anti-inflammatory effect (Batista et al., 2010; Li et al., 2015). Linalool can also reduce mechanical pain and hypersensitivity in neuropathic animals (Batista et al., 2010; Berliocchi et al., 2009). Some studies speculate that linalool has anti-migraine effects (Prachayasittikul et al., 2018; Delavar

Kasmaei et al., 2016). Based on the aforementioned studies, we studied the effects of linalool on the behavior of NTG-induced migraine rats and found that applying the same amount of linalool to CO_2-ZSE could reduce the number of head scratching in rats to the same extent, that is, linalool may be the main active component of CO_2-ZSE against migraine. Using the same animal model, the therapeutic effects of oral administration, transdermal administration, and inhalation administration of linalool were compared by detecting the animal behavior and the contents of serum NO, ET-1, and CGRP. It was determined that transdermal administration of linalool was the preferred mode of administration because it significantly restored the levels of NO, CGRP, and ET-1 in the serum of migraine-induced mice to normal, followed by inhalation administration, and oral administration was the worst. This study indicates that linalool can also regulate the activation of upstream inflammatory pathways and the accumulation of inflammatory mediators by regulating vasomotor retraction, and finally play an anti-migraine role. This mechanism is similar to the main mechanism of other known effective molecules, such as parthenolide (Tassorelli et al., 2005).

At present, oral administration, acupuncture, massage, and aromatherapy are mostly used in the treatment of migraine, or they are used together (Yuan et al., 2021). There are few therapeutic drugs for percutaneous and sniffing administration, which limited the choice of medication for migraine patients. Our research has proved that linalool can play a good therapeutic effect on migraine through percutaneous administration, which will provide guiding significance for the research and development of migraine drugs in the future. However, we only studied the effect of linalool on migraine caused by the dysregulation of the inflammatory pathway. Indeed, the etiology of migraine is complex. We can study the therapeutic effect of linalool on other migraine models and expand the therapeutic range of linalool.

CONCLUSION

CO_2-ZSE can effectively treat migraine, increase the expression of 5-HT, decrease the expression of NO, CGRP, and ET-1 to regulate vasomotor and inhibit the expression of NF-κBp65, IκBα, and IL-1β to alleviate neurogenic inflammation. This effect mainly contributes to the high concentration of linalool. These findings reveal the scientific connotation, mechanism of action, and material basis of *Z. schinifolium* for the treatment of migraine.

DATA AVAILABILITY STATEMENT

The raw data supporting the conclusions of this article will be made available by the authors, without undue reservation.

ETHICS STATEMENT

The animal study was reviewed and the protocol and experimental designs were approved by the Ethical Committee of Hospital of Chengdu University of Traditional Chinese Medicine (Approval ID: 2019KY-082).

AUTHOR CONTRIBUTIONS

RY performed the animal experiments and wrote the article. YS performed the animal experiments and analyzed the data. JZ and MY helped design the study and revised the article. QH, XW, CL, and YW performed the animal experiments. JY prepared the ZSSE. DZ, FW, and CZ supervised the project and reviewed the article.

FUNDING

We are grateful to the support of *Zanthoxylum bungeanum* Special Project of Sichuan Provincial Administration of Traditional Chinese Medicine (2018HJZX023, 2018HJZX008), Jiangxi University of Traditional Chinese Medicine Doctoral Initiation Fund Project (2018WBZR012), and the International Cooperation Project of Sichuan Science and Technology Program (2019YFH0152).

REFERENCES

Antonova, M., Wienecke, T., Olesen, J., and Ashina, M. (2013). Prostaglandins in Migraine: Update. *Curr. Opin. Neurol.* 26 (3), 269–275. doi:10.1097/WCO.0b013e328360864b

Batista, P. A., Werner, M. F., Oliveira, E. C., Burgos, L., Pereira, P., Brum, L. F., et al. (2010). The Antinociceptive Effect of (-)-linalool in Models of Chronic Inflammatory and Neuropathic Hypersensitivity in Mice. *J. Pain* 11 (11), 1222–1229. doi:10.1016/j.jpain.2010.02.022

Berliocchi, L., Russo, R., Levato, A., Fratto, V., Bagetta, G., Sakurada, S., et al. (2009). (-)-Linalool Attenuates Allodynia in Neuropathic Pain Induced by Spinal Nerve Ligation in C57/bl6 Mice. *Int. Rev. Neurobiol.* 85, 221–235. doi:10.1016/S0074-7742(09)85017-4

Cao, L. H., Lee, Y. J., Kang, D. G., Kim, J. S., and Lee, H. S. (2009). Effect of Zanthoxylum Schinifolium on TNF-Alpha-Induced Vascular Inflammation in Human Umbilical Vein Endothelial Cells. *Vascul. Pharmacol.* 50 (5-6), 200–207. doi:10.1016/j.vph.2009.01.008

Chen, L., Zhang, F. L., Sun, D. F., and Zhang, W. M. (2016). Research Progress on Biological Activity and Mechanism of Zanthoxylum Schinifolium. *Chin. Wild Plant Resour.* 35, 43–47. doi:10.3969/j.issn.1006-9690.2016.04.012

de Vries, T., Villalón, C. M., and MaassenVanDenBrink, A. (2020). Pharmacological Treatment of Migraine: CGRP and 5-HT beyond the Triptans. *Pharmacol. Ther.* 211, 107528. doi:10.1016/j.pharmthera.2020.107528

Deen, M., Hougaard, A., Hansen, H. D., Svarer, C., Eiberg, H., Lehel, S., et al. (2019). Migraine Is Associated with High Brain 5-HT Levels as Indexed by 5-HT4 Receptor Binding. *Cephalalgia* 39 (4), 526–532. doi:10.1177/0333102418793642

Delavar Kasmaei, H., Ghorbanifar, Z., Zayeri, F., Minaei, B., Kamali, S. H., Rezaeizadeh, H., et al. (2016). Effects of Coriandrum Sativum Syrup on Migraine: A Randomized, Triple-Blind, Placebo-Controlled Trial. *Iran Red Crescent Med. J.* 18 (1), e20759. doi:10.5812/ircmj.20759

Goadsby, P. (2005). Migraine Pathophysiology Headache. *J. Head Face* 45 (Supplement s1), S14–S24. doi:10.1111/j.1526-4610.2005.4501003.x

Harada, H., Kashiwadani, H., Kanmura, Y., and Kuwaki, T. (2018). Linalool Odor-Induced Anxiolytic Effects in Mice. *Front. Behav. Neurosci.* 12, 241. doi:10.3389/fnbeh.2018.00241

Hougaard, A., Younis, S., Iljazi, A., Sugimoto, K., Ayata, C., and Ashina, M. (2020). Intravenous Endothelin-1 Infusion Does Not Induce Aura or Headache in Migraine Patients with Aura. *Headache* 60 (4), 724–734. doi:10.1111/head.13753

Huo, M., Cui, X., Xue, J., Chi, G., Gao, R., Deng, X., et al. (2013). Anti-inflammatory Effects of Linalool in RAW 264.7 Macrophages and Lipopolysaccharide-Induced Lung Injury Model. *J. Surg. Res.* 180 (1), e47–54. doi:10.1016/j.jss.2012.10.050

Iljazi, A., Ayata, C., Ashina, M., and Hougaard, A. (2018). The Role of Endothelin in the Pathophysiology of Migraine-A Systematic Review. *Curr. Pain Headache Rep.* 22 (4), 27. doi:10.1007/s11916-018-0682-8

Li, L., Wang, X. Y., Li, N., and Zhang, H. (2019). Research of Mitogen-Activated Protein Kinase (MAPK) and Nuclear Transcriptionfactor-κB(NF-κB) Pathway in the Pathogenesis of Migraine. *Chin. J. Clin. Pharmacol.* 35, 153–156.

Li, Y., Lv, O., Zhou, F., Li, Q., Wu, Z., and Zheng, Y. (2015). Linalool Inhibits LPS-Induced Inflammation in BV2 Microglia Cells by Activating Nrf2. *Neurochem. Res.* 40 (7), 1520–1525. doi:10.1007/s11064-015-1629-7

Lou, Z. H., Huang, Y. F., Lv, G. Y., and Yu, F. (2012). Effect of Tianma Gouteng Granule on Reserpine Induced Migraine in Mice. *China J. Tradit. Chin. Med. Pharm.* 27, 1412–1415.

Martins, L. B., Teixeira, A. L., and Domingues, R. B. (2017). Neurotrophins and Migraine. *Vitam. Horm.* 104, 459–473. doi:10.1016/bs.vh.2016.10.003

Meng, X. H., Shang, X. Y., and Yang, J. L. (2020). Chemical Constituents of Phenols in Zanthoxylum Schinifolium and Their Antioxidant Activity. *Chin. Tradit. Herbal Drugs* 51, 2095–2101. doi:10.7501/j.issn.0253-2670.2020.08.015

Ni, N., Wang, Q., Lin, X., Hong, Y., Feng, Y., and Shen, L. (2019). Studies on the Mechanism of Glutamate Metabolism in NTG-Induced Migraine Rats Treated with DCXF. *Evid. Based Complement. Alternat. Med.* 2019, 1324797. doi:10.1155/2019/1324797

Olesen, J. (2008). The Role of Nitric Oxide (NO) in Migraine, Tension-type Headache and Cluster Headache. *Pharmacol. Ther.* 120 (2), 157–171. doi:10.1016/j.pharmthera.2008.08.003

Prachayasittikul, V., Prachayasittikul, S., Ruchirawat, S., and Prachayasittikul, V. (2018). Coriander (Coriandrum Sativum): A Promising Functional Food toward the Well-Being. *Food Res. Int.* 105, 305–323. doi:10.1016/j.foodres.2017.11.019

Pu, Z. H., Peng, C., Xie, X. F., Luo, M., Zhu, H., Feng, R., et al. (2019). Alkaloids from the Rhizomes of Ligusticum Striatum Exert Antimigraine Effects through Regulating 5-HT1B Receptor and C-Jun. *J. Ethnopharmacol.* 237, 39–46. doi:10.1016/j.jep.2019.03.026

Reuter, U., Chiarugi, A., Bolay, H., and Moskowitz, M. A. (2002). Nuclear Factor-kappaB as a Molecular Target for Migraine Therapy. *Ann. Neurol.* 51 (4), 507–516. doi:10.1002/ana.10159

Sirri, L., Pierangeli, G., Cevoli, S., Cortelli, P., Grandi, S., and Tossani, E. (2018). Illness Perception in Patients with Migraine: An Exploratory Study in a Tertiary Care Headache centre. *J. Psychosom. Res.* 111, 52–57. doi:10.1016/j.jpsychores.2018.05.011

Sohn, I., Sheykhzade, M., Edvinsson, L., and Sams, A. (2020). The Effects of CGRP in Vascular Tissue - Classical Vasodilation, Shadowed Effects and Systemic Dilemmas. *Eur. J. Pharmacol.* 881, 173205. doi:10.1016/j.ejphar.2020.173205

Song, L., and Liu, Y. P. (2009). Comparative Study on Analgesic Effect and Pharmacokinetics of Zanthoxylum Bungeanum and green Pepper. *Pharmacol. Clin. Chin. Materia Med.* 25 (06), 64–66.

Sun, Y. Y., Zhang, W. J., Dong, C. L., Zhang, X. F., Ji, J., Wang, X., et al. (2017). Baicalin Alleviates Nitroglycerin-Induced Migraine in Rats via the Trigeminovascular System. *Phytother. Res.* 31 (6), 899–905. doi:10.1002/ptr.5811

Tassorelli, C., Greco, R., Morazzoni, P., Riva, A., Sandrini, G., and Nappi, G. (2005). Parthenolide Is the Component of Tanacetum Parthenium that Inhibits Nitroglycerin-Induced Fos Activation: Studies in an Animal Model of Migraine. *Cephalalgia* 25 (8), 612–621. doi:10.1111/j.1468-2982.2005.00915.x

Tong, R. X., and Wang, P. M. (1995). Comparative Study on Acute Toxicity Pharmacological Action of Liaoning Zanthoxylum Zanthoxylum Schinifolium and Sichuan Pepper. *Liaoning J. Tradit. Chin. Med.* 22, 371–373.

Vila-Pueyo, M. (2018). Targeted 5-HT1F Therapies for Migraine. *Neurotherapeutics* 15 (2), 291–303. doi:10.1007/s13311-018-0615-6

Vos, T., Abajobir, A. A., Abate, K. H., Abbafati, C., Abbas, K. M., Abd-Allah, F., et al. (2017). Global, Regional, and National Incidence, Prevalence, and Years Lived with Disability for 328 Diseases and Injuries for 195 Countries, 1990-2016: a Systematic Analysis for the Global Burden of Disease Study 2016. *Lancet* 390 (10100), 1211–1259. doi:10.1016/S0140-6736(17)32154-2

Wang, J., Wu, S., Xu, Y. S., Liu, R., Xiao, H., Luo, S. Y., et al. (2019). Pharmacodynamics of Xiongfu Recipe on Reserpine Induced Migraine Model Mice. *Chin. Arch. Tradit. Chin. Med.* 37 (12), 4.

Wu, G., and Wu, H. (2014). Analgesia Synergism of Essential Oil from Pericarp of Zanthoxylum Schinifolium and Verapamil. *Evid. Based Complement. Alternat. Med.* 2014, 505876. doi:10.1155/2014/505876

Yao, G., Man, Y. H., Li, A. R., Guo, Y., Dai, Y., Wang, P., et al. (2020). NO Up-Regulates Migraine-Related CGRP via Activation of an Akt/GSK-3β/nf-κB Signaling cascade in Trigeminal Ganglion Neurons. *Aging (Albany NY)* 12, 6370–6384. doi:10.18632/aging.103031

Yuan, R., Zhang, D., Yang, J., Wu, Z., Luo, C., Han, L., et al. (2021). Review of Aromatherapy Essential Oils and Their Mechanism of Action against Migraines. *J. Ethnopharmacol.* 265, 113326. doi:10.1016/j.jep.2020.113326

Conflict of Interest: Author JY was employed by SBJ Biotechnology Co.,Ltd.

The remaining authors declare that the research was conducted in the absence of any commercial or financial relationships that could be construed as a potential conflict of interest.

Publisher's Note: All claims expressed in this article are solely those of the authors and do not necessarily represent those of their affiliated organizations, or those of the publisher, the editors, and the reviewers. Any product that may be evaluated in this article, or claim that may be made by its manufacturer, is not guaranteed or endorsed by the publisher.

frontiers in Pharmacology

SYSTEMATIC REVIEW
published: 30 November 2021
doi: 10.3389/fphar.2021.768268

Plectranthus ecklonii Benth: A Comprehensive Review Into its Phytochemistry and Exerted Biological Activities

Ana Ribeirinha Antão[1], *Gabrielle Bangay*[1,2†], *Eva María Domínguez-Martín*[1,2†], *Ana María Díaz-Lanza*[2] *and Patrícia Rijo*[1,3*]

[1]CBIOS -Research Center for Biosciences and Health Technologies, Universidade Lusófona de Humanidades e Tecnologias, Lisbon, Portugal, [2]University of Alcalá de Henares, Faculty of Pharmacy, Department of Biomedical Sciences, Pharmacology Area (Pharmacognosy Laboratory), New Antitumor Compounds: Toxic Action on Leukemia Cells Research Group, Campus University, Alcalá de Henares, Spain, [3]Instituto de Investigação do Medicamento (iMed.ULisboa), Faculdade de Farmácia, University of Lisbon, Lisbon, Portugal

OPEN ACCESS

Edited by:
Valentina Echeverria Moran,
Bay Pines VA Healthcare System,
United States

Reviewed by:
Mohamed L. Ashour,
Ain Shams University, Egypt
Adeyemi Oladapo Aremu,
North-West University, South Africa

***Correspondence:**
Patrícia Rijo
patricia.rijo@ulusofona.pt

[†]These authors have contributed equally to this work and share second authorship

Specialty section:
This article was submitted to Ethnopharmacology, a section of the journal Frontiers in Pharmacology

Received: 31 August 2021
Accepted: 15 October 2021
Published: 30 November 2021

Citation:
Antão AR, Bangay G, Domínguez-Martín EM, Díaz-Lanza AM and Rijo P (2021) Plectranthus ecklonii Benth: A Comprehensive Review Into its Phytochemistry and Exerted Biological Activities. Front. Pharmacol. 12:768268. doi: 10.3389/fphar.2021.768268

Ethnopharmacological Relevance: *Plectranthus* genus (*Lamiaceae* family) contain several species with acknowledged ethnopharmacological uses, such as, for gastrointestinal and respiratory-related problems, due to their anti-inflammatory, antibacterial and antifungal properties. The bioactivity of isolated medicinal compounds from this genus justifies the increased interest in recent times for species of *Plectranthus*, placing them in the spotlight for natural product drug development.

Aim of the study: To the best of our knowledge, this is the first review on the biological activities of *Plectranthus ecklonii* Benth. As such, the aim of this review was three-fold: 1) to summarize the chemical compounds isolated from *P. ecklonii*; 2) to collate the biological activities and mechanisms of action of these compounds from *in vitro* studies; and 3) to evaluate the documented uses and potential applications of this species, in order to postulate on the direction of pharmaceutical uses of this species.

Materials and methods: An extensive database retrieval was performed using the electronic databases Web of Science, PubMed, Google Scholar and ScienceDirect. The search criteria consisted of the keywords "*Plectranthus ecklonii*", "*Plectranthus ecklonii* + review", "*Plectranthus ecklonii* + diterpenes" or "*Plectranthus ecklonii* + abietanes", "*ecklonii* + parviflorone D", searched individually and as combinations. Eligibility criteria were set out and titles in English, Portuguese and Spanish were reviewed, with all references included dating from 1970 to 2021. A total of 169 papers were selected and included. Chemical structures were drawn using ChemDraw 20.0, CID numbers were searched in PubChem and the PRISMA diagram was created using PowerPoint 2012.

Results: To date, a total of 28 compounds have been isolated from *P. ecklonii*, including diterpenes, triterpenes, flavonoids, and hydroxycinnamic acids. Most focused on the antimicrobial action of its constituents, although compounds have demonstrated other

bioactivities, namely antioxidant, anti-inflammatory and antitumor. The most recent studies emphasize the diterpenoids, particularly parviflorone D, with the help of nanotechnology.

Conclusions: The widespread ethnobotanical and traditional uses of *P. ecklonii* can be scientifically justified by a range of biological activities, demonstrated by isolated secondary metabolites. These bioactivities showcase the potential of this species in the development of economically important active pharmaceutical ingredients, particularly in anticancer therapy.

Keywords: Plectranthus ecklonii, phytochemistry, pharmacology, bioactivity, plectranthus

INTRODUCTION

Since ancient times, plants have been used for the prevention and treatment of a variety of ailments. Across different cultures, they have been the basis of traditional medicine practices and they continue to be important sources of drugs, especially in developing countries that still use herbal medicine as a first line of healthcare (Salim et al., 2008). Members of the *Lamiaceae* family are considered relevant, due to their therapeutic and culinary uses throughout the world (Srancikova et al., 2013).

Plectranthus spp. (Lamiaceae) have long been used in traditional medicine, likely due to the many bioactive compounds found in the genus, having several activities, such as anti-inflammatory, antimicrobial and antifungal (Abdel-Mogib et al., 2002; Lukhoba et al., 2006; de Albuquerque et al., 2007). These properties suggest *Plectranthus* as a likely genus of bioactive compounds suitable for medicinal drug development. The isolation and understanding of the secondary metabolites from *Plectranthus* species' responsible for biological activity are important, not only to validate the popular common uses of this genus, but also to discover novel drug sources with important economic potential, or compounds that can be transformed into active ingredients.

The genus *Plectranthus* belongs to the Angiosperms family, Lamiaceae (Nepetoideae subfamily, Ocimeae tribe, Plectranthinae subtribe) and includes about 350 species, distributed mainly in subtropical Africa, Asia, and Australia (Dellar et al., 1996; Narukawa et al., 2001; Gaspar-Marques et al., 2008). The genus was first described by the French botanist L'Heritier in 1788 (Lukhoba et al., 2006) and, since then, the total number of species belonging to this genus has been increasing. Nowadays, *Plectranthus* spp. are known all over the world for their horticultural uses as they grow fast, produce beautiful flowers, and are resistant to most plant pests and diseases. *Plectranthus* spp. exist as herbs, sub bushes, or shrubs. In Europe, several species of *Plectranthus* are grown as ornamental plants (Abdel-Mogib et al., 2002). The potential medicinal and economic uses of *Plectranthus* spp. are of great interest. Hidden in this genus are potential treatments for many conditions. The most frequently cited use of *Plectranthus* spp. is for its medicinal properties. They have been used for different digestive disorders, skin and respiratory conditions, genitourinary infections, general infections and fever, pain, and musculoskeletal conditions (Narukawa et al., 2001; Abdel-Mogib et al., 2002; Lukhoba et al., 2006). Other applications include insect repellents, spells, and culinary herbs (Lukhoba et al., 2006; Pal et al., 2011). The main phytochemical constituents of the *Plectranthus* genus are diterpenes, phenolic compounds, and essential oils, the latter giving this genus its natural aroma (Abdel-Mogib et al., 2002; Rice et al., 2011).

The species *Plectranthus ecklonii* Benth. was first collected in 1813 by the naturalist William Burchel in the Eastern Cape. It is a fast-growing shrub, perennial or annual (1–3 m high), with ovate to elliptical leaves, arranged in pairs, and flowers from March to May, with a peak in April (Van Jaarsveld, 2006). It is easily propagated using cuttings or seeds and the young plants should be pruned after flowering, or at least before spring. There are three cultivable species available: the blue-flowered "Medley Wood", the white-flowered "Tommy", and the pink-flowered "Erma" (**Figure 1**). *P. ecklonii* is commonly known as Ecklon spur flower or Ecklon spoorsalie and is widely distributed in South Africa, Australia, New Zealand, Mexico, and the United States (Van Jaarsveld, 2006; Nyila et al., 2009).

P. ecklonii Benth. is traditionally used in South Africa to treat stomach aches, nausea, vomiting, and meningitis, symptoms usually associated with listeriosis infection (Lukhoba et al., 2006; Chassagne and Morgan, 2020). The leaves are used for tuberculosis-related problems and, in Zimbabwe, aerial parts are applied for skin diseases and skin hyperpigmentation problems. The activity of *P. ecklonii* against *Escherichia coli* justifies the use of *Plectranthus* spp. in traditional medicine for the treatment of gastrointestinal infections (Nyila et al., 2009). Similarly, the traditional use of this plant for skin infections may be related to the antibacterial activity of two of its diterpenes, parviflorone D (Salim et al., 2008) and parviflorone F (Srancikova et al., 2013), against *Staphylococcus aureus* (Simões et al., 2010).

Since the 1960s, the number of papers published on *P. ecklonii* has been increasing, demonstrating the interest and importance of investigating this species. In fact, the number of published biological and chemical composition studies on *P. ecklonii* cited in this paper is 16 times higher in the years from 2012 to 2021 compared to that of the previous two decades (**Figure 2**). Growing intertest, lack of review paper on this species and recent developments in active antitumour compounds isolated from *P. ecklonii* justify and warrant a comprehensive up-to-date review. Consequently, the main aim of this review is to provide and evaluate the first complete compilation of the biological activities exerted by active compounds isolated, thus far, their mechanisms of action

FIGURE 1 | *Plectranthus ecklonii* "Medley-Wood" (blue), *P. ecklonii* "Tommy" (white), and *P. ecklonii* "Erma" (pink) (Van Jaarsveld, 2006).

FIGURE 2 | Number of published papers on *P. ecklonii* included in this review.

and, finally, offer an insight into their potential future use in natural product drug development.

METHODOLOGY

For the preparation of this manuscript, an exhaustive bibliographic review among a variety of databases, including Google Scholar, PubMed, Web of Science and ScienceDirect was carried out to retrieve information on the phytochemical and pharmacological uses of *P. ecklonii*, up to January 2021. Books and other digital resources were also used, and key search terms included, "*Plectranthus ecklonii*", "*Plectranthus ecklonii* + review", "*Plectranthus ecklonii* + diterpenes" or "*Plectranthus ecklonii* + abietanes", "*ecklonii* + parviflorone D", among others. After collating all records relating to compounds

TABLE 1 | The compounds isolated to date from *P. ecklonii* Benth.

	Isolated compounds	IUPAC name and CID number	Isolation and/or identification methods	Biological Activity[a]	Solvent extractor/plant part(s)	Ref.
	Terpenes and sterols					
Diterpenes	Parviflorone D **(1)**	11-hydroxy-2α-(4-hydroxybenzoyloxy)-abieta-5,7,9(11),13-tetraene-12-one **(1)** **[**101967011]	MS + NMR	Antibacterial	DCM:EtAc	Gurlal (2005)
			NMR	Antiplasmodic	DCM/ap	Van Zyl et al. (2008)
					EtAc/ap	Nyila et al. (2009), Nyila et al. (2012)
			MS + NMR	Antibacterial	Acetone/wp	Simões et al. (2010)
				Antitumour	Acetone	Martens and Mithöfer (2005), Ozgen et al. (2008), Falé et al. (2009), Bhatt et al. (2013), Kumar and Pandey, (2013), Petersen (2013), Burmistrova et al. (2015), Andrade et al. (2018), Costa et al. (2018), Sitarek et al., (2020), Śliwiński et al. (2020)
				Antioxidant		Wellsow et al. (2006)
			-	Enzyme inhibition	-	(Nyila et al., 2009; Dai and Mumper, 2010)
	Parviflorone F **(2)**	11-hydroxy-2α-(3,4-dihydroxybenzoyloxy)-abieta-5,7,9(11),13-tetraene-12-one **(2)** [10389067]	NMR	N/A	Ether/ap	Uchida et al. (1980)
				Antiplasmodic	DCM/ap	van Zyl et al. (2007), Van Zyl et al., (2008)
				Antibacterial	EtAc/ap	(Nyila et al., 2009; Nyila, 2010)
			NMR	Antitumour	EtAc/ap	Nyila et al. (2009)
			-	Antioxidant	-	Narukawa et al. (2001)
			-	Enzyme inhibition	-	Nyila et al. (2009), Dai and Mumper, (2010)
	Parviflorone E **(3)**	11-Hydroxy-19-(3,4-dihydroxybenzoyloxy)-abieta-5,7,9(11),13-tetraene-12-one **(3)** **[**10366501]	NMR	Antiplasmodic	ap	Van Zyl et al. (2008)
			HPLC-DAD/MS	Anticariogenic	Metanol/ap	Figueiredo et al. (2014)
			-	Antioxidant	-	Narukawa et al. (2001)
	Sugiol**(4)**	12-hydroxyabieta-8,11,13-trien-7-one **(4)** [94162**]**	MS + NMR	Antibacterial, antiplasmodic	Acetone/wp	van Zyl et al., (2007), Simões et al., (2010)
				Antioxidant		Chao et al. (2005), Bajpai et al. (2014)
				Antiinflammatory		Chao et al. (2005)
				Antitumoral		Son et al. (2005)
Triterpenes	Mix of Ursolic acid **(5)** and Oleanolic acid **(6)**	3β-hydroxy-urs-12-en-28-oic acid **(5)** **[**64945**]** 3β-hydroxyolean-12-en-28-oic acid **(6)** **[**10494**]**		Antiinflammatory **(5)** Antibacterial, antiviral, antiplasmodic **(5 and 6)**, Antitumoral		Andersson et al. (2003), Checker et al. (2012)
Sterols	Mix of *ß*-sitosterol **(7)** and Stigmasterol **(8)**	3β-stigmast-5-en-3-ol **(7)** **[**222284**]** stigmasta-5,22(*E*)-dien-3*ß*-ol **(8)** **[**5280794**]**		Antibacterial		Liu et al. (2019)
	Phenolic compounds					
Hydroxyccinamic acids	Caffeic acid **(9)**	3,4-dihydroxycinnamic acid **(10)** **[**689043**]**	NMR	Antimicrobial	Methanol: Water/ap	Hawas et al. (2008)
			HPLC-DAD	Antioxidant, enzyme inhibition	Water (decoction)	Gomes et al. (2012)
			-	Antiinflammatory	-	Da Cunha et al. (2004), Gamaro et al. (2011), Yang et al. (2013)
			-	Antitumoral	-	Hawas et al. (2008), Gomes et al. (2012)

(Continued on following page)

TABLE 1 | (*Continued*) The compounds isolated to date from *P. ecklonii* Benth.

	Isolated compounds	IUPAC name and CID number	Isolation and/or identification methods	Biological Activity[a]	Solvent extractor/plant part(s)	Ref.
	Caffeic acid derivatives					
	Rosmarinic acid **(10)**					
	3,4-Dihydroxycinnamic acid	N/A	Antibacterial	Water (decoction)/ap	Figueiredo et al. (2010)	
	(R)-1-carboxy-2-(3,4-dihydroxyphenyl)ethyl ester **(10)** [5281792]	HPLC-DAD	Antioxidant, enzyme inhibition	Water (decoction)	Falé et al. (2009), Gomes et al. (2012)	
		-	Antiinflammatory		Gamaro et al. (2011)	
		-	Antitumoral		Figueiredo et al. (2010)	
Nepetoidin A **(11)**	(Z,E)-[2-(3,5-dihydroxyphenyl)ethenyl] 3-(3,4-dihydroxyphenyl)-2-propenoate **(11)** [5316820]	HPLC-DAD/NMR	Anticariogenic	Methanol/ap	Figueiredo et al. (2014)	
			Antifungal and antioxidant	Diethyl ether/ap	Grayer et al. (2003)	
Nepetoidin B **(12)**	(Z,E)-[2-(3,4-dihydroxyphenyl)ethenyl] 3-(3,4-dihydroxyphenyl)-2-propenoate **(12)** [5316819]		Anti-inflammatory (**11** and **12**)	-	Grayer et al. (2003)	
Chlorogenic acid **(13)**	5-*O*-cafeoilquinic acid **(13)** [1794427]	HPLC-DAD	Antioxidant, enzyme inhibition	Water (decoction)	Gomes et al. (2012)	
Flavones	Apigenin **(19)**	4′,5,7-trihydroxyflavone **(19)** [5280443]	NMR	Antimicrobial	Methanol: Water/ap	Hawas et al. (2008)
			HPLC/LC-MS	N/A	Diethyl ether/ap	Grayer et al. (2010)
			No information provided	Antiplasmodic	-	Lehane and Saliba, (2008)
			-	Antioxidant	-	Velioglu et al. (1998), Pietta (2000)
			-	Anti-inflammatory	-	Nakanishi et al. (1990), Hirano et al., (2004), Kim et al. (2004), Choi et al. (2014), Lago et al. (2014)
			-	Antitumoral	-	Wu et al. (2014)
	Apigenin derivatives					
	Apigetrin **(15)**	apigenin 7-O-β-glucoside **(15)** [5280704]	NMR	Antimicrobial	Methanol: Water/ap	Hawas et al. (2008)
	Apigenin 4′,6-dimethoxy -7-O-β-glucoside **(16)**	apigenin 4′,6-dimethoxy-7-O-β-glucoside **(16)** [44257792]				
	Vitexin **(17)**	Apigenin-8-*C*-glucoside **(17)** [5280441]	-	Antioxidant	-	Borghi et al. (2013)
	Isovitexin **(18)**	Apigenin-6-*C*-glucoside **(18)** [162350]	NMR	Antimicrobial	Methanol: Water/ap	Lin et al. (2002), Choi et al. (2014)
	Luteolin **(19)**	3′,4′,5,7-tetrahydroxyflavone **(19)** [5280445]	-	Anti-inflammatory	-	Kim et al. (1999), Lin et al. (2008), Chen et al. (2014)
			-	Antitumoral	-	Lin et al. (2008)
	Cynaroside **(20)**	luteolin 7-*O*-glucoside **(20)** [5280637]	NMR	Antimicrobial, antioxidant	Methanol: Water/ap	Hawas et al. (2008) Odontuya et al. (2005)
	Cirsiol **(21)**	6-Hydroxyluteolin 6,7-dimethyl ether **(21)** [160237]	-	Antitumoral (acts as radiosensitizer)	-	Kang et al. (2013)
	Genkwanin **(22)**	4′,5-Dihydroxy-7-methoxyflavone **(22)** [5281617]	HPLC/LC-MS	N/A	Diethyl ether/ap	Grayer et al. (2010)

(Continued on following page)

TABLE 1 | (*Continued*) The compounds isolated to date from *P. ecklonii* Benth.

	Isolated compounds	IUPAC name and CID number	Isolation and/or identification methods	Biological Activity[a]	Solvent extractor/plant part(s)	Ref.
	Ladanein **(23)**	scutellarein-5,7,4'-trimethyl ether **(23)** [3084066]				
	Salvigenin **(24)**	Scutellarein 6,7,4'-trimethylether **(24)** [161271]		Antioxidant		Grayer et al. (2010)
	Cirsimaritin **(25)**	Scutellarein 6,7-dimethylether **(25)** [188323]		N/A		Grayer et al. (2010)
Flavanone	2(S)-4',5-dihydroxy-6,7-dimethoxyflavanone **(26)**	2(S)-4',5-dihydroxy-6,7-dimethoxyflavanone **(26)** [14078484]	NMR		Ether/ap	Uchida et al. (1980)
	Quinones					
	Ecklonoquinone A **(27)**	[4,6-dimethyl-7,8-dioxo-1,9-di(propan-2-yl)dibenzo-p-dioxin-2-yl] 3-methylbutanoate **(27)** [21576878]	NMR	N/A	Ether/ap	Uchida et al. (1980)
	Ecklonoquinone B **(28)**	[4,9-Dimethyl-7,8-dioxo-1,6-di(propan-2-yl)dibenzo-p-dioxin-2-yl] 3-methylbutanoate **(28)** [21576879]				

N/A, Not Applicable; ap, aerial parts (leaves); wp, the whole plant.

HPLC, High performance liquid chromatography; LC-MS, Liquid Chromatography-Mass Spectrometry; NMR, Nuclear Magnetic Resonance.

[a]*Biological activity presented in table is related to the compound (can be isolated from P. ecklonii and other species)*

isolated from the species *P. ecklonii*, the search was developed further on each compound individually, including studies on other *Plectranthus* species, and species belonging to the Lamiaceae family, were considered. Titles in English, Portuguese and Spanish were reviewed, and all references included dated from 1970 to 2021. A final total of 169 references were selected and included. Chemical structures were drawn using ChemDraw 20.0, CID numbers were searched in PubChem and the PRISMA flow chart was created using PowerPoint 2012.

ISOLATED COMPOUNDS FROM *PLECTRANTHUS ECKLONII* BENTH

Plants produce a vast range of compounds originating from different biosynthetic pathways, with ranging molecular weights, which can be classified into different categories, such as primary and secondary metabolites. The relevance and application of secondary metabolites extends further than just medicine, including areas of agriculture and industry. Exploration into the different biosynthetic pathways and biological activities of these metabolites has led to the accepted categorization of their main, yet broad, categories of plant compounds: 1) terpenes or terpenoids, 2) alkaloids, and 3) phenolic compounds (Devappa et al., 2011). Terpenes are undoubtedly the largest, most distributed, and, from a structural point of view, the most diverse class of secondary metabolites. Their importance, particularly at the therapeutic level, justifies the numerous efforts made over the last few decades to clarify their biosynthesis (Devappa et al., 2011).

The main phytochemical constituents of the genus *Plectranthus* are diterpenes, essential oils, and phenolic compounds (Abdel-Mogib et al., 2002). Abietane diterpenoids of the species *Plectranthus* are specific antimicrobial and cytotoxic compounds (Teixeira et al., 1997; Gaspar-Marques et al., 2006). The main compound of the polar extract of *P. ecklonii* is rosmarinic acid (RA) (Rice et al., 2011), a common phenolic ester in the *Lamiaceae* family (Amoah et al., 2016). RA (Rice et al., 2011) together with two other esters of caffeic acid (CA) (Pal et al., 2011), nepetoidine A (Van Jaarsveld, 2006) and nepetoidine B (Nyila et al., 2009), are used as chemotaxonomic markers of the Nepetoideae subfamily (Grayer et al., 2003; Kubínová et al., 2013). Until now, a total of 28 compounds have been isolated from *P. ecklonii*, constituting a variety of different classes of plant compounds. In 1980, Uchida and colleagues were the first to report the isolation and identification of compounds from *P. ecklonii* (Uchida et al., 1980). At that time, they detected the presence of the abietane parviflorone F (Srancikova et al., 2013) and ecklonoquinones A (Śliwiński et al., 2020) and B (Andrade et al., 2018). After 40 years of research, the composition of this species is still not completely clear, however, here we have enumerated the compounds discovered thus far (**Table 1** and **Figure 3**).

Except for one study, in which the whole plant (wp) was used (Simões et al., 2010), all other studies reported using aerial parts (leaves), possibly to mimic more faithfully the traditional use of this plant. Besides, the harvesting of leaves for medicinal purposes is more sustainable than that of other parts of the plant, such as roots and stems, whose excessive harvesting could even threaten the survival of the plant (Zschocke et al., 2000).

Diterpenes

Diterpenes, a heterogeneous class of natural compounds based on a skeleton with 20 carbon atoms (C_{20}), are the most common group of secondary compounds in the genus *Plectranthus*, most of which are highly modified abietanoids containing phenolic or quinone rings, in addition to some labdanes, ent-kaurenes, and seco-kaurenes (Abdel-Mogib et al., 2002). Regarding the type of hydrocarbon skeleton, diterpenes can be acyclic or cyclic. Most belong to the cyclic group, and it is precisely the diversity in the cyclization of the hydrocarbon skeleton, combined with the diversity of functional groups with oxygen (e.g., hydroxyl, carbonyl, epoxides, quinones, acids, and acid derivatives) which defines their multiple biological properties (Wang et al., 2002; Rijo et al., 2013). In general, diterpenes are compounds with medium to low polarity, although, they often occur in plants in a glycosylated form, in which case, they are polar substances. Medium polar solvents such as dichloromethane (DCM), ethyl acetate (EtOAc), and acetone are usually used for their extraction, or strong polar solvents, such as methanol, mixtures of alcohols and water, or even pure water (Waksmundzka-Hajnos and Sherma, 2011).

From the ethyl acetate extract of *P. ecklonii*, two abietanes, parviflorone D (Salim et al., 2008) and parviflorone F (Srancikova et al., 2013) have been isolated (Nyila et al., 2009). In 2008, in a study published by Van Zyl and colleagues, these two abietanes were also isolated from a DCM extract of *P. ecklonii* (Van Zyl et al., 2008). The detection of parviflorone E (Abdel-Mogib et al., 2002) required a stronger polar solvent, in this case, methanol (Figueiredo et al., 2014). In another study, parviflorone D (Salim et al., 2008) was isolated from an acetonic extract of *P. ecklonii*, together with the diterpene sugiol (de Albuquerque et al., 2007) and mixtures of ursolic acid (UA) (Lukhoba et al., 2006) with oleanolic acid (OA) (Dellar et al., 1996) and ß-sitosterol (Gaspar-Marques et al., 2008) with stigmasterol (Narukawa et al., 2001) (Simões et al., 2010). Meanwhile, the compounds OA (Dellar et al., 1996), ß-sitosterol (Gaspar-Marques et al., 2008), and stigmasterol (Narukawa et al., 2001) have also been isolated in *Plectranthus bishopianus* Benth., but from a methanolic extract (Syamasundar et al., 2012).

Interest in diterpenoid isolation continues to grow due to its wide range of biological activities (Hanson, 2005). Abietane diterpenoids have attracted interest on account of their antibacterial (Dellar et al., 1996; Teixeira et al., 1997; Figueiredo et al., 2014), antioxidant (Rijo et al., 2009) and insect antifeedant activities (Wellsow et al., 2006), as well as their inhibitory effects on different human cancer cell lines (Marques et al., 2002). Abietane is the skeleton with the highest occurrence and most widespread in *Lamiaceae* (Vestri Alvarenga et al., 2001). Abietane diterpenoids account for the most common secondary metabolites in *Plectranthus*. Abietanoids in *Plectranthus* mostly consist of royleanones, spirocoleons, and quinines (Abdel-Mogib et al., 2002). In 2007, Van Zyl and colleagues isolated seven abietane diterpenes, including parviflorone D (Salim et al., 2008) and F (Srancikova et al., 2013), from the leaves of five different *Plectranthus* species (van Zyl et al., 2007).

Triterpenes

Triterpenes and sterols are two groups genetically engineered from the same precursor, squalene. Triterpenes, with the molecular formula $C_{30}H_{48}$, belong to the terpene group and may have acyclic carbon skeletons or contain mono-, bi-, tri-, tetra-, and pentacyclic structures (Dewick, 2002; Xu et al., 2004). From a biological point of view, the most important triterpenoid structures are those with the carbon skeletons of dammarane and euphane (tetracyclic triterpenes), oleanane, ursane, and lupane (pentacyclic triterpenes) (Dzubak et al., 2006).

For a long period of time, triterpenes were disregarded due to their low hydrophilicity. However, multiple studies, supporting their broad range of pharmacological activities and beneficial effects against several types of human diseases, including cancers, has been emerging (Patlolla and Rao, 2012). The chemistry of oleanane- and ursane-type triterpenoids have been actively explored in recent years, and their biological and pharmacological activities have been found to span a variety of properties, namely, antitumor, anti-viral, anti-inflammatory, hepato- and gastroprotective, antimicrobial, antidiabetic, and haemolytic properties (Sun et al., 2006). These triterpenoids are relatively non-toxic but their structural similarity to cholesterol gives them low water solubility, a major disadvantage in terms of bioavailability and, therefore, reduced therapeutic potential (Soica et al., 2014). However, studies of structure activity relationships (SAR) have shown that modifications in certain areas of the nuclei of these compounds can lead to significantly more active new derivatives (Sun et al., 2006). In Asian countries, the traditional applications of plants containing OA (Dellar et al., 1996) or UA (Lukhoba et al., 2006) in folk medicine are also multiple, including for anti-inflammatory, analgesic, sedative, hepatoprotective and cardiotonic effects (Liu, 1995; Poolier and Goossens, 2012). Other studies have also demonstrated their antioxidant, antiallergic, antipruritic, and antimicrobial potential (Jesus et al., 2015). For example, plant-based medicines with UA (Lukhoba et al., 2006) and OA (Dellar et al., 1996) are widely used in the treatment and prevention of type II *diabetes mellitus* in Traditional Chinese Medicine (TCM) and Indian medicines (Wang et al., 2013).

In the *Plectranthus* genus, common triterpenes have been isolated, such as UA (Lukhoba et al., 2006) OA (Dellar et al., 1996), betulin, and betulinic acid. Triterpenic acids exhibit important biological and pharmacological activities, including anti-inflammatory, antimicrobial, antiviral, cytotoxic, and cardiovascular effects (Lin et al., 2002; Odjakova et al., 2012). UA (Lukhoba et al., 2006) and OA (Dellar et al., 1996) are isomeric triterpenic acids that only differ in the position of the

methyl (CH_3) group on C_{29} and always exist simultaneously in the same plant (Xu et al., 2004). In 1971, Misra and colleagues reported the isolation of triterpenes UA (Lukhoba et al., 2006), OA (Dellar et al., 1996) from the methanolic extract of *P. bishopianus* Benth., which are also found in *P. ecklonii* (Misra et al., 1971; Andrade et al., 2021).

One of the traditional uses of *P. ecklonii* is for skin ailments and, in recent years, collagenase inhibitors, compounds that prevent the enzymatic degradation of the dermal matrix, have been identified in extracts of *Plectranthus* spp. as OA (Dellar et al., 1996) and UA (Lukhoba et al., 2006). In organic extracts of *P. ecklonii,* high collagenase inhibition has been reported and, further to this, the isolated compounds, OA (Dellar et al., 1996), and UA (Lukhoba et al., 2006), demonstrated higher anti-elastase activity when compared to the extract. This is most probably due to the compounds binding to the catalytic site of the enzyme, justifying its use in dermatology and cosmetics (Andrade et al., 2021). As they share similar structural features, OA (Dellar et al., 1996) and its isomer, UA (Lukhoba et al., 2006), frequently occur simultaneously (Jesus et al., 2015).

Phytosterols

Phytosterols or plant sterols are fatty acids contained in plants. Their nutritional interest stems from their structural similarity to cholesterol (Van Jaarsveld, 2006), and their ability to lower plasma cholesterol and low-density lipoprotein (LDL) levels. Unlike sterols, triterpenes do not occur in the animal kingdom (Gabay et al., 2010). In recent decades, phytosterols have received much attention due to their capability to inhibit intestinal cholesterol absorption, resulting in lower total serum cholesterol and LDL cholesterol levels (Feng et al., 2017). β-sitosterol (Gaspar-Marques et al., 2008) and stigmasterol (Narukawa et al., 2001) are the most abundant plant sterols and occur in complex mixtures. The nutritional interest in sterols is due to their similarity in structure to cholesterol (Gabay et al., 2010).

Various activities have been attributed to β-sitosterol (Gaspar-Marques et al., 2008), including anti-hyperlipidaemia, anti-inflammatory and anti-tumoral. Some studies suggested that β-sitosterol (Gaspar-Marques et al., 2008) could be used as an antibacterial agent and possess the ability to protect the gastric mucosa from acetic acid- or aspirin-induced damage (Liu et al., 2019). In 2017, Feng and colleagues reported less severity of mucosal colitis in mice treated with β-sitosterol (Gaspar-Marques et al., 2008) and stigmasterol (Narukawa et al., 2001) (Feng et al., 2017). ß-sitosterol (Gaspar-Marques et al., 2008) is used as a herbal treatment for benign prostatic hyperplasia. This application is described in the literature in four randomized, placebo-controlled, double-blind studies and included a total of 519 men. Three of the studies reported significant benefits in the perception of symptoms and measurable parameters, such as urinary flow rate. In one study, during an 18-months follow-up period, the beneficial effects of treatment with β-sitosterol were maintained (Berges et al., 2000). However, further clinical trials are needed to establish the real efficacy and long-term effects of ß-sitosterol (Gaspar-Marques et al., 2008). Stigmasterol (Narukawa et al., 2001) is used in several chemical processes, which are designed to yield numerous synthetic and semi-synthetic compounds for the pharmaceutical industry. It acts as a precursor in the synthesis of progesterone and as an intermediate in the biosynthesis of androgens, oestrogens, corticoids, and in the synthesis of vitamin D3 (Sandhar et al., 2011). Although most studies have focused on the cholesterol-lowering activity of stigmasterol (Narukawa et al., 2001), other bioactivities have been attributed to this plant sterol compound, one of which is a potential anti-inflammatory effect (Gabay et al., 2010). In a more recent study, β-Sitosterol (Gaspar-Marques et al., 2008) and stigmasterol (Narukawa et al., 2001) did not demonstrate anti-inflammatory responses through the NO scavenging pathways, however, further studies on the response through other mechanisms, such as COX-2, should be explored to identify the mediators responsible for the anti-inflammatory effect (Andrade et al., 2018). Parviflorone D (Salim et al., 2008) in mixtures of plant sterols, such as β-sitosterol (Gaspar-Marques et al., 2008) and stigmasta-5,22(*E*)-dien-3ß-ol (Narukawa et al., 2001), have been isolated from *P. ecklonii* (Simões et al., 2010).

Phenolics

Phenolic compounds are important plant secondary metabolites that play a key role in disease-resistance, pest protection, and species dissemination. They are widespread constituents of plant foods (fruits, vegetables, cereals, chocolate, etc.) and beverages (tea, coffee, beer, wine, etc.). There are ten main classes of phenolic compounds, which includes phenolic acids, flavonoids, and tannins, and are generally involved in the defence against ultraviolet (UV) radiation or aggression by pathogens, parasites, and predators, as well as contributing to plants' colours (Dai and Mumper, 2010). Flavonoids and phenolic acids (mainly hydroxycinnamic acids) are the most abundant compounds found in plant extracts (Ramu et al., 2012). The biological effects of hydroxycinnamic acids in humans are mainly related to their antioxidant function, although many other bioactivities have been reported for these compounds, such as antidiabetic, antigenotoxic and antimicrobial activities (Vinholes et al., 2015). However, and despite their abundance in diet and credible effects on the prevention of various OS-related diseases, only recently have dietary polyphenols been truly recognised by nutritionists, researchers and food manufacturers. Their preventive effects, in terms of cardiovascular, neurodegenerative diseases, and cancer, have been deduced from epidemiologic data (*in vitro* and *in vivo*) and result in nutritional recommendation (Dai and Mumper, 2010). The most recently identified property of polyphenols is their effect on long-term diabetes complications, including retinopathy, nephropathy, and neuropathy (Bahadoran et al., 2013).

The main phenolic compounds identified in the extracts of *Salvia* and *Plectranthus* are the hydroxycinnamic acids and their derivatives, such as rosmarinic (Rice et al., 2011), chlorogenic (Chassagne and Morgan, 2020), carnosic, and salvianolic acids. Among the most abundant cinnamic acids is caffeic acid (CA) (3,4-dihydroxycinnamic acid) (Pal et al., 2011), described as having a wide variety of biological activities, including

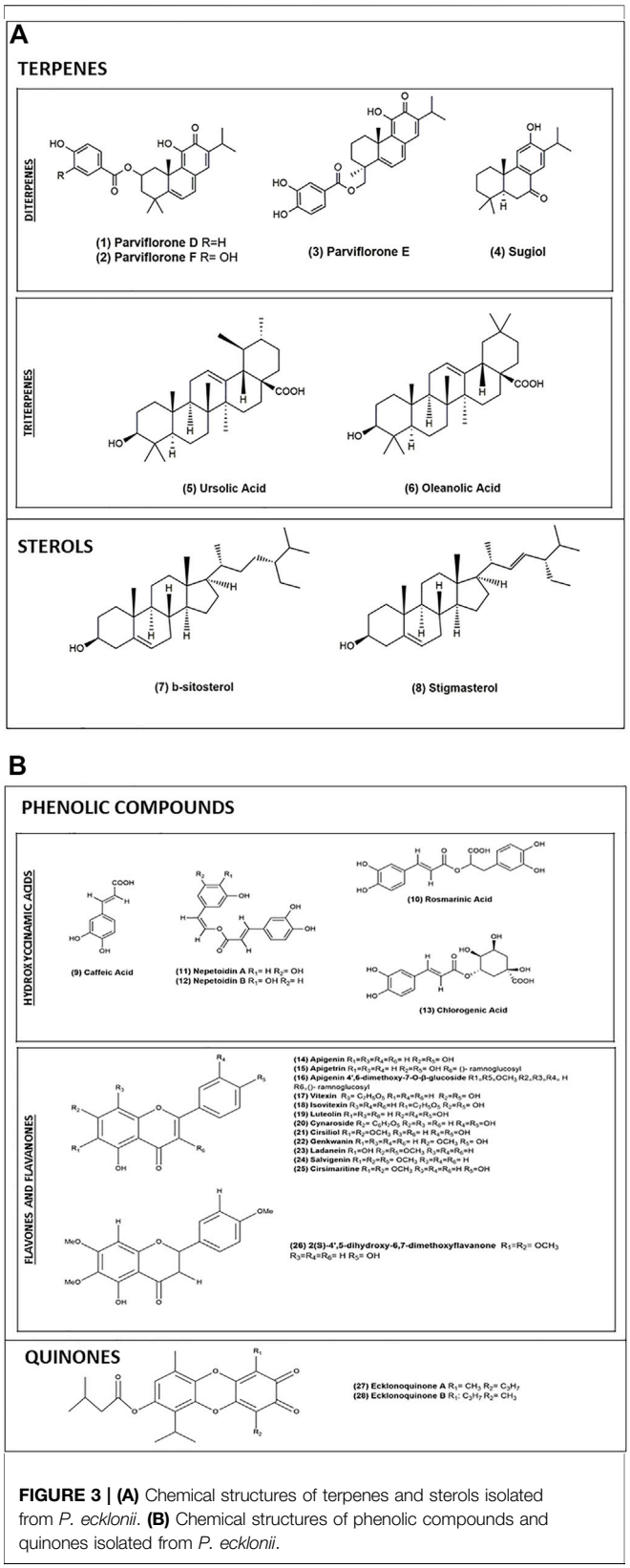

FIGURE 3 | (A) Chemical structures of terpenes and sterols isolated from *P. ecklonii*. **(B)** Chemical structures of phenolic compounds and quinones isolated from *P. ecklonii*.

antioxidant, antithrombotic, antihypertensive, antifibrotic, antiviral, and antitumour properties (Rajendra Prasad et al., 2011). While the isolation of hydroxycinnamic acids is mostly described in the literature in aqueous extracts, in the case of *P. ecklonii* there have been attempts by scientists to test other extracts, specifically hydroalcoholic extracts. Despite traditional preparations of plant extracts using water (e.g., infusions, decoctions, and poultices) (Rabe and Van Staden, 1997), there are reports of studies in which methanolic extracts have shown a higher content of phenolic compounds when compared to aqueous ones (Krishnaiah et al., 2011). RA (Rice et al., 2011) is an ester of CA (Pal et al., 2011) with 3,4-dihydroxyphenyl lactic acid (Petersen, 2013), the major component of polar extracts from many plants of the *Lamiaceae* family (Falé et al., 2009) and, presumably, one of the main compounds responsible for the potent antioxidant activity of *Lamiaceae* plants (Ozgen et al., 2008). Besides its well-studied antioxidant activity, RA acts as an enzyme inhibitor. It is known to interfere with gene expression and signalling pathways related to cancer prevention and presents antiviral, antibacterial, and anti-inflammatory properties (Bhatt et al., 2013). In 2010, Figueiredo and colleagues pointed out the presence of RA (Rice et al., 2011) in the aqueous extract of *P. ecklonii* as responsible for the antibacterial activity against *Streptococcus* spp. and for the inhibition of the enzyme glycosyltransferase (GTF) (Figueiredo et al., 2010). Furthermore, in 2009, Falé and colleagues also linked the presence of this compound to the observed effects of AChE inhibition and antioxidant activity (Falé et al., 2009). Besides its well-studied antioxidant activity, RA (Rice et al., 2011) acts as an enzyme inhibitor. It is known to interfere with gene expression and signalling pathways related to cancer prevention and presents antiviral, antibacterial, and anti-inflammatory properties (Bhatt et al., 2013). Whereas CA (Pal et al., 2011) and its derivatives are widespread in the *Labiatae* family, RA (Rice et al., 2011) is restricted to the *Nepetoideae* subfamily (Abdel-Mogib et al., 2002). For this reason, RA (Rice et al., 2011) and two other esters of CA (Pal et al., 2011), known as nepetoidin A (Van Jaarsveld, 2006) and nepetoidin B (Nyila et al., 2009) are used as chemotaxonomic markers for the subfamily *Nepetoideae* (Grayer et al., 2003).

Flavonoids

Flavonoids are low molecular weight aromatic compounds characterized by a flavanic nucleus and a carbon skeleton with a C6-C3-C6 configuration. Flavonoids contain a skeleton made up of fifteen-carbon atoms, consisting of two benzene rings, joined by a heterocyclic pyrane ring (Kumar and Pandey, 2013). The individual numbering of the flavonoid skeleton is shown in **Figure 4** (Martens and Mithöfer, 2005). Flavonoids are well-known for their antioxidant, anti-inflammatory, and cytoprotective activities. Most importantly, they appear in all green plants and constitute a large part of our common daily diet, making them vital components in the prevention of human diseases (Schmidt et al., 2012). Variations in the C ring replacement configurations result in the various subclasses of flavonoids: flavones (e.g., apigenin (Simões et al., 2010) and luteolin (Grayer et al., 2003)), flavanones, isoflavones, flavonols, flavanols (or catechins), and anthocyanidins (Sandhar et al., 2011).

Research reports flavonoids as having many activities (anti-inflammatory, antibacterial, cytotoxic, antitumour, effects on the

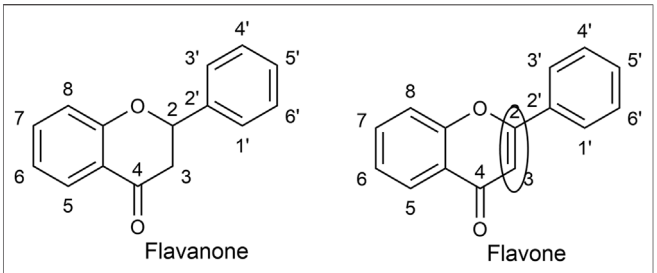

FIGURE 4 | The double bond between C2 and C3 makes it possible to distinguish flavones from flavanones.

treatment of neurodegenerative diseases), but the best-described characteristic of the majority of flavonoids is their ability to behave as antioxidants scavenging free radicals and/or chelating metal ions. They are also known to inhibit lipid peroxidation, platelet aggregation, and enzyme activity of COX and LOX enzymes (Asif and Khodadadi, 2013). Flavonoids lacking hydroxyl groups on their B-rings are more active against microorganisms than are those with the -OH groups (Cowan, 1999). Flavones differ from flavanones by the presence of a double bond between C2 and C3 in the heterocyclic flavonoid skeleton. The B ring is connected to C2 and there are usually no C3 substitutes. Flavones occur mainly as 7-*O*-glucosides, although substitution can be found in any other hydroxylated position (Martens and Mithöfer, 2005).

A study with the hydroalcoholic extract of *P. ecklonii* leaf extract showed varying degrees of antimicrobial activity and resulted in the identification of the flavones: vitexin (Gaspar-Marques et al., 2006), isovitexin (Amoah et al., 2016), apigenin 7-*O*-*β*-glucoside (Devappa et al., 2011), apigenin 4',6-dimethoxy-7-*O*-*β*-glucoside (Teixeira et al., 1997), luteolin 7-*O*-glucoside (Kubínová et al., 2013), apigenin (Simões et al., 2010) and luteolin (Grayer et al., 2003) (Hawas et al., 2008). Since then, the flavones cirsimaritin (Nyila et al., 2012), ladanein (Gurlal, 2005), and salvigenin (Van Zyl et al., 2008) have been isolated from *P. ecklonii* (Grayer et al., 2010). Apigenin (Simões et al., 2010) and luteolin (Grayer et al., 2003) are frequently found in several plant species. Apigenin (Simões et al., 2010) (4',5,7-trihydroxyiflavone) has gained particular interest in recent years as a beneficial and health promoting agent due to its low intrinsic toxicity. Plants rich in luteolin (Grayer et al., 2003) (3′,4′,5,7-tetrahydroxyflavone) have been used in TCM for treating various diseases such as hypertension, inflammatory disorders and cancer (Lin et al., 2008). Vitexin (Gaspar-Marques et al., 2006) and isovitexin (Amoah et al., 2016), naturally occurring C-glycosylated derivatives of apigenin (Simões et al., 2010), have been known to possess potent anti-diabetic, anti-Alzheimer's disease (anti-AD), and anti-inflammatory activities (Choi and Lee, 2009). Plant extracts containing vitexin (Gaspar-Marques et al., 2006) (apigenin-8-*C*-*β*-D-glucopyranoside) are reported to possess anti-inflammatory, and antioxidant activities (Borghi et al., 2013). Phytochemical studies that have been reported investigating *P. ecklonii* also include the isolation of two isomeric ortho-quinones, ecklonoquinones A (Śliwiński et al., 2020) and B (Andrade et al., 2018) (Uchida et al., 1980), twelve flavones (Hawas et al., 2008), as well as salvigenin (Van Zyl et al., 2008), cirsimiratin (Nyila et al., 2012) and the corresponding flavanone, 2(*S*)-4',5-dihydroxy-6,7-dimethoxyflavanone (Costa et al., 2018) (Uchida et al., 1980; Grayer et al., 2003). Flavonoids with a 5-hydroxy-6,7-dimethoxy-type substitution in the A-ring, such as salvigenin (Van Zyl et al., 2008), cirsimaritin (Nyila et al., 2012) and cirsiliol (Uchida et al., 1980) flavones, are considered typical in the Labiateae family (Gaspar-Marques et al., 2006). No reference to any bioactivities exercised by ecklonoquinones A (Śliwiński et al., 2020) and B (Andrade et al., 2018) has been found in the literature and therefore they are not discussed in this review.

In the following section, some of the biological activities attributed to the different constituents of *P. ecklonii* will be evaluated and discussed (**Figure 5**), to try to understand not only its traditional applications, but also the future implications for this plant.

BIOLOGICAL ACTIVITIES OF ISOLATED COMPOUNDS FROM *P. ECKLONII* BENTH

Antibacterial

The most studied bioactivity in *P. ecklonii* isolated compounds was antimicrobial, such that, different types of microorganisms have been tested. The compounds showed varying degrees of activity against Gram-positive bacteria, Gram-negative bacteria (*Pseudomonas aeruginosa* and *E. coli*), and fungi, such as *Aspergillus niger* and *Candida albicans*. In general, the compounds exert greater antibacterial activity on Gram-positive bacteria (*Staphylococcus*, *Enterococcus*, *Listeria*, and *Streptococcus*).

Parviflorones are natural diterpenes widely distributed among several *Plectranthus* species (Simões et al., 2010).The pigments parviflorone D (Salim et al., 2008) and parviflorone F (Srancikova et al., 2013) were isolated for the first time from an ethereal extract of *Plectranthus parviflorus* (Rüedi and Eugster, 1978). Since then, parviflorone D (Salim et al., 2008) [2α-(4-hydroxy)benzoyloxy-11-hydroxy-5,7,9(11),13-abietatetraen-12-one], has been isolated from *P. strigosus* Benth. (Gaspar-Marques et al., 2008) and *P. ecklonii* Benth. and reported antibacterial activity, including against methicillin- and vancomycin-resistant strains (Simões et al., 2010). Parviflorone F (Srancikova et al., 2013) [11-hydroxy-2α-(3,4-dihydroxybenzoyloxy)-abieta5,7,9(11),13-tetraene-12-one] was also isolated from *P. ecklonii* and *Plectranthus nummularius* Briq. (Narukawa et al., 2001), as well as parviflorone E (Abdel-Mogib et al., 2002) [11-hydroxy-19-(3,4-dihydroxybenzoiloxy)-abieta-5,7,9(11),13-tetraene-12-one] (Figueiredo et al., 2014).

The leaves of members of the *Lamiaceae* family are known to contain terpenoids with antifungal, antibacterial, and insect repellent activities (Cole, 1994). Extracts obtained from the leaves of some *Plectranthus* species in South Africa have shown antibacterial activity (Rabe and Van Staden, 1997). Abietane diterpenes isolated from *Plectranthus elegans* inhibited the growth of Gram-positive bacteria *Bacillus subtilis* (Dellar et al., 1996). The diterpenes isolated from *Plectranthus grandidentatus* and *Plectranthus hereroensis* also proved to be active against resistant Gram-positive bacteria, *Enterococcus*

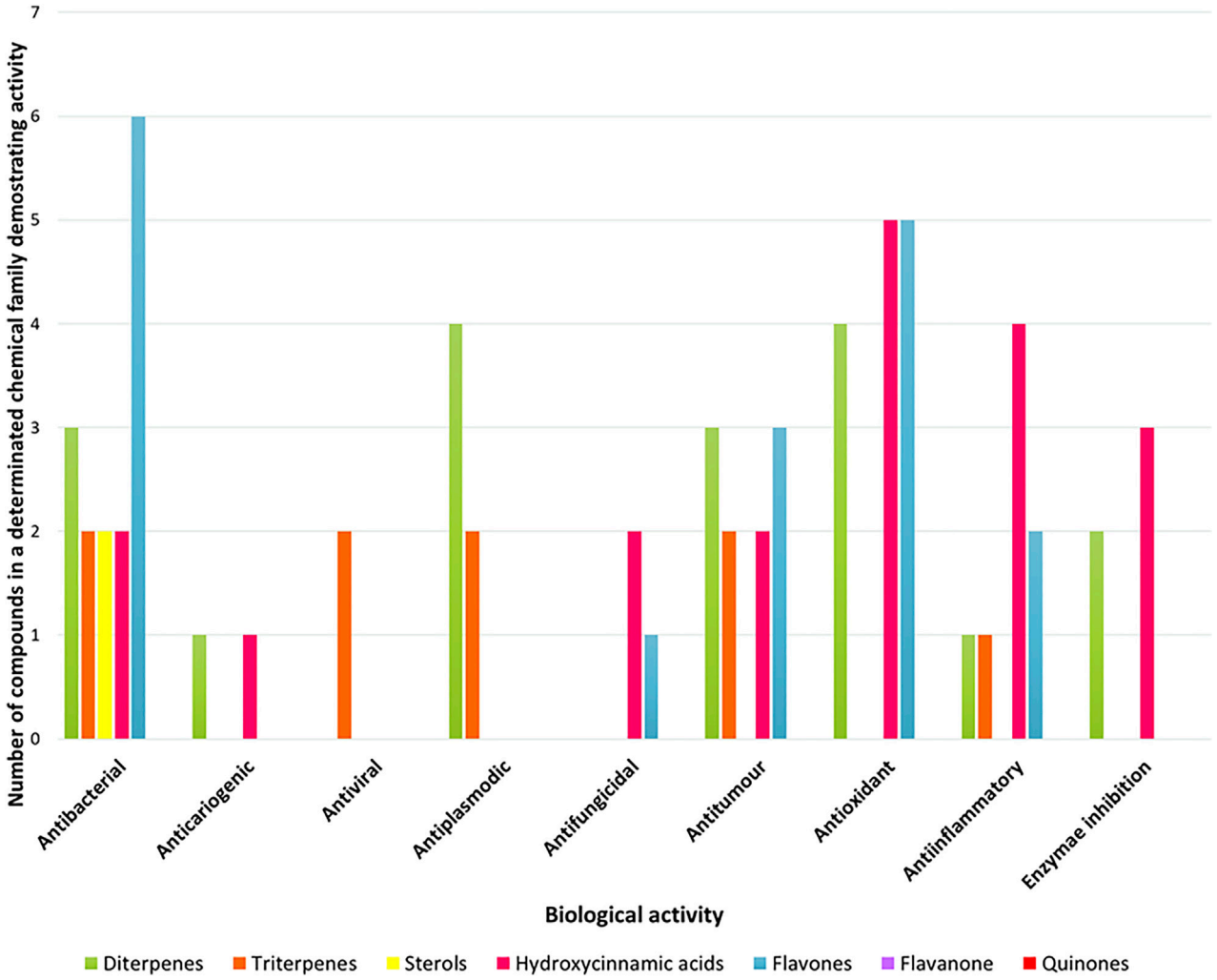

FIGURE 5 | Summary diagram of biological activities demonstrated by each family of compounds.

faecalis vancomycin-resistant (VRE) and Methicillin-resistant *Staphylococcus aureus* (MRSA) (Gibbons, 2004; Gaspar-Marques et al., 2006). Concerning ethyl acetate extracts of *P. ecklonii*, two known abietanes, parviflorone D (Salim et al., 2008) and parviflorone F (Srancikova et al., 2013), were isolated and both compounds demonstrated effective activity against *Listeria monocytogenes* (Nyila et al., 2009). The traditional use of *P. ecklonii* for the treatment of gastrointestinal disorders may also be related to its activity against *E. coli* (Nyila et al., 2012), although further studies are needed to support this hypothesis.

Abietanes parviflorone D (Salim et al., 2008) and F (Srancikova et al., 2013) were also active against *Mycobacterium smegmatis*, *P. aeruginosa*, and *E. faecalis* (Nyila et al., 2009). The antibacterial activity of sugiol (de Albuquerque et al., 2007) was also tested, although authors reported very low activity against Gram-positive *E. faecalis* bacteria (Simões et al., 2010). The leaves of the plant are used for respiratory symptoms, chest pain, and coughing (problems related to tuberculosis), which may be due to the inhibitory growth activity of *M. tuberculosis* presented by parviflorones D (Salim et al., 2008) and F (Srancikova et al., 2013) (Nyila et al., 2009). Parviflorone D (Salim et al., 2008) has also inhibited the growth of *S. aureus* (Nyila et al., 2009; Simões et al., 2010), which possibly justifies the use of the aerial parts of the plant in Zimbabwe for skin diseases and hyperpigmentation problems (Lukhoba et al., 2006). Antibacterial activity of parviflorone D (Salim et al., 2008) has been reported against *Staphylococcus* and *Enterococcus* species, including against MRSA and VRE strains (Simões et al., 2010). Even the rearranged abietane 2ß-(4-hydroxy)benzoyloxy (**Figure 6**) obtained in 2010 by Simões and colleagues from parviflorone D (Salim et al., 2008) showed antibacterial activity against some *Staphylococcus* and *Enterococcus* strains when tested against Gram-negative and Gram-positive bacteria (Simões et al., 2010).

According to Cowan, the mechanism responsible for the antibacterial activity of diterpenes may be associated with the breakdown of the bacterial membrane by lipophilic compounds (Cowan, 1999).

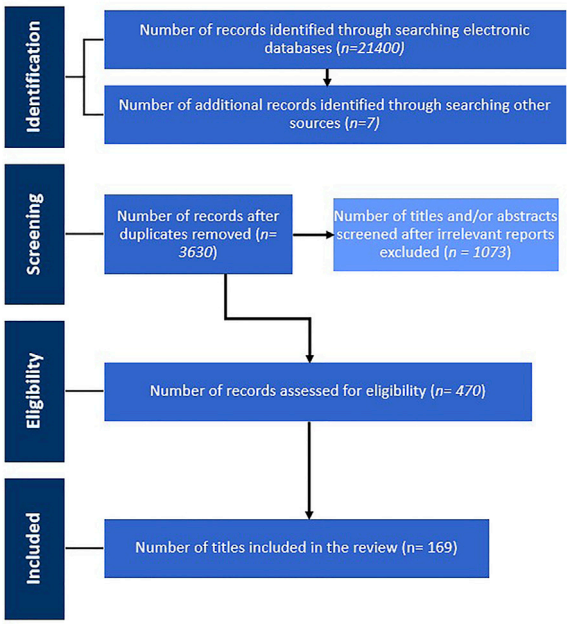

FIGURE 6 | PRISMA flow chart demonstrating the selection process and criteria.

The high cost of synthetic drugs and the problem of multidrug resistance has increased the need to exploit the anti-Listeria potential of medicinal plants. Plant extracts are affordable and accessible, which has led to the use of medicinal plants as an alternative in the treatment of listeriosis. *P. ecklonii* Benth. is one of the plants traditionally used to treat the symptoms associated with listeriosis infection (Lukhoba et al., 2006). Many organisms, including the opportunistic pathogen *Listeria monocytogenes*, appear more often as biofilms, such as in healthcare-acquired "hospital" infections. An ethyl acetate extract from *P. ecklonii* showed anti-*Listeria* activity with a minimum inhibitory concentration (MIC) of 0.5 mg/ml. Parviflorone D (Salim et al., 2008) and F (Srancikova et al., 2013) showed even higher activity in the breakdown of *L. monocytogenes* biofilm with a MIC of 15.6 μg/ml and 31.25 μg/ml, respectively (**Table 2**) (Nyila, 2010). Although the results illustrate a possible use of the compounds as disinfection agents, further studies should be carried out to investigate their potential for effectively removing *Listeria* biofilm from contaminated surfaces.

Different reports have shown that UA (Lukhoba et al., 2006) and OA (Dellar et al., 1996) exhibit antimycotic, antitumoral, antibacterial, antiviral, and antiparasitic properties. UA (Lukhoba et al., 2006) and OA (Dellar et al., 1996) present remarkable antimicrobial activities and they act against important human pathogens, such as mycobacteria, HIV, and different protozoal species (Jesus et al., 2015). UA (Lukhoba et al., 2006) and its derivatives have been shown to possess antimicrobial activity, for example, as inhibitors of Gram-positive *S. aureus*, Gram-negative organisms (*P. aeruginosa* and *E. coli*), and *Microsporium lenosum* (Zaletova et al., 1986). OA (Dellar et al., 1996) showed antimicrobial activity against *Bacillus subtilis*, methicillin-sensitive *S. aureus* (MSSA), and MRSA (Sun et al., 2006). When used against *M. tuberculosis*, both OA (Dellar et al., 1996) and UA (Lukhoba et al., 2006) presented anti-tuberculosis potential (Jiménez-Arellanes et al., 2007). In 2010, Figueiredo and colleagues pointed out that the presence of RA (Rice et al., 2011) in the aqueous extract of *P. ecklonii* is responsible for the antibacterial activity against *Streptococcus* spp. (Falé et al., 2009).

Anticariogenic

Dental caries has been the oral pathology most responsible for the loss of tooth structure with *Streptococcus mutans* being considered the main cause of this dental disease. Despite the diversity of human oral flora composition, two *Streptococci* strains, *Streptococcus mutans* and *Streptococcus sobrinus*, have been implicated as the primary etiologic agents of dental caries (Hamada and Slade, 1980; Song et al., 2006; Bernardes et al., 2010). One of the most important virulence factors of these species is their ability to produce glucosyltransferases (GTFs) and multiple glucan-binding proteins (Gbp proteins), which are thought to promote adhesion of bacteria to the tooth surface, contributing to the formation of dental plaque (Song et al., 2006; Matsumoto-Nakano, 2018). For biofilm formation, *S. sobrinus* and *S. mutans* must have the ability to adhere to a surface. Therefore, if compounds make such adherence impossible, both the biofilm formation process and its subsistence will be compromised.

The aqueous extract of *P. ecklonii* has been reported to have antibacterial activity against *S. mutans* and *S. sobrinus* and inhibited the enzyme GTF. The main compound present in *P. ecklonii* said to be responsible for this action is RA (Rice et al., 2011), however, the authors have noted that the inhibitory effect of the acid on biofilm formation did not differ significantly from the effect observed for the aqueous extract (Figueiredo et al., 2010). The methanol extract from *P. ecklonii* leaves revealed the presence of parviflorone E (Narukawa et al., 2001), together with RA (Rice et al., 2011), resulted in higher anti-cariogenic activity (Figueiredo et al., 2014), confirming this species importance in the prevention of oral diseases. Furthermore, the antimicrobial activity of an aqueous extract of *P. ecklonii*, containing RA (Rice et al., 2011), showed the extract as being active in bacteria, particularly against Gram-positive *S. epidermidis*, normally found in skin flora, justifying its traditional use and demonstrating its potential for skin application (Nicolai et al., 2020). By contrast, in an *in vitro* study of the antimicrobial activity of hydroalcoholic extracts ($EtOH/H_2O$) of *Rosmarinus officinalis* against *S. mutans*, *S. salivarius*, *S. sobrinus*, *S. mitis*, *S. sanguinis*, and *E. faecalis*, neither RA (Rice et al., 2011) nor the two ester derivatives prepared from it showed antimicrobial activity against the selected microorganisms (Bernardes et al., 2010). Further studies should therefore be carried out to confirm the true action of the compound (Rice et al., 2011) against the species *Streptococcus* concerned.

Antiviral

Among the various important pharmacological properties attributed to OA (Dellar et al., 1996) is its hepatoprotective

TABLE 2 | MICs and IC_{50} values of the compounds Parviflorone D, Parviflorone F and Sugiol against different tested microorganisms.

Microorganism	Parviflorone D Salim et al. (2008)		Parviflorone F Srancikova et al. (2013)		Sugiol de Albuquerque et al. (2007)		Ref.
	MIC (μg/ml)	IC50 (μM)	MIC (μg/ml)	IC50 (μM)	MIC (μg/ml)	IC50 (μM)	
S. aureus ATCC 43866	15.62	-	-	-	-	-	Simões et al. (2010)
S. aureus CIP 106760	15.62						
E. faecalis ATCC 51299	7.81				62.5		
E. faecalis FFHB	3.90				-		
M. smegmatis	39.06		39.06				Nyila et al. (2009)
M. tuberculosis	190		95				
L. monocytogenes	15.6		31.25				
E. coli	31.25		31.25				Nyila, (2010)
P. aeruginosa	31.25		31.25				
P. falciparum	-	5.3		3.11		1.4–3.4	Van Zyl et al. (2008), Bero et al. (2009)

S, Staphylococcus; E. faecalis, Enterococcus faecalis*; M, Mycobacterium; L, Listeria;* E. coli, Escherichia coli*;* P. aeruginosa, Pseudomonas aeruginosa*; P. falciparum, Plasmodium falciparum; ATCC, American Type Culture Collection; MIC, Minimal Inhibitory Concentration; IC_{50}, Half maximal inhibitory concentration; Ref, Reference(s)*

effect. It has been shown that OA (Dellar et al., 1996) is not only effective in protecting the liver from acute chemically induced liver injury but also protects the liver from fibrosis and cirrhosis caused by chronic liver diseases (Poolier and Goossens, 2012). OA (Dellar et al., 1996) has been marketed in China as a human over-the-counter (OTC) drug for the treatment of liver diseases such as acute and chronic hepatitis and a recent report shows that an extract, containing both acids (Lukhoba et al., 2006) and (Dellar et al., 1996), has significantly suppressed the replication of the hepatitis C virus (Kong et al., 2013). Given the anti-viral potential of these compounds, the authors propose the inclusion of these two compounds in clinical trials as monotherapy or combination with other hepatitis C antivirals. Furthermore, considering the extensive antiviral activites shown by *P. ecklonii*, it could be interesting to further investigate the effect of its active compounds for the treatment of other common viral infections, such as, Herpes simplex virus (HSV) and Hand-foot-and-mouth disease (caused by the coxsackievirus virus).

Antiplasmodic

Malaria is currently one of the world's public health concerns due to factors such as resistance to chemotherapy, poor hygiene conditions, poorly managed vector control programs, and lack of approved vaccines. There has been a general call for the use of natural products (NPs) as medicines or as a basis for the development of new antimalarials, to avoid the problems related to drug resistance (Amoa Onguéné et al., 2013). Of the four types of parasite associated with human malaria, *Plasmodium falciparum* is responsible for the most severe cases and is therefore used in most studies assessing compound activity in these species (Bero et al., 2009).

The antimalarial properties of *Plectranthus* species were determined by Van Zyl and colleagues in 2008; seven abietane diterpenes, including parviflorones D (Salim et al., 2008), F (Srancikova et al., 2013), and E (Abdel-Mogib et al., 2002), were isolated and their antiplasmodial activity and ability to inhibit the formation of β-haematin were tested (Van Zyl et al., 2008). Parviflorones D (Salim et al., 2008) and F (Srancikova et al., 2013) were isolated from *P. ecklonii* leaves and exhibited antiplasmodial activity (van Zyl et al., 2007). The lipophilic nature of abietane diterpenes allows them to easily cross erythrocyte and parasitic membranes to accumulate in the parasite vacuole. It is believed that the inhibitory effect of these compounds is related to their ability to inhibit the formation of β-haematin. This is an important effect since the malaria parasite degrades haemoglobin and the released haem, which is toxic to the parasite, is normally converted to the inert malaria pigment, β-haematin. Parviflorone F (Srancikova et al., 2013) was more effective than quinine and 62% as active as chloroquine, two conventional antimalarials. Parviflorone E (Abdel-Mogib et al., 2002), isolated from *P. purpuratus* (subspecies tongaensis) (compound also existing in *P. ecklonii*), has also been shown to be more active than quinine. When combined with quinine, the compounds Parviflorone F (Srancikova et al., 2013) and E (Abdel-Mogib et al., 2002) interacted in an additive manner (Van Zyl et al., 2008). With (Srancikova et al., 2013) and (Abdel-Mogib et al., 2002) showing higher efficacy than quinine in treating malaria, and the fact that *P. ecklonii* grows in Africa where other parasitic diseases exist, studies on other parasitic diseases should be performed, for example, sleeping sickness produced by *Trypanosoma brucei rhodesiense* and *Trypanosoma brucei gambiense*. Furthermore, it would be appropriate to suggest investigation of these compounds on other diseases also treated by quinine. Most diterpenes are known to combine high antiprotozoal activity with high toxicity to mammalian cells (e.g., kidney epithelial cells), hepatoma cells, and colon carcinoma cells. The cytotoxic profile of these compounds indicated a low degree of specificity towards the malaria parasite, making them weak candidates for the development of antimalarial agents. However, the authors suggested that further chemical modifications of these naturally-derived compounds and analogues of Parviflorone F (Srancikova et al., 2013) could result in more active antiprotozoal agents with decreased toxicity (Van Zyl et al., 2008). According to Bero and colleagues, the diterpene sugiol (de Albuquerque et al., 2007) is also a promising antimalarial agent with half-maximal inhibitory concentration (IC_{50}) between 1.4 and 3.4 μM, determined *in vitro* on *P. falciparum* strains (Bero

et al., 2009). Combinations of compounds (Srancikova et al., 2013), (Abdel-Mogib et al., 2002) and (de Albuquerque et al., 2007), should be carried out in specific formulations to identify any additive properties.

Several studies have demonstrated a growth inhibitory effect of flavonoids, in particular flavonol quercetin and flavone luteolin (Grayer et al., 2003), in protozoa of the genera *Toxoplasma*, *Trypanosoma* and *Leishmania*. Most studies involve malaria and flavonoids isolated by biologic studies of species used in traditional medicine (Lehane and Saliba, 2008). The *in vitro* antiplasmodial activity of eleven flavonoids, including the flavones apigenin (Simões et al., 2010) and luteolin (Grayer et al., 2003), has been tested against a chloroquine sensitive strain (3D7) and a chloroquine resistant strain (7G8) of *P. falciparum*. The most active compound against both strains was luteolin (Grayer et al., 2003), with IC_{50} values of 11 ± 1 μM and 12 ± 1 μM for the 3D7 and 7G8 strains, respectively. It was also found that luteolin (Grayer et al., 2003) prevents the parasite's growth progression beyond the trophotozoic phase and does not affect the parasite's susceptibility to chloroquine or artemisinin antimalarial drugs. The combination of low concentrations of different flavonoids appears to produce an additive antiplasmodic effect (Lehane and Saliba, 2008). When isolated from *P. strigosus*, the flavone salvigenin (Van Zyl et al., 2008) showed low activity against *P. aeruginosa* (Gaspar-Marques et al., 2006). It also proved to be a very weak inhibitor of *S. aureus*, as opposed to apigenin (Simões et al., 2010), which was active in MSSA and MRSA-type strains (MIC 3,9–15,6 μg/ml) (Sato et al., 2000).

Acids (Lukhoba et al., 2006) and (Dellar et al., 1996) have also been described as potent agents against *Leishmania* species. These triterpenic acids are active against amastigotes (IC_{50} 7–120 nM) and display moderate activity in the promastigotes (IC_{50} 51-137 nM) of *Leishmania donovani* and *L. major* (Tan et al., 2002). To establish anti-Leishmania SAR, in 2011, Peixoto and colleagues prepared OA (Dellar et al., 1996) derivatives and compared their IC_{50} values (Peixoto et al., 2011). The results of this *in vitro* study suggested that an increase in lipophilicity in the carbon 17 (C17) is more relevant to anti-*Leishmania* activity than an increase in lipophilicity in C3.

Anti-fungicidal

Dichloromethane extracts of *P. ecklonii* were screened for antibacterial and antifungal activities using the agar well and trench diffusion methods. Although both methods produced inconsistent results, high biological activity was observed when *P. ecklonii* was tested against *Candida* species by the trench diffusion technique (Gurlal, 2005). Abietane diterpenes isolated from *Plectranthus elegans* inhibited spore germination of the fungus *Cladosporium cucumerinum* (Dellar et al., 1996). Anti-fungicidal activity of the rearranged abietane 2ß-(4-hydroxy)benzoyloxy (**Figure 7**), obtained by Simões and colleagues in 2010, from parviflorone D (Salim et al., 2008), showed promising results against *C. albicans* (Simões et al., 2010). The flavone salvigenin (Van Zyl et al., 2008), isolated from *P. strigosus,* showed low activity against *C. albicans* (Gaspar-Marques et al., 2006). Antifungal activity against *Aspergillus niger* has also been reported for the compounds nepetoidin A (Van Jaarsveld, 2006) and nepetoidin B (Nyila et al., 2009) (Grayer et al., 2003). Nepetoidin B has also shown activity against *Cladosporium herbarum*. (Figueiredo et al., 2010).

Antitumour

Abietane diterpenes display an array of biological activities including cytotoxic and antiproliferative activities against human tumour cells (Burmistrova et al., 2013). Abietane diterpenes, especially those containing quinone moieties, deserve greater attention because several cancer chemotherapeutic agents also possess the quinone structural feature (Fronza et al., 2012). Biological membranes are potential targets of abietane diterpenes due to their lipophilic character. Studies show that cell death induced by these compounds may not follow a single mechanism, but rather several ones. It is also possible that the structural properties of diterpenes can influence or determine their molecular mode of cell death (Spiridonov et al., 2003; Fronza et al., 2012).

Sugiol (de Albuquerque et al., 2007) was reported to exhibit modest growth inhibitory activity against human breast, lung, and colon cancer cell lines (Son et al., 2005). In a study involving human pancreatic cancer cell line MIA PaCa-2, sugiol (de Albuquerque et al., 2007) influenced the relaxation activity of human DNA topoisomerases I and II. This compound showed preferential inhibition of topoisomerase I (IC_{50} of 2.8 μM) and demonstrated lower IC_{50} values than camptothecin, a classical topoisomerase I inhibitor (28.0 μM) (Fronza et al., 2012).

Recently, the anticancer effect of parviflorone D (Salim et al., 2008) was also evaluated in human breast cancer cells (Costa et al., 2018) and the results indicated further studies should be done towards a potentially therapeutic application. Furthermore, since parviflorone D (Salim et al., 2008) demonstrates limited water solubility, the formulation of parviflorone D (Salim et al., 2008) into hybrid nanoparticles to assist in longer-term drug delivery and therapeutic effect has been documented. It was reported that parviflorone D (Salim et al., 2008) showed cytotoxic activity towards human melanoma cells (A375), human 'normal-like' fibroblasts (Detroit 551 cell line), and mouse cell lines (B16V5). Further to this, α-MSH-conjugated hyaluronic and oleic acid-coated nanoparticles were formulated and showed promising results as long-term drug-release platforms in the targeted and localized therapeutic action towards melanoma cell lines (Silva et al., 2016). Additionally, studies investigating the use of optimized nanosystems for parviflorone D (Salim et al., 2008) delivery to pancreatic tumour cells, using erlotinib nanoparticles conjugated to parviflorone D (**1**) loaded albumin nanoparticles showed promising delivery to the tumour site and high antiproliferative effect in BxPC3 cell lines (Santos-Rebelo et al., 2018; Santos-Rebelo et al., 2019). During a study into the *in vitro* anti-inflammatory activity of *Plectranthus* NPs, parviflorone D (Salim et al., 2008), along with royleanone isolated from *P. grandidentatus*, demonstrated cytotoxic activity two times greater than the compound with the lowest viability. This cytotoxic evaluation showed parviflorone D (Salim et al., 2008) as having high toxicity for RAW 264.7 cells (Andrade et al., 2018).

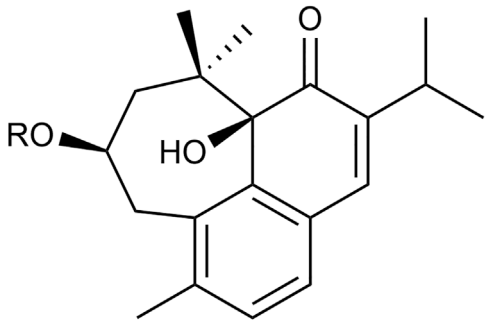

FIGURE 7 | Abietane 2ß-(4-hydroxy)benzoyloxy.

Parviflorone D (Salim et al., 2008) isolated from *P. ecklonii* showed cytotoxicity against human leukaemia cell lines CCRF-CEM and lung adenocarcinoma cell lines A549, by inducing apoptosis and influencing ROS levels (Śliwiński et al., 2020). In another recent study, parviflorone D (Salim et al., 2008) induced apoptosis in a human H7PX glioma cell line, obtained from brain tumour glioblastoma multiforme cells and demonstrated the highest amount of cytotoxicity against CCRF-CEM and A459 cell lines, when compared to other royleanone abietane diterpenes. Parviflorone D (Salim et al., 2008) produced 73% of early and late apoptosis when compared to untreated cells. The authors suggest that the high levels of phosphorylated histone in the H7PX cell lines, indicative of double-strand breaks, a decrease in the mitochondrial membrane potential and a change in pro and anti-apoptotic gene expression all contributed to apoptosis (Śliwiński et al., 2020). Furthermore, a study into the *in vitro* bioactivity of parviflorone D (Salim et al., 2008) highlighted the different pathways involved in the cytotoxic activity of the compound against multiple human cancer cell lines, including HL-60, U-937, MOLT-3, and K-562. The apoptosis induced by parviflorone D (Salim et al., 2008) was also attributed to the reduction in the mitochondrial membrane potential and influencing the levels of ROS. However, also, the inhibition of extracellular signal-regulated kinases (ERKs) enhanced tumorous cell death (Burmistrova et al., 2015). These results, along with those previously listed indicate parviflorone D (Salim et al., 2008) as having huge potential as a chemotherapeutic drug. Protein kinases C (PKC), which are involved in a variety of carcinogenic processes, have become a popular target for cancer therapy over the years. By using molecular docking studies, it has been possible to predict the enhanced activity of derivatized royleanones in cancer cell lines. Parviflorone D (Salim et al., 2008) showed activity against aggressive breast cancer cells, such as SUM159 sphere stem cells, as well as inhibiting MCF-7, SkBr3, and SUM159 cell lines, but also demonstrated a large interaction profile when binding sites were substituted with different moieties. Parviflorone D (Salim et al., 2008) PKC isoforms demonstrated the highest interaction profile when compared to other diterpene isoforms studied (Isca et al., 2020). Triple-negative breast cancer (TNBC), a rare and more aggressive cancer, in which the tests for estrogen receptors, progesterone receptors, and excess HER2 protein come back negative, has been studied with parviflorone D (Salim et al., 2008) to assess the therapeutic action of (Salim et al., 2008) in a model of TNBP, MDA-MB-231 cell lines. Overall, it was reported that (Salim et al., 2008) reduced the cell mobility and chemotactic invasion and induced apoptosis, once again demonstrating the potential of Parviflorone D (Salim et al., 2008) in chemotherapeutic drugs (Saraiva et al., 2020).

As opposed to parviflorone D (Salim et al., 2008), parviflorone F (Srancikova et al., 2013) has been shown to induce cell death by avoiding the mitochondrial permeability and initiating an alternative pathway that does not involve inhibiting anti-apoptotic proteins Bcl-2 and Bcl-X_L. Parviflorone F (Srancikova et al., 2013) showed anti-proliferative activity ranging from IC_{50} values of 4.49 - 4.99 μM, across a variety of human cell lines, including TNBC MDA-MB231, breast cancer MCF-7 and lung carcinoma A549. It has been suggested that the oxidation level of the abietane ring affects the antiproliferative selectivity of the compound. When compared to parviflorone D (Salim et al., 2008), parviflorone F (Srancikova et al., 2013) demonstrated higher cytotoxicity in Vero cell lines (Garcia et al., 2019).

Since *P. ecklonii* is a common species of South Africa, antitumour drug development using isolated compounds (Salim et al., 2008) and (Srancikova et al., 2013) could be of importance for countries with less access to other resources. When compared to the preparation of the common anticancer treatment paclitaxel, extracting parviflorones D (Salim et al., 2008) and F (Srancikova et al., 2013) from the aerial parts of *P. ecklonii* could be more accessible than, for example, from the bark of the Pacific yew tree (*Taxus brevifolia*). *P. ecklonii* is a source of different bioactive compounds, not just one of key interest, as in the case of *T. brevifolia*, therefore, in terms of economising and sustainable use of resources from natural products, *P. ecklonni* could be a legitamate alternative. Furthermore, with parviflorones D (Salim et al., 2008) and F (Srancikova et al., 2013) being recorded as demonstarting even higher antitumour activity than standard antitumour agents, the appliaction of using these compounds for *in vitro* investigation standards could be considered. The diterpene sugiol (de Albuquerque et al., 2007) demonstrated preferential inhibition of topoisomerase 1, with an IC_{50} value of 2.8 μM, lower than that of camptothecin (28.0 μM) (Fronza et al., 2012). Reported adverse effects of camptothecin have reduced it's clinical use, providing the oppourtity for alternative drug leads. Given its recorded potency, (de Albuquerque et al., 2007) should be further investigated for use in cancer therapy. Compounds, such as abietane diterpenes, could be studied in combination with current clinical drugs, to improve their activity, overcome resistances or mitigate and/or prevent adverse effects. All these results suggests potential therapeutic properties for Parvifloron D (Salim et al., 2008), specially with the help of the nanotechnology to enhance its solubility.With parviflorones D (Salim et al., 2008) and F (Srancikova et al., 2013) being recorded as demonstrating even higher antitumour activity than standard antitumour agents, the appliaction of these compounds for *in vitro* standard studies could be considered, as well as in combination with current clinical drugs, to improve their activity, overcome resistances or mitigate and/or prevent adverse effects.

The antitumour activity and multifunctionality of triterpenoids is attributed to different mechanisms, including, inhibiting NF-κB and topoisomerases activation, inducing an apoptotic response, blocking signal transducer and activating angiogenesis and transcription (D'yakonov et al., 2017). The use of triterpenic compounds, such as UA (Lukhoba et al., 2006) and OA (Dellar et al., 1996), has long been recommended in Japan as a skin cancer therapy (Muto et al., 1990) since both acids have effectively inhibited the promotion and initiation of skin tumours in rats. Cosmetic preparations containing one or both acids are even patented in Japan for topical preventive use of skin cancer (Liu, 1995). There is at least one patented pharmaceutical preparation containing OA (Dellar et al., 1996) for the treatment of non-lymphatic leukaemia (granulocytic and monocytic) without adverse side effects (Liu, 1986). Several studies have indicated that UA (Lukhoba et al., 2006) and its derivatives inhibit the growth of cancer cells by interrupting the cell cycle and stimulating apoptosis (Liu, 2005). In HT-29 colon cancer cells, UA (Lukhoba et al., 2006) decreased cell proliferation in a dose- and time-dependent manner, suggesting that it may be a potent agent for the treatment of colorectal cancer (Andersson et al., 2003; Shan et al., 2009). Another study suggests UA (Lukhoba et al., 2006) as a potential chemopreventive agent in metastatic breast cancer (Yoeh et al., 2010). Cancer is a multifactorial disease, with multiple symptoms and targets; interest in drugs possessing multiple biological actions, such as antitumour and anti-inflammatory, are of increasing interest for their combinations of action, rather than single modes of action. As an example, COX-2 and Leukotrienes (LTs) are involved in the inflammatory process, which have also been linked to the mechanisms of action involved in cancer. In colon cancer HT-29 cells, antitumour effects of RA (Rice et al., 2011) have been related to its ability to inhibit COX-2 activation by AP-1 inducing agents (Hossan et al., 2014). LTs are significantly involved in the immunoregulation process of various inflammatory-dependent diseases, including asthma, and various allergic conditions They are initially biosynthesized by 5-LOX from arachidonic acid. CA (Pal et al., 2011) has been shown to have anti-inflammatory properties as a selective inhibitor of 5-LOX and thus of LT biosynthesis (Yasuko et al., 1984). CA (Pal et al., 2011) also inhibits PKC (Gamaro et al., 2011) and the activation of NF-kB, induced by ceramides in human myeloid leukaemia cell line U937 (Nardini et al., 2001). CA (Pal et al., 2011) was found to diminish NO and prostaglandin E2 (PGE2) production in LPS-stimulated RAW264.7 cells. Additionally, mRNA levels of TNF-α, COX-2, and iNOS were downregulated by CA (Pal et al., 2011) (Yang et al., 2013).

Due to the multiple biological activities of flavonoids (anti-inflammatory, antioxidant, antiproliferative, and antibacterial), there have been many studies towards their application as anti-tumour and radiosensitizing agents. For example, cirsiliol (Uchida et al., 1980) has been investigated as a possible radiosensitizer in non-small cell lung cancer (NSCLC) (Kang et al., 2013). Most lung cancer patients are diagnosed at an advanced and inoperable stage, with radiotherapy being their only effective treatment option. Unfortunately, radioresistance of tumours remains a critical obstacle (Provencio et al., 2010). Results show that cirsiliol (Uchida et al., 1980) reduces the proliferation of NSCLC by inhibiting the expression (but not activation) of the Notch-1 gene (Kang et al., 2013).

Several studies have shown that many flavonoids, including luteolin (Grayer et al., 2003) and apigenin (Simões et al., 2010), inhibit the proliferation of various normal and tumoral cells, derived from almost all tissues (Packer et al., 2004). Apigenin (Simões et al., 2010) is a powerful inhibitor of cell proliferation and angiogenesis in human endothelial cells. It inhibits the expression of vascular endothelial growth factor (VEGF) via alpha-1 hypoxia inducing factor degradation (HIF-1α) (Osada et al., 2004) and the growth of human cervical carcinoma HeLa cells and neuroblastoma cell lines, a paediatric tumour (Zheng et al., 2005). Apoptosis of HeLa cells by inducing p53 gene expression suggests the potential of apigenin (Simões et al., 2010) in the development of a preventive agent for cervical cancer. Another study confirmed this chemopreventive action of apigenin (Simões et al., 2010), this time in the treatment of pancreatic cancer, by the inhibition of NF-κB activation (Wu et al., 2014). Although it does not appear so, the anti-proliferative cell activity of flavonoids is specific, depending on the type of cell and the structure of the flavonoid. For example, neither apigenin (Simões et al., 2010) nor luteolin (Grayer et al., 2003) shows the significant growth-inhibiting activity of 4A5 cells in melanoma B16 (Packer et al., 2004).

Antioxidant

The current modern-day lifestyle causes excessive free radical production and reactive oxygen and/or nitrogen species (ROS/RNS). Antioxidants are defined as compounds that can delay, inhibit, or prevent the oxidation of oxidizable materials by scavenging free radicals and diminishing oxidative stress (OS) (Dai and Mumper, 2010). The production of free radicals is common place during normal aerobic cellular metabolism and can perform various functions as signalling and provide protection against infections (Sharma et al., 2012). However, free radical overproduction results in OS, a detrimental process that can cause oxidative damage of different biomolecules (such as enzymes, proteins, lipids, and nucleic acids) inhibiting their normal function and causing many diseases (Valko et al., 2007). OS has been implicated in the development of chronic degenerative diseases, including cardiovascular and respiratory diseases, neurodegenerative disorders (Alzheimer's disease (AD) and Parkinson's disease (PD)), *diabetes mellitus*, rheumatoid arthritis, and different types of cancer, as well as in the aging process (Phaniendra et al., 2015), discovering natural compounds with good scavenging capacity against ROS imperative.

Plant antioxidants are composed of a broad variety of different substances like ascorbic acid (vitamin C) and tocopherols, polyphenolic compounds, or terpenoids (Graßmann, 2005). Evidence of terpene antioxidant behaviour comes from the increasing number of publications published in recent years, focusing on their source, structures, and mechanisms, through which they exert their pharmacological and possible therapeutic

activities (Gonzalez-Burgos and Gomez-Serranillos, 2012). One of the most frequently employed methods used to detect the presence of antioxidant compounds is the 2,2-Diphenyl-1-picrylhydrazyl (DPPH•) radical scavenging assay (Akar et al., 2017). In 2005, Chao and colleagues reported that although sugiol (de Albuquerque et al., 2007) had low inhibitory activity against DPPH radical, it could effectively reduce intracellular production of ROS in lipopolysaccharide (LPS) stimulated macrophages (Chao et al., 2005). When compared to the standard compound, ascorbic acid, sugiol (de Albuquerque et al., 2007) showed significant scavenging activities of DPPH, nitric oxide (NO), superoxide, and hydroxyl free radicals in a concentration-dependent manner (Bajpai et al., 2014). Besides, sugiol (de Albuquerque et al., 2007) showed an inhibitory effect of lipid peroxidation of 76.5% compared with α-tocopherol (80.13%) and butylated hydroxyanisole (BHA) (76.5%), two well-known synthetic antioxidants. However, increasing concern concerning these synthetic antioxidants in promoting liver damage and carcinogenic processes merits the search for alternative antioxidant sources, such as, from *Plectranthus* spp. Another diterpene isolated from *P. ecklonii* which demonstrated dose-dependent anti-radical activity was parviflorone D (Salim et al., 2008). This compound had antioxidant properties equivalent to hydroxyl butyltoluene (BHT), but lower than quercetin, two other synthetic antioxidants (Rijo et al., 2009). The antioxidant activity of parviflorone F (Srancikova et al., 2013) and E (Abdel-Mogib et al., 2002), isolated from the leaves of *P. nummularius* Briq., was also evaluated by the DPPH method. Both compounds showed a higher uptake capacity of the DPPH radical than that of the α-tocopherol (Narukawa et al., 2001). It is most probable that the quinone moiety present in the abietane diterpenes, such as in parviflorone D (Salim et al., 2008), aids in stabilizing free radicals.

Phenolic acids, tannins and flavonoid compounds, which are subgroups of phenolics, are known to be potent antioxidants (Ramu et al., 2012). Studies demonstrate a positive and highly significant relationship between total phenolics and antioxidant activity (Velioglu et al., 1998; Pulido et al., 2000; Zheng and Wang, 2001; Özgen et al., 2006). Phenolic compounds have been recognized as powerful antioxidants *in vitro* and have proven to be more potent antioxidants than Vitamin C, E, and carotenoids (Pulido et al., 2000). Authors suggest phenolic antioxidant properties to be mediated by three main mechanisms: 1. scavenging radical species such as ROS/RNS; 2. suppressing ROS/RNS formation by the inhibition of several enzymes or chelating trace metals involved in the production of free radical production; 3. upregulating or protecting antioxidant defence (Dai and Mumper, 2010).

The structure of phenolic compounds is a key determinant of their radical scavenging and metal chelating activity, and this is referred to as SAR (Aberoumand and Deokule, 2008). Hydroxycinnamic acids have higher antioxidant activity than the corresponding hydroxybenzoic acids, which may be a result of the CH=CH-COOH group, which guarantees the greater capacity to donate hydrogen ions (H+) and stabilize radicals than the carboxyl group. CA (Pal et al., 2011) acts particularly well as a donor of hydrogen atoms, mainly thanks to the extra stability given to the phenoxy radical, resulting from interaction with the adjacent hydroxyl group(s) by hydrogen bonds (Balasundram et al., 2006). By having a hydroxyl in *para*-position relative to the lateral chain, it also easily captures a radical. Besides, it can fluctuate between hydrophilic and lipophilic, which makes it easier for the compound to access areas where there is oxidized vitamin E and, subsequently, can regenerate it (Scott, 1997). *In vitro* and *in vivo* experiments have demonstrated the exceptional antioxidant activity of RA (Rice et al., 2011) against peroxidative damage to biological membranes. RA (Rice et al., 2011) is an ester of CA (Pal et al., 2011) with 3,4-dihydroxyphenyl lactic acid (Petersen, 2013), the major component of polar extracts from many plants of the *Lamiaceae* family (Falé et al., 2009) and, presumably, one of the main compounds responsible for the potent antioxidant activity of *Lamiaceae* plants (Ozgen et al., 2008). The four phenolic hydrogens account for this compound's ability to modulate free radical scavenging. In combination with two catechol moieties, that provide the suitable polarity for (Rice et al., 2011) to penetrate the lipid bilayers, RA (Rice et al., 2011) has shown to protect against oxidation, without disturbing the molecular structure (Amoah et al., 2016). RA (Rice et al., 2011) protects neurons from OS by significantly reducing H_2O_2-induced ROS production and apoptosis cell death, showing the potential application in neurodegenerative diseases, such as PD and Huntingdon's Disease (HD) (Bhatt et al., 2013). In 2003, Grayer and colleagues demonstrated that the CA (Pal et al., 2011) derivative, nepetoidin B (Nyila et al., 2009), isolated from the aqueous extracts of *P. ecklonii* leaves, has a potent free radical trapping activity (Grayer et al., 2003). Compound (Nyila et al., 2009), nepetoidin B, has been tested, together with three known antioxidants (gallic acid, RA (Rice et al., 2011), and CA (Pal et al., 2011), using the DPPH test. Nepetoidin B (Nyila et al., 2009) showed a higher capacity to capture free radicals than acids (Rice et al., 2011) and (Pal et al., 2011). Nepetoidin A (Van Jaarsveld, 2006) has not been tested enough to gather sufficient evidence. However, even low concentrations of the substance have resulted in a considerable colour loss of a DPPH solution, indicating that nepetoidin A (Van Jaarsveld, 2006) is likely to have strong antioxidant activity as well.

Flavonoid antioxidant activity is attributed to their capability to recapture free radicals and chelate metals (Bilto et al., 2012), as well as their effects on cell signalling and gene expression (Soobrattee et al., 2005). The *in vitro* antioxidant capacity of flavonoids has been intensively studied over the past years and, based on SAR studies, it is predicted that their antioxidant activity depends on its chemical structure, corresponding to the number and position of hydroxyl groups (Amic et al., 2007). *In vivo* antioxidant efficacy of flavonoids appears less in the literature (Pietta, 2000). The antioxidant activity improves notably when C-3' and C-4' positions in ring "B" are occupied by hydroxyl groups (**Figure 4**). As for ring "A", phenolic hydroxyl groups contribute somewhat to the antioxidant activity, due to the electrophilic effect of ring "C" (Lin et al., 2014). The presence of ortho-di-hydroxyl (catechol) group on the "B" ring and the double bond between C2-C3 in conjugation with an oxo group at C4 are key structural features of antioxidant flavonoids, since the catechol group stabilizes radical species. Luteolin (Grayer et al., 2003) and its glycosides (e.g. luteolin 7-O-glucoside (Kubínová et al., 2013)) satisfy these structural necessities, therefore, it is not surprising

that many luteolin-containing plants possess antioxidant properties, through their ability to scavenge ROS and RNS (López-Lázaro, 2009). In a study of the copper chelating properties of luteolin-7-*O*-glucoside (Kubínová et al., 2013) and luteolin (Grayer et al., 2003), the ortho-3',4'-dihydroxy substitution in the B-ring, in the case of luteolin (Grayer et al., 2003), was suggested as being important for copper chelation, thereby influencing its antioxidant activity (Brown and Rice-Evans, 1998).

There is also evidence in the literature that simultaneous hydroxylation of C3 and C5 flavonoids is another important structural feature involved in maximizing the potential for free radical scavenging, in determining antioxidant activity (Bors et al., 1990; Soobrattee et al., 2005). Besides, the existence of a portion of sugar in the C8 position of vitexin (Gaspar-Marques et al., 2006) significantly decreases the antioxidant efficacy of this compound compared to its non-glycosylated derivative (Simões et al., 2010) (Soobrattee et al., 2005). The antioxidant activity of the flavones salvigenin (Van Zyl et al., 2008), cirsimaritin (Nyila et al., 2012), and genkwanin (Zschocke et al., 2000) have been evaluated by the qualitative tests of DPPH and the discoloration of ß-carotene. They all tested negative for DPPH, which means that they do not pick-up radicals by this method. Salvigenin (Van Zyl et al., 2008) was the only one to test positive for beta-carotene bleaching, which may indicate preventive antioxidant activity, possibly related to the absorption of UV radiation (Gaspar-Marques et al., 2006). Preventive antioxidants can be compounds with the ability to absorb UV rays, superoxide dismutase enzymes, catalases, and peroxidases, or compounds with the ability to chelate or reduce transition metals (Scott, 1997). The use of flavones in the treatment of Alzheimer's disease focuses on the inflammation process underlying the progression of the disease. This therapeutic approach is based on the preventive action of flavones in the face of OS and consequent inflammation by acting as antioxidants by capturing free radicals.

Anti-inflammatory

Several studies have shown that triterpenoids significantly suppress chronic inflammation by modulating proinflammatory mediators. The anti-inflammatory effects of pentacyclic triterpenoids are largely ascribed to their ability to inhibit molecular targets such as 5-lipoxygenase (LOX), inducible nitric oxide synthase (iNOS), cyclooxygenase (COX) - 2, and nuclear factor-kappa B (NF-κB) activities (Yap and Lim, 2015). The anti-inflammatory effects of UA (Lukhoba et al., 2006) have been attributed to its ability to suppress nuclear factor-kappa B (NF-κB) activation, which, together with NF-AT (nuclear factor of activated T cells) and AP-1 (activator protein-1), regulate inflammatory genes (Checker et al., 2012). Another potential application of this compound could be in the treatment of osteoarthritis since the activation of NF-kB is critical in the pathophysiology of osteoarthritis (Gabay et al., 2010). The potential anti-inflammatory activity of sugiol (de Albuquerque et al., 2007) and the relationship between signal transduction and inflammatory cytokines was evaluated *in vitro* (Chao et al., 2005). A dose of 30 μM of sugiol effectively inhibited the production of pro-inflammatory cytokines, prointerleukin-1beta, IL-1β, and tumour necrosis factor-alpha (TNF-α), suggesting that sugiol (de Albuquerque et al., 2007) is bioactive against inflammation. The authors suggested that the efficacy of sugiol (de Albuquerque et al., 2007) in inhibiting inflammatory cytokines IL-1ß and TNF-α could be attributed to a reduction of ROS, which in turn causes a decrease in the phosphorylation of mitogen-activated protein kinases (MAPKs).

The anti-inflammatory properties of RA (Rice et al., 2011) are thought to be based on the inhibition of LOX and COX, on the interference with the complement cascade and the inhibition of expression of inflammatory cytokines. Another study has shown that CA (Pal et al., 2011) derivatives exert anti-inflammatory action *in vitro* and *in vivo* and their action is mediated, at least partially, by NO recapture (Da Cunha et al., 2004). Nakanishi and colleagues reported potent inhibition of xanthine oxidase by both Nepetoidin A (Van Jaarsveld, 2006) and B (Nyila et al., 2009) and particularly by nepetedoin B (Nyila et al., 2009), suggesting that this compound could have the potential for the control of hyperuricemia in human gout (Nakanishi et al., 1990).

The anti-inflammatory effect of phenolic compounds is related to the ability to modulate the expression of pro-inflammatory enzymes such as phospholipase A2, nitric oxide synthase (NOS), COX, and LOX. Inhibition of these enzymes by flavonoids reduces the production of arachidonic acid, prostaglandins (PG), LTs, and NO, crucial mediators of inflammation. In general, flavones have a greater inhibitory effect on NO production than flavonols (Kim et al., 2004). Different flavonoids, such as quercetin, apigenin (Simões et al., 2010) and luteolin (Grayer et al., 2003), have been reported to possess anti-inflammatory and analgesic effects (Kumar and Pandey, 2013). Apigenin (Simões et al., 2010) showed strong anti-inflammatory activity through inhibition of NO and iNOS production, and inhibition of COX-2 expression. Inhibition of iNOS and NO production is also attributed to luteolin (Grayer et al., 2003) (Choi et al., 2014). Apigenin (Simões et al., 2010) and luteolin (Grayer et al., 2003) also inhibit interleukin (IL)-5, which promotes the growth and survival of eosinophils and plays an important role in allergic inflammation associated with eosinophilia (Packer et al., 2004). In an *in vitro* study, both flavones showed potent inhibition of IL-4 and IL-13 synthesis (Hirano et al., 2004), and both have an inhibitory action on LOX and pro-inflammatory cytokines TNF-α and IL-1 (Lago et al., 2014). On a structural level, the requirements for the anti-inflammatory activity of the flavonoids include unsaturation in the C-ring (between C2 and C3); the number and position of hydroxyl groups (e.g., the catechol group in the B-ring); the carbonyl group in C4; and the non-glycosylation of the molecule. However, compounds that do not have these structural characteristics also exhibit anti-inflammatory activity, affecting enzymes of the inflammatory cascade (Lago et al., 2014). Data in the literature strongly suggest that the double bond between C2 and C3 is crucial for inhibiting NO production and that hydroxyl substitutions in the A and B rings influence inhibitory activity **(Figure 4)**. Hydroxylation on positions 5- and/or 7- of the A-ring, and in positions 3'- and/or 4'- of the B-ring provide favourable results for inhibition of production, the opposite if hydroxylation is in carbon 3 (C-ring) (Kim et al., 1999). Apigenin (Simões et al., 2010) and luteolin (Grayer et al., 2003) are among the flavonoids cited as the most active inhibitors. The anti-inflammatory effect

of luteolin (Grayer et al., 2003), its glucosides and plants containing luteolin (Grayer et al., 2003) have been tested *in vitro* and *in vivo* (López-Lázaro, 2009). In an *in vitro* SAR study, luteolin (Grayer et al., 2003) showed high inhibitory activity of thromboxane and LT synthesis, and in particular against the enzyme activity of LTs. Cinaroside (Kubínová et al., 2013) (luteolin-7-*O*-ßglucoside) showed only moderate inhibitory activity against both enzyme synthesis pathways (Odontuya et al., 2005). These results support the idea that the hydroxyl substitute in the C5 position and the non-glycosylation of the molecule contribute significantly to the anti-inflammatory activity of the flavonoids. *In vivo* studies have shown that luteolin (Grayer et al., 2003) effectively protects mouse induced LPS lethality, suggesting the application of this compound as a potential therapeutic agent in septic decay treatment (Kuo et al., 2011; Chen et al., 2014).

Enzyme Inhibition

Tyrosinase is one of the keys enzymes in the biosynthesis of melanin, the pigment responsible for determining skin and hair colour. The inhibition of tyrosinase is one of the major strategies to treat skin hyperpigmentation, one of the common skin complaints that affect people of all skin types. Inhibitors of the tyrosinase enzyme, such as hydroquinone, kojic acid, and azelaic acid, have been used to treat hyperpigmentation disorders but despite their efficacy, many of these agents are frequently reported to have numerous limitations, such as high cytotoxicity, poor skin penetration, and low stability in formulations (Otang-Mbeng and Sagbo, 2020). Therefore, there has been a growing demand for products that act safely and effectively when inhibiting enzymatic oxidation, to prevent hyperpigmentation (Nerya et al., 2004). One of the traditional preparations, a paste made from the leaves of *P. ecklonii*, is used in Zimbabwe for skin diseases and skin hyperpigmentation problems.

P. ecklonii ethyl acetate extract and its isolated compounds, parviflorone D (Salim et al., 2008) and F (Srancikova et al., 2013), were tested for their tyrosinase inhibitory action in comparison to kojic acid. The concentration at which half the tyrosinase activity was inhibited (IC_{50}) by the extract was 61.7 ± 2.7 µg/ml. During cytotoxicity evaluation, compounds (Salim et al., 2008) and (Srancikova et al., 2013), were toxic against monkey kidney Vero cell lines, as shown by their IC_{50} values (Nyila et al., 2009). Nevertheless, the activity demonstrated by the raw extract of *P. ecklonii* in the tyrosinase test, together with its antibacterial activity against *S. aureus*, helps to justify the traditional use of the plant in skin-related diseases (Lukhoba et al., 2006). In a more recent study, the high chelating ability of abietane diterpenes, found in *P. ecklonii,* was attributed to the observed anti-tyrosinase activity, *in vitro*, and was considered almost as efficient as kojic acid, the positive control. The combination of polyphenolic compounds, such as quercetin, with abietane diterpenes, has shown a synergistic effect that promotes both anti-tyrosinase and antioxidant activity, suitable for skin treatment, such as, anti-pigmentation (Andrade et al., 2021).

Acetylcholinesterase (AChE) is the enzyme that catalyses the hydrolysis of the neurotransmitter acetylcholine (ACh) (Dvir et al., 2010). Nowadays, the most effective therapy for Alzheimer's disease (AD) consists of increasing the levels of ACh through the inhibition of AChE activity (Falé et al., 2009). The literature indicates that terpenoids and, in particular, some diterpenoids, may have anti-acetylcholinesterase activity (Dvir et al., 2010). To date, no references to the inhibitory effect of AChE by diterpenes with an abietane skeleton isolated from *P. ecklonii* have been found in the literature.

AChE is the target of cholinesterase (ChE) inhibitors used when addressing the cholinergic deficit in AD patients. The leading AD therapeutics involve AChE inhibitors, which produce an increase of the acetylcholine concentrations in the synaptic cleft, enhancing the cholinergic transmission. Despite decades of research, current pharmacotherapeutic options for AD are still very limited and represent an area of need that is currently unmet. Studies indicate that species of the *Lamiaceae* family are a bountiful source of varying natural AChE inhibitors and antioxidants that could be useful in the prevention and treatment of AD and other related diseases (Vladimir-Knežević et al., 2014). In a study with *P. barbatus*, the presence of RA (Rice et al., 2011), a compound which is also found in *P. ecklonii*, has been attributed to the antioxidant activity found *in vitro* and the inhibition of AChE, where high inhibition activity was demonstrated in the decoction (31% inhibition). The authors also analysed other *Plectranthus* spp., *P. ecklonii*, *P. fructicosus*, *P. lanuginosus*, and *P. verticillatus*, where they compared the RA (Rice et al., 2011) content of the plants. *P. ecklonii* was the species studied that gave the highest inhibition activity (62.8%) (Falé et al., 2009). In a study looking for new treatment strategies for AD, the *in vitro* AChE inhibition, antioxidant activity, and bioactive components of five different spp. of *Plectranthus* (*P. ecklonii* including) were investigated. The main components of the aqueous extracts, rosmarinic (Rice et al., 2011), chlorogenic (Chassagne and Morgan, 2020) and caffeic (Pal et al., 2011) acids, were quantified. The decoctions showed high AChE inhibitory and antioxidant activities for *P. ecklonii* and *P. saccatus* (Gomes et al., 2012). According to these studies, the aqueous extracts and decoction method is the best way to evaluate the AChE activity of *P. ecklonii*. It has also been stated that the most active extracts were obtained from the leaves as opposed to the flowers (Falé et al., 2009). The activity of other enzymes, such as collagenase inhibition, in aqueous extracts of *P. ecklonii*, has recently been established with rosmarinic (Rice et al., 2011) being attributed to promoting the highest amount of biological activity at 4.5%. However, the presence of CA (Pal et al., 2011) in the extracts could also be considered accountable for the increased activity and further studies would be required to positively identify the compounds responsible for the enzyme inhibition (Andrade et al., 2021). RA's (Rice et al., 2011) inhibitory activity of the enzyme glycosyltransferase (GTF) has been highlighted (Figueiredo et al., 2010) and the presence of this compound has also been linked to the observed effects of AChE inhibition and antioxidant activity (Falé et al., 2009). The flavones vitexin (Gaspar-Marques et al., 2006), isovitexin (Amoah et al., 2016) and naturally occurring C-glycosylated derivatives of apigenin (Simões et al., 2010) have demonstrated anti-AD activity (Choi et al., 2014), again

promptly the need for further studies of this species to corroborate these findings.

CONCLUSION

With the growing acceptance of alternative forms of health care, such as traditional medicine, new requirements are also emerging. Compound screening is needed to clarify which molecules are responsible for biological activities, to scientifically validate popular plant uses. Secondary metabolites found in plants provide an immeasurable wealth of structurarly diverse compounds with associated bioactivities The genus *Plectranthus*, for its diverse ethnobotanical applications and the several biological effects (antimicrobial, antioxidant, anti-inflammatory and anti-tumour), has been suggested as a promising source for the discovery of bioactive compounds. In this sense, the isolation of secondary metabolites from *Plectranthus* species and the understanding of the origin of their therapeutic properties is imperative and can guarantee effective and safe use. In this work not only have some of the traditional uses of *P. ecklonii* been validated, but the potential of this plant as a prospective source of new drug leads has been demonstrated. From the species *P. ecklonii* Benth., 28 compounds have been isolated to date. As observed in other *Plectranthus* species studied over the years, the predominant classes are terpenes and phenolic compounds. Eight diterpenes were identified in *P. ecklonii*, four of them being diterpenes with an abietane skeleton (**1**, **2**, **9**, and **27**), two being triterpenes (**12** and **13**) and two being identified as sterols (**14** and **15**). Regarding phenolic compounds, twelve flavones (**19**-**24**, **26** and **28**-**31**) and one flavanone (Costa et al., 2018) were isolated, in addition to CA (Pal et al., 2011) and four of its derivatives (**3**, **4**, **5**, and **16**). The literature reports RA (Rice et al., 2011) as the predominant compound in the aqueous extracts of *P. ecklonii*. Phytochemical studies have reported the isolation of two isomeric *o*-quinones, ecklonoquinones A (Śliwiński et al., 2020) and B (Andrade et al., 2018) from *P. ecklonii* which have not been analysed in this work because no reference was found in the literature concerning any bioactivities (Uchida et al., 1980). Among the diterpenes, the most recent studies emphasise the major abietane diterpenoid, parviflorone D (Salim et al., 2008), for its potential in cancer therapy, particularly when combined with nanotechnology, and sugiol (de Albuquerque et al., 2007) has also demonstrated its anticancer potential as an effective topoisomerase 1 inhibitor. The main phenolic compound, rosmarinic acid (Rice et al., 2011), mainly exhibited antioxidant and anti-inflammatory activity, although photoprotective and melanogenic properties have also been described. Anti-inflammatory activity has also been attributed to sugiol (de Albuquerque et al., 2007), caffeic acid (Pal et al., 2011), apigenin (Simões et al., 2010) and luteolin (Grayer et al., 2003). The diterpenes parviflorone D (Salim et al., 2008), E (Abdel-Mogib et al., 2002), F (Srancikova et al., 2013) and sugiol (de Albuquerque et al., 2007) all showed antioxidant activity as well as oleanolic acid (Dellar et al., 1996), caffeic acid (Pal et al., 2011) and Nepetoidin B (Nyila et al., 2009).The antimicrobial activity of *Plectranthus ecklonii* has been attributed to parviflorone D (Salim et al., 2008) and F (Srancikova et al., 2013), the latter also showing similar antimalarial activity similar to that of chloroquine. Adittionally, (2) and (Abdel-Mogib et al., 2002) were reported to be more effective than quinine. As an ornamental plant, with multiple compounds showing anticancer activity, *P. ecklonii* could become an accessible source for antitumour drugs. Since *P. ecklonii* is a common species of South Africa, in terms of economising and the sustainable use of resources from natural products, *P. ecklonii* could be a legitamate alternative to current antitumour drugs. However, the lack of data and information on possible side effects and saftey of this species warrants further investigation, to assess the safety of this plant for clinical and therapeutic use.

AUTHOR CONTRIBUTIONS

Conceptualization, AMA and PR; methodology, AMA, GB and ED; formal analysis, AMA, GB, and ED, investigation, AMA and GB; re-writing of original draft preparation, AMA; review-writing and editing, GB and ED; figures preparation, ED; supervision, AD, and PR; funding acquisition, AD and PR. All authors have read and agreed to the published version of the manuscript.

FUNDING

This work was financially supported in part by FCT – *Fundacão para a Ciência e Tecnologia* grants PEst-OE/SAU/UI4013/2014, UID/DTP/04567/2016, UIDB/04567/2020 and UIDP/04567/2020; and INSTITUTO LUSÓFONO DE INVESTIGAÇÃO E DESENVOLVIMENTO (ILIND) for the project COFAC/ILIND/CBIOS/1/2020.

ACKNOWLEDGMENTS

ED-M gratefully acknowledges being the recipient of a predoctoral FPU 2019 fellowship from the University of Alcalá de Henares.

REFERENCES

Abdel-Mogib, M., Albar, H., and Batterjee, S. (2002). Chemistry of the Genus Plectranthus. *Molecules* 7, 271–301. doi:10.3390/70200271

Aberoumand, A., and Deokule, S. S. (2008). Comparison of Phenolic Compounds of Some Edible Plants of Iran and India. *Pakistan J. Nutr.* 7 (4), 582–585. doi:10.3923/pjn.2008.582.585

Akar, Z., Küçük, M., and Doğan, H. (2017). A New Colorimetric DPPH• Scavenging Activity Method with No Need for a Spectrophotometer Applied on Synthetic and Natural Antioxidants and Medicinal Herbs. *J. Enzyme Inhib. Med. Chem.* 32 (1), 640–647. doi:10.1080/14756366.2017.1284068

Amic, D., Davidovic-Amic, D., Beslo, D., Rastija, V., Lucic, B., and Trinajstic, N. (2007). SAR and QSAR of the Antioxidant Activity of Flavonoids. *Cmc* 14 (7), 827–845. doi:10.2174/092986707780090954

Amoa Onguéné, P., Ntie-Kang, F., Lifongo, L. L., Ndom, J. C., Sippl, W., and Mbaze, L. M. (2013). The Potential of Anti-malarial Compounds Derived from African Medicinal Plants, Part I: A Pharmacological Evaluation of Alkaloids and Terpenoids. *Malar. J.* 12, 449. doi:10.1186/1475-2875-12-449

Amoah, S., Sandjo, L., Kratz, J., and Biavatti, M. (2016). Rosmarinic Acid - Pharmaceutical and Clinical Aspects. *Planta Med.* 82, 388–406. doi:10.1055/s-0035-1568274

Andersson, D., Liu, J. J., Nilsson, A., and Duan, R. D. (2003). Ursolic Acid Inhibits Proliferation and Stimulates Apoptosis in HT29 Cells Following Activation of Alkaline Sphingomyelinase. *Anticancer Res.* 23 (4), 3317–3322.

Andrade, J. M., Custódio, L., Romagnoli, A., Reis, C. P., Rodrigues, M. J., Garcia, C., et al. (2018). Antitubercular and Anti-inflammatory Properties Screening of Natural Products from *Plectranthus* Species. *Future Med. Chem.* 10 (14), 1677–1691. doi:10.4155/fmc-2018-0043

Andrade, J. M., Domínguez-Martín, E. M., Nicolai, M., Faustino, C., Rodrigues, L. M., and Rijo, P. (2021). Screening the Dermatological Potential of *Plectranthus* Species Components: Antioxidant and Inhibitory Capacities over Elastase, Collagenase and Tyrosinase. *J. Enzyme Inhib. Med. Chem.* 36 (1), 257–269. doi:10.1080/14756366.2020.1862099

Asif, M., and Khodadadi, E. (2013). Medicinal Uses and Chemistry of Flavonoid Contents of Some Common Edible Tropical Plants. *J. Paramed Sci.* 4 (3), 119–138. doi:10.22037/jps.v4i3.4648

Bahadoran, Z., Mirmiran, P., and Azizi, F. (2013). Dietary Polyphenols as Potential Nutraceuticals in Management of Diabetes: a Review. *J. Diabetes Metab. Disord.* 12. doi:10.1186/2251-6581-12-43

Bajpai, V. K., Sharma, A., Kang, S. C., and Baek, K. H. (2014). Antioxidant, Lipid Peroxidation Inhibition and Free Radical Scavenging Efficacy of a Diterpenoid Compound Sugiol Isolated from *Metasequoia Glyptostroboides*. *Asian Pac. J. Trop. Med.* 7 (1), 9–15. doi:10.1016/S1995-7645(13)60183-2

Balasundram, N., Sundram, K., and Samman, S. (2006). Phenolic Compounds in Plants and Agri-Industrial By-Products: Antioxidant Activity, Occurrence, and Potential Uses. *Food Chem.* 99 (1), 191–203. doi:10.1016/j.foodchem.2005.07.042

Berges, R. R., Kassen, A., and Senge, T. (2000). Treatment of Symptomatic Benign Prostatic Hyperplasia with Beta-Sitosterol: an 18-month Follow-Up. *BJU Int.* 85, 842–846. doi:10.1046/j.1464-410x.2000.00672.x

Bernardes, W. A., Lucarini, R., Tozatti, M. G., Souza, M. G., Silva, M. L., Filho, A. A., et al. (2010). Antimicrobial Activity of *Rosmarinus Officinalis* against Oral Pathogens: Relevance of Carnosic Acid and Carnosol. *Chem. Biodivers* 7 (7), 1835–1840. doi:10.1002/cbdv.200900301

Bero, J., Frédérich, M., and Quetin-Leclercq, J. (2009). Antimalarial Compounds Isolated from Plants Used in Traditional Medicine. *J. Pharm. Pharmacol.* 61 (11), 1401–1433. doi:10.1211/jpp/61.11.0001

Bhatt, R., Mishra, N., and Bansal, P. K. (2013). Phytochemical, Pharmacological and Pharmacokinetics Effects of Rosmarinic Acid. *J. Pharm. Sci. Innov.* 2 (2), 28–34. doi:10.7897/2277-4572.02215

Bilto, Y. Y., Suboh, S., Aburjai, T., and Abdalla, S. (2012). Structure-activity Relationships Regarding the Antioxidant Effects of the Flavonoids on Human Erythrocytes. *Ns* 04 (09), 740–747. doi:10.4236/ns.2012.49098

Borghi, S. M., Carvalho, T. T., Staurengo-Ferrari, L., Hohmann, M. S., Pinge-Filho, P., Casagrande, R., et al. (2013). Vitexin Inhibits Inflammatory Pain in Mice by Targeting TRPV1, Oxidative Stress, and Cytokines. *J. Nat. Prod.* 76 (6), 1141–1149. doi:10.1021/np400222v

Bors, W., Heller, W., Michel, C., and Saran, M. (1990). Flavonoids as Antioxidants: Determination of Radical-Scavenging Efficiencies. *Methods Enzymol.* 186 (C), 343–355. doi:10.1016/0076-6879(90)86128-I

Brown, J. E., and Rice-Evans, C. A. (1998). Luteolin-rich Artichoke Extract Protects Low Density Lipoprotein from Oxidation *In Vitro*. *Free Radic. Res.* 29 (3), 247–255. doi:10.1080/10715769800300281

Burmistrova, O., Perdomo, J., Simões, M. F., Rijo, P., Quintana, J., and Estévez, F. (2015). The Abietane Diterpenoid Parvifloron D from *Plectranthus Ecklonii* Is a Potent Apoptotic Inducer in Human Leukemia Cells. *Phytomedicine* 22 (11), 1009–1016. doi:10.1016/j.phymed.2015.06.013

Burmistrova, O., Simões, M. F., Rijo, P., Quintana, J., Bermejo, J., and Estévez, F. (2013). Antiproliferative Activity of Abietane Diterpenoids against Human Tumor Cells. *J. Nat. Prod.* 76 (8), 1413–1423. doi:10.1021/np400172k

Chao, K. P., Hua, K. F., Hsu, H. Y., Su, Y. C., and Chang, S. T. (2005). Anti-inflammatory Activity of Sugiol, a Diterpene Isolated from *Calocedrus Formosana* Bark. *Planta Med.* 71 (4), 300–305. doi:10.1055/s-2005-864094

Chassagne, F., and Morgan, M. (2020). Book Review: Underexplored Medicinal Plants from Sub-saharan Africa: Plants with Therapeutic Potential for Human Health. *Front. Pharmacol.* 11, 229–233. doi:10.3389/fphar.2020.00965

Checker, R., Sandur, S. K., Sharma, D., Patwardhan, R. S., Jayakumar, S., Kohli, V., et al. (2012). Potent Anti-inflammatory Activity of Ursolic Acid, a Triterpenoid Antioxidant, Is Mediated through Suppression of NF-Kb, AP-1 and NF-AT. *PLoS One* 7, e31318. doi:10.1371/journal.pone.0031318

Chen, D., Bi, A., Dong, X., Jiang, Y., Rui, B., Liu, J., et al. (2014). Luteolin Exhibits Anti-inflammatory Effects by Blocking the Activity of Heat Shock Protein 90 in Macrophages. *Biochem. Biophys. Res. Commun.* 443 (1), 326–332. doi:10.1016/j.bbrc.2013.11.122

Choi, J. S., Islam, M. N., Ali, M. Y., Kim, E. J., Kim, Y. M., and Jung, H. A. (2014). Effects of C-Glycosylation on Anti-diabetic, Anti-alzheimer's Disease and Anti-inflammatory Potential of Apigenin. *Food Chem. Toxicol.* 64, 27–33. doi:10.1016/j.fct.2013.11.020

Choi, Y., and Lee, J. (2009). Antioxidant and Antiproliferative Properties of a Tocotrienol-Rich Fraction from Grape Seeds. *Food Chem.* 114 (4), 1386–1390. doi:10.1016/j.foodchem.2008.11.018

Cole, M. D. (1994). Key Antifungal, Antibacterial and Anti-insect Assays-A Critical Review. *Biochem. Syst. Ecol.* 22, 837–856. doi:10.1016/0305-1978(94)90089-2

Costa, J., Saraiva, N., Rijo, P., Almeida, N., Reis, C., and Fernandes, A. S. (2018). Anti-tumor Properties of the Redox-Active Compound Parvifloron D in Breast Cancer Cells. *Free Radic. Biol. Med.* 120, S119–S120. doi:10.1016/j.freeradbiomed.2018.04.394

Cowan, M. M. (1999). Plant Products as Antimicrobial Agents. *Clin. Microbiol. Rev.* 12, 564–582. doi:10.1128/cmr.12.4.564

D'yakonov, V. A., Dzhemileva, L. U., and Dzhemilev, U. M. 2017. Advances in the Chemistry of Natural and Semisynthetic Topoisomerase I/II Inhibitors. *Studies in Natural Products Chemistry*. 54, 21–86. doi:10.1016/B978-0-444-63929-5.00002-4

Da Cunha, F. M., Duma, D., Assreuy, J., Buzzi, F. C., Niero, R., Campos, M. M., et al. (2004). Caffeic Acid Derivatives: *In Vitro* and *In Vivo* Anti-inflammatory Properties. *Free Radic. Res.* 38 (11), 1241–1253. doi:10.1080/10715760400016139

Dai, J., and Mumper, R. J. (2010). Plant Phenolics: Extraction, Analysis and Their Antioxidant and Anticancer Properties. *Molecules* 15, 7313–7352. doi:10.3390/molecules15107313

de Albuquerque, R. L., de Vasconcelos Silvade, M. G. V., Machado, M. I. L., de A. Matosde, F. J. A., de Morais, S. M., and Neto, J. S. (2007). Chemical Composition and Antioxidant Activity of *Plectranthus Grandis* and *P. Ornatus* Essential Oils from north-eastern Brazil. *Flavour Fragr. J.* 22 (1), 24–26. doi:10.1002/ffj.1730

Dellar, J. E., Cole, M. D., and Waterman, P. G. (1996). Antimicrobial Abietane Diterpenoids from *Plectranthus Elegans*. *Phytochemistry* 41 (3), 735–738. doi:10.1016/0031-9422(95)00694-X

Devappa, R. K., Makkar, H. P. S., and Becker, K. (2011). Jatropha Diterpenes: a Review. *J. Am. Oil Chem. Soc.* 88, 301–322. doi:10.1007/s11746-010-1720-9

Dewick, P. M. (2002). Medicinal Natural Products. A Biosynthetic Approach P.M. Dewick; Wiley, Chichester, UK. *Phytochemistry* 60 (6), 648. doi:10.1016/s0031-9422(02)00176-0

Dvir, H., Silman, I., Harel, M., Rosenberry, T. L., and Sussman, J. L. (2010). Acetylcholinesterase: From 3D Structure to Function. *Chem. Biol. Interact* 187 (1–3), 10–22. doi:10.1016/j.cbi.2010.01.042

Dzubak, P., Hajduch, M., Vydra, D., Hustova, A., Kvasnica, M., Biedermann, D., et al. (2006). Pharmacological Activities of Natural Triterpenoids and Their Therapeutic Implications. *Nat. Prod. Rep.* 23, 394–411. doi:10.1039/b515312n

Falé, P. L., Borges, C., Madeira, P. J. A., Ascensão, L., Araújo, M. E. M., Florêncio, M. H., et al. (2009). Rosmarinic Acid, Scutellarein 4′-methyl Ether 7-O-Glucuronide and (16S)-Coleon E Are the Main Compounds Responsible for the Antiacetylcholinesterase and Antioxidant Activity in Herbal tea of Plectranthus Barbatus ("falso Boldo"). *Food Chem.* 114 (3), 798–805. doi:10.1016/j.foodchem.2008.10.015

Feng, S., Dai, Z., Liu, A., Wang, H., Chen, J., Luo, Z., et al. (2017). β-Sitosterol and Stigmasterol Ameliorate Dextran Sulfate Sodium-Induced Colitis in Mice Fed a High Fat Western-Style Diet. *Food Funct.* 8 (11), 4179–4186. doi:10.1039/c7fo00375g

Figueiredo, N., Falé, P. L., and Madeira, P. J. A. (2014). Phytochemical Analysis of Plectranthus Sp. Extracts and Application in Inhibition of Dental Bacteria, *Streptococcus Sobrinus* and *Streptococcus Mutans*. *Ejmp* 4 (7), 794–809. doi:10.9734/ejmp/2014/7544

Figueiredo, N. L., de Aguiar, S. R. M. M., Falé, P. L., Ascensão, L., Serralheiro, M. L. M., and Lino, A. R. L. (2010). The Inhibitory Effect of *Plectranthus Barbatus* and *Plectranthus Ecklonii* Leaves on the Viability, Glucosyltransferase Activity and Biofilm Formation of *Streptococcus Sobrinus* and *Streptococcus Mutans*. *Food Chem.* 119 (2), 664–668. doi:10.1016/j.foodchem.2009.07.008

Fronza, M., Lamy, E., Günther, S., Heinzmann, B., Laufer, S., and Merfort, I. (2012). Abietane Diterpenes Induce Cytotoxic Effects in Human Pancreatic Cancer Cell Line MIA PaCa-2 through Different Modes of Action. *Phytochemistry* 78, 107–119. doi:10.1016/j.phytochem.2012.02.015

Gabay, O., Sanchez, C., Salvat, C., Chevy, F., Breton, M., Nourissat, G., et al. (2010). Stigmasterol: a Phytosterol with Potential Anti-osteoarthritic Properties. *Osteoarthritis Cartilage* 18 (1), 106–116. doi:10.1016/j.joca.2009.08.019

Gamaro, G. D., Suyenaga, E., Borsoi, M., Lermen, J., Pereira, P., and Ardenghi, P. (2011). Effect of Rosmarinic and Caffeic Acids on Inflammatory and Nociception Process in Rats. *ISRN Pharmacol.* 2011, 451682–451686. doi:10.5402/2011/451682

Garcia, C., Teodósio, C., Oliveira, C., Oliveira, C., Díaz-Lanza, A., Reis, C., et al. (2019). Naturally Occurring *Plectranthus*-Derived Diterpenes with Antitumoral Activities. *Curr. Pharm. Des.* 24 (36), 4207–4236. doi:10.2174/1381612825666190115144241

Gaspar-Marques, C., Simões, M. F., Valdeira, M. L., and Rodríguez, B. (2008). Terpenoids and Phenolics from *Plectranthus Strigosus*, Bioactivity Screening. *Nat. Prod. Res.* 22 (2), 167–177. doi:10.1080/14786410701654560

Gaspar-Marques, C. (2006). *Univeristy of Lisbon*. "*Phytochemical Studies and Biological Activities of Plectranthus Grandidentatus Gürke*,". Editors P. strigosus Benth and P. fruticosus L'Hérit.

Gibbons, S. (2004). Anti-staphylococcal Plant Natural Products. *Nat. Prod. Rep.* 21, 263–277. doi:10.1039/b212695h

Gomes, A., Jerónimo, A., Reis, C., and Rijo, P. (2012). New Treatment Strategies with Plant Extracts Teas for Alzheimer's Disease. *Biomed. Biopharm. Res.* 2 (9), 242.

Gonzalez-Burgos, E., and Gomez-Serranillos, M. P. (2012). Terpene Compounds in Nature: A Review of Their Potential Antioxidant Activity. *Cmc* 19 (31), 5319–5341. doi:10.2174/092986712803833335

Grayer, R. J., Eckert, M. R., Veitch, N. C., Kite, G. C., Marin, P. D., Kokubun, T., et al. (2003). The Chemotaxonomic Significance of Two Bioactive Caffeic Acid Esters, Nepetoidins A and B, in the Lamiaceae. *Phytochemistry* 64 (2), 519–528. doi:10.1016/S0031-9422(03)00192-4

Grayer, R. J., Eckert, M. R., Lever, A., Veitch, N. C., Kite, G. C., and Paton, A. J. (2010). Distribution of Exudate Flavonoids in the Genus *Plectranthus*. *Biochem. Syst. Ecol.* 38 (3), 335–341. doi:10.1016/j.bse.2010.01.014

Graßmann, J. (2005). Terpenoids as Plant Antioxidants. *Plant Antioxid.* 72, 505–535. doi:10.1016/S0083-6729(05)72015-X

Gurlal, P. (2005). *Testing for Microbiologically Active Compounds Extracted from Members of the Family Lamiaceae and Other Indigenous Plants*. KwaZulu-Natal, South Africa.

Hamada, S., and Slade, H. D. (1980). Biology, Immunology, and Cariogenicity of Streptococcus Mutans. *Microbiol. Rev.* 44, 331–384. doi:10.1128/mmbr.44.2.331-384.1980

Hanson, J. R. (2005). Diterpenoids. *Nat. Prod. Rep.* 22, 594–602. doi:10.1039/b501834j

Hawas, U., El-Toumy, S., and Meyer, J. (2008). Phenolic Constituents and Antimicrobial Studies on the Aqueous Methanolic Extract of the *Plectranthus Ecklonii* Leaves. *Planta Med.* 74, 74. doi:10.1055/s-0028-1084349

Hirano, T., Higa, S., Arimitsu, J., Naka, T., Shima, Y., Ohshima, S., et al. (2004). Flavonoids Such as Luteolin, Fisetin and Apigenin Are Inhibitors of Interleukin-4 and Interleukin-13 Production by Activated Human Basophils. *Int. Arch. Allergy Immunol.* 134 (2), 135–140. doi:10.1159/000078498

Hossan, M. S., Rahman, S., Bashar, A. B. M. A., Jahan, R., Al-Nahain, A., and Rahmatullah, M. (2014). Rosmarinic Acid: A Review of its Anticancer Action. *World J. Pharm. Pharm. Sci.* 3 (9), 57–70.

Isca, V. M. S., Sencanski, M., Filipovic, N., Dos Santos, D. J. V. A., Čipak Gašparović, A., Saraíva, L., et al. (2020). Activity to Breast Cancer Cell Lines of Different Malignancy and Predicted Interaction with Protein Kinase C Isoforms of Royleanones. *Int. J. Mol. Sci.* 21, 21. doi:10.3390/ijms21103671

Jesus, J. A., Lago, J. H. G., Laurenti, M. D., Yamamoto, E. S., and Passero, L. F. D. (2015). Antimicrobial Activity of Oleanolic and Ursolic Acids: An Update. *Evidence-Based Complement. Altern. Med.* 2015, 1–14. doi:10.1155/2015/620472

Jiménez-Arellanes, A., Meckes, M., Torres, J., and Luna-Herrera, J. (2007). Antimycobacterial Triterpenoids from *Lantana Hispida* (Verbenaceae). *J. Ethnopharmacol* 111 (2), 202–205. doi:10.1016/j.jep.2006.11.033

Kang, J., Kim, E., Kim, W., Seong, K. M., Youn, H., Kim, J. W., et al. (2013). Rhamnetin and Cirsiliol Induce Radiosensitization and Inhibition of Epithelial-Mesenchymal Transition (EMT) by miR-34a-Mediated Suppression of Notch-1 Expression in Non-small Cell Lung Cancer Cell Lines. *J. Biol. Chem.* 288 (38), 27343–27357. doi:10.1074/jbc.M113.490482

Kim, H. K., Cheon, B. S., Kim, Y. H., Kim, S. Y., and Kim, H. P. (1999). Effects of Naturally Occurring Flavonoids on Nitric Oxide Production in the Macrophage Cell Line RAW 264.7 and Their Structure-Activity Relationships. *Biochem. Pharmacol.* 58 (5), 759–765. doi:10.1016/S0006-2952(99)00160-4

Kim, H. P., Son, K. H., Chang, H. W., and Kang, S. S. (2004). Anti-inflammatory Plant Flavonoids and Cellular Action Mechanisms. *J. Pharmacol. Sci.* 96, 229–245. doi:10.1254/jphs.crj04003x

Kong, L., Li, S., Liao, Q., Zhang, Y., Sun, R., Zhu, X., et al. (2013). Oleanolic Acid and Ursolic Acid: Novel Hepatitis C Virus Antivirals that Inhibit NS5B Activity. *Antivir. Res.* 98 (1), 44–53. doi:10.1016/j.antiviral.2013.02.003

Krishnaiah, D., Sarbatly, R., and Nithyanandam, R. (2011). A Review of the Antioxidant Potential of Medicinal Plant Species. *Food Bioproducts Process.* 89, 217–233. doi:10.1016/j.fbp.2010.04.008

Kubínová, R., Švajdlenka, E., Schneiderová, K., Hanáková, Z., Dall'Acqua, S., and Farsa, O. (2013). Polyphenols and Diterpenoids from Plectranthus Forsteri 'Marginatus'. *Biochem. Syst. Ecol.* 49, 39–42. doi:10.1016/j.bse.2013.03.029

Kumar, S., and Pandey, A. K. (2013). Chemistry and Biological Activities of Flavonoids: An Overview. *Scientific World J.* 2013, 1–16. doi:10.1155/2013/162750

Kuo, M. Y., Liao, M. F., Chen, F. L., Li, Y. C., Yang, M. L., Lin, R. H., et al. (2011). Luteolin Attenuates the Pulmonary Inflammatory Response Involves Abilities of Antioxidation and Inhibition of MAPK and NFκB Pathways in Mice with Endotoxin-Induced Acute Lung Injury. *Food Chem. Toxicol.* 49 (10), 2660–2666. doi:10.1016/j.fct.2011.07.012

Lago, J. H., Toledo-Arruda, A. C., Mernak, M., Barrosa, K. H., Martins, M. A., Tibério, I. F., et al. (2014). Structure-Activity Association of Flavonoids in Lung Diseases. *Molecules* 19 (3), 3570–3595. doi:10.3390/molecules19033570

Lehane, A. M., and Saliba, K. J. (2008). Common Dietary Flavonoids Inhibit the Growth of the Intraerythrocytic Malaria Parasite. *BMC Res. Notes* 1, 26. doi:10.1186/1756-0500-1-26

Lin, C. M., Chen, C. S., Chen, C. T., Liang, Y. C., and Lin, J. K. (2002). Molecular Modeling of Flavonoids that Inhibits Xanthine Oxidase. *Biochem. Biophys. Res. Commun.* 294 (1), 167–172. doi:10.1016/S0006-291X(02)00442-4

Lin, C. Z., Zhu, C. C., Hu, M., Wu, A. Z., Bairu, Z. D., and Kangsa, S. Q. (2014). Structure-activity Relationships of Antioxidant Activity *In Vitro* about Flavonoids Isolated from *Pyrethrum Tatsienense*. *J. Intercult Ethnopharmacol* 3 (3), 123–127. doi:10.5455/jice.20140619030232

Lin, Y., Shi, R., Wang, X., and Shen, H. M. (2008). Luteolin, a Flavonoid with Potential for Cancer Prevention and Therapy. *Curr. Cancer Drug Targets* 8 (7), 634–646. doi:10.2174/156800908786241050

Liu, J. (1995). Pharmacology of Oleanolic Acid and Ursolic Acid. *J. Ethnopharmacol* 49, 57–68. doi:10.1016/0378-8741(95)90032-2

Liu, J. (2005). Oleanolic Acid and Ursolic Acid: Research Perspectives. *J. Ethnopharmacology* 100, 92–94. doi:10.1016/j.jep.2005.05.024

Liu, R., Hao, D., Xu, W., Li, J., Li, X., Shen, D., et al. (2019). β-Sitosterol Modulates Macrophage Polarization and Attenuates Rheumatoid Inflammation in Mice. *Pharm. Biol.* 57 (1), 161–168. doi:10.1080/13880209.2019.1577461

Liu, Y. G. (1986). Pharmaceutical Composition for Treating Nonlymphatic Leukemia and its Components. *Chem. Abstr.*

López-Lázaro, M. (2009). Distribution and Biological Activities of the Flavonoid Luteolin. *Mrmc* 9, 31–59. doi:10.2174/138955709787001712

Lukhoba, C. W., Simmonds, M. S. J., and Paton, A. J. (2006). Plectranthus: A Review of Ethnobotanical Uses. *J. Ethnopharmacology* 103, 1–24. doi:10.1016/j.jep.2005.09.011

Marques, C. G., Pedro, M., Simões, M. F., Nascimento, M. S., Pinto, M. M., and Rodríguez, B. (2002). Effect of Abietane Diterpenes from *Plectranthus Grandidentatus* on the Growth of Human Cancer Cell Lines. *Planta Med.* 68 (9), 839–840. doi:10.1055/s-2002-34407

Martens, S., and Mithöfer, A. (2005). Flavones and Flavone Synthases. *Phytochemistry* 66, 2399–2407. doi:10.1016/j.phytochem.2005.07.013

Matsumoto-Nakano, M. (2018). Role of *Streptococcus Mutans* Surface Proteins for Biofilm Formation. *Jpn. Dent Sci. Rev.* 54, 22–29. doi:10.1016/j.jdsr.2017.08.002

Misra, P. S., Misra, G., Nigam, S. K., and Mitra, C. R. (1971). Constituents of *Diospyros Peregrina* Fruit and Seed. *Phytochemistry* 10 (4), 904–905. doi:10.1016/S0031-9422(00)97175-9

Muto, Y., Ninomiya, M., and Fujiki, H. (1990). Present Status of Research on Cancer Chemoprevention in Japan. *JJCO* 20, 219–224. doi:10.1093/oxfordjournals.jjco.a039391

Nakanishi, T., NIshi, M., Inada, A., Obata, H., Tanabe, N., Abe, S., et al. (1990). Two New Potent Inhibitors of Xanthine Oxidase from Leaves of Perilla Frutescens Britton Var. Acuta Kudo. *Chem. Pharm. Bull. (Tokyo)* 38 (6), 1772–1774. doi:10.1248/cpb.38.1772

Nardini, M., Leonardi, F., Scaccini, C., and Virgili, F. (2001). Modulation of Ceramide-Induced NF-kappaB Binding Activity and Apoptotic Response by Caffeic Acid in U937 Cells: Comparison with Other Antioxidants. *Free Radic. Biol. Med.* 30 (7), 722–733. doi:10.1016/s0891-5849(00)00515-3

Narukawa, Y., Shimizu, N., Shimotohno, K., and Takeda, T. (2001). Two New Diterpenoids from *Plectranthus Nummularius* Briq. *Chem. Pharm. Bull. (Tokyo)* 49 (9), 1182–1184. doi:10.1248/cpb.49.1182

Nerya, O., Musa, R., Khatib, S., Tamir, S., and Vaya, J. (2004). Chalcones as Potent Tyrosinase Inhibitors: The Effect of Hydroxyl Positions and Numbers. *Phytochemistry* 65 (10), 1389–1395. doi:10.1016/j.phytochem.2004.04.016

Nicolai, M., Mota, J., Fernandes, A. S., Pereira, F., Pereira, P., P Reis, C., et al. (2020). Assessment of the Potential Skin Application of *Plectranthus Ecklonii* Benth. *Pharmaceuticals (Basel)* 13 (6), 1–10. doi:10.3390/ph13060120

Nyila, M. A. (2010). Antilisterial Bioactivity and/or Biofilm-Formation by Compounds from Plectranthus Ecklonii Benth. And Acacia Karroo Hayne Submitted in partial fulfillment of the requirements. PhD thesis. South Africa: Department of Plant Science, Faculty of Natural and Agricultural Sciences, University of Pretoria.

Nyila, M. A., Leonard, C. M., Hussein, A. A., and Lall, N. (2009). Bioactivities of *Plectranthus Ecklonii* Constituents. *Nat. Prod. Commun.* 4 (9), 1177–1180. doi:10.1177/1934578x0900400903

Nyila, M. A., Leonard, C. M., Hussein, A. A., and Lall, N. (2012). Activity of South African Medicinal Plants against Listeria Monocytogenes Biofilms, and Isolation of Active Compounds from Acacia Karroo. *South Afr. J. Bot.* 78, 220–227. doi:10.1016/j.sajb.2011.09.001

Odjakova, M., Popova, E., Al, M., and Mironov, R. (2012). Plant-Derived Agents with Anti-glycation Activity. *Glycosylation*. doi:10.5772/48186

Odontuya, G., Hoult, J. R., and Houghton, P. J. (2005). Structure-activity Relationship for Antiinflammatory Effect of Luteolin and its Derived Glycosides. *Phytother Res.* 19 (9), 782–786. doi:10.1002/ptr.1723

Osada, M., Imaoka, S., and Funae, Y. (2004). Apigenin Suppresses the Expression of VEGF, an Important Factor for Angiogenesis, in Endothelial Cells via Degradation of HIF-1alpha Protein. *FEBS Lett.* 575 (1–3), 59–63. doi:10.1016/j.febslet.2004.08.036

Otang-Mbeng, W., and Sagbo, I. J. (2020). Anti-melanogenesis, Antioxidant and Anti-tyrosinase Activities of *Scabiosa Columbaria* L. *Processes* 8, 236. doi:10.3390/pr8020236

Ozgen, M., Durgaç, C., Serçe, S., and Kaya, C. (2008). Chemical and Antioxidant Properties of Pomegranate Cultivars Grown in the Mediterranean Region of Turkey. *Food Chem.* 111 (3), 703–706. doi:10.1016/j.foodchem.2008.04.043

Özgen, U., Mavi, A., Terzi, Z., Yıldırım, A., Coşkun, M., and Houghton, P. J. (2006). Antioxidant Properties of Some Medicinal Lamiaceae (Labiatae) Species. *Pharm. Biol.* 44 (2), 107–112. doi:10.1080/13880200600592061

Packer, L., Ong, C., and Halliwell, B. (2004). *Herbal Traditional Medicine, Molecular Aspects of Health*. New York: Marcel Dekker.

Pal, M., Kumar, A., and Tewari, K. (2011). Chemical Composition and Mosquito Repellent Activity of the Essential Oil of Plectranthus Incanus Link. *Facta Univ. Phys. Chem. Technol.* 9 (1), 57–64. doi:10.2298/fupct1101057p

Patlolla, J. M., and Rao, C. V. (2012). Triterpenoids for Cancer Prevention and Treatment: Current Status and Future Prospects. *Curr. Pharm. Biotechnol.* 13 (1), 147–155. doi:10.2174/138920112798868719

Peixoto, J. A., Andrade E Silva, M. L., Crotti, A. E., Cassio Sola Veneziani, R., Gimenez, V. M., Januário, A. H., et al. (2011). Antileishmanial Activity of the Hydroalcoholic Extract of *Miconia Langsdorffii*, Isolated Compounds, and Semi-synthetic Derivatives. *Molecules* 16 (2), 1825–1833. doi:10.3390/molecules16021825

Petersen, M. (2013). Rosmarinic Acid: New Aspects. *Phytochem. Rev.* 12, 207–227. doi:10.1007/s11101-013-9282-8

Phaniendra, A., Jestadi, D. B., and Periyasamy, L. (2015). Free Radicals: Properties, Sources, Targets, and Their Implication in Various Diseases. *Ind. J. Clin. Biochem.* 30, 11–26. doi:10.1007/s12291-014-0446-0

Pietta, P.-G. (2000). Flavonoids as Antioxidants. *J. Nat. Prod.* 63, 1035–1042. doi:10.1021/np9904509

Poolier, J., and Goossens, A. (2012). Molecules of Interest – Oleanolic Acid. *Phytochemistry* 77, 10.

Provencio, M., Sánchez, A., Garrido, P., and Valcárcel, F. (2010). New Molecular Targeted Therapies Integrated with Radiation Therapy in Lung Cancer. *Clin. Lung Cancer* 11, 91–97. doi:10.3816/clc.2010.n.012

Pulido, R., Bravo, L., and Saura-Calixto, F. (2000). Antioxidant Activity of Dietary Polyphenols as Determined by a Modified Ferric Reducing/antioxidant Power Assay. *J. Agric. Food Chem.* 48 (8), 3396–3402. doi:10.1021/jf9913458

Rabe, T., and Van Staden, J. (1997). Antibacterial Activity of South African Plants Used for Medicinal Purposes. *J. Ethnopharmacol* 56 (1), 81–87. doi:10.1016/S0378-8741(96)01515-2

Rajendra Prasad, N., Karthikeyan, A., Karthikeyan, S., and Reddy, B. V. (2011). Inhibitory Effect of Caffeic Acid on Cancer Cell Proliferation by Oxidative Mechanism in Human HT-1080 Fibrosarcoma Cell Line. *Mol. Cel Biochem* 349 (1–2), 11–19. doi:10.1007/s11010-010-0655-7

Ramu, G., Mohan, G. K., Jayaveera, K. N., Dhanapal, S. P., and Senthilkumar, G. (2012). Preliminary Phytochemical and Antioxidant Study of Hydroalcoholic Extracts from Selected Genera of Indian Lamiaceae. *Asian Pac. J. Trop. Biomed.*, 2. doi:10.1016/S2221-1691(12)60296-2

Rice, L. J., Brits, G. J., Potgieter, C. J., and Van Staden, J. (2011). *Plectranthus*: A Plant for the Future? *South Afr. J. Bot.* 77 (4), 947–959. doi:10.1016/j.sajb.2011.07.001

Rijo, P., Chumbo, J., and Oliveira, A. (2009). Antioxidant Activity of Two Abietane Diterpenoids from *Plectranthus* Spp. *5o Congreso da la SEFIR*. Lisbon.

Rijo, P., Faustino, C., and Simões, M. F. (2013). "Antimicrobial Natural Products from *Plectranthus* Plants," in *Microbial Pathogens and Strategies for Combating Them: Science, Technology and Education*. Editor A. Méndez-Vilas, 933–1031.

Rüedi, P., and Eugster, C. H. (1978). Diterpenoide Drüsenfarbstoffe aus Labiaten: 6 neuep-Chinomethane aus Plectranthus parviflorus WILLD. *Hca* 61 (2), 709–715. doi:10.1002/hlca.19780610219

Salim, A., Chin, Y., and Kingthorn, A. (2008). *Drug Discovery from Plants*. in *Bioactive Molecules and Medicinal Plants*. Editors K. G. Ramawat and J. M. Merillon (Berlin: Springer), 1–25. doi:10.1007/978-3-540-74603-4

Sandhar, H. K., Kumar, B., Prasher, S., Tiwari, P., Salhan, M., and Sharma, P. (2011). A Review of Phytochemistry and Pharmacology of Flavonoids. *Int. Pharm. Sci. Internet* 1 (1), 25–41. Available from: http://www.ipharmsciencia.com.

Santos-Rebelo, A., Garcia, C., Eleutério, C., Bastos, A., Coelho, S. C., Coelho, M. A. N., et al. (2018). Development of Parvifloron D-Loaded Smart Nanoparticles to Target Pancreatic Cancer. *Pharmaceutics* 10, 10. doi:10.3390/pharmaceutics10040216

Santos-Rebelo, A., Kumar, P., Pillay, V., Choonara, Y. E., Eleutério, C., Figueira, M., et al. (2019). Development and Mechanistic Insight into the Enhanced Cytotoxic Potential of Parvifloron D Albumin Nanoparticles in EGFR-Overexpressing Pancreatic Cancer Cells. *Cancers* 11, 1733. doi:10.3390/cancers11111733

Saraiva, N., Costa, J. G., Reis, C., Almeida, N., Rijo, P., and Fernandes, A. S. (2020). Anti-migratory and Pro-apoptotic Properties of Parvifloron D on Triple-Negative Breast Cancer Cells. *Biomolecules* 10, 10. doi:10.3390/biom10010158

Sato, Y., Suzaki, S., Nishikawa, T., Kihara, M., Shibata, H., and Higuti, T. (2000). Phytochemical Flavones Isolated from *Scutellaria Barbata* and Antibacterial Activity against Methicillin-Resistant *Staphylococcus aureus*. *J. Ethnopharmacol* 72 (3), 483–488. doi:10.1016/S0378-8741(00)00265-8

Schmidt, T. J., Khalid, S. A., Romanha, A. J., Alves, T. M. A., Biavatti, M. W., Brun, R., et al. (2012). The Potential of Secondary Metabolites from Plants as Drugs or

Leads against Protozoan Neglected Diseases - Part II. *Cmc* 19 (14), 2176–2228. doi:10.2174/092986712800229087

Scott, G. (1997). *Antioxidants in Science, Technology, Medicine and Nutrition.* Chichester, UK: Albion Publishing. doi:10.1533/9780857099938

Shan, J. Z., Xuan, Y. Y., Zheng, S., Dong, Q., and Zhang, S. Z. (2009). Ursolic Acid Inhibits Proliferation and Induces Apoptosis of HT-29 colon Cancer Cells by Inhibiting the EGFR/MAPK Pathway. *J. Zhejiang Univ. Sci. B* 10 (9), 668–674. doi:10.1631/jzus.B0920149

Sharma, P., Jha, A. B., Dubey, R. S., and Pessarakli, M. (2012). Reactive Oxygen Species, Oxidative Damage, and Antioxidative Defense Mechanism in Plants under Stressful Conditions. *J. Bot.* 2012, 1–26. doi:10.1155/2012/217037

Silva, C. O., Molpeceres, J., Batanero, B., Fernandes, A. S., Saraiva, N., Costa, J. G., et al. (2016). Functionalized Diterpene Parvifloron D-Loaded Hybrid Nanoparticles for Targeted Delivery in Melanoma Therapy. *Ther. Deliv.* 7 (8), 521–544. doi:10.4155/tde-2016-0027

Simões, M. F., Rijo, P., Duarte, A., Matias, D., and Rodríguez, B. (2010). An Easy and Stereoselective Rearrangement of an Abietane Diterpenoid into a Bioactive Microstegiol Derivative. *Phytochemistry Lett.* 3 (4), 234–237. doi:10.1016/j.phytol.2010.09.001

Sitarek, P., Toma, M., Ntungwe, E., Kowalczyk, T., Skała, E., Wieczfinska, J., et al. (2020). Insight the Biological Activities of Selected Abietane Diterpenes Isolated from Plectranthus Spp. *Biomolecules* 10, 10. doi:10.3390/biom10020194

Śliwiński, T., Sitarek, P., Skała, E., Isca, V. M. S., Synowiec, E., Kowalczyk, T., et al. (2020). Diterpenoids from *Plectranthus* Spp. As Potential Chemotherapeutic Agents via Apoptosis. *Pharmaceuticals (Basel)* 13 (6), 1–16. doi:10.3390/ph13060123

Soica, C., Oprean, C., Borcan, F., Danciu, C., Trandafirescu, C., Coricovac, D., et al. (2014). The Synergistic Biologic Activity of Oleanolic and Ursolic Acids in Complex with Hydroxypropyl-γ-Cyclodextrin. *Molecules* 19 (4), 4924–4940. doi:10.3390/molecules19044924

Son, K. H., Oh, H. M., Choi, S. K., Han, D. C., and Kwon, B. M. (2005). Anti-tumor Abietane Diterpenes from the Cones of *Sequoia Sempervirens*. *Bioorg. Med. Chem. Lett.* 15 (8), 2019–2021. doi:10.1016/j.bmcl.2005.02.057

Song, J. H., Kim, S. K., Chang, K. W., Han, S. K., Yi, H. K., and Jeon, J. G. (2006). *In Vitro* inhibitory Effects of Polygonum Cuspidatum on Bacterial Viability and Virulence Factors of *Streptococcus Mutans* and *Streptococcus Sobrinus*. *Arch. Oral Biol.* 51 (12), 1131–1140. doi:10.1016/j.archoralbio.2006.06.011

Soobrattee, M. A., Neergheen, V. S., Luximon-Ramma, A., Aruoma, O. I., and Bahorun, T. (2005). Phenolics as Potential Antioxidant Therapeutic Agents: Mechanism and Actions. *Mutat. Res.* 579 (1–2), 200–213. doi:10.1016/j.mrfmmm.2005.03.023

Spiridonov, N. A., Arkhipov, V. V., Foigel, A. G., Shipulina, L. D., and Fomkina, M. G. (2003). Protonophoric and Uncoupling Activity of Royleanones from Salvia Officinalis and Euvimals from Eucalyptus viminalis. *Phytother Res.* 17 (10), 1228–1230. doi:10.1002/ptr.1403

Srancikova, A., Horvathova, E., and Kozics, K. (2013). Biological Effects of Four Frequently Used Medicinal Plants of Lamiaceae. *Neoplasma* 60, 585–597. doi:10.4149/neo_2013_076

Sun, H., Fang, W. S., Wang, W. Z., and Hu, C. (2006). Structure-activity Relationships of Oleanane- and Ursane-type Triterpenoids. *Bot. Stud.* 47, 339–368.

Syamasundar, K. V., Vinodh, G., Srinivas, K. V. N. S., and Srinivasulu, B. (2012). A New Abietane Diterpenoid from Plectranthus bishopianusBenth. *Hca* 95 (4), 643–646. doi:10.1002/hlca.201100425

Tan, N., Kaloga, M., Radtke, O. A., Kiderlen, A. F., Oksüz, S., Ulubelen, A., et al. (2002). Abietane Diterpenoids and Triterpenoic Acids from *Salvia Cilicica* and Their Antileishmanial Activities. *Phytochemistry* 61 (8), 881–884. doi:10.1016/S0031-9422(02)00361-8

Teixeira, A. P., Batista, O., Fátima Simões, M., Nascimento, J., Duarte, A., De La Torre, M. C., et al. (1997). Abietane Diterpenoids from *Plectranthus Grandidentatus*. *Phytochemistry* 44 (2), 325–327. doi:10.1016/S0031-9422(96)00467-0

Uchida, V. M., Riiedi, P., Eugster, H., Zurich-irchel, O. I. D. U., and Zurich, C. (1980). 21. Driisenfarbstoffe aus Labiaten : Ecklonochinone A und B, zwei neuartige aus *Plectranthus ecklonii* BENTH. *Helv. Chim. Acta* 63 (21), 18–19. doi:10.1002/hlca.19800630122

Valko, M., Leibfritz, D., Moncol, J., Cronin, M. T. D., Mazur, M., and Telser, J. (2007). Free Radicals and Antioxidants in normal Physiological Functions and Human Disease. *Int. J. Biochem. Cel Biol.* 39, 44–84. doi:10.1016/j.biocel.2006.07.001

Van Jaarsveld, E. (2006). *Southern African Plectranthus*. South Africa: Fernwood Press (Pty) Ltd.

van Zyl, R., Khan, F., Drewes, S., and Edwards, T. (2007). Antiplasmodial Activity of Abietane Diterpenes Isolated from Five Southern African *Plectranthus* Species. *Planta Med.* 73, 73. doi:10.1055/s-2007-986911

Van Zyl, R. L., Khan, F., Edwards, T. J., and Drewes, S. E. (2008). Antiplasmodial Activities of Some Abietane Diterpenes from the Leaves of Five *Plectranthus* Species. *S Afr. J. Sci.* 104 (1–2), 62–64.

Velioglu, Y. S., Mazza, G., and Gao, L., (1998). Antioxidant Activity and Total Phenolics in Selected Fruits, Vegetables, and Grain Products. *J. Agric. Food Chem.* 46 (10), 4113–4117. doi:10.1021/jf9801973

Vestri Alvarenga, S. A., Pierre Gastmans, J., do Vale Rodrigues, G., Moreno, P. R., and de Paulo Emerenciano, V. (2001). A Computer-Assisted Approach for Chemotaxonomic Studies-Dditerpenes in Lamiaceae. *Phytochemistry* 56 (6), 583–595. doi:10.1016/s0031-9422(00)00424-6

Vinholes, J., Silva, B. M., and Silva, L. R. (2015). Hydroxycinnamic Acids (HCAS): Structure, Biological Properties and Health Effects. *Advances in Medicine and Biology*. 88, 105–130.

Vladimir-Knežević, S., Blažeković, B., Kindl, M., Vladić, J., Lower-Nedza, A., and Brantner, A. (2014). Acetylcholinesterase Inhibitory, Antioxidant and Phytochemical Properties of Selected Medicinal Plants of the Lamiaceae Family. *Molecules* 19 (1), 767–782. doi:10.3390/molecules19010767

Waksmundzka-Hajnos, M., and Sherma, J. (2011). *High Performance Liquid Chromatography in Phytochemical Analysis*. Boca Raton: Taylor & Francis, 102.

Wang, S.-Y., Wu, J.-H., Shyur, L.-F., Kuo, Y.-H., and Chang, S.-T. (2002). Antioxidant Activity of Abietane-type Diterpenes from Heartwood of Taiwania Cryptomerioides Hayata. *Holzforschung* 56 (5), 487–492. doi:10.1515/hf.2002.075

Wang, Z., Wang, J., and Chan, P. (2013). Treating Type 2 Diabetes Mellitus with Traditional Chinese and Indian Medicinal Herbs. *Evidence-Based Complement. Altern. Med.* 2013, 1–17. doi:10.1155/2013/343594

Wellsow, J., Grayer, R. J., Veitch, N. C., Kokubun, T., Lelli, R., Kite, G. C., et al. (2006). Insect-antifeedant and Antibacterial Activity of Diterpenoids from Species of *Plectranthus*. *Phytochemistry* 67 (16), 1818–1825. doi:10.1016/j.phytochem.2006.02.018

Wu, D. G., Yu, P., Li, J. W., Jiang, P., Sun, J., Wang, H. Z., et al. (2014). Apigenin Potentiates the Growth Inhibitory Effects by IKK-β-Mediated NF-Kb Activation in Pancreatic Cancer Cells. *Toxicol. Lett.* 224 (1), 157–164. doi:10.1016/j.toxlet.2013.10.007

Xu, R., Fazio, G. C., and Matsuda, S. P. T. (2004). On the Origins of Triterpenoid Skeletal Diversity. *Phytochemistry* 65, 261–291. doi:10.1016/j.phytochem.2003.11.014

Yang, W. S., Jeong, D., Yi, Y. S., Park, J. G., Seo, H., Moh, S. H., et al. (2013). IRAK1/4-targeted Anti-inflammatory Action of Caffeic Acid. *Mediators Inflamm.* 2013, 518183. doi:10.1155/2013/518183

Yap, W. H., and Lim, Y. M. (2015). Mechanistic Perspectives of Maslinic Acid in Targeting InflammationBiochemistry Research International. 2015. *Biochem. Res. Int.* 2015, 1–9. doi:10.1155/2015/279356

Yasuko, K., Tomohiro, N., Sei-Itsu, M., Ai-Na, L., Yasuo, F., and Takashi, T. (1984). Caffeic Acid Is a Selective Inhibitor for Leukotriene Biosynthesis. *Biochim. Biophys. Acta (Bba) - Lipids Lipid Metab.* 792 (1), 92–97. doi:10.1016/0005-2760(84)90287-X

Yoeh, C. T., Wu, C. H., and Yen, G. C. (2010). Ursolic Acid, a Naturally Occurring Triterpenoid, Suppresses Migration and Invasion of Human Breast Cancer Cells by Modulating C-Jun N-Terminal Kinase, Akt and Mammalian Target of Rapamycin Signaling. *Mol. Nutr. Food Res.* 54 (9), 1285–1295. doi:10.1002/mnfr.200900414

Zaletova, N. I., Shchavlinskii, A. N., Tolkachev, O. N., Vichkanova, S. A., Fateeva, T. V., Krutikova, N. M., et al. (1986). Preparation of Certain Derivatives of Ursolic Acid and Their Antimicrobial Activity. *Pharm. Chem. J.* 20 (5), 345–348. doi:10.1007/BF00758617

Zheng, P. W., Chiang, L. C., and Lin, C. C. (2005). Apigenin Induced Apoptosis through P53-dependent Pathway in Human Cervical Carcinoma Cells. *Life Sci.* 76 (12), 1367–1379. doi:10.1016/j.lfs.2004.08.023

Zheng, W., and Wang, S. Y. (2001). Antioxidant Activity and Phenolic Compounds in Selected Herbs. *J. Agric. Food Chem.* 49 (11), 5165–5170. doi:10.1021/jf010697n

Zschocke, S., Rabe, T., Taylor, J. L., Jäger, A. K., and van Staden, J. (2000). Plant Part Substitution-A Way to Conserve Endangered Medicinal Plants? *J. Ethnopharmacol* 71 (1–2), 281–292. doi:10.1016/S0378-8741(00)00186-0

Conflict of Interest: The authors declare that the research was conducted in the absence of any commercial or financial relationships that could be construed as a potential conflict of interest.

Publisher's Note: All claims expressed in this article are solely those of the authors and do not necessarily represent those of their affiliated organizations, or those of the publisher, the editors and the reviewers. Any product that may be evaluated in this article, or claim that may be made by its manufacturer, is not guaranteed or endorsed by the publisher.

frontiers in Pharmacology

REVIEW
published: 23 December 2021
doi: 10.3389/fphar.2021.809994

Approaches to Decrease Hyperglycemia by Targeting Impaired Hepatic Glucose Homeostasis Using Medicinal Plants

Gerardo Mata-Torres, Adolfo Andrade-Cetto and Fernanda Espinoza-Hernández*

Laboratorio de Etnofarmacología, Departamento de Biología Celular, Facultad de Ciencias, Universidad Nacional Autónoma de México, Mexico City, Mexico

Liver plays a pivotal role in maintaining blood glucose levels through complex processes which involve the disposal, storage, and endogenous production of this carbohydrate. Insulin is the hormone responsible for regulating hepatic glucose production and glucose storage as glycogen, thus abnormalities in its function lead to hyperglycemia in obese or diabetic patients because of higher production rates and lower capacity to store glucose. In this context, two different but complementary therapeutic approaches can be highlighted to avoid the hyperglycemia generated by the hepatic insulin resistance: 1) enhancing insulin function by inhibiting the protein tyrosine phosphatase 1B, one of the main enzymes that disrupt the insulin signal, and 2) direct regulation of key enzymes involved in hepatic glucose production and glycogen synthesis/breakdown. It is recognized that medicinal plants are a valuable source of molecules with special properties and a wide range of scaffolds that can improve hepatic glucose metabolism. Some molecules, especially phenolic compounds and terpenoids, exhibit a powerful inhibitory capacity on protein tyrosine phosphatase 1B and decrease the expression or activity of the key enzymes involved in the gluconeogenic pathway, such as phosphoenolpyruvate carboxykinase or glucose 6-phosphatase. This review shed light on the progress made in the past 7 years in medicinal plants capable of improving hepatic glucose homeostasis through the two proposed approaches. We suggest that Coreopsis tinctoria, Lithocarpus polystachyus, and Panax ginseng can be good candidates for developing herbal medicines or phytomedicines that target inhibition of hepatic glucose output as they can modulate the activity of PTP-1B, the expression of gluconeogenic enzymes, and the glycogen content.

Keywords: medicinal plants, hyperglycemia, hepatic glucose output, insulin resistance, PTP-1B inhibitors, natural products

OPEN ACCESS

Edited by:
Valentina Echeverria Moran, Bay Pines VA Healthcare System, United States

Reviewed by:
Luis Goya, Spanish National Research Council (CSIC), Spain
Sakina Mohamed Yagi, University of Khartoum, Sudan

****Correspondence:***
Adolfo Andrade-Cetto
aac@ciencias.unam.mx

Specialty section:
This article was submitted to Ethnopharmacology, a section of the journal Frontiers in Pharmacology

Received: *05 November 2021*
Accepted: *30 November 2021*
Published: *23 December 2021*

Citation:
Mata-Torres G, Andrade-Cetto A and Espinoza-Hernández F (2021) Approaches to Decrease Hyperglycemia by Targeting Impaired Hepatic Glucose Homeostasis Using Medicinal Plants. Front. Pharmacol. 12:809994. doi: 10.3389/fphar.2021.809994

INTRODUCTION

Diabetes mellitus (DM) is a chronic metabolic disease characterized by high blood sugar levels (hyperglycemia), caused by insulin malfunctioning, deficient insulin secretion, or both (Liu et al., 2019). Type 2 diabetes (T2D) is the most important type of DM due to its high worldwide prevalence (American Diabetes Association, 2021). It is characterized by insulin resistance, which is defined as a

poor response of insulin-sensitive tissues to normal insulin concentration (Mlinar et al., 2007). The main cause of insulin resistance has been associated to an obesogenic environment in which large amounts of free fatty acids and adipokines are responsible for impairing insulin signaling by increasing serine phosphorylation that inhibits tyrosine phosphorylation of insulin receptor (IR) and insulin receptor substrates (IRSs) (DeFronzo et al., 2015). However, it has also been reported that protein tyrosine phosphatases (PTPs) could have a more important role since they are upregulated in insulin resistant states. Insulin action is negative regulated by PTPs, particularly the PTP-1B, because they promote the dephosphorylation of tyrosine residues of IR and IRSs (Saltiel and Kahn, 2001). When insulin signaling is impaired in liver by either insulin resistance or low insulin levels, the glucose storage and production is dysregulated, increasing the hepatic glucose output rates yielding hyperglycemia in diabetic patients.

Liver represents a crucial therapeutic target for treating hyperglycemia in T2D because hepatic glucose output is the pathophysiological abnormality that contributes the most to the hyperglycemic state in fasting and postprandial state as a consequence of hepatic insulin resistance (Sharabi et al., 2015). During the overnight fast (postabsorptive state), the liver of a normal person produces glucose at a rate of approximately 1.8–2 mg/kg. min. However, this rate increases around 0.5 mg/kg min in a patient with T2D, promoting a significant rise in the basal state of glucose production (Cersosimo et al., 2018). After food ingestion and the subsequent increase in insulin levels, the suppression of glucose production is slower in a diabetic patient, promoting an evident postprandial hyperglycemia due to the excess of glucose produced in addition to that from the exogenous source (Rizza, 2010).

Medicinal plants and natural products have shown to have numerous benefits on processes involved in glucose and lipid metabolism, leading to correct homeostasis imbalances that promote metabolic diseases such as T2D (Li J. et al., 2018; Xu L. et al., 2018; Saadeldeen et al., 2020). Unlike the classic "on-target" paradigm in pharmacology, namely a drug with a specific target, the polypharmacology approach, or the binding of a drug to more than one target, could be more effective against a disease as complex as T2D due to its multiple pathophysiological abnormalities (Reddy and Zhang, 2013). In this context, extract plants and phytochemicals isolated from medicinal plants exhibit multiple mechanisms of action on assorted metabolic targets that are involved in glucose homeostasis. Therefore, efforts have been made to describe all the beneficial effects on metabolism of these extracts and molecules in recent years.

The current review summarizes the medicinal plants reported from 2015 that can potentially decrease hyperglycemia resulting from imbalance in hepatic glucose metabolism by two different approaches: improving hepatic insulin resistance by inhibiting PTP-1B and decreasing hepatic glucose output by inhibiting rate-limiting enzymes involved in the storage and production of glucose.

METHODOLOGY

Two separate searches were performed based on the Preferred Reporting Items for Systematic Review and Meta-Analysis (PRISMA) (Page et al., 2021) in the following databases: Scopus, Clarivate and PubMed (**Figure 1**). The first involved studies related to extracts or phytochemicals tested against the activity or expression of PTP-1B enzyme, while in the second, studies with extracts or phytochemicals with an effect on the glucose-producing pathways were sought. Only records related to the study of medicinal plants and their isolated compounds were considered.

THERAPEUTIC APPROACHES TO REDUCE HYPERGLYCEMIA RESULTING FROM IMPAIRED HEPATIC GLUCOSE HOMEOSTASIS

Each insulin-sensitive tissue presents abnormal characteristics that contribute to hyperglycemia in an insulin-resistant state. The underlying mechanisms that give rise to insulin resistance converge on deficient insulin signalling that limits the activation of factors involved in energy metabolism. In obesity and T2D, insulin resistance has been linked mainly to defects in the signalling pathway of phosphatidylinositol 3-kinase and protein kinase B (PI3K/Akt), particularly to the Akt2 isoform (Cusi et al., 2000; Krook et al., 2000).

In normal conditions, the insulin secreted by pancreatic β cell binds to its receptor in the target cell, activating the tyrosine kinase activity, which promotes the receptor autophosphorylation and the subsequent phosphorylation of IRSs, mainly IRS-1 and IRS-2, in tyrosine residues. Afterwards, the enzyme P13K is recruited and activated by IRS to convert phosphatidylinositol 4,5-bisphosphate (PIP2) from the plasma membrane to phosphatidylinositol 3,4,5-triphosphate (PIP3), which facilitates the phosphorylation and activation of Akt at two important sites: by phosphoinositide-dependent kinase 1 (PDK1) at residue Thr308 of the catalytic domain, and by mammalian target rapamycin complex 2 (mTORC2) at residue Ser473 of the regulatory domain (Schultze et al., 2012). Specifically in liver, the activated Akt enzyme is responsible for phosphorylating different factors that are involved in the regulation of processes such as glycogen synthesis, gluconeogenesis, and glycogenolysis, which are activated or inhibited under different nutritional circumstances (Dimitriadis et al., 2021).

Due to hepatic insulin resistance, this hormone losses its ability to regulate glucose metabolism in liver, resulting in enhanced glucose output that contributes greatly to fasting and postprandial hyperglycemia, namely glycogen synthesis is reduced, and production of glucose is increased (**Figure 2**). Therefore, we proposed two approaches by which medicinal plants could ameliorated hyperglycemia through enhancing hepatic glucose metabolism: improving the function of insulin in the liver by inhibiting the enzyme PTP-1B and modulating the

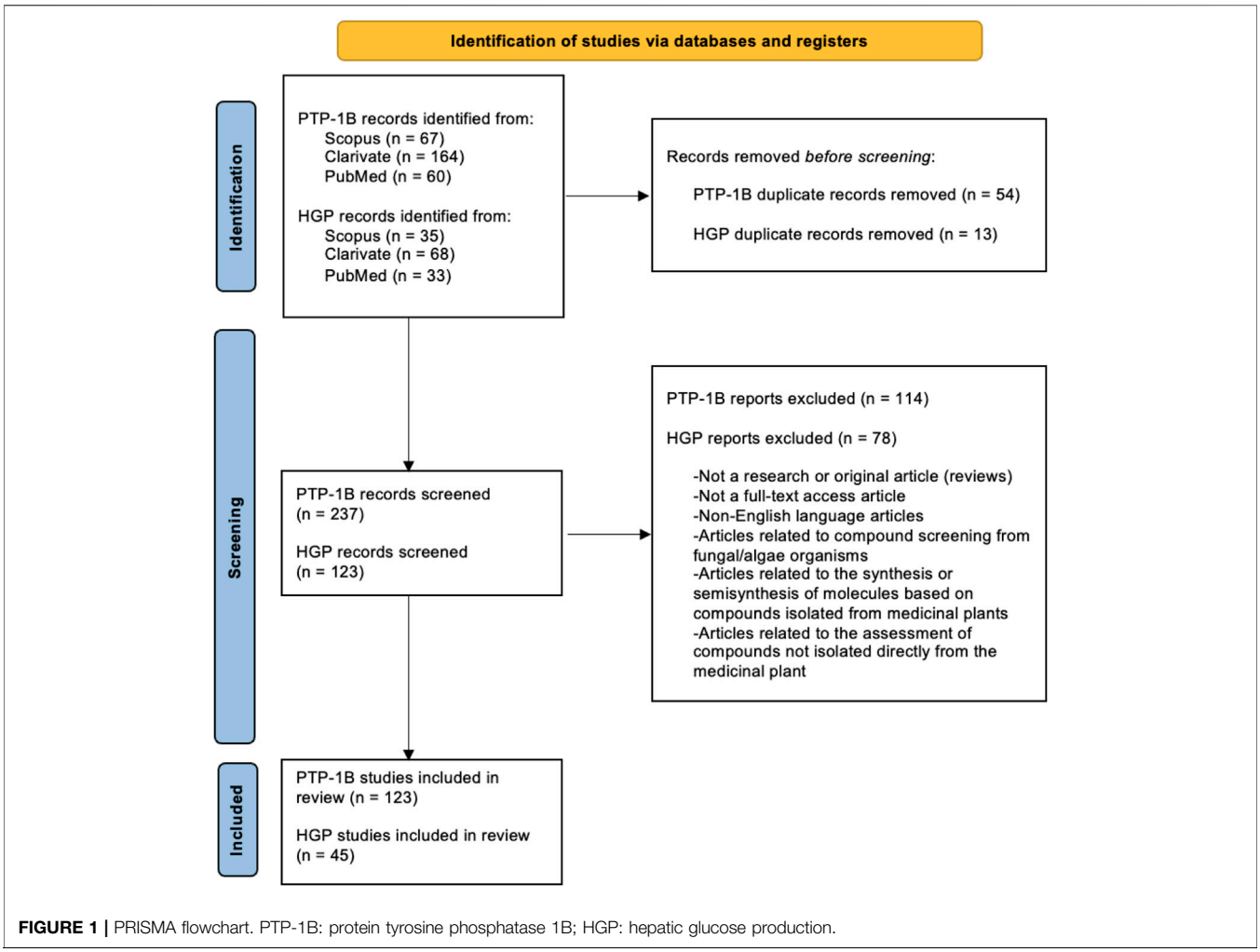

FIGURE 1 | PRISMA flowchart. PTP-1B: protein tyrosine phosphatase 1B; HGP: hepatic glucose production.

hepatic production/storage of glucose by regulating the enzymes involved in gluconeogenesis, glycogenolysis, and glycogenesis.

Inhibition of Protein Tyrosine Phosphatase 1B

The modification of proteins through phosphorylation and dephosphorylation of tyrosine residues represents one of the main mechanisms of cell signaling regulation (Alonso et al., 2016), which is carried out by two superfamilies of enzymes: protein tyrosine kinases (PTKs), and PTPs. In this regard, the classical PTP subfamily possess a domain of 240–250 amino acids characterized by a conserved site that exhibits a catalytic mechanism based on cysteine (Denu and Dixon, 1998). Specifically, the enzyme PTP-1B is a classic intracellular PTP widely distributed in mammalian tissues that is anchored on the cytoplasmic side of the endoplasmic reticulum membrane. Despite its localization, the PTP-1B enzyme can access its substrates located on the surface of the plasma membrane during endocytosis, biosynthesis, and by the movement of the endoplasmic reticulum towards the plasma membrane in specific regions (Bakke and Haj, 2015).

Since its first isolation from the human placenta in 1988 by Tonks et al., 1988 PTP-1B has become an attractive research object due to its direct link with the etiopathogenesis of insulin resistance. In addition to the processes promoted by the obesogenic inflammatory environment, such as the serine/threonine phosphorylation of IR and IRS, and their proteasomal degradation (Mlinar et al., 2007; Ahmed et al., 2021), the dephosphorylation of these components by PTP-1B has also been implied to the termination of the insulin signal (Ahmad et al., 1995; Kenner et al., 1996; Chen et al., 1997).

Experimental data obtained from various studies have shown that the PTP-1B enzyme is one of the main negative regulators of the insulin signaling pathway. For instance, studies performed in PTP-1B knock-out mice have been shown that the absence of this enzyme produces healthy organisms that exhibit enhanced insulin sensitivity, protection against the weight gain generated by high-fat diet, and increased hepatic phosphorylation of IR and IRS after an intraperitoneal insulin injection (Elchebly et al., 1999; Klaman et al., 2000). On the other hand, it has been reported an increased PTP-1B activity in hepatic cytosolic fractions isolated from streptozotocin (STZ)-hyperglycemic rats (Meyerovitch et al., 1989), while augmented hepatic microsomal enzyme

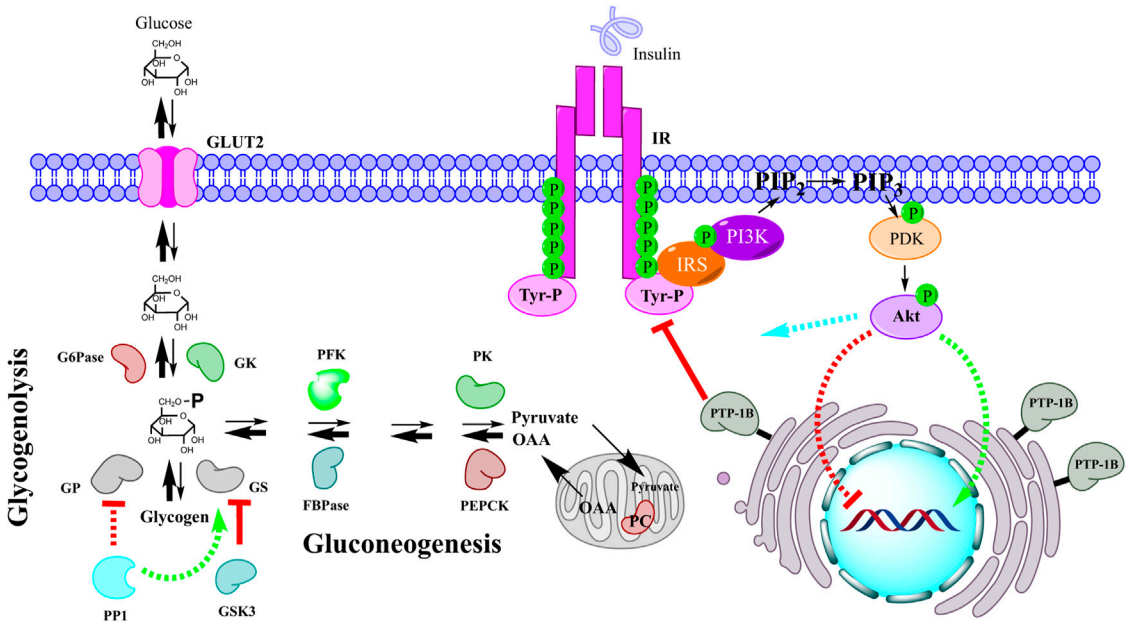

FIGURE 2 | Impaired hepatic glucose homeostasis by insulin resistance. When insulin does not work properly either due to overexpression of PTP-1B or other factors, glucose production in liver is upregulated generating a hyperglycemic state. Both gluconeogenesis and glycogenolysis are enhanced due to poor insulin signaling, namely genetic expression of gluconeogenic enzymes is not repressed and enzymes related to glycogen metabolism are not adequately regulated. Akt functions: green color indicates positive regulation, red color indicates negative regulation, and blue color represents direct or indirect regulation by phosphorylation or allosterism. IR: insulin receptor; IRS: insulin receptor substrate; PI3K: phosphoinositide 3-kinase; PIP2: phosphatidylinositol 4,5-bisphosphate; PIP3: phosphatidylinositol 3,4,5-triphosphate; PDK: phosphoinositide-dependent kinase; Akt: protein kinase B; PTP-1B: protein tyrosine phosphatase 1B; PC: pyruvate carboxylase; OAA: oxalacetate; PEPCK: phosphoenolpyruvate carboxykinase; PK: pyruvate kinase; FBPase: fructose 1,6-bisphosphatase; PFK: phosphofructokinase; GS: glycogen synthase; GP: glycogen phosphorylase; PP1: protein phosphatase 1; GSK3: glycogen synthase kinase-3; GK: glucokinase; G6Pase: glucose 6-phosphatase; GLUT2: glucose transporter 2.

activity, content of protein, and mRNA levels have only been observed after 2 weeks of insulin treatment in these insulinopenic organisms, suggesting that elevated insulin levels are necessary to modify PTP-1B content and activity, namely hyperinsulinemia caused by insulin resistance may lead to altered PTP-1B expression and activity (Ahmad and Goldstein, 1995). Additionally, it has also been shown that insulin rises hepatic microsomal PTP-1B activity in rat hepatoma cells (Hashimoto and Goldstein, 1992). Likewise, abnormal expression and activity of PTP-1B have been reported in skeletal muscle of insulin-resistant obese people (Ahmad et al., 1997), as well as in non-obese Goto-Kakizaki rats with spontaneously generated insulin resistance (Dadke et al., 2000), and in STZ-hyperglycemic rats fed with high-fat diet (Wu et al., 2005).

Based on the aforementioned, the PTP-1B inhibition represents a good therapeutic target for the treatment of insulin resistance-related diseases, such as DM2 (Zhang et al., 2006). Hence, an arsenal of molecules with inhibitory capacity of PTP-1B activity has been generated in recent years. The methodological approaches that have been applied are the rational design of synthetic phospho-(tyrosine)-mimetic molecules to be used as competitive inhibitors, considering the structural characteristics of the protein, and the search for molecules from natural sources (Sun et al., 2018). The latter is based on the statement that nature has a great variety of structures that present diverse pharmacological effects (Atanasov et al., 2021), so natural products can be used as a starting point for the creation of powerful inhibitors.

Table 1 summarizes all medicinal plants and their identified compounds that have proved to inhibit the activity or expression of PTP-1B since 2015. It was obtained a total of 125 medicinal plants used in various traditional medicine systems around the world, mainly represented in eastern folk, such as Chinese and Vietnamese. *Morus alba* L. (Moraceae), a plant used in the traditional Chinese system, has been the most evaluated for this purpose. In addition to direct PTP-1B activity inhibition and molecular docking studies, some extracts and compounds were assessed to improve glucose and lipid metabolism *in vivo*, such as lowering blood glucose levels, improved insulin resistance and glucose intolerance, and improved lipid profile. Furthermore, their effect on glucose uptake and phosphorylation of some components of insulin signaling, such as IR, IRS, and Akt, was evaluated in cell cultures under insulin-resistant conditions.

Inhibition of Hepatic Glucose Output by Modulating Glucose Metabolism in Liver

The liver is a key organ that plays a crucial role in the regulation of blood glucose because it manages both storage and synthesis of glucose. The latter involves two metabolic pathways: glycogenolysis and gluconeogenesis, which constitute total hepatic glucose production (HGP) (Lee et al., 2015).

TABLE 1 | Medicinal plants and their phytochemicals with PTP-1B inhibitory capacity.

Medicinal plant (scientific name [Family]/Traditional medicine system or places where it is used)	Part/Extract	Isolated compounds	Experiment/Outcome	References
Acmella paniculata (Wall. ex DC.) R.K.Jansen [Asteraceae]/ Indonesian	Aerial parts/EtOH	N-isobutyl-2E-decenamide	*In vitro*: PTP-1B enzyme assay/IC_{50} = 24 μM	Abdjul et al. (2018)
Agrimonia pilosa Ledeb. [Rosaceae]/Chinese	Aerial parts/EtOH	Apigenin-7-O-b-D-glucuronide-6″-methyl ester Quercetin-3-O-b-D-glycoside Kaempferol Kaempferol-3-O-a-L-rhamnoside b-sitosterol Ursolic acid Tormentic acid Methyl 2-hydroxyl tricosanoate Palmitic acid	*In vitro*: PTP-1B enzyme assay/IC_{50} = 14.35, 27.73, 42.93, 12.16, 49.78, 3.47, 0.5, 36.39, 0.1 μM	Na et al. (2016)
		Apigenin 7-O-b-D-glucuronide Ellagic acid Agritannin	*In vitro*: PTP-1B enzyme assay/IC_{50} = 7.14, 7.73, 17.03 μM	Nguyen et al. (2017)
Akebia quinata (Thunb. ex Houtt.) Decne. [Lardizabalaceae]/Chinese	Stems/MeOH	Cyrtophyllones B Uncinatone 3-*O*-α-L-arabinopyranosyl olean-12-en-28-oic acid 3-*O*-[β-D-glucopyranosyl (1–4)-α-L-arabinopyranosyl)]olean-12-en-28-oic acid 2α,3α,23-trihydroxyoleane-12-en-28-oic acid	*In vitro*: PTP-1B enzyme assay/IC_{50} = 6.77, 5.41, 4.08, 21.8, 7.78 μM	An et al. (2016)
Allium cepa L. [Amaryllidaceae]	Outer skins/MeOH	Cepadial B, C Cepabifla A–C Cepadial D	*In vitro*: PTP-1B enzyme assay/IC_{50} = 22.55, 22.33, 17.01, 24.07, 14.29, 1.68 μM	Vu et al. (2020)
Allophylus cominia (L.) Sw. [Sapindaceae]/Cuban	Leaves/MeOH	Pheophytin A, B	*In vitro*: PTP-1B enzyme assay/ Activity inhibition by 65 and 57% at 30 μg/ml *In vitro*: cell culture (L6 myotubes)/↑insulin-dependent glucose uptake (pheophytin extract) *In vitro*: cell culture (3T3-L1)/↓lipid accumulation on the differentiation phase, ↓lipid droplets (phaeophytin extract)	Semaan et al., 2017, 2018
Angelica decursiva (Miq.) Franch. & Sav. [Apiaceae]/ Korean	Whole plant/MeOH	*cis*-3′-Acetyl-4′-angeloylkhellactone Isorutarine	*In vitro*: PTP-1B enzyme assay/IC_{50} = 86.95, 80.09 μM	Yousof Ali et al. (2015)
Anoectochilus chapaensis Gagnep. [Orchidaceae]/ Chinese	Whole plant/EtOH	Friedelin Sorghumol Epifriedelanol Friedelane 2a,3b-dihydroxyolean-12-en-23, 28, 30-trioic acid Quercetin Isorhamnetin Isorhamnetin-3-O-b-D-glucoside Isorhamnetin-3-O-b-D-rutinoside	*In vitro*: PTP-1B enzyme assay/IC_{50} = 6.21, 3.5, 3.75, 4.6, 2.65, 5.63, 1.75, 1.16, 1.2 μM	Cai et al. (2015)
Artocarpus nanchuanensis S.S.Chang S.C.Tan & Z.Y.Liu [Moraceae]/Chinese	Stems/EtOH	Hypargystilbene B, D, E	*In vitro*: PTP-1B enzyme assay/IC_{50} = 3.23, 37.31, 2.53 nM	Zhang et al. (2015)
Artocarpus styracifolius Pierre [Moraceae]/Chinese	Roots/EtOH	(±)-Styrastilbene A Styrastilbene B (±)-Styrastilbene C	*In vitro*: PTP-1B enzyme assay/IC_{50} = 4.52, 2.4, 8.23 μM	Li et al. (2019b)
Astragalus mongholicus Bunge [Fabaceae]/Chinese	Root/Aqueous	Astragaloside IV	*In vitro*: PTP-1B enzyme assay/IC_{50} = 10.34 μM *In vitro:* cell culture (insulin-resistant HepG2)/↑glucose consumption, ↓PTP-1B, ↑pIR, ↑pIRS1 protein levels	Zhou et al. (2021)
Bidens pilosa L. [Asteraceae]/ Chinese	Whole plant/Aqueous In combination with *Euonymus alatus* (Thunb.) Siebold [Celastraceae] winged branchlet *Coptis chinensis* Franch. [Ranunculaceae] rhizome *Cornus officinalis* Siebold & Zucc. [Cornaceae] fruit *Ligustrum lucidum* W.T.Aiton [Oleaceae] fruit *Scrophularia ningpoensis* Hemsl. [Scrophulariaceae] root	Full extract	*In vivo:* hypertensive rats fed with HFD (2020 mg/kg b.w.)/prevention of increased body weight, ↓triglycerides, ↓LDL, ↓insulin resistance, ↑glucose tolerance, ↓ PTP-1B expression in adipose tissue	Zhu et al. (2018)

(Continued on following page)

TABLE 1 | (*Continued*) Medicinal plants and their phytochemicals with PTP-1B inhibitory capacity.

Medicinal plant (scientific name [Family]/Traditional medicine system or places where it is used)	Part/Extract	Isolated compounds	Experiment/Outcome	References
Bistorta officinalis Delarbre [Polygonaceae]/Chinese	Rhizome/EtOAc	Full extract	*In vitro*: PTP-1B enzyme assay/IC_{50} = 17.43 μg/ml	Zhao et al. (2019b)
Boehmeria nivea (L.) Gaudich. [Urticaceae]/Chinese	Root/EtOAc	Full extract Hederagenin Pomolic acid	*In vitro*: PTP-1B enzyme assay/IC_{50} = 20.19 μg/ml, 9.53, 4.89 μM	Zhao et al. (2019b)
Camellia crapnelliana Tutcher [Theaceae]/Chinese	Twigs and leaves/MeOH	Camellianol B, C, E–G A_1- barrigenol 22-O-angeloyl-A_1-barrigenol Camelliagenin A 16-O-acetylcamelliagenin A 3β,11α,13β-trihydroxyolean-12-one α-amyrin Lupeol 3β,20-dihydroxylupane	*In vitro*: PTP-1B enzyme assay/IC_{50} = 4.87, 7.4, 20.03, 14.36, 11.08, 16.79, 2.56, 8.93, 10.16, 1.34, 19.26, 3.68, 12.44 μM	Xiong et al. (2017)
Cassia fistula L. [Fabaceae]/Vietnamese	Leaves/EtOAc	Full extract	*In vitro*: PTP-1B enzyme assay/IC_{50} = 24.1 μg/ml	Trinh et al. (2017a)
Catharanthus roseus (L.) G.Don [Apocynaceae]/Malaysia, India, China, South Africa, and Mexico	Leaves/DCM	Vindogentianine	*In vitro*: PTP-1B enzyme assay/IC_{50} = 15.28 μg/ml *In vitro:* cell culture (β-TC6, C2C12)/↑glucose uptake	Tiong et al. (2015)
Cedrus deodara (Roxb. ex D.Don) G.Don [Pinaceae]/Aryuveda	Needles/Essential oil	Caryophyllene oxide	*In vitro*: PTP-1B enzyme assay/IC_{50} = 31.32 μM	Wang et al. (2017a)
Centella asiatica (L.) Urb. [Apiaceae]/Jamu	Aerial parts/Aqueous	Full extract	*In vitro*: PTP-1B enzyme assay/IC_{50} = 13.2 μg/ml	Saifudin et al. (2016b)
Chaenomeles japonica (Thunb.) Lindl. ex Spach [Rosaceae]/Japanese and Chinese	Fruits/acetone	Polyphenolic extract	*In vitro:* cell culture (HepG2)/↓PTP-1B mRNA expression level, ↓PEPCK mRNA expression level, ↑GLUT4 mRNA expression level, ↑IRS-2 mRNA expression level, ↑pAMPK, ↑glycogen synthesis, ↓glucose production	Zakłos-Szyda and Pawlik, (2018)
Cinnamomum osmophloeum Kaneh. [Lauraceae]/Taiwan	Twigs and leaves/acetone	Full extract *n*-hexane soluble fraction ethyl acetate soluble fraction *n*-butanol soluble fraction water soluble fraction	*In vitro*: PTP-1B enzyme assay/IC_{50} = 1.9, 3.2, 2, 1.7, 1.9 μg/ml	Lin et al. (2016)
Cipadessa baccifera (Roth) Miq. [Meliaceae]/Chinese	Leaves/EtOH	Cipacinoid A	*In vitro*: PTP-1B enzyme assay/IC_{50} = 16.7 μM	Yu et al. (2016a)
Clausena sanki (Perr.) Molino [Rutaceae]/Chinese	Fruits/EtOH	Clausenanisines A–C, E, F Euchrestifoline Dihydromupamine Clauraila B Kurryame Clausenaline F 3-formyl-1-hydroxycarbazole Clausine Z, I Clauszoline N, M	*In vitro*: PTP-1B enzyme assay/IC_{50} = 0.58, 0.87, 28.79, 27.96, 2.47, 1.28, 15.26, 23.89, 27.93, 28.42, 4.36, 5.39, 3.96, 24.43, 26.37 μM	Liu et al. (2021)
Coptis chinensis Franch. [Ranunculaceae]/Chinese	Rhizome/MeOH	Berberine Epiberberine Magnoflorine Coptisine	*In vitro*: PTP-1B enzyme assay/IC_{50} = 16.43, 21.19, 28.14, 51.04 μM	Choi et al. (2015)
Coreopsis tinctoria Nutt. [Asteraceae]/North American and Chinese	Capitula/EtOH	Butin Taxifolin 7,3′,4′-trihydroxyflavone Quercetagitin-7-O-b-D-glucoside	*In vitro*: PTP-1B enzyme assay/IC_{50} = 20.92, 7.73, 27.93, 24.5 μM	Begmatov et al. (2020)
Cymbopogon nardus (L.) Rendle [Poaceae]/Jamu	Leaves/Aqueous	Full extract	*In vitro*: PTP-1B enzyme assay/IC_{50} = 10.63 μg/ml	Saifudin et al. (2016b)
Dioscorea bulbifera L. [Dioscoreaceae]/Chinese	Rhizome/EtOAc	Full extract 9,10-Dihydro-2,4,6,7-phenanthrenetetrol [1,1'-Biphenanthren]-2,2',3,3',6,6',7,7'-octaol Cassigarol D	*In vitro*: PTP-1B enzyme assay/IC_{50} = 32.21 μg/ml, 23.79, 3.36, 13.16 μM	Zhao et al. (2019b)
Dracaena cochinchinensis (Lour.) S.C.Chen [Asparagaceae]/Chinese	Red resin/MeOH	Biflavocochin B, F, G	*In vitro*: PTP-1B enzyme assay/IC_{50} = inhibition of 75.8, 66.7, 74.9% at 10 μM	Lang et al. (2020)
Duranta erecta L. [Verbenaceae]/Aryuveda	Whole plant/EtOH	Full extract	*In silico:* Network pharmacology/phytoconstituents targeting PTP-1B *In silico:* molecular docking/PTP-1B binding energy: 8.9 kcal/mol (durantanin I) *In vivo:* diabetic rats (100, 200, and 400 mg/kg b.w.)/chronic hypoglycemic effect, ↓HbA1c, ↑glucose tolerance,	Khanal and Patil, (2020)

(Continued on following page)

TABLE 1 | (*Continued*) Medicinal plants and their phytochemicals with PTP-1B inhibitory capacity.

Medicinal plant (scientific name [Family]/Traditional medicine system or places where it is used)	Part/Extract	Isolated compounds	Experiment/Outcome	References
			↓G6Pase and FBPase activity, ↑hexokinase activity, ↓triglycerides, LDL, VLDL, and total cholesterol, ↑HDL, ↑hepatic glycogen content, ↑glucose uptake in isolated rat hemidiaphragm	
Elaeocarpus grandiflorus Sm. [Elaeocarpaceae]/Jamu	Fruits/Aqueous	Full extract	*In vitro*: PTP-1B enzyme assay/IC_{50} = 6.9 μg/ml	Saifudin et al. (2016b)
Elephantopus scaber L. [Asteraceae]/Jamu	Aerial parts/Aqueous	Full extract	*In vitro*: PTP-1B enzyme assay/IC_{50} = 2.64 μg/ml	Saifudin et al. (2016b)
Eleutherococcus senticosus (Rupr. & Maxim.) Maxim. [Araliaceae]/Chinese	Stems/MeOH	(7S,8R)-3-hy- droxyl-4-methoxyl-balanophonin (7S,8R)-5-methoxyl-balanophonin Balanophonin Curcasinlignan A–C	*In vitro*: PTP-1B enzyme assay/IC_{50} = 15.2, 12.6, 16.1, 17.1, 31, 29.4 μM	Li et al. (2017)
Epimedium koreanum Nakai [Berberidaceae]/Chinese	Aerial parts/MeOH	Icaritin Icariside II	*In vitro*: PTP-1B enzyme assay/IC_{50} = 11.59, 9.94 μM	Kim et al. (2017a)
Eremophila bignoniiflora (Benth.) F. Muell. [Scrophulariaceae]/Australian	Leaves/EtOAc	7-hydroxy-6-methyl-4-oxo-2-(3-(5-oxo-2,5- dihydrofuran-3-yl)propyl) hept-5-en-1-yl (E)-3-(3,4-dihydroxyphenyl) acrylate Galangin 3-methyl ether	*In vitro*: PTP-1B enzyme assay/IC_{50} = 52.4, 41.4 μM	Zhao et al. (2019a)
Eremophila lucida Chinnock [Scrophulariaceae]	Leaves/EtOAc	5-hydroxyviscida-3,14-dien-20-oic acid	*In vitro*: PTP-1B enzyme assay/IC_{50} = 42 μM	Tahtah et al. (2016)
Eremophila oppositifolia R.Br. [Scrophulariaceae]/Australian	Leaves/CH_3CN	Type B dimeric fatty acids related to the branched-chain fatty acid (2E,4Z,6E)-5-(acetoxymethyl) tetradeca-2,4,6-trienoic acid (Compounds 9, 12, 13a, 13b)	*In vitro*: PTP-1B enzyme assay/IC_{50} = 24, 2.4, 12, 12 μM	Pedersen et al. (2020)
Eriobotrya japonica (Thunb.) Lindl. [Rosaceae]/Chinese	Leaves/EtOH	Extract of triterpenoid acids (maslinic acid, corosolic acid, oleanolic acid, and ursolic acid)	*In vivo:* insulin-resistant mice (200 mg/kg b.w.)/↓insulin resistance, ↑glucose tolerance, ↓triglycerides, LDL, VLDL, and total cholesterol, ↑HDL; in liver: ↑PPARg, GLUT2, and glucokinase mRNA expression levels, ↓PTP-1B mRNA expression levels	Li et al. (2020b)
Eucalyptus robusta Sm. [Myrtaceae]/Chinese	Leaves/EtOH	Eucarobustol A–I Macrocarpal C	*In vitro*: PTP-1B enzyme assay/IC_{50} = 1.3, 4.3, 4.3, 2.9, 4.1, 5.6, 1.8, 3.0, 1.6, 4.5 μM	Yu et al. (2016b)
Euphorbia hirta L. [Euphorbiaceae]/Vietnamese	Whole plant/EtOAc and *n*-BuOH	Full extracts	*In vitro*: PTP-1B enzyme assay/IC_{50} = 29.2, 38.3 μg/ml	Trinh et al. (2017a)
Ficus deltoidea Jack [Moraceae]/Malay	Leaves/EtOH	70% EtOH extract Lupeol 3β,11β-dihydroxyolean-12-en-23-oic acid	*In vitro*: PTP-1B enzyme assay/IC_{50} = 92%, 2.88, 4.55 μM *In vivo:* diabetic rats (125, 250, and 500 mg/kg b.w. of 70% EtOH extract)/chronic hypoglycemic effect, ↓triglycerides, LDL, and total cholesterol, ↑HDL; in liver: ↑GLUT2 levels, ↓PEPCK, G6Pase, and PTP-1B mRNA expression levels	Abdel-Rahman et al. (2020)
Ficus racemosa L. [Moraceae]/ Vietnamese	Fruit/EtOAc	Isoderrone Derrone Alpinumisoflavone Mucusisoflavone B	*In vitro*: PTP-1B enzyme assay/IC_{50} = 22.7, 12.6, 21.2, 2.5 μM	Trinh et al. (2017a)
Garcinia mangostana L. [Clusiaceae]/Southeast Asia and India	Fruits/EtOH	γ-Mangostin 8-Deoxyartanin 1,3,7-Trihydroxy-2,8-di-(3-methylbut-2-enyl)- xanthone α-Mangostin Garcinone E 9-Hydroxycalabaxanthone	*In vitro*: PTP-1B enzyme assay/IC_{50} = 0.86, 1.57, 3.28, 1.34, 0.43, 12.89 μM	Hu et al. (2021)
Garcinia oblongifolia Champ. ex Benth [Clusiaceae]/Vietnamese	Twigs/EtOAc	Norcowanin	*In vitro*: PTP-1B enzyme assay/IC_{50} = 14.1 μM	Trinh et al. (2017b)

(Continued on following page)

TABLE 1 | (*Continued*) Medicinal plants and their phytochemicals with PTP-1B inhibitory capacity.

Medicinal plant (scientific name [Family]/Traditional medicine system or places where it is used)	Part/Extract	Isolated compounds	Experiment/Outcome	References
Geranium collinum Stephan ex Willd. [Geraniaceae]/Chinese and Tajik	Root/EtOH In combination with *Hypericum scabrum* aerial parts (ratio: 7:3)	Full extract	*In vitro*: PTP-1B enzyme assay/IC_{50} = 0.48 μg/ml *In vitro:* cell culture (L6 myotubes, in the presence of insulin)/↓PTP-1B protein, ↑IR, ↑pAkt, ↑pIRS-1, ↑pGSK3β, ↑pAMPK, ↑glucose consumption	Edirs et al. (2018)
	Roots/EtOH	3,3′,4,4′-Tetra-O-methylellagic acid 3,3′-Di-O-methylellagic acid Caffeic acid Quercetin Catechin Epicatechin Corilagin	*In vitro*: PTP-1B enzyme assay/IC_{50} = 21.64, 6.26, 35.81, 2.19, 0.62, 0.23, 0.87 μM	Numonov et al. (2017)
Glycyrrhiza inflata Batalin [Fabaceae]/Japanese and Chinese	Roots and rhizomes/EtOAc	Licoagrochalcone A Kanzonol C Glyurallin B Gancaonin H 2′-hydroxyisolupalbigenin Gancaonin Q Glisoflavanone Glabrol Macarangaflavanone B	*In vitro*: PTP-1B enzyme assay/IC_{50} = 0.97, 0.45, 4.5, 1.48, 0.5, 0.55, 0.84, 0.31, 1.03 μM	Lin et al. (2017)
Glycyrrhiza uralensis Fisch. ex DC. [Fabaceae]/Chinese	Rhizomes/EtOH	Licochalcone A Licoflavone B	*In vitro*: PTP-1B enzyme assay/IC_{50} = 27.95, 15.62 μM	Guo et al. (2015)
		Isoangustone A Angustone A	*In vitro*: PTP-1B enzyme assay/IC_{50} = 3, 0.4 μM	Ji et al. (2016)
Glyptostrobus pensilis (Staunton ex D.Don) K.Koch [Cupressaceae]/Chinese	Trunk barks/MeOH	Spiropensilisol A, B 3-*epi*-larixinol 3,2′-*epi*-larixinol Abiesinol F Larixinol (Abiesinol E)	*In vitro*: PTP-1B enzyme assay/IC_{50} = 3.3, 11.2, 17.1, 4.6, 12.9, 8.1 μM	Xiong et al. (2020)
Gymnema latifolium Wall. ex Wight [Apocynaceae]/ Vietnamese	Aerial parts/EtOH	Gymlatinoside GL2, GL3	*In vitro*: PTP-1B enzyme assay/IC_{50} = 22.66, 19.83 μM	Pham et al. (2020)
Gynostemma pentaphyllum (Thunb.) Makino [Cucurbitaceae]/Chinese	Aerial parts/EtOH	Gypenoside 2–6	*In vitro*: PTP-1B enzyme assay/IC_{50} = 18.2, 23.5, 28.6, 8.2, 12.5 μM	Wang et al. (2017b)
Helicteres isora L. [Malvaceae]/ Jamu	Gum/Aqueous	Full extract	*In vitro*: PTP-1B enzyme assay/IC_{50} = 3.49 μg/ml	Saifudin et al. (2016b)
Houttuynia cordata Thunb. [Saururaceae]/Korea, Japan, India, and China	Aerial parts/EtOH	3-hydroxy-1,2-dimethoxy-5-methyl-5H-dibenzoindol-4- one 4-hydroxy-1,2,3-trimethoxy- 7H-dibenzo-quinolin-7-one 7-oxodehy-droasimilobine Cepharadione B	*In vitro*: PTP-1B enzyme assay/IC_{50} = 1.254, 2.016, 2.672, 1.862 μM	Ma et al. (2017)
Hypericum longistylum Oliv. [Hypericaceae]/Chinese	Aerial parts/MeOH	Longistylione A–D	*In vitro*: PTP-1B enzyme assay/IC_{50} = 18.87, 16.76, 24.56, 15.96 μM	Cao et al. (2017)
Hypericum perforatum L. [Hypericaceae]/Chinese	Aerial parts/EtOH	Full extract	*In vitro*: PTP-1B enzyme assay/IC_{50} = 1.08 μg/ml *In vivo:* insulin-resistant mice (50 and 200 mg/kg b.w.)/↓PTP-1B expression, ↑hepatic pAkt, ↑hepatic pIRS-1, ↑glucose tolerance, ↑insulin sensitivity, ↓triglycerides, improvement of lipid metabolism	Tian et al. (2015)
Hypericum scabrum L. [Hypericaceae]/Chinese	Aerial parts/EtOH	Quercetin	*In vitro*: PTP-1B enzyme assay/IC_{50} = 2.19 μM	Jiang et al. (2015)
Iris sanguinea Hornem. [Iridaceae]/Chinese	Seeds/MeOH	Kikkanol F monoacetate	*In vitro*: PTP-1B enzyme assay/IC_{50} = 7.3 μM *In vitro:* cell culture/ ↑glucose uptake (3T3-L1), ↑pAMPK (C2C12)	Yang et al. (2017)
Juniperus chinensis L. [Cupressaceae]/Chinese	Heartwood/MeOH	a-methyl artoflavanocoumarin	*In vitro*: PTP-1B enzyme assay/IC_{50} = 25.27 μM *In vitro:* cell culture (insulin-resistant HepG2)/↓PTP-1B protein, ↑pPI3K, ↑pAkt, ↑pERK1, ↑insulin-stimulated glucose uptake	Jung et al. (2017)
Kandelia candel (L.) Druce [Rhizophoraceae]/Vietnamese	Bark/EtOAc and *n*-BuOH	Full extracts	*In vitro*: PTP-1B enzyme assay/IC_{50} = 12.9, 0.02 μg/ml	Trinh et al. (2017a)
	Leaves/*n*-BuOH	Full extract		Trinh et al. (2017a)

(Continued on following page)

TABLE 1 | (*Continued*) Medicinal plants and their phytochemicals with PTP-1B inhibitory capacity.

Medicinal plant (scientific name [Family]/Traditional medicine system or places where it is used)	Part/Extract	Isolated compounds	Experiment/Outcome	References
Lagerstroemia speciosa (L.) Pers. [Lythraceae]/Vietnamese			*In vitro*: PTP-1B enzyme assay/IC_{50} = 19.6 μg/ml	
Lantana camara L. [Verbenaceae]/Indonesian and Japanese	Aerial parts/EtOH	24- hydroxy-lantadene B 3-hydroxy-lantadene C Icterogenin 4-epi-hederagonic acid Oleanolic acid 22b-oleanolic acid 3b-hydroxy-lantadene A 3b-hydroxy-lantadene B 22-hydroxy-oleanonic acid Lantadene B, A Oleanonic acid Lantadene D Pomonic acid Pomolic acid Lantanilic acid Camaric acid Lantanolic acid	*In vitro*: PTP-1B enzyme assay/IC_{50} = 7.3, 7.3, 11, 8.1, 2, 7.9, 7.2, 5.1, 6.9, 5.5, 5.2, 6.9, 7.9, 10.5, 10.6, 7.5, 5.1, 13 μM	Abdjul et al. (2017)
Lanxangia tsao-ko (Crevost & Lemarié) M.F. Newman & Škorničk [Zingiberaceae]/Asian countries	Fruits/EtOH	Tsaokoflavanol F, J, K, L, S	*In vitro*: PTP-1B enzyme assay/IC_{50} = 56.4, 75.1, 80.4, 73, 69.8 μM *In vivo: db/db* mice (200 and 400 mg/kg b.w.)/chronic hypoglycemic effect (full extract)	He et al. (2020)
Leonurus sibiricus L. [Lamiaceae]/Mongolian	Aerial parts/MeOH	Full extract	*In vitro*: PTP-1B enzyme assay/ Activity inhibition by 40% at 10 μg/ml *In vitro:* cell culture (C2C12, in the presence of insulin)/↑glucose uptake	Pitschmann et al. (2016)
Lithocarpus polystachyus (Wall. ex A.DC.) Rehder [Fagaceae]/ Chinese	Leaves/MeOH	Full extracts from five localities in China	*In vitro*: PTP-1B enzyme assay/IC_{50} = inhibition rate ranging from 84.3 to 90.3% at 1.25 mg/ml	Meng et al. (2020)
Litsea cubeba (Lour.) Pers. [Lauraceae]/Chinese	Twigs/EtOAc	(+)-9,9′-O-di-(E)-feruloyl-5,5′-dimethoxy secoisolariciresinol	*In vitro*: PTP-1B enzyme assay/IC_{50} = 13.5 μM	Li et al. (2019c)
Lonicera japonica Thunb. [Caprifoliaceae]/Chinese	Flower buds/EtOH	Lonjaponspiroside A, B	*In vitro*: PTP-1B enzyme assay/IC_{50} = 6.14, 8.42 μM	Liu et al. (2016)
Ludwigia octovalvis (Jacq.) P.H.Raven [Onagraceae]/ Vietnamese	Aerial parts/EtOAc and *n*-BuOH	Full extracts	*In vitro*: PTP-1B enzyme assay/IC_{50} = 16.9, 3.3 μg/ml	Trinh et al. (2017a)
Macaranga denticulata (Blume) Müll.Arg. [Euphorbiaceae]/ Chinese	Twings and leaves/EtOH	Macdentichalcone 1-(5,7-dihydroxy-2,2,6-trimethyl-2H-1-benzopyran-8-yl)-3-phenyl-2-propen-1-one	*In vitro*: PTP-1B enzyme assay/IC_{50} = 21, 22 μM	Lei et al. (2016)
Macleaya cordata (Willd.) R.Br. [Papaveraceae]/Chinese	Aerial parts/EtOH	Macleayine	*In silico*: molecular docking	Sai et al. (2016)
Maclura tricuspidata Carrière [Moraceae]/Korean, Japanese, and Chinese	Leaves/Aqueous	Full extract	*In vitro*: PTP-1B enzyme assay/IC_{50} = 65 μg/ml *In vitro*: PTP-1B enzyme assay (protein chip screening method)/↓PTP-1B activity *In vitro*: cell culture (3T3-L1)/↓lipid droplets, ↑pIRS-1, ↑pAkt *In vivo:* obese mice (20 and 100 mg/kg b.w.)/↑hepatic pIRS-1, ↑hepatic pAkt ↓tryglicerides, ↓glucose tolerance	Kim et al. (2016)
	Root barks/MeOH	Cudratricusxanthone N 1,6,7-trihydroxy-2-(1,1-dimethyl-2-propenyl)-3-methoxyxanthone Cudratricusxanthone L, A Cudraxanthone L Macluraxanthone B Cudracuspixanthone A Cudraxanthone D, M Cudraflavanone D Euchrestaflavanone C Cudraflavone C Kuwanon C	*In vitro*: PTP-1B enzyme assay/IC_{50} = 2, 3, 3, 4.3, 4.6, 3.8, 1.9, 2.8, 3.5, 5.7, 12.3, 9.4, 13.6 μM	Quang et al. (2015)
Magnolia aromatica (Dandy) V.S.Kumar [Magnoliaceae]/ Chinese	Twigs and leaves/EtOH	(1R,6S,7S)-1-hydroxy- cadin-4,9-dien-8-onea	*In vitro*: PTP-1B enzyme assay/IC_{50} = 83.5 μM	Wang et al. (2016b)
	Root barks/MeOH	Full extract	*In vitro*: PTP-1B enzyme assay/IC_{50} = 55.96 μg/ml *In vitro:* cell culture	Sun et al. (2015)

(Continued on following page)

TABLE 1 | (*Continued*) Medicinal plants and their phytochemicals with PTP-1B inhibitory capacity.

Medicinal plant (scientific name [Family]/Traditional medicine system or places where it is used)	Part/Extract	Isolated compounds	Experiment/Outcome	References
Magnolia officinalis Rehder & E.H.Wilson [Magnoliaceae]/ Chinese			(3T3-L1 and C2C12, in the presence of insulin)/↑pIRb, ↑pERK, ↑GLUT4 translocation *In vivo:* db/ db mice (0.5 g/kg b.w.)/chronic hypoglycemic effect	
Magnolia officinalis var. *biloba* Rehder & E.H.Wilson [Magnoliaceae]/Chinese	Barks/EtOH	Magterpenoid A, C	*In vitro*: PTP-1B enzyme assay/IC_{50} = 1.44, 0.81 μM	Li et al. (2018)
		Magmenthane E, H	*In vitro*: PTP-1B enzyme assay/IC_{50} = 4.38, 3.8 μM	Li et al. (2019a)
	Root and stem bark/EtOH	(±)-Mooligomers B, D, E	*In vitro*: PTP-1B enzyme assay/IC_{50} = 0.47, 2.1, 0.35, 1.22, 0.89, 0.14 μM	Li et al. (2020a)
Melaleuca leucadendra (L.) L. [Myrtaceae]/Jamu	Fruit/MeOH	Betulinic acid Ursolic acid	*In vitro*: PTP-1B enzyme assay/IC_{50} = 1.5, 2.3 μM	Saifudin et al. (2016a)
	Leaves/Aqueous	Full extract	*In vitro*: PTP-1B enzyme assay/IC_{50} = 2.05 μg/ml	Saifudin et al. (2016b)
Melicope pteleifolia (Champ. ex Benth.) T.G. Hartley [Rutaceae]/ Chinese	Roots/CH_2Cl_2/CH_3OH (1:1)	Melicoptelin B1/B2, D1/D2, E	*In vitro*: PTP-1B enzyme assay/IC_{50} = 34.4, 55.2, 66.6 μM	Xu et al. (2019b)
Momordica charantia L. [Cucurbitaceae]	Fruits/EtOH	25- O-methylkaraviagein D (19R,23E)-5b,19-epox y-19,25-dimethoxycucurbita-6,23-dien-3b-ol	*In vitro*: PTP-1B enzyme assay/IC_{50} = 51.8, 54.95 μM	Yue et al. (2017)
Morus alba L. [Moraceae]/ Chinese	Leaves/Aqueous	Full extract (mulberry leaves polysaccharide)	*In vivo:* insulin-resistant rats (200 mg/kg b.w.)/↑glucose tolerance, ↓insulin resistance, ↑hepatic glycogen synthesis, ↓hepatic PTP-1B expression, ↑hepatic pIRS-2, ↑hepatic pAkt-2, ↑hepatic PI3K	Ren et al. (2015)
	Fruits/EtOH	Full extract	*In vitro*: PTP-1B enzyme assay/IC_{50} = 11.89 μg/ml	Xiao et al. (2017b)
	Leave cell culture/EtOH	Morusalone A–D	*In vitro*: PTP-1B enzyme assay/IC_{50} = 2.51, 1.14, 0.35, 1.99 μM *In vitro:* cell culture (HepG2)/↑pIRβ and pAkt protein levels	Su et al. (2019)
		Morusalisin A–F	*In vitro*: PTP-1B enzyme assay/IC_{50} = 1.55, 2.24, 1.58, 1.52, 1.60, 1.14 μM	Su et al. (2020)
	Leaves/EtOH	mortatarin E 3′-geranyl-3-prenyl-2′,4′,5,7- tetrahydroxyflavone	*In vitro*: PTP-1B enzyme assay/IC_{50} = 4.53, 10.53 μM *In vitro:* cell culture (insulin-resistant HepG2)/ ↑glucose uptake, ↑glycogen synthesis, ↓PTP-1B, ↑IRS1, ↑IRS2, ↓GSK3β, and ↑GLUT4 mRNA expression levels, ↓PTP-1B, ↑pIRS1, ↑PI3K, ↑pAkt, and ↑GLUT4 protein levels (mortatarin E)	Niu et al. (2020)
	Root bark/MeOH	Morusalfuran A–C, F Morusalnol B Morusibene A	*In vitro*: PTP-1B enzyme assay/IC_{50} = 11.02, 8.92, 7.26, 18.02, 26.56, 17.64 μM	Ha et al. (2020)
	Roots/EtOAc	Kuwanon L Mulberrofuran G Moracenin B (Kuwanon G) Morusinol Sanggenon G Kuwanon C Moracenin A (Kuwanon H) Kuwanon T, F, M Morusin Mulberrofuran B Cyclomorusin Sanggenofuran A	*In vitro*: PTP-1B enzyme assay/IC_{50} = 21.67, 20.03, 13.07, 30.49, 10.87, 17.48, 4.04, 9.83, 9.52, 10.71, 19.63, 4.69, 13.28, 12.72 μg/ml	Zhao et al. (2018)
Morus macroura Miq. [Moraceae]/Chinese	Twigs/EtOH	Notabilisin E Taxifolin Hultenin	*In vitro*: PTP-1B enzyme assay/IC_{50} = 0.87, 5.3, 1.04 μM	Wang et al. (2015)

(Continued on following page)

TABLE 1 | (*Continued*) Medicinal plants and their phytochemicals with PTP-1B inhibitory capacity.

Medicinal plant (scientific name [Family]/Traditional medicine system or places where it is used)	Part/Extract	Isolated compounds	Experiment/Outcome	References
Myrtus communis L. [Myrtaceae]/Italian	Leaves/chloroform	3β-cis-*p*-coumaroyloxy-2α,23-dihydroxyolean-12-en-28-oic acid 3β-trans-*p*-coumaroyloxy-2α,24-dihydroxy-urs-12-en-28-oic acid Maslinic acid Corosolic acid Isomyrtucommulone B 3β-O-cis-*p*-coumaroyl-2α-hydroxy-urs-12-en-28-oic acid Jacoumaric acid Betulinic acid Oleanolic acid Ursolic acid	*In vitro*: PTP-1B enzyme assay/IC_{50} = 15.38, 14.89, 25.73, 12.21, 8.93, 26.67, 11.93, 16.05, 8.92, 14.93 μM	Liang et al. (2020)
Nepenthes mirabilis (Lour.) Druce [Nepenthaceae]/ Vietnamese	Whole plant/EtOAc and *n*-BuOH	Full extracts	*In vitro*: PTP-1B enzyme assay/IC_{50} = 1.4, 0.4 μg/ml	Trinh et al. (2017a)
Nigella sativa L. [Ranunculaceae]/From Turkey to India	Aerial parts/MeOH	3-O-[α-L-Rhamnopyranosyl-(1→2)-α-l-arabinopyranpsyl]hederagenin	*In vitro*: PTP-1B enzyme assay/IC_{50} = 91.3 μM	Parveen et al. (2020)
Nigella sativa var. *hispidula* Boiss. [Ranunculaceae]/Uighur	Seeds/Petroleum ether	Nigelladine A–C	*In vitro:* cell culture (L6 myotubes, in the presence of insulin)/↓PTP-1B protein, ↑pAkt, ↑pIRS-1, ↑pGSK-3b, ↑pAMPK, ↑glucose consumption, ↑lactic acid production, ↑glycogen synthesis, ↑hexokinase activity	Tang et al. (2017)
Orthosiphon aristatus (Blume) Miq. [Lamiaceae]/Vietnamese and Indonesian	Aerial parts/MeOH	Siphonol B, D Orthosiphol B, F, G, I, N	*In vitro*: PTP-1B enzyme assay/IC_{50} = 8.18, 24.75, 9.84, 27.56, 3.82, 0.33, 1.6 μM *In vitro:* cell culture (3T3-L1)/↑glucose uptake	Nguyen et al. (2019)
Ouret lanata (L.) Kuntze [Amaranthaceae]/Ayurveda	Leaves/EtOH	Full extract	*In vitro*: PTP-1B enzyme assay/IC_{50} = 94.66 μg/ml *In vitro:* cell culture (L6 myotubes)/↑adipogenesis, ↑insulin-mediated glucose uptake *In vivo:* diabetic rats (500 mg/kg b.w.)/antihyperglycemic effect in OSTTs by 18.44%	Riya et al. (2015)
Paeonia lactiflora Pall. [Paeoniaceae]/Chinese	Seeds/EtOH	Paeonilactiflorol *trans*-gnetin H	*In vitro*: PTP-1B enzyme assay/IC_{50} = 27.23, 27.81 μM	Zhang et al. (2019a)
Panax ginseng C.A.Mey. [Araliaceae]/Eastern Asia	Stems, flowers, and fruits/EtOH	20(R)-25-methoxydammarane-3β,12β, 20-tetrol 20(R)-dammarane-3β,6α,12β, 20, 25-pentol 20(R)-protopanaxatriol 20(S)-panaxatriol 20(R)-protopanaxadiol	*In vitro*: PTP-1B enzyme assay/IC_{50} = 16.54, 10.07, 17.98, 21.02, 21.27 μM	Yang et al. (2016)
Panax quinquefolius L. [Araliaceae]/Chinese	Crude saponins/EtOH	20(S)-panaxadiol (20S,24R)-dammarane-20,24-epoxy-3 β,6 α, 12 β,25- tetraol 20(R)-dammarane-3 β, 12 β,20,25-tetraol 20(S)-dammarane-3 β,6 α, 12 β,20,25-pentol 20(R)-dammarane-3 β, 12 β,20,25-tetrahydroxy-3 β-O- β-D–glucopyranoside Oleanolic acid 20(S)-protopanaxadiol	*In vitro*: PTP-1B enzyme assay/IC_{50} = 27.23, 23.63, 10.39, 6.21, 5.91, 18.99, 13.38 μM	Han et al. (2020)
Pandanus odorifer (Forssk.) Kuntze [Pandanaceae]/ Vietnamese	Fruit/EtOAc and *n*-BuOH	Full extracts	*In vitro*: PTP-1B enzyme assay/IC_{50} = 20.8, 40.4 μg/ml	Trinh et al. (2017a)
Phyllanthus amarus Schumach. & Thonn. [Phyllanthaceae]/ Vietnamese	Whole plant/EtOAc	Full extract	*In vitro*: PTP-1B enzyme assay/IC_{50} = 74.4 μg/ml	Trinh et al. (2017a)
Phyllanthus niruri L. [Phyllanthaceae]/Jamu	Aerial parts/Aqueous	Full extract	*In vitro*: PTP-1B enzyme assay/IC_{50} = 10.99 μg/ml	Saifudin et al. (2016b)
Phyllanthus urinaria L. [Phyllanthaceae]/Vietnamese	Whole plant/EtOAc and *n*-BuOH	Full extracts	*In vitro*: PTP-1B enzyme assay/IC_{50} = 14, 10.8 μg/ml	Trinh et al. (2017a)

(Continued on following page)

TABLE 1 | (*Continued*) Medicinal plants and their phytochemicals with PTP-1B inhibitory capacity.

Medicinal plant (scientific name [Family]/Traditional medicine system or places where it is used)	Part/Extract	Isolated compounds	Experiment/Outcome	References
Pithecellobium dulce (Roxb.) Benth. [Fabaceae]/Vietnamese	Stem/EtOAc	Full extract	*In vitro*: PTP-1B enzyme assay/IC_{50} = 26.1 μg/ml	Trinh et al. (2017a)
Prunus amygdalus Batsch [Rosaceae]	Fruits/EtOH	Hexane fraction Chloroform fraction	*In vitro*: PTP-1B enzyme assay/IC_{50} = 9.66, 37.95 μg/ml	Qureshi et al. (2019)
Psidium guajava L. [Myrtaceae]/Worldwide	Leaves/EtOAc	Psiguadiol A–J	*In vitro*: PTP-1B enzyme assay/IC_{50} = 4.7, 11, 11.9, 10.7, 19.1, 18.9, 6.2, 9.2, 22.8, 22.8 μM	Hou et al. (2019)
	Leaves/EtOH	Jejuguajavone A, C	*In vitro*: PTP-1B enzyme assay/IC_{50} = 10.52, 9.4 μM	Ryu et al. (2021)
Psydrax subcordatus (DC.) Bridson [Rubiaceae]/African	Leaves and bark/EtOH	Subcordatanol I, III, IV	*In vitro*: PTP-1B enzyme assay/IC_{50} = 22.2, 8.9, 9.8 μM	Zhou et al. (2019)
Pueraria montana var. *lobata* (Willd.) Maesen & S.M.Almeida ex Sanjappa & Predeep [Fabaceae]/Chinese	Root/MeOH	Puerarin	*In silico:* molecular docking/PTP-1B binding energy: 6.4 kcal/mol	Ojo, (2021)
	Roots/EtOH	Lupeol Lupenone	*In vitro*: PTP-1B enzyme assay/IC_{50} = 38.89, 15.11 μM	Seong et al. (2016)
		Full extract	*In vitro*: PTP-1B enzyme assay/IC_{50} = 0.046 mg/ml *In vitro:* cell culture (insulin resistant HepG2 cells)/↑glucose uptake *In vivo:* insulin resistant mice (0.25, 0.5, 1, and 2 g/kg b.w.)/↓AUC in OGTTs by 5.7, 10, 20, and 21%	Sun et al. (2019)
Quercus infectoria G.Olivier [Fagaceae]/Jamu	Fruits/Aqueous	Full extract	*In vitro*: PTP-1B enzyme assay/IC_{50} = 4.68 μg/ml	Saifudin et al. (2016b)
Quercus wutaishanica Mayr [Fagaceae]/Chinese and Mexican	Acorn/EtOH	3-O-galloyloleanolic acid 23- acetoxy-3-O-galloyloleanolic acid 3-acetoxy-23-O-galloyloleanolic acid Oleanolic acid 3-O-galloylursolic acid Ursolic acid	*In vitro*: PTP-1B enzyme assay/IC_{50} = 2.10, 4.17, 4.52, 17.25, 1.86, 17.37 μM	Xu et al. (2018a)
	Leaves/EtOH	Quercetin-3-O-(2″-O-galloyl)-β-galactopyranoside Kaempferol-3-O-rutinoside Quercetin-3-O-rutinoside Quercetin Kaempferol Myricetin Dihydromyricetin 4′,5,7-trihydroxyflavanone 4′-methoxy-5′,5,7-trihydroxyflavanone Ellagic acid	*In vitro*: PTP-1B enzyme assay/IC_{50} = 5.56, 24.89, 20.56, 4.16, 3.92, 3.53, 9.58, 15.38, 20.16, 1.03 μM *In vitro:* cell culture (MIN6)/Protective effect on pancreatic b cells damaged by H_2O_2 (Quercetin-3-O-(2″-O-galloyl)-β-galactopyranoside)	Xu et al. (2018b)
Reynoutria japonica Houtt. [Polygonaceae]/Japanese, South Korean, and Chinese	Roots/EtOAc	(*trans*)-emodin-physcion bianthrone (*cis*)-emodin-physcion bianthrone	*In vitro*: PTP-1B enzyme assay/IC_{50} = 2.77, 7.29 μM	Zhao et al. (2017)
Reynoutria multiflora (Thunb.) Moldenke [Polygonaceae]/Chinese	Roots/EtOH	Multiflorumiside H–K	*In vitro*: PTP-1B enzyme assay/IC_{50} = 1.2, 1.7, 1.5, 4.6 μM	Yang et al. (2020)
Rhizophora apiculata Blume [Rhizophoraceae]/India	Leaves/EtOH	Glycosin	*In silico:* molecular docking/PTP-1B binding energy: 6.35 kcal/mol *In vivo:* diabetic rats (50 mg/kg b.w.)/↓blood glucose reduction by 25% in OGTTs, ↓chronic hypoglycemic effect, ↓HbA1c, ↓triglycerides, ↓cholesterol, ↑HDL, ↑hexokinase activity, ↓G6Pase activity, ↑FBPase activity	Selvaraj et al. (2016)
Rhizophora mucronata Poir. [Rhizophoraceae]/Vietnamese	Bark/EtOAc and *n*-BuOH	Full extracts	*In vitro*: PTP-1B enzyme assay/IC_{50} = 17.2, 1.8 μg/ml	Trinh et al. (2017a)
Rhodiola rosea L. [Crassulaceae]/Chinese	Whole plant/MeOH	Arbutin	*In vitro*: PTP-1B enzyme assay/IC_{50} = 20.5 μM	Yuan et al. (2021)
Rhododendron fastigiatum Franch. [Ericaceae]	Aerial parts/EtOH	(+)-fastinoid B (-)-fastinoid B Rubiginosin A (-)-rubiginosin A Grifolinone A	*In vitro*: PTP-1B enzyme assay/IC_{50} = 47, 54.9, 40.9, 49.2, 13 μM	Huang et al. (2019)

(Continued on following page)

TABLE 1 | (*Continued*) Medicinal plants and their phytochemicals with PTP-1B inhibitory capacity.

Medicinal plant (scientific name [Family]/Traditional medicine system or places where it is used)	Part/Extract	Isolated compounds	Experiment/Outcome	References
Ricinus communis L. [Euphorbiaceae]/Chinese	Rhizomes/EtOH	3α,19-dihydroxyl-ent-pimara-8 (14),15-diene	*In vitro*: PTP-1B enzyme assay/IC_{50} = 49.49% at 20 μg/ml	Zhang et al. (2019b)
Rubus chingii Hu [Rosaceae]/ Chinese	Fruits/MeOH	Ursolic acid 2-oxopomolic acid 2α,19α-dihydroxy-3-oxo-urs- 12-en-28-oic acid	*In vitro*: PTP-1B enzyme assay/IC_{50} = 7.1, 23.7, 52.3 μM	Zhang et al. (2019c)
Rubus idaeus L. [Rosaceae]	Leaves/MeOH	Full extract	*In vitro*: PTP-1B enzyme assay/IC_{50} = 3.41 μg/ml	Li et al. (2016)
Rubus occidentalis L. [Rosaceae]	Fruits/EtOH	Cyanidin-3-O-xylosilutinoside Cyanidin-3-O -rutinoside Quercetin-3-O-rutinoside Ellagic acid	*In vitro*: PTP-1B enzyme assay/IC_{50} = 2.58, 1.88, 2.12, 0.03 μM	Xiao et al. (2017a)
Salvia circinnata Cav. [Lamiaceae]/Mexican	Aerial parts/Aqueous	6-hydroxyluteolin Pedalitin	*In vitro*: PTP-1B enzyme assay/IC_{50} = 80.1, 62 μM	Salinas-Arellano et al. (2020)
Salvia miltiorrhiza Bunge [Lamiaceae]/Chinese	Roots/EtOH	Cryptotanshinone Tanshinol B Tanshinonal 15,16-dihydrotanshinone I Tanshinone I Dehydrodanshenol A	*In vitro*: PTP-1B enzyme assay/IC_{50} = 5.5, 4.7, 37.6, 18.6, 27.1, 8.5 μM	Kim et al. (2017b)
	Selected compounds of Tangzhiqing herbal formula In combination with *Morus alba* L. (Moraceae) *Nelumbo nucifera* Gaertn. (Nelumbonaceae) *Crataegus pinnatifida* Bunge (Rosaceae) *Paeonia lactiflora* Pall. (Paeoniaceae)	Nuciferine Rutin 1-Deoxynojirimycin Salvianolic acid A Salvianolic acid C Danshensu Rosmarinic acid Tanshinone IIA Cryptotanshinone Dihydrotanshinone I Quercitrin Paeoniflori	*In silico:* molecular docking/PTP-1B binding energy: 26.49, 86.52, 17.57, 72.09, 95.07, 49.37, 54.44, 25.66, 33.08, 22.27, 83.52, 44.46 kcal/mol	Hao et al. (2020)
Selaginella rolandi-principis Alston [Selaginellaceae]/ Vietnamese	Aerial parts/EtOH	Selaginolide A 2′-hydroxygenistein 6,7-dimethoxy-2′,4′-dihydroxyisoflavone	*In vitro*: PTP-1B enzyme assay/IC_{50} = 7.4, 23.02, 11.08 μM *In vitro:* cell culture (3T3-L1)/↑glucose uptake, ↑pIRS-1, ↑pPI3K, pAkt	Nguyen et al. (2021)
Selaginella tamariscina (P.Beauv.) Spring [Selaginellaceae]/Chinese	Aerial parts/MeOH	Selariscinin D Selariscinin E Amentoflavone Robustaflavone Cupressuflavone Taiwaniaflavone 3,8″-biapigenin	*In vitro*: PTP-1B enzyme assay/IC_{50} = 13.2, 9.8, 7.4, 6.2, 9.6, 5.4, 4.5 μM *In vitro:* cell culture (3T3-L1)/↑glucose uptake	Nguyen et al. (2015)
		Sellaginellin U–W Sellaginellin Selariscinin A	*In vitro*: PTP-1B enzyme assay/IC_{50} = 13.8, 14.5, 14.6, 15.9, 4.8 μM	Le et al. (2017)
Selaginella uncinata (Desv.) Spring [Selaginellaceae]/ Chinese	Whole plant/EtOH	Uncinatabiflavone C 7-methyl ether Robustaflavone 4′-methyl ether Robustaflavone 7- methyl ether (2R) 2, 3-dihy- droamentoflavone Amentoflavone Bilobetin (2″S) chrysocauloflavone I Delicaflavone (2S) 2,3-dihydro- 5,5″,7,7″,4′-pentahydroxy-6,6″-dimethyl-[3′-O-4‴]-biflavone	*In vitro*: PTP-1B enzyme assay/IC_{50} = 7.7, 9.2, 9.8, 16.1, 10.6, 14.6, 5.5, 6.2, 4.6 μM *In vitro:* cell culture (insulin-resistant HepG2)/↑glucose uptake, ↑pIRS-1, ↑pPI3K, pAkt (Uncinatabiflavone C 7-methyl ether)	Xu et al. (2019a)
Senna obtusifolia (L.) H.S.Irwin & Barneby [Fabaceae]/Chinese	Seeds/MeOH	Physcion Chrysophanol Emodin Alaternin Obtusin Questin Chryso-obtusin Aurantio-obtusin 2-Hydroxyemodin-1 methylether	*In vitro*: PTP-1B enzyme assay/IC_{50} = 7.28, 5.86, 3.51, 1.22, 6.44, 5.69, 14.88, 27.19, 5.22 μM *In vitro:* cell culture (insulin-resistant HepG2)/↑insulin-stimulated glucose uptake (alaternin and emodin)	Jung et al. (2016)
Silybum marianum (L.) Gaertn. [Asteraceae]	Seeds/EtOAc	Taxifolin Dihydrokaempferol Dihydroquercetin-4′-methylether Kaempferol	*In vitro*: PTP-1B enzyme assay/IC_{50} = 24.23, 27.83, 21.30, 6.79 μM	Qin et al. (2017)
Smilax china L. [Smilacaceae]/ Thai	Leaves/EtOH	Morin Kaempferol 7-O-α-L-rhamnoside Quercetin-4′-O-β-D-glucoside 4′-methoxy-5,7-dihydroxyflavone-(3-O-7″)-4‴,5″,7″-trihydroxyflavone Partensein 1,3,6-trihydroxyxanthone	*In vitro*: PTP-1B enzyme assay/IC_{50} = 7.62, 10.80, 0.92, 2.68, 9.77, 24.17 μM	Zhao et al. (2016)

(Continued on following page)

TABLE 1 | (*Continued*) Medicinal plants and their phytochemicals with PTP-1B inhibitory capacity.

Medicinal plant (scientific name [Family]/Traditional medicine system or places where it is used)	Part/Extract	Isolated compounds	Experiment/Outcome	References
Sophora flavescens Aiton [Fabaceae]	Roots/EtOH	Sophobiflavonoid A, C	*In vitro*: PTP-1B enzyme assay/IC_{50} = 0.33, 0.35 μM	Yan et al. (2019)
Symplocos cochinchinensis (Lour.) S. Moore. [Symplocaceae]/Ayurveda	Bark/EtOH	Full extract	*In vivo:* insulin-resistant rats (250 and 500 mg/kg b.w.)/↓hepatic PTP-1B activity and expression, ↑hepatic pAkt, ↑hepatic pIRS-1, ↑glucose tolerance, ↑insulin sensitivity, ↓hepatic triglycerides, ↓expression of gluconeogenic enzymes	Antu et al. (2016)
Syzygium cumini (L.) Skeels [Myrtaceae]/Vietnamese,	Seeds/MeOH	Valoneic acid dilactone Rubuphenol Ellagic acid	*In vitro*: PTP-1B enzyme assay/IC_{50} = 9.37, 28.14, 25.96 μM	Sawant et al. (2015)
Ayurveda, Unani, and Chinese	Fruit/EtOAc	Full extract	*In vitro*: PTP-1B enzyme assay/IC_{50} = 27.5 μg/ml	Trinh et al. (2017a)
Tetradium ruticarpum (A.Juss.) T.G.Hartley [Rutaceae]/East Asia	Buds/MeOH	Schinifoline Intergrifoliodiol	*In vitro*: PTP-1B enzyme assay/IC_{50} = 24.3, 47.7 μM	To et al. (2021)
Thonningia sanguinea Vahl [Balanophoraceae]/Angola	Rhizomes/MeOH	2′-O- (3-O-galloyl-4,6-O-Sa-hexahydroxydiphenoyl-β-D-glucopyranosyl)-3-hydroxyphloretin 4′-O-(4,6-O-Sa-hexahydroxydiphenoyl-β-D-glucopyranosyl)- phloretin 2′-O-(3-O-galloyl-4,6-O-Sa-hexahydroxydiphenoyl-β-D-glucopyranosyl)phloretin Thonningianin B, A	*In vitro*: PTP-1B enzyme assay/IC_{50} = 24.7, 23.8, 19.3, 21.7, 4.4 μM *In vitro:* cell culture (HepG2)/↑insulin-stimulated IR phosphorylation (Thonningianin A)	Pompermaier et al. (2018)
Tinospora sagittata (Oliv.) Gagnep. [Menispermaceae]/ Chinese	Rhizome/EtOAc	Full extract	*In vitro*: PTP-1B enzyme assay/IC_{50} = 38.5 μg/ml	Zhao et al. (2019b)
Tradescantia spathacea Sw. [Commelinaceae]/Vietnamese	Aerial parts/MeOH	Bracteanolide A Latifolicinin C, A Oresbiusin A	*In vitro*: PTP-1B enzyme assay/IC_{50} = 7.82, 6.80, 4.55, 6.38 μM	Vo et al. (2015)
Ugni molinae Turcz. [Myrtaceae]/Chilean	Leaves/EtOAc	Full extract Madecassic acid Myricetin	*In vitro*: PTP-1B enzyme assay/IC_{50} = 97.2% at 2 μg/ml (full extract) *In vivo:* Insulin resistant mice (20, 20, and 20 mg/kg b.w.)/↓PTP-1B mRNA expression in aorta (full extract), ↑glucose tolerance (full extract and madecassic acid), ↑aortic insulin sensitivity	Arancibia-Radich et al. (2019)
Vaccinium myrtillus L. [Ericaceae]	Fruits/EtOH	Full extract	*In vitro*: PTP-1B enzyme assay/IC_{50} = 6.96 μg/ml	Xiao et al. (2017b)
Vaccinium uliginosum L. [Ericaceae]	Fruits/EtOH	Full extract	*In vitro*: PTP-1B enzyme assay/IC_{50} = 3.06 μg/ml	Xiao et al. (2017b)
		Phenolic compounds Cyanidin-3-arabinoside Delphinidin-3-glucoside Cyanidin-3-galactoside Cyanidin-3-glucoside Malvidin-3-galactoside Petunidin-3-glucoside	*In vitro*: PTP-1B enzyme assay/IC_{50} = 8.91, 17.8, 19.8, 25.9, 34, 31.1 μM *In vitro:* cell culture (PTP-1B-overexpressed HepG2)/ ↑glucose consumption, ↑glycogen synthesis, ↓PTP-1B mRNA expression and protein level, ↑IRS1 and ↓GSK3β mRNA expression, ↑pIRS1, PI3K, pAkt, pAMPK, and pGSK3β protein level (cyanidin-3-arabinoside)	Tian et al. (2019)
		Procyanidin B1, B2	*In vitro*: PTP-1B enzyme assay/IC_{50} = 0.6, 4.79 μM *In vitro:* cell culture (HepG2)/↓PTP-1B mRNA expression and protein level	Li et al. (2021)

(Continued on following page)

TABLE 1 | (*Continued*) Medicinal plants and their phytochemicals with PTP-1B inhibitory capacity.

Medicinal plant (scientific name [Family]/Traditional medicine system or places where it is used)	Part/Extract	Isolated compounds	Experiment/Outcome	References
Viburnum macrocephalum Fortune [Viburnaceae]/Chinese	Fruits/EtOH	Viburmacrosides C Viburmacrosideand D (+)-8′-hydroxypinoresinol 4-O-b-D-glucoside (-)-olivil 4′-O-b-D-glucoside	*In vitro*: PTP-1B enzyme assay/IC_{50} = 25.8, 8.9, 28.7, 27.5 μM	Zhao et al. (2020)
Vigna radiata (L.) R.Wilczek [Fabaceae]	Seeds/Aqueous	Full extract	*In vitro*: PTP-1B enzyme assay/IC_{50} = 10 μg/ml *In vitro:* cell culture (insulin-resistant HepG2)/↑glucose uptake, ↓PEPCK and GSK3β mRNA expression level	Saeting et al. (2021)

EtOH: ethanolic extract; MeOH: methanolic extract; EtOAc; ethyl acetate extract; PTP-1B: protein tyrosine phosphatase 1B; OSTT: oral sucrose tolerance test; OGTT: oral glucose tolerance test; IR: insulin receptor; IRS1: insulin receptor substrate 1; IRS2: insulin receptor substrate 2; GSK3β: glycogen synthase kinase 3 beta; Akt: protein kinase B; PI3K: phosphoinositide 3-kinase; ERK1: extracellular signal-regulated kinase 1; HFD: high-fat diet; HDL: high-density lipoprotein; LDL: low-density lipoprotein; VLDL: very low-density lipoprotein; PEPCK: phosphoenolpyruvate carboxykinase; FBPase: fructose 1,6-bisphosphatase; G6Pase: glucose 6-phosphatase; GLUT2: glucose transporter 2; GLUT4: glucose transporter 4; AMPK: AMP-activated protein kinase; PPARγ: peroxisome proliferator-activated receptor gamma; HbA1c: glycated hemoglobin.

Glycogenolysis consists of glycogen breakdown into glucose, being half of the basal HGP in fasting and decreasing the glycogen concentration at an almost linear rate during the first 22 h (Rothman et al., 1991; Cersosimo et al., 2018). In fasting, it is controlled by glucagon and epinephrine that activate glycogen phosphorylase (GP), the major enzyme responsible for digesting glycogen by releasing glucose 1-phosphate. In feeding condition, insulin inhibits glycogen breakdown and promotes glycogen synthesis through the activation of Akt and protein phosphatase 1 (PP1), leading the deactivation of both GP and glycogen synthase kinase-3 (GSK3), which in its active form (dephosphorylated), inactivates glycogen synthase (GS) (Han et al., 2016).

Gluconeogenesis, on the other hand, is defined as the production of glucose from a molecule that is not a carbohydrate. Its main substrates are pyruvate, glycerol, and amino acids such as alanine (Hanson and Owen, 2013). Another way to denote gluconeogenesis is as "reverse glycolysis" since both share not only substrates and final products, but also many enzymes. However, the direction of the reactions catalyzed in gluconeogenesis goes in the opposite direction, so the steps that are not shared with glycolysis can be determined as regulatory steps. These reactions are catalyzed by four rate-limiting enzymes: pyruvate carboxylase (PC), which is responsible for converting pyruvate into oxaloacetate; phosphoenolpyruvate carboxykinase (PEPCK), that converts oxaloacetate to phosphoenolpyruvate; fructose 1,6-bisphosphatase (FBPase), that dephosphorylates fructose 1,6-bisphosphate obtaining fructose 6-phosphate; and glucose 6-phosphatase (G6Pase), which is responsible for removing the phosphate group from glucose 6-phosphate, yielding *novo* synthesized glucose (Postic et al., 2004).

In the diabetic state, increased rates of HGP are observed as a result of an imbalance of various factors, such as the augmented availability of gluconeogenic substrates, the resistance of the liver to the action of insulin, and elevated levels of glucagon that activate HGP (Sharabi et al., 2015). Due to all these factors, the inhibition of HGP turns out to be an important therapeutic target for the reduction of hyperglycemia observed in T2D patients. In this regard, **Table 2** summarizes the works made between 2015 and 2021 with extracts or natural products from 47 medicinal plants that showed to modulate hepatic glucose metabolism by inhibiting glucose production or promoting glycogen synthesis. As it can be observed, decreasing the expression of PEPCK and G6Pase is the principal mechanism related to gluconeogenesis inhibition, while phosphorylation of GSK3, promotion of GS activity, and inhibition of GP are the main mechanisms involved in glycogen breakdown and synthesis. Furthermore, although PI3K/Akt pathway stands out as a good pharmacological target to reduce insulin resistance, medicinal plants and their phytochemicals can also decrease HGP through AMP-activated protein kinase (AMPK).

DISCUSSION

Insulin resistance in liver leads to the release of large amounts of glucose into the bloodstream that affects long-term homeostasis. The regulation of hepatic glucose output represents a good pharmacological target for the control of metabolic diseases such as T2D, which are characterized by the presence of this pathophysiological phenomenon. The search for new molecules capable of regulating hepatic glucose metabolism from medicinal plants has focused on screening for phytochemicals that can directly inhibit key enzymes in glucose-producing pathways. However, considering compounds with the ability to also decrease the activity of the enzymes involved in terminating the insulin signal could result in more effective glycemic control.

According to the bibliographic search, plants used in different systems of traditional medicine have shown the ability to inhibit the activity or expression of PTP-1B, which could indicate that

TABLE 2 | Medicinal plants and their phytochemicals capable to modulate hepatic glucose metabolism.

Medicinal plant (scientific name [Family]/Traditional medicine system or places where it is used)	Part/Extract	Isolated compounds	Experiment/Outcome	References
Abelmoschus esculentus (L.) Moench [Malvaceae]/Chinese	Whole plant/EtOH	Polysaccharides	*In vivo:* insulin-resistant mice (200 and 400 mg/kg b.w.)/↑pAkt and pGSK3β	Liao et al. (2019)
Ageratina petiolaris (Moc. & Sessé ex DC.) R.M.King & H.Rob. [Asteraceae]/Mexican	Aerial parts/Aqueous	Full extract	*In vivo:* diabetic rats (160 mg/kg b.w.)/↓Glucose production in PTTs *In vitro:* G6Pase inhibition assay/IC_{50} = 223 μg/ml	Mata-Torres et al. (2020)
Aloe vera (L.) Burm.f. [Asphodelaceae]/Aryuveda	Gel/EtOH	Carbohydrate fraction	*In vivo:* diabetic rats (27 and 54 mg/kg b.w.)/↑Liver glycogen content, ↑GS protein levels, ↓G6Pase activity	Govindarajan et al. (2021)
Alsophila firma (Baker) D.S.Conant [Cyatheaceae]/Mexican	Rhizome/Aqueous	Full extract	*In vitro:* G6Pase inhibition assay/IC_{50} = 341 μg/ml *In vitro:* FBPase inhibition assay/IC_{50} = 45 μg/ml	Andrade-Cetto et al. (2021b)
Aster spathulifolius Maxim. [Asteraceae]/Korean	Whole plant/EtOH	Full extract	*In vivo: db/db* mice (50, 100, and 200 mg/kg b.w.)/↑GK, ↓G6Pase and PEPCK expression	Yin et al. (2015)
Averrhoa bilimbi L. [Oxalidaceae]/Indian	Fruits/Aqueous	EtOAc fraction	*In vivo:* diabetic rats (25 mg/kg b.w.)/↓G6Pase and FBPase activity	Kurup and S, (2017)
Bromelia karatas L. [Bromeliaceae]/Mexican	Aerial parts/Aqueous	Full extract	*In vitro:* G6Pase inhibition assay/IC_{50} = 1,136 μg/ml	Mata-Torres et al. (2020)
Calea urticifolia (Mill.) DC. [Asteraceae]/Mexican	Aerial parts/Aqueous	Full extract	*In vivo:* diabetic rats (41 mg/kg b.w.)/↓Glucose production in PTTs *In vitro:* G6Pase inhibition assay/IC_{50} = 406 μg/ml	Andrade-Cetto et al. (2021a)
Calotropis procera (Aiton) W.T.Aiton [Apocynaceae]/Indian	Aerial parts/Latex	Protein fraction	*In vivo:* Wistar rats (5 mg/kg b.w.)/↑pAMPK, ↓PEPCK expression, ↓blood glucose in PTTs	de Oliveira et al. (2019)
Caralluma fimbriata Wall. [Apocynaceae]/Indian	Stems/EtOH	Full extract	*In vivo:* insulin-resistant rats (200 mg/kg b.w.)/↓G6Pase and FBPase activity	Gujjala et al. (2017)
Caralluma quadrangula (Forssk.) N.E.Br./Apocynaceae/Saudi	Whole plant/MeOH	Russelioside B	*In vivo:* diabetic rats (50 mg/kg b.w.)/↑Glycogen content, ↓GP activity, ↓GS and GSK3β expression, ↓G6Pase activity and expression	Abdel-Sattar et al. (2016)
Chrysobalanus icaco L. [Chrysobalanaceae]/Nigerian	Leaves/Aqueous	Full extract	*In vivo:* diabetic rats (11.076, 22.134, and 44.268 mg/kg b.w.)/↑Liver glycogen content, ↓G6Pase activity	Ekakitie et al. (2021)
Cola nitida (Vent.) Schott & Endl. [Malvaceae]/African	Seeds/Aqueous	Full extract	*In vivo*: diabetic rats (300 mg/kg b.w.)/↓GP, G6Pase, and FBPase activities	Erukainure et al. (2019b)
Combretum lanceolatum Pohl ex Eichler [Combretaceae]/Brazilian	Flowers/EtOH	Full extract	*In vivo:* diabetic rats (500 mg/kg b.w.)/↑pAMPK and pAkt, ↓PEPCK expression	Siqueira et al. (2016)
Coreopsis tinctoria Nutt. [Asteraceae]/Chinese and Portuguese	Flowers/EtOAc	Marein	*In vitro:* cell culture (insulin-resistant HepG2)/↑Glycogen content, ↓G6Pase and PEPCK expression and protein levels	Jiang et al. (2018a)
Corispermum squarrosum L. [Amaranthaceae]/Mongol	Whole plant/EtOH	Oligosaccharides	*In vivo: db/db* mice (380 and 750 mg/kg b.w.)/In liver: ↑pIRS2, ↑pAkt, ↑IRS2, PI3K, Akt, and IR expression and protein levels	Bao et al. (2020)
Couroupita guianensis Aubl. [Lecythidaceae]	Leaves/Aqueous	Full extract Gold nanoparticles	*In vivo:* diabetic rats (100 and 2.5 mg/kg b.w.)/↑Glycogen storage, ↓G6Pase activity and expression	Manimegalai et al. (2020)
Edgeworthia gardneri (Wall.) Meisn. [Thymelaeaceae]/Chinese	Flowers/Aqueous	Full extract	*In vitro:* cell culture (insulin-resistant HepG2)/↑Glucose uptake and consumption, ↑Glycogen content, ↓Gluconeogenesis, ↑pIR, ↑pIRS1, ↑pAkt, ↑pGSK3	Zhang et al. (2020)
Equisetum myriochaetum Schltdl. & Cham. [Equisetaceae]/Mexican	Aerial parts/Aqueous	Full Extract	*In vivo:* diabetic rats (330 mg/kg b.w.)/↓Glucose production in PTTs	Mata-Torres et al. (2020)

(Continued on following page)

TABLE 2 | (*Continued*) Medicinal plants and their phytochemicals capable to modulate hepatic glucose metabolism.

Medicinal plant (scientific name [Family]/Traditional medicine system or places where it is used)	Part/Extract	Isolated compounds	Experiment/Outcome	References
Eryngium cymosum F.Delaroche [Apiaceae]/Mexican	Aerial parts/Aqueous	Full extract	*In vivo:* diabetic rats (470 mg/kg b.w.)/↓ Glucose production in PTTs *In vitro:* G6Pase inhibition assay/IC_{50} = 782 μg/ml *In vitro:* FBPase inhibition assay/IC_{50} = 57.4 μg/ml	Espinoza-Hernández et al. (2021)
Eryngium longifolium Cav. [Apiaceae]/Mexican	Aerial parts/EtOH	Full extract	*In vitro:* G6Pase inhibition assay/IC_{50} = 780 μg/ml *In vitro:* FBPase inhibition assay/IC_{50} = 93 μg/ml	Andrade-Cetto et al. (2021b)
Ficus carica L. [Moraceae]/Spain	Leaves/EtOH	Full extract	*In vivo:* diabetic mice (2 g/kg b.w.)/↓PEPCK and G6Pase expression, ↑pAMPK *In vitro:* cell culture (HepG2)/↓PEPCK and G6Pase expression, ↑pAMPK	Zhang et al. (2019d)
Forsythia suspensa (Thunb.) Vahl [Oleaceae]/Chinese	Fruit/MeOH	Full extract	*In vivo:* diabetic mice (200 mg/kg b.w.)/↓PEPCK expression	Zhang et al. (2016b)
Graptopetalum paraguayense (N.E.Br.) E.Walther [Crassulaceae]/Taiwan	Leaves/MeOH	Full extract Partially purified fraction (HH-F3)	*In vitro:* cell culture (Hep3B/T2)/↓PEPCK and G6Pase expression	Jhuang et al. (2015)
Hyoscyamus albus L. [Solanaceae]/Mediterranean	Seeds/MeOH	Calystegine fraction	*In vitro:* cell culture (insulin-resistant HepG2)/↑Glucose consumption, ↓G6Pase (catalytic subunit) expression, ↑IR, IRS1/2, PI3K, Akt1/2 expression and protein levels	Kowalczuk et al. (2021)
Hypericum attenuatum Fisch. ex Choisy [Hypericaceae]/Chinese	Whole plant/EtOH	Full extract	*In vivo:* insulin-resistant mice (100, 200, and 300 mg/kg b.w.)/↓PEPCK and G6Pase expression and protein levels, ↑GS expression and protein levels, ↑pIRS, ↑PI3K, ↑pAkt, ↑GSK3	Jin et al. (2019)
Iris domestica (L.) Goldblatt & Mabb. [Iridaceae]/Chinese	Leaves/EtOH	Saponins and polysaccharide fraction Flavonoid fraction	*In vivo:* KK-A^y-mice (200 mg/kg b.w.)/↓G6Pase and PEPCK activities, ↑Glycogen content	Guo et al. (2019)
Launaea acanthodes (Boiss.) Kuntze [Asteraceae]/Iran	Aerial parts/EtOH	Full extract	*In vivo:* diabetic rats (100, 200, and 400 mg/kg b.w.)/↑GK and GLUT2 expression, ↓PEPCK and G6Pase expression	Marvibaigi et al. (2021)
Lithocarpus polystachyus (Wall. ex A.DC.) Rehder [Fagaceae]/Chinese	Leaves/Aqueous	Full extract	*In vivo:* insulin-resistant mice (800 mg/kg b.w.)/↑Glycogen content, ↑Liver glucose influx,/↓G6Pase and PEPCK expression, ↑IR and IRS expression	Wang et al. (2016a)
Lupinus mutabilis Sweet [Fabaceae]/Andean	Seeds/Aqueous	Protein fraction	*In vitro:* cell culture (HepG2)/↓glucose production and PEPCK expression	Muñoz et al. (2018)
Myrianthus arboreus P.Beauv. [Urticaceae]/African	Root bark/EtOH	EtOAc fraction Isoorientin Orientin Chlorogenic acid	*In vitro:* cell culture (H4IIE hepatocytes)/↓G6Pase activity, ↑pAMPK	Kasangana et al. (2019)
	Root bark/Aqueous, EtOH (EtOAc and hexane fractions), Alkaloid rich, and DCM extracts	Full extracts or fractions	*In vitro:* cell culture (H4IIE hepatocytes)/↓G6Pase activity, ↑pAkt, ↑pAMPK *In vitro:* cell culture (HepG2)/↑GS activity, ↑GSK3	Kasangana et al. (2018)
Myrica rubra (Lour.) Siebold & Zucc. [Myricaceae]/Chinese	Fruits/EtOH	Full extract	*In vivo:* KK-A^y mice (200 mg/kg b.w.)/↑pAMPK. ↓ PEPCK and G6Pase expression *In vitro:* cell culture (HepG2)/↑pAMPK, ↓PEPCK and G6Pase expression	Zhang et al. (2016a)
Pachylobus edulis G.Don [Burseraceae]/African and Nigerian	Leaves/EtOH	BuOH fraction	*In vivo:* diabetic rats (150 and 300 mg/kg b.w.)/↓GP, FBPase, and G6Pase activities	Erukainure et al. (2020)
	Leaves/EtOAc, EtOH, and Aqueous	Full extracts	*In vitro:* G6Pase inhibition assay/IC_{50} = 0.66, 3.59, 0.05 μg/ml	Erukainure et al. (2017)

(Continued on following page)

TABLE 2 | (*Continued*) Medicinal plants and their phytochemicals capable to modulate hepatic glucose metabolism.

Medicinal plant (scientific name [Family]/Traditional medicine system or places where it is used)	Part/Extract	Isolated compounds	Experiment/Outcome	References
Panax ginseng C.A.Mey. [Araliaceae]/Korean	Roots/EtOH	Black ginseng extract	*In vivo:* diabetic mice (300 and 900 mg/kg b.w.)/↓G6Pase, PEPCK and GP expression, ↑GS expression	Seo et al. (2016)
Plantago depressa Willd [Plantaginaceae]/Chinese	Seeds/EtOH	Plantadeprate A Plumbagine D Plantagoguanidinic acid	*In vitro:* cell culture (rat hepatocytes)/↓Gluconeogenesis inhibition by 8.2, 18.5, and 12.5% at 40 μM	Zheng et al. (2015)
Raphia hookeri G.Mann & H.Wendl. [Arecaceae]	Raffia palm wine/ Concentrated in water bath	Concentrated wine	*In vivo:* diabetic rats (150 and 300 mg/kg b.w.)/↓GP, FBPase and G6Pase activity	Erukainure et al. (2019)
Rhizophora mangle L. [Rhizophoraceae]/Mexican	Bark/EtOH	Full Extract	*In vivo:* diabetic rats (90 mg/kg b.w.)/↓Glucose production in PTTs *In vitro:* G6Pase inhibition assay/IC_{50} = 99 μg/ml	Mata-Torres et al. (2020)
Rhodiola crenulata (Hook.f. & Thomson) H.Ohba [Crassulaceae]/ Asian and Eastern European countries	Roots/EtOH	Full extract	*In vivo:* Sprague–Dawley rats (50 mg/kg b.w.)/↓PEPCK expression, ↑pAMPK *In vitro:* cell culture (HepG2)/↑pGSK3β and AMPK, ↓PEPCK and G6Pase expression	Lee et al. (2015)
Sarcopoterium spinosum (L.) Spach [Rosaceae]/Israel, Palestine, and Jordan	Root/Aqueous	Full extract	*In vivo:* insulin-resistant mice (35 and 100 mg/kg b.w.)/↑pIR, ↑pAkt, ↑GSK3, ↑glycogen content *In vivo:* KK-Ay mice (35 and 100 mg/kg b.w.)/↑pIR, ↑pAkt, ↓PEPCK expression	Rozenberg and Rosenzweig, (2018)
Senna alata (L.) Roxb. [Fabaceae]/ Asia, Africa and South America	Leaves/EtOH	Full extract	*In vivo:* diabetic rats (400 mg/kg b.w.)/↑Liver glycogen content, ↑GS activity, ↓GP and FBPase activities	Mohanasundaram et al. (2021)
	Flowers/Aqueous	Full extract EtOAc fraction *n*-butanol fraction Aqueous fraction	*In vivo:* diabetic rats (75 mg/kg b.w.)/↑Glycogen storage	Uwazie et al. (2020)
Sesbania grandiflora (L.) Poir. [Fabaceae]/Aryuveda	Flowers/MeOH	Full extract	*In vivo:* diabetic rats (250 mg/kg b.w.)/↑Liver glycogen content, ↑GS activity, ↓GP, G6Pase, and FBPase activities	Sureka et al. (2021)
Shirakiopsis elliptica (Hochst.) Esser [Euphorbiaceae]/Nigerian	Leaves/EtOH	Full extract	*In vivo:* diabetic rats (400 and 800 mg/kg b.w.)/↑GK activity by 40.31%, ↓G6Pase activity by 37.29%, ↑Glycogen content	Ighodaro et al. (2017)
Smilax moranensis M.Martens & Galeotti [Smilacaceae]/Mexican	Roots/EtOH	Full Extract	*In vitro:* G6Pase inhibition assay/IC_{50} = 84 μg/ml	Mata-Torres et al. (2020)
Swietena humilis Zucc. [Meliaceae]/ Mexican	Seeds/Aqueous	Dried aqueous extract Mexicanolide 1 Mexicanolide 2 Mexicanolide 3	*In vitro:* G6Pase inhibition assay in H4IIE hepatocytes Extract: 100 μg/ml = 40.67%; 200 μg/ml = 61.11 1: 9.46 μM = 42.68% 2: 8.79 μM = 56.51% 3: 8.13 μM = 41.79%	Ovalle-Magallanes et al. (2019)
Tephrosia tinctoria (L.) Pers. [Fabaceae]/Aryuveda	Stems/EtOAc	EtOAc fraction	*In vivo:* diabetic rats (100 and 200 mg/kg b.w.)/↑Liver glycogen content, ↓G6Pase and FBPase activity	Krishnasamy and Periyasamy, (2019)
Terminalia catappa L. [Combretaceae]/Aryuveda	Leaves/EtOH	Full extract	*In vivo:* diabetic rats (300 and 500 mg/kg b.w.)/↓G6Pase and FBPase activity	Divya et al. (2019)
Trigonella foenum-graecum L. [Fabaceae]/Asia, Africa, and the Mediterranean region	Seeds/EtOH	Fenugreek flavonoids	*In vivo:* diabetic rats (0.5 g in 10 ml/kg)/↑Liver glycogen content, ↓G6Pase and FBPase activity	Jiang et al. (2018b)

EtOH: ethanolic extract; MeOH: methanolic extract; EtOAc; ethyl acetate extract; PTT: pyruvate tolerance test; IR: insulin receptor; IRS1: insulin receptor substrate 1; IRS2: insulin receptor substrate 2; GSK3: glycogen synthase kinase 3; Akt: protein kinase B; PI3K: phosphoinositide 3-kinase; PEPCK: phosphoenolpyruvate carboxykinase; FBPase: fructose 1,6-bisphosphatase; G6Pase: glucose 6-phosphatase; GLUT4: glucose transporter 4; AMPK: AMP-activated protein kinase; GS: glycogen synthase; GP: glycogen phosphorylase.

they have a potential inhibitory effect on HGP. The determination of biological activity of full extracts and compounds isolated from medicinal plants has been approached through different perspectives. Generally, the medicinal plant is first identified using an ethnopharmacological approach. Afterwards, different types of extracts are elaborated (aqueous, ethanolic, methanolic, etc.) and then tested on the biological activity to be evaluated following several paths: 1) direct inhibition enzymatic assays, which can be complemented with structure-activity relationship (SAR) studies and molecular docking analysis to find the possible structures responsible for the bioactivity, relating them with the binding of amino acid residues present at the catalytic or regulatory sites (regarding isolated compounds); 2) the use of cell cultures to evaluate the effect of the extract or compound on the expression and protein levels of key enzymes; and 3) *in vivo* studies, where diabetic (hyperglycemic) animals induced with STZ or alloxan, or insulin-resistant animals generated by the consumption of high-fat diet are used.

Regarding PTP-1B, most of the studies published between 2015 and 2021 focused on conducting enzyme activity assays, and few of them had a multidisciplinary approach that encompassed enzyme assays and *in vitro* or *in vivo* studies. The main problem with the first type of studies is that, although the inhibition potency and selectivity of the molecule over the enzyme are directly evaluated, the pharmacokinetic properties of the compound are omitted. This particularity stands out since it has been reported that, despite having excellent inhibitory activity, many compounds lack adequate cellular permeability, namely they present poor absorption and low bioavailability (Zhang et al., 2017). Another aspect to highlight is that PTP-1B is almost identical to TC-PTP, another member of the PTP family with 74% identity at the catalytic site, so it is important that the identified inhibitors have a high selectivity towards PTP-1B to avoid unwanted effects (Dewang et al., 2005). Considering these facts, it would be necessary in the future to carry out more studies involving as many approaches as possible to obtain a more integrative panorama and to be able to evaluate potential inhibitors considering their pharmacokinetic properties and selectivity. Also, it is encouraged to directly evaluate the effect of medicinal plants and their compounds with reported PTP-1B inhibitory capacity on hepatic glucose metabolism.

In addition to exhibiting PTP-1B inhibitory capacity, some of the medicinal plants reported in **Table 1** also improved hepatic glucose metabolism by promoting glucose consumption and glycogen synthesis, upregulating activity or expression of GS, decreasing activity or expression of key enzymes involved in glycogenolysis and gluconeogenesis such as GSK3, GP, PEPCK, FBPase, and G6Pase, and by modulating insulin signaling. The compounds isolated from these plants could have a greater modulatory capacity of hepatic glucose metabolism because they are capable of directly reducing both insulin resistance and glucose production. These species were *Astragalus mongholicus* (astragaloside IV), *Chaenomeles japonica*, *Duranta erecta*, *Eriobotrya japonica* (maslinic acid, corosolic acid, oleanolic acid, and ursolic acid), *Symplocos cochinchinensis*, *Thonningia sanguinea* (2′-O- (3-O-galloyl-4,6-O-Sa-hexahydroxydiphenoyl-β-D-glucopyranosyl)-3-hydroxyphloretin, 4′-O-(4,6-O-Sa-hexahydroxydiphenoyl-β-D-glucopyranosyl)- phloretin, 2′-O-(3-O-galloyl-4,6-O-Sa-hexahydroxydiphenoyl-β-D-glucopyranosyl) phloretin, thonningianin A, and thonningianin B), *Vaccinium uliginosum* (cyanidin-3-arabinoside, delphinidin-3-glucoside, cyanidin-3-galactoside, cyanidin-3-glucoside, malvidin-3-galactoside, petunidin-3-glucoside, procyanidin B1, and procyanidin B2), and *Vigna radiata*. On the other hand, since *Coreopsis tinctoria*, *Lithocarpus polystachyus*, and *Panax ginseng* were documented in both **Tables 1**, **2**, their isolated compounds may have better glycemic control.

This work focused on summarizing the medicinal plants with the potential capacity to reduce hyperglycemia resulting from an imbalance in the hepatic metabolism of glucose, encompassing two different approaches: the inhibition of PTP-1B (improvement of hepatic insulin resistance), and the modulation of enzymes involved in gluconeogenesis and glycogenolysis/glycogenesis (decreased hepatic glucose output). In recent years, PTP-1B research has focused on the characterization of different phytochemicals from medicinal plants, such as phenolic compounds, terpenes, and alkaloids. The main methodology used was to carry out direct enzyme inhibition tests to evaluate the potency of these molecules, omitting important aspects such as selectivity or pharmacokinetics. Therefore, it is proposed to use of multidisciplinary approaches that involve *in vitro* studies, such as the use of cell lines or primary culture to evaluate the effect of the extracts and compounds on expression and protein levels, and *in vivo* studies, where the concentration of the compound in systemic circulation and its duration is determined, as well as the transformation processes involved. In this regard, not only the inhibitory activity of the compounds is evaluated, but also the impact on other pharmacological aspects that can only be observed using animal models.

On the other hand, research on medicinal plants that modulate hepatic glucose metabolism has primary focused on testing full extracts rather than compounds. However, it is worth mentioning that mixtures could have synergistic effects capable of regulating multiple targets (Caesar and Cech, 2019) and therefore compound fractions may exhibit more bioactivity than isolated molecules. Further studies are needed to identify potential multi-target phytochemicals in plants listed in **Table 2**. Finally, it is expected that this review will provide greater knowledge of medicinal plants and compounds for the development of drugs that improving hepatic glucose metabolism as a therapeutic target for the treatment of T2D.

We suggest that *Coreopsis tinctoria*, *Lithocarpus polystachyus*, and *Panax ginseng* can be good candidates for developing herbal medicines or phytomedicines that target inhibition of hepatic glucose output as they can modulate the activity of PTP-1B, the expression of gluconeogenic enzymes, and the glycogen content. However, only their full extracts are tested until now. Therefore, compounds responsible for the effects mentioned above have not been identified, and pharmacological and toxicological tests in animal models are

required to assess their efficacy and safety, with the aim of moving forward to carry out clinical studies.

AUTHOR CONTRIBUTIONS

GM-T and FE-H performed the bibliographical research summarized in tables and wrote the first version of the manuscript. AA-C reviewed and edited the manuscript. All authors have read and agreed to the published version of the manuscript.

FUNDING

This project was partially sponsored by DGAPA PAPIIT IN226719 and IN213222.

ACKNOWLEDGMENTS

Authors acknowledge "Consejo Nacional de Ciencia y Tecnología (CONACyT)" for the doctoral scholarship of GM-T and FE-H.

REFERENCES

Abdel-Rahman, R. F., Ezzat, S. M., Ogaly, H. A., Abd-Elsalam, R. M., Hessin, A. F., Fekry, M. I., et al. (2020). Ficus Deltoidea Extract Down-Regulates Protein Tyrosine Phosphatase 1B Expression in a Rat Model of Type 2 Diabetes Mellitus: a New Insight into its Antidiabetic Mechanism. *J. Nutr. Sci.* 9, e2. doi:10.1017/jns.2019.40

Abdel-Sattar, E., El-Maraghy, S. A., El-Dine, R. S., and Rizk, S. M. (2016). Russelioside B, a Pregnane Glycoside Ameliorates Hyperglycemia in Streptozotocin Induced Diabetic Rats by Regulating Key Enzymes of Glucose Metabolism. *Chem. Biol. Interact.* 252, 47–53. doi:10.1016/j.cbi.2016.03.033

Abdjul, D. B., Yamazaki, H., Maarisit, W., Rotinsulu, H., Wewengkang, D. S., Sumilat, D. A., et al. (2017). Oleanane Triterpenes with Protein Tyrosine Phosphatase 1B Inhibitory Activity from Aerial Parts of Lantana Camara Collected in Indonesia and Japan. *Phytochemistry* 144, 106–112. doi:10.1016/j.phytochem.2017.08.020

Abdjul, D. B., Yamazaki, H., Maarisit, W., Kirikoshi, R., Takahashi, O., Losung, F., et al. (2018). Protein Tyrosine Phosphatase 1B Inhibitory Components and a New Unique N -alkylamide Derivative with an Endoperoxide Bridge from Aerial Parts of Indonesian Spilanthes Paniculata. *Phytochemistry Lett.* 24, 71–74. doi:10.1016/j.phytol.2018.01.013

Ahmad, F., Azevedo, J. L., Cortright, R., Dohm, G. L., and Goldstein, B. J. (1997). Alterations in Skeletal Muscle Protein-Tyrosine Phosphatase Activity and Expression in Insulin-Resistant Human Obesity and Diabetes. *J. Clin. Invest.* 100, 449–458. doi:10.1172/JCI119552

Ahmad, F., and Goldstein, B. J. (1995). Alterations in Specific Protein-Tyrosine Phosphatases Accompany Insulin Resistance of Streptozotocin Diabetes. *Am. J. Physiol.* 268, E932–E940. doi:10.1152/ajpendo.1995.268.5.e932

Ahmad, F., Li, P. M., Meyerovitch, J., and Goldstein, B. J. (1995). Osmotic Loading of Neutralizing Antibodies Demonstrates a Role for Protein-Tyrosine Phosphatase 1B in Negative Regulation of the Insulin Action Pathway. *J. Biol. Chem.* 270, 20503–20508. doi:10.1074/jbc.270.35.20503

Ahmed, B., Sultana, R., and Greene, M. W. (2021). Adipose Tissue and Insulin Resistance in Obese. *Biomed. Pharmacother.* 137, 111315. doi:10.1016/j.biopha.2021.111315

Alonso, A., Nunes-Xavier, C. E., Bayón, Y., and Pulido, R. (2016). "The Extended Family of Protein Tyrosine Phosphatases," in *Methods in Molecular Biology*. Editor R. Pulido (New York: Humana Press), 1–23. doi:10.1007/978-1-4939-3746-2_1*Protein Tyrosine Phosphatases*

American Diabetes Association (2021). 2. Classification and Diagnosis of Diabetes: Standards of Medical Care in Diabetes-2021. *Diabetes Care* 44, S15–S33. doi:10.2337/dc21-S002

An, J. P., Ha, T. K., Kim, J., Cho, T. O., and Oh, W. K. (2016). Protein Tyrosine Phosphatase 1B Inhibitors from the Stems of Akebia Quinata. *Molecules* 21. doi:10.3390/molecules21081091

Andrade-Cetto, A., Espinoza-Hernández, F., Mata-Torres, G., and Escandón-Rivera, S. (2021b). Hypoglycemic Effect of Two Mexican Medicinal Plants. *Plants (Basel)* 10, 2060. doi:10.3390/plants10102060

Andrade-Cetto, A., Espinoza-Hernández, F., and Mata-Torres, G. (2021a). Hypoglycemic Effect of *Calea Urticifolia* (Mill.) DC. *Evidence-Based Complement. Altern. Med.* 2021, 1–10. doi:10.1155/2021/6625009

Antu, K. A., Riya, M. P., Nair, A., Mishra, A., Srivastava, A. K., and Raghu, K. G. (2016). Symplocos Cochinchinensis Enhances Insulin Sensitivity via the Down Regulation of Lipogenesis and Insulin Resistance in High Energy Diet Rat Model. *J. Ethnopharmacol.* 193, 500–509. doi:10.1016/j.jep.2016.09.050

Arancibia-Radich, J., González-Blázquez, R., Alcalá, M., Martín-Ramos, M., Viana, M., Arribas, S., et al. (2019). Beneficial Effects of Murtilla Extract and Madecassic Acid on Insulin Sensitivity and Endothelial Function in a Model of Diet-Induced Obesity. *Sci. Rep.* 9, 599. doi:10.1038/s41598-018-36555-1

Atanasov, A. G., Zotchev, S., Zotchev, S. B., Dirsch, V. M., and Supuran, C. T. (2021). The International Natural Product Sciences Taskforce, and Supuran, CNatural Products in Drug Discovery: Advances and Opportunities. *Nat. Rev. Drug Discov.* 20, 200–216. doi:10.1038/s41573-020-00114-z

Bakke, J., and Haj, F. G. (2015). Protein-tyrosine Phosphatase 1B Substrates and Metabolic Regulation. *Semin. Cel Dev Biol* 37, 58–65. doi:10.1016/j.semcdb.2014.09.020

Bao, S., Wu, Y. L., Wang, X., Han, S., Cho, S., Ao, W., et al. (2020). Agriophyllum Oligosaccharides Ameliorate Hepatic Injury in Type 2 Diabetic Db/db Mice Targeting INS-R/IRS-2/PI3K/AKT/PPAR-γ/Glut4 Signal Pathway. *J. Ethnopharmacol.* 257, 112863. doi:10.1016/j.jep.2020.112863

Begmatov, N., Li, J., Bobakulov, K., Numonov, S., and Aisa, H. A. (2020). The Chemical Components of Coreopsis Tinctoria Nutt. And Their Antioxidant, Antidiabetic and Antibacterial Activities. *Nat. Prod. Res.* 34, 1772–1776. doi:10.1080/14786419.2018.1525377

Caesar, L. K., and Cech, N. B. (2019). Synergy and Antagonism in Natural Product Extracts: When 1 + 1 Does Not Equal 2. *Nat. Prod. Rep.* 36, 869–888. doi:10.1039/c9np00011a

Cai, J., Zhao, L., and Tao, W. (2015). Potent Protein Tyrosine Phosphatase 1B (PTP1B) Inhibiting Constituents from Anoectochilus Chapaensis and Molecular Docking Studies. *Pharm. Biol.* 53, 1030–1034. doi:10.3109/13880209.2014.957781

Cao, X., Yang, X., Wang, P., Liang, Y., Liu, F., Tuerhong, M., et al. (2017). Polycyclic Phloroglucinols as PTP1B Inhibitors from Hypericum Longistylum: Structures, PTP1B Inhibitory Activities, and Interactions with PTP1B. *Bioorg. Chem.* 75, 139–148. doi:10.1016/j.bioorg.2017.09.001

Cersosimo, E., Triplitt, C., Solis-Herrera, C., Mandarino, L. J., and DeFronzo, R. A. (2018). "Pathogenesis of Type 2 Diabetes Mellitus," in *" in* Endotext. Editor K. R. Feingold (South Dartmouth: MDText.com, Inc.). . http://www.ncbi.nlm.nih.gov/pubmed/25905339 (Accessed September 1, 2021).

Chen, H., Wertheimer, S. J., Lin, C. H., Katz, S. L., Amrein, K. E., Burn, P., et al. (1997). Protein-tyrosine Phosphatases PTP1B and Syp Are Modulators of Insulin-Stimulated Translocation of GLUT4 in Transfected Rat Adipose Cells. *J. Biol. Chem.* 272, 8026–8031. doi:10.1074/jbc.272.12.8026

Choi, J. S., Ali, M. Y., Jung, H. A., Oh, S. H., Choi, R. J., and Kim, E. J. (2015). Protein Tyrosine Phosphatase 1B Inhibitory Activity of Alkaloids from Rhizoma Coptidis and Their Molecular Docking Studies. *J. Ethnopharmacol.* 171, 28–36. doi:10.1016/j.jep.2015.05.020

Cusi, K., Maezono, K., Osman, A., Pendergrass, M., Patti, M. E., Pratipanawatr, T., et al. (2000). Insulin Resistance Differentially Affects the PI 3-kinase- and MAP Kinase-Mediated Signaling in Human Muscle. *J. Clin. Invest.* 105, 311–320. doi:10.1172/JCI7535

Dadke, S. S., Li, H. C., Kusari, A. B., Begum, N., and Kusari, J. (2000). Elevated Expression and Activity of Protein-Tyrosine Phosphatase 1B in Skeletal Muscle of Insulin-Resistant Type II Diabetic Goto-Kakizaki Rats. *Biochem. Biophys. Res. Commun.* 274, 583–589. doi:10.1006/bbrc.2000.3188

de Oliveira, K. A., Moreira Gomes, M. D., Vasconcelos, R. P., de Abreu, E. S., Fortunato, R. S., Carneiro Loureiro, A. C., et al. (2019). Phytomodulatory Proteins Promote Inhibition of Hepatic Glucose Production and Favor Glycemic Control via the AMPK Pathway. *Biomed. Pharmacother.* 109, 2342–2347. doi:10.1016/j.biopha.2018.11.139

DeFronzo, R. A., Ferrannini, E., Groop, L., Henry, R. R., Herman, W. H., Holst, J. J., et al. (2015). Type 2 Diabetes Mellitus. *Nat. Rev. Dis. Primers* 1, 15019–15022. doi:10.1038/nrdp.2015.19

Denu, J. M., and Dixon, J. E. (1998). Protein Tyrosine Phosphatases: Mechanisms of Catalysis and Regulation. *Curr. Opin. Chem. Biol.* 2, 633–641. doi:10.1016/S1367-5931(98)80095-1

Dewang, P. M., Hsu, N. M., Peng, S. Z., and Li, W. R. (2005). Protein Tyrosine Phosphatases and Their Inhibitors. *Curr. Med. Chem.* 12, 1–22. doi:10.2174/978160805207310940103711O.2174/0929867053363504

Dimitriadis, G. D., Maratou, E., Kountouri, A., Board, M., and Lambadiari, V. (2021). Regulation of Postabsorptive and Postprandial Glucose Metabolism by Insulin-dependent and Insulin-independent Mechanisms: An Integrative Approach. *Nutrients* 13, 1–33. doi:10.3390/nu13010159

Divya, N., Rengarajan, R. L., Radhakrishnan, R., Fathi Abd Allah, E., Alqarawi, A. A., Hashem, A., et al. (2019). Phytotherapeutic Efficacy of the Medicinal Plant *Terminalia catappa* L. *Saudi J. Biol. Sci.* 26, 985–988. doi:10.1016/j.sjbs.2018.12.010

Edirs, S., Jiang, L., Xin, X., and Aisa, H. A. (2018). Anti-diabetic Effect and Mechanism of Kursi Wufarikun Ziyabit in L6 Rat Skeletal Muscle Cells. *J. Pharmacol. Sci.* 137, 212–219. doi:10.1016/j.jphs.2018.06.011

Ekakitie, L. I., Oyinloye, B. E., and Ajiboye, B. O. (2021). The Ameliorative Activity of Chrysobalanus Orbicularis in Streptozotocin-Induced Type II Diabetes Mellitus Rat Model. *Heliyon* 7, e06596. doi:10.1016/j.heliyon.2021.e06596

Elchebly, M., Payette, P., Michaliszyn, E., Cromlish, W., Collins, S., Loy, A. L., et al. (1999). Increased Insulin Sensitivity and Obesity Resistance in Mice Lacking the Protein Tyrosine phosphatase-1B Gene. *Science* 283, 1544–1548. doi:10.1126/science.283.5407.1544

Erukainure, O. L., Ijomone, O. M., Chukwuma, C. I., Xiao, X., Salau, V. F., and Islam, M. S. (2020). Dacryodes Edulis (G. Don) H.J. Lam Modulates Glucose Metabolism, Cholinergic Activities and Nrf2 Expression, while Suppressing Oxidative Stress and Dyslipidemia in Diabetic Rats. *J. Ethnopharmacol.* 255, 112744. doi:10.1016/j.jep.2020.112744

Erukainure, O. L., Mopuri, R., Oyebode, O. A., Koorbanally, N. A., and Islam, M. S. (2017). Dacryodes Edulis Enhances Antioxidant Activities, Suppresses DNA Fragmentation in Oxidative Pancreatic and Hepatic Injuries; and Inhibits Carbohydrate Digestive Enzymes Linked to Type 2 Diabetes. *Biomed. Pharmacother.* 96, 37–47. doi:10.1016/j.biopha.2017.09.106

Erukainure, O. L., Oyebode, O. A., Ijomone, O. M., Chukwuma, C. I., Koorbanally, N. A., and Islam, M. S. (2019a). Raffia palm (Raphia Hookeri G. Mann & H. Wendl) Wine Modulates Glucose Homeostasis by Enhancing Insulin Secretion and Inhibiting Redox Imbalance in a Rat Model of Diabetes Induced by High Fructose Diet and Streptozotocin. *J. Ethnopharmacol.* 237, 159–170. doi:10.1016/j.jep.2019.03.039

Erukainure, O. L., Sanni, O., Ijomone, O. M., Ibeji, C. U., Chukwuma, C. I., and Islam, M. S. (2019b). The Antidiabetic Properties of the Hot Water Extract of Kola Nut (Cola Nitida (Vent.) Schott & Endl.) in Type 2 Diabetic Rats. *J. Ethnopharmacol.* 242, 112033. doi:10.1016/j.jep.2019.112033

Espinoza-Hernández, F., Andrade-Cetto, A., Escandón-Rivera, S., Mata-Torres, G., and Mata, R. (2021). Contribution of Fasting and Postprandial Glucose-Lowering Mechanisms to the Acute Hypoglycemic Effect of Traditionally Used Eryngium Cymosum F.Delaroche. *J. Ethnopharmacology* 279, 114339. doi:10.1016/j.jep.2021.114339

Govindarajan, S., Babu, S. N., Vijayalakshmi, M. A., Manohar, P., and Noor, A. (2021). Aloe Vera Carbohydrates Regulate Glucose Metabolism through Improved Glycogen Synthesis and Downregulation of Hepatic Gluconeogenesis in Diabetic Rats. *J. Ethnopharmacol.* 281, 114556. doi:10.1016/j.jep.2021.114556

Gujjala, S., Putakala, M., Nukala, S., Bangeppagari, M., Rajendran, R., and Desireddy, S. (2017). Modulatory Effects of Caralluma Fimbriata Extract against High-Fat Diet Induced Abnormalities in Carbohydrate Metabolism in Wistar Rats. *Biomed. Pharmacother.* 92, 1062–1072. doi:10.1016/j.biopha.2017.06.016

Guo, Y., Dai, R., Deng, Y., Sun, L., Meng, S., and Xin, N. (2019). Hypoglycemic Activity of the Extracts of Belamcanda Chinensis Leaves (BCLE) on KK-Ay Mice. *Biomed. Pharmacother.* 110, 449–455. doi:10.1016/j.biopha.2018.11.094

Guo, Z., Niu, X., Xiao, T., Lu, J., Li, W., and Zhao, Y. (2015). Chemical Profile and Inhibition of α-glycosidase and Protein Tyrosine Phosphatase 1B (PTP1B) Activities by Flavonoids from Licorice (Glycyrrhiza Uralensis Fisch). *J. Funct. Foods* 14, 324–336. doi:10.1016/j.jff.2014.12.003

Ha, M. T., Shrestha, S., Tran, T. H., Kim, J. A., Woo, M. H., Choi, J. S., et al. (2020). Inhibition of PTP1B by Farnesylated 2-arylbenzofurans Isolated from Morus alba Root Bark: Unraveling the Mechanism of Inhibition Based on *In Vitro* and In Silico Studies. *Arch. Pharm. Res.* 43, 961–975. doi:10.1007/s12272-020-01269-4

Han, H. S., Kang, G., Kim, J. S., Choi, B. H., and Koo, S. H. (2016). Regulation of Glucose Metabolism from a Liver-Centric Perspective. *Exp. Mol. Med.* 48, e218–10. doi:10.1038/emm.2015.122

Han, S.-w., Shi, S.-m., Zou, Y.-x., Wang, Z.-c., Wang, Y.-q., Shi, L., et al. (2020). Chemical Constituents from Acid Hydrolyzates of Panax Quinquefolius Total Saponins and Their Inhibition Activity to α-glycosidase and Protein Tyrosine Phosphatase 1B. *Chin. Herbal Medicines* 12, 195–199. doi:10.1016/j.chmed.2020.03.003

Hanson, R. W., and Owen, O. E. (2013). *"Gluconeogenesis," in* Metabolism Vitamins And Hormones. Elsevier, 381–386. doi:10.1016/B978-0-12-378630-2.00040-2

Hao, J., Han, L., Zhang, Y., and Wang, T. (2020). Docking Studies on Potential Mechanisms for Decreasing Insulin Resistance by the Tangzhiqing Herbal Formula. *Evidence-Based Complement. Altern. Med.* 2020, 1–11. doi:10.1155/2020/1057648

Hashimoto, N., and Goldstein, B. J. (1992). Differential Regulation of mRNAs Encoding Three Protein-Tyrosine Phosphatases by Insulin and Activation of Protein Kinase C. *Biochem. Biophys. Res. Commun.* 188, 1305–1311. doi:10.1016/0006-291X(92)91373-X

He, X. F., Chen, J. J., Li, T. Z., Zhang, X. K., Guo, Y. Q., Zhang, X. M., et al. (2020). Nineteen New Flavanol-Fatty Alcohol Hybrids with α-Glucosidase and PTP1B Dual Inhibition: One Unusual Type of Antidiabetic Constituent from Amomum Tsao-Ko. *J. Agric. Food Chem.* 68, 11434–11448. doi:10.1021/acs.jafc.0c04615

Hou, J. Q., Fan, C. L., Pei, X., Zhang, P. L., Deng, F., Jiang, W. Q., et al. (2019). Psiguadiols A-J, Rearranged Meroterpenoids as Potent PTP1B Inhibitors from Psidium Guajava. *J. Nat. Prod.* 82, 3267–3278. doi:10.1021/acs.jnatprod.9b00333

Hu, Y., Li, J., Chang, A. K., Li, Y., Tao, X., Liu, W., et al. (2021). Screening and Tissue Distribution of Protein Tyrosine Phosphatase 1B Inhibitors in Mice Following Oral Administration of Garcinia Mangostana L. Ethanolic Extract. *Food Chem.* 357, 129759–129768. doi:10.1016/j.foodchem.2021.129759

Huang, G. H., Lei, C., Zhu, K. X., Li, J. Y., Li, J., and Hou, A. J. (2019). Enantiomeric Pairs of Meroterpenoids from Rhododendron Fastigiatum. *Chin. J. Nat. Med.* 17, 963–969. doi:10.1016/S1875-5364(19)30119-0

Ighodaro, O. M., Akinloye, O. A., Ugbaja, R. N., and Omotainse, S. O. (2017). Sapium Ellipticum (Hochst) Pax Ethanol Leaf Extract Modulates Glucokinase and Glucose-6-Phosphatase Activities in Streptozotocin Induced Diabetic Rats. *Asian Pac. J. Trop. Biomed.* 7, 544–548. doi:10.1016/j.apjtb.2017.05.009

Jhuang, H. J., Hsu, W. H., Lin, K. T., Hsu, S. L., Wang, F. S., Chou, C. K., et al. (2015). Gluconeogenesis, Lipogenesis, and HBV Replication Are Commonly Regulated by PGC-1α-dependent Pathway. *Oncotarget* 6, 7788–7803. doi:10.18632/oncotarget.3050

Ji, S., Li, Z., Song, W., Wang, Y., Liang, W., Li, K., et al. (2016). Bioactive Constituents of Glycyrrhiza Uralensis (Licorice): Discovery of the Effective Components of a Traditional Herbal Medicine. *J. Nat. Prod.* 79, 281–292. doi:10.1021/acs.jnatprod.5b00877

Jiang, B.-p., Lv, Q.-y., Xiang, J.-m., Le, L., Hu, K.-p., Xu, L.-j., et al. (2018a). Inhibition of Metabolic Disorders *In Vivo* and *In Vitro* by Main Constituent of Coreopsis Tinctoria. *Chin. Herbal Medicines* 10, 157–168. doi:10.1016/j.chmed.2018.03.004

Jiang, L., Numonov, S., Bobakulov, K., Qureshi, M. N., Zhao, H., and Aisa, H. A. (2015). Phytochemical Profiling and Evaluation of Pharmacological Activities of Hypericum Scabrum L. *Molecules* 20, 11257–11271. doi:10.3390/molecules200611257

Jiang, W., Si, L., Li, P., Bai, B., Qu, J., Hou, B., et al. (2018b). Serum Metabonomics Study on Antidiabetic Effects of Fenugreek Flavonoids in Streptozotocin-Induced Rats. *J. Chromatogr. B Analyt Technol. Biomed. Life Sci.* 1092, 466–472. doi:10.1016/j.jchromb.2018.06.041

Jin, D.-X., He, J.-F., Luo, X.-G., and Zhang, T.-C. (2019). Hypoglycemic Effect of Hypericum Attenuatum Choisy Extracts on Type 2 Diabetes by Regulating Glucolipid Metabolism and Modulating Gut Microbiota. *J. Funct. Foods* 52, 479–491. doi:10.1016/j.jff.2018.11.031

Jung, H. A., Ali, M. Y., and Choi, J. S. (2016). Promising Inhibitory Effects of Anthraquinones, Naphthopyrone, and Naphthalene Glycosides, from Cassia Obtusifolia on α-Glucosidase and Human Protein Tyrosine Phosphatases 1B. *Molecules* 22, 28. doi:10.3390/molecules22010028

Jung, H. J., Seong, S. H., Ali, M. Y., Min, B. S., Jung, H. A., and Choi, J. S. (2017). α-Methyl Artoflavanocoumarin from Juniperus Chinensis Exerts Anti-diabetic Effects by Inhibiting PTP1B and Activating the PI3K/Akt Signaling Pathway in Insulin-Resistant HepG2 Cells. *Arch. Pharm. Res.* 40, 1403–1413. doi:10.1007/s12272-017-0992-0

Kasangana, P. B., Eid, H. M., Nachar, A., Stevanovic, T., and Haddad, P. S. (2019). Further Isolation and Identification of Anti-diabetic Principles from Root Bark of Myrianthus Arboreus P. Beauv.: The Ethyl Acetate Fraction Contains Bioactive Phenolic Compounds that Improve Liver Cell Glucose Homeostasis. *J. Ethnopharmacol.* 245, 112167. doi:10.1016/j.jep.2019.112167

Kasangana, P. B., Nachar, A., Eid, H. M., Stevanovic, T., and Haddad, P. S. (2018). Root Bark Extracts of Myrianthus Arboreus P. Beauv. (Cecropiaceae) Exhibit Anti-diabetic Potential by Modulating Hepatocyte Glucose Homeostasis. *J. Ethnopharmacol.* 211, 117–125. doi:10.1016/j.jep.2017.09.017

Kenner, K. A., Anyanwu, E., Olefsky, J. M., and Kusari, J. (1996). Protein-tyrosine Phosphatase 1B Is a Negative Regulator of Insulin- and Insulin-like Growth Factor-I-Stimulated Signaling. *J. Biol. Chem.* 271, 19810–19816. doi:10.1074/jbc.271.33.19810

Khanal, P., and Patil, B. M. (2021). Integration of Network and Experimental Pharmacology to Decipher the Antidiabetic Action of Duranta Repens L. *J. Integr. Med.* 19, 66–77. doi:10.1016/j.joim.2020.10.003

Kim, D. H., Jung, H. A., Sohn, H. S., Kim, J. W., and Choi, J. S. (2017a). Potential of Icariin Metabolites from Epimedium Koreanum Nakai as Antidiabetic Therapeutic Agents. *Molecules* 22. doi:10.3390/molecules22060986

Kim, D. H., Lee, S., Chung, Y. W., Kim, B. M., Kim, H., Kim, K., et al. (2016). Antiobesity and Antidiabetes Effects of a Cudrania Tricuspidata Hydrophilic Extract Presenting PTP1B Inhibitory Potential. *Biomed. Res. Int.* 2016, 8432759. doi:10.1155/2016/8432759

Kim, D. H., Paudel, P., Yu, T., Ngo, T. M., Kim, J. A., Jung, H. A., et al.(2017b). Characterization of the Inhibitory Activity of Natural Tanshinones from Salvia Miltiorrhiza Roots on Protein Tyrosine Phosphatase 1B. *Chem. Biol. Interact.* 278, 65–73. doi:10.1016/j.cbi.2017.10.013

Klaman, L. D., Boss, O., Peroni, O. D., Kim, J. K., Martino, J. L., Zabolotny, J. M., et al. (2000). Increased Energy Expenditure, Decreased Adiposity, and Tissue-specific Insulin Sensitivity in Protein-Tyrosine Phosphatase 1B-Deficient Mice. *Mol. Cel. Biol.* 20, 5479–5489. doi:10.1128/mcb.20.15.5479-5489.2000

Kowalczuk, A., Bourebaba, N., Kornicka-Garbowska, K., Turlej, E., Marycz, K., and Bourebaba, L. (2021). Hyoscyamus Albus Nortropane Alkaloids Reduce Hyperglycemia and Hyperinsulinemia Induced in HepG2 Cells through the Regulation of SIRT1/NF-kB/JNK Pathway. *Cell Commun. Signal.* 19, 61. doi:10.1186/s12964-021-00735-w

Krishnasamy, R., and Periyasamy, S. (2019). Regulating Role of Ethyl Acetate Fraction of Tephrosia Tinctoria Pers. In Carbohydrate Metabolism and Oxidative Stress in Diabetic Rats. *Biomed. Pharmacother.* 114, 108842. doi:10.1016/j.biopha.2019.108842

Krook, A., Björnholm, M., Galuska, D., Jiang, X. J., Fahlman, R., Myers, M. G., et al. (2000). Characterization of Signal Transduction and Glucose Transport in Skeletal Muscle from Type 2 Diabetic Patients. *Diabetes* 49, 284–292. doi:10.2337/diabetes.49.2.284

Kurup, S. B., and Mini, S. (2017). Protective Potential of Averrhoa Bilimbi Fruits in Ameliorating the Hepatic Key Enzymes in Streptozotocin-Induced Diabetic Rats. *Biomed. Pharmacother.* 85, 725–732. doi:10.1016/j.biopha.2016.11.088

Lang, G. Z., Li, C. J., Gaohu, T. Y., Li, C., Ma, J., Yang, J. Z., et al. (2020). Bioactive Flavonoid Dimers from Chinese Dragon's Blood, the Red Resin of Dracaena Cochinchinensis. *Bioorg. Chem.* 97, 103659. doi:10.1016/j.bioorg.2020.103659

Le, D. D., Nguyen, D. H., Zhao, B. T., Seong, S. H., Choi, J. S., Kim, S. K., et al. (2017). PTP1B Inhibitors from Selaginella Tamariscina (Beauv.) Spring and Their Kinetic Properties and Molecular Docking Simulation. *Bioorg. Chem.* 72, 273–281. doi:10.1016/j.bioorg.2017.05.001

Lee, S. Y., Lai, F. Y., Shi, L. S., Chou, Y. C., Yen, I. C., and Chang, T. C. (2015). Rhodiola Crenulata Extract Suppresses Hepatic Gluconeogenesis via Activation of the AMPK Pathway. *Phytomedicine* 22, 477–486. doi:10.1016/j.phymed.2015.01.016

Lei, C., Zhang, L.-B., Yang, J., Gao, L.-X., Li, J.-Y., Li, J., et al. (2016). Macdentichalcone, a Unique Polycyclic Dimeric Chalcone from Macaranga Denticulata. *Tetrahedron Lett.* 57, 5475–5478. doi:10.1016/j.tetlet.2016.10.090

Li, B., Fu, R., Tan, H., Zhang, Y., Teng, W., Li, Z., et al. (2021). Characteristics of the Interaction Mechanisms of Procyanidin B1 and Procyanidin B2 with Protein Tyrosine phosphatase-1B: Analysis by Kinetics, Spectroscopy Methods and Molecular Docking. *Spectrochimica Acta A: Mol. Biomol. Spectrosc.* 259, 119910. doi:10.1016/j.saa.2021.119910

Li, C., Li, C. J., Ma, J., Chen, F. Y., Li, L., Wang, X. L., et al. (2018a). Magterpenoids A-C, Three Polycyclic Meroterpenoids with PTP1B Inhibitory Activity from the Bark of Magnolia Officinalis Var. Biloba. *Org. Lett.* 20, 3682–3686. doi:10.1021/acs.orglett.8b01476

Li, C., Li, C. J., Ma, J., Huang, J. W., Wang, X. Y., Wang, X. L., et al. (2019a). Magmenthanes A-H: Eight New Meroterpenoids from the Bark of Magnolia Officinalis Var. Biloba. *Bioorg. Chem.* 88, 102948. doi:10.1016/j.bioorg.2019.102948

Li, C., Li, C. J., Xu, K. L., Ma, J., Huang, J. W., Ye, F., et al. (2020a). Novel Oligomeric Neolignans with PTP1B Inhibitory Activity from the Bark of Magnolia Officinalis Var. Biloba. *Bioorg. Chem.* 104, 104319. doi:10.1016/j.bioorg.2020.104319

Li, F., Li, Y., Li, Q., and Shi, X. (2020b). Eriobotrya Japonica Leaf Triterpenoid Acids Ameliorate Metabolic Syndrome in C57BL/6J Mice Fed with High-Fat Diet. *Biomed. Pharmacother.* 132, 110866. doi:10.1016/j.biopha.2020.110866

Li, J., Yu, H., Wang, S., Wang, W., Chen, Q., Ma, Y., et al. (2018b). Natural Products, an Important Resource for Discovery of Multitarget Drugs and Functional Food for Regulation of Hepatic Glucose Metabolism. *Drug Des. Devel. Ther.* 12, 121–135. doi:10.2147/DDDT.S151860

Li, J. L., Li, N., Xing, S. S., Zhang, N., Li, B. B., Chen, J. G., et al. (2017). New Neo-Lignan from Acanthopanax Senticosus with Protein Tyrosine Phosphatase 1B Inhibitory Activity. *Arch. Pharm. Res.* 40, 1265–1270. doi:10.1007/s12272-015-0659-7

Li, W., Pu, Z., Yi, W., Ma, Q., Lin, Q., Zhong, G., et al. (2019b). Unusual Prenylated Stilbene Derivatives with PTP1B Inhibitory Activity from Artocarpus Styracifolius. *Planta Med.* 85, 1263–1274. doi:10.1055/a-1013-1417

Li, X., Xia, H., Wang, L., Xia, G., Qu, Y., Shang, X., et al. (2019c). Lignans from the Twigs of Litsea Cubeba and Their Bioactivities. *Molecules* 24. doi:10.3390/molecules24020306

Li, Z. H., Guo, H., Xu, W. B., Ge, J., Li, X., Alimu, M., et al. (2016). Rapid Identification of Flavonoid Constituents Directly from PTP1B Inhibitive Extract of Raspberry (Rubus Idaeus L.) Leaves by HPLC-ESI-QTOF-MS-MS. *J. Chromatogr. Sci.* 54, 805–810. doi:10.1093/chromsci/bmw016

Liang, C., Staerk, D., and Kongstad, K. T. (2020). Potential of Myrtus Communis Linn. As a Bifunctional Food: Dual High-Resolution PTP1B and α-glucosidase Inhibition Profiling Combined with HPLC-HRMS and NMR for Identification of Antidiabetic Triterpenoids and Phloroglucinol Derivatives. *J. Funct. Foods* 64, 103623. doi:10.1016/j.jff.2019.103623

Liao, Z., Zhang, J., Liu, B., Yan, T., Xu, F., Xiao, F., et al. (2019). Polysaccharide from Okra (Abelmoschus Esculentus (L.) Moench) Improves Antioxidant Capacity via PI3K/AKT Pathways and Nrf2 Translocation in a Type 2 Diabetes Model. *Molecules* 24, 1906. doi:10.3390/molecules24101906

Lin, G. M., Chen, Y. H., Yen, P. L., and Chang, S. T. (2016). Antihyperglycemic and Antioxidant Activities of Twig Extract from Cinnamomum Osmophloeum. *J. Tradit. Complement. Med.* 6, 281–288. doi:10.1016/j.jtcme.2015.08.005

Lin, Y., Kuang, Y., Li, K., Wang, S., Song, W., Qiao, X., et al. (2017). Screening for Bioactive Natural Products from a 67-compound Library of Glycyrrhiza Inflata. *Bioorg. Med. Chem.* 25, 3706–3713. doi:10.1016/j.bmc.2017.05.009

Liu, Y., Wang, C., Li, J., Mei, Y., and Liang, Y. (2019). Hypoglycemic and Hypolipidemic Effects of Phellinus Linteus Mycelial Extract from Solid-State Culture in A Rat Model of Type 2 Diabetes. *Nutrients* 11, 296. doi:10.3390/nu11020296

Liu, Y. P., Li, Y. J., Zhao, Y. Y., Guo, J. M., Liu, Y. Y., Wang, X. P., et al. (2021). Carbazole Alkaloids from the Fruits of Clausena Anisum-Olens with Potential PTP1B and α-glucosidase Inhibitory Activities. *Bioorg. Chem.* 110, 104775. doi:10.1016/j.bioorg.2021.104775

Liu, Z., Cheng, Z., He, Q., Lin, B., Gao, P., Li, L., et al. (2016). Secondary Metabolites from the Flower Buds of *Lonicera japonica* and Their *In Vitro* Anti-diabetic Activities. *Fitoterapia* 110, 44–51. doi:10.1016/j.fitote.2016.02.011

Ma, Q., Wei, R., Wang, Z., Liu, W., Sang, Z., Li, Y., et al. (2017). Bioactive Alkaloids from the Aerial Parts of Houttuynia Cordata. *J. Ethnopharmacol.* 195, 166–172. doi:10.1016/j.jep.2016.11.013

Manimegalai, S., Mahboob, S., Al-Ghanim, K. A., Al-Misned, F., Govindarajan, M., Anbarasu, K., et al. (2020). Down-regulation of Hepatic G-6-Pase Expression in Hyperglycemic Rats: Intervention with Biogenic Gold Nanoconjugate. *Saudi J. Biol. Sci.* 27, 3334–3341. doi:10.1016/j.sjbs.2020.09.026

Marvibaigi, M., Hosseini, S. M., and Amini, N. (2021). Launaea Acanthodes (Boiss) O. Kuntze Mediates Hepatic Glucose Metabolism and Ameliorates Impaired Pancreatic Function in Streptozotocin-Induced Diabetic Rats. *J. Ethnopharmacol.* 268, 113577. doi:10.1016/j.jep.2020.113577

Mata-Torres, G., Andrade-Cetto, A., Espinoza-Hernández, F. A., and Cárdenas-Vázquez, R. (2020). Hepatic Glucose Output Inhibition by Mexican Plants Used in the Treatment of Type 2 Diabetes. *Front. Pharmacol.* 11, 215–219. doi:10.3389/fphar.2020.00215

Meng, Y., Ding, L., Wang, Y., Nie, Q. T., Xing, Y. Y., and Ren, Q. (2020). Phytochemical Identification of Lithocarpus Polystachyus Extracts by Ultra-high-performance Liquid Chromatography-Quadrupole Time-Of-Flight-MS and Their Protein Tyrosine Phosphatase 1B and α-glucosidase Activities. *Biomed. Chromatogr.* 34, e4705. doi:10.1002/bmc.4705

Meyerovitch, J., Backer, J. M., and Kahn, C. R. (1989). Hepatic Phosphotyrosine Phosphatase Activity and its Alterations in Diabetic Rats. *J. Clin. Invest.* 84, 976–983. doi:10.1172/JCI114261

Mlinar, B., Marc, J., Janez, A., and Pfeifer, M. (2007). Molecular Mechanisms of Insulin Resistance and Associated Diseases. *Clin. Chim. Acta* 375, 20–35. doi:10.1016/j.cca.2006.07.005

Mohanasundaram, S., Rangarajan, N., Sampath, V., Porkodi, K., and Pennarasi, M. (2021). GC-MS and HPLC Analysis of Antiglycogenolytic and Glycogenic Compounds in Kaempferol 3-O-Gentiobioside Containing *Senna alata* L Leaves in Experimental Rats. *Translational Metab. Syndr. Res.* 4, 10–17. doi:10.1016/j.tmsr.2021.07.001

Muñoz, E. B., Luna-Vital, D. A., Fornasini, M., Baldeón, M. E., and Gonzalez de Mejia, E. (2018). Gamma-conglutin Peptides from Andean Lupin Legume (Lupinus Mutabilis Sweet) Enhanced Glucose Uptake and Reduced Gluconeogenesis *In Vitro*. *J. Funct. Foods* 45, 339–347. doi:10.1016/j.jff.2018.04.021

Na, B., Nguyen, P. H., Zhao, B. T., Vo, Q. H., Min, B. S., and Woo, M. H. (2016). Protein Tyrosine Phosphatase 1B (PTP1B) Inhibitory Activity and Glucosidase Inhibitory Activity of Compounds Isolated from Agrimonia Pilosa. *Pharm. Biol.* 54, 474–480. doi:10.3109/13880209.2015.1048372

Nguyen, D. H., Seo, U. M., Zhao, B. T., Le, D. D., Seong, S. H., Choi, J. S., et al. (2017). Ellagitannin and Flavonoid Constituents from Agrimonia Pilosa Ledeb. With Their Protein Tyrosine Phosphatase and Acetylcholinesterase Inhibitory Activities. *Bioorg. Chem.* 72, 293–300. doi:10.1016/j.bioorg.2017.04.017

Nguyen, D. T., To, D. C., Tran, T. T., Tran, M. H., and Nguyen, P. H. (2021). PTP1B and α-glucosidase Inhibitors from Selaginella Rolandi-Principis and Their Glucose Uptake Stimulation. *J. Nat. Med.* 75, 186–193. doi:10.1007/s11418-020-01448-z

Nguyen, P. H., Ji, D. J., Han, Y. R., Choi, J. S., Rhyu, D. Y., Min, B. S., et al. (2015). Selaginellin and Biflavonoids as Protein Tyrosine Phosphatase 1B Inhibitors from Selaginella Tamariscina and Their Glucose Uptake Stimulatory Effects. *Bioorg. Med. Chem.* 23, 3730–3737. doi:10.1016/j.bmc.2015.04.007

Nguyen, P. H., Tuan, H. N., Hoang, D. T., Vu, Q. T., Pham, M. Q., Tran, M. H., et al. (2019). Glucose Uptake Stimulatory and PTP1B Inhibitory Activities of Pimarane Diterpenes from Orthosiphon Stamineus Benth. *Biomolecules* 9, 859. doi:10.3390/biom9120859

Niu, S. L., Tong, Z. F., Zhang, Y., Liu, T. L., Tian, C. L., Zhang, D. X., et al. (2020). Novel Protein Tyrosine Phosphatase 1B Inhibitor-Geranylated Flavonoid from Mulberry Leaves Ameliorates Insulin Resistance. *J. Agric. Food Chem.* 68, 8223–8231. doi:10.1021/acs.jafc.0c02720

Numonov, S., Edirs, S., Bobakulov, K., Qureshi, M. N., Bozorov, K., Sharopov, F., et al. (2017). Evaluation of the Antidiabetic Activity and Chemical Composition of Geranium Collinum Root Extracts-Computational and Experimental Investigations. *Molecules* 22. doi:10.3390/molecules22060983

Ojo, O. A. (2021). Puerarin as a Potential Drug Candidate for the Management of Type-2 Diabetes: Molecular Docking and Pharmacophore Modeling Studies. *Biointerface Res. Appl. Chem.* 11, 8751–8759. doi:10.33263/BRIAC112.87518759

Ovalle-Magallanes, B., Navarrete, A., Haddad, P. S., Tovar, A. R., Noriega, L. G., Tovar-Palacio, C., et al. (2019). Multi-target Antidiabetic Mechanisms of Mexicanolides from Swietenia Humilis. *Phytomedicine* 58, 152891. doi:10.1016/j.phymed.2019.152891

Page, M. J., Moher, D., Bossuyt, P. M., Boutron, I., Hoffmann, T. C., Mulrow, C. D., et al. (2021). PRISMA 2020 Explanation and Elaboration: Updated Guidance and Exemplars for Reporting Systematic Reviews. *BMJ* 372, n160. doi:10.1136/bmj.n160

Parveen, A., Farooq, M. A., and Kyunn, W. W. (2020). A New Oleanane Type Saponin from the Aerial Parts of Nigella Sativa with Anti-oxidant and Anti-diabetic Potential. *Molecules* 25, 1–13. doi:10.3390/molecules25092171

Pedersen, H. A., Ndi, C., Semple, S. J., Buirchell, B., Møller, B. L., and Staerk, D. (2020). PTP1B-Inhibiting Branched-Chain Fatty Acid Dimers from Eremophila Oppositifolia Subsp. Angustifolia Identified by High-Resolution PTP1B Inhibition Profiling and HPLC-PDA-HRMS-SPE-NMR Analysis. *J. Nat. Prod.* 83, 1598–1610. doi:10.1021/acs.jnatprod.0c00070

Pham, H. T. T., Ryu, B., Cho, H. M., Lee, B. W., Yang, W. Y., Park, E. J., et al. (2020). Oleanane Hemiacetal Glycosides from Gymnema Latifolium and Their Inhibitory Effects on Protein Tyrosine Phosphatase 1B. *Phytochemistry* 170, 112181. doi:10.1016/j.phytochem.2019.112181

Pitschmann, A., Zehl, M., Heiss, E., Purevsuren, S., Urban, E., Dirsch, V. M., et al. (2016). Quantitation of Phenylpropanoids and Iridoids in Insulin-Sensitising Extracts of Leonurus Sibiricus L. (Lamiaceae). *Phytochem. Anal.* 27, 23–31. doi:10.1002/pca.2583

Pompermaier, L., Heiss, E. H., Alilou, M., Mayr, F., Monizi, M., Lautenschlaeger, T., et al. (2018). Dihydrochalcone Glucosides from the Subaerial Parts of Thonningia Sanguinea and Their *In Vitro* PTP1B Inhibitory Activities. *J. Nat. Prod.* 81, 2091–2100. doi:10.1021/acs.jnatprod.8b00450

Postic, C., Dentin, R., and Girard, J. (2004). Role of the Liver in the Control of Carbohydrate and Lipid Homeostasis. *Diabetes Metab.* 30, 398–408. doi:10.1016/S1262-3636(07)70133-7

Qin, N. B., Jia, C. C., Xu, J., Li, D. H., Xu, F. X., Bai, J., et al. (2017). New Amides from Seeds of Silybum marianum with Potential Antioxidant and Antidiabetic Activities. *Fitoterapia* 119, 83–89. doi:10.1016/j.fitote.2017.04.008

Quang, T. H., Ngan, N. T., Yoon, C. S., Cho, K. H., Kang, D. G., Lee, H. S., et al. (2015). Protein Tyrosine Phosphatase 1B Inhibitors from the Roots of Cudrania Tricuspidata. *Molecules* 20, 11173–11183. doi:10.3390/molecules200611173

Qureshi, M. N., Numonov, S., and Aisa, H. A. (2019). Chemical and Pharmacological Evaluation of Hulls of Prunus Dulcis Nuts. *Int. J. Anal. Chem.* 2019, 5861692. doi:10.1155/2019/5861692

Reddy, A. S., and Zhang, S. (2013). Polypharmacology: Drug Discovery for the Future. *Expert Rev. Clin. Pharmacol.* 6, 41–47. doi:10.1586/ECP.12.74

Ren, C., Zhang, Y., Cui, W., Lu, G., Wang, Y., Gao, H., et al. (2015). A Polysaccharide Extract of mulberry Leaf Ameliorates Hepatic Glucose Metabolism and Insulin Signaling in Rats with Type 2 Diabetes Induced by High Fat-Diet and Streptozotocin. *Int. J. Biol. Macromol.* 72, 951–959. doi:10.1016/j.ijbiomac.2014.09.060

Riya, M. P., Antu, K. A., Pal, S., Chandrakanth, K. C., Anilkumar, K. S., Tamrakar, A. K., et al. (2015). Antidiabetic Property of Aerva Lanata (L.) Juss. Ex Schult. Is Mediated by Inhibition of Alpha Glucosidase, Protein Glycation and Stimulation of Adipogenesis. *J. Diabetes* 7, 548–561. doi:10.1111/1753-0407.12216

Rizza, R. A. (2010). Pathogenesis of Fasting and Postprandial Hyperglycemia in Type 2 Diabetes: Implications for Therapy. *Diabetes* 59, 2697–2707. doi:10.2337/db10-1032

Rothman, D. L., Magnusson, I., Katz, L. D., Shulman, R. G., and Shulman, G. I. (1991). Quantitation of Hepatic Glycogenolysis and Gluconeogenesis in Fasting Humans with 13C NMR. *Science* 254, 573–576. doi:10.1126/science.1948033

Rozenberg, K., and Rosenzweig, T. (2018). Sarcopoterium Spinosum Extract Improved Insulin Sensitivity in Mice Models of Glucose Intolerance and Diabetes. *PLoS One* 13, e0196736. doi:10.1371/journal.pone.0196736

Ryu, B., Cho, H. M., Zhang, M., Lee, B. W., Doan, T. P., Park, E. J., et al. (2021). Meroterpenoids from the Leaves of Psidium Guajava (Guava) Cultivated in Korea Using MS/MS-based Molecular Networking. *Phytochemistry* 186, 112723. doi:10.1016/j.phytochem.2021.112723

Saadeldeen, F. S. A., Niu, Y., Wang, H., Zhou, L., Meng, L., Chen, S., et al. (2020). Natural Products: Regulating Glucose Metabolism and Improving Insulin Resistance. *Food Sci. Hum. Wellness* 9, 214–228. doi:10.1016/j.fshw.2020.04.005

Saeting, O., Chandarajoti, K., Phongphisutthinan, A., Hongsprabhas, P., and Sae-Tan, S. (2021). Water Extract of Mungbean (Vigna Radiata L.) Inhibits Protein Tyrosine Phosphatase-1B in Insulin-Resistant HepG2 Cells. *Molecules* 26, 1452. doi:10.3390/molecules26051452

Sai, C.-M., Qin, N.-B., Jia, C.-C., Li, D.-H., Wang, K.-B., Pei, Y.-H., et al. (2016). Macleayine, a New Alkaloid from Macleaya Cordata. *Chin. Chem. Lett.* 27, 1717–1720. doi:10.1016/j.cclet.2016.06.017

Saifudin, A., Lallo, S. A., and Tezuka, Y. (2016a). The Potent Inhibitors of Protein Tyrosine Phosphatase 1B from the Fruits of Melaleuca Leucadendron. *Pharmacognosy Res.* 8, S38–S41. doi:10.4103/0974-8490.178644

Saifudin, A., Usia, T., AbLallo, S., Morita, H., Tanaka, K., and Tezuka, Y. (2016b). Potent Water Extracts of Indonesian Medicinal Plants against PTP1B. *Asian Pac. J. Trop. Biomed.* 6, 38–43. doi:10.1016/j.apjtb.2015.09.021

Salinas-Arellano, E., Pérez-Vásquez, A., Rivero-cruz, I., Torres-Colin, R., González-Andrade, M., Rangel-Grimaldo, M., et al. (2020). Flavonoids and Terpenoids with PTP-1B Inhibitory Properties from the Infusion of Salvia Amarissima Ortega. *Molecules* 25, 1–18. doi:10.3390/molecules25153530

Saltiel, A. R., and Kahn, C. R. (2001). Insulin Signalling and the Regulation of Glucose and Lipid Metabolism. *Nature* 414, 799–806. doi:10.1038/414799a

Sawant, L., Singh, V. K., Dethe, S., Bhaskar, A., Balachandran, J., Mundkinajeddu, D., et al. (2015). Aldose Reductase and Protein Tyrosine Phosphatase 1B Inhibitory Active Compounds from Syzygium Cumini Seeds. *Pharm. Biol.* 53, 1176–1182. doi:10.3109/13880209.2014.967784

Schultze, S. M., Hemmings, B. A., Niessen, M., and Tschopp, O. (2012). PI3K/AKT, MAPK and AMPK Signalling: Protein Kinases in Glucose Homeostasis. *Expert Rev. Mol. Med.* 14, e1–21. doi:10.1017/S1462399411002109

Selvaraj, G., Kaliamurthi, S., and Thirugnasambandan, R. (2016). Effect of Glycosin Alkaloid from *Rhizophora apiculata* in Non-insulin Dependent Diabetic Rats and its Mechanism of Action: *In Vivo* and In Silico Studies. *Phytomedicine* 23, 632–640. doi:10.1016/j.phymed.2016.03.004

Semaan, D. G., Igoli, J. O., Young, L., Gray, A. I., Rowan, E. G., and Marrero, E. (2018). *In Vitro* anti-diabetic Effect of Flavonoids and Pheophytins from Allophylus Cominia Sw. On the Glucose Uptake Assays by HepG2, L6, 3T3-L1 and Fat Accumulation in 3T3-L1 Adipocytes. *J. Ethnopharmacol.* 216, 8–17. doi:10.1016/j.jep.2018.01.014

Semaan, D. G., Igoli, J. O., Young, L., Marrero, E., Gray, A. I., and Rowan, E. G. (2017). *In Vitro* anti-diabetic Activity of Flavonoids and Pheophytins from Allophylus Cominia Sw . On PTP1B, DPPIV, Alpha-Glucosidase and Alpha-Amylase Enzymes. *J. Ethnopharmacol.* 203, 39–46. doi:10.1016/j.jep.2017.03.023

Seo, Y. S., Shon, M. Y., Kong, R., Kang, O. H., Zhou, T., Kim, D. Y., et al. (2016). Black Ginseng Extract Exerts Anti-hyperglycemic Effect via Modulation of Glucose Metabolism in Liver and Muscle. *J. Ethnopharmacol.* 190, 231–240. doi:10.1016/j.jep.2016.05.060

Seong, S. H., Roy, A., Jung, H. A., Jung, H. J., and Choi, J. S. (2016). Protein Tyrosine Phosphatase 1B and α-glucosidase Inhibitory Activities of Pueraria Lobata Root and its Constituents. *J. Ethnopharmacol.* 194, 706–716. doi:10.1016/j.jep.2016.10.007

Sharabi, K., Tavares, C. D., Rines, A. K., and Puigserver, P. (2015). Molecular Pathophysiology of Hepatic Glucose Production. *Mol. Aspects Med.* 46, 21–33. doi:10.1016/j.mam.2015.09.003

Siqueira, J. T., Batistela, E., Pereira, M. P., da Silva, V. C., de Sousa Junior, P. T., Andrade, C. M., et al. (2016). Combretum Lanceolatum Flowers Ethanol Extract Inhibits Hepatic Gluconeogenesis: an *In Vivo* Mechanism Study. *Pharm. Biol.* 54, 1671–1679. doi:10.3109/13880209.2015.1120321

Su, C., Duan, Y., Tian, J., Liu, J., Xie, K., Chen, D., et al. (2020). Morusalisins A-F, Six New Diels-Alder Type Adducts, as Potential PTP1B Inhibitors from Cell Cultures of Morus alba. *Fitoterapia* 146, 104682. doi:10.1016/j.fitote.2020.104682

Su, C., Tao, X., Yin, Z., Zhang, X., Tian, J., Chen, R., et al. (2019). Morusalones A-D, Diels-Alder Adducts with 6/7/6/6/6/6 Hexacyclic Ring Systems as Potential PTP1B Inhibitors from Cell Cultures of Morus alba. *Org. Lett.* 21, 9463–9467. doi:10.1021/acs.orglett.9b03664

Sun, J., Wang, Y., Fu, X., Chen, Y., Wang, D., Li, W., et al. (2015). Magnolia Officinalis Extract Contains Potent Inhibitors against PTP1B and Attenuates Hyperglycemia in Db/db Mice. *Biomed. Res. Int.* 2015, 139451. doi:10.1155/2015/139451

Sun, J., Qu, C., Wang, Y., Huang, H., Zhang, M., Li, H., et al. (2018). PTP1B, A Potential Target of Type 2 Diabetes Mellitus. *Mol. Biol.* 05. doi:10.4172/2168-9547.1000174

Sun, R., Deng, X., Zhang, D., Xie, F., Wang, D., Wang, J., et al. (2019). Anti-diabetic Potential of Pueraria Lobata Root Extract through Promoting Insulin Signaling by PTP1B Inhibition. *Bioorg. Chem.* 87, 12–15. doi:10.1016/j.bioorg.2019.02.046

Sureka, C., Elango, V., Al-Ghamdi, S., Aldossari, K. K., Alsaidan, M., Geddawy, A., et al. (2021). Ameliorative Property of Sesbania Grandiflora on Carbohydrate Metabolic Enzymes in the Liver and Kidney of Streptozotocin-Induced Diabetic Rats. *Saudi J. Biol. Sci.* 28, 3669–3677. doi:10.1016/j.sjbs.2021.05.002

Tahtah, Y., Wubshet, S. G., Kongstad, K. T., Heskes, A. M., Pateraki, I., Møller, B. L., et al. (2016). High-resolution PTP1B Inhibition Profiling Combined with High-Performance Liquid Chromatography-High-Resolution Mass Spectrometry-solid-phase Extraction-Nuclear Magnetic Resonance Spectroscopy: Proof-Of-Concept and Antidiabetic Constituents in Crude Extract of Eremophila Lucida. *Fitoterapia* 110, 52–58. doi:10.1016/j.fitote.2016.02.008

Tang, D., Chen, Q. B., Xin, X. L., and Aisa, H. A. (2017). Anti-diabetic Effect of Three New Norditerpenoid Alkaloids *In Vitro* and Potential Mechanism via PI3K/Akt Signaling Pathway. *Biomed. Pharmacother.* 87, 145–152. doi:10.1016/j.biopha.2016.12.058

Tian, J. L., Liao, X. J., Wang, Y. H., Si, X., Shu, C., Gong, E. S., et al. (2019). Identification of Cyanidin-3-Arabinoside Extracted from Blueberry as a Selective Protein Tyrosine Phosphatase 1B Inhibitor. *J. Agric. Food Chem.* 67, 13624–13634. doi:10.1021/acs.jafc.9b06155

Tian, J. Y., Tao, R. Y., Zhang, X. L., Liu, Q., He, Y. B., Su, Y. L., et al. (2015). Effect of *Hypericum perforatum* L. Extract on Insulin Resistance and Lipid Metabolic Disorder in High-Fat-Diet Induced Obese Mice. *Phytother. Res.* 29, 86–92. doi:10.1002/ptr.5230

Tiong, S. H., Looi, C. Y., Arya, A., Wong, W. F., Hazni, H., Mustafa, M. R., et al. (2015). Vindogentianine, a Hypoglycemic Alkaloid from Catharanthus Roseus (L.) G. Don (Apocynaceae). *Fitoterapia* 102, 182–188. doi:10.1016/j.fitote.2015.01.019

To, D. C., Bui, T. Q., Nhung, N. T. A., Tran, Q. T., Do, T. T., Tran, M. H., et al. (2021). On the Inhibitability of Natural Products Isolated from Tetradium Ruticarpum towards Tyrosine Phosphatase 1B (PTP1B) and α-Glucosidase (3W37): An *In Vitro* and In Silico Study. *Molecules* 26. doi:10.3390/molecules26123691

Tonks, N. K., Diltz, C. D., and Fischer, E. H. (1988). Characterization of the Major Protein-Tyrosine-Phosphatases of Human Placenta. *J. Biol. Chem.* 263, 6731–6737. doi:10.1016/s0021-9258(18)68703-4

Trinh, B. T., Quach, T. T., Bui, D. N., Staerk, D., Nguyen, L. D., and Jäger, A. K. (2017b). Xanthones from the Twigs of Garcinia Oblongifolia and Their Antidiabetic Activity. *Fitoterapia* 118, 126–131. doi:10.1016/j.fitote.2017.03.003

Trinh, B. T. D., Jäger, A. K., and Staerk, D. (2017a). High-Resolution Inhibition Profiling Combined with HPLC-HRMS-SPE-NMR for Identification of PTP1B Inhibitors from Vietnamese Plants. *Molecules* 22. doi:10.3390/molecules22071228

Uwazie, J. N., Yakubu, M. T., Ashafa, A. O. T., and Ajiboye, T. O. (2020). Identification and Characterization of Anti-diabetic Principle in *Senna alata* (Linn.) Flower Using Alloxan-Induced Diabetic Male Wistar Rats. *J. Ethnopharmacol.* 261, 112997. doi:10.1016/j.jep.2020.112997

Vo, Q. H., Nguyen, P. H., Zhao, B. T., Ali, M. Y., Choi, J. S., Min, B. S., et al. (2015). Protein Tyrosine Phosphatase 1B (PTP1B) Inhibitory Constituents from the Aerial Parts of Tradescantia Spathacea Sw. *Fitoterapia* 103, 113–121. doi:10.1016/j.fitote.2015.03.017

Vu, N. K., Kim, C. S., Ha, M. T., Ngo, Q. T., Park, S. E., Kwon, H., et al. (2020). Antioxidant and Antidiabetic Activities of Flavonoid Derivatives from the Outer Skins of Allium cepa L. *J. Agric. Food Chem.* 68, 8797–8811. doi:10.1021/acs.jafc.0c02122

Wang, H., Gu, D., Wang, M., Guo, H., Wu, H., Tian, G., et al. (2017a). A Strategy Based on Gas Chromatography-Mass Spectrometry and Virtual Molecular Docking for Analysis and Prediction of Bioactive Composition in Natural Product Essential Oil. *J. Chromatogr. A.* 1501, 128–133. doi:10.1016/j.chroma.2017.04.031

Wang, J., Huang, Y., Li, K., Chen, Y., Vanegas, D., McLamore, E. S., et al. (2016a). Leaf Extract from Lithocarpus Polystachyus Rehd. Promote Glycogen Synthesis in T2DM Mice. *PLoS One* 11, e0166557. doi:10.1371/journal.pone.0166557

Wang, J., Yang, J. L., Zhou, P. P., Meng, X. H., and Shi, Y. P. (2017b). Further New Gypenosides from Jiaogulan (Gynostemma Pentaphyllum). *J. Agric. Food Chem.* 65, 5926–5934. doi:10.1021/acs.jafc.7b01477

Wang, L.-J., Xiong, J., Zou, Y., Mei, Q.-B., Wang, W.-X., and Hu, J.-F. (2016b). Sesquiterpenoids from the Chinese Endangered Plant Manglietia Aromatica. *Phytochemistry Lett.* 18, 202–207. doi:10.1016/j.phytol.2016.10.018

Wang, M., Yu, B. W., Yu, M. H., Gao, L. X., Li, J. Y., Wang, H. Y., et al. (2015). New Isoprenylated Phenolic Compounds from Morus Laevigata. *Chem. Biodivers.* 12, 937–945. doi:10.1002/cbdv.201400210

Wu, Y., Ouyang, J. P., Wu, K., Wang, S. S., Wen, C. Y., and Xia, Z. Y. (2005). Rosiglitazone Ameliorates Abnormal Expression and Activity of Protein Tyrosine Phosphatase 1B in the Skeletal Muscle of Fat-Fed, Streptozotocin-Treated Diabetic Rats. *Br. J. Pharmacol.* 146, 234–243. doi:10.1038/sj.bjp.0706306

Xiao, T., Guo, Z., Sun, B., and Zhao, Y. (2017b). Identification of Anthocyanins from Four Kinds of Berries and Their Inhibition Activity to α-Glycosidase and Protein Tyrosine Phosphatase 1B by HPLC-FT-ICR MS/MS. *J. Agric. Food Chem.* 65, 6211–6221. doi:10.1021/acs.jafc.7b02550

Xiao, T., Guo, Z., Bi, X., and Zhao, Y. (2017a). Polyphenolic Profile as Well as Anti-oxidant and Anti-diabetes Effects of Extracts from Freeze-Dried Black Raspberries. *J. Funct. Foods* 31, 179–187. doi:10.1016/j.jff.2017.01.038

Xiong, J., Hu, C. L., Wang, P. P., Gao, D. D., Huang, F., Li, J., et al. (2020). Spirobiflavonoid Stereoisomers from the Endangered conifer Glyptostrobus Pensilis and Their Protein Tyrosine Phosphatase 1B Inhibitory Activity. *Bioorg. Med. Chem. Lett.* 30, 126943. doi:10.1016/j.bmcl.2019.126943

Xiong, J., Wan, J., Ding, J., Wang, P. P., Ma, G. L., Li, J., et al. (2017). Camellianols A-G, Barrigenol-like Triterpenoids with PTP1B Inhibitory Effects from the Endangered Ornamental Plant Camellia Crapnelliana. *J. Nat. Prod.* 80, 2874–2882. doi:10.1021/acs.jnatprod.7b00241

Xu, J., Wang, X., Yue, J., Sun, Y., Zhang, X., and Zhao, Y. (2018b). Polyphenols from Acorn Leaves (Quercus Liaotungensis) Protect Pancreatic Beta Cells and Their Inhibitory Activity against α-Glucosidase and Protein Tyrosine Phosphatase 1B. *Molecules* 23. doi:10.3390/molecules23092167

Xu, J., Yang, L., Wang, R., Zeng, K., Fan, B., and Zhao, Z. (2019a). The Biflavonoids as Protein Tyrosine Phosphatase 1B Inhibitors from Selaginella Uncinata and Their Antihyperglycemic Action. *Fitoterapia* 137, 104255. doi:10.1016/j.fitote.2019.104255

Xu, J., Cao, J., Yue, J., Zhang, X., and Zhao, Y. (2018a). New Triterpenoids from Acorns of Quercus Liaotungensis and Their Inhibitory Activity against α -glucosidase, α -amylase and Protein-Tyrosine Phosphatase 1B. *J. Funct. Foods* 41, 232–239. doi:10.1016/j.jff.2017.12.054

Xu, L., Li, Y., Dai, Y., and Peng, J. (2018c). Natural Products for the Treatment of Type 2 Diabetes Mellitus: Pharmacology and Mechanisms. *Pharmacol. Res.* 130, 451–465. doi:10.1016/j.phrs.2018.01.015

Xu, Q. Q., Chen, X. L., Xu, J. F., Wang, S. B., Luo, J. G., and Kong, L. Y. (2019b). Acetophenone Derivatives from the Roots of Melicope Ptelefolia. *Fitoterapia* 132, 40–45. doi:10.1016/j.fitote.2018.11.013

Yan, H. W., Zhu, H., Yuan, X., Yang, Y. N., Feng, Z. M., Jiang, J. S., et al. (2019). Eight New Biflavonoids with Lavandulyl Units from the Roots of Sophora Flavescens and Their Inhibitory Effect on PTP1B. *Bioorg. Chem.* 86, 679–685. doi:10.1016/j.bioorg.2019.01.058

Yang, J. B., Ye, F., Tian, J. Y., Song, Y. F., Gao, H. Y., Liu, Y., et al. (2020). Multiflorumisides HK, Stilbene Glucosides Isolated from Polygonum Multiflorum and Their *In Vitro* PTP1B Inhibitory Activities. *Fitoterapia* 146, 104703. doi:10.1016/j.fitote.2020.104703

Yang, J. L., Ha, T. K. Q., Lee, B. W., Kim, J., and Oh, W. K. (2017). PTP1B Inhibitors from the Seeds of Iris Sanguinea and Their Insulin Mimetic Activities via AMPK and ACC Phosphorylation. *Bioorg. Med. Chem. Lett.* 27, 5076–5081. doi:10.1016/j.bmcl.2017.09.031

Yang, N., Zhang, S., Yang, S., Guo, Z., Zhang, X., and Zhao, Y. (2016). The Inhibition of α-glycosidase and Protein Tyrosine Phosphatase 1B (PTP1B) Activities by Ginsenosides from Panax Ginseng C.A. Meyer and Simultaneous Determination by HPLC-ELSD. *J. Funct. Foods* 23, 188–197. doi:10.1016/j.jff.2015.12.018

Yin, X., Huang, Y., Jung, D. W., Chung, H. C., Choung, S. Y., Shim, J. H., et al. (2015). Anti-Diabetic Effect of Aster Sphathulifolius in C57BL/KsJ-Db/db Mice. *J. Med. Food* 18, 987–998. doi:10.1089/jmf.2014.3416

Yousof Ali, M., Jung, H. A., and Choi, J. S. (2015). Anti-diabetic and Anti-alzheimer's Disease Activities of Angelica Decursiva. *Arch. Pharm. Res.* 38, 2216–2227. doi:10.1007/s12272-015-0629-0

Yu, J. H., Liu, Q. F., Sheng, L., Wang, G. C., Li, J., and Yue, J. M. (2016a). Cipacinoids A-D, Four Limonoids with Spirocyclic Skeletons from Cipadessa Cinerascens. *Org. Lett.* 18, 444–447. doi:10.1021/acs.orglett.5b03487

Yu, Y., Gan, L. S., Yang, S. P., Sheng, L., Liu, Q. F., Chen, S. N., et al. (2016b). Eucarobustols A-I, Conjugates of Sesquiterpenoids and Acylphloroglucinols from Eucalyptus Robusta. *J. Nat. Prod.* 79, 1365–1372. doi:10.1021/acs.jnatprod.6b00090

Yuan, Y. C., Bai, X. L., Liu, Y. M., Tang, X. Y., Yuan, H., and Liao, X. (2021). Ligand Fishing Based on Cell Surface Display of Enzymes for Inhibitor Screening. *Anal. Chim. Acta* 1156, 338359. doi:10.1016/j.aca.2021.338359

Yue, J., Xu, J., Cao, J., Zhang, X., and Zhao, Y. (2017). Cucurbitane Triterpenoids from Momordica Charantia L. And Their Inhibitory Activity against α-glucosidase, α-amylase and Protein Tyrosine Phosphatase 1B (PTP1B). *J. Funct. Foods* 37, 624–631. doi:10.1016/j.jff.2017.07.041

Zakłos-Szyda, M., and Pawlik, N. (2018). Japanese Quince (Chaenomeles Japonica L.) Fruit Polyphenolic Extract Modulates Carbohydrate Metabolism in HepG2 Cells via AMP-Activated Protein Kinase. *Acta Biochim. Pol.* 65, 67–78. doi:10.18388/abp.2017_1604

Zhang, C. C., Geng, C. A., Huang, X. Y., Zhang, X. M., and Chen, J. J. (2019a). Antidiabetic Stilbenes from Peony Seeds with PTP1B, α-Glucosidase, and DPPIV Inhibitory Activities. *J. Agric. Food Chem.* 67, 6765–6772. doi:10.1021/acs.jafc.9b01193

Zhang, P. Z., Gu, J., and Zhang, G. L. (2015). Novel Stilbenes from Artocarpus Nanchuanensis. *J. Asian Nat. Prod. Res.* 17, 217–223. doi:10.1080/10286020.2015.1006202

Zhang, R., Yu, R., Xu, Q., Li, X., Luo, J., Jiang, B., et al. (2017). Discovery and Evaluation of the Hybrid of Bromophenol and Saccharide as Potent and Selective Protein Tyrosine Phosphatase 1B Inhibitors. *Eur. J. Med. Chem.* 134, 24–33. doi:10.1016/j.ejmech.2017.04.004

Zhang, S. N., Zeng, J., Tan, Y. N., Ma, R. J., Zhang, G. J., Wang, H. S., et al. (2019b). 3α,19-Dihydroxyl-ent-pimara-8(14),15-diene, a New Diterpenoid from the Rhizomes of Ricinus communis. *J. Asian Nat. Prod. Res.* 21, 522–527. doi:10.1080/10286020.2018.1461087

Zhang, W., Hong, D., Zhou, Y., Zhang, Y., Shen, Q., Li, J. Y., et al. (2006). Ursolic Acid and its Derivative Inhibit Protein Tyrosine Phosphatase 1B, Enhancing Insulin Receptor Phosphorylation and Stimulating Glucose Uptake. *Biochim. Biophys. Acta* 1760, 1505–1512. doi:10.1016/j.bbagen.2006.05.009

Zhang, X., Lv, Q., Jia, S., Chen, Y., Sun, C., Li, X., et al. (2016a). Effects of flavonoid-rich Chinese bayberry (Morella rubra Sieb. et Zucc.) fruit extract on regulating glucose and lipid metabolism in diabetic KK-A(y) mice. *Food Funct.* 7, 3130–3140. doi:10.1039/c6fo00397d

Zhang, X. Y., Li, W., Wang, J., Li, N., Cheng, M. S., and Koike, K. (2019c). Protein Tyrosine Phosphatase 1B Inhibitory Activities of Ursane-type Triterpenes from Chinese Raspberry, Fruits of Rubus Chingii. *Chin. J. Nat. Med.* 17, 15–21. doi:10.1016/S1875-5364(19)30004-4

Zhang, Y., Chen, J., Zeng, Y., Huang, D., and Xu, Q. (2019d). Involvement of AMPK Activation in the Inhibition of Hepatic Gluconeogenesis by Ficus Carica Leaf Extract in Diabetic Mice and HepG2 Cells. *Biomed. Pharmacother.* 109, 188–194. doi:10.1016/j.biopha.2018.10.077

Zhang, Y., Feng, F., Chen, T., Li, Z., and Shen, Q. W. (2016b). Antidiabetic and Antihyperlipidemic Activities of Forsythia Suspensa (Thunb.) Vahl (Fruit) in Streptozotocin-Induced Diabetes Mice. *J. Ethnopharmacol.* 192, 256–263. doi:10.1016/j.jep.2016.07.002

Zhang, Y., Yan, L. S., Ding, Y., Cheng, B. C. Y., Luo, G., Kong, J., et al. (2020). Edgeworthia Gardneri (Wall.) Meisn. Water Extract Ameliorates Palmitate Induced Insulin Resistance by Regulating IRS1/GSK3β/FoxO1 Signaling Pathway in Human HepG2 Hepatocytes. *Front. Pharmacol.* 10, 1666. doi:10.3389/fphar.2019.01666

Zhao, B. T., Le, D. D., Nguyen, P. H., Ali, M. Y., Choi, J. S., Min, B. S., et al. (2016). PTP1B, α-glucosidase, and DPP-IV Inhibitory Effects for Chromene Derivatives from the Leaves of Smilax china L. *Chem. Biol. Interact.* 253, 27–37. doi:10.1016/j.cbi.2016.04.012

Zhao, C. C., Chen, J., Shao, J. H., Zhang, X. H., Gu, W. Y., Shen, J., et al. (2020). Lignan Constituents from the Fruits of Viburnum Macrocephalum F. Keteleeri and Their α-Amylase, α-Glucosidase, and Protein Tyrosine Phosphatase 1B Inhibitory Activities. *J. Agric. Food Chem.* 68, 11151–11160. doi:10.1021/acs.jafc.0c03353

Zhao, Y., Chen, M. X., Kongstad, K. T., Jäger, A. K., and Staerk, D. (2017). Potential of Polygonum Cuspidatum Root as an Antidiabetic Food: Dual High-Resolution α-Glucosidase and PTP1B Inhibition Profiling Combined with HPLC-HRMS and NMR for Identification of Antidiabetic Constituents. *J. Agric. Food Chem.* 65, 4421–4427. doi:10.1021/acs.jafc.7b01353

Zhao, Y., Kjaerulff, L., Kongstad, K. T., Heskes, A. M., Møller, B. L., and Staerk, D. (2019a). 2(5H)-Furanone Sesquiterpenes from *Eremophila bignoniiflora*: High-Resolution Inhibition Profiling and PTP1B Inhibitory Activity. *Phytochemistry* 166, 112054. doi:10.1016/j.phytochem.2019.112054

Zhao, Y., Kongstad, K. T., Liu, Y., He, C., and Staerk, D. (2019b). Unraveling the Complexity of Complex Mixtures by Combining High-Resolution Pharmacological, Analytical and Spectroscopic Techniques: Antidiabetic Constituents in Chinese Medicinal Plants. *Faraday Discuss.* 218, 202–218. doi:10.1039/c8fd00223a

Zhao, Y., Kongstad, K. T., Jäger, A. K., Nielsen, J., and Staerk, D. (2018). Quadruple High-Resolution α-glucosidase/α-amylase/PTP1B/radical Scavenging Profiling Combined with High-Performance Liquid Chromatography-High-Resolution Mass Spectrometry-solid-phase Extraction-Nuclear Magnetic Resonance Spectroscopy for Identification of Antidiabetic Constituents in Crude Root Bark of Morus alba L. *J. Chromatogr. A* 1556, 55–63. doi:10.1016/j.chroma.2018.04.041

Zheng, X. M., Meng, F. W., Geng, F., Qi, M., Luo, C., Yang, L., et al. (2015). Plantadeprate A, a Tricyclic Monoterpene Zwitterionic Guanidium, and Related Derivatives from the Seeds of Plantago Depressa. *J. Nat. Prod.* 78, 2822–2826. doi:10.1021/acs.jnatprod.5b00368

Zhou, J., Wu, Z., Oyawaluja, B. O., Coker, H. A. B., Odukoya, O. A., Yao, G., et al. (2019). Protein Tyrosine Phosphatase 1B Inhibitory Iridoids from Psydrax Subcordata. *J. Nat. Prod.* 82, 2916–2924. doi:10.1021/acs.jnatprod.9b00770

Zhou, X., Wang, L. L., Tang, W. J., and Tang, B. (2021). Astragaloside IV Inhibits Protein Tyrosine Phosphatase 1B and Improves Insulin Resistance in Insulin-Resistant HepG2 Cells and Triglyceride Accumulation in Oleic Acid (OA)-treated HepG2 Cells. *J. Ethnopharmacol.* 268, 113556. doi:10.1016/j.jep.2020.113556

Zhu, Y., Huang, J. J., Zhang, X. X., Yan, Y., Yin, X. W., Ping, G., et al. (2018). Qing Gan Zi Shen Tang Alleviates Adipose Tissue Dysfunction with Up-Regulation of SIRT1 in Spontaneously Hypertensive Rat. *Biomed. Pharmacother.* 105, 246–255. doi:10.1016/j.biopha.2018.05.022

Conflict of Interest: The authors declare that the research was conducted in the absence of any commercial or financial relationships that could be construed as a potential conflict of interest.

Publisher's Note: All claims expressed in this article are solely those of the authors and do not necessarily represent those of their affiliated organizations, or those of the publisher, the editors and the reviewers. Any product that may be evaluated in this article, or claim that may be made by its manufacturer, is not guaranteed or endorsed by the publisher.

frontiers in Pharmacology

ORIGINAL RESEARCH
published: 19 January 2022
doi: 10.3389/fphar.2021.773957

Integrating Network Analysis and Metabolomics to Reveal Mechanism of Huaganjian Decoction in Treatment of Cholestatic Hepatic Injury

Qin Dong[1], Jiao Chen[1], Yan-Ping Jiang[1], Zong-Ping Zhu[1], Yong-Feng Zheng[1], Jin-Ming Zhang[1], Zhen Zhang[1], Wen-Qing Chen[2], Shi-Yi Sun[1], Lan Pang[1], Xin Yan[3], Wan Liao[1] and Chao-Mei Fu[1]**

[1]State Key Laboratory of Southwestern Chinese Medicine Resources, Pharmacy College, Chengdu University of Traditional Chinese Medicine, Chengdu, China, [2]Department of Biology, Hong Kong Baptist University, Hong Kong, China, [3]Chengdu Institute of Chinese Herbal Medicine, Chengdu, China

OPEN ACCESS

Edited by:
Zhong-qiu Liu,
Guangzhou University of Chinese Medicine, China

Reviewed by:
Elisa Lozano,
University of Salamanca, Spain
Gang Cao,
Zhejiang Chinese Medical University, China

***Correspondence:**
Wan Liao
liaowan@cdutcm.edu.cn
Chao-Mei Fu
chaomeifu@126.com

Specialty section:
This article was submitted to Ethnopharmacology, a section of the journal Frontiers in Pharmacology

Received: 10 September 2021
Accepted: 22 December 2021
Published: 19 January 2022

Citation:
Dong Q, Chen J, Jiang Y-P, Zhu Z-P, Zheng Y-F, Zhang J-M, Zhang Z, Chen W-Q, Sun S-Y, Pang L, Yan X, Liao W and Fu C-M (2022) Integrating Network Analysis and Metabolomics to Reveal Mechanism of Huaganjian Decoction in Treatment of Cholestatic Hepatic Injury. Front. Pharmacol. 12:773957. doi: 10.3389/fphar.2021.773957

Huaganjian decoction (HGJD) was first recorded in the classic "*Jing Yue Quan Shu*" during the Ming dynasty, and it has been extensively applied in clinical practice to treat liver diseases for over 300 years in China. However, its bioactive constituents and relevant pharmacological mechanism are still unclear. In this study, a strategy integrating network analysis and metabolomics was applied to reveal mechanism of HGJD in treating cholestatic hepatic injury (CHI). Firstly, we observed the therapeutic effect of HGJD against CHI with an alpha-naphthylisothiocyanate (ANIT) induced CHI rat model. Then, we utilized UPLC-Q-Exactive MS/MS method to analyze the serum migrant compounds of HGJD in CHI rats. Based on these compounds, network analysis was conducted to screen for potential active components, and key signaling pathways interrelated to therapeutic effect of HGJD. Meanwhile, serum metabolomics was utilized to investigate the underlying metabolic mechanism of HGJD against CHI. Finally, the predicted key pathway was verified by western blot and biochemical analysis using rat liver tissue from *in vivo* efficacy experiment. Our results showed that HGJD significantly alleviated ANIT induced CHI. Totally, 31 compounds originated from HGJD have been identified in the serum sample. PI3K/Akt/Nrf2 signaling pathway related to GSH synthesis was demonstrated as one of the major pathways interrelated to therapeutic effect of HGJD against CHI. This research supplied a helpful strategy to determine the potential bioactive compounds and mechanism of traditional Chinese medicine.

Keywords: huaganjian decoction, cholestatic hepatic injury, metabolomics, serum pharmacochemistry, network analysis

1 INTRODUCTION

Cholestatic hepatic injury (CHI) occurs mainly due to intrahepatic cholestasis. Its main characteristics are aberrant metabolism of bile acid and accumulating of toxic bile acids in the liver. Signals such as oxidative stress and inflammatory responses are activated, leading to parenchymal cell death of liver and bile duct (Cai and Boyer, 2021). Without proper treatment, CHI may further develop into fibrosis, cirrhosis, hepatocellular carcinoma and eventually liver failure

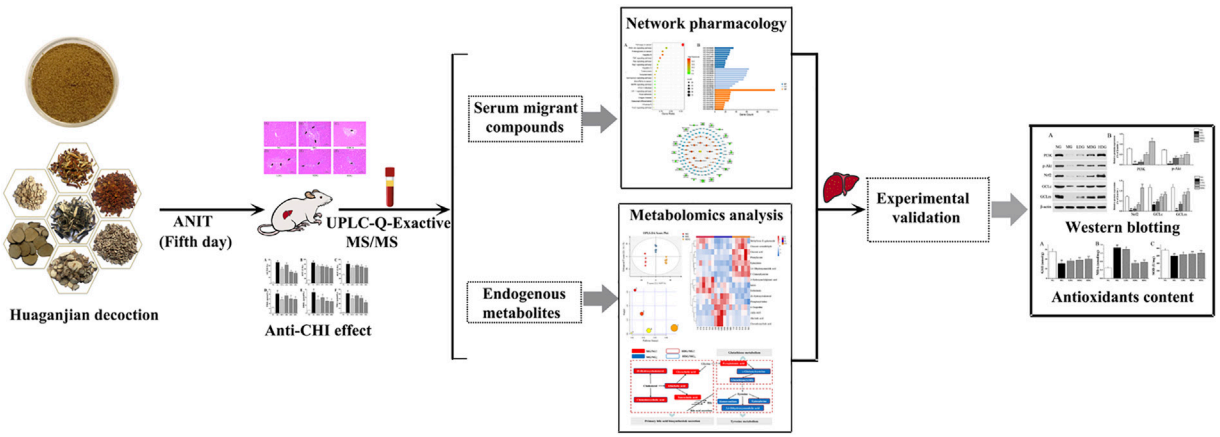

FIGURE 1 | The graphical abstract of this study.

(Pollock and Minuk, 2017). Currently, ursodeoxycholic acid (UDCA), and obeticholic acid (OCA) are main therapeutic options for CHI (Hohenester and Beuers, 2017). However, some patients have an inadequate response to UDCA therapy and the side effects of OCA in this treatment remain to be improved (Hirschfield et al., 2015; Kowdley et al., 2018).

In recent years, with rapid preclinical and clinical research of traditional Chinese medicine (TCM), TCM has shown advantage in clinical practice to treat CHI. Huaganjian decoction (HGJD) is a classic Chinese medicine formula, which is first recorded in the classic "*Jing Yue Quan Shu*" during the Ming dynasty. This formula is composed of 7 botanical drugs: Citri Reticulatae Pericarpium Viride (*Citrus reticulata* Blanco, Qingpi, 7.5 g), Gardeniae Fructus (*Gardenia jasminoides* Ellis, Zhizi, 5.6 g), Paeoniae Radix Alba (*Paeonia lactiflora* Pall., Baishao, 7.5 g), Moutan Cortex (*Paeonia suffruticosa* Andr., Mudanpi, 5.6 g), Alismatis Rhizaoma (*Alisma plantago-aquatica* Linn., Zexie, 5.6 g), Fritillariae Thunbergii Bulbus (*Fritillaria thunbergii* Miq., Zhebeimu, 11.2 g), and Citri Reticulatae Pericarpium (*Citrus reticulata* Blanco., Chenpi, 7.5 g). It is characterized by comprehensive therapy, which can relieve stagnation of liver qi, extenuate liver fire, and invigorate liver blood. It was widely used in the clinical practice to protect against liver injury (He, 2009; Liu L F et al., 2019; Li, 2021). Moreover, HGJD has been listed as one of the 100 ancient classic prescriptions highly valued by the Chinese government. According to modern medical research, HGJD could promote bile excretion, protect liver cells, and inhibit the proliferation of activated hepatic stellate cells HSC-T6 (Gao et al., 2019). Qingpi was the principle drug of HGJD, which could protect against liver damage caused by carbon tetrachloride and promote bile excretion (Jin et al., 2007). Zhizi was the minister drug of HGJD, which could attenuate live cell injury and fibrosis as demonstrated in both animal and human studies (Chen et al., 2012). However, the specific mechanism of HGJD protecting against CHI is still not revealed. Besides, the bioactive compounds that contribute to its therapeutic efficacy remain unclear.

In this research, a comprehensive method integrating network analysis and metabolomics was used to illustrate mechanism of HGJD in treating CHI. Firstly, we observed the therapeutic effect of HGJD against CHI by evaluating the serum biochemical indices and histopathology of liver with an ANIT induced CHI rat model. Then, we utilized UPLC-Q-Exactive MS/MS method to analyze the serum migrant compounds of HGJD in ANIT induced CHI rat model. Network analysis based on serum migrant compounds of HGJD was used to explore the correlations among potential active ingredients, targets and signaling pathways interrelated to therapeutic effect of HGJD. Meanwhile, non-target serum metabolomics were applied to investigate the underlying metabolic mechanism of HGJD against CHI. Finally, we further validated the predicted pathway by western blot and biochemical analysis using rat liver tissue from *in vivo* efficacy experiment. This research would offer experimental basis for further research on HGJD in treatment of CHI, and offer a novel insight into improving the treatment for CHI. A graphical abstract of this study is presented in **Figure 1**.

2 MATERIALS AND METHODS

2.1 Chemicals and Reagents

All 22 standard compounds used in this study (synephrine, gallic acid, chlorogenic acid, geniposide, peimine, peiminine, albiflorin, paeoniflorin, rutin, narirutin, crocin, naringin, hesperidin, neohesperidin, didymin, quercetin, benzoylpaeoniflorin, paeonol, sinensetin, nobiletin, hepta-3, and alisol B 23-acetate) were supplied by Weikeqi Biotechnology Co., Ltd (Chengdu, China), and the purity were all greater than 98%. UDCA administrated as positive control was supplied by Shanghai Aladdin Biochemical Co., Ltd. (Shanghai, China). ANIT and medical-grade soybean oil were purchased from Shanghai Aladdin Biochemical Co., Ltd. (Shanghai, China). β-actin was obtained from Wuhan Servicebio Technology Co., Ltd. (Wuhan, China). Antibody PI3K was purchased from Beijing Boaosen

Biotechnology Co., Ltd. (Beijing, China). Antibody p-AKT was bought from Affinity Biosciences Ltd. (Jiangsu, China). Antibody Nrf2 was purchased from Wuhan Sanying Biotechnology Co., Ltd. (Wuhan, China). Antibody GCLc and GCLm were obtained from abcam (Cambridge, United Kingdom). Commercially available kits were provided by Nanjing Jian cheng Institute of Biotechnology (Nanjing, China) and Changchun Huili Biological Technology Co., Ltd. (Changchun, China). All other chemicals and reagents were belonged to analytical grade, and were purchased from commercial sources.

All botanical drugs in the HGJD formula were bought from Sichuan Neautus TCM Co., Ltd (Chengdu, China) and identified by Professor Guihua Jiang of the School of Pharmacy, Chengdu University of Traditional Chinese Medicine.

2.2 Preparation of HGJD Samples

The botanical drug mixture of Citri Reticulatae Pericarpium Viride, Gardeniae Fructus, Paeoniae Radix Alba, Moutan Cortex, Alismatis Rhizaoma, Fritillariae Thunbergii Bulbus, and Citri Reticulatae Pericarpium (4: 3: 4: 3: 3: 6: 4) was soaked with 9 vol. distilled water for 30 min and maintained boiling for 25 min. The extraction solution was filtered and evaporated under reduced pressure to the weight of the original mixture. Finally, freeze drying was carried out for concentrated extract to obtain lyophilized powder. The lyophilized powder yield was about 33.12%. The lyophilized powder was stored in different airtight packages before chemical and pharmacological studies. Quality control of the sample was led according to our previous research (Nie et al., 2020). Moreover, UPLC-Q-Exactive MS/MS was used to analyze the chemical composition of HGJD sample (**Supplementary Figure S1**; **Supplementary Table S1**). Every day before administration, lyophilized powder of HGJD was dissolved in different volumes of water to prepare low (0.15 g/ml), medium (0.30 g/ml) and high dosage (0.60 g/ml) samples.

2.3 Animals

SPF Male Sprague-Dawley (SD) rats (220 ± 20 g) were purchased from Beijing Sibefu Biotechnology Co., Ltd. (Beijing, China) (Certificate No. SCXK (Jing) 2019–0010). Animal Ethics Committee of Chengdu University of TCM (Chengdu, China) approved this experiment, and international rules for care and use of laboratory animals were strictly followed. The room temperature was regulated at 20 ± 2°C with 50 ± 20% humidity and equipped with a 12 h light/dark cycle. We allowed the rats to eat pure water and food freely. All animals were adapted to the conditions for 1 week.

2.4 Anti-CHI Effect of HGJD

2.4.1 Animal Treatment

Thirty-six rats were randomly divided into six groups on average. Normal group (NG) and model group (MG) were received gavage of saline once daily for seven consecutive days. UDCA treated positive group (UDCA, 100 mg/kg), and three HGJD groups treated with low (LDG, 1.50 g/kg, extracts), medium (MDG, 3.01 g/kg, extracts), and high dosages (HDG, 6.02 g/kg, extracts) were received oral administration once daily for seven consecutive days. The adult dosage of HGJD is 50.50 g (crude drug) daily. Based on the body surface area index and lyophilized powder yield (33.12%) (Nair et al., 2018), the animal dosage of HGJD is calculated, and low animal dosage equals to the clinical dosage. On the fifth day, normal group was received the vehicle (soybean oil) treatment by gavage, and the other groups were received 60 mg/kg ANIT dissolved in an equal volume of soybean oil by gavage. According to previous studies, this dose was known to induce cholestasis.

The rats were maintained fasting for 12 h before receiving the last dose of HGJD. 1 h after the last dose, rats were anesthetized with pentobarbital. Blood samples were collected from abdominal aorta. After that, the rats were sacrificed. Liver samples were dissected, and rinsed once with ice-cold normal saline. One part of each liver sample was stored at −80°C for western blot and biochemical index analysis, and the remaining specimens were set in 10% PBS-buffered formalin for histopathological analysis.

2.4.2 Assays of the Serum Enzymes and Components

The contents of alanine transaminase (ALT), aspartate transaminase (AST), alkaline phosphatase (ALP), γ-glutamyltranspeptidase (γ-GT), total bilirubin (TBIL), direct bilirubin (DBIL), and total bile acid (TBA) in serum were determined by commercial test kits.

2.4.3 Histological Examination

The liver tissue fixed with 10% PBS-buffered formalin, were embedded in paraffin, serially sectioned (5 μm), and stained with nuclear dye (hematoxylin) and counterstain (eosin) for histological examination. Optical microscopy was applied to examine the histological section.

2.5 Identification of Serum Migrant Compounds of HGJD

2.5.1 Animal Treatment

Six rats received oral administration of HGJD (6.02 g/kg) for 7 consecutive days. At fifth day, ANIT was orally administrated to rats in both the model group and the dose group. On the seventh day, after the orally administration of HGJD at 15 min, 30 min, 1, 2, 4, and 6 h, blood samples were taken from the angular vein of each rat. The serum samples collected from each rat at the different time points were mixed before sample processing.

2.5.2 Preparation of Samples

10 ml of 50% methanol was applied to dissolve HGJD powder (0.1 g), and then the samples were extracted for 30 min by ultrasonic extraction. The mixture was centrifuged at 13,000 rpm maintained for 15 min. Filter membrane (0.22 μm) was used to filter the supernatant to obtain an injection sample.

1 ml serum sample was added with 3 ml methanol, then vortexed for 30 s and centrifuged at 13,000 rpm 4°C for 15 min to precipitate the protein. The supernatant was collected and dried with a nitrogen blowing concentrator. The residue was dissolved with 500 μl of 50% methanol, and repeated the centrifugation procedure. Then, a filter membrane (0.22 μm) was used to filter the supernatant to obtain an injection sample.

2.5.3 UPLC-Q-Exactive MS/MS Analysis

The Vanquish UHPLC system (Thermo Fisher Scientific, United States) equipped with Q Exactive quadrupole-electrostatic field orbitrap high-resolution mass spectrometer was applied to analyze HGJD powder and serum samples. Samples were separated on an ACQUITY UPLC®BEH C_{18} column (2.1 × 100 mm 1.7 μm, Waters, United States). The mobile phase consisted of deionized water with 0.1% formic acid (A) and acetonitrile (B). The gradient elution procedure was as follows: 0–35 min, 5–95% B; 35–40 min, 95% B. The column temperature was maintained at 30°C. The flow rate was set at 0.4 ml/min.

All samples were analyzed in positive and negative ion modes, respectively. Mass spectrometry parameters were set as follows: nitrogen was selected as auxiliary gas and sheath gas. Flow rate was 10 L/min in positive mode and 35 L/min in negative mode. The voltage of the ion spray was 3 kV and −2.5 kV separately. The ion source temperature was kept at 320°C. Auxiliary gas heating temperature was maintained at 350°C. The fragment voltage was 50 V. Scan mass ratio was within the mass range of m/z 50–1000.

Compound Discoverer software (Thermo Fisher Scientific) was applied to analyze the LC-MS data. Components were identified by comparison of chemical information of reference substances, and initially identified with online databases (MZ cloud, MZ vault) and literatures.

2.6 Network Analysis

2.6.1 Target Prediction of the Active Ingredients of HGJD Against CHI

The serum migrant components which were regarded as potential effective ingredients were applied to identify potential treatment targets of HGJD against CHI. Meanwhile, several online databases have contributed to the research of possible therapeutic targets. We first searched the CAS and 3D molecular structures of the serum migrant components on PubChem. Secondly, the CAS or 3D molecular structures were imported into TCMSP (http://tcmsp-e.com), Swiss Target Prediction (http://www.swisstargetprediction.ch/), and PharmMapper Server (Version 2017) (http://www.lilab-ecust.cn/pharmmapper/index.html) (Wang et al., 2017) to explore potential targets of the compounds. Then, "cholestasis", "cholestatic hepatic injury" and "cholestatic liver injury" were used as keywords in the online database, including GeneCards (http://www.genecards.org/), Disgenet (https://www.disgenet.org/), OMIM (https://omim.org/), and TTD (Wang et al., 2020) (http://bidd.nus. edu. sg/group/ttd/) to screen for disease targets. Besides, standardization of all targets was conducted on the Uniprot database (https://www.uniprot.org/). Finally, intersection targets of CHI and HGJD were picked out by an online Venn analysis tool (http://bioinformatics.psb.ugent.be/webtools/Venn/).

2.6.2 KEGG Pathways Analysis and GO Biological Process Enrichment

To clarify the function of the targets and their functions in signaling transduction, the DAVID 6.8 database was applied to evaluate the KEGG pathways and GO enrichment of the targets of HGJD against CHI.

2.6.3 Network Construction

Three visualized networks were visualized by Cytoscape 3.7.1: 1) Drug-components-targets network was the interaction network among HGJD, potential active components of HGJD, and intersection targets; 2) Protein-Protein Interaction (PPI) network showed the importance of the targets of the potential active compounds of HGJD associated with CHI; 3) Components-Targets-Pathways network provided a systematic understanding of the complex network among drug, components, targets, pathways, and disease.

2.7 Metabolomics Analysis

2.7.1 Sample Preparation

100 μl of thawed serum sample and 300 μl of methanol (precooled at −20°C) were added into 1.5 ml centrifuge tubes, and vortexed for 60 s, then solution was allowed to stand for 30 min at 4°C. Samples were centrifuged for 15 min at 12,000 rpm and 4°C to obtain supernatant. Each supernatant was added with internal standard (2-chlorophenoalanine 1 mg/ml), oscillated, mixed and filtered through 0.22 μm membrane to get the prepared sample for UPLC-MS analysis. Ultimately, 20 μl of each prepared sample was taken and mixed to obtain the QC sample (Dunn et al., 2011).

2.7.2 Chromatography and Mass Spectrometry Conditions

Chromatographic separation was completed on Thermo Ultimate 3000 system which was equipped with a Hyper gold C_{18} (100 × 2.1 mm, 1.9 μm, and Thermo) column. Gradient elution of analyses was conducted with 0.1% formic acid in 5% acetonitrile(C) and 0.1% formic acid in acetonitrile (D) for positive ion mode. While, 0.05% acetic acid in 5% acetonitrile (A) and 0.05% acetic acid in acetonitrile (B) for negative mode. An incremental linear gradient of solvent B or D (v/v) was used as follows: 0–1.5 min, 0–20% B/D; 1.5–9.5 min, 20–100% B/D; 9.5–14.5 min, 100% B/D; 14.5–14.6 min, 100–5% B/D; 14.6–18 min, 5% B/D. The column flow rate and temperature were respectively set at 0.3 ml/min and 45°C. 3 μl of each sample was injected into UPLC-Q-Exactive MS/MS for analysis.

The experiments of ESI-MS^n were conducted on the Thermo Q Exactive mass spectrometer in positive and negative ion modes, respectively. Mass spectrometry parameters were set as follows: spray voltage was 3.0 kV in positive mode and −3.2 kV in negative mode. Sheath gas was kept at 45 arbitrary units, while auxiliary gas was 15 arbitrary units. The capillary temperature was maintained at 350°C. Full mass scan (m/z 70–1050) and HCD MS/MS spectra were recorded at a resolution of 70,000.

2.7.3 Data Processing and Analysis

Raw data acquired by Proteowizard software (v3.0.8789) was transformed into mzXML format (Smith et al., 2006). Peaks recognition, filtration and comparison were executed by R (v3.3.2) XCMS package. Besides, peak intensity has been normalized, so as to facilitate comparison of different magnitudes of data. Then, Principal Component Analysis (PCA), Partial Least Squares Discriminant Analysis (PLS-DA), and Orthogonal-Partial Least Squares-Discriminant Analysis (OPLS-DA) methods were conducted by software SIMCA-P (v13.0) and R language ropes package to analyze data in different groups.

Components with marked changes in the groups ($p < 0.05$ and VIP >1) were chosen as differential biomarkers, which were tentatively identified with the exact molecular weight (error <20 ppm). Moreover, the MS/MS fragmentation patterns of compounds were matched by METLIN database (http://www.metlin.scipps.edu/) and MoNA database (https://mona.fiehnlab.ucdavis.edu//).

To reveal the changing trends of the potential biomarkers and the callback effect of HGJD, the heatmap analysis was carried out by MetaboAnalyst 5.0 (https://www.metaboanalyst.ca/MetaboAnalyst/) and R version 3.0.3. The pathways analysis of differential metabolites was conducted with MetaboAnalyst 5.0.

2.8 Regulation of PI3K/Akt/Nrf2 Pathway

2.8.1 Western Blotting Assay

Samples have been processed and determined the concentrations of total protein with BCA kit, before western blotting assay to test the level of PI3K, p-Akt, GCLc, GCLm, and Nrf2. As for Nrf2, the nuclear and cytoplasmic extractions were carefully performed by extraction kits. Then, these extractions were detected by Western blot analysis for the presence of Nrf2. The samples with equal amount of total protein (100 μg) were electrophoresed on a twelve alkyl sulfate polyacrylamide gel system consisted of 5% stacking gel and 8–15% resolving gel. The electrophoresed products were transferred onto polyvinylidene fluoride membrane. The membranes were blocked in 5% skimmed milk powder for 0.5 h at room temperature, subsequently incubated with specific primary antibodies overnight, including PI3K (1:1000), p-Akt (1:1000), Nrf2 (1:1000), GCLc (1:1000), GCLm (1:1000), and β-actin (1:3000). Next, washed and incubated with appropriate secondary antibody for 30 min. Ultimately, membranes were developed with chemiluminescent detection reagents and visualized with film. The relative expressions of PI3K, p-Akt, Nrf2, GCLc, and GCLm were quantified through optical density value utilizing an image processing system.

2.8.2 Biochemical Analysis of Antioxidant Compounds in Liver Tissue

Equal amount of Liver tissue (0.4 g) was carefully homogenized on ice with normal saline using a high speed tissue grinder to get a 1:10 (w/v) solution. Then the supernatants were tested using the GSH, MDA, and SOD assay kit according to the manufacturer's instructions.

3 RESULTS

3.1 Anti-CHI Effect Evaluation

The levels of ALT, AST, ALP, TBIL, DBIL, TBA, and γ-GT in the model group were significantly higher than that in the normal group ($p < 0.01$), indicating that ANIT successfully induced the CHI in rats. The levels of all factors in HGJD treatment groups were dose dependently lower than those in model group (**Figure 2**). In addition, the high dose and medium dose of HGJD groups showed similar preventive effect with UDCA group on CHI ($p < 0.01$), while low dose showed weaker. As shown in **Figure 3,** liver tissue of normal group displayed normal structure, while the specimens in the ANIT group observed spotty necrosis of liver cells. Administrating with 3.01 and 6.02 g/kg HGJD significantly reduced the trauma of liver tissue. The results showed that HGJD had a protective effect against ANIT-induced CHI.

3.2 Identification of Serum Migrant Compounds of HGJD

We established a UPLC-Q-Exactive MS/MS analysis method to analyze HGJD extracts and serum samples from rats after treatment of HGJD. The typical base peak chromatographs were shown in **Supplementary Figure S1**. On the basis of standards and related literatures, 31 compounds from HGJD in total were identified initially (**Table 1**). These compounds involved flavonoids, organic acids, phenols, alkaloids, and terpenoids. According to previous research, above compounds might originate from Citri Reticulatae Pericarpium Viride, Gardeniae Fructus, Paeoniae Radix Alba, Moutan Cortex, Alismatis Rhizaoma, Fritillariae Thunbergii Bulbus, and Citri Reticulatae Pericarpium in HGJD. Detailed source for each compound was shown in **Table 1**. In this study, prototype compounds absorbed into serum were mainly focused on. However, the metabolites in serum have not been identified and classified.

3.3 Network Analysis

3.3.1 Targets Prediction of Potential Active Compounds of HGJD Against CHI

On the basis of 31 serum migrant compounds of HGJD, 596 targets of HGJD were picked. According to database analysis of disease targets, we obtained 962 targets. Subsequently, an online Venn analysis tool was applied to generate the Venn diagram. 159 common targets were regarded as potential targets of HGJD against CHI (**Supplementary Figure S2**, **Table S2**).

3.3.2 KEGG Pathways Analysis and Gene Ontology (GO) Enrichment

The enrichment of signaling pathways was performed on DAVID database, and top 20 KEGG pathways which were selected according to the order of p value from small to large, were shown in **Figure 4A**; **Supplementary Table S3**. The results demonstrated that HGJD treating CHI mainly involved

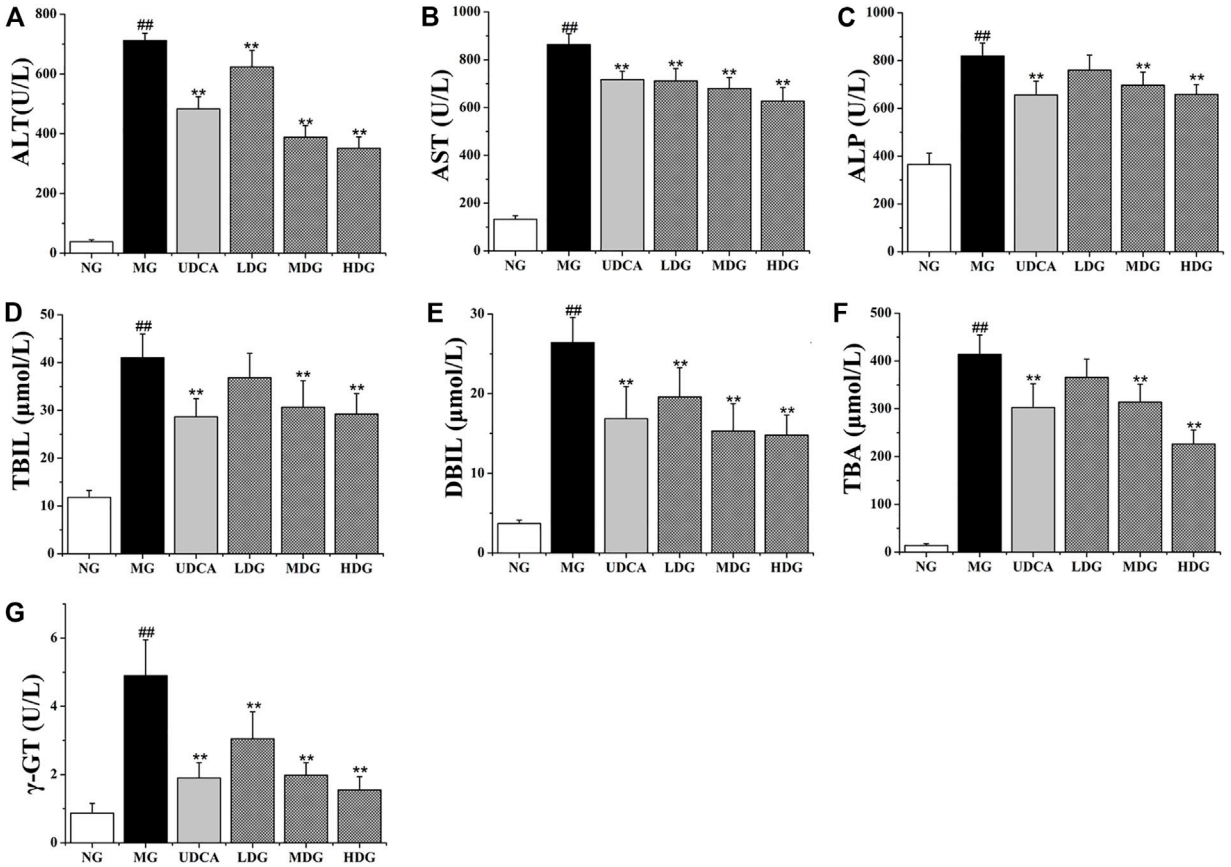

FIGURE 2 | The effects of HGJD on serum biochemistry. The biomarkers of liver injury and biliary cell damage in the serum biochemistry were ALT **(A)**, AST **(B)**, ALP **(C)**, TBIL **(D)**, DBIL **(E)**, TBA **(F)** and γ-GT **(G)**. Data are expressed as the Mean ± SD (n = 6 in each group). ##p < 0.01 compared with the normal group; **p < 0.01 compared with the model group.

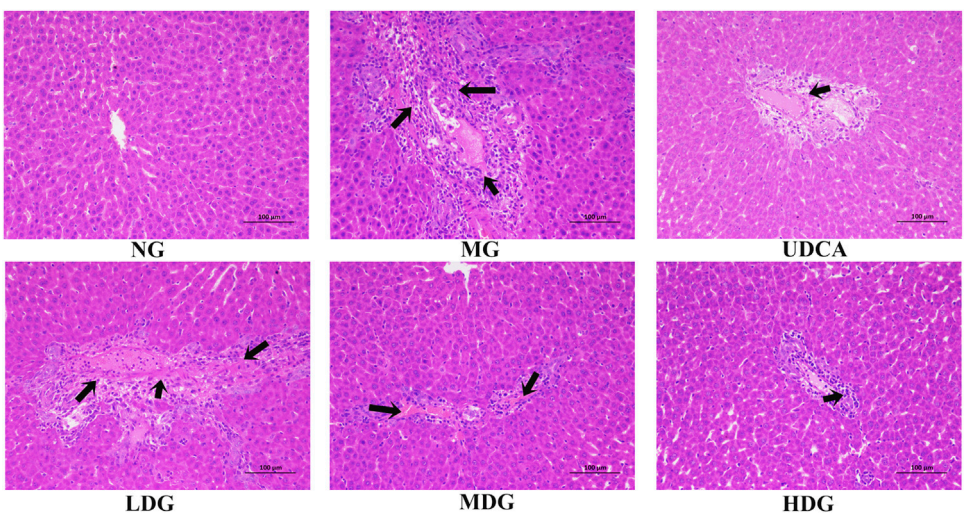

FIGURE 3 | Representative histopathological section photos of liver specimens of rat with H&E staining (200 × magnification). Damage to hepatocytes is pointed by black arrows.

TABLE 1 | Characterization of serum migrant compounds of HGJD by UPLC-Q-Exactive MS/MS.

NO.	Compound	RT (min)	Formula	Precursor ion	Predictived	Measured	Error (ppm)	MS2	Source	Reference
S1	Acetophenone	1.88	C_8H_8O	$[M + H]^+$	121.0647	121.0652	4.13	103.0539, 91.0548, and 53.0391	CP	Zheng et al. (2020)
S2	Quinic acid	1.94	$C_7H_{12}O_6$	$[M–H]^–$	191.0561	191.0559	–1.05	173.0453, 85.0285	ZZ	Zhou et al. (2020)
S3	Nicotinamide	2.46	$C_6H_6N_2O$	$[M + H]^+$	123.0552	123.0554	1.63	88.0236, 80.0500, 56.9654, and 53.0392	CP	Zheng et al. (2020)
S4	Citric acid	3.23	$C_6H_8O_7$	$[M–H]^–$	191.0197	191.0195	–1.05	111.0080, 87.0078	BS	Xu et al. (2018)
S5	Geniposidic acid	4.67	$C_{16}H_{22}O_{10}$	$[M–H]^–$	373.114	373.1147	1.88	211.0611, 167.070, 123.0444, and 149.0602	ZZ	Wang et al. (2016)
S6	Shanzhiside	4.71	$C_{16}H_{24}O_{11}$	$[M–H]^–$	391.1245	391.1254	2.30	193.0507	ZZ	Zhou et al. (2020)
S7	Gardenoside	5.64	$C_{17}H_{24}O_{11}$	$[M–H]^–$	403.1245	403.1274	7.19	241.0719	ZZ	Fu et al. (2014)
S8	Jasminoside B	6.47	$C_{16}H_{26}O_8$	$[M + H]^+$	347.17	347.1700	0	185.1172, 167.1066	ZZ	Zhou et al. (2020)
S9	Methyl gallate	6.63	$C_8H_8O_5$	$[M–H]^–$	183.0298	183.0296	–1.09	168.0059, 124.0158	BS MDP	Li et al. (2018)
S10	Oxypaeoniflorin	7.02	$C_{23}H_{28}O_{12}$	$[M–H]^–$	495.1508	495.1514	1.21	165.0555	BS MDP	Zhan et al. (2018)
S11	Chlorogenic acid*	7.66	$C_{16}H_{18}O_9$	$[M + H]^+$	355.1023	355.1022	–0.28	—	ZZ	Wang et al., 2016; Zhou et al. (2020)
S12	Geniposide*	8.01	$C_{17}H_{24}O_{10}$	$[M + H]^+$	389.1442	389.1446	1.03	—	ZZ	Zhou et al. (2020)
S13	Peimisine	8.27	$C_{27}H_{41}NO_3$	$[M + H]^+$	428.3159	428.3157	–0.47	67.0549, 84.0813, 81.0704, and 79.0550	ZBM	Zhou et al. (2013)
S14	Peimine*	8.35	$C_{27}H_{45}NO_3$	$[M + H]^+$	432.3472	432.3470	–0.46	414.3004, 95.0860, and 67.0548	ZBM	Wang et al. (2014)
S15	Peiminine*	8.71	$C_{27}H_{43}NO_3$	$[M + H]^+$	430.3315	430.3313	–0.46	412.3204, 98.0967	ZBM	Zhou et al. (2013)
S16	Albiflorin*	8.78	$C_{23}H_{28}O_{11}$	$[M–H]^–$	525.1613	525.1619	1.28	357.1193, 121.0287	BS	Qi et al., 2014; Xiang et al. (2016)
S17	Paeoniflorin*	9.23	$C_{23}H_{28}O_{11}$	$[M–H]^–$	525.1613	525.1621	1.52	449.1466, 327.1079, 165.0550, and 121.0300	BS,MDP	Qi et al. (2014)
S18	Ebeiedinone	10.32	$C_{27}H_{43}NO_2$	$[M + H]^+$	414.3366	414.3364	–0.48	67.0548, 81.070, 91.0547, 93.0702, 105.0702, and 119.0857	ZBM	Zhou et al. (2013)
S19	Isoquercitrin	10.48	$C_{21}H_{20}O_{12}$	$[M + H]^+$	465.1027	465.1032	1.08	303.0497	CP,ZZ	Fu et al. (2014); Zhang et al. (2018)
S20	Puqiedinone	10.63	$C_{27}H_{43}NO_2$	$[M + H]^+$	414.3366	414.3359	–1.69	105.0702, 91.0547, 81.0704, 67.0548, and 55.0549	ZBM	Zhou et al. (2013)
S21	Narirutin*	10.90	$C_{27}H_{32}O_{14}$	$[M + H]^+$	581.1864	581.1855	–1.55	273.0750, 153.0181	CP,QP	Zheng et al. (2019)
S22	Hesperetin	11.43	$C_{16}H_{14}O_6$	$[M + H]^+$	303.0863	303.0859	–1.32	219.0640,171.0288,153.0181, 135.0439, 89.0390, and 67.0185	CP,QP	Zheng et al. (2020)
S23	Galloylpaeoniflorin	11.43	$C_{30}H_{32}O_{15}$	$[M + H]^+$	633.1814	633.1783	–4.90	153.0184	BS,MDP	(Xiang et al., 2016; Zhan et al., 2018)
S24	Hesperidin*	11.45	$C_{28}H_{34}O_{15}$	$[M–H]^–$	609.1824	609.1832	1.31	301.0719, 286.0480	CP,QP	(Xu et al., 2018; Zheng et al., 2019)
S25	Didymin*	13.90	$C_{28}H_{34}O_{14}$	$[M + H]^+$	595.2021	595.2021	0	287.0908	CP,QP	Tong et al. (2018)
S26	Naringenin	16.85	$C_{15}H_{12}O_5$	$[M–H]^-$	271.0611	271.0615	1.48	151.0041	CP,QP	Zheng et al. (2019)
S27	Paeonol*	19.10	$C_9H_{10}O_3$	$[M + H]^+$	167.0702	167.0701	–0.60	149.0596, 121.0648	BS,MDP	Xu et al. (2018)
S28	Nobiletin*	20.71	$C_{21}H_{22}O_8$	$[M + H]^+$	403.1387	403.1383	–0.99	403.1383, 388.1152, and 373.0914	CP,QP	Cai et al. (2019)
S29	Hepta-3*	21.72	$C_{22}H_{24}O_9$	$[M + H]^+$	433.1493	433.1489	–0.92	418.1256, 403.1018, and 385.0910	CP,QP	Cai et al. (2019)

(Continued on following page)

TABLE 1 | (*Continued*) Characterization of serum migrant compounds of HGJD by UPLC-Q-Exactive MS/MS.

NO.	Compound	RT (min)	Formula	Precursor ion	Predictived	Measured	Error (ppm)	MS2	Source	Reference
S30	Tangeretin	22.45	$C_{20}H_{20}O_7$	$[M + H]^+$	373.1281	373.1276	−1.34	373.1280, 343.0809	CP,QP	Xu et al. (2018)
S31	Alisol B	25.97	$C_{30}H_{48}O_4$	$[M + H]^+$	473.3625	473.3626	0.21	437.342	ZX	Li et al. (2017)

*CP, Citri Reticulatae Pericarpium (*Citrus reticulata *Blanco); QP, Citri Reticulatae Pericarpium Viride (*Citrus reticulata *Blanco); BS, Paeoniae Radix Alba (*Paeonia lactiflora *Pall); MDP, Moutan Cortex (*Paeonia suffruticosa *Andr.); ZZ, Gardeniae Fructus (*Gardenia jasminoides *Ellis); ZX, Alismatis Rhizaoma (*Alisma plantago-aquatica *Linn.); ZBM, Fritillariae Thunbergii Bulbus (*Fritillaria thunbergii *Miq.).*

*The substances with * in the table have been compared with the reference substance.*

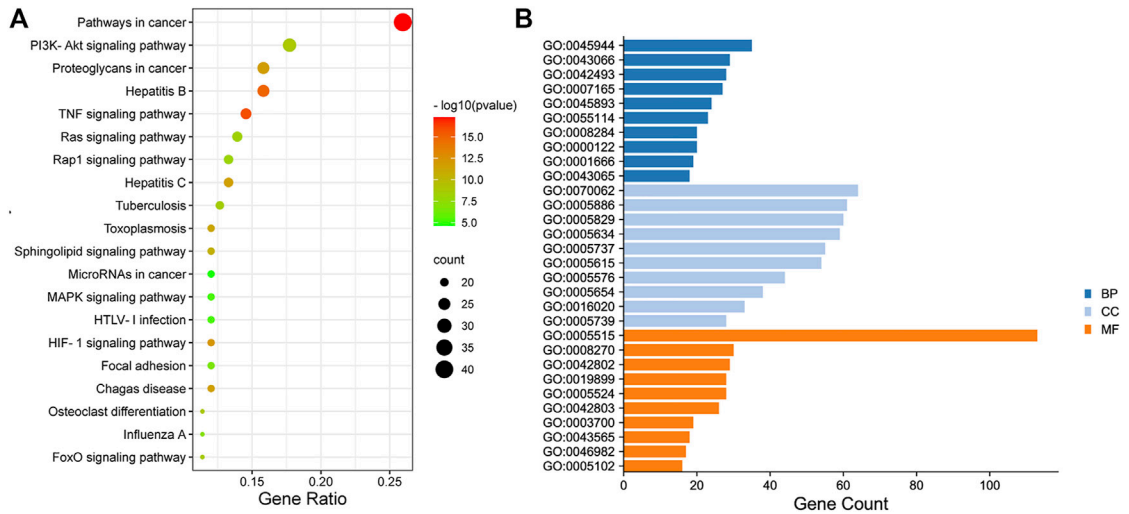

FIGURE 4 | The Dotplot for KEGG pathway **(A)** and GO enrichment analysis of the predicted targets in Biological Process, Molecular Function, and Cell Composition **(B)**. In **Figure 4A**, the size of each node represents plentiful counts. Color indicates plentiful *p*-value. In **Figure 4B**, BP represents Biological Processes, CC represents Cellular Components, MF represents Molecular Functions.

following pathways: pathways in cancer, PI3K-Akt signaling pathway and hepatitis B, *etc.*

The top10 results enriched by GO were displayed in **Figure 4B**; **Supplementary Table S4**. It was found that the target genes were involved in Cellular Components (CC), including extracellular exosome, plasma membrane, cytosol, and nucleus, *etc.* As for Biological Processes (BP), the key genes were mainly concentrated in negative regulation of apoptotic process, response to drug, signal transduction, and oxidation-reduction process. These functions closely correlated with protein binding, zinc ion binding, enzyme binding, and ATP binding in Molecular Functions (MF).

3.3.3 Network Construction

Drug-components-targets network was conducted based on 31 serum migrant compounds of HGJD and 159 targets with therapeutic potential. (**Supplementary Figure S3A**; **Supplementary Table S5**). Besides, the protein-protein interaction network was established to screen the key targets of HGJD against CHI. As shown in **Supplementary Figure S3B**, the key targets involving in the anti-CHI effects of HGJD included MAPK1, AKT, MAPK3, and PIK3R1.

The top 20 signaling pathways enriched by KEGG, targets involved in the top 20 signaling pathways, and the corresponding ingredients in HGJD were submitted to Cytoscape 3.7.1 to construction of the components-targets-pathways network (**Figure 5**). The network was consisted of 127 nodes (including 1 drug, 30 serum migrant compounds, 76 targets, and 20 pathways) and 728 edges. In addition, the network analysis result indicated that serum migrant compounds which had high degree value include hepta-3, alisol B, naringenin, nobiletin, albiflorin, tangeretin, paeonol, and galloylpaeoniflorin, might be the potential active ingredients of HGJD treating CHI.

3.4 Metabolomics

3.4.1 Multivariable Data Analysis

The typically based peak intensity chromatograms of serum samples in different groups were shown in **Supplementary Figure S4, S5**. Meanwhile, QC samples could cluster

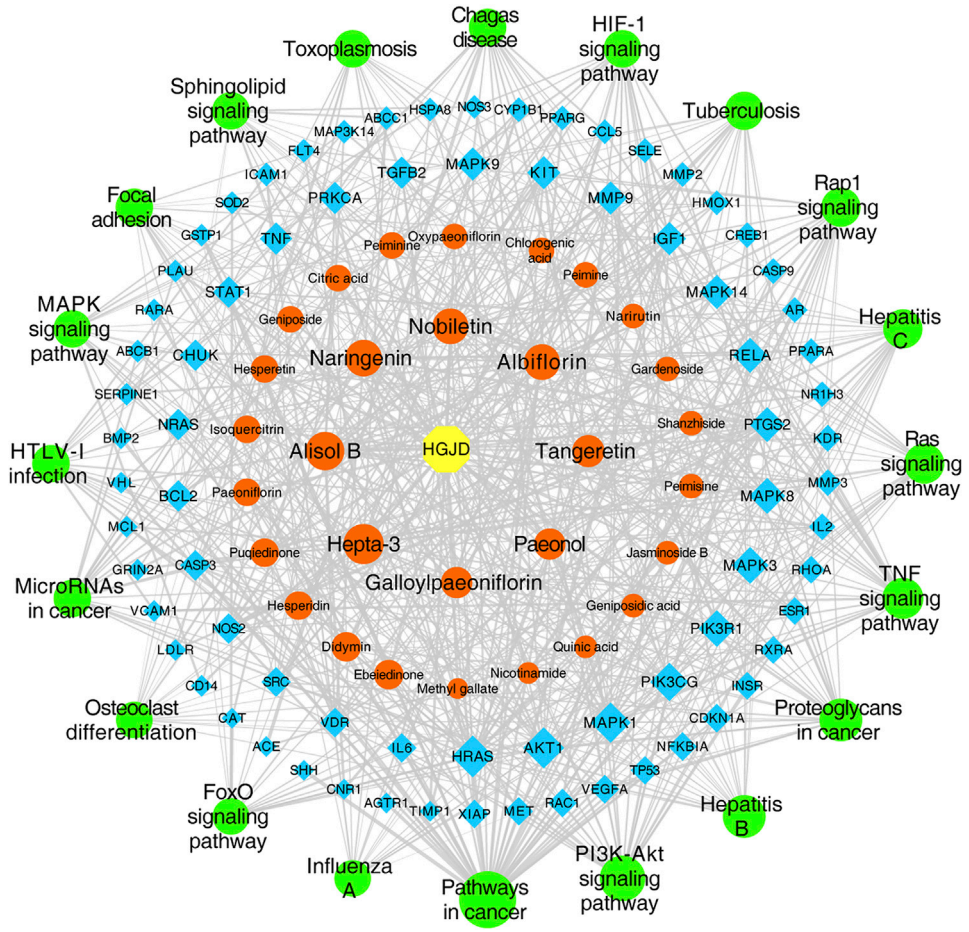

FIGURE 5 | Network of drug components-targets-pathways. The yellow hexagon node represents drug, the orange round shape nodes represent absorbed ingredients in blood, the blue diamonds represent targets, the green round shape nodes represent pathways, and the edges represent the interactions between them. The size of nodes is proportional to their degree value.

together, indicating that the instrument was stable (**Supplementary Figure S6**). The PCA and PLS-DA score plots (ESI+: R2X = 0.435, R2Y = 0.994, and Q2 = 0.898; ESI-: R2X = 0.480, R2Y = 0.997, and Q2 = 0.92) indicated that the normal group, model group and high dose of HGJD treatment group were separated from each other (**Figures 6A–D**), the combination of histological and biochemical examination confirmed the reliability of the CHI model and reflected the regulatory effect of HGJD on metabolites. Simultaneously, permutation test indicated that PLS-DA model was not over-fitted. **(Figures 6E,F)**. The complexity of the model was reduced using OPLS-DA and the interpretation of the model was improved (**Figures 6G,H**). The results showed that the metabolites in each group have achieved complete separation (ESI+: R2X = 0.372, R2Y = 0.999, Q2 = 0.859; ESI-: R2X = 0.356, R2Y = 0.985, and Q2 = 0.901) in two ion modes. Further, VIP value in OPLS-DA was one of the important factors for identifying differential metabolites.

3.4.2 Identification of Differential Biomarkers

OPLS-DA models and *t*-test were applied to distinguish the differential metabolites induced by ANIT and improved by HGJD. Differential biomarkers were screened by a criterion of p-value < 0.05 and VIP >1. Based on literature reports and four online databases including Human Metabolome Database (HMDB) (http://www.hmdb.ca), Metlin (http://metlin.scripps.edu), massbank (http://www.massbank.jp/), LipidMaps (http://www.lipidmaps.org), and mzclound (https://www.mzcloud.org), the differential biomarkers were tentatively identified. In total, 16 differential metabolites were screened out. As shown in **Table 2,** 7 metabolites were up-regulated and 9 metabolites were down-regulated with ANIT intervention in model group. Compared to this trend, the level of 13 metabolites was significantly reversed (p < 0.05) in the high dose of HGJD treatment group. The heatmap of 16 biomarkers was displayed in **Figure 7**, which demonstrated that ANIT treatment could influence the level of endogenous metabolites notably, while HGJD treatment had beneficial effects for the recovery of metabolite disorders.

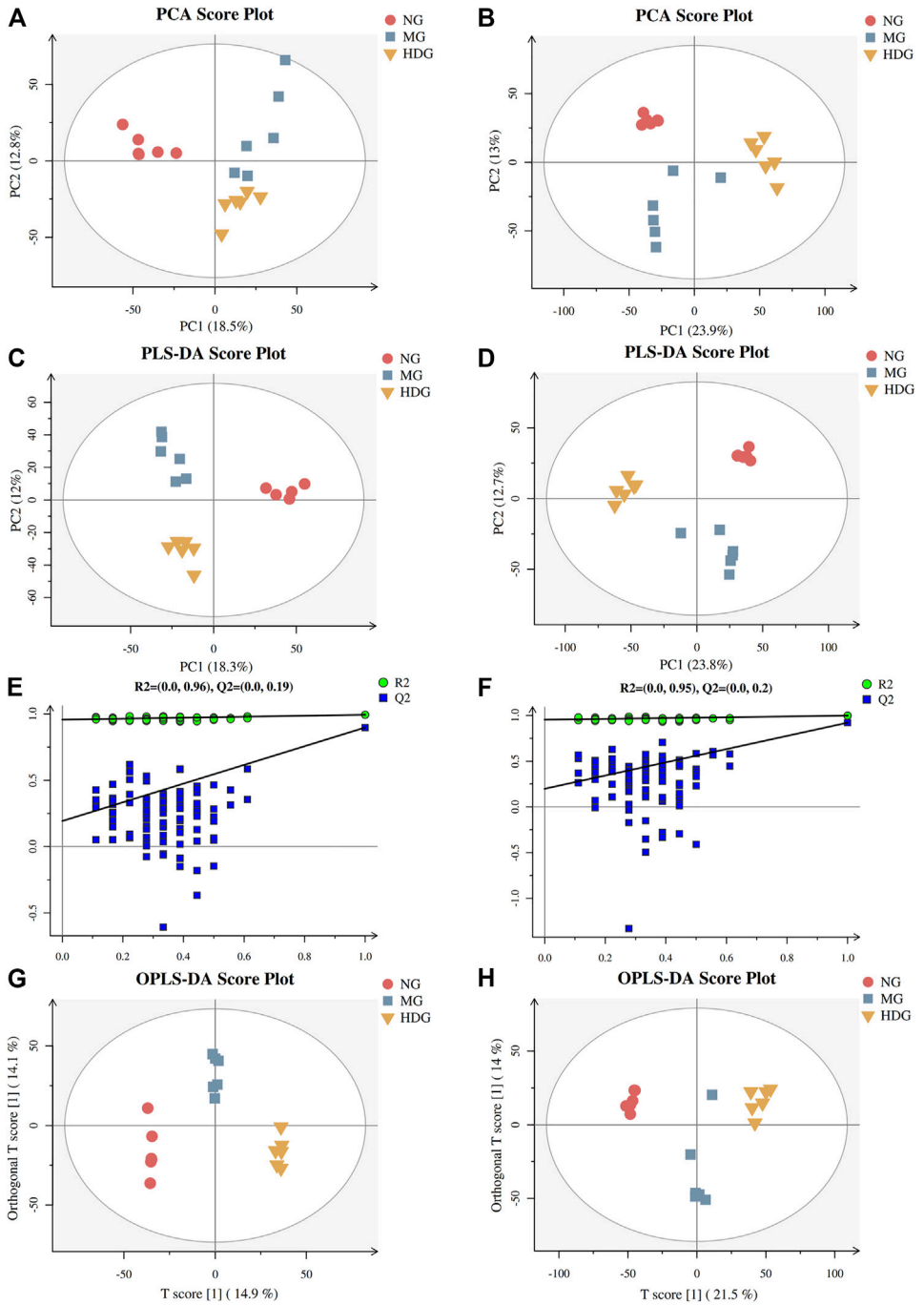

FIGURE 6 | The results of multivariate statistical analysis. The PCA score graph in positive **(A)** and negative **(B)** ion mode. The PLS-DA score graph in positive **(C)** and negative **(D)** ion mode. Permutations graph in positive **(E)** and negative **(F)** ion mode. The OPLS-DA score graph in positive **(G)** and negative **(H)** ion mode.

3.4.3 Metabolic Pathway Analysis

Metabolic pathway analysis was carried out to explore the underlying molecular functions of these serum differential metabolites. The result revealed that 5 pathways were affected by the administration of HGJD, including primary bile acid biosynthesis, tyrosine metabolism, pentose phosphate pathway, glutathione metabolism and glycerophospholipid metabolism (**Figure 8**; **Table 3**).

3.4.4 Signaling Networks

We imported the identified differential metabolites into the KEGG (http://www.kegg.jp/) to find signaling pathways

TABLE 2 | List and change trends of differential metabolites in the rats serum induced by ANIT.

No	Name	RT(min)	Formula	Exact mass	Error (ppm)	KEGG	Type	Trend	
								MG *vs* NG	HDG *vs* MG
1	Methyl beta-D-galactoside	0.69	$C_7H_{14}O_6$	194.0790	6.69	C03619	$[M + H]^+$	↓	↑
2	Epinephrine	1.03	$C_9H_{13}NO_3$	183.0895	12.25	C00788	$[M + H]^+$	↓	↑
3	3-Hydroxymethylglutaric acid	1.10	$C_6H_{10}O_5$	162.0528	8.96	C03761	$[M–H]^-$	↓	↑
4	Gluconic acid	1.27	$C_6H_{12}O_7$	196.0583	2.79	C00257	[M–H]–	↑	↑
5	Glutarate semialdehyde	2.81	$C_5H_8O_3$	116.0473	14.90	C03273	[M–H]–	↓	↑
6	3,4-Dihydroxymandelic acid	2.97	$C_8H_8O_5$	184.0370	3.54	C05580	[M–H]–	↓	↑
7	Indole	3.02	C_8H_7N	117.0578	4.05	C00463	$[M + H]^+$	↓	↓
8	Phenyllactate	4.18	$C_9H_{10}O_3$	166.0630	5.06	C05607	[M–H]–	↓	↑
9	25-Hydroxycholesterol	5.62	$C_{27}H_{46}O_2$	402.3498	2.56	C15519	[M–H]–	↑	↓
10	Allocholic acid	6.14	$C_{24}H_{40}O_5$	408.2876	7.46	C00695	$[M + H]^+$	↑	↓
11	Chenodeoxycholic acid	6.14	$C_{24}H_{40}O_4$	392.2927	15.10	C02528	$[M + H]^+$	↑	↓
12	Dethiobiotin	6.54	$C_{10}H_{18}N_2O_3$	214.1317	11.18	C01909	[M–H]–	↓	↓
13	Phosphorylcholine	7.27	$C_5H_{15}NO_4P$	184.0739	1.02	C00588	$[M + H]^+$	↑	↓
14	4-Oxoproline	8.57	$C_5H_7NO_3$	129.0426	1.54	C01877	$[M + H]^+$	↑	↓
15	13(S)-HOT	8.65	$C_{18}H_{30}O_3$	294.2195	1.04	C16316	$[M + H]^+$	↑	↓
16	Γ-Glutamylcysteine	9.63	$C_8H_{14}N_2O_5S$	250.0623	0.97	C00669	[M–H]–	↓	↑

↑: *Compound is up-regulated.* ↓: *Compound is down-regulated.*

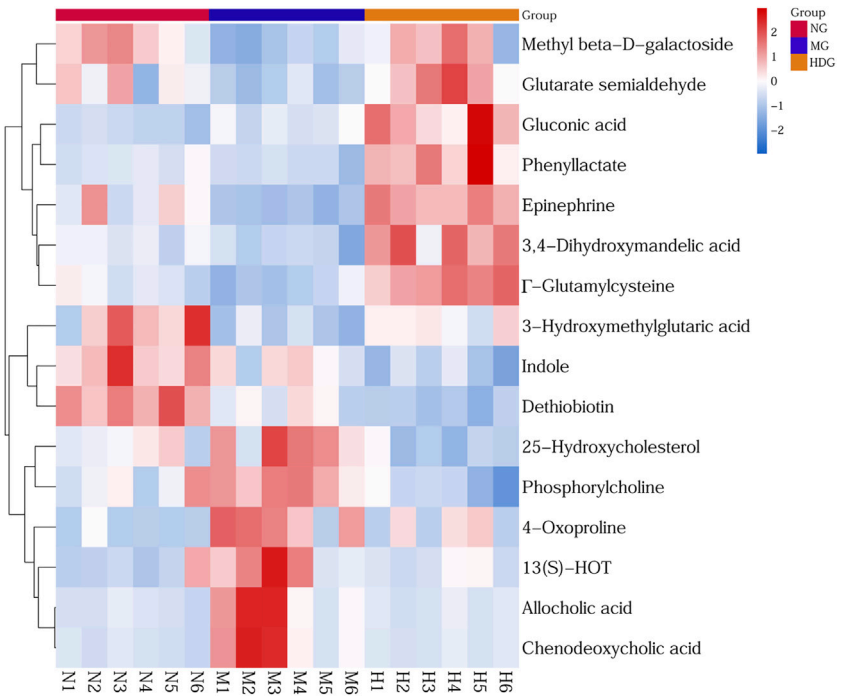

FIGURE 7 | Heatmap of differential metabolites. Color changed from blue to red, corresponding to a progressive increase in concentration.

correlated with them. Moreover, relationships among different signaling pathways were analyzed based on literatures. As shown in **Figure 9**, primary bile acid biosynthesis, tyrosine metabolism and glutathione metabolism might be related to the anti-CHI effect of HGJD. Meanwhile, when compared with model group, the levels of 25-Hydroxycholesterol, cholic acid, and chenodeoxycholic acid were significantly down-regulated by HGJD. Conversely, the levels of Γ-Glutamylcysteine, Epinephrine and 3, 4-Dihydroxymandelic acid were significantly increased by HGJD.

3.5 Regulation of PI3K/Akt/Nrf2 Pathway

3.5.1 Western Blotting Assay

Integrating liver biochemistry, network analysis and metabolomics results, PI3K/Akt pathway, primary bile acid biosynthesis as well as secretion, and glutathione metabolism

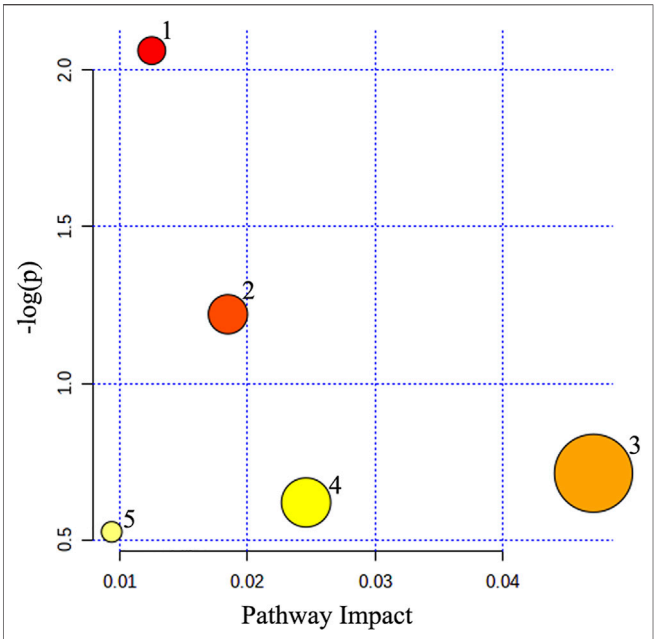

FIGURE 8 | Pathway analyses of differential metabolites in serum sample.

might be involved in the anti-CHI effect of HGJD. Meanwhile, accumulated evidence has shown that activation of PI3K/Akt pathway could induce nuclear translocation of Nrf2, and then affect GSH synthesis, which was an important mechanism of nature product protection against hepatic oxidative injury (Ma et al., 2015; Jin et al., 2019; Mukherjee et al., 2021). Therefore, western blotting was used to test and verify the effect of HGJD on PI3K/Akt/Nrf2 signaling pathway. As displayed in **Figure 10**, the protein expressions of PI3K, p-Akt, Nrf2, GCLc, and GCLm were decreased in ANIT induced model group. Whereas, these reduced protein levels were significantly increased after the treatment with HGJD.

3.5.2 Biochemical Analysis of Antioxidant Compounds in Liver Tissue

As reported in literatures, activation of PI3K/Akt/Nrf2 pathway could promote the imbalance between antioxidant system and oxidative system, which was closely related to mitigation of oxidative stress-induced injuries (Shi et al., 2018). Antioxidant compounds content (GSH, SOD) which could scavenge ROS, were significantly reduced with treatment of ANIT ($p < 0.01$). In UDCA group, medium dose and high dose of HGJD group, the levels of these compounds in liver were significantly reversed, while the antioxidant effect of low dose of HGJD was weak (**Figures 11A,C**). The hepatic MDA which was one of oxidative stress products was significantly increased in the model group ($p < 0.01$). The treatment with different dose of HGJD significantly reversed the increase of MDA induced by ANIT (**Figure 11B**). These results demonstrated that the potential mechanism of HGJD to alleviate CHI might correlate with the activation of PI3K/Akt/Nrf2 pathway to induce antioxidant synthesis.

4 DISCUSSION

In this study, HGJD significantly decreased the biochemical indicators which were related to CHI, and improved the inflammatory infiltration induced by ANIT. The results suggested that HGJD had a protective effect against ANIT-induced CHI. In terms of biochemical results, the effect of HGJD was not as good as UDCA, which might be related to overall regulation, slowness, and long-lasting characteristics of TCM treatment. In addition, serum pharmacochemistry combined with network analysis was applied to analyze drug-target interactions and identify potentially active components of HGJD. Moreover, mechanisms of anti-CHI effect of HGJD were explored by integrating network analysis and metabolomics, and the predicted main pathway was validated in the level of molecular biology. Although dosage in our study is within the range stipulated by Chinese Pharmacopoeia (2020 Edition), it is still lager than the dosage recommends for animal studies (Heinrich et al., 2020). Further pharmacological and toxicological studies are needed to guide the determination of clinical dose range.

Through literature research, we found that metabolic enzyme activity and gut microbiota might change under disease conditions, which could affect the absorption of pharmaceutical ingredients (Feng et al., 2020; Kummen and Hov, 2019; Pang et al., 2017; Qi et al., 2020). Therefore, in this experiment, the ANIT-induced CHI rats were selected to study serum pharmacochemistry, so as to better reflect absorption of HGJD components under the pathological state of CHI. Moreover, the network analysis was used to screen for potential active components of HGJD. The present results showed that hepta-3, alisol B, naringenin, nobiletin, albiflorin, tangeretin, paeonol, and galloylpaeoniflorin were the pivotal compounds of the compound-target network of HGJD against CHI. As reported in literature, hepta-3, naringenin, tangeretin,

TABLE 3 | Results of metabolic pathway analysis.

No	Pathway name	Total	Hits	*p*-value	–log(*p*)	Impact
1	Primary bile acid biosynthesis	46	3	0.008671	2.0619	0.0125
2	Tyrosine metabolism	42	2	0.060225	1.2202	0.0185
3	Pentose phosphate pathway	22	1	0.193790	0.7127	0.0471
4	Glutathione metabolism	28	1	0.240200	0.6194	0.0246
5	Glycerophospholipid metabolism	36	1	0.298210	0.5255	0.0094

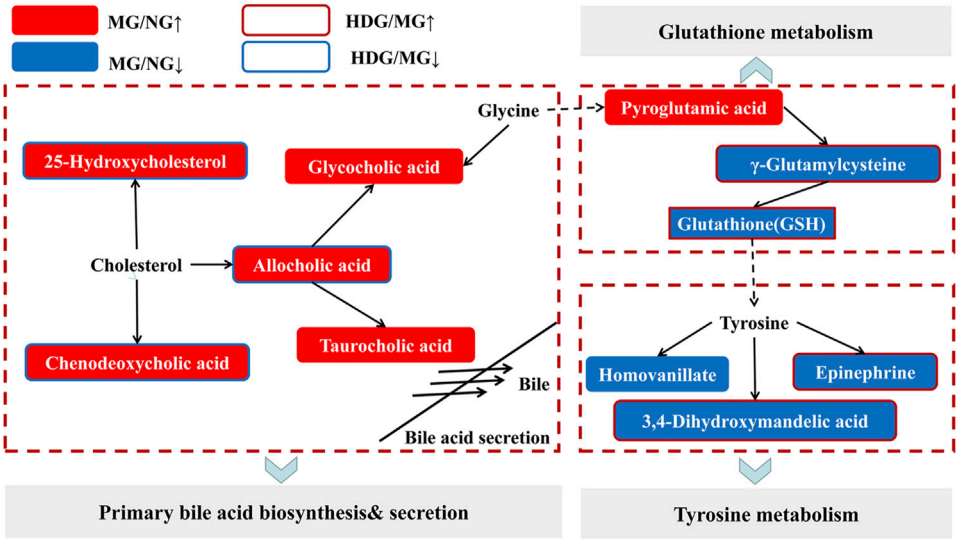

FIGURE 9 | Sketch map of the metabolic pathway correlated with CHI and HGJD therapy. The red and blue solid boxes represent that metabolites were significantly elevated or reduced in the model group when contrasted with normal group, respectively. The boxes with red and blue border indicated that metabolites were significantly increased or decreased in the HGJD group when compared with model group, respectively.

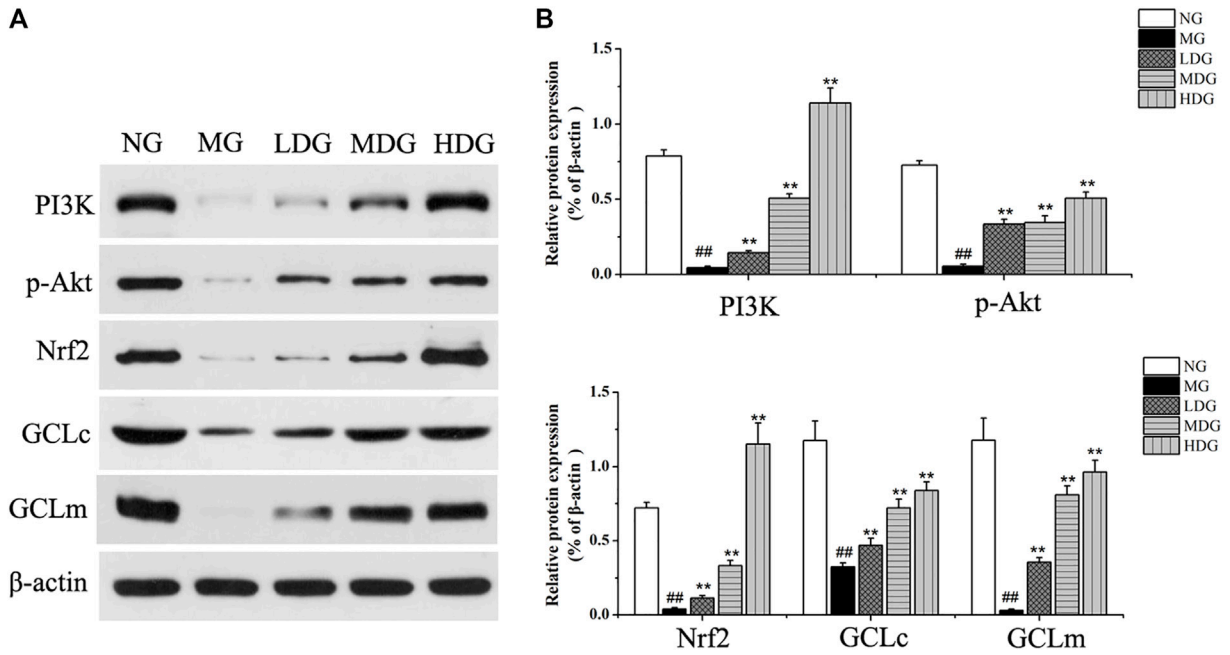

FIGURE 10 | The effects of HGJD on the expression of PI3K/Akt/Nrf2 signaling pathway. The effect of HGJD pretreatment on PI3K p-Akt, Nrf2, GCLc, and GCLm protein expression after ANIT treatment **(A)** and the optical density analysis of the protein bands intensity **(B)**. Data are expressed as the mean ± SD, ##$p < 0.01$ contrasted with the normal group. **$p < 0.01$ contrasted with the model group.

and nobiletin could reduce oxidative stress-induced liver injury by Nrf2 related pathway (Lin et al., 2019). Due to the regulation of transporters and enzymes mediated by FXR, Alisol B 23-acetate has shown the anti-CHI effect in animal experiment (Meng et al., 2015). Albiflorin was the one of the main active compounds of *Paeonia lactiflora* Pall against CHI (Jiang et al., 2012). Paeonol could alleviate live injury via anti-inflammatory, anti-oxidative and anti-apoptosis activity (Ding et al., 2016; Gong et al., 2017). These active components and their mixtures might play a vital role in protecting effect of HGJD against ANIT-induced CHI. However, the relationships among those compounds were complex, which needed to be explored in future work.

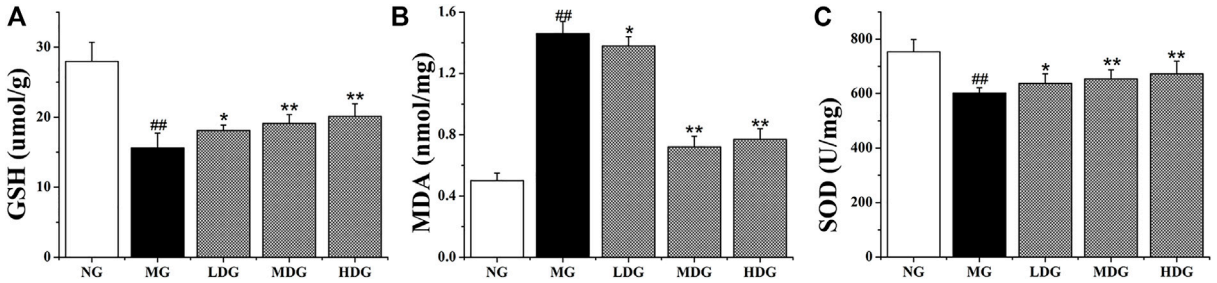

FIGURE 11 | Effects of HGJD on GSH **(A)**, MDA **(B)**, and SOD **(C)** in liver specimens in ANIT-induced CHI rats. Data are expressed as the Mean ± SD ($n = 6$ in each group). ##$p < 0.01$ contrasted with the normal group; *$p < 0.05$ compared with the model group; **$p < 0.01$ contrasted with the model group.

Past work has shown that inhibition of PI3K/Akt pathway might aggravate liver damage (Han et al., 2010; Liu W et al., 2019). Besides, natural products have been demonstrated to have hepatoprotective activity via up-regulated the expression of Nrf2 by activating the PI3K/Akt pathway (Zhang et al., 2017). From the results of network analysis, PI3K/Akt signaling pathway had a significant correlation with the key targets identified in our study. Furthermore, as reported in literature, under acute and chronic liver disease conditions, Nrf2 was activated and relieved oxidative stress-induced injuries by regulating genes expression of cytoprotective enzymes, which promoted GSH synthesis, and inhibited ROS generation (Bataille and Manautou, 2012; Xu et al., 2019). Based on our serum metabolomics research, glutathione metabolism might contribute to the anti-CHI effect of HGJD. Thus integrating results from network analysis and metabolomics showed that PI3K/Akt/Nrf2 signaling pathway related to glutathione (GSH) synthesis might be one of the major pathways interrelated to anti-CHI function of HGJD. Therefore, we further studied the connection among GSH synthesis, Nrf2 expression, and PI3K/Akt signaling pathways. As demonstrated in this study, HGJD could improve the protein expressions of PI3K, p-Akt, Nrf2, GCLc and GCLm, and increase GSH and SOD content. The results effectively corroborated the above prediction results, suggested that this integrated strategy was feasible.

As for CHI, excessive accumulation of bile acids in liver and systemic circulation could induce live cell damage (Gonzalez-Sanchez et al., 2016), which was related to bile acid-induced initiation of apoptosis and oxidative stress increase in liver cells (Sokolovic et al., 2013). The non-targeted metabolomics in our research showed that the therapeutic effect of HGJD was correlated with primary bile acid biosynthesis as well as secretion, and glutathione metabolism. Moreover, as reported in literature, farnesoid X receptor (FXR) played an important role in regulating bile acid. Meanwhile, oxidative stress in FXR-null mice increased spontaneously, which might be attributed to the continuous increase in hepatic bile acids level (Nomoto et al., 2009). However, there was a complex network of biological signaling pathways, and might be a clear tissue-specific role of FXR in the liver and intestine (Cheng, et al., 2021; Stofan and Guo, 2020). FXR and the molecular mechanism by which it regulates bile acid and oxidative stress are valuable for further research.

In conclusion, this study showed that HGJD could alleviate CHI. A comprehensive method based on network analysis, metabolomics and *in vivo* validation experiment was used to investigate the mechanism of HGJD in treatment of CHI. PI3K/Akt/Nrf2 signaling pathway related to GSH synthesis has been identified as the staple pathway correlated with the effects of HGJD against CHI. Totally, 31 compounds originated from HGJD have been identified in the serum sample. The pivotal compounds in the network analysis were predicted as potential active components. In the future, other signaling pathways predicted in our study should be investigate, and the potential active ingredients can be used to improve the quality control of HGJD.

DATA AVAILABILITY STATEMENT

The original contribution presented in the study are included in the article/**Supplementary Material**; further inquiries can be directed to the corresponding authors.

ETHICS STATEMENT

The animal study was reviewed and approved by The Animal Ethics Committee of Chengdu University of Traditional Chinese Medicine (Chengdu, China).

AUTHOR CONTRIBUTIONS

C-MF and WL designed the study. QD, Y-PJ, S-YS, and LP performed the experiments, JC, Z-PZ, Y-FZ, and W-QC recorded the experimental data. QD wrote the manuscript. QD and XY made the charts. WL, ZZ, and J-MZ reviewed and edited the manuscript. All authors have read and approved the manuscript.

FUNDING

This work was supported by the Sichuan Provincial Key Research and Development Program (No. 2020YFS0567); the National Natural Science Foundation of China (Grant Nos. 81403103, 82073994); the International Cooperation Project of Science and Technology Department of Sichuan Province (Grant No. 2018HH0122); Chengdu Science and Technology Bureau International Science and Technology Cooperation Project (Grant No. 2017-GH02-00054-HZ).

SUPPLEMENTARY MATERIAL

The Supplementary Material for this article can be found online at: https://www.frontiersin.org/articles/10.3389/fphar.2021.773957/full#supplementary-material

REFERENCES

Bataille, A. M., and Manautou, J. E. (2012). Nrf2: a Potential Target for New Therapeutics in Liver Disease. *Clin. Pharmacol. Ther.* 92 (3), 340–348. doi:10.1038/clpt.2012.110

Cai, H., Xu, Y., Xie, L., Duan, Y., Zhou, J., Liu, J., et al. (2019). Investigation on Spectrum-Effect Correlation between Constituents Absorbed into Blood and Bioactivities of Baizhu Shaoyao San before and after Processing on Ulcerative Colitis Rats by UHPLC/Q-TOF-MS/MS Coupled with Gray Correlation Analysis. *Molecules* 24 (5), 940. doi:10.3390/molecules24050940

Cai, S. Y., and Boyer, J. L. (2021). The Role of Bile Acids in Cholestatic Liver Injury. *Ann. Transl. Med.* 9 (8), 737. doi:10.21037/atm-20-5110

Chen, Y. H., Lan, T., Li, J., Qiu, C. H., Wu, T., Gou, H. J., et al. (2012). *Gardenia Jasminoides* Attenuates Hepatocellular Injury and Fibrosis in Bile Duct-Ligated Rats and Human Hepatic Stellate Cells. *World J. Gastroenterol.* 18 (48), 7158–7165. doi:10.3748/wjg.v18.i48.7158

Cheng, H., Liu, J., Tan, Y., Feng, W., and Peng, C. (2021). Interactions between Gut Microbiota and Berberine, a Necessary Procedure to Understand the Mechanisms of Berberine. *J. Pharm. Anal.* doi:10.1016/j.jpha.2021.10.003

Ding, Y., Li, Q., Xu, Y., Chen, Y., Deng, Y., Zhi, F., et al. (2016). Attenuating Oxidative Stress by Paeonol Protected against Acetaminophen-Induced Hepatotoxicity in Mice. *PLoS One* 11 (5), e0154375. doi:10.1371/journal.pone.0154375

Dunn, W. B., Broadhurst, D., Begley, P., Zelena, E., Francis-McIntyre, S., Anderson, N., et al. (2011). Procedures for Large-Scale Metabolic Profiling of Serum and Plasma Using Gas Chromatography and Liquid Chromatography Coupled to Mass Spectrometry. *Nat. Protoc.* 6 (7), 1060–1083. doi:10.1038/nprot.2011.335

Feng, W. W., Liu, J., Ao, H., Yue, S. J., and Peng, C. (2020). Targeting gut microbiota for precision medicine: Focusing on the efficacy and toxicity of drugs. *Theranostics* 10 (24), 11278–11301. doi:10.7150/thno.47289

Fu, Z., Ling, Y., Li, Z., Chen, M., Sun, Z., and Huang, C. (2014). HPLC-Q-TOF-MS/MS for Analysis of Major Chemical Constituents of Yinchen-Zhizi Herb Pair Extract. *Biomed. Chromatogr.* 28 (4), 475–485. doi:10.1002/bmc.3057

Gao, Y. F., Xia, W. Z., Xia, L., and Ouyang, R. (2019). Effect of Huaganjian on the Function of Hepatocytes and Activated Hepatic Stellate Cells. *Lishizhen Med. Mater. Med. Res.* 30 (12), 2879–2881.

Gong, X., Yang, Y., Huang, L., Zhang, Q., Wan, R. Z., Zhang, P., et al. (2017). Antioxidation, Anti-inflammation and Anti-apoptosis by Paeonol in LPS/d-GalN-induced Acute Liver Failure in Mice. *Int. Immunopharmacol.* 46, 124–132. doi:10.1016/j.intimp.2017.03.003

Gonzalez-Sanchez, E., Perez, M. J., Nytofte, N. S., Briz, O., Monte, M. J., Lozano, E., et al. (2016). Protective Role of Biliverdin against Bile Acid-Induced Oxidative Stress in Liver Cells. *Free Radic. Biol. Med.* 97, 466–477. doi:10.1016/j.freeradbiomed.2016.06.016

Han, J. W., Zhan, X. R., Li, X. Y., Xia, B., Wang, Y. Y., Zhang, J., et al. (2010). Impaired PI3K/Akt Signal Pathway and Hepatocellular Injury in High-Fat Fed Rats. *World J. Gastroenterol.* 16 (48), 6111–6118. doi:10.3748/wjg.v16.i48.6111

He, Y. Z. (2009). Observation on Curative Effect of 80 Cases of Chronic Cholecystitis Treated by Chinese and Western Medicine. *Guangming Tradit. Chin. Med.* 24 (10), 1959. doi:10.3969/j.issn.1003-8914.2009.10.078

Heinrich, M., Appendino, G., Efferth, T., Fürst, R., Izzo, A. A., Kayser, O., et al. (2020). Best Practice in Research - Overcoming Common Challenges in Phytopharmacological Research. *J. Ethnopharmacol.* 246, 112230. doi:10.1016/j.jep.2019.112230

Hirschfield, G. M., Mason, A., Luketic, V., Lindor, K., Gordon, S. C., Mayo, M., et al. (2015). Efficacy of Obeticholic Acid in Patients with Primary Biliary Cirrhosis and Inadequate Response to Ursodeoxycholic Acid. *Gastroenterology* 148 (4), 751–e8. doi:10.1053/j.gastro.2014.12.005

Hohenester, S., and Beuers, U. (2017). Chronic Cholestatic Liver Diseases : Differential Diagnosis, Pathogenesis and Current Treatment in Adults. *Internist (Berl)* 58 (8), 805–825. doi:10.1007/s00108-017-0287-z

Jiang, F., Zhao, Y., Wang, J., Wei, S., Wei, Z., Li, R., et al. (2012). Comparative Pharmacokinetic Study of Paeoniflorin and Albiflorin after Oral Administration of *Radix Paeoniae Rubra* in normal Rats and the Acute Cholestasis Hepatitis Rats. *Fitoterapia* 83 (2), 415–421. doi:10.1016/j.fitote.2011.12.009

Jin, J., Zheng, C., Lin, L., Luo, D. S., Liu, Q. Z., and Liu, Q. (2007). Dose-effect Relationship of Protective Effect of Qingpi on Acute Carbon Tetrachloride Induced Liver Injury in Rats. *Lishizhen Med. Mater. Med. Res.* (12), 2977–2978. doi:10.3969/j.issn.1008-0805.2007.12.064

Jin, Y., Huang, Z. L., Li, L., Yang, Y., Wang, C. H., Wang, Z. T., et al. (2019). Quercetin Attenuates Toosendanin-Induced Hepatotoxicity through Inducing the Nrf2/GCL/GSH Antioxidant Signaling Pathway. *Acta Pharmacol. Sin.* 40 (1), 75–85. doi:10.1038/s41401-018-0024-8

Kowdley, K. V., Luketic, V., Chapman, R., Hirschfield, G. M., Poupon, R., Schramm, C., et al. (2018). A Randomized Trial of Obeticholic Acid Monotherapy in Patients with Primary Biliary Cholangitis. *Hepatology* 67 (5), 1890–1902. doi:10.1002/hep.29569

Kummen, M., and Hov, J. R. (2019). The gut microbial influence on cholestatic liver disease. *Liver Int.* 39 (7), 1186–1196. doi:10.1111/liv.14153

Li, C. R., Li, M. N., Yang, H., Li, P., and Gao, W. (2018). Rapid Characterization of Chemical Markers for Discrimination of *Moutan Cortex* and its Processed Products by Direct Injection-Based Mass Spectrometry Profiling and Metabolomic Method. *Phytomedicine* 45, 76–83. doi:10.1016/j.phymed.2018.04.003

Li, D. (2021). Discussion on Clinical Application of Huagan Jian Based on Treatment of Liver Depression by Relief Therapy. *J. Guangzhou Univ. Tradit. Chin. Med.* 38 (04), 842–845. doi:10.13359/j.cnki.gzxbtcm.2021.04.035

Li, S., Jin, S., Song, C., Jia, S., Zhang, Y., Feng, Y., et al. (2017). The Strategy for Establishment of the Multiple Reaction Monitoring Based Characteristic Chemical Profile of Triterpenes in *Alismatis Rhizoma* Using Two Combined Tandem Mass Spectrometers. *J. Chromatogr. A.* 1524, 121–134. doi:10.1016/j.chroma.2017.09.057

Lin, Z. H., Chan, Y. F., Pan, M. H., Tung, Y. C., and Su, Z. Y. (2019). Aged Citrus Peel (Chenpi) Prevents Acetaminophen-Induced Hepatotoxicity by Epigenetically Regulating Nrf2 Pathway. *Am. J. Chin. Med.* 47 (8), 1833–1851. doi:10.1142/S0192415X19500939

Liu, L. F., Liang, H. Z., and Bin, J. P. (2019). Clinical Observation on Hyperthyroidism Liver Damage Treated with Therapy Integrated Traditional Chinese Medicine and Western Medicine. *J. Pract. Tradit. Chin. Med.* 35 (09), 1073–1075.

Liu, W., Jing, Z. T., Xue, C. R., Wu, S. X., Chen, W. N., Lin, X. J., et al. (2019). PI3K/AKT Inhibitors Aggravate Death Receptor-Mediated Hepatocyte Apoptosis and Liver Injury. *Toxicol. Appl. Pharmacol.* 381, 114729. doi:10.1016/j.taap.2019.114729

Ma, X., Zhao, Y. L., Zhu, Y., Chen, Z., Wang, J. B., Li, R. Y., et al. (2015). *Paeonia Lactiflora Pall.* Protects against ANIT-Induced Cholestasis by Activating Nrf2 via PI3K/Akt Signaling Pathway. *Drug Des. Devel. Ther.* 9, 5061–5074. doi:10.2147/DDDT.S90030

Meng, Q., Chen, X. L., Wang, C. Y., Liu, Q., Sun, H. J., Sun, P. Y., et al. (2015). Alisol B 23-acetate Protects against ANIT-Induced Hepatotoxity and Cholestasis, Due

to FXR-Mediated Regulation of Transporters and Enzymes Involved in Bile Acid Homeostasis. *Toxicol. Appl. Pharmacol.* 283 (3), 178–186. doi:10.1016/j.taap.2015.01.020

Mukherjee, S., Ghosh, S., Choudhury, S., Gupta, P., Adhikary, A., and Chattopadhyay, S. (2021). Pomegranate Polyphenols Attenuate Inflammation and Hepatic Damage in Tumor-Bearing Mice: Crucial Role of NF-Kb and the Nrf2/GSH Axis. *J. Nutr. Biochem.* 97, 108812. doi:10.1016/j.jnutbio.2021.108812

Nair, A., Morsy, M. A., and Jacob, S. (2018). Dose Translation between Laboratory Animals and Human in Preclinical and Clinical Phases of Drug Development. *Drug Dev. Res.* 79 (8), 373–382. doi:10.1002/ddr.21461

Nie, X., Pang, L., Jiang, H. J., Chen, Y., Wang, L., Wang, S. J., et al. (2020). Study on Specific Chromatogram and Content Determination of Multi-index Components about Material Reference of Classic Prescription of Huaganjian. *China Tradit. Herb Drugs* 51 (20), 5177–5186. doi:10.7501/j.issn.0253-2670.2020.20.009

Nomoto, M., Miyata, M., Yin, S., Kurata, Y., Shimada, M., Yoshinari, K., et al. (2009). Bile Acid-Induced Elevated Oxidative Stress in the Absence of Farnesoid X Receptor. *Biol. Pharm. Bull.* 32 (2), 172–178. doi:10.1248/bpb.32.172

Peng, H. Q., Tang, Y. P., Cao, Y. J., Tan, Y. J., Jin, Y., Shi, X. Q., et al. (2017). Comparatively evaluating the pharmacokinetic of fifteen constituents in normal and blood deficiency rats after oral administration of Xin-Sheng-Hua Granule by UPLC-MS/MS. *J. Chromatogr. B Analyt. Technol. Biomed. Life Sci.* 1061-1062, 372–381. doi:10.1016/j.jchromb.2017.07.042

Pollock, G., and Minuk, G. Y. (2017). Diagnostic Considerations for Cholestatic Liver Disease. *J. Gastroenterol. Hepatol.* 32 (7), 1303–1309. doi:10.1111/jgh.13738

Qi, Y., Cheng, X. H., Jing, H. T., Yan, T. X., Xiao, F., Wu, B., et al. (2020). Comparative pharmacokinetic study of the components in Alpinia oxyphylla Miq.-Schisandra chinensis (Turcz.) Baill. herb pair and its single herb between normal and Alzheimer's disease rats by UPLC-MS/MS. *J. Pharm. Biomed. Anal.* 177, 112874. doi:10.1016/j.jpba.2019.112874

Qi, Y., Li, S., Pi, Z., Song, F., Lin, N., Liu, S., et al. (2014). Chemical Profiling of Wu-tou Decoction by UPLC-Q-TOF-MS. *Talanta* 118, 21–29. doi:10.1016/j.talanta.2013.09.054

Shi, A., Shi, H., Wang, Y., Liu, X., Cheng, Y., Li, H., et al. (2018). Activation of Nrf2 Pathway and Inhibition of NLRP3 Inflammasome Activation Contribute to the Protective Effect of Chlorogenic Acid on Acute Liver Injury. *Int. Immunopharmacol.* 54, 125–130. doi:10.1016/j.intimp.2017.11.007

Smith, C. A., Want, E. J., O'Maille, G., Abagyan, R., and Siuzdak, G. (2006). XCMS: Processing Mass Spectrometry Data for Metabolite Profiling Using Nonlinear Peak Alignment, Matching, and Identification. *Anal. Chem.* 78 (3), 779–787. doi:10.1021/ac051437y

Sokolovic, D., Nikolic, J., Kocic, G., Jevtovic-Stoimenov, T., Veljkovic, A., Stojanovic, M., et al. (2013). The Effect of Ursodeoxycholic Acid on Oxidative Stress Level and DNase Activity in Rat Liver after Bile Duct Ligation. *Drug Chem. Toxicol.* 36 (2), 141–148. doi:10.3109/01480545.2012.658919

Stofan, M., and Guo, G. L. (2020). Bile Acids and FXR: Novel Targets for Liver Diseases. *Front. Med. (Lausanne)* 7, 544. doi:10.3389/fmed.2020.00544

Tong, C., Peng, M., and Shi, S. (2018). Rapid Identification of Flavonoid Compounds in Pericarpium Citri Reticulatae by Online Extraction-High Performance Liquid Chromatography-Diode Array Detection-Quadrupole Time-Of-Flight Mass Spectrometry. *Se. Pu.* 36 (3), 278–284. doi:10.3724/SP.J.1123.2017.11031

Wang, G. W., Bao, B., Han, Z. Q., Han, Q. Y., and Yang, X. L. (2016). Metabolic Profile of *Fructus Gardeniae* in Human Plasma and Urine Using Ultra High-Performance Liquid Chromatography Coupled with High-Resolution LTQ-Orbitrap Mass Spectrometry. *Xenobiotica* 46 (10), 901–912. doi:10.3109/00498254.2015.1132793

Wang, X., Shen, Y., Wang, S., Li, S., Zhang, W., Liu, X., et al. (2017). PharmMapper 2017 Update: a Web Server for Potential Drug Target Identification with a Comprehensive Target Pharmacophore Database. *Nucleic Acids Res.* 45 (W1), W356–w360. doi:10.1093/nar/gkx374

Wang, Y., Zhang, S., Li, F., Zhou, Y., Zhang, Y., Wang, Z., et al. (2020). Therapeutic Target Database 2020: Enriched Resource for Facilitating Research and Early Development of Targeted Therapeutics. *Nucleic Acids Res.* 48 (D1), D1031–D1041. doi:10.1093/nar/gkz981

Wang, Y., Li, C. M., Huang, L., Liu, L., Guo, Y. L., Ma, L., et al. (2014). Rapid Identification of Traditional Chinese Herbal Medicine by Direct Analysis in Real Time (DART) Mass Spectrometry. *Anal. Chim. Acta* 845, 70–76. doi:10.1016/j.aca.2014.06.014

Xiang, H., Zhang, L., Song, J., Fan, B., Nie, Y., Bai, D., et al. (2016). The Profiling and Identification of the Absorbed Constituents and Metabolites of Guizhi Decoction in Rat Plasma and Urine by Rapid Resolution Liquid Chromatography Combined with Quadrupole-Time-Of-Flight Mass Spectrometry. *Int. J. Mol. Sci.* 17 (9), 1409. doi:10.3390/ijms17091409

Xu, D., Xu, M., Jeong, S., Qian, Y., Wu, H., Xia, Q., et al. (2019). The Role of Nrf2 in Liver Disease: Novel Molecular Mechanisms and Therapeutic Approaches. *Front. Pharmacol.* 9, 1428. doi:10.3389/fphar.2018.01428

Xu, Y., Cai, H., Cao, G., Duan, Y., Pei, K., Tu, S., et al. (2018). Profiling and Analysis of Multiple Constituents in Baizhu Shaoyao San before and after Processing by Stir-Frying Using UHPLC/Q-TOF-MS/MS Coupled with Multivariate Statistical Analysis. *J. Chromatogr. B Analyt. Technol. Biomed. Life Sci.* 1083, 110–123. doi:10.1016/j.jchromb.2018.03.003

Zhan, Z. L., Deng, A. P., Kang, L. P., Tang, J. F., Nan, T. G., Chen, T., et al. (2018). Chemical Profiling in *Moutan Cortex* after Sulfuring and Desulfuring Processes Reveals Further Insights into the Quality Control of TCMs by Nontargeted Metabolomic Analysis. *J. Pharm. Biomed. Anal.* 156, 340–348. doi:10.1016/j.jpba.2018.04.045

Zhang, X., Pi, Z., Zheng, Z., Liu, Z., and Song, F. (2018). Comprehensive Investigation of *In-Vivo* Ingredients and Action Mechanism of Iridoid Extract from *Gardeniae Fructus* by Liquid Chromatography Combined with Mass Spectrometry, Microdialysis Sampling and Network Pharmacology. *J. Chromatogr. B Analyt. Technol. Biomed. Life Sci.* 1076, 70–76. doi:10.1016/j.jchromb.2018.01.023

Zhang, Y., Wei, Z., Liu, W., Wang, J., He, X., Huang, H., et al. (2017). Melatonin Protects against Arsenic Trioxide-Induced Liver Injury by the Upregulation of Nrf2 Expression through the Activation of PI3K/AKT Pathway. *Oncotarget* 8 (3), 3773–3780. doi:10.18632/oncotarget.13931

Zheng, G., Liu, M., Chao, Y., Yang, Y., Zhang, D., Tao, Y., et al. (2020). Identification of Lipophilic Components in *Citri Reticulatae Pericarpium* Cultivars by Supercritical CO2 Fluid Extraction with Ultra-high-performance Liquid Chromatography-Q Exactive Orbitrap Tandem Mass Spectrometry. *J. Sep. Sci.* 43 (17), 3421–3440. doi:10.1002/jssc.202000490

Zheng, Y. Y., Zeng, X., Peng, W., Wu, Z., and Su, W. W. (2019). Characterisation and Classification of *Citri Reticulatae Pericarpium Varieties* Based on UHPLC-Q-TOF-MS/MS Combined with Multivariate Statistical Analyses. *Phytochem. Anal.* 30 (3), 278–291. doi:10.1002/pca.2812

Zhou, J., Zhang, Y., Li, N., Zhao, D., Lu, Y., Wang, L., et al. (2020). A Systematic Metabolic Pathway Identification of Common Gardenia Fruit (*Gardeniae Fructus*) in Mouse Bile, Plasma, Urine and Feces by HPLC-Q-TOF-MS/MS. *J. Chromatogr. B Analyt. Technol. Biomed. Life Sci.* 1145, 122100. doi:10.1016/j.jchromb.2020.122100

Zhou, J. L., Liu, W., Guo, Z. X., and Chen, B. L. (2013). Fingerprint Analysis of Fritillaria Thunbergii Using Rapid Resolution Liquid Chromatography Coupled with Electrospray Ionization Quadrupole Time-Of-Flight Tandem Mass Spectrometry. *Zhongguo Zhong Yao Za Zhi* 38 (17), 2832–2837. doi:10.4268/cjcmm20131717

Conflict of Interest: The authors declare that the research was conducted in the absence of any commercial or financial relationships that could be construed as a potential conflict of interest.

Publisher's Note: All claims expressed in this article are solely those of the authors and do not necessarily represent those of their affiliated organizations, or those of the publisher, the editors and the reviewers. Any product that may be evaluated in this article, or claim that may be made by its manufacturer, is not guaranteed or endorsed by the publisher.

frontiers in Pharmacology

SYSTEMATIC REVIEW
published: 04 February 2022
doi: 10.3389/fphar.2021.787084

Bupleuri radix for Acute Uncomplicated Respiratory Tract Infection: A Systematic Review of Randomized Controlled Trials

Li-Jiao Yan[1], Zhi-Jie Wang[2], Min Fang[1], Hui-Di Lan[1,3], Michael Moore[4], Merlin Willcox[4], Jeanne Trill[4], Xiao-Yang Hu[4,5] and Jian-Ping Liu[1]**

[1]Centre for Evidence-Based Chinese Medicine, Beijing University of Chinese Medicine, Beijing, China, [2]Department of Oncology, Shanxi Provincial Hospital of Traditional Chinese Medicine, Shanxi, China, [3]Ruikang Hospital Affiliated to Guangxi University of Chinese Medicine, Nanning, China, [4]Primary Care and Population Sciences, Faculty of Medicine, University of Southampton, Southampton, United Kingdom, [5]Research Design Service South Central, National Institute of Health Research, Southampton, United Kingdom

OPEN ACCESS

Edited by:
Michael Heinrich, University College London, United Kingdom

Reviewed by:
Weihong Cong, China Academy of Chinese Medical Sciences, China
Qinxiu Zhang, Chengdu University of Traditional Chinese Medicine, China

***Correspondence:**
Jian-Ping Liu
Liujp@bucm.edu.cn
Xiao-Yang Hu
X.hu@soton.ac.uk

Specialty section:
This article was submitted to Ethnopharmacology, a section of the journal Frontiers in Pharmacology

Received: *30 September 2021*
Accepted: *28 December 2021*
Published: *04 February 2022*

Citation:
Yan L-J, Wang Z-J, Fang M, Lan H-D, Moore M, Willcox M, Trill J, Hu X-Y and Liu J-P (2022) Bupleuri radix for Acute Uncomplicated Respiratory Tract Infection: A Systematic Review of Randomized Controlled Trials. Front. Pharmacol. 12:787084. doi: 10.3389/fphar.2021.787084

Objective: To evaluate the efficacy, clinical effectiveness, and safety of the Chinese herb *Bupleuri radix* for the treatment of acute uncomplicated respiratory tract infections (ARTIs).

Methods: Four English and four Chinese databases were searched from their inception to June 2021. Randomized controlled trials (RCTs) assessing therapeutic effects of *Bupleuri radix* on ARTI were eligible for inclusion. The risk of bias for each trial was assessed using the Cochrane Risk of Bias Tool 2.0. RevMan 5.4 software was used for data analyses with effects estimated as risk ratios (RR) or mean differences (MD) with 95% confidence intervals (CI). The certainty of the evidence was assessed using the online GRADEpro tool.

Results: Seven randomized trials involving 910 patients with acute upper respiratory tract infection (AURTI) were included. The review identified *Bupleuri radix* agents with four administration routes (oral, acupoint injection, intramuscular injection, nebulized inhalation). *Bupleuri radix* acupoint injection compared with placebo showed statistically significant effects in reducing fever resolution time (MD: −33.32 h, 95%CI: −35.71, −30.93), and in increasing the proportion of participants with fever resolved within 48 h from treatment onset (RR: 14, 95%CI: 1.96, 99.94). *Bupleuri radix* acupoint injection combined with usual care is more effective in reducing the temperature at day 1 from treatment onset (MD: −1.00°C, 95%CI: −1.19, −0.81) compared with usual care alone. *Bupleuri radix* pills showed similar antipyretic effects to acetaminophen. However, *Bupleuri radix* intramuscular injection plus vitamins failed to demonstrate an effect in reducing fever, when compared with ribavirin plus vitamins. It suggested that oral administration of *Bupleuri radix* solution for injections, pills, and *Bupleuri radix* decoction have a similar effect on improving global AURTI symptoms including two key symptoms (nasal discharge and cough), when compared with usual care alone. Only two trials reported whether or not there were any AEs and found no occurrence of adverse events in the herbal group.

Conclusion: Low-certainty or very low-certainty evidence demonstrated that *Bupleuri radix* (solution for injections and pills) has an antipyretic effect on febrile patients with

AURTI, but it has no effect on other AURTI symptoms. However, these findings need to be further confirmed by well-designed clinical trials with adequate sample sizes.

Systematic review registration: (https://www.crd.york.ac.uk/prospero/#recordDetails), PROSPERO registration number: CRD42021234066.

Keywords: bupleuri radix, herbal medicine, Chinese herbal medicine, acute respiratory tract infection, systematic-review

INTRODUCTION

Acute uncomplicated respiratory tract infections (ARTIs) involve both upper and lower airways; they include the common cold, influenza, otitis media, sinusitis, tonsillitis, laryngitis, pharyngitis, and bronchitis (Acute, 1998). Symptoms include nasal congestion and discharge, sneezing, sore throat, cough, sputum production, shortness of breath, chest pain, earache, and fever (Acute, 1998). Generally, typical common colds are self-limiting and last 7–10 days, whereas acute (rhino)sinusitis can last for up to 4 weeks (Acute, 1998). On average, acute bronchitis takes 3 weeks to resolve (NICE, N.I.f.H.a.C.E, 2010). ARTI is one of the most common reasons for primary care consultations. Treatments for ARTI are mainly symptomatic, and often include antipyretics, mucolytics, expectorants, decongestants, and educational interventions. Although ARTIs are predominantly viral infections and antibiotics show little benefit in symptom improvement for ARTI, antibiotics are frequently prescribed in primary care settings (Pouwels et al., 2018). Antimicrobial resistance (AMR) is an evolving major global threat to public health (Limmathurotsakul et al., 2019). The marginal benefit of antibiotics for ARTI is outweighed by increasing AMR and common adverse reactions leading to unnecessary increases in healthcare costs (Gonzales et al., 2001; Naylor et al., 2019). However, many patients believe in antibiotics and want a prescription (Cabral et al., 2015). Findings also suggest that many patients and doctors are willing to consider alternatives (Soilemezi et al., 2020; Willcox et al., 2020). Research is warranted to explore other alternatives that may offer symptomatic relief and reduce unnecessary antibiotic prescribing for ARTI.

The Chinese herb Chai hu (*Bupleuri radix*) is derived from the dried roots of *Bupleurum* L. There are approximately 200 genera and 2,500 species in different regions and herbal markets (Huang et al., 2017). Most notably the roots of *Bupleurum chinense* DC, *Bupleurum scorzonerifolium* Willd (China), and *Bupleurum falcatum* L (Japan) are commonly used in Traditional Chinese Medicine (TCM) and Kampo medicine.

With a 2000-years medicinal history, *Bupleuri radix* is believed to be one of the most important herbal medicines in China. The earliest record of *Bupleuri radix* in China appeared in the Divine Farmer's Classic of Materia Medica (Han dynasty, 202 BC ~ 220 AD) (Chen and Chen, 2004). Since then, *Bupleuri radix,* as an ingredient alone (Fang and Zhang, 2003) and within particular formulations (such as Chaihuang granule (Zhu et al., 2017)), has been widely used for the treatment of ARTIs in China, Japan, Korea, as well as other countries (Wyk and Wink, 2004; Klein et al., 2012; Yang et al., 2017). *Bupleuri radix* is often processed into pieces for easy use, but since the 1940s, *Bupleuri radix* injection has been formulated using steam distillation of the volatile oils from the herb. This is for treating influenza, the common cold, and malaria. With more recent developments of TCM, other *Bupleuri radix* preparations have been developed, such as pills and nasal sprays.

There is encouraging evidence demonstrating the potential mechanism for the effects of *Bupleuri radix* for ARTI. The active constituents of *Bupleuri radix* comprise mainly triterpenoid saponins, flavonoids, and essential oil (Yang et al., 2017). They possess anti-inflammatory activity by inhibiting some inflammation-associated cytokines, proteins, and enzymes, and regulating inflammation-related signal pathways. For example, the crude polysaccharides (80 mg/kg) isolated from the roots of *Bupleurum chinense* DC. significantly attenuated lung injury by inhibiting the activity of myeloperoxidase (MPO), reducing the production of tumor necrosis factor-α (TNF-α) in the bronchoalveolar lavage fluid (BALF) and of NO in serum (Xie et al., 2012). *Bupleuri radix* demonstrates antipyretic effects via adjustment of intracellular level of cyclic adenosine monophosphate (cAMP) and synthesis and exudation of arginine vasopressin (AVP). *Bupleuri radix* injection (5 ml/kg, 2.5 ml/kg, and 1.25 ml/kg) can significantly reduce the body temperature of rats (in the lipopolysaccharide fever model), and the dose-effect relationship is significant (Gao et al., 2012). It has also been shown to be effective against human coronavirus and influenza A virus through interference in the early stage of viral replication, such as absorption and penetration, and attenuating aberrant pro-inflammatory cytokine production *in vitro* (Yang et al., 2017). The ethanol extract of *Bupleurum chinense* DC. exerted a remarkable bacteriostatic effect on the Gram-negative microorganism *Helicobacter pylori in vitro* (Gao et al., 2012). The bioactive minimum inhibitory concentration (MIC) value was 60 μg/ml (Li et al., 2005). However, the toxic effects of *Bupleuri radix* in clinical applications have been gradually reported, especially for the preparation of *Bupleuri radix* injection. It has been implicated in multiple cases of acute hepatitis both as an ingredient alone and within a particular formulation "Xiao-Chai-Hu-Tang" (also known as Syo-Saiko-To in Japanese) (Itoh et al., 1995). A systematic review conducted in 2010 identified 203 ADR/AE cases in patients using *Radix Bupleuri* injection, such as anaphylactic shock, acute hepatitis, and acute hepatic necrosis, and for most intramuscular cases, ADR/AE happened within 30 min from injection (Kong et al., 2010). However, there is uncertainty about the side effects of other preparations of *Bupleuri radix*. Moreover, the Ministry of Health revised the Standards of

Bupleuri radix injection (Administration, S.F.a.D., 2012) in 2011, which require it not to exceed 60 μg furfural (one of the main harmful ingredients) per 1 ml of the product. So far, there is uncertainty about the safety of *Bupleuri Radix* injection which follows the new standards.

OBJECTIVES

This systematic review aims to evaluate the efficacy, clinical effectiveness, and safety of *Bupleuri radix* for the treatment of ARTI in randomized controlled trials (RCTs).

METHODS

Criteria for Considering Studies for This Review

Types of Studies

All RCTs were eligible for inclusion.

Types of Participants

Trials with patients of any age, with either an ARTI diagnosis or symptoms of ARTI, were included. Diagnoses of ARTI included the common cold, influenza, rhinosinusitis, laryngitis, tonsillitis, pharyngitis, croup, acute otitis media, bronchitis, and acute exacerbations of chronic obstructive pulmonary disease (AECOPD). Symptoms of ARTI were defined as having symptoms such as cough, sore throat, fever, runny nose, and discolored sputum for less than 4 weeks (King et al., 2015).

We excluded any condition for which a specific therapy was recommended, such as streptococcal infections, pneumonia, diphtheria, tuberculosis, infections in immunocompromised, or any life-threatening condition. Also, studies restricted to patients with underlying chronic disease, such as asthma, or any other condition potentially impacting on the management and outcome of ARTI were not included.

Types of Interventions

Any form of preparation of *Bupleuri radix*, as monotherapy was included. Trials were included irrespective of the route of administration, e.g. oral, intramuscular injection or acupoint injection, or topical use. A preparation prescribed alone or as an adjunct treatment was only relevant if *Bupleuri radix* could be isolated as the intervention. Other treatments were permitted, such as additional symptomatic treatment, but this needed to follow national guidelines, and needed to be the same in both intervention and control groups. *Bupleuri radix* combined with other TCM therapies such as acupuncture were excluded.

Types of Control

No intervention, placebo; usual care such as antipyretics, antivirals, antibiotics, anti-inflammatories, steroids, or corticosteroids were included.

Prespecified Outcomes Included

Primary outcomes:

1) Change in global symptoms, which is measured as time to complete resolution of global symptoms (in days) or the proportion of patients resolved at a predefined time.
2) Change in some key symptoms (e.g. fever, cough, and sore throat), which measured as time to complete resolution of symptoms (in days), or the proportion of patients with symptoms resolved at a predefined time.

Secondary outcomes:

1) Need for antibiotics at follow-up.
2) Days off work or school.
3) Length of hospitalization.
4) Adverse events (AEs): These included any anaphylactic, allergic reactions, hypersensitivity reactions, or complications of taking *Bupleuri radix*. Information regarding AEs due to interactions of *Bupleuri radix* either as a monotherapy or in combination with other remedies, as well as potential interactions with medications for patients with comorbidities was collected.

We defined serious AEs according to the International Council on Harmonization of Technical Requirements for Registration of Pharmaceuticals for Human Use (ICH) guidelines as any event that leads to death, is life-threatening, requires hospitalization, or leads to persistent or significant disability, or leads to abnormal laboratory results such as liver or renal function tests (ICH, T.I.C.f.H., 1994).

Search Methods for Identification of Studies

A wide range of sources were searched (by LJY and MF) to find both published and unpublished studies via the following electronic databases and grey literature sources from their inception to June 2021. The major Chinese electronic databases included China national knowledge infrastructure (CNKI), Chinese Scientific Journal Database (VIP), Chinese BioMedical Literature Database (Sinomed), and Wanfang Database (Wanfang). The international databases searched were: PubMed, the Cochrane Library (Issue 6), Embase, Allied, and Complementary Medicine Database, Web of Science, and trial registries via ClinicalTrials. The references of all identified reviews or clinical trials were searched for additional studies.

Search terms included "*Bupleuri radix*" AND "respiratory tract infection" AND "randomized controlled trials". Additional search terms and strategies in different languages with different databases are listed in the **Supplementary Material** search strategy.

No language restrictions were applied.

Study Selection and Data Extraction

All titles and abstracts of studies retrieved from the electronic searches were reviewed by two authors (LJY and MF), who selected the relevant articles by title and abstract. Full-texts of each publication were independently reviewed by the two authors to determine their inclusion based on the criteria. Two authors (LJY and HDL) independently carried out data extraction using a pre-tested data extraction form. A third author (JPL) resolved disagreements between the two authors in consultation with them. For included trials, we abstracted the

following data as recommended in the Cochrane Handbook for Systematic Reviews of Interventions: 1) General information: published or unpublished, author, country, publication language, publication year, journal citation; 2) Participants: inclusion and exclusion criteria, the total number enrolled and number in each comparison group, baseline characteristics, setting; 3) Interventions: details of interventions in all trial arms including type and dose of therapy, according to the CONSORT 2010 extension for reporting Chinese herbal medicine formulas (CHM) checklist (Cheng et al., 2017); 4) Risk of bias in trials (see Assessment of risk of bias in included studies); 5) Follow-up: length of follow-up, the reason for and the number of dropouts and withdrawals, method of analysis; 6) Outcome measures, as the mean and standard deviation (SD) for continuous outcomes, and the number of events for dichotomous outcomes; 7) Safety and adverse events.

Assessment of Risk of Bias in Included Studies

The risk of bias for each trial was assessed by using version 2 of the Cochrane tool for assessing the risk of bias in randomized trials (RoB 2) (Sterne et al., 2019). It included assessment of the randomization process, deviations from intended interventions, missing outcome data, measurement of the outcome, and selection of the reported result. Any disagreements were resolved by discussion.

Measures of Treatment Effect

Statistical analyses were performed by using RevMan 5.4 (The Cochrane Collaboration, 2020). Dichotomous outcomes were expressed as risk ratio (RR) with 95% confidence interval (CI); Continuous data were presented as mean difference (MD) with 95% CI, or as standardized mean differences (SMDs) if outcomes were conceptually the same but measured in different ways in the different trials.

Unit of Analysis Issues

The individual participant was the unit of analysis. For multiple treatment groups, we separated the arms into different comparisons that met our inclusion criteria. For example, one trial (Song, 2020) was multi-armed comparing *Bupleuri radix* injection with different administration routes (acupoint injection and intramuscular injection) versus placebo (acupoint injection with saline solution), and usual care (intramuscular injection with ribavirin). They were separated into two comparison groups: acupoint injection with *Bupleuri radix* versus acupoint injection with saline solution; and intramuscular injection with *Bupleuri radix* versus intramuscular injection with ribavirin.

Dealing With Missing Data

We contacted authors where data was missing or incomplete. Where standard deviation was not reported with means, it was calculated from the information reported such as confidence intervals (CI), *p*-values, or F-values. The number of participants whose data was available at baseline and the last follow-up and the rate of loss to follow-up were recorded.

Assessment of Heterogeneity

We planned to assess between-study heterogeneity using the I^2 statistic which describes the percentage of variation across studies that is due to heterogeneity rather than chance. A rule of thumb for interpretation of this statistic suggests that $I^2 > 30\%$ represents moderate heterogeneity, $I^2 > 50\%$ represents substantial heterogeneity, and $I^2 > 75\%$ represents considerable heterogeneity (Higgins et al., 2020). As high levels of heterogeneity were expected due to complexity in the form of *Bupleurum* (e.g. the various forms of preparation), a random-effects model was utilized to pool the overall effects.

Assessment of Reporting Biases

We conducted funnel plot tests for asymmetry to investigate potential reporting bias where this was feasible and there were sufficient studies under a single meta-analysis.

Data Synthesis

Where possible, the analyses were planned to be based on intention to treat (ITT) data on each outcome provided for every randomized participant from the individual trials. Where possible, for continuous outcomes, the end of treatment scores rather than change from baseline scores was extracted. Due to the expected variability in the populations and interventions of included trials, a generic inverse variance random-effects model was used to pool the data to incorporate heterogeneity.

Subgroup Analysis and Investigation of Heterogeneity

We planned to conduct the following subgroup analyses for the primary outcome if there were sufficient trials:

- Adults (over 18) versus children
- *Bupleuri radix* in different preparations, e.g. granule versus capsule
- ARTI types regarding pathogen (bacterial or viral infection)

Sensitivity Analysis

We planned to perform sensitivity analyses for the primary outcome to determine whether the conclusions were different if eligibility was restricted to trials with a low risk of overall bias.

Where substantial heterogeneity exists, sensitivity analysis was planned to be conducted to further investigate potential sources of heterogeneity.

RESULTS

Results of the Search

In total 2,546 papers were identified, of which a total of 7 RCTs (Xu and Mao, 2001; Lv, 2010; Li et al., 2011; Cao, 2012; Gui et al., 2012; Huang, 2014; Song, 2020) comprising 910 patients, met the inclusion criteria (**Figure 1** and **Supplementary Material**

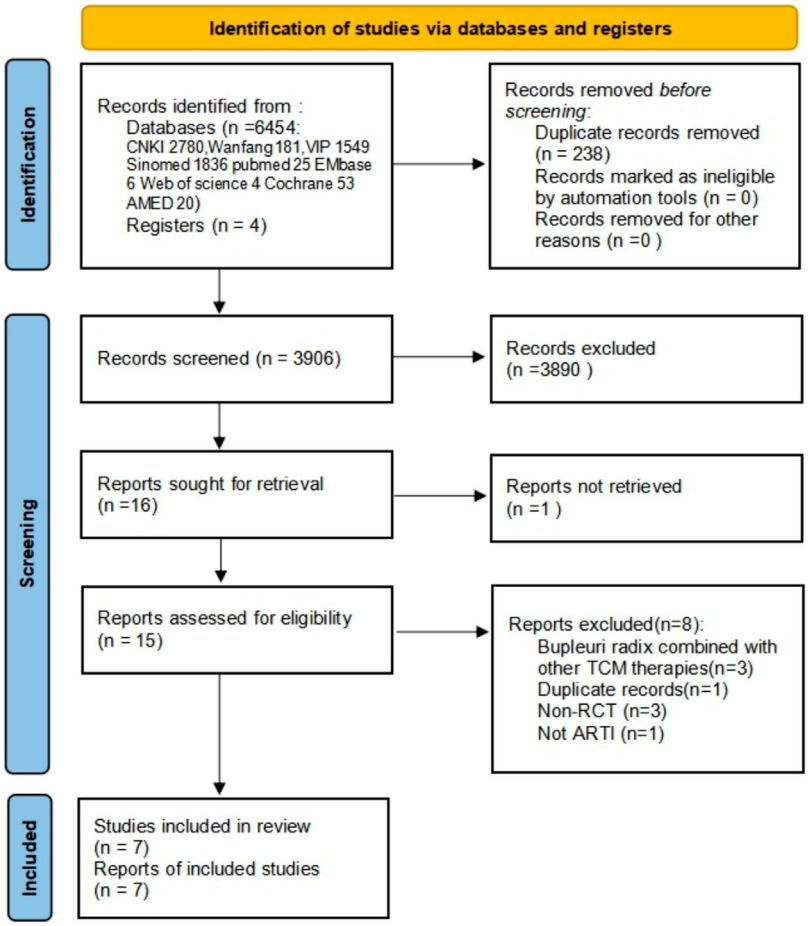

FIGURE 1 | Flow and identification of trials included. CNKI: China national knowledge infrastructure; VIP: Chinese Scientific Journal Database; AMED: The Allied and Complementary Medicine Database; CBM: Chinese Bio Medical Literature Database; ARTI: Acute uncomplicated respiratory tract infections; RCT: randomized controlled trial.

Characteristics of excluded studies). The included trials were published between 2001 and 2020, and all were from China.

Description of Included Trials

All included trials studied patients with clinically diagnosed acute upper respiratory tract infection (AURTI—see **Table 1**). One was on the common cold in patients aged 16–37 years old (Huang, 2014), and the other six trials included children with fever without specifying the type of AURTI. One(Lv, 2010) study diagnosed AURTI according to the Chinese medicine clinical research guidelines (CMCRG) (China, M.o.H.o.t.p.s.R.o, 1997) and the diagnosis in Practical Pediatrics (Wu and Hu, 1995). Another study (Cao, 2012) diagnosed AURTI where the patient had "WBC<10.0×10^9/L, neutrophils<0.70, fever, nasal congestion (or nasal discharge, cough, or dry mouth) red tongue, and yellow coating on the tongue, no complications, and onset within 24 h". Others didn't specify the diagnostic criteria. Only four studies (Cao, 2012; Gui et al., 2012; Huang, 2014; Song, 2020) specified a threshold of less than 24 h-5.5 days from the onset of symptoms for acute disease. Two trials (Cao, 2012; Gui et al., 2012) recruited patients from outpatient clinics, one from both outpatient clinics and inpatient wards (Lv, 2010), the remaining four did not specify the setting. Only two trials reported the source of funding (Lv, 2010; Huang, 2014), and both of them received funding from the government. None of the included trials stated whether or not a conflict of interest existed.

Comparisons were usual care or placebo. All trials involving usual care included some form of active intervention such as antibacterial drugs, antivirals, vitamins, or antipyretics.

Treatment duration in the included clinical trials ranged from 3 to 7 days.

One trial (Lv, 2010) was multi-armed comparing *Bupleuri radix* injection with acupoint injection and intramuscular injection versus placebo (acupoint injection with saline solution), and usual care. All others were two-arm parallel trials, of which one (Cao, 2012) used *Bupleuri radix* injection solution taken orally, one (Gui et al., 2012) used inhaled nebulized *Bupleuri radix* solution, one (Xu and Mao, 2001) used *Bupleuri radix* injection for intramuscular injection, two (Li et al., 2011;

TABLE 1 | Characteristics of included trials.

Study ID	Diagnosis (syndrome differentiation)	Setting	Funding sources	Course of symptoms: mean ± SD	Sample size (TG/CG)	Age: Mean ± SD (y)	Gender (Male/ Total)	Name of the TG product and cointervention if available	Details of control group	Duration of treatment	Outcome measures
Cao (2012)	AURTI[a]	China, Clinic	NR	Within 24 h	109 (70/39)	NR, Children as reported	TG:34/ 70 CG: 19/39	*Bupleuri radix* solution for injections (PO,1~2 ml for children<3 years,2–3 ml for children≥3 years, tid)+ Usual care	Usual care: vitamin C (PO,0.1 g for children<3 years,0.2 g for children ≥3 years, tid), constant indoor temperature, maintains a level of humidity, physically cooling down when high fever occurs	72 h	systematic symptom resolution rate within 3 days from treatment onset[b]
Gui et al. (2012)	Infant, AURTI, fever	China, Clinic	NR	Within 24 h	108 (52/56)	42 days-12 m	TG:28/ 52 CG: 30/56	*Bupleuri radix* solution for injections (aerosol inhalation for 15 min,2 ml, 1/d)+ Usual care	Usual care: Nebulised ribavirin (aerosol inhalation for 15 min, 10–15 mg/(kg.d), 1/d), penicillin (for children with increased leukocytes and neutrophils), metamizole sodium (if necessary)	5 d	3 days symptom resolution rate cough, nasal discharge),1d-2 days-3 days temperature, adverse effect
Huang (2014)	viral cold	China	Hainan Provincial Administration of Traditional Chinese Medicine	2–5.5 (2.46 ±0.37)d	80 (54/26)	16-37 (22.0 ±2.2)	NR	*Bupleuri radix* (raw herb) (15g, Decoction, 2/d, PO)	Ribavirin (30 mg,1/d)	7 d	Cure rate[c]
Lv (2010)	AURTI, fever	China, Clinic and ward	Taishan (Shandong province) Science and Technology Development Plan	NR	253 (100/50/ 52/51)	NR, Children as reported	NR	T1:*Bupleuri radix* injection (acupoint injection, 0.4 ml for children 1-2 years,0.6 ml for children 3-6 years, 1 ml for children 6 years,2/d) +Usual care T2:*Bupleuri radix* injection, intramuscular injection, regimens same as TG)+Usual care	C1:placebo (normal saline, acupoint injection, regimens same as TG)+Usual care, C2: Usual care: (ribavirin, intramuscular injection,10 mg/kg/d)+Usual care; Usual care: vitamin C、vitamin B6 (IV), metamizole sodium (intramuscular injection,10 mg/kg, if temperature >39 °C)	48 h (indicated by the outcome24–48 h symptom resolution)	Time to resolution (fever); 24–48 h symptom resolution rate (fever)
Song (2020)	Febrile children, caused by AURTI	China	NR	2h-3 d	100 (50/50)	5-14 y	TG:29/ 50 CG: 27/50	*Bupleuri radix* (pill, 25mg/kg, PO)	Acetaminophen (PO,5–10 mg/kg, if temperature >38.5 C)	3 d	30min-60min–120min temperature, 3 days global symptom resolution rate (GPCR)
Xu and Mao (2001)	AURTIs, hyperpyrexia (rectal temperature: 39.5–40.8°C)	China	NR	NR	140 (78/62)	NR, children as reported	TG:42/ 78 CG: 38/62	*Bupleuri radix* injection, IM, 1 ml for children <3 years, 2 ml for children >3 years)+ Usual care	Usual care:acetaminophen (Suspension,10–15 mg/kg, PO)	1 d	1h-2h-4h–8 h temperature
		China	NR	NR		1-8 y					

(Continued on following page)

TABLE 1 | (*Continued*) Characteristics of included trials.

Study ID	Diagnosis (syndrome differentiation)	Setting	Funding sources	Course of symptoms: mean ± SD	Sample size (TG/CG)	Age: Mean ± SD (y)	Gender (Male/ Total)	Name of the TG product and cointervention if available	Details of control group	Duration of treatment	Outcome measures
Li et al. (2011)	Febrile children, caused by AURTI (temperature: 38.5–40.0				120 (60/60)		TG:32/ 60 CG: 34/60	*Bupleuri radix* (pills, 25mg/kg, PO, if temperature >38.5°C)+ Usual care	Acetaminophen (po,5–10 mg/kg, if temperature >38.5 °C) + Usual care Usual care: antibacterial drugs (in compliance with the "Guiding Principles for the Clinical Application of Antibacterial Drugs"), antiviral drugs etc.	96 h (indicated by the outcome 48–96 h symptom resolution)	30mim-1h–2 h temperature, 4 days global symptom resolution rate

[a]*Diagnosed AURTI, with the criteria: WBC<10.0 × 109/L, neutrophils<0.70, fever, nasal congestion and discharge, cough, dry mouth, red tongue, yellow coating on the tongue, no complications, onset within 24 h.*

[b]*Definition of global symptom resolution is "no symptom and normal temperature".*

[c]*Definition of cure rate is "no symptoms or sign of ARTI, normal laboratory checks".*

AURTI: acute upper respiratory tract infection; PO: oral; NR: not reported, TG: treatment group, CG: control group, SD: standard deviation, y: year, m: month, d: day, h: hour.

Song, 2020) used oral pills, one (Huang, 2014) used a decoction of *Bupleuri radix* pieces. Included trials seldom reported manufacturing or quality control details (see **Table 2**).

The reported outcome measures included change in global symptoms (Li et al., 2011; Cao, 2012; Huang, 2014; Song, 2020) and relief of symptoms including nasal discharge (Gui et al., 2012), cough (Gui et al., 2012), and fever (Xu and Mao, 2001; Lv, 2010; Gui et al., 2012; Song, 2020). These were defined as time to complete resolution of the symptom, the severity of symptoms, or the number of patients resolved at a pre-defined time. One trial (Lv, 2010) reported the definition of global symptom resolution based on the "Guiding principles of clinical research on the treatment of children with exogenous fever by new Chinese medicine" (Medicine, 1994). Three trials that assessed global symptoms improvement, used self-defined criteria. Only two (Li et al., 2011; Gui et al., 2012) trials reported any information about adverse events. No trials reported antibiotic usage, length of hospitalization, and days off work or school. All the outcomes were measured during treatment or at the completion of treatment.

Risk of Bias in Included Studies

All the studies which reported the change in fever had "some concerns" in their risk of overall bias. All were described as "randomized," one (Li et al., 2011) used the lottery method, randomly divided the participants into two groups according to odd and even numbers. Others did not report the method of random sequence generation or provided information on allocation concealment. Only one trial compared *Bupleuri radix* with placebo (Lv, 2010), there is a possibility that participants were aware of their assigned intervention during the trial, and there was no information about whether or not researchers were blinded. Researchers and participants in six trials (Xu and Mao, 2001; Lv, 2010; Li et al., 2011; Cao, 2012; Huang, 2014; Song, 2020) were likely aware of participants' assigned intervention during the trial, as they assessed two interventions that were different in dosage, or form of preparation, or two types of interventions, or compared *Bupleuri radix* plus usual care versus usual care, without any blinding information given. No included trials reported any losses to follow-up; thus all were judged as low risk of bias in deviations from the intended intervention and missing outcome data. No trial provided sufficient information to determine whether blinding of outcome assessment was achieved. It was, therefore, assumed that assessors may be aware of the intervention received by study participants. Thus, there are "some concerns" regarding the measurement of the outcome. No trial had a protocol available, accordingly, there were "some concerns" of the risk of bias in the selection of the reported result (see **Figure 2**).

All the studies which reported changes in global symptoms or nasal discharge and cough, had a high risk of overall bias, as all outcome measures were at risk of bias due to lack of blinding in the assessors (see **Figure 3**).

Effects of Interventions

The included trials featured four comparison groups: *Bupleuri radix* plus Vitamins versus placebo plus Vitamins (Lv, 2010),

TABLE 2 | Details of *Bupleuri radix* preparations in the included studies.

For patent proprietary CHM formulas

Study ID	Preparations	Reference to publicly available materials, such as pharmacopeia, for the details about the composition, dosage, efficacy, safety	Details of the formula, namely 1) the proprietary product name (i.e., brand name), 2) name of manufacturer, 3) lot number, 4) production date and expiry date, 5) name and percentage of added materials	Statement of whether the patent proprietary formula used in the trial is for a condition that is identical to the publicly available reference(Y/N)	Chemical analysis reported? (Y/N)	Quality control reported? (Y/N)
Cao (2012)	Injection	Take l000 g of Bupleuri radix (raw herb), cut into sections, soak in water. After steam distillation, the initial distillate was collected, and then re-distillation was conducted to collect about 1,000 ml of the heavy distillate. Add 3 g polysorbide 80, stir to dissolve the oil completely, add 9 g sodium chloride, dissolve, filter, add water for injection with 1,000 ml, adjust pH value, then fine filtration, poach, and sterilize[a]	Prepared by Wanrong Sanjiu Pharmaceutical Co., LTD. (Shanxi, China) Added materials: 3 g polysorbide 80, 9 g sodium chloride, water Other information: NA	Y	N	N
Gui et al. (2012)	Injection		Added materials: 3 g polysorbide 80, 9 g sodium chloride, water Other information: NA	Y	N	N
Lv (2010)	Injection		Prepared by Shanxi Jinxin Shuanghe Pharmaceutical Co., LTD. (Shanxi, China) Added materials: 3 g polysorbide 80, 9 g sodium chloride, water Other information: NA	Y	N	N
Xu and Mao (2001)	Injection		Name and percentage of added materials: 3 g polysorbide 80, 9 g sodium chloride, water Other information: NA	Y	N	N
Song (2020), Li et al. (2011)	Pills	[Pharmacopeia] Bupleuri radix (raw herb) 3571 g, add water and decoct twice, filter the decoction, and concentrate the filtrate to a relative density of 1.15–1.20 C80°C), add ethanol to make the alcohol content reach 70%, add an appropriate amount of polyethylene glycol, heat to melt and mix. Makes 1000 g film-coated pill	Brand name: Bupleurum pill Prepared by Tianjin Tasly Pharmaceutical Co., LTD. (Tianjin, China) lot number:100206 SFDA approval number: Z19990,024 Name and percentage of added materials: water, ethanol, polyethylene glycol Other information: NA	Y	N	N

For fixed CHM formulas

Study ID	Preparations	Name, source, processing method, and dosage of each medical substance	The authentication method of each ingredient and how, when, where, and by whom it was conducted; statement of whether any voucher specimen was retained, and if so, where they were kept and whether they are accessible	Principles, rationale, and interpretation of forming the formula	The production method of the formula	Safety assessment of the formula	References (s) as to the efficacy of the formula	Chemical analysis reported? (Y/N)	Quality control reported? (Y/N)
Huang (2014)	Decoction	Name: *Bupleuri radix* Other information: NA	*Bupleuri radix* (Chaihu) Other information: NA	Not relevant	Decoct with water	NA	NA	N	N

NA: Not available Y:Yes N:No SFDA: state food and drug administration.

[a]*The* Bupleuri radix *injection used in the four studies may not be prepared by the same manufacturer. The process methods were extracted from Volume 17 Drug Standards for Traditional Chinese Medicine Patent Preparation issued by the Ministry of Health in 1998(NO. WS3-B-3297-98), which had been valid until 2011 (China, P.C.o.t.M.o.H.o.t.P.s.R.o, 1998).*

Bupleuri radix plus usual care versus usual care (Xu and Mao, 2001; Cao, 2012; Gui et al., 2012), *Bupleuri radix* versus usual care (Huang, 2014; Song, 2020), *Bupleuri radix* plus usual care versus symptomatic treatment plus usual care (Lv, 2010; Li et al., 2011). Not all subgroup analyses were conducted due to insufficient data.

FIGURE 2 | Risk of bias in the studies which reported the outcome of fever.

Bupleuri radix Plus Usual Care Versus Placebo Plus Usual Care (1 Trial)

One trial (Lv, 2010), including 150 children with AURTI and fever, reported a statistically significant effect in favor of *Bupleuri radix* acupoint injection plus vitamins compared to placebo plus vitamins. The intervention shortened fever clearance time (FCT), defined as the time between the onset of treatment and sustained resolution of fever, i.e. the return of temperature to normal (<37.5°C) without recurrence during the same illness (MD: −33.32 h, 95%CI: −35.71, −30.93). It also improved the chance of fever resolution within 48 h (RR:14.00, 95%CI: 1.96, 99.94).

Bupleuri radix Plus Usual Care Versus Usual Care (3 Trials)

One trial (Cao, 2012) including 109 children with AURTI showed no difference between oral administration of *Bupleuri radix* solution for injections plus vitamins, versus vitamins alone, in global symptom resolution rate within 3 days from treatment onset (RR:1.42, 95%CI: 0.73, 2.76). Another trial (Gui et al., 2012) including 108 infants with AURTI used nebulized inhalation of *Bupleuri radix* solution for injections plus nebulized ribavirin compared with nebulized ribavirin alone. It showed an equivalent effect in relieving the symptom of nasal discharge and cough. However, it showed significant treatment effects for temperature reduction. A third trial (Xu and Mao, 2001), including 140 children with ARTI and fever, assessed the change of temperature with time from treatment onset, and demonstrated intramuscular injection of *Bupleuri radix* injection plus oral acetaminophen when compared with oral acetaminophen alone had larger effects on temperature reduction. See **Table 3**.

Bupleuri radix Versus Usual Care (2 Trials)

One trial (Huang, 2014) including 80 adults with the common cold, showed the effect of *Bupleuri radix* decoction on cure rate (no symptom or sign of AURTI, normal laboratory checks) after 7 days of continuous treatment was no different to ribavirin. Another trial (Song, 2020) including 100 AURTI children with fever, showed that *Bupleuri radix* pills when compared with acetaminophen had an inferior effect on temperature reduction at 30 min from treatment onset, but there wasn't a statistically significant effect at 60 min or 120 min from treatment onset. After 3 days of treatment, the pills demonstrated a higher global symptom resolution rate. See **Table 4**.

Bupleuri radix Plus Usual Care Versus Symptomatic Treatment Plus Usual Care (2 Trials)

One trial (Lv, 2010) including 103 children with AURTI and fever reported no significant difference in Fever Clearance Time FCT (MD: 0.99h, 95%CI: −6.31, 4.33) and the chance of fever resolution within 48 h (RR: 0.78, 95%CI: 0.22, 2.76), when comparing *Bupleuri radix* injection (intramuscular injection) plus vitamins with ribavirin plus vitamins. The other trial (Li et al., 2011) including 120 children with AURTI and fever compared *Bupleuri radix* pills plus usual care (antibacterial and antiviral drugs) with acetaminophen plus usual care, also had a similar result on improving the symptom of fever, regarding the temperature at 30 min from treatment onset (MD: −0.03°C, 95%CI: −0.14, 0.08), the temperature at 1st hour (MD: 0.05°C, 95%CI: −0.12, 0.22), the temperature at 2nd h (MD: −0.04 °C, 95%CI: −0.16, 0.08). Moreover, *Bupleuri radix* pills plus usual care also failed to show a statistically significant effect on global symptom

FIGURE 3 | Risk of bias in the studies which reported the outcome of improvement in global symptoms or nasal discharge and cough.

resolution rate within 4 days from treatment onset (RR: 1.25, 95%CI: 0.89, 1.76).

Adverse Events

Only two trials reported the occurrence of AEs; one of which (Gui et al., 2012) reported that there were no AEs in either the intervention or control groups. The other one (Li et al., 2011) reported 2 cases had skin rash, 2 cases sweated profusely in the control group. The other trials did not report whether or not there were any AEs.

Certainty Assessment of Evidence Using GRADE

All outcomes were evaluated as low-certainty or very low-certainty using the GRADE system approach. The details of the certainty of the available evidence can be found in **Supplementary Tables**. The certainty of the evidence was downgraded mainly due to the following reasons: 1) Risk of bias (high risk of detection bias and/or attrition bias); and 2) imprecision (small sample size or only one trial was included).

DISCUSSION

Summary of Main Results

Seven randomized trials involving 910 patients with AURTI were included in this review, with no language restrictions. The review identified three *Bupleuri radix* preparations (*Bupleuri radix* solution for injections, pills, decoction) with four administration routes: oral, acupoint injection, intramuscular injection, and nebulized inhalation. There were no trials that evaluated the effectiveness and safety of *Bupleuri radix* injection, with the administration routes of oral, acupoint injection, intramuscular injection, and nebulized inhalation, according to the Ministry of Health 2011 standards. *Bupleuri radix* acupoint injection demonstrated a statistically significant effect in reducing fever when compared with placebo, measured by both fever clearance time (MD: −33.32 h, 95%CI: −35.71, −30.93), and the chance of fever resolution within a predefined time after treatment (RR:14, 95%CI:1.96, 99.94). Nebulised inhalation of *Bupleuri radix* solution for injections was more effective when combined with usual care in improving fever, compared with usual care alone. However, *Bupleuri radix* injection (intramuscular injection) plus vitamins failed to demonstrate an effect in reducing fever, when compared with ribavirin plus vitamins. *Bupleuri radix* pills showed similar antipyretic effects with acetaminophen (mean temperature at 30 min from treatment onset: 38.61 ± 0.26; at 1st hour: 37.51 ± 0.24; at 2nd hour: 36.74 ± 0.24) (Song, 2020). Included trials also suggested that oral administration of *Bupleuri radix* solution for injections, pills, and *Bupleuri radix* decoction have a similar effect on improving global AURTI symptoms and two key symptoms (nasal discharge and cough), when compared with usual care. Some usual care involved in the included trials were not usual care in

TABLE 3 | *Bupleuri radix* plus usual care versus usual care (3 trials).

Study ID	Participants	Intervention	Control	Outcomes	Measures	Effect estimate
Cao (2012)	109 AURTI children	*Bupleuri radix* solution for injections (po) plus vitamin C	Vitamin C	Global symptom resolution rate within 3 days from treatment onset	RR (95% CI)	1.42 [0.73, 2.76]
Gui et al. (2012)	108 AURTI infants	*Bupleuri radix* solution for injections (nebulized inhalation) plus nebulized ribavirin	Nebulised ribavirin	Resolution rate of nasal discharge within 3 days from treatment onset	RR (95% CI)	1.13 [0.70, 1.83]
				Resolution rate of cough within 3 days from treatment onset	RR (95% CI)	1.62 [0.80, 3.27]
				The temperature at day 1 from treatment onset	MD (95% CI)	−1.00°C [−1.19, −0.81]
				The temperature at day 2 from treatment onset	MD (95% CI)	−0.60°C [−0.77, −0.43]
				The temperature at day 3 from treatment onset	MD (95% CI)	−0.10°C [−0.23, 0.03]
Xu and Mao (2001)	140 children with AURTI and fever	*Bupleuri radix* injection (IM) plus oral acetaminophen	Oral acetaminophen	The temperature at 1st hour from treatment onset	MD (95% CI)	−0.27°C [−0.47, −0.07]
				The temperature at 2 nd h from treatment onset	MD (95% CI)	−0.41°C [−0.61, −0.21]
				The temperature at the 4th hour from treatment onset	MD (95% CI)	−0.10°C [−0.28, 0.08]
				The temperature at the 8th hour from treatment onset	MD (95% CI)	−0.74°C [−0.96, −0.52]

AURTI: acute upper respiratory tract infection; PO: oral; IM: intramuscular injection; RR: risk ratio; MD: mean difference; CI: confidence interval.

the UK and many other countries, such as nebulized ribavirin is not usual care for the common cold. However, in China, they were usual care as some form of active intervention at the time of trials conducted. To facilitate the sorting of the results, they were all named "usual care". Only two trials reported on the occurrence of adverse events; they did not record any adverse events in the intervention groups.

Quality of the Evidence

There were no high-quality trials of *Bupleuri radix* for ARTI, and the quality of reporting was poor for all trials. None of the included trials were blinded; reporting indicated that the outcomes could have been influenced by a lack of blinding, and consequently were rated at a high risk of bias. There were no diagnostic or inclusion/exclusion criteria provided in most of the studies. This may have impacted the homogeneity of participants included in the trials, and the severity of symptoms. This makes the trials difficult to replicate.

As a natural product, the source of herb and the production method (plant extraction and whether the product is standardized) determine the proportion of constituents and resulting dose, thus influencing the effectiveness and safety of *Bupleuri radix*. This review identified three *Bupleuri radix* preparations, but most of them did not provide manufacturing details to ensure the quality and consistency of the products. The quality of evidence using GRADE was low for fever-related outcomes and very low for other symptom-related outcomes.

Strengths and Limitations

This is the first systematic review evaluating the effects of *Bupleuri radix* on ARTI. The Cochrane methodology was

TABLE 4 | *Bupleuri radix* versus usual care (2 trial).

Study ID	Participants	Intervention	Control	Outcomes	Measures	Effect estimate
Huang (2014)	80 adults with the common cold	*Bupleuri radix* decoction (po)	Ribavirin	Cure rate after 7 days continuous treatment	RR (95% CI)	0.78 [0.42, 1.43]
Song (2020)	100 children with AURTI and fever	*Bupleuri radix* pill (po)	Acetaminophen	Global symptom resolution rate within 3 days from treatment onset	RR (95% CI)	2.23 [1.32, 3.77]
				Temperature at 30 min from treatment onset	MD (95% CI)	0.13°C [0.03, 0.23]
				Temperature at 1st hour from treatment onset	MD (95% CI)	0.04°C [−0.05, 0.13]
				The temperature at 2 nd h from treatment onset	MD (95% CI)	0.07°C [−0.03, 0.17]

AURTI: acute upper respiratory tract infection; PO: oral; RR: risk ratio; MD: Mean Difference; CI: Confidence interval.

followed and a protocol of this systematic review was registered and published online. We searched for RCTs using a broad search of different databases without language restrictions. Although we performed a broad search for ARTI in both children and adults, only trials involving AURTI qualified for inclusion. There were no trials on acute lower respiratory tract infections such as acute bronchitis. As all authors running the searches are Chinese, there may be a bias in that studies published in Chinese or Chinese journals, may have been more likely to be identified than articles in other non-English languages, even though language restrictions were not applied.

Comparison With Other Studies or Reviews

Contemporary experimental research suggests that *Bupleuri radix* acts on various targets and pathways to produce significant antiviral effects on ARTI, but it is usually used with other herbals such as *Scutellariae Radix*, which are reported to be effective in improving the AURTI symptoms, such as fever and cough (Li and Deng, 2018; Wei et al., 2021). However, this review only included *Bupleuri radix* as a single herb and it failed to detect a statistically significant effect on global symptom resolution rate and some respiratory symptoms including cough and nasal discharge. Moreover, *Bupleuri radix* has been reported to exhibit mild to a severe adverse drug reaction or adverse events (ADR/AE) such as anaphylactic shock, acute hepatitis, and acute hepatic necrosis (Kong et al., 2010). However, the studies included in this review reported no side effects. Due to the relatively small number of studies combined with the short duration of treatment included in this review, we cannot draw any conclusions about the safety of *Bupleuri radix*.

Implications for Future Studies

Future well-designed trials evaluating effectiveness and safety of *Bupleuri radix* for AURTI and reported according to the CONSORT checklist (Schulz et al., 2010) are vital. The potential for antibiotic sparing should also be studied in future trials. Concerning the assessment of safety, other data sources may be necessary to complement our findings.

Implications for Practice

This review shows that *Bupleuri radix* may have a superior antipyretic effect on febrile adults or children who suffer from AURTI compared with placebo and usual care. However, fever management in AURTI with antipyretic drugs remains a common practice. There is currently insufficient evidence to recommend a change in practice.

CONCLUSION

Low-certainty or very low-certainty evidence demonstrated that *Bupleuri radix* pill and solution for injections may have an antipyretic effect on febrile patients who suffer from AURTI, but it failed to show effects on other AURTI symptoms. However, the quality of included trials was generally low as many were poorly designed and inadequately blinded. Insufficient adverse event data was available to comment on its safety. Therefore, we could not draw more firm conclusions.

DATA AVAILABILITY STATEMENT

The original contributions presented in the study are included in the article/**Supplementary Material**, further inquiries can be directed to the corresponding authors.

AUTHOR CONTRIBUTIONS

JPL, XYH, and LJY conceived and designed the review. LJY, MF, and HDL were responsible for the searching, screening, and selection of studies. HDL and LJY participated in the data extraction. Z-JW and LJY were responsible for the risk of bias assessment. LJY performed the statistical analysis. LJY drafted the manuscript. MF completed the PRISMA checklist. JPL, MM, MW, JT, and XYH were involved in critically revising the manuscript. All authors have contributed to and approved the manuscript, including the authorship list.

FUNDING

This review is funded by the National Key Research and Development Project (Grant No. 2018YFE0102300) and Innovate UK (Grant No. 104287-610239).

SUPPLEMENTARY MATERIAL

The Supplementary Material for this article can be found online at: https://www.frontiersin.org/articles/10.3389/fphar.2021.787084/full#supplementary-material

REFERENCES

Acute (1998). Acute Respiratory Infections: the Forgotten Pandemic. *Bull. World Health Organ.* 76 (1), 101-7–105-107.

Administration, S.F.a.D. (2012). "National Drug Standards Issued by the State Food and Drug Administration [Revision] (ZGB2011-46), Drug Standards of China".

Cabral, C., Lucas, P. J., Ingram, J., Hay, A. D., and Horwood, J. (2015). "It's Safer to . . ." Parent Consulting and Clinician Antibiotic Prescribing Decisions for Children with Respiratory Tract Infections: An Analysis across Four Qualitative Studies. *Soc. Sci. Med.* 136-137, 156–164. doi:10.1016/j.socscimed.2015.05.027

Cao, C. Y. (2012). Analysis of 70 Cases of Upper Respiratory Tract Infection Treated with Chaihu Injection. *Chin. Pharm. Clin.* 12 (S1), 66. doi:10.3969/j.issn.1671-2560.2012.z1.036

Chen, J. K., Chen, T. T., and Crampton, L. (2004). "Wind-Heat Releasing Herb-Section 2 ChaiHu (Radix Bupleuri)," in *Chinese Medical Herbology and Pharmacology*. City of Industry, CA: Art of Medicine Press, Chap. 2, 83–85.

Cheng, C. W., Wu, T. X., Shang, H. C., Li, Y. P., Altman, D. G., Moher, D., et al. (2017). CONSORT Extension for Chinese Herbal Medicine Formulas 2017:

Recommendations, Explanation, and Elaboration (Traditional Chinese Version). *Ann. Intern. Med.* 167 (2), W7–W121. doi:10.7326/M16-2977

China, M.o.H.o.t.p.s.R.o. (1997). "Guiding Principles of Clinical Research on the Treatment of Exogenous Fever in Children with New Drugs of Traditional Chinese Medicine".

China, P.C.o.t.M.o.H.o.t.P.s.R.o. (1998). "Pharmaceutical Standards of the Ministry of Health of the People's Republic of China".

Fang, J. L., and Zhang, Y. P. (2003). Observation on the Curative Effect of Fast Cure of 50 Cases of Cold with Chaihu Acupoint Block Therapy. *Chin. J. Clin. Med. (Beijing)* 4 (20), 56.

Gao, Y., Wang, Z. B., Zuo, Z. P., Yu-Chi, H. U., Cao, C. R., Guo, Y. D., et al. (2012). Antipyretic Effect of Chaihu Injection in Rat Model with Lps-Induced Fever. *J. Beijing Univ. Traditional Chin. Med.* 35 (10), 696–698.

Gonzales, R., Malone, D. C., Maselli, J. H., and Sande, M. A. (2001). Excessive Antibiotic Use for Acute Respiratory Infections in the United States. *Clin. Infect. Dis.* 33 (6), 757–762. doi:10.1086/322627

Gui, C. K., Kang, Y. H., and Gui, C. G. (2012). Analysis of the Efficacy of Bupleurum and Ribavirin Oxygen Atomization Inhalation in the Treatment of Upper Respiratory Tract Infection in Infants. *Chin. foreign Med. Res.* 10 (05), 38–39. doi:10.14033/j.cnki.cfmr.2012.05.107

Huang, H. Q., Wang, X., H., Fu, H., Wang, Y., and Yang, S., H. (2017). Research Progress on Medicinal Plant Resources of Bupleurum L. *Chin. Traditional Herbal Drugs* 48 (14), 2989–2996. doi:10.7501/j.issn.0253-2670.2017.14.030

Huang, J. B. (2014). 54 Cases of Viral Cold Were Treated with a Single Bupleurum Decoction. *Traditional Chin. Med.* 34 (09), 1790–1791. doi:10.16367/j.issn.1003-5028.2014.09.062

Higgins, Julian., James, Thomas., Chandler, Jacqueline., Miranda, Cumpston., Li, Tianjing., Page, Matthew., et al. (2020). Cochrane Handbook for Systematic Reviews of Interventions Version 6.1 [Online]. [Accessed December 8, 2021].

ICH, T.I.C.f.H. (1994). CLINICAL SAFETY DATA MANAGEMENT: DEFINITIONS and STANDARDS for EXPEDITED REPORTING E2A [Online]. [Accessed December 8, 2021].

Itoh, S., Marutani, K., Nishijima, T., Matsuo, S., and Itabashi, M. (1995). Liver Injuries Induced by Herbal Medicine, Syo-Saiko-To (Xiao-chai-hu-tang). *Dig. Dis. Sci.* 40 (8), 1845–1848. doi:10.1007/BF02212712

King, D., Mitchell, B., Williams, C. P., and Spurling, G. K. (2015). Saline Nasal Irrigation for Acute Upper Respiratory Tract Infections. *Cochrane Database Syst. Rev.* 4, CD006821. doi:10.1002/14651858.CD006821.pub3

Klein, S. D., Becker, S., and Wolf, U. (2012). Occurrence of Chai Hu (Bupleuri Radix) in Prescriptions of Chinese Herbal Medicine in Switzerland. *Forsch Komplementmed* 19 (5), 242–246. doi:10.1159/000343506

Kong, X. Y., Hao, Y., Wu, T. X., and Xie, Y. M. (2010). Adverse Drug Reactions or Adverse Events of Chaihu Injection: a Systematic Review. *Zhong Xi Yi Jie He Xue Bao* 8 (12), 1124–1132. doi:10.3736/jcim20101204

Li, W. H., and Deng, Z. H. (2018). Clinical Study of Chaihuang Granule Combined with Ribavirin Aerosol in the Treatment of Acute Upper Respiratory Tract Infection in Children. *Mod. Med. Clinic* 33 (11), 2884–2887. doi:10.7501/j.issn.1674-5515.2018.11.027

Li, Y., Xu, C., Zhang, Q., Liu, J. Y., and Tan, R. X. (2005). *In Vitro* anti-Helicobacter pylori Action of 30 Chinese Herbal Medicines Used to Treat Ulcer Diseases. *J. Ethnopharmacol* 98 (3), 329–333. doi:10.1016/j.jep.2005.01.020

Li, Y. J., Xiao, Y., and Me, H. X. (2011). Comparison of Antipyretic Efficacy of Chaihu Pills and Paracetamol. *Chin. Pharmacist* 14 (12), 1796–1797. doi:10.3969/j.issn.1008-049X.2011.12.038

Limmathurotsakul, D., Dunachie, S., Fukuda, K., Feasey, N. A., Okeke, I. N., Holmes, A. H., et al. (2019). Improving the Estimation of the Global burden of Antimicrobial Resistant Infections. *Lancet Infect. Dis.* 19 (11), e392–e398. doi:10.1016/S1473-3099(19)30276-2

Lv, G. Q. (2010). Clinical Nursing Care of Children with Exogenous Fever Treated by Quchi Acupoint Sealing with Bupleurum Injection. *Inner Mongolia traditional Chin. Med.* 29 (24), 151–152. doi:10.16040/j.cnki.cn15-1101.2010.24.042

Medicine, S.A.o.T.C (1994). *Diagnostic and Curative Effect Standard of Disease and Syndrome of Traditional Chinese Medicine*. Nanjing: Nanjing University Press.

Naylor, N. R., Pouwels, K. B., Hope, R., Green, N., Henderson, K. L., Knight, G. M., et al. (2019). The Health and Cost burden of Antibiotic Resistant and Susceptible Escherichia coli Bacteraemia in the English Hospital Setting: A National Retrospective Cohort Study. *PLoS One* 14 (9), e0221944. doi:10.1371/journal.pone.0221944

NICE, N.I.f.H.a.C.E. (2010). NHS [Online]. [Accessed December 8, 2021].

Pouwels, K. B., Dolk, F. C. K., Smith, D. R. M., Robotham, J. V., and Smieszek, T. (2018). Actual versus 'ideal' Antibiotic Prescribing for Common Conditions in English Primary Care. *J. Antimicrob. Chemother.* 73 (Suppl. l_2), 19–26. doi:10.1093/jac/dkx502

Schulz, K. F., Altman, D. G., Moher, D., and Group, C. (2010). CONSORT 2010 Statement: Updated Guidelines for Reporting Parallel Group Randomized Trials. *Obstet. Gynecol.* 115 (11), 1063–1070. doi:10.1097/AOG.0b013e3181d9d421

Soilemezi, D., Leydon, G. M., Yan, R., Simpson, C., Bell, M., Bostock, J., et al. (2020). Herbal Medicine for Acute Bronchitis: A Qualitative Interview Study of Patients' and Health Professionals' Views. *Complement. Ther. Med.* 55, 102613. doi:10.1016/j.ctim.2020.102613

Song, l. J. (2020). Study on the Efficacy of Chaihu Dropping Pills in the Treatment of Infantile Fever. *China Health Nutr.* 30 (36), 270.

Sterne, J. A. C., Savović, J., Page, M. J., Elbers, R. G., Blencowe, N. S., Boutron, I., et al. (2019). RoB 2: a Revised Tool for Assessing Risk of Bias in Randomised Trials. *BMJ* 366, l4898. doi:10.1136/bmj.l4898

The Cochrane Collaboration (2020). Review Manager (RevMan) [Computer program]. Version 5.4.

Wei, J. R., Zhang, B., Zhang, G. Y., Shen, D. X., and Zhou, J. J. (2021). Clinical Study of Chaihuang Granule Combined with Oseltamivir in the Treatment of Acute Upper Respiratory Tract Infection in Children. *Mod. Med. Clinic* 36 (01), 72–75. doi:10.7501/j.issn.1674-5515.2021.01.014

Willcox, M., Donovan, E., Hu, X. Y., Elboray, S., Jerrard, N., Roberts, N., et al. (2020). Views Regarding Use of Complementary Therapies for Acute Respiratory Infections: Systematic Review of Qualitative Studies. *Complement. Ther. Med.* 50, 102382. doi:10.1016/j.ctim.2020.102382

Wu, R. P., and Hu, Y. M. (1995). *Practical Pediatrics*. Beijing: people's Health Publishing House.

Wyk, B. E. V., and Wink, M. (2004). *Medicinal Plants of the World: An Illustrated Scientific Guide to Important Medicinal Plants and Their Uses*. Portland, Oregon: Timber Press, 480.

Xie, J. Y., Di, H. Y., Li, H., Cheng, X. Q., Zhang, Y. Y., and Chen, D. F. (2012). Bupleurum Chinense DC Polysaccharides Attenuates Lipopolysaccharide-Induced Acute Lung Injury in Mice. *Phytomedicine* 19 (2), 130–137. doi:10.1016/j.phymed.2011.08.057

Xu, F. Z., and Mao, C. F. (2001). Observation on the Efficacy of Bupleurum and Tylenol in the Treatment of 78 Cases of Infantile Upper Fever. *Handan Med. Coll. academical Bull.* 14 (05), 403.

Yang, F., Dong, X., Yin, X., Wang, W., You, L., and Ni, J. (2017). Radix Bupleuri: A Review of Traditional Uses, Botany, Phytochemistry, Pharmacology, and Toxicology. *Biomed. Res. Int.* 2017, 7597596. doi:10.1155/2017/7597596

Zhu, W. W., Yu, Y., and Peng, Z. P. (2017). The Therapeutic Effect of Chaihuang Granule on Children with Repeated Respiratory Infections and its Influence on Immune Function. *Mod. J. Integrated Traditional Chin. West. Med.* 26 (32), 3587–3589. doi:10.3969/j.issn.1008-8849.2017.32.018

Conflict of Interest: The authors declare that the research was conducted in the absence of any commercial or financial relationships that could be construed as a potential conflict of interest.

Publisher's Note: All claims expressed in this article are solely those of the authors and do not necessarily represent those of their affiliated organizations, or those of the publisher, the editors and the reviewers. Any product that may be evaluated in this article, or claim that may be made by its manufacturer, is not guaranteed or endorsed by the publisher.

frontiers in Pharmacology

ORIGINAL RESEARCH
published: 23 February 2022
doi: 10.3389/fphar.2022.801350

An Integrative Pharmacology Model for Decoding the Underlying Therapeutic Mechanisms of Ermiao Powder for Rheumatoid Arthritis

Jie Wu[1,2†], Kexin Wang[1,3†], Qinwen Liu[1,2], Yi Li[4†], Yingying Huang[5], Yujie Liu[1,2], Jieqi Cai[1,2], Chuanhui Yin[1,2†], Xiaowei Li[1,2], Hailang Yu[1,2], Wei Meng[1,2], Handuo Wang[1,2], Aiping Lu[6,7], Yazi Li[1,2]* and Daogang Guan[1,2]**

[1]Department of Biochemistry and Molecular Biology, School of Basic Medical Sciences, Southern Medical University, Guangzhou, China, [2]Guangdong Provincial Key Laboratory of Single Cell Technology and Application, Guangzhou, China, [3]Neurosurgery Institute, Department of Neurosurgery, Zhujiang Hospital, Southern Medical University, Guangzhou, China, [4]Department of Radiology, Nanfang Hospital, Southern Medical University, Guangzhou, China, [5]Department of Obstetrics and Gynecology, Nanfang Hospital, Southern Medical University, Guangzhou, China, [6]Institute of Integrated Bioinformedicine and Translational Science, Hong Kong Baptist University, Hong Kong, China, [7]Guangdong-Hong Kong-Macau Joint Lab on Chinese Medicine and Immune Disease Research, Guangzhou, China

OPEN ACCESS

Edited by:
Shuai Ji,
Xuzhou Medical University, China

Reviewed by:
Wildan Khairi Muhtadi,
Sekolah Tinggi Ilmu Farmasi Riau, Indonesia
Nut Koonrungsesomboon,
Chiang Mai University, Thailand

***Correspondence:**
Aiping Lu
aipinglu@hkbu.edu.hk
Yazi Li
liyazi@smu.edu.cn
Daogang Guan
guandg0929@hotmail.com

†These authors have contributed equally to this work

Specialty section:
This article was submitted to Ethnopharmacology, a section of the journal Frontiers in Pharmacology

Received: *25 October 2021*
Accepted: *04 January 2022*
Published: *23 February 2022*

Citation:
Wu J, Wang K, Liu Q, Li Y, Huang Y, Liu Y, Cai J, Yin C, Li X, Yu H, Meng W, Wang H, Lu A, Li Y and Guan D (2022) An Integrative Pharmacology Model for Decoding the Underlying Therapeutic Mechanisms of Ermiao Powder for Rheumatoid Arthritis. Front. Pharmacol. 13:801350. doi: 10.3389/fphar.2022.801350

As a systemic inflammatory arthritis disease, rheumatoid arthritis (RA) is complex and hereditary. Traditional Chinese medicine (TCM) has evident advantages in treating complex diseases, and a variety of TCM formulas have been reported that have effective treatment on RA. Clinical and pharmacological studies showed that Ermiao Powder, which consists of *Phellodendron amurense* Rupr. (PAR) and *Atractylodes lancea* (*Thunb.*) DC. (ALD), can be used in the treatment of RA. Currently, most studies focus on the anti-inflammatory mechanism of PAR and ALD and are less focused on their coordinated molecular mechanism. In this research, we established an integrative pharmacological strategy to explore the coordinated molecular mechanism of the two herbs of Ermiao Powder in treating RA. To explore the potential coordinated mechanism of PAR and ALD, we firstly developed a novel mathematical model to calculate the contribution score of 126 active components and 85 active components, which contributed 90% of the total contribution scores that were retained to construct the coordinated functional space. Then, the knapsack algorithm was applied to identify the core coordinated functional components from the 85 active components. Finally, we obtained the potential coordinated functional components group (CFCG) with 37 components, including wogonin, paeonol, ethyl caffeate, and magnoflorine. Also, functional enrichment analysis was performed on the targets of CFCG to explore the potential coordinated molecular mechanisms of PAR and ALD. The results indicated that the CFCG could treat RA by coordinated targeting to the genes involved in immunity and inflammation-related signal pathways, such as phosphatidylinositol 3-kinase/protein kinase B signaling pathway, mitogen-activated protein kinase signaling pathway, tumor necrosis factor signaling pathway, and nuclear factor-kappa B signaling pathway. The docking and *in vitro* experiments were used to predict the affinity and validate the effect of CFCG and further confirm the reliability of our method. Our integrative pharmacological strategy, including CFCG identification and verification, can provide the methodological

references for exploring the coordinated mechanism of TCM in treating complex diseases and contribute to improving our understanding of the coordinated mechanism.

Keywords: rheumatoid arthritis (RA), traditional Chinese medicine (TCM), Ermiao Powder (EMP), coordinated functional components group (CFCG), coordinated molecular mechanisms

INTRODUCTION

Rheumatoid arthritis (RA) is autoimmune arthritis with the characteristics of systemic inflammation, persistent synovitis, and autoantibodies (Scott et al., 2010; Wasserman 2011; Smolen et al., 2017). It is related to the aberrant immune network, which consists of complex inflammatory signaling pathways underlying its pathogenesis (Scott et al., 2010; Xu et al., 2018). The factors that contribute to RA are multiple and bring challenges to the treatment of RA (MacGregor et al., 2000; Wasserman 2011). This hereditary disease is common in the elderly and women (Scott et al., 2010). Early diagnosis of RA plays a key role in effective treatment. Also, in the earlier treatment, disease-modifying antirheumatic drugs (DMARDs) are applied (Quinn et al., 2001; Choi et al., 2002; Donahue et al., 2008). DMARDs are usually combined to control the disease (Simon 2000; Garrood and Scott 2001; Kremer 2001; O'Dell 2001; Choy et al., 2005). When DMARDs are not suitable for the patients, biological agents can be used to relieve the symptoms, such as tumor necrosis factor (TNF) inhibitors, abatacept, rituximab, and tocilizumab (Kristensen et al., 2007; Alonso-Ruiz et al., 2008; Singh et al., 2009; Scott et al., 2010). However, the costs of biological agents are high for patients, and they may have the risk of infections (Bansback et al., 2009; Leombruno et al., 2009; Strangfeld et al., 2009).

Traditional Chinese medicine (TCM) has a long history of development, and it has accumulated a large number of theories and rich clinical experience. TCM can effectively treat RA with high safety and few adverse effects (Shi et al., 2020). Increasing studies about RA have paid attention to the effects of TCM on the treatment of RA, and more and more evidence confirms that a variety of TCM formulas can have effective treatment on RA (Wang et al., 2011; Zhang et al., 2015; Guo et al., 2016; Cheng et al., 2017; Guo et al., 2017; Wang et al., 2018; Wang et al. 2020a; Wang et al. 2020b; Liu et al., 2020), such as Ermiao Powder (EMP) (Li et al., 2020), Danggui-Sini-decoction (Cheng et al., 2017; Wang L. et al., 2020), Huangqi-Guizhi Wuwu-Decoction (Wang et al., 2020a; Wang et al., 2020b; Liu et al., 2020), Bi-Qi capsule (Wang et al., 2011; Wang et al., 2018), Wu-Tou Decoction (Zhang et al., 2015; Guo et al., 2017), and Guizhi-Shaoyao-Zhimu (Guo et al., 2016). Among these formulas, EMP is widely used in clinical.

EMP is comprised of two herbs: *Phellodendron amurense* Rupr. (PAR) (15 g) and *Atractylodes lancea* (*Thunb.*) DC. (ALD) (15 g). Due to the function of anti-inflammatory, EMP has been widely used in treating RA. More studies focused on analyzing the anti-inflammatory mechanism of PAR and ALD separately or the anti-inflammatory effects of EMP. Chen et al. (2014) explored EMP's anti-inflammatory effects through the activation of NO and the production of pro-inflammatory cytokine in lipopolysaccharide (LPS)-induced RAW264.7 cells, and they found that EMP could inhibit the mitogen-activated protein kinase (MAPK) and nuclear factor-kappa B (NF-κB) pathway to decrease the inflammatory events and downregulate the expression of inducible nitric oxide synthase. To analyze EMP's effect on rats with RA, Li et al. (2020) tested joint swelling and arthritis index in different experimental groups of rats. The result of Masson staining showed that the joints of collagen-induced arthritis rats had pathological features of arthritis, such as synovial hyperplasia, articular cartilage, and bone erosion. The rats in the EMP group displayed significantly alleviated symptoms compared with the collagen-induced arthritis group, such as the swelling of the hind paws and the joint damage. Their results indicated that EMP could treat RA by regulating the cholinergic anti-inflammatory pathway (Li et al., 2020). However, the coordinated molecular mechanism of PAR and ALD in treating RA remains unclear.

Toward this end, we explored the coordinated molecular mechanisms of EMP in treating RA through a network pharmacology method. We screened active components from the components of PAR and ALD obtained from the Traditional Chinese Medicine Database and Analysis Platform (TCMSP), and 126 components that meet Lipinski's rules were retained. Then, the coordinated functional space prediction model was applied to quantify the effect of 126 active components on RA, and we identified the coordinated functional space composed of 85 components. Through the knapsack algorithm, we identified A coordinated functional components group (CFCG) from the 85 active components. We also explored the potential coordinated mechanism of CFCG by the functional enrichment analysis and molecular docking. The results indicated the potential co-functional effect of CFCG, and they can target genes related to inflammation and immunity. Finally, we validated the effect of CFCG through *in vitro* experiments. The results demonstrated the coordinated mechanism of CFCG from PAR and ALD in treating RA. Our study's principal novelty is the design of a reliable optimization model and reverse-engineering strategy, which can obtain the core components group with the smallest number of components and the most extensive coverage of function from EMP. It could provide a methodologic reference for exploring the coordinated mechanism of TCM in treating complex diseases and prescriptions optimization.

METHODS

Dataset Collection

The chemical components of PAR and ALD were collected from the TCMSP (https://tcmsp-e.com/) (Ru et al., 2014). Open Babel

toolkit (version 2.4.1) was applied to convert the components' chemical structure to canonical SMILES (O'Boyle et al., 2011).

Absorption, Distribution, Metabolism, and Excretion Screening

From SwissADME (http://www.swissadme.ch/index.php) (Daina et al., 2017), we obtained the properties of all components, including molecular weight (MW), rotatable bonds (RBN), number of hydrogen bonds acceptors (nHAcc), number of hydrogen bonds donors (nHDon), and the Consensus LogP (ClogP). Lipinski's rules were applied to filter active components of PAR and ALD: 1) MW lower than 500 Da, 2) RBN lower than 11, 3) nHAcc lower than 10, 4) nHDon lower than 5, and 5) the ClogP value over −2 and lower than 5 (Lipinski et al., 2001).

Target Prediction

The target genes of active components were predicted through Similarity Ensemble Approach (SEA) (http://sea.bkslab.org/) (Keiser et al., 2007), HitPick (http://mips.helmholtz-muenchen.de/hitpick/cgi-bin/index.cgi?content=targetPrediction.html) (Liu et al., 2013), and SwissTargetPrediction (http://www.swisstargetprediction.ch/) (Gfeller et al., 2014). Then, the prediction results from the three databases were merged.

Component-Target Networks Construction

The component-target (C-T) network was constructed based on active components and their target genes by Cytoscape (version 3.6.0) (Shannon et al., 2003). The Cytoscape plugin NetworkAnalyzer was then used to obtain and analyze the C-T networks' topological properties.

Coordinated Functional Space Prediction Model

To analyze the effect of each active component of PAR and ALD on RA, a coordinated functional space prediction model was constructed to calculate the contribution score of each component to the coordinated functional space as follows:

$$CSC(i) = \sum_{ij}^{n} \left(NL\left(C_{ij}\right) + NL\left(dose_i\right) \right)$$

$$NL\left(C_{ij}\right) = \frac{C_{ij} - C_{min}}{C_{max} - C_{min}}$$

$$NL\left(dose_i\right) = \frac{dose_i - dose_{min}}{dose_{max} - dose_{min}}$$

$$C_{ij} = Comp_i \times \left[\left(\frac{C_{edge}}{T_{edge}} + \left| \frac{Comp_{Hi} - Comp_{Ci}}{Comp_{Hi} + Comp_{Ci}} \right| \right) \times Tar_j \right]$$

In the equation discussed earlier, i represents the component, and j is one of its targets. For each component, CSC represents the contribution score, and $Comp_i$ represents the eccentricity. $Comp_{Hi}$ represents the eccentricity of each component only in PAR, and $Comp_{Ci}$ represents components that only consist in ALD. C_{edge} is the edge count of each component, T_{edge} is the edge count of all the component's targets, and Tar_j represents the sum eccentricity value of all the component's targets. NL (C_{ij}) represents the value of min–max normalization to C_{ij}, and NL ($dose_i$) represents the value of min–max normalization to each component's dose in EMP.

According to the coordinated functional space prediction models, we obtained each component's contribution score. The top 85 components were selected; the sum of their contribution score accounts for 90% of the total contribution score of all components.

Function Enrichment Analysis

Gene Ontology (GO) and Kyoto Encyclopedia of Genes and Genomes (KEGG) pathway analysis for targets of components in this study and RA-related genes was performed by R package "clusterProfiler," respectively (Yu et al., 2012).

Identification of Key Coordinated Function Components

To identify the core coordinated functional components of the top 85 active components that have the greatest effects in EMP, we applied the knapsack algorithm. For the 900 targets of the 85 active components, the target–target interaction was identified according to the protein–protein interaction (PPI) network. Then, the degrees of the 85 active components and the 900 targets were obtained by the Cytoscape plugin NetworkAnalyzer. The 473 targets whose degrees were over the median degree of 900 targets and 85 components were retained.

Next, the knapsack algorithm was performed for the 85 components and their 473 targets.

$$f_{iN} = \begin{cases} 0 & i = 0 \; or \; N = 0 \\ \sum_{N<n_i}^{i-1} k_{i-1} D_{i-1} & 0 < i < 85 \\ \max\left\{ f_{(i-1)N},\; f_{(i-1)(N-n_i)} + D_i \right\} & 0 < i \le 85, N \ge n_i \end{cases}$$

$$k_i = 0/1, i = 1, 2, \ldots, 85$$

In the formula, k_i represents the component i that was selected or not, and D_i is the sum degree of its targets. N is set to 426, which is the largest number of targets in the knapsack. n_i represents the count of targets of component i. f_{iN} represents the largest sum degrees of the targets of components in the knapsack, whereas the number of targets is N. In short, when the number of targets in the knapsack accounts for 90% (426) of the 473 targets, the number of components put in the knapsack is the least, and the sum of the degrees of these 426 targets is the largest. CFCG, which consists of 37 components, was identified.

Prediction of Coordinated Mechanism by Molecular Docking

The three-dimensional conformer of CFCG was collected from ZINC (https://zinc.docking.org/) (Sterling and Irwin 2015) and PubChem (https://pubchem.ncbi.nlm.nih.gov) databases (Kim et al., 2021). The proteins coded by the target genes of CFCG

were acquired from the protein data bank (http://www.rcsb.org) (wwPDB Consortium, 2019). Auto Dock Tools (Morris et al., 2009) and Autodock Vina (Trott and Olson 2010) were used to docking with the seed of docking set to 10,000, the energy range is four, and the exhaustiveness is 96. The affinity method and pyMOL (Delano, 2002; Mura et al., 2010) were used to estimate and perform the docking result.

EXPERIMENTAL VERIFICATION OF COORDINATED FUNCTIONAL COMPONENTS GROUP

Materials

Wogonin (≥98% purity by high-performance liquid chromatography) was purchased from Jingzhu Biotechnology Co., Ltd. (Nanjing, China). Paeonol, magnoflorine (≥98% purity by high-performance liquid chromatography), and ethyl caffeate were purchased from Jiangsu Yongjian Pharmaceutical Co., Ltd. (Jiangsu, China). Moreover, fetal bovine serum and Dulbecco's modified Eagle's medium, which were required for the experiments, were obtained from Gibco (Grand Island, United States). Also, LPS was acquired from Sigma-Aldrich Co., Ltd. (St. Louis, United States).

Cell Culture and Treatment

Mouse macrophage RAW264.7 cells were acquired from the cell bank of the Chinese Academy of Sciences (Shanghai, China). The RAW264.7 cells were cultured in complete Dulbecco's modified Eagle's medium with 8% fetal bovine serum, then incubated in a constant temperature incubator at 37°C with an atmosphere of 5% CO_2. The culture medium needed to change every 1–2 days. RAW264.7 cells were blown down and passaged at a ratio of 1:2 or 1:3 when they had reached approximately 80% confluence. The cells (2×10^4 per/well) were then seeded in 96-well plates until they reached 80% confluence. Next, the cells were treated with wogonin, paeonol, ethyl caffeate, and magnoflorine for 2 h and treated with LPS (1 μg/ml) for 24 h subsequently.

Cell Viability Measure

The CCK-8 was used to assay the cell viability. To test the cytotoxicity of four components in our experiment, RAW264.7 cells were placed in 96-well plates with a density of 1×10^5 cells/ml. The cells reached approximately 80% confluence after 24 h of incubation. Then, the cells were treated with various concentrations of wogonin (6.25, 12.5, 25, 50, and 100 μM), paeonol (10, 50, 100, 200, and 400 μM), ethyl caffeate (75, 150, 300, 500, and 800 nM), and magnoflorine (0.1, 1, 5, 10, and 50 μM). Subsequently, we added 10-μl CCK8 (Dojindo) in each well. After incubation for 3 h, cell viability (CCK8 activity) was quantified through the absorbance at 450 nm measured by a microplate reader (Tecan infinite M200).

Assay the Content of NO

After 2 h of incubation of the RAW264.7 cells with caffeic acid, wogonin, paeonol, ethyl caffeate, and magnoflorine and 24 h of incubation with LPS (1 μg/ml), we collected the culture supernatant and mixed it with total nitric oxide assay kit (Beyotime) for NO assay. Then, the microplate reader (Tecan infinite M200) was used to assay the absorbance at 540 nm.

Western Blot

RAW264.7cells were lysed in radioimmunoprecipitation assay lysis buffer (Beyotime, China) containing protease suppressor. The protein concentration was quantified by the bicinchoninic acid protein assay kit (Thermo Fisher Scientific, United States). An equal amount of protein was separated by sodium dodecyl sulfate–polyacrylamide gel electrophoresis and then transferred onto polyvinylidene fluoride membranes (Millipore, Bedford, MA). After blocking in 5% blocking in QuickBlock Western (Beyotime, cat. no. P0252) for 10 min, the proteins on the membrane were incubated with following primary antibodies at 4°C overnight: Akt (1:1,000; cat. no. 4691T; Cell Signaling Technology, United States), p-Akt (1:1,000; cat. no. 4060T; Cell Signaling Technology), p38 MAPK (1:1,000; cat. no. 8690T; Cell Signaling Technology), p-p38 MAPK (1:1,000; cat. no.4511T; Cell Signaling Technology), p44/42 MAPK (Erk1/2) (1:1,000; cat. no.4695T; Cell Signaling Technology), p-p44/42 MAPK (Erk1/2) (1:1,000; cat. no.4370T; Cell Signaling Technology), NF-κB p65 (1:1,000; cat. no. 8242T; Cell Signaling Technology), p-NF-κB p65 (1:1,000; cat. no. 3033T; Cell Signaling Technology), and TNF-α (1:1,000; cat. no. 17590-1-AP; Proteintech, United States). Following four washes in Tris-buffered saline with Tween, proteins were incubated with secondary antibodies for 1 h at room temperature. Antibody signal was detected using Clarity Western enhanced chemiluminescence substrate (Abbkine Scientific, China). The β-actin served as an endogenous reference.

Statistical Analysis

To compare the anti-inflammatory effects of four components, GraphPad Prism 5 was used for statistical analysis. Student's t-test for the comparison of two groups was utilized to analyze the significance of differences, whereas a one-way analysis of variance followed by a Dunnett *post-hoc* test was used to compare more than two groups. Results were considered statistically significant if the p-value was <0.05.

RESULTS

An integrative pharmacological model explored the underlying therapeutic mechanism of PAR and ALD for RA. The components of the two herbs in EMP were obtained from the TCMSP. Next, the active components were screened by absorption, distribution, metabolism, and excretion. These active components' targets were predicted by SEA, HitPick, and SwissTargetPrediction. The C-T networks were constructed by these components and their targets. Then, a coordinated functional space prediction model and knapsack algorithm were applied to demonstrate the co-functional mechanism of components from EMP in treating RA (**Figure 1**). Finally, we performed molecular docking to predict the co-functional effect of CFCG and further explore the coordinated mechanism. Also, the experiment results confirmed the reliability of CFCG, which was identified by our pharmacological strategy.

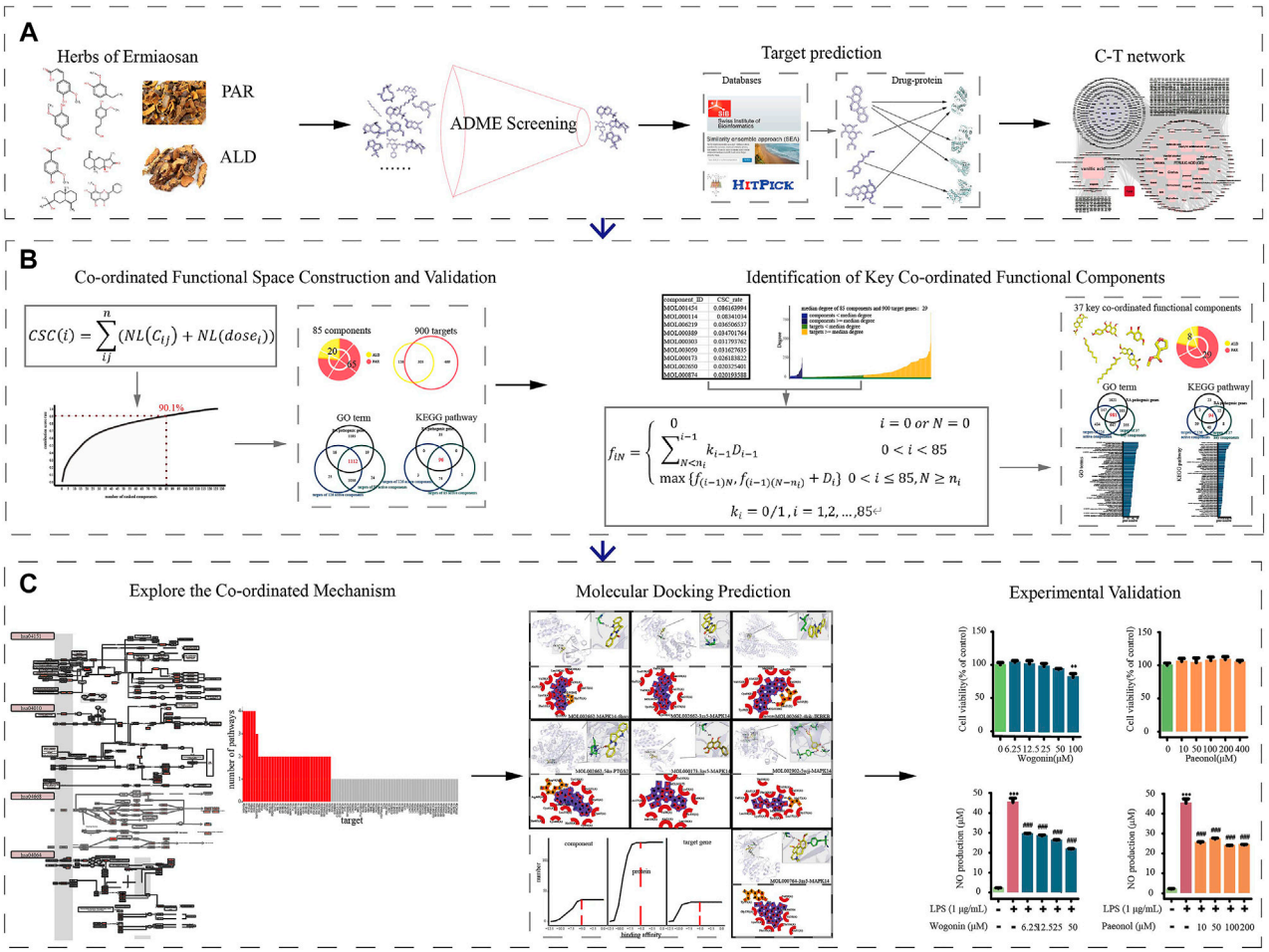

FIGURE 1 | Workflow for systematic pharmacological strategy. Through integrative pharmacological strategy based on system pharmacological model, knapsack algorithm, molecular docking, and in vitro experiments, molecular mechanisms of ESM in treating RA were decoded and validated. **(A)** Components collection, ADME screening, target prediction and C-T networks construction. **(B)** Using the co-ordinated functional space prediction model and knapsack algorithm to identified the potential co-ordinated functional components group (CFCG). **(C)** Validation of CFCG and potential co-ordinated mechanism exploration.

TABLE 1 | Information of EMP's chemical components from literature.

Formula	Method	Component	Concentration	References
Ermiaosan	UPLC-MS/MS	Chlorogenic acid	3.884 ± 0.178 mg/g	Feng et al., 2017
		Ferulic acid	4.058 ± 0.09 mg/g	
		Berberine	69.857 ± 3.965 mg/g	
		Phellodendrine	7.002 ± 0.165 mg/g	
		Palmatine	1.045 ± 0.028 mg/g	
		Magnoflorine	2.221 ± 0.078 mg/g	
		Jatrorrhizine	0.894 ± 0.019 mg/g	
		Tetrahydropalmatine	0.0165 ± 0.0005 mg/g	
		Tetrahydroberberine	0.0035 ± 0.0005 mg/g	
		Obaculactone	3.244 ± 0.167 mg/g	
		Obacunone	0.213 ± 0.026 mg/g	
		Atractylenolide I	0.3295 ± 0.0235 mg/g	
		Atractylenolide II	0.131 ± 0.015 mg/g	
		AtractylenolideIII	0.144 ± 0.023 mg/g	

TABLE 2 | The 126 active components ofactive components of PAR and ALD after ADME screening.

Molecule name	MW	RBN	nHAcc	nHDon	ClogP	Source
Undecenal	168.28	8	1	0	3.41	PAR
Furol	96.08	1	2	0	0.69	
Myrcene	136.23	4	0	0	3.43	
(S)-(+)-α-Phellandrene	136.23	1	0	0	2.97	
L-Limonen	136.23	1	0	0	3.35	
Eugenol	164.2	3	2	1	2.25	
Caprylic acid	144.21	6	2	1	2.23	
4-[(Z)-3-hydroxyprop-1-enyl]-2,6-dimethoxyphenol	210.23	4	4	2	1.47	
Ferulic Acid (CIS)	194.18	3	4	2	1.36	
Magnograndiolide	266.33	0	4	2	1.7	
Vanillin	152.15	2	3	1	1.2	
Pentylfuran	138.21	4	1	0	2.83	
WLN: VHR	106.12	1	1	0	1.57	
Trans-2-nonenal	140.22	6	1	0	2.66	
(2S,3S)-3,5,7-trihydroxy-2-(4-hydroxyphenyl)chroman-4-one	288.25	1	6	4	1	
Magnoflorine	342.41	2	4	2	1.89	
Menisporphine	321.33	3	5	0	2.98	
Palmatine	352.4	4	4	0	2.51	
STOCK1N-14407	355.43	4	5	0	3.1	
Fumarine	353.37	0	6	0	2.67	
Jatrorrizine	338.38	3	4	1	2.23	
Isocorypalmine	341.4	3	5	1	2.75	
Menisperine	356.44	3	4	1	2.19	
Paeonol	166.17	2	3	1	1.63	
Beta-elemene	204.35	3	0	0	4.65	
Mnk	170.29	8	1	0	3.48	
Phellamurin_qt	356.37	3	6	4	2.59	
Pisol	186.33	10	1	1	3.94	
Oxophorone	152.19	0	2	0	1.47	
Berberine	336.36	2	4	0	2.41	
(S)-Canadine	339.39	2	5	0	2.96	
Columbamine	338.38	3	4	1	2.23	
Coptisine	320.32	0	4	0	2.32	
EUG	150.17	2	2	1	2.14	
Isovanillin	152.15	2	3	1	1.12	
Methyl 3-furoate	126.11	2	3	0	1.06	
N-Methylflindersine	241.29	0	2	0	2.65	
Homocresol	152.19	2	2	1	2.02	
(s)-carvone	150.22	1	1	0	2.43	
Beta-Rhodinol	156.27	5	1	1	2.93	
Phlorol	122.16	1	1	1	2.11	
(±)-lyoniresinol	420.45	7	8	4	2	
Obacunoic acid	472.53	4	8	2	2.65	
Phellodendrine	342.41	2	4	2	1.68	
Phellopterin	300.31	4	5	0	3.36	
PEA	121.18	2	1	1	1.6	
Vanillyl alcohol	154.16	2	3	2	0.86	
(4R)-limonene 1beta, 2beta-epoxide	152.23	1	1	0	2.71	
Coniferol	180.2	3	3	2	1.62	
Dehydrotanshinone II A	292.33	0	3	0	3.61	
Delta7-Dehydrosophoramine	242.32	0	2	0	1.81	
Dictamine	199.21	1	3	0	2.63	
Kihadanin A	486.51	1	9	1	2	
Rutaecarpine	287.32	0	2	1	3.1	
Skimmianin	259.26	3	5	0	2.58	
Fagarine	229.23	2	4	0	2.59	
Ferulic Acid	192.21	3	3	2	2.15	
Chelerythrine	332.35	2	4	0	4.37	
Worenine	334.35	0	4	0	2.52	
Cavidine	353.41	2	5	0	3.23	
Hispidone	472.7	1	4	2	4.86	
Berberrubine	322.33	1	4	1	2.14	
Noroxyhydrastinine	191.18	0	3	1	1.23	
Ethyl caffeate	208.21	4	4	2	1.82	

(Continued on following page)

TABLE 2 | (*Continued*) The 126 active components ofactive components of PAR and ALD after ADME screening.

Molecule name	MW	RBN	nHAcc	nHDon	ClogP	Source
Guasol	124.14	1	2	1	1.4	
IPH	94.11	0	1	1	1.41	
Nonanoic acid	158.24	7	2	1	2.6	
Dodec-2-enal	182.3	9	1	0	3.78	
Naphthalene	128.17	0	0	0	3.1	
Limonin	470.51	1	8	0	2.54	
5-Methylfurfural	110.11	1	2	0	1.02	
Maruzen M	122.16	1	1	1	2.11	
O-cresol	108.14	0	1	1	1.78	
Creosol	138.16	1	2	1	1.7	
Methyl naphthalene	142.2	0	0	0	3.46	
Isoferulic acid	194.18	3	4	2	1.39	
Cyclopentenone	82.1	0	1	0	0.96	
Methyl caffeate	194.18	3	4	2	1.35	
Clorius	136.15	2	2	0	1.84	
Ptelein	229.23	2	4	0	2.62	
SMR000232320	474.72	5	4	3	4.86	
Canthin-6-one	220.23	0	2	0	2.39	
4,10-dimethylene-7-isopropyl-5(E)-cyclodecenol	220.35	1	1	1	3.47	
4-[(1R,3aS,4R,6aS)-4-(4-hydroxy-3,5-dimethoxyphenyl)-1,3,3a,4,6,6a-hexahydrofuro (4,3-c)furan-1-yl]-2,6-dimethoxyphenol	418.44	6	8	2	2.33	
Guanidine	59.07	0	1	3	-1.01	
7-hydroxy-6-(2-hydroxyethyl)coumarin	206.19	2	4	2	1.35	
Thalifendine	322.33	1	4	1	2.14	
Furfuranol	98.1	1	2	1	0.62	
(S)-4-Nonanolide	156.22	4	2	0	2.24	
2,4,6-trimethyl-Octane	156.31	5	0	0	4.26	
Methyl atratate	196.2	2	4	2	1.77	
Acetylfuran	110.11	1	2	0	1.01	
Candicine	180.27	3	1	1	1.19	
2-undecenoic acid	184.28	8	2	1	3.18	
Homoveratrole	152.19	2	2	0	2.05	
Obacunone	454.51	1	7	0	3.19	
Auraptene	298.38	6	3	0	4.51	
Tetrahydropalmatine	355.43	4	5	0	3.08	
Jatrorrhizine	380.46	6	4	1	3.05	
Obaculactone	470.51	1	8	0	2.54	
Alpha-humulene	204.35	0	0	0	4.26	ALD
Beta-Eudesmol	222.37	1	1	1	3.61	
2-[(1R,3S,4S)-3-isopropenyl-4-methyl-4-vinylcyclohexyl]propan-2-ol	222.37	3	1	1	3.77	
Atractylenolide i	230.3	0	2	0	3.25	
Atractylenolide II	232.32	0	2	0	3.2	
Selina-4(14),7(11)-dien-8-one	218.33	0	1	0	3.65	
Vanillic acid	168.15	2	4	2	1.08	
Beta-Chamigrene	204.35	0	0	0	4.39	
Atractylone	216.32	0	1	0	3.81	
2-[(2S,5S,6S)-6,10-dimethylspiro [4.5]dec-9-en-2-yl]propan-2-ol	222.37	1	1	1	3.54	
ZINC01609418	222.37	4	1	1	3.76	
3β-hydroxyatractylone	232.32	0	2	1	2.87	
()-2-Carene	136.23	0	0	0	3.12	
Alpha-Guaiene	204.35	1	0	0	4.3	
Guaiene	204.35	0	0	0	4.23	
Guaiol	222.37	1	1	1	3.42	
Furol	96.08	1	2	0	0.69	
Wogonin	284.26	2	5	2	2.54	
Cyperene	204.35	0	0	0	4.4	
Atractylenolide iii	248.32	0	3	1	2.65	
2-Hydroxyisoxypropyl-3-hydroxy-7-isopentene-2,3-dihydrobenzofuran-5-carboxylic	306.35	4	5	3	2.37	
Beta-Eudesmol	222.37	1	1	1	3.61	
Butenolide B	234.29	0	3	1	2.21	
3β-acetoxyatractylone	274.35	2	3	0	3.3	
3,5-dimethoxy-4-glucosyloxyphenylallylalcohol_qt	210.23	4	4	2	1.55	
(Z)-caryophyllene	204.35	0	0	0	4.25	
Patchoulene	204.35	0	0	0	4.35	

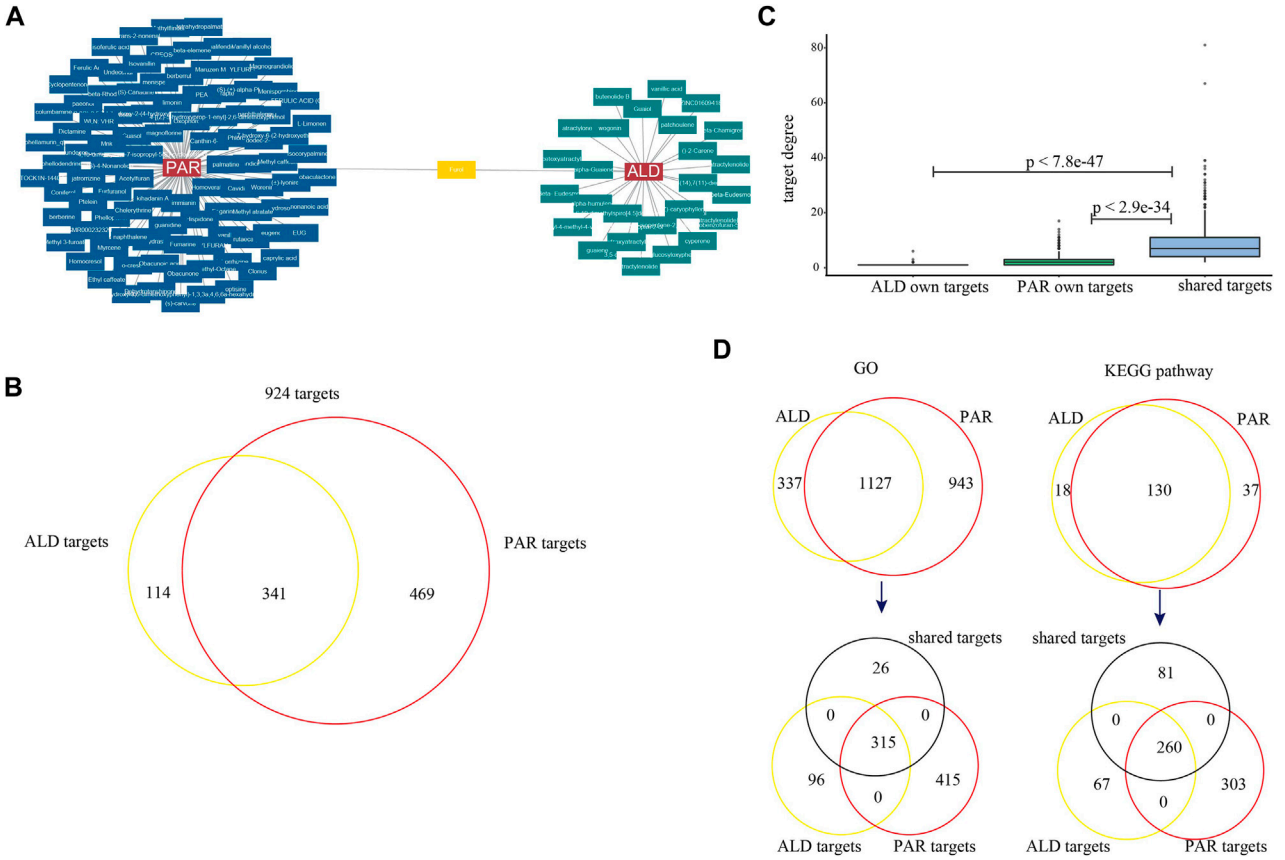

FIGURE 2 | C-T networks of 127 active components and their target genes. **(A)** Active components of *Phellodendron amurense* Rupr. (PAR) and *Atractylodes lancea* (Thunb.) DC. (ALD). **(B)** Venn diagrams for target genes of active components of two herbs. **(C)** Box plots for degrees of targets in C-T network. **(D)** Venn diagrams for GO terms and KEGG pathways mapped by target genes of two herbs. Two Venn diagrams show target genes enriched in 1,127 GO terms and 130 KEGG pathways (black represents 341 shared target genes of two herbs, yellow represents genes targeted by ALD, and red represents genes targeted by PAR).

Components in *Phellodendron amurense* Rupr. and *Atractylodes lancea* (*Thunb.*) DC.

For EMP, we collected 140 components of PAR and 49 of ALD from the TCSMP. Among the 187 components, 138 components were only in PAR, and 47 components were only in ALD, whereas two components were shared by the two herbs (**Supplementary Table S1**). It indicated the potential co-functional effect of the two herbs in EMP. The information of chemical components' identification and concentration of EMP was collected through searching the literature. As shown in **Table 1**, the information collected earlier provided an experiment-aided chemical space for the identification of active components in the following analysis.

Filtration of Active Components in *Phellodendron amurense* Rupr. and *Atractylodes lancea* (*Thunb.*) DC.

By integrating the components of PAR and ALD from the TCSMP and **Table 1**, 191 components were finally obtained. However, not all of the components have effective pharmacodynamic and pharmacokinetic characteristics in EMP. So, absorption, distribution, metabolism, and excretion screening was performed to filter out active components from them. As shown in **Table 2**, 100 active components of PAR and 27 of ALD were identified for the following analysis. Among the 126 active components, only Furol is shared by PAR and ALD. The result suggested that the components of the two herbs may play a co-functional effect on the treatment of RA *via* their specific space.

Component-Target Networks Construction

To explore whether the potential coordinated functional space of PAR and ALD exists, we constructed the C-T networks composed of active components and their targets (**Figure 2**). The targets of the 126 active components were obtained from SEA, HitPick, and SwissTargetPrediction. The PAR C-T network consisted of 3,839 components–targets, which included 100 active components and 810 targets. The ALD C-T network contains 776 components–targets, including 27 active components and 455 targets. The C-T networks indicated that one component might target multiple genes, and several components may intend to act

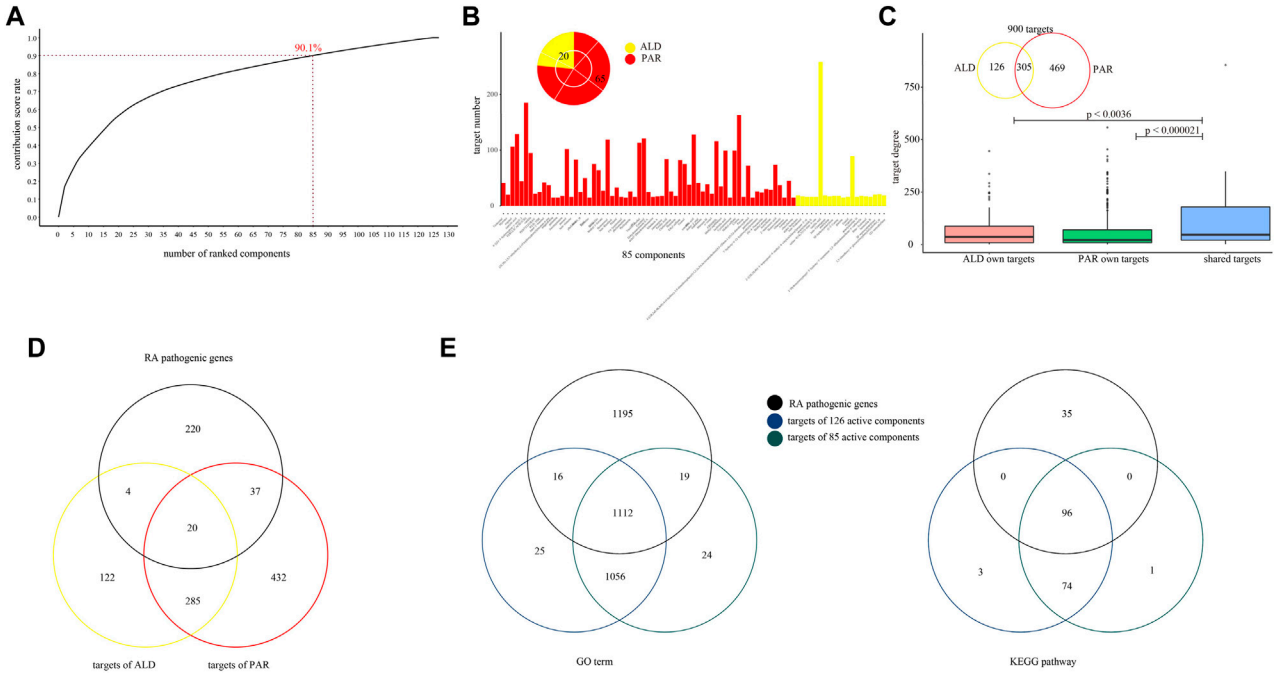

FIGURE 3 | Coordinated functional space constructed by 85 active components. **(A)** Coordinated functional space prediction models obtained top 85 active components with 90.1% of sum contribution score. **(B)** Number of 85 active components' targets. Among 85 components, 65 come from PAR, and 20 belong to ALD. **(C)** Degree of 85 active components' targets in network converged by PPI network and C-T network. **(D)** Venn diagrams for two herbs' targets and RA pathogenic genes. **(E)** Venn diagrams for GO-BP terms and KEGG pathways with RA pathogenic genes, 126 components' targets, and 85 components' targets mapped in.

on the same target. We also found that 341 targets were shared by the PAR C-T network and the ALD C-T network (**Figures 2B,C**), suggesting that some active components of PAR and some of ALD play roles on the same targets together. Also, in the C-T network constructed by 126 components and 924 targets, the degrees of these 341 targets were significantly greater than other targets (Student's t-test, 341 targets *vs.* PAR own targets, $p < 2.9e^{-34}$; 341 targets *vs.* ALD own targets, $p < 7.8e^{-47}$) (**Figures 2B,C**). We then performed GO and KEGG pathway enrichment analysis for the targets of the two herbs, respectively, and the results showed that 1,127 GO terms and 130 KEGG pathways were shared by the targets of the two herbs (**Figure 2D**). In the shared GO terms and pathways, we found that 92.4 and 76.2% of the 341 shared targets were enriched, respectively. These results revealed that PAR and ALD might play the principal co-functional effect through their shared target genes, which is consistent with the complex multi-target and multicomponent mediated coordinated mechanism of TCM.

Construction and Validation of Coordinated Functional Space

To further analyze the co-functional effect of active components from PAR and ALD on RA, coordinated functional space prediction models were constructed to quantify the effect of each component. According to the results of models, the top 85 active components have the greatest effects of EMP on RA with 90.1% of the sum contribution score of 126 components (**Figure 3A**, **Supplementary Table S1**). Among the 14 components in **Table 1**, nine components (including berberine, phellodendrine, palmatine, magnoflorine, jatrorrhizine, ferulic acid, obaculactone, obacunone, and atractylenolideIII) were included in the 85 active components. We also found that the number of the 85 components' targets covers 97.4% of 126 components (900 of 924). These results indicated that the 85 components constitute the coordinated functional space of PAR and ALD in EMP. Among the 85 components, 65 come from PAR with 774 of 900 targets, and 20 belong to ALD with 431 of 900 targets, whereas 305 targets were shared by the components of the two herbs (**Figures 3B,C**). We further converged the PPI network and C-T network, which included 85 components and 900 targets, and the result showed that the degrees of the shared 305 targets were significantly greater than others (Student's t-test, 305 targets *vs.* PAR own targets, $p < 0.000021$; 341 targets *vs.* ALD own targets, $p < 0.0036$) (**Figure 3C**). It also demonstrated the co-functional effect of PAR and ALD in EMP on RA and indicated that the two herbs might perform their potential coordinated effect through their shared target genes.

To explore the potential effect of the 85 active components, we performed GO and KEGG pathway analysis for RA pathogenic genes, 924 targets of the 126 active components and 900 targets of the 85 active components, respectively. The RA pathogenic genes set contains 281 known pathogenic genes which have been

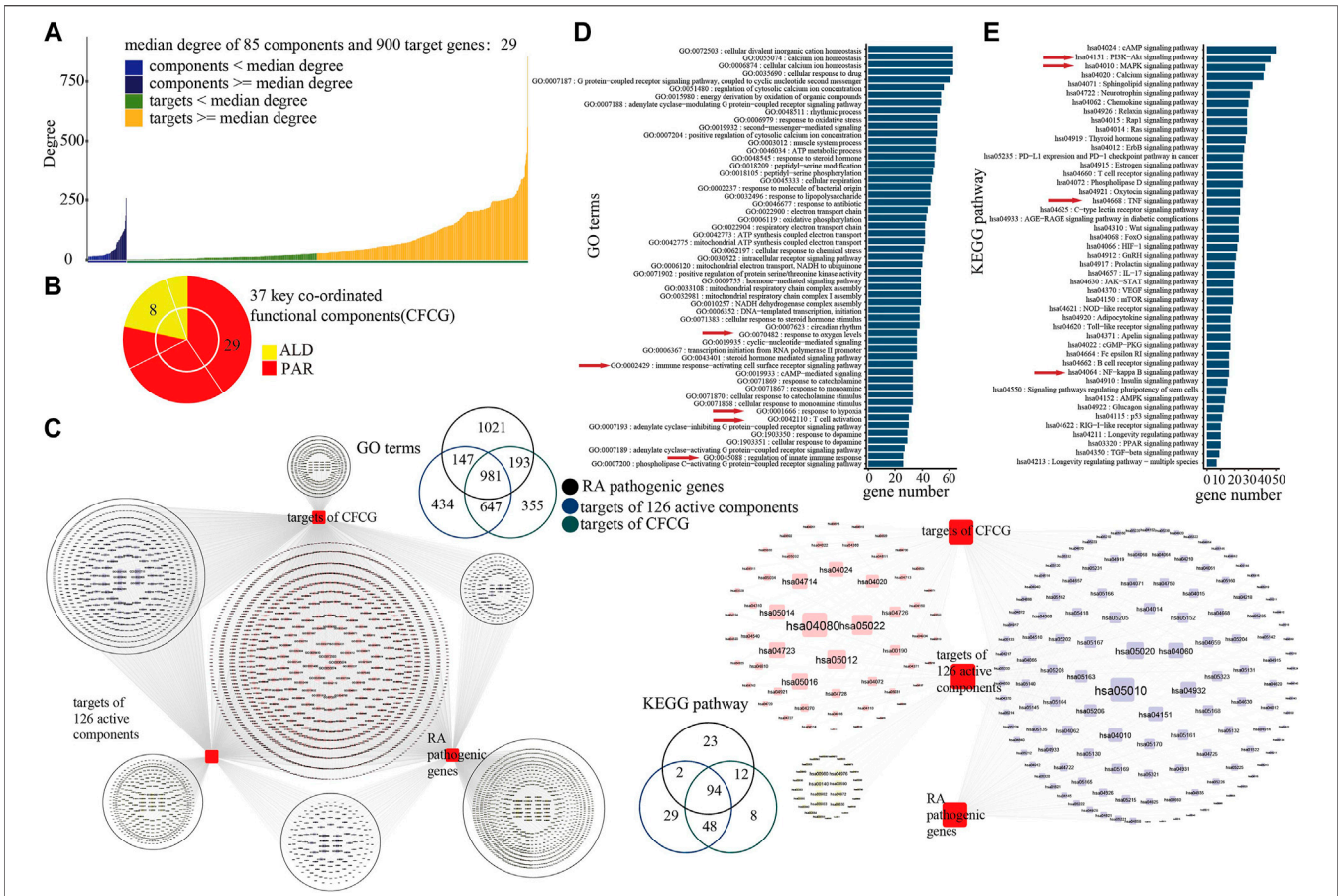

FIGURE 4 | Identification of key coordinated functional components group (CFCG). **(A)** Degrees of 85 active components and their 900 target genes in network. Median degree of network was 29, and 473 targets with degrees over median degree were retained for following analysis. **(B)** CFCG composed of 37 active components. Among them, 29 components belong to PAR, and eight belong to ALD. **(C)** GO-BP terms and KEGG pathways with RA pathogenic genes, 126 components' targets, and CFCG's targets mapped in. **(D,E)** Results of GO **(D)** and KEGG pathway **(E)** enrichment analysis performed on target genes of CFCG.

confirmed by at least five previous studies. We found that the targets of 85 components contain 61 of the 281 RA pathogenic genes (**Figure 3D**). The results showed that 924 target genes of 126 active components were enriched in 2,209 GO-BP terms and mapped in 173 KEGG pathways and shared 1,128 GO-BP terms and 96 KEGG pathways with the RA pathogenic genes. Also, among these 1,128 GO-BP terms and 96 KEGG pathways, 98.6 and 100% of them were mapped by 900 targets of 85 active components, respectively (**Figure 3E**). These results suggested that the coordinated functional space consisted of 85 active components that have a potential correlation with RA pathogenic genes and may play an important role in EMP treatment of RA.

Identification of Key Coordinated Functional Components From Coordinated Functional Space of Ermiao Powder

It is known that the characteristics of the TCM mechanism are multicomponent and multi-target; the results of our analysis for the co-functional effect of PAR and ALD in EMP demonstrated the phenomenon. We found that 305 of the 85 actives components' targets were shared by components in PAR and others in ALD (**Figure 3B**). The result indicated that the 85 active components contain the main co-functional components, and further analysis was needed to identify the key co-functional components of EMP. According to the network converged by PPI network and C-T network, the 473 key targets with degrees over the median degree of the 900 targets and 85 components were retained for the following analysis (**Figure 4A**).

Based on the knapsack algorithm performed for the 85 components and their 473 key targets, we identified 37 active components as the key coordinated functional components (**Figure 4B**). GO and KEGG pathway analysis was performed for the 426 targets of the CFCG. The 426 targets were enriched in 2,176 GO-BP terms and mapped in 162 KEGG pathways, and they mapped in 86.96 and 97.92% of GO-BP terms and KEGG pathway of the overlap of RA-related genes and 924 targets of 126 active components (**Figure 4C**). The results demonstrated that the CFCG retained the main functions of the formulas of EMP

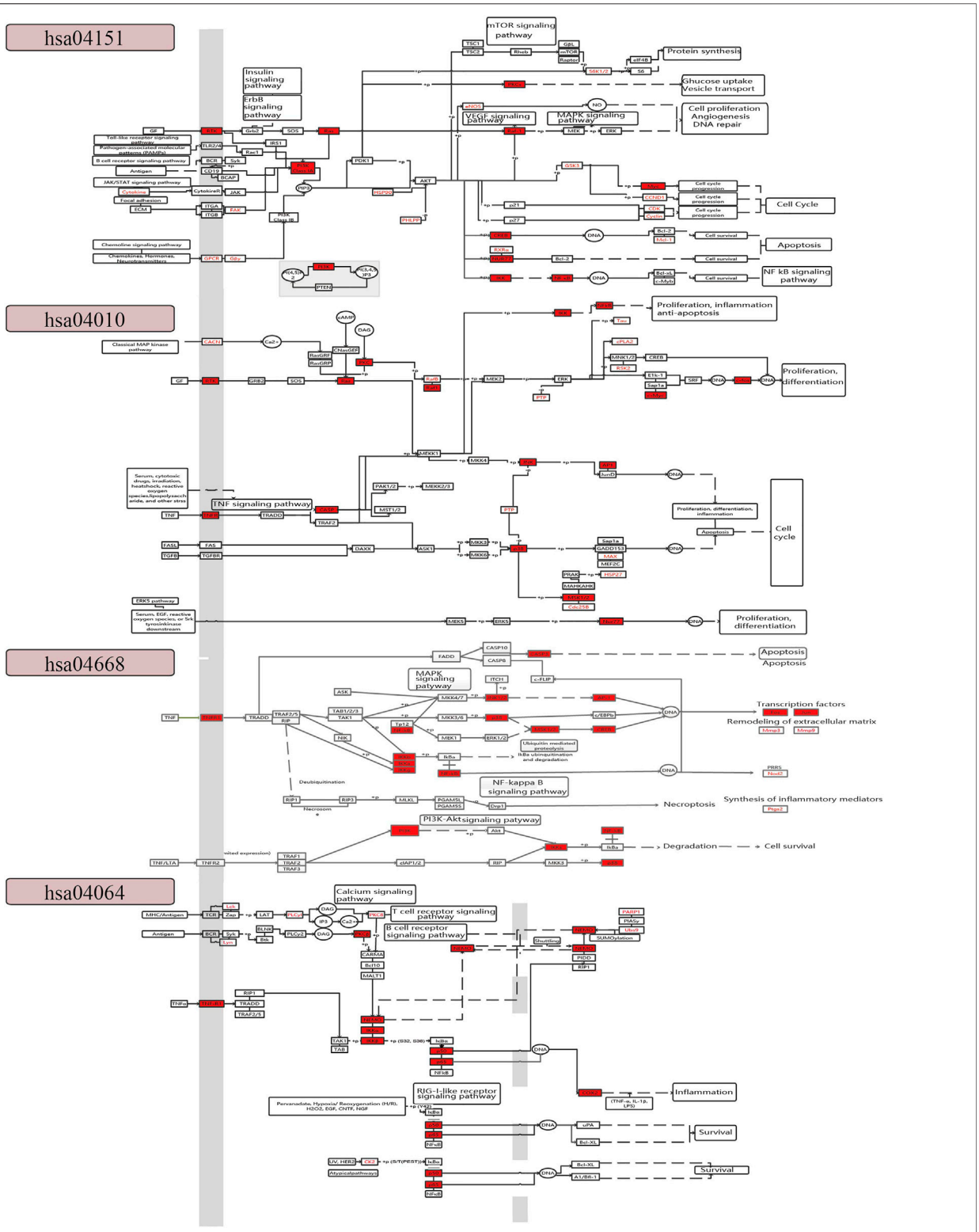

FIGURE 5 | Comprehensive pathway with four pathways: hsa04151, hsa04010, hsa04668, and hsa04064.

and had the main coordinated effects in the treatment of EMP on RA.

Analysis of Coordinated Mechanisms

To further explore the co-functional effects of CFCG, we dissect the results of GO and KEGG pathway enrichment analysis performed on the 426 targets (**Figures 4D,E**).

The results of the GO analysis showed that the targets were enriched in biological processes which play an important role in RA, such as response to oxygen levels (GO:0070482), response to hypoxia (GO:0001666), regulation of innate immune response (GO:0045088), immune response-activating cell surface receptor signaling pathway (GO:0002429), and T cell activation (GO: 0042110) (Hu et al., 2014; Torices et al., 2017; Bartlett et al., 2018; Gong et al., 2019; Leite Pereira et al., 2019) (**Figure 4D**). RA is a systemic autoimmune inflammatory disease, which is related to the aberrant immune network (Xu et al., 2018). The inflammation of the synovium of the joint is the main pathological feature of RA. Angiogenesis plays a major role in the development of synovitis, whereas the hypoxic environment of the RA joint is closely related to the excessive formation of synovial vessels (Elshabrawy et al., 2015; Gong et al., 2019). CFCG may inhibit angiogenesis and reduce the production and expression of inflammatory cytokines by targeting the hypoxia-inducible factor-1α. Angiogenesis can contribute to the infiltration of inflammatory cells (such as neutrophils, monocytes, and macrophages) into the joint, and the pro-inflammatory environment can enhance the pathology of RA by extending the lifespan of inflammatory cells in the joint. Inhibition of joint angiogenesis can reduce the inflammation of the synovium. CFCG may also inhibit the inflammatory response and repair the damage of RA through regulating the expression of targets involved in immunity and inflammation, such as interleukin (IL)-6 and NF-κB. The results indicated that the CFCG could treat RA by targeting the genes related to inflammation and immunity.

The result of KEGG pathway enrichment analysis also indicated that the targets were involved in pathways related to inflammation and immunity, such as the PI3K-Akt signaling pathway (hsa04151), MAPK signaling pathway (hsa04010), TNF signaling pathway (hsa04668), NF-κB signaling pathway (hsa04064), T cell receptor (TCR) signaling pathway (hsa04660), and cyclic adenosine 3',5'-monophosphate signaling pathway (hsa04024) (**Figure 4E**).

To further explore the coordinated mechanism of the CFCG in treating RA, we constructed a comprehensive pathway with four pathways, including hsa04151, hsa04010, hsa04668, and hsa04064 (**Figure 5**). We defined the first three columns of targets as upstream target genes and others as downstream targets in the comprehensive pathway. The CFCG can regulate upstream targets of the PI3K-Akt signaling pathway such as RTK and FAK and downstream targets such as Ras, PI3K, Raf-1, Myc, CREB, IKK, and NF-κB. These targets are involved in cell proliferation, cell cycle, cell survival, and so on, which are involved in the development and progression of RA. The targets in the MARK signaling pathway are mainly associated with cell proliferation, differentiation, apoptosis, and inflammation, such as RTK, TNFR, Ras, CASP, p38, JNK, and Nur77. In the TNF signaling pathway, the CFCG can regulate targets such as TNFR1, NF-κB, p38, PI3K, Fos, Jun, and ptgs2 to affect cell survival and synthesis of inflammatory mediators. In the NF-κB signaling pathway, the proteins involved in immunity, inflammation, and cell survival are targeted by the CFCG, such as TNFR1, NEMO, p50, p65, and COX2. All the targets mentioned earlier play different roles in the four pathways, which indicate the coordinated therapeutic effect of the CFCG from PAR and ALD in treating RA.

Prediction of Coordinated Mechanism by Molecular Docking

To explore the co-functional effect of the CFCG, we also conducted molecular docking for 37 components with a three-dimensional conformer and 131 proteins coded by the 32 target genes (**Figures 6A–C**). A total of 42,842 binding relationships in the docking results were obtained. Each binding relationship has a binding affinity value, and the smaller affinity value represents better binding. Among them, 25,802 binding relationships with binding affinity < −5 were retained, where components could bind with proteins effectively. The 25,802 binding relationships contained 37 components, 32 genes, and 130 proteins. Among these bindings, MOL002662 can bind best with protein 6 hwv coded by gene MAPK14 with the binding affinity of −11.2 kcal/mmol, followed by MOL002662-3zs5-MAPK14 (−11 kcal/mmol) and MOL002662-4kik-IKBKB (−10.8 kcal/mmol). Among the 37 components in 25,802 binding relationships, MOL000173 and MOL002662 could bind the most, with 130 proteins coded by 32 genes, whereas MOL000764 could bind the 127 proteins coded by 32 genes, MOL002902 could bind the 122 proteins coded by 31 genes, MOL000874 could bind the 106 proteins coded by 28 genes. MAPK14 and PTGS2 could bind the most, with 36 components. These results indicated that the CFCG could effectively bind with the proteins in the comprehensive pathway and suggested their potential co-functional effect in the treatment of RA.

Verification of Coordinated Functional Components Group by *In Vitro* Experiment

To further validate the results of the identification of CFCG, four components (wogonin, paeonol, ethyl caffeate, and magnoflorine) from CFCG were selected for *in vitro* experiments. We detected the four components' anti-inflammatory effects through RAW264.7 cells induced by LPS.

NO assay was applied to detect the effects of wogonin, paeonol, ethyl caffeate, and magnoflorine with different concentrations on RAW264.7 cells' viability. As compared with the control group, the four concentrations of wogonin (6.25, 12.5, 25, and 50 μM), paeonol (10, 50, 100, and 200 μM), ethyl caffeate (75, 150, 300, and 500 nM), and magnoflorine (0.1, 1, 5, and 10 μM) had no influence on cell viability; the four concentrations of these components were used for following experiments (**Figures 7A–D**).

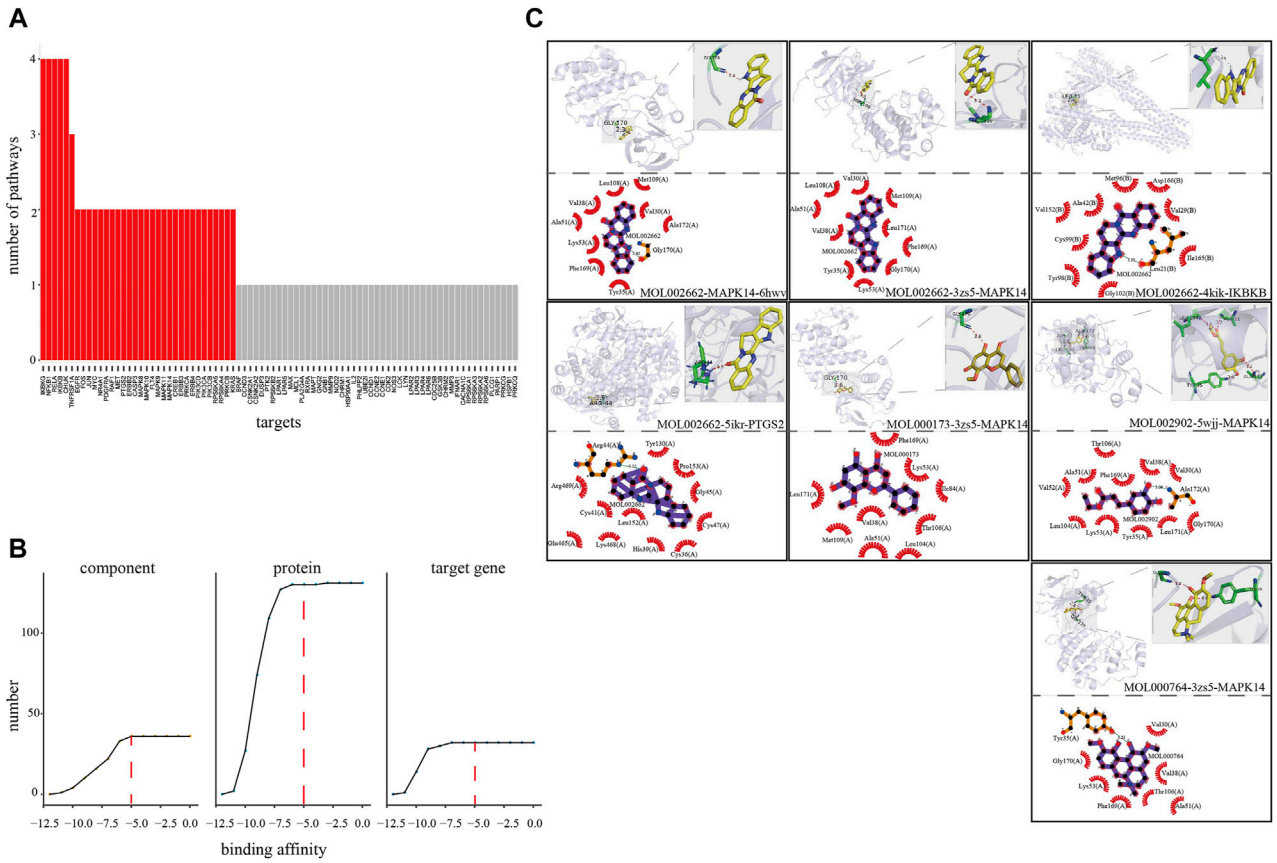

FIGURE 6 | Verification of coordinated mechanism by molecular docking. **(A)** Number of pathways where target mapped in four pathways (hsa04151, hsa04010, hsa04668, and hsa04064). **(B)** Screening threshold of effective binding affinity. **(C)** Docking result visualization.

Compared with the control group, we found that the NO level significantly increased by 2,034.2% in the culture medium of LPS-treated cells, whereas wogonin (6.25, 12.5, 25, and 50 μM), paeonol (10, 50, 100, and 200 μM), ethyl caffeate (75, 150, 300, and 500 nM), and magnoflorine (0.1, 1, 5, and 10 μM) significantly decreased the extracellular NO levels with $p < 0.0001$ in a concentration-dependent manner (**Figures 7E–H**). The results demonstrated that wogonin, paeonol, ethyl caffeate, and magnoflorine could effectively reduce the production of NO in RAW264.7 cells induced by LPS.

Furthermore, to validate the results of the comprehensive pathway, Western blotting was applied to detect the activities of the PI3K-Akt signaling pathway, MAPK signaling pathway, NF-κB signaling pathway, and TNF signaling pathway in RAW264.7 cells (**Figure 7I**). Compared with the control group, it was observed that the four pathways were all activated in LPS-induced RAW264.7 cells. However, the expression level of p-Akt, p-p38 MAPK, p-Erk1/2, p-NF-κB, and TNF-α were decreased in dosing groups, which supported that wogonin (50 μM), paeonol (200 μM), ethyl caffeate (500 nM), and magnoflorine (10 μM) can inhibit the activities of the four pathways in LPS-induced RAW264.7 cells. The results indicated that the CFCG plays a role in treating RA at least partially *via* reducing the activities of the PI3K-Akt signaling pathway, MAPK signaling pathway, TNF signaling pathway, and NF-κB signaling pathway. Also, it also validated the reliability and accuracy of the identification of CFCG.

DISCUSSION

As a chronic and systemic autoimmune inflammatory disease (Scott et al., 2010; Wasserman 2011; Smolen et al., 2017), the multiple factors contributing to RA and its complex pathogenesis bring challenges for therapeutic interventions. TCM has evident advantages in treating complex diseases, such as multi-target and multicomponent treatment (Wang L. et al., 2020; Shi et al., 2020; Yang et al., 2021). EMP is comprised of PAR and ALD, which have been widely applied in the treatment of rheumatic diseases (Resch et al., 1998; Kim et al., 2011; Xian et al., 2011; Tang et al., 2018; Wan 2018; Zhang et al., 2018; Li et al., 2020; Zhang et al., 2021). Clinical and pharmacological studies have demonstrated PAR's function as an anti-inflammatory (Kim et al., 2011; Xian et al., 2011; Wan 2018; Zhang et al., 2018). ALD can exhibit anti-inflammatory activity by inhibiting MPO activity and inflammatory cell infiltration and reducing the secretion of TNF-α, IL-1β, and IL-6 (Resch et al., 1998; Tang et al., 2018;

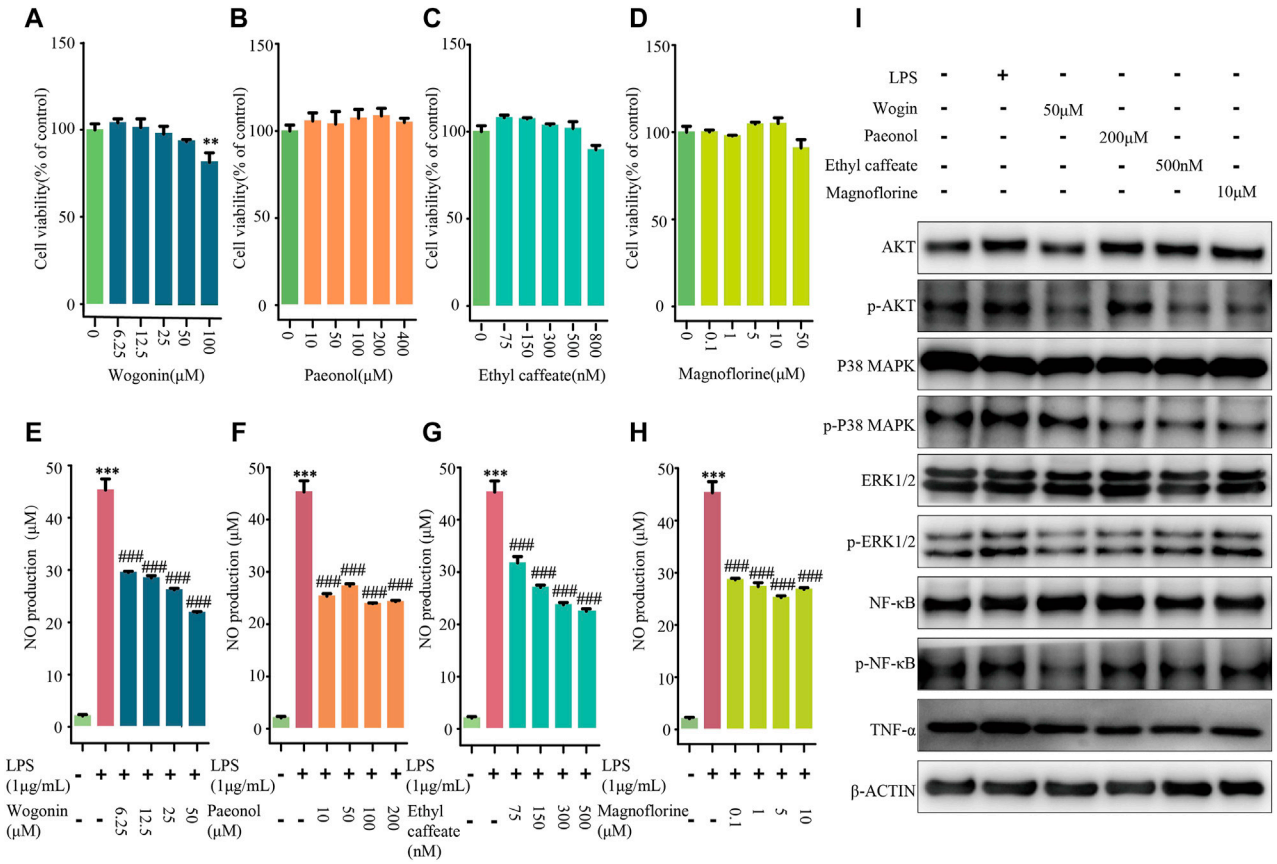

FIGURE 7 | Experiments validation of four components from CFCG. Effects of wogonin **(A,E)**, paeonol **(B,F)**, ethyl caffeate **(C,G)**, and magnoflorine **(D,H)** on viabilities and NO production of RAW264.7 cells induced by LPS. $^{**}p < 0.01$, $^{***}p < 0.001$ compared with control group. $^{###}p < 0.001$ compared with LPS group. **(I)** LPS-induced RAW264.7 cells were treated with wogonin (50 μM), paeonol (200 μM), ethyl caffeate (500 nM), and magnoflorine (10 μM). Also, Western blotting was performed to detect activities of four pathways in RAW264.7 cells, including PI3K-Akt signaling pathway, MAPK signaling pathway, NF-κB signaling pathway, and TNF signaling pathway.

Zhang et al., 2021). Currently, most studies have focused on analyzing the anti-inflammatory effects of PAR and ALD separately and the anti-inflammatory effects of EMP. Due to the unclear coordinated molecular mechanism of PAR and ALD in treating RA, we systematically explored the mechanisms of EMP in treating RA based on a network pharmacology method.

Recently, the flourishing development of network pharmacology has contributed to an emerging trend of TCM network pharmacology (Hao da and Xiao 2014; Zhou et al., 2020). TCM formula contains multiple herbs and treats complex diseases with the characteristic of multi-targets and multiomponents, which is consistent with the multi-target action network characteristic of network pharmacology. Many studies have been made in mechanism research of TCM by network pharmacology approach, while mostly inferred the potential mechanism by decoding the network constructed by the selected active components and their targets. For example, Tao et al. (2013) decoded the mechanism of the Curcumae Radix formula for preventing cardiovascular and cerebrovascular diseases based on 58 active components and 32 potential targets related to cerebrovascular diseases. Based on network pharmacology assays, Hong et al. (2017) constructed two drug-target networks of herb-induced liver injury of Xiao-Chai-Hu-Tang and Polygoni Multiflori Radix (Heshouwu) and identified the three potential hepatotoxic components from the networks. Zhou et al. (2018) applied network pharmacology and molecular docking technology to identify possible active components in Qingdai and explored their molecular mechanisms in treating chronic myelogenous leukemia based on the 19 key gene nodes in the PPI and nine components of Qingdai. These studies have proved the reliability of network pharmacology. Based on these models, we proposed a new model with two main advantages. The first point was that our model considered whether the selected components are the better component group in the original formula. The second point was that we not only paid attention to the key gene nodes and component nodes in the complex network but also considered the coverage of the information of the original network after components screening. Our strategy can avoid information redundancy and noise as well as the loss of effective information.

In this study, we explored the potential coordinated functional space of PAR and ALD based on the C-T networks. We found

that 341 targets were shared by the two herbs. It indicated the potential co-functional therapeutic effect of PAR and ALD in EMP. Then, we constructed the coordinated functional space prediction models and performed the knapsack algorithm to identify the key coordinated functional components of the potential coordinated functional space. Thirty-seven components were defined as the key coordinated functional components. The results of GO and KEGG pathway enrichment analysis on the targets of CFCG showed that the 426 targets were enriched in 86.96 and 97.92% of GO-BP terms and KEGG pathway of the overlap of RA-related genes and 924 targets of 126 active components. The CFCG identified by our method can cover the most function information of the original active components from EMP. The functional enrichment analysis results also indicated that the CFCG could coordinate the treatment of RA by regulating the genes that involved in biological processes and signaling pathways related to inflammation and immunity, such as oxygen levels (GO: 0070482), response to hypoxia (GO:0001666), regulation of innate immune response (GO:0045088), immune response-activating cell surface receptor signaling pathway (GO: 0002429), T cell activation (GO:0042110), PI3K-Akt signaling pathway (hsa04151), MAPK signaling pathway (hsa04010), TNF signaling pathway (hsa04668), and NF-κB signaling pathway (hsa04064). It has been reported that the PI3K-Akt signaling pathway is involved in regulating the expression of inflammatory cytokines and plays an important role in the development and progression of various types of inflammation (Liu et al., 2019; Gao et al., 2020). The development and progression of RA can be attenuated by inhibiting PI3K/Akt/mTOR signaling pathway activity (Wu et al., 2017; Liu et al., 2019; Li and Wang 2020). The MAPK signaling pathway can contribute to the development and progression of RA by mediating the proliferation and migration of RA fibroblast-like synoviocytes (Ralph and Morand 2008; Sujitha and Rasool 2017; Liu et al., 2018). The symptoms of RA, such as synovial tissue hyperplasia and articular cartilage tissue injury, can be relieved by inhibiting the MAPK signaling pathway (Bao et al., 2018; Liu et al., 2018; Yang et al., 2018). The TNF signaling pathway is associated with osteoarthritis activity and pathology, including bone loss, osteoblasts proliferation, and inflammation (Yu et al., 2018; Li et al., 2019; Jiang et al., 2020). The inhibition of the TNF signaling pathway can decrease inflammation and bone destruction (Yu et al., 2018). The NF-κB signaling pathway has been reported to be related to the pathogenesis of RA (Xia et al., 2018). It can regulate proliferation, apoptosis, and angiogenesis of human fibroblast-like synovial cells in RA (Zhang et al., 2017; Mitchell and Carmody 2018; Xia et al., 2018; Cao et al., 2019). Multiple studies have shown that T cell dysregulation appeared during the pathogenesis of RA (Fournier 2005; Larbi et al., 2008; Park et al., 2020). The activation and differentiation of T cells partly depend on the signal strength received by TCR (Goronzy and Weyand 2008), whereas altered TCR signaling thresholds can promote the occurrence and development of autoimmune arthritis (Larbi et al., 2008; Sakaguchi et al., 2012). RA is associated with uncontrolled transendothelial migration of leukocytes, and the cyclic adenosine 3',5'-monophosphate signaling pathway is involved in the molecular mechanisms that regulate the migration of leukocytes across the endothelium (Lorenowicz et al., 2006; Lorenowicz et al., 2007). These results demonstrated the reliability and accuracy of our strategy. Also, the result of molecular docking showed that the CFCG could bind well with the proteins coded by target genes in the comprehensive pathway and supported their important roles in the treatment of RA. All these results suggested the coordinated function mechanism of the CFCG identified from PAR and ALD in EMP treatment of RA. Finally, our experiment results also demonstrated the reliability and accuracy of the coordinated functional space prediction models and the knapsack algorithm.

In summary, we decoded and validated the molecular mechanisms of EMP in treating RA based on system pharmacological model, knapsack algorithm, molecular docking, and *in vitro* experiments. PAR and ALD play a coordinating role by regulating genes related to oxygen levels, immune response, synthesis of inflammatory mediators, and so on. Our strategy has the function of compound optimization and can further explore the coordinated mechanism of the CFCG, which was identified in the optimization process. Specifically, the components screened by the coordinated functional space prediction model can cover the most information of the original active components from EMP, and the reverse optimization method based on the targets of CFCG can also retain most targets of the screened components from our model. The identification of CFCG may contribute to improving our understanding of the coordinated mechanism of TCM in treating complex diseases. Moreover, the strategy can reduce the experiment time and cost of the studies on the mechanisms of TCM formulas. It can provide a reference for TCM mechanism research and ideas for the development of new drugs. However, our research lacks sufficient experimental verification. More components from CFCG and their targets should be selected to verify the reliability of our strategy. The determination of the content of herbs' components is also a difficult problem, and the effect of the components is related to the content. It requires further experimental verification. Our research mainly focuses on exploring the coordinated mechanism of herbs and the identification of CFCG. Although the CFCG plays a major therapeutic role, the effect of other components cannot be ignored. Further research is needed to analyze the effect of non-CFCG.

DATA AVAILABILITY STATEMENT

The original contributions presented in the study are included in the article/**Supplementary Material**; further inquiries can be directed to the corresponding authors.

AUTHOR CONTRIBUTIONS

Conceptualization: JW, KW, and DG.; Methodology: DG and AL; Software: JW, YiL, and XL; Validation: CY, YH, QL, and WM; Investigation: HY, HW, YaL, and AL; Data curation: JW and KW; Writing—Original draft: JW, QL and CY; Writing—Review and editing: DG, AL, and YaL; Visualization: JW, YuL, and JC Funding acquisition: DG. All authors have read and agreed to the published version of the manuscript.

FUNDING

This study is supported by the Startup fund from the Southern Medical University (grant No. G820282016), the Natural Science Foundation Council of China (grant No. 31501080, 32070676, 31900886), Natural Science Foundation of Guangdong Province (grant No. 2021A1515010737), Hong Kong Baptist University Strategic Development Fund (grant No. SDF13-1209-P01, SDF15-0324-P02(b) and SDF19-0402-P02), Hong Kong Baptist University Interdisciplinary Research Matching Scheme (grant No. RC/IRCs/17-18/04), the 2020 Guangdong Provincial Science and Technology Innovation Strategy Special Fund (grant No: 2020B1212030006), Guangzhou Basic and Applied Basic Research Foundation (202102020550), Guangdong Basic and Applied Basic Research Foundation (2018A030313392).

SUPPLEMENTARY MATERIAL

The Supplementary Material for this article can be found online at: https://www.frontiersin.org/articles/10.3389/fphar.2022.801350/full#supplementary-material

REFERENCES

Alonso-Ruiz, A., Pijoan, J. I., Ansuategui, E., Urkaregi, A., Calabozo, M., and Quintana, A. (2008). Tumor Necrosis Factor Alpha Drugs in Rheumatoid Arthritis: Systematic Review and Metaanalysis of Efficacy and Safety. *BMC Musculoskelet. Disord.* 9, 52. doi:10.1186/1471-2474-9-52

Bansback, N., Marra, C. A., Finckh, A., and Anis, A. (2009). The Economics of Treatment in Early Rheumatoid Arthritis. *Best Pract. Res. Clin. Rheumatol.* 23 (1), 83–92. doi:10.1016/j.berh.2008.11.005

Bao, C. X., Chen, H. X., Mou, X. J., Zhu, X. K., Zhao, Q., and Wang, X. G. (2018). GZMB Gene Silencing Confers protection against Synovial Tissue Hyperplasia and Articular Cartilage Tissue Injury in Rheumatoid Arthritis through the MAPK Signaling Pathway. *Biomed. Pharmacother.* 103, 346–354. doi:10.1016/j.biopha.2018.04.023

Bartlett, D. B., Willis, L. H., Slentz, C. A., Hoselton, A., Kelly, L., Huebner, J. L., et al. (2018). Ten Weeks of High-Intensity Interval Walk Training Is Associated with Reduced Disease Activity and Improved Innate Immune Function in Older Adults with Rheumatoid Arthritis: a Pilot Study. *Arthritis Res. Ther.* 20 (1), 127. doi:10.1186/s13075-018-1624-x

Cao, Y. X., Huang, D., Liu, J., Zong, R. K., Wan, L., Huang, C. B., et al. (2019). A Novel Chinese Medicine, Xinfeng Capsule, Modulates Proinflammatory Cytokines via Regulating the Toll-like Receptor 4 (TLR4)/Mitogen-Activated Protein Kinase (MAPK)/Nuclear Kappa B (NF-Kb) Signaling Pathway in an Adjuvant Arthritis Rat Model. *Med. Sci. Monit.* 25, 6767–6774. doi:10.12659/MSM.916317

Chen, G., Li, K. K., Fung, C. H., Liu, C. L., Wong, H. L., Leung, P. C., et al. (2014). Er-Miao-San, a Traditional Herbal Formula Containing Rhizoma Atractylodis and Cortex Phellodendri Inhibits Inflammatory Mediators in LPS-Stimulated RAW264.7 Macrophages through Inhibition of NF-Kb Pathway and MAPKs Activation. *J. Ethnopharmacol* 154 (3), 711–718. doi:10.1016/j.jep.2014.04.042

Cheng, B., Zheng, H., Wu, F., Wu, J., Liu, X., Tang, C., et al. (2017). Metabolomics Analysis of Danggui Sini Decoction on Treatment of Collagen-Induced Arthritis in Rats. *J. Chromatogr. B Analyt Technol. Biomed. Life Sci.* 1061-1062, 282–291. doi:10.1016/j.jchromb.2017.07.043

Choi, H. K., Hernán, M. A., Seeger, J. D., Robins, J. M., and Wolfe, F. (2002). Methotrexate and Mortality in Patients with Rheumatoid Arthritis: a Prospective Study. *Lancet* 359 (9313), 1173–1177. doi:10.1016/S0140-6736(02)08213-2

Choy, E. H., Smith, C., Doré, C. J., and Scott, D. L. (2005). A Meta-Analysis of the Efficacy and Toxicity of Combining Disease-Modifying Anti-rheumatic Drugs in Rheumatoid Arthritis Based on Patient Withdrawal. *Rheumatology (Oxford)* 44 (11), 1414–1421. doi:10.1093/rheumatology/kei031

Daina, A., Michielin, O., and Zoete, V. (2017). SwissADME: a Free Web Tool to Evaluate Pharmacokinetics, Drug-Likeness and Medicinal Chemistry Friendliness of Small Molecules. *Sci. Rep.* 7, 42717. doi:10.1038/srep42717

Delano, W. L. J. P. S. F. and Bioinformatics (2002). "The PyMol Molecular Graphics System." 30: 442–454.

Donahue, K. E., Gartlehner, G., Jonas, D. E., Lux, L. J., Thieda, P., Jonas, B. L., et al. (2008). Systematic Review: Comparative Effectiveness and Harms of Disease-Modifying Medications for Rheumatoid Arthritis. *Ann. Intern. Med.* 148 (2), 124–134. doi:10.7326/0003-4819-148-2-200801150-00192

Elshabrawy, H. A., Chen, Z., Volin, M. V., Ravella, S., Virupannavar, S., and Shahrara, S. (2015). The Pathogenic Role of Angiogenesis in Rheumatoid Arthritis. *Angiogenesis* 18 (4), 433–448. doi:10.1007/s10456-015-9477-2

Feng, X., Zhao, W. J., Hou, T., and Zhang, N. (2017). Simultaneous Determination of 14 Compounds in Ermiaosan Extracts by Uplc-ms/ms *Chin. J. Exp. Tradit. Med. Formulae* 23 (21), 79–85. doi:10.13422/j.cnki.syfjx.2017210079

Fournier, C. (2005). Where Do T Cells Stand in Rheumatoid Arthritis? *Jt. Bone Spine* 72 (6), 527–532. doi:10.1016/j.jbspin.2004.12.012

Gao, Y., Wang, K. X., Wang, P., Li, X., Chen, J. J., Zhou, B. Y., et al. (2020). A Novel Network Pharmacology Strategy to Decode Mechanism of Lang Chuang Wan in Treating Systemic Lupus Erythematosus. *Front. Pharmacol.* 11, 512877. doi:10.3389/fphar.2020.512877

Garrood, T., and Scott, D. L. (2001). Combination Therapy with Disease Modifying Anti-rheumatic Drugs in Rheumatoid Arthritis. *BioDrugs* 15 (8), 543–561. doi:10.2165/00063030-200115080-00006

Gfeller, D., Grosdidier, A., Wirth, M., Daina, A., Michielin, O., and Zoete, V. (2014). SwissTargetPrediction: a Web Server for Target Prediction of Bioactive Small Molecules. *Nucleic Acids Res.* 42 (Web Server issue), W32–W38. doi:10.1093/nar/gku293

Gong, Y., Yu, Z., Wang, Y., Xiong, Y., Zhou, Y., Liao, C. X., et al. (2019). Effect of Moxibustion on HIF-1α and VEGF Levels in Patients with Rheumatoid Arthritis. *Pain Res. Manag.* 2019, 4705247. doi:10.1155/2019/4705247

Goronzy, J. J., and Weyand, C. M. (2008). T-cell Co-stimulatory Pathways in Autoimmunity, *Arthritis Res. Ther.* Suppl. 1, 10 Suppl 1. S3, S3. doi:10.1186/ar2414

Guo, Q., Mao, X., Zhang, Y., Meng, S., Xi, Y., Ding, Y., et al. (2016). Guizhi-Shaoyao-Zhimu Decoction Attenuates Rheumatoid Arthritis Partially by Reversing Inflammation-Immune System Imbalance. *J. Transl Med.* 14 (1), 165. doi:10.1186/s12967-016-0921-x

Guo, Q., Zheng, K., Fan, D., Zhao, Y., Li, L., Bian, Y., et al. (2017). Wu-tou Decoction in Rheumatoid Arthritis: Integrating Network Pharmacology and *In Vivo* Pharmacological Evaluation. *Front. Pharmacol.* 8, 230. doi:10.3389/fphar.2017.00230

Hao, da. C., and Xiao, P. G. (2014). Network Pharmacology: a Rosetta Stone for Traditional Chinese Medicine. *Drug Dev. Res.* 75 (5), 299–312. doi:10.1002/ddr.21214

Hong, M., Li, S., Tan, H. Y., Cheung, F., Wang, N., Huang, J., et al. (2017). A Network-Based Pharmacology Study of the Herb-Induced Liver Injury Potential of Traditional Hepatoprotective Chinese Herbal Medicines. *Molecules* 22 (4), 632. doi:10.3390/molecules22040632

Hu, F., Mu, R., Zhu, J., Shi, L., Li, Y., Liu, X., et al. (2014). Hypoxia and Hypoxia-Inducible Factor-1α Provoke Toll-like Receptor Signalling-Induced Inflammation in Rheumatoid Arthritis. *Ann. Rheum. Dis.* 73 (5), 928–936. doi:10.1136/annrheumdis-2012-202444

Jiang, F., Zhou, H. Y., Zhou, L. F., Zeng, W., and Zhao, L. H. (2020). IRF9 Affects the TNF-Induced Phenotype of Rheumatoid-Arthritis Fibroblast-like Synoviocytes via Regulation of the SIRT-1/nf-Kb Signaling Pathway. *Cells Tissues Organs* 209 (2-3), 110–119. doi:10.1159/000508405

Keiser, M. J., Roth, B. L., Armbruster, B. N., Ernsberger, P., Irwin, J. J., and Shoichet, B. K. (2007). Relating Protein Pharmacology by Ligand Chemistry. *Nat. Biotechnol.* 25 (2), 197–206. doi:10.1038/nbt1284

Kim, J. H., Huh, J. E., Baek, Y. H., Lee, J. D., Choi, D. Y., and Park, D. S. (2011). Effect of Phellodendron Amurense in Protecting Human Osteoarthritic Cartilage and Chondrocytes. *J. Ethnopharmacol* 134 (2), 234–242. doi:10.1016/j.jep.2010.12.005

Kim, S., Chen, J., Cheng, T., Gindulyte, A., He, J., He, S., et al. (2021). PubChem in 2021: New Data Content and Improved Web Interfaces. *Nucleic Acids Res.* 49 (D1), D1388–D1395. doi:10.1093/nar/gkaa971

Kremer, J. M. (2001). Rational Use of New and Existing Disease-Modifying Agents in Rheumatoid Arthritis. *Ann. Intern. Med.* 134 (8), 695–706. doi:10.7326/0003-4819-134-8-200104170-00013

Kristensen, L. E., Christensen, R., Bliddal, H., Geborek, P., Danneskiold-Samsøe, B., and Saxne, T. (2007). The Number Needed to Treat for Adalimumab, Etanercept, and Infliximab Based on ACR50 Response in Three Randomized Controlled Trials on Established Rheumatoid Arthritis: a Systematic Literature Review. *Scand. J. Rheumatol.* 36 (6), 411–417. doi:10.1080/03009740701607067

Larbi, A., Fülöp, T., and Pawelec, G. (2008). Immune Receptor Signaling, Aging and Autoimmunity. *Adv. Exp. Med. Biol.* 640, 312–324. doi:10.1007/978-0-387-09789-3_21

Leite Pereira, A., Bitoun, S., Paoletti, A., Nocturne, G., Marcos Lopez, E., Cosma, A., et al. (2019). Characterization of Phenotypes and Functional Activities of Leukocytes from Rheumatoid Arthritis Patients by Mass Cytometry. *Front. Immunol.* 10, 2384. doi:10.3389/fimmu.2019.02384

Leombruno, J. P., Einarson, T. R., and Keystone, E. C. (2009). The Safety of Anti-tumour Necrosis Factor Treatments in Rheumatoid Arthritis: Meta and Exposure-Adjusted Pooled Analyses of Serious Adverse Events. *Ann. Rheum. Dis.* 68 (7), 1136–1145. doi:10.1136/ard.2008.091025

Li, X., and Wang, Y. (2020). Cinnamaldehyde Attenuates the Progression of Rheumatoid Arthritis through Down-Regulation of PI3K/AKT Signaling Pathway. *Inflammation* 43 (5), 1729–1741. doi:10.1007/s10753-020-01246-5

Li, Y., Yuan, L., Jiang, S., Liu, S., Xia, L., Shen, H., et al. (2019). Interleukin-35 Stimulates Tumor Necrosis Factor-α Activated Osteoblasts Differentiation through Wnt/β-Catenin Signaling Pathway in Rheumatoid Arthritis. *Int. Immunopharmacol* 75, 105810. doi:10.1016/j.intimp.2019.105810

Li, Z., Liu, J., Hao, H. Q., Gao, Y. T., and Wang, Z. (2020). Chinese Herbal Formula Ermiao Powder () Regulates Cholinergic Anti-inflammatory Pathway in Rats with Rheumatoid Arthritis. *Chin. J. Integr. Med.* 26 (12), 905–912. doi:10.1007/s11655-020-3471-2

Lipinski, C. A., Lombardo, F., Dominy, B. W., and Feeney, P. J. (2001). Experimental and Computational Approaches to Estimate Solubility and Permeability in Drug Discovery and Development Settings. *Adv. Drug Deliv. Rev.* 46 (1-3), 3–26. doi:10.1016/s0169-409x(00)00129-0

Liu, F., Feng, X. X., Zhu, S. L., Huang, H. Y., Chen, Y. D., Pan, Y. F., et al. (2018). Sonic Hedgehog Signaling Pathway Mediates Proliferation and Migration of Fibroblast-like Synoviocytes in Rheumatoid Arthritis via MAPK/ERK Signaling Pathway. *Front. Immunol.* 9, 2847. doi:10.3389/fimmu.2018.02847

Liu, K., Zhang, Y., Liu, L., and Yuan, Q. (2019). miR-125 Regulates PI3K/Akt/mTOR Signaling Pathway in Rheumatoid Arthritis Rats via PARP2. *Biosci. Rep.* 39 (1). doi:10.1042/BSR20180890

Liu, W., Fan, Y., Tian, C., Jin, Y., Du, S., Zeng, P., et al. (2020). Deciphering the Molecular Targets and Mechanisms of HGWD in the Treatment of Rheumatoid Arthritis via Network Pharmacology and Molecular Docking. *Evid. Based Complement. Alternat Med.* 2020, 7151634. doi:10.1155/2020/7151634

Liu, X., Vogt, I., Haque, T., and Campillos, M. (2013). HitPick: a Web Server for Hit Identification and Target Prediction of Chemical Screenings. *Bioinformatics* 29 (15), 1910–1912. doi:10.1093/bioinformatics/btt303

Lorenowicz, M. J., Fernandez-Borja, M., and Hordijk, P. L. (2007). cAMP Signaling in Leukocyte Transendothelial Migration. *Arterioscler Thromb. Vasc. Biol.* 27 (5), 1014–1022. doi:10.1161/ATVBAHA.106.132282

Lorenowicz, M. J., van Gils, J., de Boer, M., Hordijk, P. L., and Fernandez-Borja, M. (2006). Epac1-Rap1 Signaling Regulates Monocyte Adhesion and Chemotaxis. *J. Leukoc. Biol.* 80 (6), 1542–1552. doi:10.1189/jlb.0506357

MacGregor, A. J., Snieder, H., Rigby, A. S., Koskenvuo, M., Kaprio, J., Aho, K., et al. (2000). Characterizing the Quantitative Genetic Contribution to Rheumatoid Arthritis Using Data from Twins. *Arthritis Rheum.* 43 (1), 30–37. doi:10.1002/1529-0131(200001)43:1<30:AID-ANR5>3.0.CO;2-B

Mitchell, J. P., and Carmody, R. J. (2018). NF-κB and the Transcriptional Control of Inflammation. *Int. Rev. Cel Mol Biol* 335, 41–84. doi:10.1016/bs.ircmb.2017.07.007

Morris, G. M., Huey, R., Lindstrom, W., Sanner, M. F., Belew, R. K., Goodsell, D. S., et al. (2009). AutoDock4 and AutoDockTools4: Automated Docking with Selective Receptor Flexibility. *J. Comput. Chem.* 30 (16), 2785–2791. doi:10.1002/jcc.21256

Mura, C., McCrimmon, C. M., Vertrees, J., and Sawaya, M. R. (2010). An Introduction to Biomolecular Graphics. *Plos Comput. Biol.* 6 (8). doi:10.1371/journal.pcbi.1000918

O'Boyle, N. M., Banck, M., James, C. A., Morley, C., Vandermeersch, T., and Hutchison, G. R. (2011). Open Babel: An Open Chemical Toolbox. *J. Cheminform* 3, 33. doi:10.1186/1758-2946-3-33

O'Dell, J. R. (2001). Combinations of Conventional Disease-Modifying Antirheumatic Drugs. *Rheum. Dis. Clin. North. Am.* 27 (2), 415–x. doi:10.1016/s0889-857x(05)70210-6

Park, J. E., Brand, D. D., Rosloniec, E. F., Yi, A. K., Stuart, J. M., Kang, A. H., et al. (2020). Leukocyte-associated Immunoglobulin-like Receptor 1 Inhibits T-Cell Signaling by Decreasing Protein Phosphorylation in the T-Cell Signaling Pathway. *J. Biol. Chem.* 295 (8), 2239–2247. doi:10.1074/jbc.RA119.011150

Quinn, M. A., Conaghan, P. G., and Emery, P. (2001). The Therapeutic Approach of Early Intervention for Rheumatoid Arthritis: what Is the Evidence? *Rheumatology (Oxford)* 40 (11), 1211–1220. doi:10.1093/rheumatology/40.11.1211

Ralph, J. A., and Morand, E. F. (2008). MAPK Phosphatases as Novel Targets for Rheumatoid Arthritis. *Expert Opin. Ther. Targets* 12 (7), 795–808. doi:10.1517/14728222.12.7.795

Resch, M., Steigel, A., Chen, Z. L., and Bauer, R. (1998). 5-Lipoxygenase and Cyclooxygenase-1 Inhibitory Active Compounds from Atractylodes Lancea. *J. Nat. Prod.* 61 (3), 347–350. doi:10.1021/np970430b

Ru, J., Li, P., Wang, J., Zhou, W., Li, B., Huang, C., et al. (2014). TCMSP: a Database of Systems Pharmacology for Drug Discovery from Herbal Medicines. *J. Cheminform* 6, 13. doi:10.1186/1758-2946-6-13

Sakaguchi, S., Benham, H., Cope, A. P., and Thomas, R. (2012). T-cell Receptor Signaling and the Pathogenesis of Autoimmune Arthritis: Insights from Mouse and Man. *Immunol. Cel Biol* 90 (3), 277–287. doi:10.1038/icb.2012.4

Scott, D. L., Wolfe, F., and Huizinga, T. W. (2010). Rheumatoid Arthritis. *Lancet* 376 (9746), 1094–1108. doi:10.1016/S0140-6736(10)60826-4

Shannon, P., Markiel, A., Ozier, O., Baliga, N. S., Wang, J. T., Ramage, D., et al. (2003). Cytoscape: a Software Environment for Integrated Models of Biomolecular Interaction Networks. *Genome Res.* 13 (11), 2498–2504. doi:10.1101/gr.1239303

Shi, Y., Shu, H., Wang, X., Zhao, H., Lu, C., Lu, A., et al. (2020). Potential Advantages of Bioactive Compounds Extracted from Traditional Chinese Medicine to Inhibit Bone Destructions in Rheumatoid Arthritis. *Front. Pharmacol.* 11, 561962. doi:10.3389/fphar.2020.561962

Simon, L. S. (2000). DMARDs in the Treatment of Rheumatoid Arthritis: Current Agents and Future Developments. *Int. J. Clin. Pract.* 54 (4), 243–249.

Singh, J. A., Christensen, R., Wells, G. A., Suarez-Almazor, M. E., Buchbinder, R., Lopez-Olivo, M. A., et al. (2009). A Network Meta-Analysis of Randomized Controlled Trials of Biologics for Rheumatoid Arthritis: a Cochrane Overview. *CMAJ* 181 (11), 787–796. doi:10.1503/cmaj.091391

Smolen, J. S., Landewé, R., Bijlsma, J., Burmester, G., Chatzidionysiou, K., Dougados, M., et al. (2017). EULAR Recommendations for the Management of Rheumatoid Arthritis with Synthetic and Biological Disease-Modifying Antirheumatic Drugs: 2016 Update. *Ann. Rheum. Dis.* 76 (6), 960–977. doi:10.1136/annrheumdis-2016-210715

Sterling, T., and Irwin, J. J. (2015). ZINC 15--Ligand Discovery for Everyone. *J. Chem. Inf. Model.* 55 (11), 2324–2337. doi:10.1021/acs.jcim.5b00559

Strangfeld, A., Listing, J., Herzer, P., Liebhaber, A., Rockwitz, K., Richter, C., et al. (2009). Risk of Herpes Zoster in Patients with Rheumatoid Arthritis Treated with Anti-TNF-alpha Agents. *JAMA* 301 (7), 737–744. doi:10.1001/jama.2009.146

Sujitha, S., and Rasool, M. (2017). MicroRNAs and Bioactive Compounds on TLR/MAPK Signaling in Rheumatoid Arthritis. *Clin. Chim. Acta* 473, 106–115. doi:10.1016/j.cca.2017.08.021

Tang, F., Fan, K., Wang, K., and Bian, C. (2018). Atractylodin Attenuates Lipopolysaccharide-Induced Acute Lung Injury by Inhibiting NLRP3 Inflammasome and TLR4 Pathways. *J. Pharmacol. Sci.* 136 (4), 203–211. doi:10.1016/j.jphs.2017.11.010

Tao, W., Xu, X., Wang, X., Li, B., Wang, Y., Li, Y., et al. (2013). Network Pharmacology-Based Prediction of the Active Ingredients and Potential Targets of Chinese Herbal Radix Curcumae Formula for Application to Cardiovascular Disease. *J. Ethnopharmacol* 145 (1), 1–10. doi:10.1016/j.jep.2012.09.051

Torices, S., Alvarez-Rodríguez, L., Varela, I., Muñoz, P., Balsa, A., López-Hoyos, M., et al. (2017). Evaluation of Toll-Like-Receptor Gene Family Variants as Prognostic Biomarkers in Rheumatoid Arthritis. *Immunol. Lett.* 187, 35–40. doi:10.1016/j.imlet.2017.04.011

Trott, O., and Olson, A. J. (2010). AutoDock Vina: Improving the Speed and Accuracy of Docking with a New Scoring Function, Efficient Optimization, and Multithreading. *J. Comput. Chem.* 31 (2), 455–461. doi:10.1002/jcc.21334

Wan, Y. (2018). Observation for Clinical Effect of Phellodendron Wet Compress in Treating the Phlebitis Caused by Infusion. *Pak J. Pharm. Sci.* 31 (3), 1099–1102. (Special).

Wang, K., Zhang, D., Liu, Y., Wang, X., Zhao, J., Sun, T., et al. (2018). Traditional Chinese Medicine Formula Bi-qi Capsule Alleviates Rheumatoid Arthritis-Induced Inflammation, Synovial Hyperplasia, and Cartilage Destruction in Rats. *Arthritis Res. Ther.* 20 (1), 43. doi:10.1186/s13075-018-1547-6

Wang, K. X., Gao, Y., Gong, W. X., Ye, X. F., Fan, L. Y., Wang, C., et al. (2020a). A Novel Strategy for Decoding and Validating the Combination Principles of Huanglian Jiedu Decoction from Multi-Scale Perspective. *Front. Pharmacol.* 11, 567088. doi:10.3389/fphar.2020.567088

Wang, K. X., Gao, Y., Lu, C., Li, Y., Zhou, B. Y., Qin, X. M., et al. (2020b). Uncovering the Complexity Mechanism of Different Formulas Treatment for Rheumatoid Arthritis Based on a Novel Network Pharmacology Model. *Front. Pharmacol.* 11, 1035. doi:10.3389/fphar.2020.01035

Wang, L., Fan, Y., Xin, P., Zhao, Y., Deng, H., and Jia, B. (2020c). The Efficacy and Safety of Huangqi Guizhi Wuwu Decoction for Rheumatoid Arthritis: A Protocol for Systematic Review and Meta-Analysis. *Medicine (Baltimore)* 99 (36), e22011. doi:10.1097/MD.0000000000022011

Wang, Q. S., Cui, Y. L., Wang, Y. F., and Chi, W. (2011). Effects of Compounds from Bi-qi Capsule on the Expression of Inflammatory Mediators in Lipopolysaccharide-Stimulated RAW 264.7 Macrophages. *J. Ethnopharmacol* 136 (3), 480–487. doi:10.1016/j.jep.2010.06.008

Wasserman, A. M. (2011). Diagnosis and Management of Rheumatoid Arthritis. *Am. Fam. Physician* 84 (11), 1245–1252.

Wu, X., Long, L., Liu, J., Zhang, J., Wu, T., Chen, X., et al. (2017). Gambogic Acid Suppresses Inflammation in Rheumatoid Arthritis Rats via PI3K/Akt/mTOR Signaling Pathway. *Mol. Med. Rep.* 16 (5), 7112–7118. doi:10.3892/mmr.2017.7459

wwPDB consortium (2019). Protein Data Bank: the Single Global Archive for 3D Macromolecular Structure Data. *Nucleic Acids Res.* 47 (D1), D520–D528. doi:10.1093/nar/gky949

Xia, Z. B., Meng, F. R., Fang, Y. X., Wu, X., Zhang, C. W., Liu, Y., et al. (2018). Inhibition of NF-Kb Signaling Pathway Induces Apoptosis and Suppresses Proliferation and Angiogenesis of Human Fibroblast-like Synovial Cells in Rheumatoid Arthritis. *Medicine (Baltimore)* 97 (23), e10920. doi:10.1097/MD.0000000000010920

Xian, Y. F., Mao, Q. Q., Ip, S. P., Lin, Z. X., and Che, C. T. (2011). Comparison on the Anti-inflammatory Effect of Cortex Phellodendri Chinensis and Cortex Phellodendri Amurensis in 12-O-Tetradecanoyl-Phorbol-13-Acetate-Induced Ear Edema in Mice. *J. Ethnopharmacol* 137 (3), 1425–1430. doi:10.1016/j.jep.2011.08.014

Xu, Y., Hong, S., Zhao, X., Wang, S., Xu, Z., Ding, S., et al. (2018). Acupuncture Alleviates Rheumatoid Arthritis by Immune-Network Modulation. *Am. J. Chin. Med.* 46 (5), 997–1019. doi:10.1142/S0192415X18500520

Yang, G., Chang, C. C., Yang, Y., Yuan, L., Xu, L., Ho, C. T., et al. (2018). Resveratrol Alleviates Rheumatoid Arthritis via Reducing ROS and Inflammation, Inhibiting MAPK Signaling Pathways, and Suppressing Angiogenesis. *J. Agric. Food Chem.* 66 (49), 12953–12960. doi:10.1021/acs.jafc.8b05047

Yang, L., Fan, L., Wang, K., Chen, Y., Liang, L., Qin, X., et al. (2021). Analysis of Molecular Mechanism of Erxian Decoction in Treating Osteoporosis Based on Formula Optimization Model. *Oxid Med. Cel Longev* 2021, 6641838. doi:10.1155/2021/6641838

Yu, F. Y., Xie, C. Q., Jiang, C. L., Sun, J. T., and Huang, X. W. (2018). TNFalpha Increases Inflammatory Factor Expression in Synovial Fibroblasts through the Tolllike Receptor3mediated ERK/AKT Signaling Pathway in a Mouse Model of Rheumatoid Arthritis. *Mol. Med. Rep.* 17 (6), 8475–8483. doi:10.3892/mmr.2018.8897

Yu, G., Wang, L. G., Han, Y., and He, Q. Y. (2012). clusterProfiler: an R Package for Comparing Biological Themes Among Gene Clusters. *OMICS* 16 (5), 284–287. doi:10.1089/omi.2011.0118

Zhang, H. J., Wei, Q. F., Wang, S. J., Zhang, H. J., Zhang, X. Y., Geng, Q., et al. (2017). LncRNA HOTAIR Alleviates Rheumatoid Arthritis by Targeting miR-138 and Inactivating NF-Kb Pathway. *Int. Immunopharmacol* 50, 283–290. doi:10.1016/j.intimp.2017.06.021

Zhang, W. J., Zhao, Z. Y., Chang, L. K., Cao, Y., Wang, S., Kang, C. Z., et al. (2021). Atractylodis Rhizoma: A Review of its Traditional Uses, Phytochemistry, Pharmacology, Toxicology and Quality Control. *J. Ethnopharmacol* 266, 113415. doi:10.1016/j.jep.2020.113415

Zhang, Y., Bai, M., Zhang, B., Liu, C., Guo, Q., Sun, Y., et al. (2015). Uncovering Pharmacological Mechanisms of Wu-tou Decoction Acting on Rheumatoid Arthritis through Systems Approaches: Drug-Target Prediction, Network Analysis and Experimental Validation. *Sci. Rep.* 5, 9463. doi:10.1038/srep09463

Zhang, Y., Sun, Y., Yan, R., Lin, Z., Zhang, Y., Lu, Y., et al. (2018). Application of Phellodendron Amurense Facial Mask for Slight to Moderate Acne Vulgaris. *Clin. Exp. Dermatol.* 43 (8), 928–930. doi:10.1111/ced.13663

Zhou, C., Liu, L., Zhuang, J., Wei, J., Zhang, T., Gao, C., et al. (2018). A Systems Biology-Based Approach to Uncovering Molecular Mechanisms Underlying Effects of Traditional Chinese Medicine Qingdai in Chronic Myelogenous Leukemia, Involving Integration of Network Pharmacology and Molecular Docking Technology. *Med. Sci. Monit.* 24, 4305–4316. doi:10.12659/MSM.908104

Zhou, Z., Chen, B., Chen, S., Lin, M., Chen, Y., Jin, S., et al. (2020). Applications of Network Pharmacology in Traditional Chinese Medicine Research. *Evid. Based Complement. Alternat Med.* 2020, 1646905. doi:10.1155/2020/1646905

Conflict of Interest: The authors declare that the research was conducted in the absence of any commercial or financial relationships that could be construed as a potential conflict of interest.

Publisher's Note: All claims expressed in this article are solely those of the authors and do not necessarily represent those of their affiliated organizations or those of the publisher, the editors, and the reviewers. Any product that may be evaluated in this article, or claim that may be made by its manufacturer, is not guaranteed or endorsed by the publisher.

frontiers in Pharmacology

SYSTEMATIC REVIEW
published: 24 February 2022
doi: 10.3389/fphar.2022.787032

Reynoutria japonica Houtt for Acute Respiratory Tract Infections in Adults and Children: A Systematic Review

Zhi-Jie Wang[1,2], Jeanne Trill[3], Lin-Lin Tan[2], Wen-Jing Chang[4], Yu Zhang[5], Merlin Willcox[3], Ru-Yu Xia[4], Yue Jiang[4], Michael Moore[3], Jian-Ping Liu[4] and Xiao-Yang Hu[3]**

[1]Department of Oncology, Shanxi Province Hospital of Tradition Chinese Medicine, Taiyuan, China, [2]The Institute of Shanxi Traditional Chinese Medicine, Taiyuan, China, [3]Primary Care Research Centre, Faculty of Medicine, University of Southampton, Southampton, United Kingdom, [4]Center for Evidence-based Chinese Medicine, Beijing University of Chinese Medicine, Beijing, China, [5]The First Affiliated Hospital of Anhui University of Chinese Medicine, Hefei, China

Introduction: Respiratory tract infections (RTIs) are a major cause of morbidity and mortality in some high-risk groups including children and older adults. There is evidence that Chinese herbal medicine has an effect on RTIs. *Reynoutria japonica* Houtt (better known under its synonym *Fallopia japonica* (Houtt.) Ronse Decr.) (*F. japonica*), a commonly used Chinese herbal medicine, has a high content of resveratrol and glycosides. In traditional Chinese medicine theory, *F. japonica* has the effect of clearing heat in the body, improving blood and qi circulation, eliminating phlegm, and relieving cough, so it may have an effect on RTIs.

Methods: This systematic review was registered under PROSPERO CRD42020188604. Databases were searched for randomized controlled trials of *F. japonica* as a single herb, or as a component of a complex herbal formula for RTIs. Quality of methodology was assessed by two reviewers independently using the Cochrane Risk of Bias Tool. The primary outcome was symptom improvement rate. The secondary outcome measures were fever clearance time, Murray lung injury score and incidence of adverse effects. The extracted data were pooled and meta-analysed by RevMan 5.3 software.

Results: Eight RCTs with 1,123 participants with acute RTIs were included in this systematic review, and all the RCTs used *F. japonica* as part of a herbal mixture. Only one included trial used *F. japonica* in a herbal mixture without antibiotics in the treatment group. The findings showed that herbal remedies that included *F. japonica* could increase the symptom improvement rate (risk ratio 1.14, 95% confidence intervals [1.09, 1.20], I^2 = 0%, $p < 0.00001$, n = 7 trials, 1,013 participants), shorten fever duration, reduce Murray

OPEN ACCESS

Edited by:
Aiping Lu,
Hong Kong Baptist University, Hong Kong SAR, China

Reviewed by:
Yuan Shiun Chang,
China Medical University (Taiwan), Taiwan
Lei Wu,
Guangdong Provincial Hospital of Chinese Medicine, China

***Correspondence:**
Xiao-Yang Hu
X.Hu@soton.ac.uk
Jian-Ping Liu
liujp@bucm.edu.cn

Specialty section:
This article was submitted to Ethnopharmacology, a section of the journal Frontiers in Pharmacology

Received: *30 September 2021*
Accepted: *31 January 2022*
Published: *24 February 2022*

Citation:
Wang Z-J, Trill J, Tan L-L, Chang W-J, Zhang Y, Willcox M, Xia R-Y, Jiang Y, Moore M, Liu J-P and Hu X-Y (2022) Reynoutria japonica Houtt for Acute Respiratory Tract Infections in Adults and Children: A Systematic Review. Front. Pharmacol. 13:787032. doi: 10.3389/fphar.2022.787032

Abbreviations: AECOPD, acute exacerbation of chronic obstructive pulmonary disease; AMED, Allied and Complementary Medicine Database; ARI, acute respiratory infection; CI, confidence intervals; CHM, Chinese herbal medicine; CNKI, China National Knowledge Infrastructure; COPD, chronic obstructive pulmonary disease; FDA, the Food and Drug Administration; *F. japonica*, *Reynoutria japonica* Houtt; GRADE, Grades of Recommendations Assessment, Development and Evaluation; ITT, intention to treat; MD, mean differences; MMP-9, matrix metalloproteinase-9; NF-Kb, κ-light chain of nuclear factor B cells; OASIS, Oriental Medicine Advanced Searching Integrated System; PD, Polydatin; PRISMA, the Preferred Reporting Items for Systematic Reviews and Meta-Analyses; RTIs, Respiratory tract infections; RISS, Sino-Med Database Research Information Service System; RCTs, randomized controlled trials; RR, risk ratio; SM, standardized mean differences; TCM, Traditional Chinese Medicine; TIMP-1, tissue inhibitor of metalloprotease-1; VIP, Chinese Science and Technology Journal Database; WHO, the World Health Organization.

lung injury score and did not increase adverse events (RR 0.33, 95% CI [0.11, 1.00], I^2 = 0%, p = 0.05, n = 5 trials, 676 participants).

Conclusion: There is limited but some evidence that *F. japonica* as part of a herbal mixture may be an effective and safe intervention for acute RTIs in clinical practice. In future studies it would be preferable to evaluate the effectiveness and safety of using *F. japonica* without antibiotics for acute RTIs.

Keywords: *reynoutria japonica*, herbal remedy, respiratory tract infections (RTIs), randomized controlled trials, meta-analysis

1 INTRODUCTION

A variety of viruses and bacteria can cause respiratory tract infections (RTIs) including upper and lower RTIs. The most frequent upper RTIs are the common cold, laryngitis, tonsillopharyngitis, and otitis media; lower RTIs include bronchitis, bronchiolitis, and pneumonia. RTIs are a major cause of morbidity and mortality in some high-risk groups including children and older adults (Shek and Lee, 2003). RTIs are the leading infectious cause of death, and the sixth-leading cause of death overall worldwide. RTIs result in millions of clinical visits and subsequent prescriptions of antibiotics every year. Globally, in 2016 there were more than 300 million cases of RTIs (GBD 2016 Lower Respiratory Infections Collaborators, 2018).

Symptom relief is often the target of treatment for RTIs. Appropriate and effective treatments may limit cough, fever, pain, congestion and other symptoms in patients with RTIs (Irwin et al., 2006). Rates of prescribing antibiotics for respiratory conditions in the United Kingdom are high with median prescribing rates of 54% (Gulliford et al., 2014). Of the antibiotics prescribed in primary care with an attributable target, nearly half were for respiratory conditions (Costelloe et al., 2010) with similar high rates reported in China (Li, 2019), despite the lack of evidence to support using antibiotics for viral infections (Weintraub, 2015). The overuse of antibiotics increases the risk of colonisation with resistant bacteria, promotes antibiotic resistance in the community, risks subsequent infection with antibiotic resistant organisms, and may cause some allergic reactions and other adverse effects (Weintraub, 2015; Bryce et al., 2016).

Chinese herbal medicine (CHM) is an important part of Traditional Chinese Medicine (TCM), and is used for almost all kinds of diseases in clinical practice in China. CHMs include one or more herbs for syndromes or disorders according to the TCM theories (Wu et al., 2008). The Food and Drug Administration (FDA) in the United States has approved the use of 13 herbal remedies, and of the total 252 drugs in the World Health Organization (WHO) essential medicine list, 11% are exclusively of plant origin, resulting in increased sales of CHMs (Wachtel-Galor and Benzie, 2011). Considering the adverse effects and resistance of antibiotics, and the diverse symptoms of RTIs, CHMs are commonly used for inflammation including RTIs (Chen et al., 2006).

Hu Zhang [虎杖] in the *Chinese Pharmacopoeia* consists of the roots and rhizomes of Japanese Knotweed. The accepted scientific name of this plant is now *Reynoutria japonica* Houtt, but it also has many synonyms, of which the most important are *Fallopia japonica* (Houtt) Ronse Decr. and *Polygonum cuspidatum Siebold & Zucc*. The herb is commonly used in CHM therapy (Jeong et al., 2010), and dates back to at least the Han Dynasty when it was recorded in the 'Supplementary Records of Famous Physicians' [名医别录]. The herb is used for clearing heat from the body, improving blood [血] and qi [气] circulation, eliminating phlegm, and relieving cough and asthma (Yan et al., 2019). It is always classed as a sovereign herb (a herb that plays a major role in the treatment of the main syndrome or main symptom) in CHM formulas for treating RTIs, an example of which is Shufeng Jiedu capsule. It is used for nervous system disorders, bronchitis, high blood pressure and jaundice (Editor Committee of Jiangsu New Medical College, 2011.).

F. japonica is reported to have antiallergic, antimutagenic, antioxidant, antibacterial and antiviral activities, and the main active compounds are believed to be resveratrol and glycosides (Bralley et al., 2008; Zahedi et al., 2013; Goc et al., 2015). Some activation of nuclear transcription factors such as Nuclear Factor kappa B (NF-κB), activator protein-1, matrix metalloproteinase-9 (MMP-9) and tissue inhibitor of metalloprotease-1 (TIMP-1) were reported in connection with RTIs, which might be activated by *F. japonica* (Manna et al., 2000; Huang, 2017). Polydatin (PD) is another major active ingredient of *F. japonica*; the herb is widely used for treating both acute and chronic lung disorders (Lin et al., 2011; Lee et al., 2015).

F. japonica and its extracts have been reported to have a positive effect on RTIs, but no systematic review has ever been conducted on its use for these conditions. In this review, we aimed to evaluate the effectiveness and safety of *F. japonica,* or herbal remedies that included *F. japonica,* for acute RTIs in adults and children.

2 METHOD

The Preferred Reporting Items for Systematic Reviews and Meta-Analyses (PRISMA) has been adhered to in reporting this review (Moher et al., 2015), and the protocol has been registered under PROSPERO (CRD42020188604).

2.1 Data Sources and Search Terms

A search was carried out across the databases MEDLINE, embase, Cochrane Central Register of Controlled Trials, Allied and Complementary Medicine Database (AMED), Web of Science,

CINAHL Plus, China National Knowledge Infrastructure (CNKI), Wan Fang, Chinese Science and Technology Journal Database (VIP), Sino-Med Database Research Information Service System (RISS), Oriental Medicine Advanced Searching Integrated System (OASIS), and the National Assembly Library from their inception to July 2021. Clinical trial registers, ClinicalTrials.gov and the World Health Organization International Clinical Trials Registry Platform, were also searched. Search terms included '*Fallopia japonica*' or 'Hu Zhang' or 'Japanese Knotweed' or '*Reynoutria japonica*' or '*Polygonum cuspidatum*', AND 'respiratory tract infections' or 'common cold' or 'cough'. Additional search terms and strategies in different languages with different databases are listed in **Supplementary Appendix S1**. We also repeated the searches including the names of the complex formulae which included *F. japonica*.

2.2 Study Selection

2.2.1 Inclusion and Exclusion Criteria

This systematic review included published and unpublished randomized controlled trials (RCTs), and data from crossover trials prior to the crossover. Controlled before and after studies, interrupted time series studies, quasi-RCTs and non-experimental studies were not included due to their potential high risk of bias.

Population: Trials with patients in all age groups, with either an acute respiratory tract infection (ARI) diagnosis or presentation with ARI symptoms were included. A clinical diagnosis of ARI was the main inclusion criterion. Diagnoses of upper or lower ARIs included the common cold, otitis media, influenza, rhinosinusitis, laryngitis, tonsillitis, pharyngitis, supraglottitis, croup, tracheitis, bronchitis, and acute exacerbations of either asthma or chronic obstructive pulmonary disease (COPD). Symptoms of ARIs are defined as having symptoms such as cough, sore throat, fever, runny nose, earache and discoloured sputum with duration of less than 3 weeks. In and out patients were both included.

Trials were excluded if they recruited participants with another non infectious condition such as asthma or participants with infections such as tuberculosis and pneumonia which require antibiotics. Exclusion was applied to trials that included patients who had a known immune deficiency.

Intervention: any form of *F. japonica*, including oral, nasal, or external use, apart from injection; either as a single herb, or within a herbal remedy. There was no limitation concerning dosage, dosing method or duration of administration.

Comparator: no intervention, placebo or usual care such as antipyretics, antivirals, antibiotics, anti-inflammatories, steroids or corticosteroids were included.

2.2.2 Outcome Measures

The primary outcome measure was effect estimation (symptom improvement rate). The secondary outcome measures were fever clearance time, lung injury score (such as the Murray lung injury score) and incidence of adverse effects.

2.2.3 Data Selection and Collection

Literature searching and screening (titles, abstracts and full texts) was conducted by three reviewers independently (WZJ, XRY, JY), and disagreements were resolved through discussion and consensus, or were assessed by a fourth reviewer (HXY). There were no restrictions on language. Researchers were not blinded to the authors' affiliations, journal of publication, or study results.

2.2.4 Data Extraction and Management

Two reviewers (WZJ, ZY) independently extracted data from the included trials including study characteristics, participants and diseases, details of interventions on all trial arms, outcome measures, and adverse events.

2.3 Assessment of Bias and Reporting Quality of Included Trials

Two reviewers (WZJ, ZY) independently assessed the risk of bias using the Cochrane Collaboration risk of bias tool (Higgins et al., 2019). The risk of bias tool assessed seven domains and for each domain the two reviewers made a judgment whether the risk of bias was high, unclear or low. Disagreements were discussed and resolved with reference to the original protocol and, if necessary, arbitration by a third reviewer (HXY). We planned to conduct funnel plot tests for asymmetry to investigate potential reporting bias if this was feasible and there existed sufficient studies (≥10) under a single meta-analysis (Egger et al., 1997). The evidence level of the included trials was assessed by Grades of Recommendations Assessment, Development and Evaluation (GRADE) with the high, moderate, low or very low level.

2.4 Measures of Treatment Effect

Where possible, the analyses were based on intention to treat (ITT) data on each outcome provided for every randomized participant from the individual trials. For continuous outcomes, the end of treatment scores rather than change from baseline scores were extracted; for continuous data, due to the anticipated variability in the populations and interventions of included trials, a generic inverse variance random effects model was used to pool the mean differences (MD) with 95% confidence intervals (CI) to incorporate heterogeneity (Murad et al., 2015). If the units of the outcome measures used across studies were not consistent, the effects as standardized mean differences (SMD) were reported. An overall effect size of 0.2–0.5 was regarded as small, 0.5–0.8 as moderate and more than 0.8 as large. For dichotomous data, a random effects method was used to pool the summary risk ratio (RR) with 95% CI.

2.5 Dealing With Missing Data

Where standard deviation was not reported with means, it was calculated from the information reported such as CI, *p*-values, or F-values. ITT analysis was utilized for all outcomes as far as possible. For the missing data, we planned to contact the corresponding author of the original study.

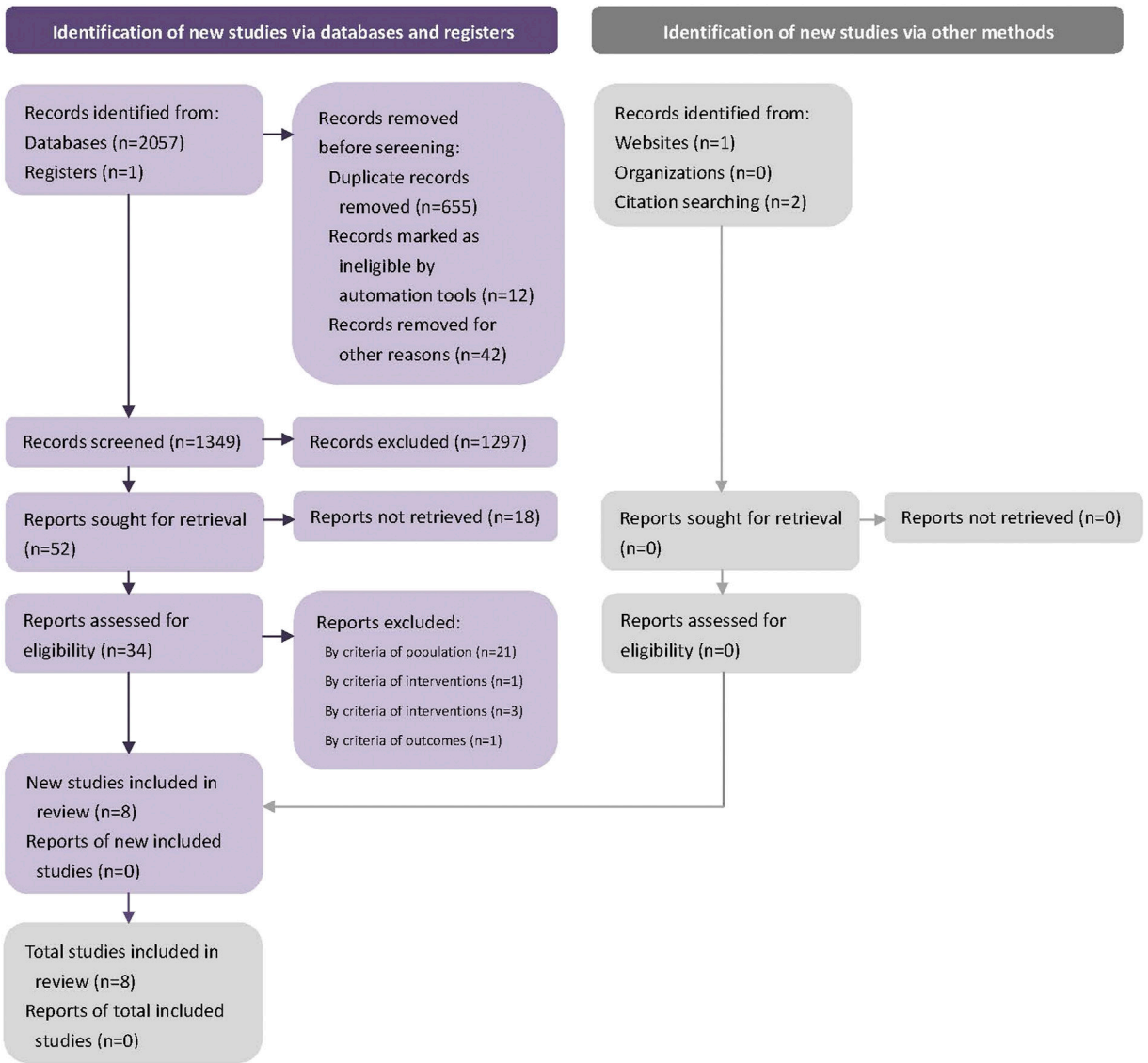

FIGURE 1 | Flow diagram.

2.6 Assessment of Heterogeneity

Between-study heterogeneity was assessed using the I^2—statistic which describes the percentage of variation across studies due to heterogeneity rather than chance. Criteria recommended for interpretation of this statistic suggested that I^2>30% represents moderate heterogeneity, I^2>50% represents substantial heterogeneity and I^2>75% represents considerable heterogeneity (Higgins et al., 2019). Where I^2 values were above 50%, potential sources of heterogeneity were further investigated in a subgroup analysis. This was taken into account when interpreting the findings. As high levels of heterogeneity were to be expected due to complexity in the form of *F. japonica* (such as variation of the type of preparation and the percentage of the active ingredient), a random effects model was utilized to pool the overall effects (Higgins et al., 2019).

2.7 Sensitivity Analysis

Sensitivity analyses were performed for the primary outcome on usage of antibiotics, as well as on the overall RTI symptoms or two target symptoms: cough and sore throat. This was to determine whether the review conclusions would have differed if eligibility was restricted to trials with low risk of selection bias (Higgins et al., 2019).

2.8 Subgroup Analysis

Where sufficient data were available, several subgroup analyses were planned to compare the effect estimates between studies that evaluated: adults versus children (younger than 18); *F. japonica* in different preparations, e.g., granule versus capsule or other forms; *F. japonica* as a monotherapy versus as part of a complex herbal remedy, or a supplement mixture; or specific ARIs (e.g., tonsillitis,

TABLE 1 | Study characteristics.

study ID	Condition	setting	sample size	Mean age (±SD)		Gender (male/female)		Treatments		Outcome measures	Adverse events	source of funding
			T/C	T	C	T	C	T	C			
URTIs												
Bi and Feng, (2015)	pediatric URTIs	inpatient	84 (42/42)	5.5 ± 1.3 Y	6.0 ± 1.5 Y	24/18	22/20	UC + SFJDC for 3d	UC	symptom improvement rate, time without fever	2 (1 nausea, 1 rash)/8 (4 nausea, 2 diarrhea, 2 rash)	NR
Chen et al. (2016)	pediatric URTIs	inpatient	156 (78/78)	6.3 ± 3.5 Y	6.5 ± 1.5 Y	35/43	41/37	UC + SFJDC for 7d	UC	symptom improvement rate, time without fever	1 (nausea)/ 1 (rash)	NR
Li et al. (2014)	pediatric URTIs	unclear	100 (50/50)	4.91 ± 0.95 Y	4.77 ± 0.77 Y	23/27	24/26	Tuire Liquid for 6d	UC	symptom improvement rate	NR	NR
Liu et al. (2020)	acute URTIs	unclear	180 (90/90)	34.77 ± 7.24 Y	32.60 ± 8.95 Y	47/43	49/41	UC + SFJDC for 3d	UC	symptom improvement rate, lung function	No/No	NR
Zhao and Wang, (2020)	acute URTIs	unclear	156 (78/78)	37.30 ± 6.50 Y	36.80 ± 6.20 Y	41/37	40/38	UC + SFJDC for 5d	UC	symptom improvement rate, time without fever	1 (1 diarrhea)/3 (2 nausea, 1 fatigue)	NR
Zhang et al. (2021)	acute URTIs	unclear	237 (118/ 119)	31.94 ± 6.50 Y	35.94 ± 3.50 Y	67/51	65/54	UC + SFJDC for 3d	UC + SFJDC placebo	symptom improvement rate	NR	NR
AECOPD												
Yang (2019)	AECOPD	inpatient	100 (50/50)	61.30 ± 4.70 Y	63.15 ± 3.71 Y	27/23	24/26	UC + SFJDC for 7d	UC	symptom improvement rate, lung function	No/No	NR
Yang, (2019)	AECOPD	unclear	110 (55/55)	71.23 ± 2.13 Y	71.30 ± 1.98 Y	30/25	31/24	UC + Xuanfei Quyu Tongluo Liquid for 45d	UC	lung function	NR	NR

SFJDC: Fallopia japonica root [虎杖], Forsythia suspensa fruit [连翘], Isatis indigotica L root [板蓝根], Bupleurum chinense root [柴胡], Patrinia scabiosaefolia flower [败酱草], Verbena officinalis L. herb [马鞭草], Phragmites communis rhizome [芦根], Glycyrrhiza uralensis Fisch root [甘草]. Tuire Liquid: Indigo naturalis [青黛], Herba Menthae [薄荷], Armeniaca amarum seed [杏仁], Fallopia japonica root [虎杖], Artemisia annua herb [青蒿], Crystalline Mirabilite [寒水石], Forsythia suspensa fruit [连翘], Uncaria spp. twigs with hooks [钩藤], Cassia occidentalis seed [望江南], Fortunes Boss Fern Rhizome [贯众], Fructus Crataegi [山楂], Massa Medicata Fermentata [神曲]. Xuanfei Quyu Tongluo Liquid: Salvia miltiorrhizae root [丹参], Deer antler glue [鹿角胶], Armeniaca amarum seed [杏仁], Pinellia ternata (Thunb.) Breit root [半夏], Wolfiporia extensa (Peck) Ginns fungus[茯苓], Trichosanthes spp. fruit[瓜蒌], Psoralea corylifolia Linn fruit [补骨脂], Fallopia japonica root [虎杖], Ephedra [麻黄], Citrus reticulata Blanco fruit peel [陈皮]. The formula of the included herbal remedies. T: treatment group; C: control group; UC: usual care; NR: not reported; URTIs: upper respiratory tract infections; AECOPD: acute exacerbation of chronic obstructive pulmonary disease; SFJDC: shufeng jiedu capsule.

otitis media, rhinosinusitis, etc.) to be grouped together according to the main symptoms depending on the number of papers found.

3 RESULTS

2061 potential studies were searched initially, and 712 duplicates were removed. The remaining 1,349 studies were screened by the title and abstract. 1,313 studies were excluded at this stage, 34 studies were screened in full text, and eight RCTs were included in the final systematic review (Li et al., 2014; Bi and Feng, 2015; Chen et al., 2016; Yang, 2019; Yang et al., 2019; Liu et al., 2020). (**Figure 1**). We contacted the corresponding author of the data missing studies, but no replies from the authors. **Figure 1**. Flow diagram.

3.1 Study Characteristics

Eight RCTs and 1,123 participants (which ranged between 84 and 237 in each trial) were included in this review (**Table 1**). All were carried out in China. No trial used *F. japonica* as a monotherapy, but all tested herbal remedies containing *F. japonica*. Three RCTs focused on children under 10 years old Li et al., 2014; Bi and Feng, 2015; Chen et al., 2016), and five focused on adults (Yang, 2019; Yang et al., 2019; Liu

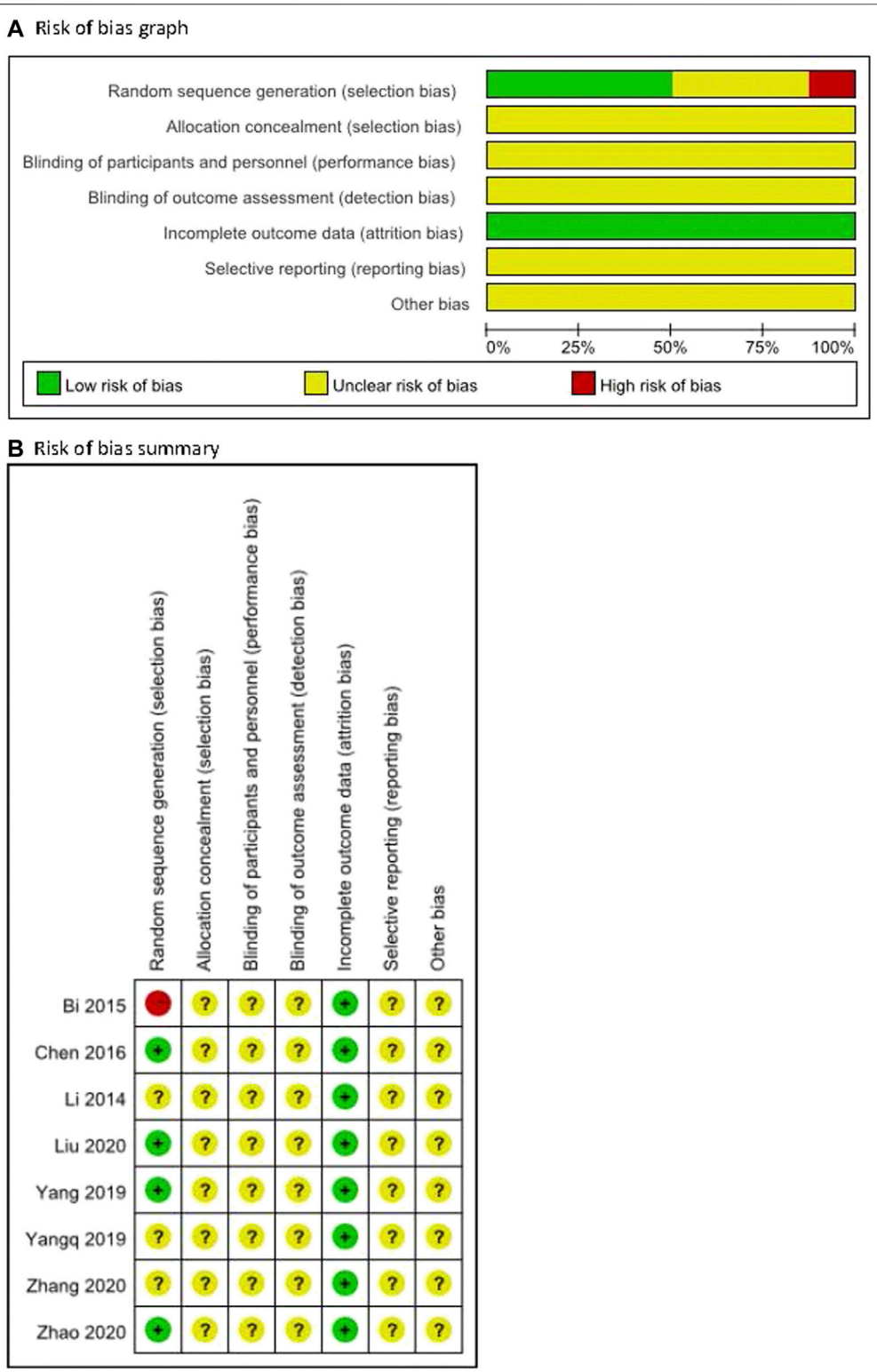

FIGURE 2 | Risk of bias of the including trials.

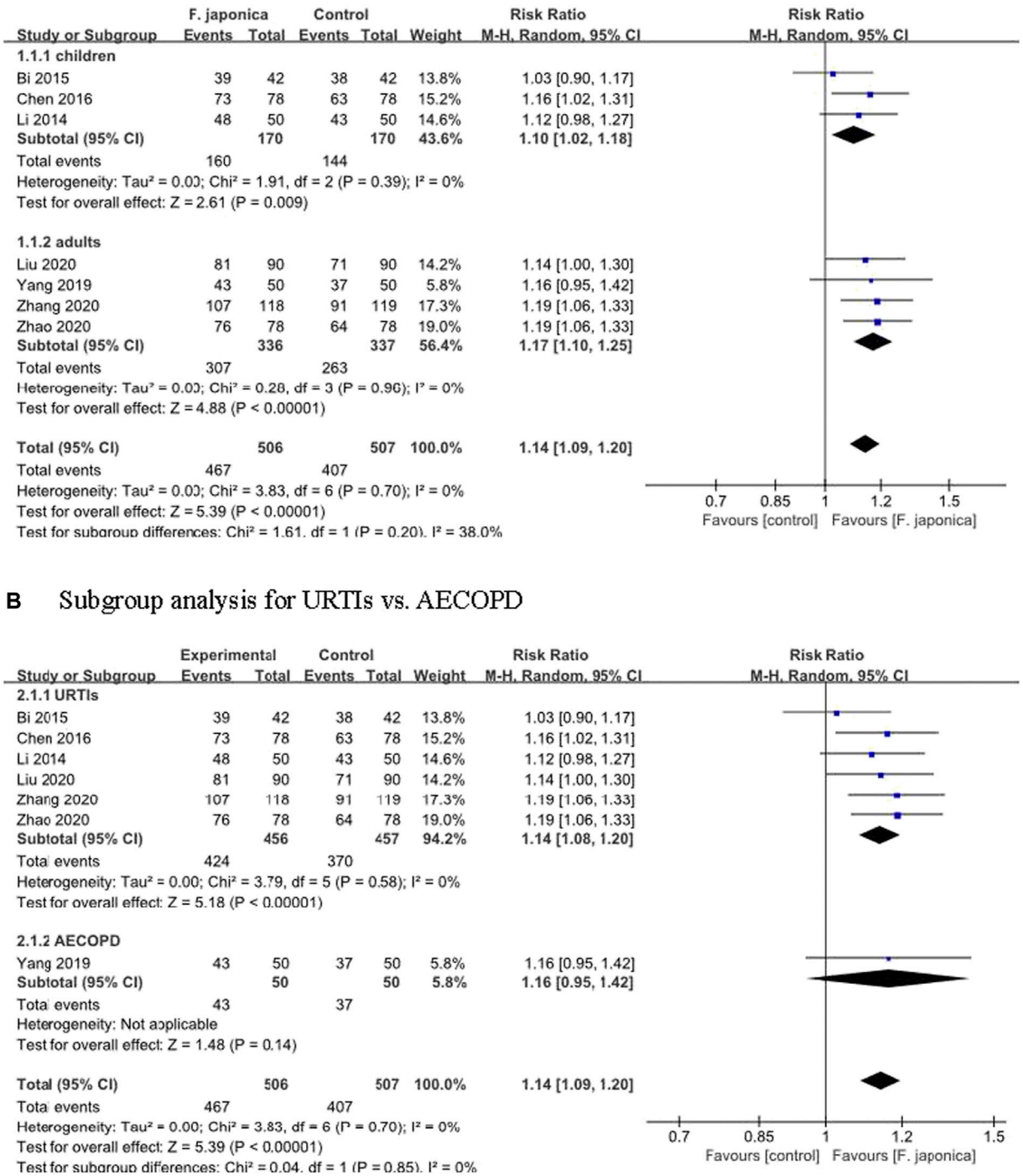

FIGURE 3 | Meta-analysis of symptom improvement rate **(A)**. Subgroup analysis for children vs. adults **(B)**. Subgroup analysis for URTIs vs. AECOPD.

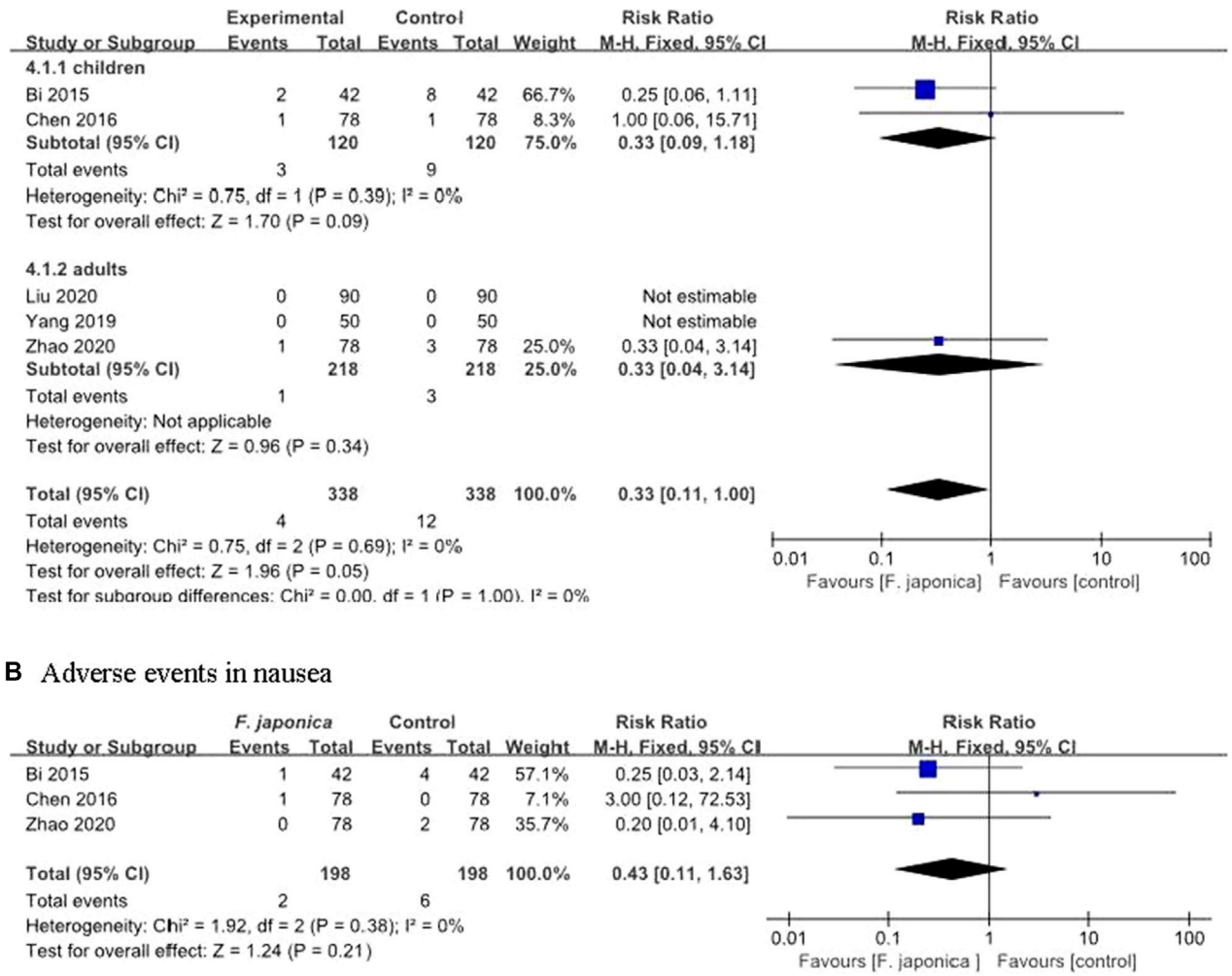

FIGURE 4 | Adverse events from the including trials **(A)**. Total adverse events **(B)**. Adverse events in nausea.

et al., 2020; Zhao and Wang, 2020; Zhang et al., 2021). Three trials (Bi and Feng, 2015; Chen et al., 2016; Yang et al., 2019) reported on treatment of inpatients, while others did not report whether patients were inpatients or outpatients. The treatment duration was from 3 to 45 days, and the most common was 3–7 days. Six trials tested Shufeng Jiedu capsule (Bi and Feng, 2015; Chen et al., 2016; Yang et al., 2019; Liu et al., 2020; Zhao and Wang, 2020; Zhang et al., 2021), one used Tuire liquid (Li et al., 2014), and one used Xuanfei Quyu Tongluo liquid (Yang, 2019). One trial (Zhang et al., 2021) used usual care plus Shufeng Jiedu capsule placebo, and other trials used usual care only in the control groups. Seven RCTs evaluated symptom improvement rate (Bi and Feng, 2015; Chen et al., 2016; Yang et al., 2019; Liu et al., 2020; Zhao and Wang, 2020; Zhang et al., 2021), three assessed the lung injury score (Yang, 2019; Yang et al., 2019; Liu et al., 2020), and three observed fever resolution time (Bi and Feng, 2015; Chen et al., 2016; Zhao and Wang, 2020). Five of the included trials reported adverse events, with two of them (Yang et al., 2019; Liu et al., 2020) reporting no adverse events. One (Bi and Feng, 2015) reported two cases (one nausea and one rash), one (Chen et al., 2016) reported one case of nausea, and one (Zhao and Wang, 2020) reported one case of diarrhoea following ingestion of Shufeng Jiedu capsule. None of the including trials reported the source of funding.

3.2 Risk of Bias

The methodological quality for all included trials was poor (**Figure 2**). For random sequence generation, four trials were judged low risk bias as random number tables or SAS software was utilized (Chen et al., 2016; Yang et al., 2019; Liu et al., 2020; Zhao and Wang, 2020). One was judged to be at high risk of bias because of an inadequate method (the sequence in relation to seeing a doctor) for random sequence generation (Bi and Feng, 2015), while others were not considered to use clear methods. For allocation concealment, the risk of all included trials was unclear because they did not report the information. For

blinding, one trial (Zhang et al., 2021) reported double blinding without detailed information so the risk was judged as unclear, and others did not report the information on blinding of outcome assessment so the risk was judged as unclear for all. All trials reported full information on outcome data, but there was incomplete information on selective reporting and other potential biases such as criteria for disease or participants, ethics for conducting a clinical trial, funding, or conflict of interest.

3.3 Effect Estimation

3.3.1 Symptom Improvement Rate

Symptom improvement rate was defined as (total number of patients—the number of patients with ineffective treatment)/total number of patients × 100%. The clinical effective of this systematic review was defined following symptom improvement rate, and the higher rate meant the better clinical effective. Seven RCTs (Li et al., 2014; Bi and Feng, 2015; Chen et al., 2016; Yang et al., 2019; Liu et al., 2020; Zhao and Wang, 2020; Zhang et al., 2021) evaluated the symptom improvement rate, and the meta-analysis result showed that herbal remedies that included *F. japonica* had a positive effect on symptom improvement rate when compared to usual care or usual care plus herbal remedy placebo (RR 1.14, 95% CI [1.09, 1.20], I^2 = 0%, p < 0.00001, n = 7 trials, 1,013 participants). Similar results were found in the subgroups: for children (RR 1.10, 95% CI [1.02, 1.18], I^2 = 0%, p < 0.00001, n = 3 trials, 340 participants) and for adults (RR 1.17, 95% CI [1.10, 1.25], I^2 = 0%, p < 0.00001, n = 4 trials, 673 participants) (**Figure 3A**). Subgroups analysis for different symptoms: for URTIs, herbal remedies that included *F. japonica* had a positive effect on symptom improvement rate when compared to usual care or usual care plus herbal remedy placebo (RR 1.14, 95% CI [1.08, 1.20], I^2 = 0%, p < 0.00001, n = 6 trials, 913 participants), while for acute exacerbations of chronic obstructive pulmonary disease (AECOPD), there was no significant difference between herbal remedies that included *F. japonica* and usual care (RR 1.16, 95% CI [0.95, 1.42], n = 1 trial, 100 participants) (**Figure 3B**).

3.3.2Fever Resolution Time

Two RCTs (Bi and Feng, 2015; Chen et al., 2016) assessed fever resolution time in children, and one (Zhao and Wang, 2020) in adults. Two of the four (Bi and Feng, 2015; Chen et al., 2016) compared Shufeng Jiedu capsule plus usual care with usual care for paediatric upper RTIs: the duration was 3 days in Bi's study and the results showed Shufeng Jiedu capsule plus usual care shortened the time with fever (MD -0.60 days, 95% CI [-0.77, -0.43]); the duration in Chen's study was 7 days and the results showed similar findings (MD -1.70 days, 95% CI [-2.13, -1.27]). One trial (Zhao and Wang, 2020) which compared usual care plus Shufeng Jiedu capsule with usual care only, found that Shufeng Jiedu capsule shortened fever clearance time for adults (MD -1.39 days, 95% CI [-1.57, -1.21]). Overall significant differences were observed in time without fever.

3.3.3 Murray Lung Injury Score

Three RCTs (Yang et al., 2019; Yang, 2019; Liu et al., 2020) evaluated the lung injury severity based simply on oxygenation criteria (PaO2/FiO2) (by calculating with PaO2/FiO2 when the fresh gas flow was off at the time of the arterial blood gas sampling, a higher score means lower percentage oxygenation and more severe lung injury) (Ntoumenopoulos et al., 2021). Those three trials focused on adults and compared herbal remedies that included *F. japonica* plus usual care with usual care: Shufeng Jiedu capsule could significantly reduce the score in acute RTIs (MD -3.49, 95% CI [-3.96 to -3.03]) (Liu et al., 2020) and in acute exacerbation of chronic obstructive pulmonary disease (AECOPD) (MD -3.49, 95% CI [-3.96 to -3.03]) (Yang et al., 2019); and Xuanfei Quyu Tongluo liquid was less likely to reduce the score in AECOPD than usual care (MD -0.60, 95% CI [-0.98 to -0.22]) (Yang Q 2019).

3.3.4 Adverse Events

Five RCTs (Bi and Feng, 2015; Chen et al., 2016; Yang, 2019; Liu et al., 2020; Zhao and Wang, 2020) assessed the adverse events of herbal remedies that included *F. japonica*. The results showed that there was no significant difference between herbal remedies that included *F. japonica* and usual care or usual care plus herbal remedy placebo (RR 0.33, 95% CI [0.11, 1.00], I^2 = 0%, p = 0.05, n = 5 trials, 676 participants) (**Figure 4A**). One (Bi and Feng, 2015) reported two AEs (one nausea and one rash), one (Chen et al., 2016) reported one case of nausea and one (Zhao and Wang, 2020) reported one case of diarrhoea after taking Shufeng Jiedu capsule. The similar results showed that there was no significant difference between herbal remedies containing *F. japonica* (such as Shufeng Jiedu capsule) and usual care with regard to nausea (RR 0.43, 95% CI [0.11, 1.63], I^2 = 0%, p = 0.21, n = 3 trials, 396 participants) (**Figure 4B**), rash (RR 0.43, 95% CI [0.06, 2.84], I^2 = 0%, p = 0.38, n = 2 trials, 240 participants), and diarrhoea (RR 0.67, 95% CI [0.11, 3.93], I^2 = 0%, p = 0.65, n = 2 trials, 240 participants).

3.4 Evidence Level Based on GRADE

Based on the results from GRADE, we found very low quality evidence on herbal remedies that included *F. japonica* for symptom improvement rate and reducing adverse events. The reasons for down-grading were an inadequate method for random sequence generation in Bi's study, lack of information on inconsistency, and poor publication quality of all the included trials (**Supplementary Appendix S2**).

4 DISCUSSION

The effectiveness and safety of *F. japonica*, which is widely used for infectious diseases such as RTIs, were evaluated in this systematic review. The results show some evidence of benefit with herbal remedies that included *F. japonica* for acute RTIs in adults and children, although the quality of all included trials was rated as poor. There were no studies on *F. japonica* as a monotherapy for acute RTIs.

4.1 Summary of the Main Results

4.1.1 *F. japonica* as a Monotherapy for RTIs

The aim of this systematic review focused on evaluating *F. japonica* for RTIs, but no trials used it as a monotherapy in the present evidence. So we could not draw any conclusions about the

effectiveness of *F. japonica* as a monotherapy for improving symptoms of RTIs.

4.1.2 *F. japonica* in Herbal Remedies for RTIs

After combining the included eight RCTs in this systematic review, the results showed that patients with acute RTIs who took *F. japonica* in a herbal remedy had faster rates of symptom improvement regardless of age. Also, *F. japonica* in a herbal mixture could reduce the duration of fever and the Murray lung injury score when comparing the herbal remedy plus usual care with usual care alone, or comparing the herbal remedy alone with usual care. For adverse events, there were no statistically significant differences between herbal remedies that included *F. japonica* and usual care. In conclusion, *F. japonica* as part of a multi herbal remedy might be an effective and safe option for acute RTIs. Only one included trial compared herbal medicine (Tuire Liquid) to usual care; all the others used herbal medicine plus usual care including antibiotics.

4.2 Previous Studies on *F. japonica* for RTIs

To our best knowledge, there has been no previous meta-analysis of clinical trials of *F. japonica* for acute RTIs. It has always been used in combination with other herbs in clinical practice: in this review, Shufeng Jiedu capsule and Qingfei liquid were the most commonly used remedies that included *F. japonica* for RTIs. Although the mechanism of *F. japonica* for RTIs is still unclear, herbal remedies treating RTIs have multiple possible active compounds, mechanisms of action, targets and pathways (Xu et al., 2020). The findings from our previous systematic review verified that Shufeng Jiedu capsule could be a therapeutic option for shortening the duration of the typical symptoms in acute URTIs without serious adverse events (Zhang et al., 2021); this previous study showed similar results to this systematic review.

4.3 Limitations

This systematic review had some limitations. Although comprehensive searches were carried out on 12 databases, this review may have missed some trials: potentially eligible trials might be missed if the duration of the condition was not reported, therefore patients with acute RTIs could not be identified, or the original trial assessed a complex herbal remedy which did not properly index *F. japonica* despite its inclusion in the remedy. All included RCTs used *F. japonica* in a multi-herbal formula, so we could not evaluate the effect of this herb alone for RTIs. All the included RCTs in this review were carried out in China and published in Chinese, which may lead to language bias and may lack generalizability of the results from this review. All included studies showed positive results for herbal remedies that included *F. japonica* therapy, but there may be publication bias because some negative results may not be published in peer-reviewed literature. Only one (12.5%) of the included trials used a herbal placebo. Finally, all included trials lacked information on their protocol or registered outcomes. Overall the quality of the included studies was rated as low, and so the results of the review should be regarded with caution.

4.4 Implications for Future Research

All the interventions in the included RCTs comprised *F. japonica* as part of a herbal formula, while no trial examined the use of *F. japonica* as a monotherapy to treat acute RTIs. Herbal remedies with *F. japonica* appear to have helpful effects in relief of RTI symptoms. Therefore, we suggest *F. japonica* in a herbal remedy could be useful in treating RTIs. *F. japonica* acts as the sovereign drug in some herbal remedies such as Shufeng Jiedu capsule for RTIs, so we suggest *F. japonica* may possibly have efficacy as a single intervention for RTIs, but more RCTs of better quality need to be conducted. High quality trials with precise methodological design and rigorous reporting on the evaluation of *F. japonica* for acute RTIs should be carried out. Using appropriate methods of random allocation, blinding, estimating the sample size of participants, and developing a detailed study protocol should be promoted for future relevant clinical trials to ensure high-quality. Future studies could compare *F. japonica* with placebo and report the details on blinding for participants, investigators and outcome assessors. Since nearly all the studies were carried out in China, multi-centre or international studies could be conducted. Children are a special population and the safety of children's medication should be critical, so the safety assessment for children should be given attention. The most important thing for future clinical trials is evaluating the effectiveness and safety of using herbal medicine without antibiotics for RTIs, or measuring antibiotic use reduction as a main outcome measure, which could really contribute to reducing the use of antibiotics.

5 CONCLUSION

There is limited but some evidence that *F. japonica* as part of an herbal mixture may be an effective and safe intervention for acute RTIs in clinical practice. Nevertheless, the findings in this review should be interpreted with caution due to the limited methodological quality of the included RCTs. It is better to evaluate the effectiveness and safety of using herbal medicine without antibiotics for acute RTIs in future studies.

DATA AVAILABILITY STATEMENT

The original contributions presented in the study are included in the article/**Supplementary Material** further inquiries can be directed to the corresponding authors.

AUTHORS' CONTRIBUTION

Z-JW and W-JC wrote the original manuscript, and it was revised by JT, WM, MM, LJP, R-YX, and X-YH. All authors contributed

to writing the protocol, and JT facilitated the registration under PROSPERO. Z-JW, R-YX, JY and L-LT addressed the search strategy. Z-JW, ZY and L-LT screened potential studies, extracted and analyzed data, and assessed the risk of bias. All authors gave approval for the final version to be published.

FUNDING

This systematic review was funded by Innovate UK (grant no. 104287-610239) and the National Key Research and Development Project, China (grant no. 2018YFE0102300). Z-JW was supported by Scientific Research Project of Shanxi Provincial Health Commission (No. 2020050), and Youth Basic Research Program of Shanxi Province (No. 20210302124087).

SUPPLEMENTARY MATERIAL

The Supplementary Material for this article can be found online at: https://www.frontiersin.org/articles/10.3389/fphar.2022.787032/full#supplementary-material

REFERENCES

Bi, M. Y., and Feng, W. W. (2015). Clinical Effect of Reduning Injection Combined with Shufeng-Jiedu Capsules on Upper Respiratory Tract Infection in Children. *Pract. J. Card. Cereb. Pneumal Vasc. Dis.* 23 (7), 118–120. doi:10.3969/j.issn.1008-5971.2015.07.036

Bralley, E. E., Greenspan, P., Hargrove, J. L., Wicker, L., and Hartle, D. K. (2008). Topical Anti-inflammatory Activity of *Polygonum Cuspidatum* Extract in the TPA Model of Mouse Ear Inflammation. *J. Inflamm. (Lond)* 5, 1. doi:10.1186/1476-9255-5-1

Bryce, A., Hay, A. D., Lane, I. F., Thornton, H. V., Wootton, M., and Costelloe, C. (2016). Global Prevalence of Antibiotic Resistance in Paediatric Urinary Tract Infections Caused by *Escherichia coli* and Association with Routine Use of Antibiotics in Primary Care: Systematic Review and Meta-Analysis. *BMJ* 352, i939. doi:10.1136/bmj.i939

Chen, H., Su, Y. M., and Luan, J. Q. (2016). Clinical Observation of Shufeng Jiedu Capsules in Treatment Pediatric Acute Upper Respiratory Tract Infection. *World J. Integrated Traditional West. Med.* 11 (5), 716–728. doi:10.13935/j.cnki.sjzx.160531

Chen, X., Wu, T., and Liu, G. (2006). Chinese Medicinal Herbs for Influenza: a Systematic Review. *J. Altern. Complement. Med.* 12 (2), 171–180. doi:10.1089/acm.2006.12.171

Costelloe, C., Metcalfe, C., Lovering, A., Mant, D., and Hay, A. D. (2010). Effect of Antibiotic Prescribing in Primary Care on Antimicrobial Resistance in Individual Patients: Systematic Review and Meta-Analysis. *BMJ* 340, c2096. doi:10.1136/bmj.c2096

Editor Committee of Jiangsu New Medical College (2001). *Encyclopedia of Traditional Chinese Medicine*. Shanghai: Shanghai Science and Technology Press, 1329.

Egger, M., Davey Smith, G., Schneider, M., and Minder, C. (1997). Bias in Meta-Analysis Detected by a Simple, Graphical Test. *BMJ* 315, 629–634. doi:10.1136/bmj.315.7109.629

GBD 2016 Lower Respiratory Infections Collaborators (2018). Estimates of the Global, Regional, and National Morbidity, Mortality, and Aetiologies of Lower Respiratory Infections in 195 Countries, 1990-2016: a Systematic Analysis for the Global Burden of Disease Study 2016. *Lancet Infect. Dis.* 18 (11), 1191–1210. doi:10.1016/S1473-3099(18)30310-4

Goc, A., Niedzwiecki, A., and Rath, M. (2015). *In Vitro* evaluation of Antibacterial Activity of Phytochemicals and Micronutrients against *Borrelia Burgdorferi* and *Borrelia Garinii*. *J. Appl. Microbiol.* 119, 1561–1572. doi:10.1111/jam.12970

Gulliford, M. C., Dregan, A., Moore, M. V., Ashworth, M., Staa, T. V., McCann, G., et al. (2014). Continued High Rates of Antibiotic Prescribing to Adults with Respiratory Tract Infection: Survey of 568 UK General Practices. *BMJ Open* 4, e006245. doi:10.1136/bmjopen-2014-006245

Huang, R. R. (2017). *Effects of Polygonum Cuspidatum on MMP-9 and TIMP-1 of Lung Tissue in Rats with COPD*. Hangzhou: Zhejiang University of Chinese Medicine.

Irwin, R. S., Baumann, M. H., Bolser, D. C., Boulet, L. P., Braman, S. S., Brightling, C. E., et al. (2006). Diagnosis and Management of Cough Executive Summary: ACCP Evidence-Based Clinical Practice Guidelines. *Chest* 129 (1 Suppl. l), 1S–23S. doi:10.1378/chest.129.1_suppl.1S

Jeong, E. T., Jin, E. T., Jin, M. H., Kim, M. S., and Chang, Y. H. (2010). Inhibition of Melanogenesis by Piceid Isolated from *Polygonum Cuspidatum*. *Arch. Pharm. Res.* 33, 1331–1338. doi:10.1007/s12272-010-0906-x

J. P. T. Higgins, J. Thomas, J. Chandler, M. Cumpston, T. Li, M. J. Page, et al. (Editors) (2019). *Cochrane Handbook for Systematic Reviews of Interventions*. 2nd Edition (Chichester, UK: John Wiley & Sons).

Lee, C. C., Chen, Y. T., Chiu, C. C., Liao, W. T., Liu, Y. C., and David Wang, H. M. (2015). Polygonum Cuspidatum Extracts as Bioactive Antioxidaion, Anti-tyrosinase, Immune Stimulation and Anticancer Agents. *J. Biosci. Bioeng.* 119 (4), 464–469. doi:10.1016/j.jbiosc.2014.09.008

Li, D. D. (2019). *Trend Analysis of Antibiotic Use in China's General Hospital during 2012-2016*. Wuhan: Huazhong University of Science and Technology.

Li, Z. W., Zhang, Y., and Gu, G. X. (2014). Tuire Liquid for Pediatric Acute Upper Respiratory Tract Infection with Wind-Heat Syndrome. *J. Pract. Traditional Chin. Med.* 30 (10), 930–931.

Lin, Y. W., Yang, F. J., Chen, C. L., Lee, W. T., and Chen, R. S. (2011). Free Radical Scavenging Activity and Antiproliferative Potential of *Polygonum Cuspidatum* Root Extracts. *J. Nat. Med.* 64, 146–152. doi:10.1007/s11418-009-0387-8

Liu, Z. Q., Wang, G. M., Pan, W. W., and Jiang, X. C. (2020). Shufeng Jiedu Capsule for Viral Upper Respiratory Tract Infection. *JETCM* 29 (5), 898–900. doi:10.3969/j.issn.1004-745X.2020.05.043

Manna, S. K., Mukhopadhyay, A., and Aggarwal, B. B. (2000). Resveratrol Suppresses TNF-Induced Activation of Nuclear Transcription Factors NF-Kappa B, Activator Protein-1, and Apoptosis: Potential Role of Reactive Oxygen Intermediates and Lipid Peroxidation. *J. Immunol.* 164, 6509–6519. doi:10.4049/jimmunol.164.12.6509

Moher, D., Shamseer, L., Clarke, M., Ghersi, D., Liberati, A., Petticrew, M., et al. (2015). Preferred Reporting Items for Systematic Review and Meta-Analysis Protocols (PRISMA-P) 2015 Statement. *Syst. Rev.* 4, 1. doi:10.1186/2046-4053-4-1

Ntoumenopoulos, G., Buscher, H., and Scott, S. (2021). Lung Ultrasound Score as an Indicator of Dynamic Lung Compliance during Veno-Venous Extra-corporeal Membrane Oxygenation. *Int. J. Artif. Organs* 44 (3), 194–198. doi:10.1177/0391398820948870

Shek, L. P., and Lee, B. W. (2003). Epidemiology and Seasonality of Respiratory Tract Virus Infections in the Tropics. *Paediatr. Respir. Rev.* 4 (2), 105–111. doi:10.1016/s1526-0542(03)00024-1

Wachtel-Galor, S., and Benzie, I. F. F. (2011). "Herbal Medicine: an Introduction to its History, Usage, Regulation, Current Trends, and Research Needs," in *Herbal Medicine: Biomolecular and Clinical Aspects* (Boca Raton, USA: CRC Press).

Weintraub, B. (2015). Upper Respiratory Tract Infections. *Pediatr. Rev.* 36 (12), 554–556. doi:10.1542/pir.36-12-554

Wu, T., Yang, X., Zeng, X., and Poole, P. (2008). Traditional Chinese Medicine in the Treatment of Acute Respiratory Tract Infections. *Respir. Med.* 102 (8), 1093–1098. doi:10.1016/j.rmed.2008.03.015

Xu, H., Li, P., Qi, X., Mo, J., Huang, Y., Fang, C., et al. (2020). Mechanism of Shufeng Jiedu Capsule in the Treatment of Novel Coronavirus Pneumonia Based on Network Pharmacology and Molecular Docking. *J. Chin. Med. Mater* 43 (08), 2053–2061. doi:10.13863/j.issn1001-4454.2020.08.049

Yan, J., Wang, Y., Wu, H., Sun, Z., Tan, S., Wang, W., et al. (2019). Development of a Method for Simultaneous Determination of Two Stilbenes and Four Anthraquinones from *Polygonum Cuspidatum* by RP-HPLC. *J. Aoac Int.* 102 (1), 69–74. doi:10.5740/jaoacint.18-0097

Yang, Q. (2019). Traditional Chinese Medicine of Xuanfei Quyu Tonglu for Acute Exacerbation of Chronic Obstructive Pulmonary Disease the Influence of Pulmonary Function and Blood Gas index. *J. Harbin Med.* 39 (5), 487–488.

Yang, T. W., Li, M. H., Ren, C. F., Huang, Q. Y., Zhao, Y. L., He, J., et al. (2019). Effect and Safety of Shufeng Jiedu Capsule for AECOPD. *JETCM* 28 (10), 1824–1827. doi:10.3969/j.issn.1004-745X.2019.10.035

Zahedi, H. S., Jazayeri, S., Ghiasvand, R., Djalali, M., and Eshraghian, M. R. (2013). Effects of Polygonum Cuspidatum Containing Resveratrol on Inflammation in Male Professional Basketball Players. *Int. J. Prev. Med.* 4, S1–S4.

Zhang, Y. Y., Xia, R. Y., Liang, S. B., Hu, X. Y., Dai, M. Y., Li, Y. L., et al. (2021). Chinese Patent Herbal Medicine (Shufeng Jiedu Capsule) for Acute Upper Respiratory Tract Infections: a Systematic Review and Meta-Analysis. *Integr. Med. Res.* 10, 100726. doi:10.1016/j.imr.2021.100726

Zhao, L. B., and Wang, Z. B. (2020). Clinical Observation of Shufeng Jiedu Capsule in Treating Acute Upper Respiratory Tract Infection (Wind-heat Syndrome). *JETCM* 29 (7), 1278–1279. doi:10.3969/j.issn.1004-745X.2020.07.044

Conflict of Interest: The authors declare that the research was conducted in the absence of any commercial or financial relationships that could be construed as a potential conflict of interest.

frontiers in Pharmacology

REVIEW
published: 28 February 2022
doi: 10.3389/fphar.2022.815742

Phytochemistry in the Ethnopharmacology of North and Central America

John Thor Arnason[1]*, *Cory S. Harris*[1] and *José A. Guerrero-Analco*[2]

[1]Biology Department, University of Ottawa, Ottawa, ON, Canada, [2]Red de Estudios Moleculares Avanzados, Instituto de Ecología A.C., Xalapa, Mexico

Traditionally the role of phytochemistry in the ethnopharmacology of North and Central America has been to characterize plant materials so that they can be produced reproducibly for commercial use or to identify active principles in unstudied traditional medicines for drug discovery. With new decolonial objectives coming from Indigenous communities, emphasis has shifted to evaluating the safety and efficacy of traditional medicines and preparations for community use. With new techniques and technologies available, scientific focus has shifted from individual bioactives to more rapid and comprehensive chemical characterizations and polypharmacy of traditional medicines. Untargeted metabolomics and associated statistical treatments have greatly expanded identification of components, improved species and cultivar identification and provided means for identifying multiple activity biomarkers, via chemometric and biochemometric analysis. New integrated techniques are available for identifying multiple active principles and synergists. The recent explosion of information is not without problems that need to be addressed including many unconfirmed tentative identifications of phytochemicals, lack of quantitative testing, superficial chemical activity testing and continuing need for dereplication.

Keywords: phytochemistry, medicinal plants, chemometrics, activity biomarkers, dereplication, untargeted metabolomics

OPEN ACCESS

Edited by:
Javier Echeverria,
University of Santiago, Chile

Reviewed by:
Marinella De Leo,
University of Pisa, Italy
Marco Leonti,
University of Cagliari, Italy

***Correspondence:**
John Thor Arnason
john.arnason@uotttawa.ca

Specialty section:
This article was submitted to Ethnopharmacology, a section of the journal Frontiers in Pharmacology

Received: *15 November 2021*
Accepted: *31 January 2022*
Published: *28 February 2022*

Citation:
Arnason JT, Harris CS and Guerrero-Analco JA (2022) Phytochemistry in the Ethnopharmacology of North and Central America. Front. Pharmacol. 13:815742. doi: 10.3389/fphar.2022.815742

INTRODUCTION

There is no shortage of medicinal and other Indigenous uses for native plants in North America and Central America, known to Haudenosaunee and Anishinaabe indigenous peoples as Turtle Island, and the place of creation (Robinson, 2018). For example, Moerman et al., 2018) records 4029 taxa for ethnobotanically used plants in North America. For Central America, the Mesoamerican Medicinal Plant Database includes a total of 2188 plant taxa (Geck et al., 2020) but more regionally focussed reviews also reveal the traditional use of many species in some individual cultures, such as 350 by the Q'eqchi' Maya (Arnason et al., 2022). Phytochemical and ethnopharmacological studies have only examined a small percentage of these plants and uses. Of these, the pharmacopeial or commercial medicinal plants are the best studied, but many Indigenous traditional medicines are now emerging as the focus of new research (Hall et al., 2022; Mata et al., 2022).

For commercial or pharmacopeial medicinal plants, characterization of the preparation is a fundamental step. Phytochemistry is essential to this so that any published experiment can be replicated or extended by others, and so that pharmacologically and clinically tested material can be shown to be consistent or comparable to preparations used in practice. Unlike single entity drugs,

traditional medicines contain multiple active principles that have additive, antagonistic and synergistic effects, so that full characterization is of value but may present a difficult, expensive and time-consuming challenge for scientists. Many excellent ethnopharmacology studies have been rejected at publication because the authors could not provide adequate information on chemical characterization.

For the less well studied non-commercial Indigenous medicinal plants and herbal medicines of the Americas, the challenge is identifying bioactive molecules in the botanical drug, often with a goal of making new compound discoveries or for the purpose of validating and providing respect for traditional knowledge. Both the scientific and cultural context of this field has evolved rapidly in the last 15 years.

The goal of this insight review is to provide a discussion of issues and advances in phytochemistry of medicinal plants of the Americas taken from our experience as well as from selected examples of high impact peer reviewed papers in the literature. For example, an important area of discussion is decolonizing research in ethnopharmacology, while technical advances in metabolomics and biochemometrics have revolutionized the field. These insights are the opinions and reviews of the authors only. They are directed to early career scientists in the field or pharmacologists without phytochemical training rather than directed to experienced phytochemists. The insights are intended to help them better understand modern phytochemical requirements in publications as well as advances in phytochemical methods which improve quality of ethnopharmacology studies.

METHODS

This article is not a comprehensive review and only a few representative examples of studies were selected from articles found using the databases, PubMed or Web of Science (Clarivate™) from January 2005-October 2021 using keywords including phytochemical methods, targeted and untargeted analysis, chemometrics, biochemometrics, phytochemical metabolomics, active principle identification, and dereplication. Technical details are limited, and readers are directed to the referenced papers for detailed information about equipment, proprietary software and statistical packages, etc. Two major areas covered are (1) pharmacopeial plant preparations and commercial medicinal plants and (2) new phytochemical studies of traditional plant medicines and plant drug discovery. While these areas could apply to medicinal plants from any part of the world, our examples come from the Americas and provide current examples from here.

PHARMACOPEIAL PLANT PREPARATIONS AND COMMERCIAL MEDICINAL PLANTS

For defined pharmacopeial plant preparations and commercial medicinal plants, a primary objective is to characterize phytochemicals for identity and quality assurance.

Identity Confirmation, Substitution and Adulteration in Commercial Medicinal Plants

Identity can be difficult to establish since raw plant products are often received by finished product formulators as internationally shipped dried powders from independent supply houses. Adulteration and substitution of species are common issues. Since plant morphological feature are absent, industry and regulators have traditionally confirmed identity by phytochemical analysis targeting one or a few species chemical markers. In industry, identity is still commonly achieved by liquid chromatography systems coupled to diode array and ultraviolet-light detector (LC-DAD, LC-UV), or mass spectrometry (LC-MS) detector using co-analysis with isolated standards of the marker compounds purified to >95%. For example alkylamides identified originally by Bauer et al. (1988) as well as well-known caffeic acid derivatives are typically used in pharmacopeial monographs as phytochemical evidence of identity of *Echinacea purpurea* L. Moench (Asteraceae) (Upton 2004). Examples of chromatograms used for distinguishing *E. purpurea* and *E. angustifolia* DC are shown in **Figure 1** (Liu et al., 2021a). High performance thin layer chromatography (HPTLC) methods are also accepted (Upton 2004; Gafner et al., 2021) but older colorimetric tests such as total content assays of phenolics, tannins, saponins, flavonoids, alkaloids are no longer accepted in this journal or by most regulators.

Identity is very important because substitutions and adulterations are often encountered that can be dangerous to consumers. A well-known case of substitution involved North American Black Cohosh [*Actea racemosa* L. (Ranunculaceae)] products used for symptoms associated with menopause. Mahady et al. (2008) identified thirty unduplicated reports concerning liver damage with the use of black cohosh products. All the reports of liver damage were assigned possible causality, and none were probable or certain causality. One high profile case of liver damage in Canada received analysis with respect to authenticity of the product because there were few confounding factors (the patient had no underlying conditions, was taking no other drugs and consumed just one identified commercial product sold as black cohosh). Identity and registration of the commercial product was originally established by the presence of two markers, actein and 23-epi-26-deoxyactein. However, these compounds are also found in several other Asian species in the genus. More rigorous analysis of the product for several chemical markers led to the discovery of the presence of cimifugin, an antipruritic compound, present in an Asian species but not black cohosh from North America. Because of this case, the analytical requirements for registration in Canada have been updated to include cimiracemide C as an *A. racemosa* marker and to exclude materials containing cimifugin and other Asian species markers to ensure the plant material has not been substituted or adulterated (Health Canda, 2018).

There have been several recent incidents of adulterations in North America due to herbal supply issues in the Covid 19 pandemic. One example is great interest in antiviral botanical extracts derived from elderberry [*Sambucus nigra* L. and *S.*

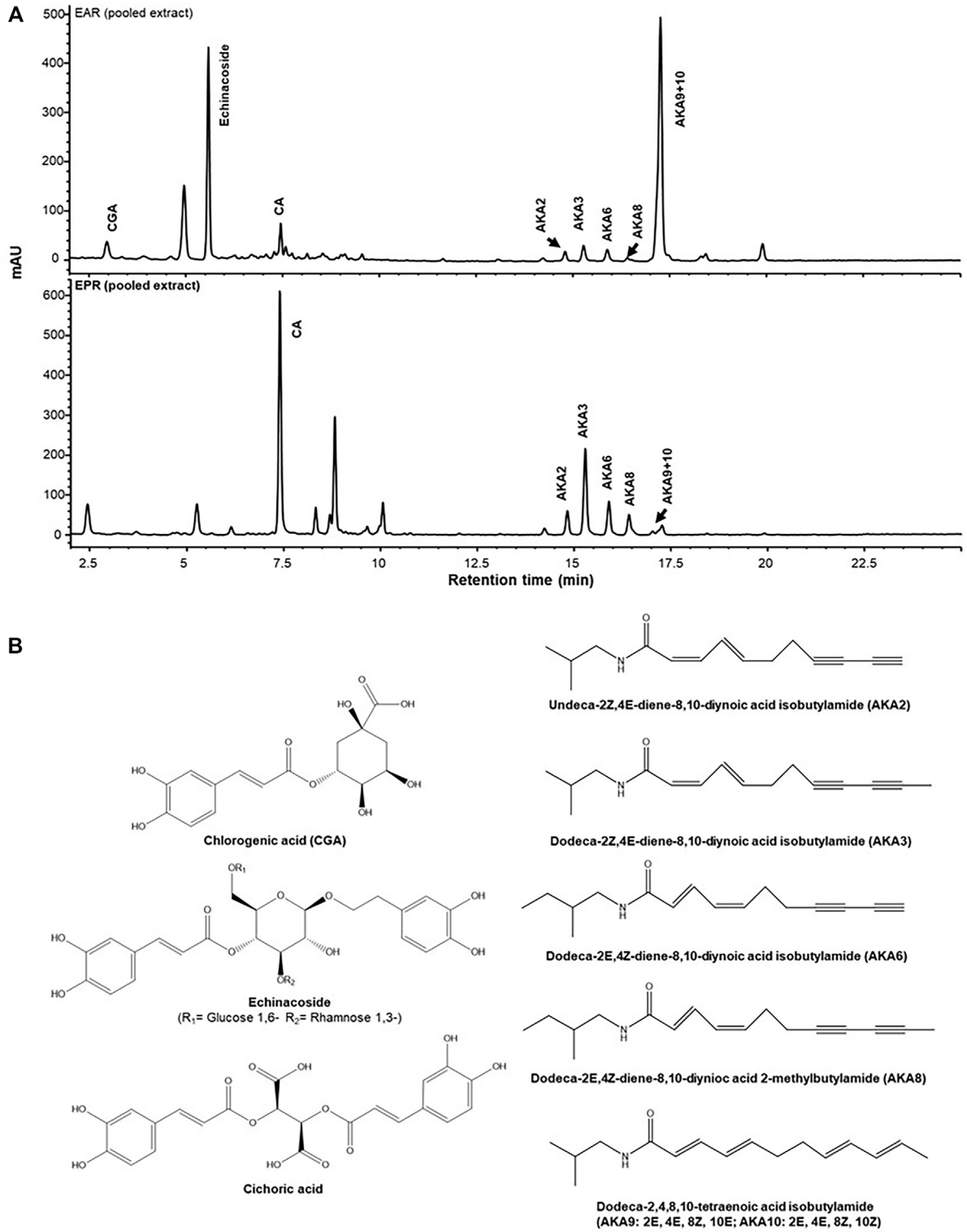

FIGURE 1 | Targeted identity analysis of *E. purpurea* (EPR) and *E angustifolia* (EAR) roots by HPLC-DAD-MS showing distinct phytochemical profiles for each species **(A)**. Quantification of these markers, **(B)** with a validated method provides quality assurance for pharmacological studies. Reproduced from Liu R., Salas N.C., Li W., Wang L., Arnason J.T., Harris C.S. Interactions of *Echinacea* spp. root extracts and alkylamides with the endocannabinoid system and peripheral inflammatory pain. *Frontiers in pharmacology.* 2021 12:776. Reproduced under the terms of a CC BY 4.0 license https://creativecommons.org/licenses/by/4.0/.

canadensis L. (Viburnaceae)] which saw great demand and short supply, leading to appearance of adulterated products (Gafner et al., 2021). Industry -independent groups such as the American Botanical Council's Botanical Adulterants Prevention Program (PAP) published in the trade magazine HerbalGram (https://www.herbalgram.org) established that adulterated products were common in elderberry products marketed in North America (58 products out of 532 analysed by collaboration independent labs by HPLC-DAD or UV-Vis, or HPTLC) and often contained black rice extract which contains the elderberry marker cyanidin-3-*O*-glucoside. The presence of peonidine-3-*O*-glucoside and other markers are indicative of black rice extract. Therefore robust analytical methods are needed to prevent substitution and identity issues in a wide variety of problem commercial products such as methods provided by United States Pharmacopeia (USP).

Metabolomics and Chemometrics

Untargeted metabolomics and chemometrics have recently accelerated the authentication of identity and identification of adulterants by high-throughput profiling (Ravaglia et al., 2019; Wallace et al., 2020). Metabolomic methods are becoming more accessible and overcome many of the limitations associated with genomic- and simple biomarker-based techniques (Simmler et al., 2018).

The availability of metabolomics platforms and methods allow rapid annotation of hundreds of small molecules by the comparison of their spectrometric features (m/z values and retention times) in spectral databases. This provides a technicolour view of plant phytochemistry where we once saw only the black and white version of extracts. In the majority of studies, the metabolome is identified by LC-MS or LC-MS/MS methods, where compounds in the injected extract are first separated by HPLC or UPLC systems and then detected either using a time of flight (TOF) or Orbitrap MS detector. Compounds are annotated from their mass spectrometry m/z ion and chromatography retention time data. They can be identified with different levels of accuracy using in house and online data deposited in spectral libraries. This analysis attempts to identify any small molecule present, it is therefore called untargeted. Each identified compound or annotated m/z signal is a chemotaxonomic character and a large number of them greatly improves identification of species, or difficult to separate varieties and different type of extracts.

Chemometrics (Statistical methods are applied to chemical analysis) can classify plant extracts into different taxa (or other categories such as type of extract) through uni or multivariate statistical methods like principal components analysis (PCA). Once a series of known extracts is analysed and classified, an unknown can be analysed and classified based on its metabolome grouping (or exclusion). Further analysis such as orthogonal partial least square discriminant analysis (OPLS-DA) or hierarchical clustering (heat maps) are very powerful statistical methods which can identify significantly different phytochemical markers in contrasted extracts subjected to metabolomic analysis.

Brown et al. (2012a and b) applied UPLC-MS-TOF chemometrics to identity three species of cranberry and in a second study five cultivars of commercial North American cranberry cultivars. Partial least squares discriminant analysis (PLS-DA) was applied to the metabolomics data and led to the separation of each species. In the cultivar study, most signals were detected in all extracts but a few were identified as associated with specific cultivars. Whereas PCA of the cultivar phytochemistry did not lead to the full separation of cultivars, PLS-DA exhibited significant clustering of extracts by cultivar, indicating that the method can separate and identify cultivars. Recently Mudge et al. (2019) have used chemometric methods to study cannabinoid and terpene chemotaxonomy in cannabis.

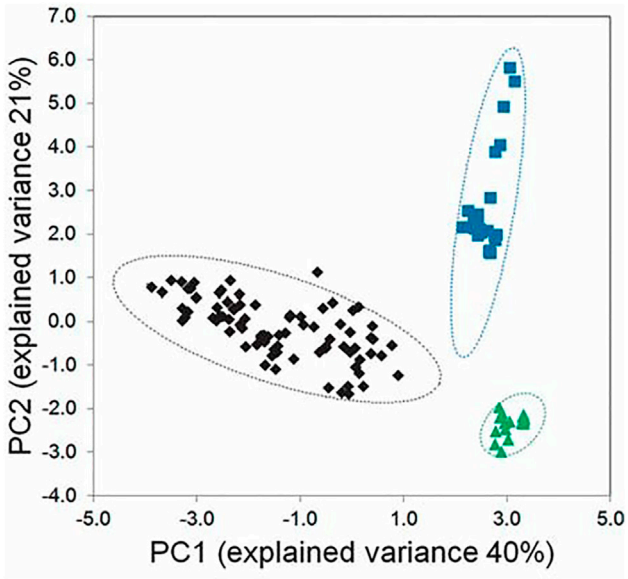

FIGURE 2 | Chemometric analysis of Vaccinium species using NMR metabolomic data. Scores plot for three species, *Vaccinium angustifolium* (black diamonds), *V. ovalifolium* (blue squares), and *V. macrocarpon* (green triangles). Hotelling ellipses, showing the region of the 95% confidence limit, are shown for each group by dashed lines of the matching color. Note that spectra for each species occupy a distinct region, with no overlap. Reproduced (**Figure 2**) with permission from Markus, M. A., Ferrier, J., Luchsinger, S. M., Yuk, J., Cuerrier, A., Balick, M. J., & Colson, K. L (2014). Distinguishing Vaccinium species by chemical fingerprinting based on NMR spectra, validated with spectra collected in different laboratories. Planta medica, 80(08/09), 732-739.

An alternative method of chemical fingerprinting is based on high-resolution nuclear magnetic resonance (NMR) spectroscopy. For example, Markus et al. (2014) studied NMR spectra of several *Vaccinium* spp. (Ericaceae). Instead of identifying specific compounds, the NMR spectra from submitted samples were binned (divided into many different subspectra) that were used as taxonomic characters for statistical analysis. Using PCA, leaf extracts of the three species were resolved in the scores plot (**Figure 2**) and analysis of variance showed that the three species differed significantly, establishing that the species can be distinguished by NMR alone. Because NMR spectra do not vary greatly from instrument to instrument when magnet size is basically the same (i.e. 500 or 600 MHz), and this equipment is available at many institutions, the method was validated with spectra collected in six different institutions. Using blinded

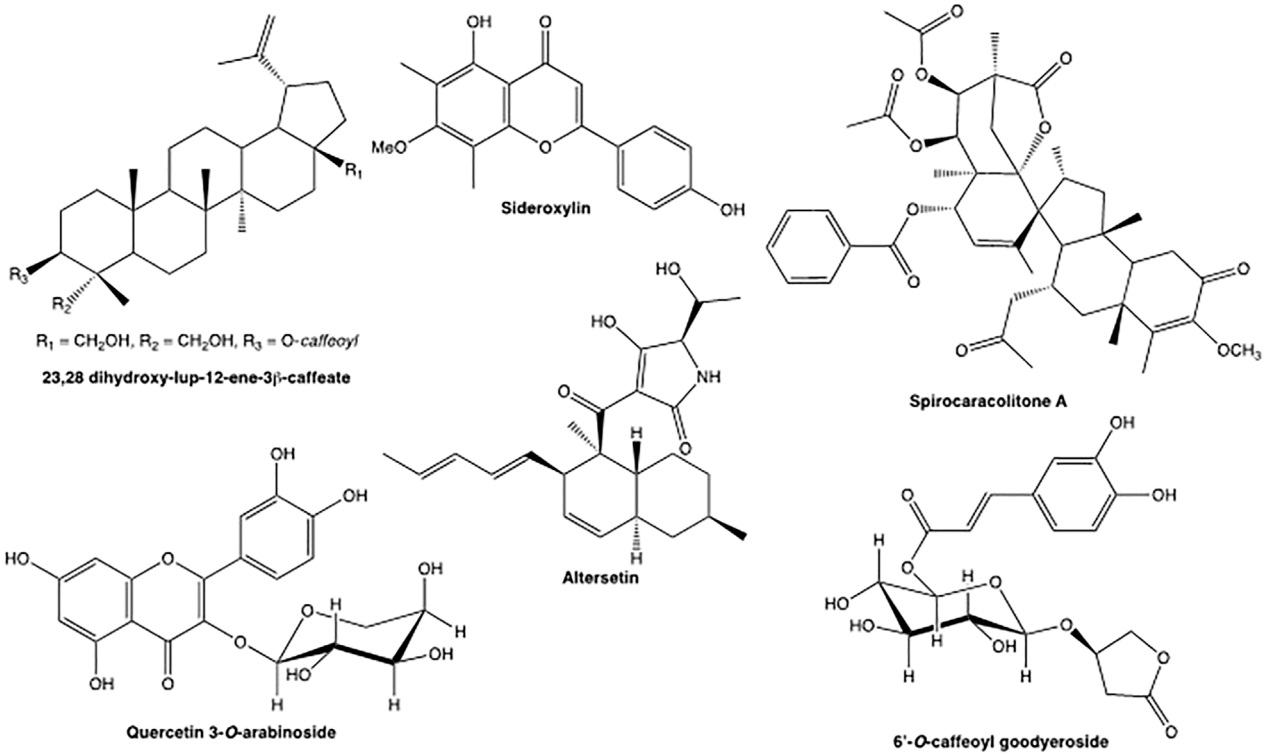

FIGURE 3 | New bioactive compounds from plants and fungi.

samples from the reference set, *V. ovalifolium Sm.* and *V. macrocarpon* Aiton were classified correctly 100% of the time and *V. angustifolium* Aiton 94% of the time. These NMR methods have high resolving power and have already been adapted for a large number of blueberry species (Ferrier, 2014) and for industrial use in the rapid identity control of fruit juices of different geographic origin.

Plant powders can also be identified by near infrared (IR) reflectance spectroscopy, since this region of the electromagnetic spectrum also provides good structural information (Türker-Kaya and Huck., 2017). This method is inexpensive and generally has good reliability for identification of different common medicinal plants.

Comparing methods, neither the NMR metabolomic nor IR methods provide the rapid identification of marker compounds afforded by LC/GC-MS methods. NMR metabolomics is somewhat limited by low sensitivity and (unresolvable) overlapping signals compared to LC-MS. LC-MS methods, specifically those with high resolution analyzers, rapidly lead to separation and identification of known compounds. Major obstacles, however, include the expensive purchase and operating costs, the need for experienced operators, and the lack of robust spectral libraries to support accurate chemical identification. Nonetheless, researchers and young scientists with early access to this equipment enthusiastically attempted to identify many new compound occurrences in plants with LC-MS techniques. Because of positional ambiguity in MS identification, a former editor of Phytochemistry (journal) was concerned that the early metabolomic papers contributed many tentative structural assignments to the published scientific literature that were incorrect. Improved procedures in the last decade and use of MS/MS and TOF data (accurate mass values) with more rigorous online spectral libraries have made identification of phytochemicals much more reliable. On the other hand, early untargeted metabolomic studies led to important new discoveries such as the identification of the animal hormone melatonin in plants, which has led to a new field in plant physiology (Murch et al., 1997).

Quality Requires Quantitative Validation Studies

While profiling of metabolites for identity may be sufficient for early mechanistic studies of plant drugs, advanced ethnopharmacological studies in animal models of clinical settings cannot be compared or repeated without quantitative assessment of the main active principle(s). There is no shortcut to quantitation which requires prior quantitative validation studies that use highly purified phytochemical standards and strict adherence to International Harmonization Standard (IHS) validation methods, usually by LC-DAD-UV or LC-MS methods. These include characterizing the method in terms of precision, accuracy,

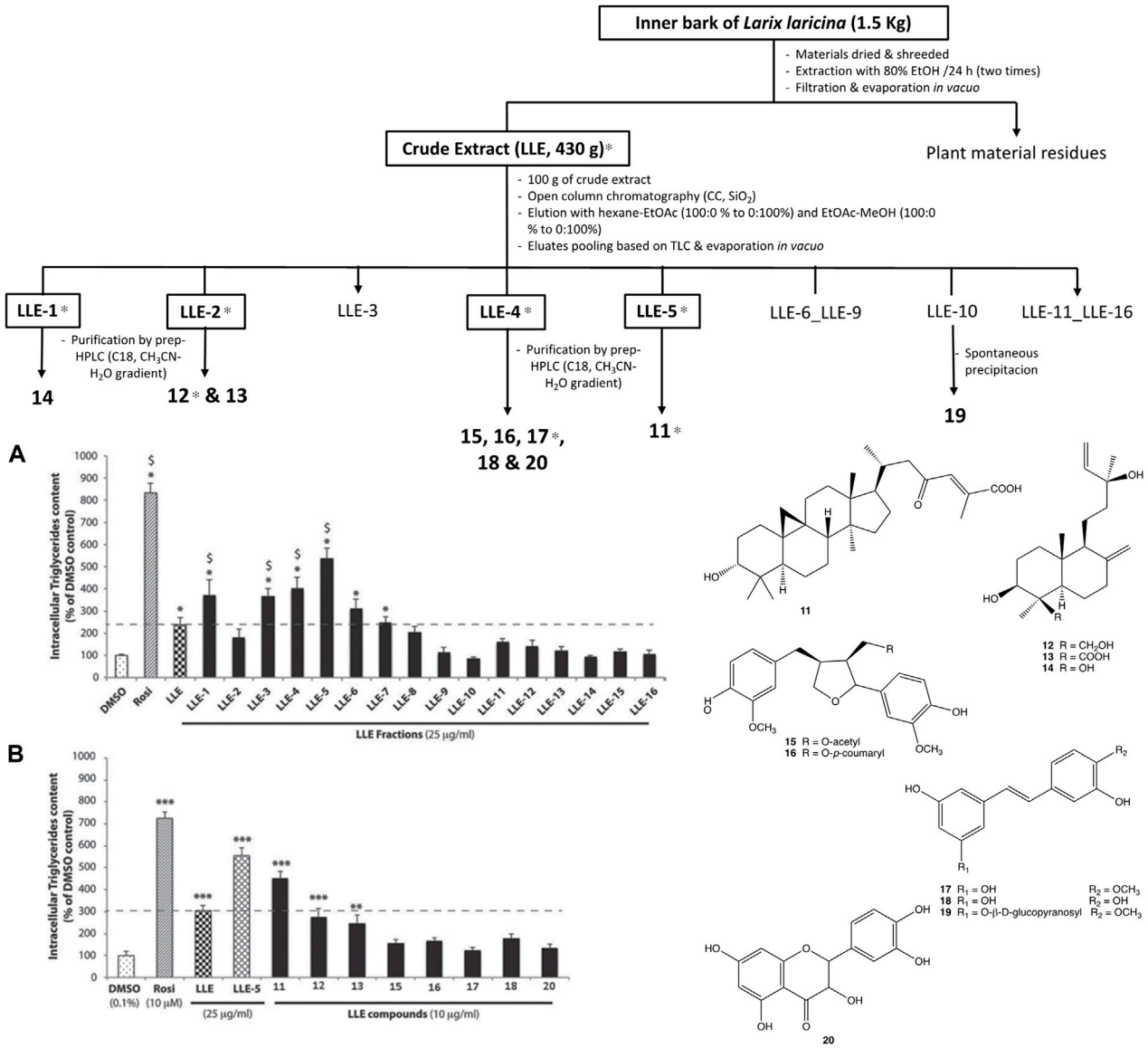

FIGURE 4 | Classic bioassay guided fractionation of *Larix larcina* (Tamarack or larch) in an adipogenic activity assay leading to identification of a novel cycloartane triterpenoid named Awashishic acid (23-oxo-3 -hydroxycycloart-24-en-26-oic acid, 11). Figure adapted with permission to use data from Shang et al., 2012. Adipogenic constituents from the bark of Larix laricina du roi (K. koch; Pinaceae), an important medicinal plant used traditionally by the Cree of eeyou istchee (Quebec, Canada) for the treatment of type 2 diabetes symptoms. J. Ethnopharmacol.141:1051-7.

linearity, interlab and intra-/inter-day variability, Limit Of Detection, Limit Of Quantification, etc. Recovery of standards from spiked samples are recommended to determine how accurately the method captures and quantifies targeted compounds. A recent example (Mamallapalli and Raju, 2021) is a validated method for kava (*Piper methisticum* G. Forst. (Piperaceae)), in which they developed a UPLC MS/MS-based analytical method for the expanded quantification of six major kavalactones (kavain, dihydrokavain, methysticin, dihydromethysticin, yangonin and desmethoxyyangonin) and two new flavokavains. They used labelled isotope standards which improved recovery estimates. Many validated methods for pharmacopeial products are published or available from USP and the Association of Official Agricultural Chemists (AOAC).

Plant Metabolomics Meets Network Pharmacology

Network pharmacology is a systems approach to pharmacology that combines systems biology, network analysis and bioinformatics, and it is characterized as "the next paradigm" in drug discovery (Hopkins, 2008). Originally it was conceived as a study of single entity drugs activating pharmacological receptor(s) leading to a network of interacting downstream

cellular events. The array of secondary metabolites identified in metabolomic studies of medicinal plants is now acknowledged to activate several signaling pathways that can lead to multiple independent and synergistic or interacting effects. This field has recently been explored in detail and is found in the special issue of Frontiers in Pharmacology: ethnopharmacology, entitled Network Pharmacology and Traditional Medicine (Lai et al., 2020). In this issue, many interesting examples of the application of network pharmacology are found in the complex formulae of Traditional Chinese medicines which provides a new strategy and powerful tool to uncover the biological basis underlying herbal formula.

NEW PHYTOCHEMICAL STUDIES OF TRADITIONAL PLANT MEDICINES AND PLANT DRUG DISCOVERY

At the turn of the millennium, major research groups were funded by US drug discovery grants for work on traditional indigenous medicines in North and South America. These programs combined drug companies, researchers and Indigenous people to find new single entity drugs for development from traditional medicines. Some of these programs were controversial and criticized by Indigenous groups as commercial appropriation of Indigenous knowledge. In response, ethical guidelines were developed internationally which led to the Nagoya protocol, an amendment to the Convention on Biological Diversity (co-chaired by Canada in 2014) which provided a framework for access to biodiversity and benefit sharing with Indigenous people. Unfortunately, the co-chair country, Canada, did not consult with Canadian Indigenous First Nations in Canada on a timely basis and did not receive their approval of the treaty. The protocol has been rejected by a consortium of First Nations (Grand Council of the Crees, 2012) as both a colonial process and document that violates their sovereignty and treaty rights. Fortunately, efforts to reset the relationship with Indigenous people are underway, in which the voices and leadership of First Nations in research are being heard (Styawat/Joseph, 2022).

As explained to our team by Cree and Maya indigenous healers with whom we have worked closely for decades, they do not wish to commercialize their plants, as they believe the healing properties of plants are a sacred gift of the creator. The priority of healers is to personally treat patients and not the development of commercial medicines or drugs. However, they value modern scientific studies, when they can provide information on the safety and efficacy of traditional medicines. They believe that this scientific translation of traditional knowledge is key to recognition and respect from government regulators and others. To achieve this goal, the identification of active principles and assessment of pharmacological effects (efficacy and safety) is appropriate.

Alternatively, some Indigenous groups including a few in Canada have accepted commercialization, if the process can be done sustainably and fairly. In the field of plant drug discovery many groups internationally believe that if the Nagoya protocols are followed and benefit sharing agreements are in place with Indigenous groups, this represents current best practice. Efforts to improve trust and partnership for research on traditional medicines are now being developed, for example in Guatemala (Berger-Gonzalez et al., 2022). In this case, plant-based traditional medicines may be studied to find new active principles, which may lead to standardized and tested medicinal plant drugs or become active lead compounds for chemical analoging to improve efficacy, availability and safety useful for the treatment of well-known diseases as well as emergent and culture-bound conditions.

Classic Bioassay Guided Isolation

The classic method to determine active principles in medicinal plants is bioactivity guided isolation (BGI). An example of classic BGI for ethnopharmacology is the isolation of antidiabetic compounds from Cree traditional medicines. Showy mountain ash bark (*Sorbus decora* (Sarg.) C.K. Scneid. (Rosaceae) is used by traditional Eyou Istchee Cree healers in the James Bay district of Northern Quebec for symptoms of diabetes. The extracts of bark were studied in a glucose uptake assay with muscle cells and found to have activity that compared favorably with metformin. The plant extract was successively fractionated by column chromatography and fractions tested to find activity (Guerrero-Analco et al., 2010), before a new round of purification was undertaken, and eventually pure compounds isolated by preparative HPLC and identified by spectroscopic methods. A new triterpenoid, 23,28-dihydroxylupan-20(29)-ene-3β-caffeate was identified with exceptional activity for stimulation of glucose uptake in muscle cells (**Figure 3**).

In a related study (Shang et al., 2012), the adipogenic active principles of the bark of Tamarack trees, *Larix larcina* (Du Roi) K. Koch. (Pinaceae) were isolated by a similar approach (BGI). The bark is used for the treatment of diabetic sores, frequent urination, and infected wounds by Cree healers. It was found to significantly enhance adipogenesis in differentiating 3T3-L1 adipocytes in a screening study using *in vitro* cell-based bioassays. *L. laricina* extract decreases hyperglycemia and insulin resistance *in vivo*, using the diet induced obese mouse model. The cell line was used to carry out a BGF of an 80% EtOH extract from the inner bark of Tamarack. A total of 16 primary fractions were separated on a normal phase silica gel column (SiO_2) and the most active one had two thirds of the activity of the reference drug rosiglitazone. Ten compounds were further isolated by preparative HPLC and the most active one was a novel cycloartane triterpenoid, 23-oxo-3α-hydroxycycloart-24-en-26-oic acid, which strongly potentiates adipogenesis with an EC_{50} of 7.7 μM (**Figure 4**). This compound was name awashishic acid to honour the contributions of a Cree elder and healer, Sam Awashish.

The action of medicinal plants is often attributed to multiple active principles and interacting synergists. Junio et al. (2011) developed a bioassay guided procedure to identify synergists of the antimicrobial alkaloids in golden seal (*Hydrastis canadensis* L. (Ranunculaceae)). Golden seal was fractionated by column chromatography and the fractions were tested in a synergy assay for antimicrobial activity against *S. aureus*. The assay combined the active principle berberine with the fraction tested over a concentration range of 5–300 μg/ml in a broth dilution assay. After two rounds of fractionation the synergist

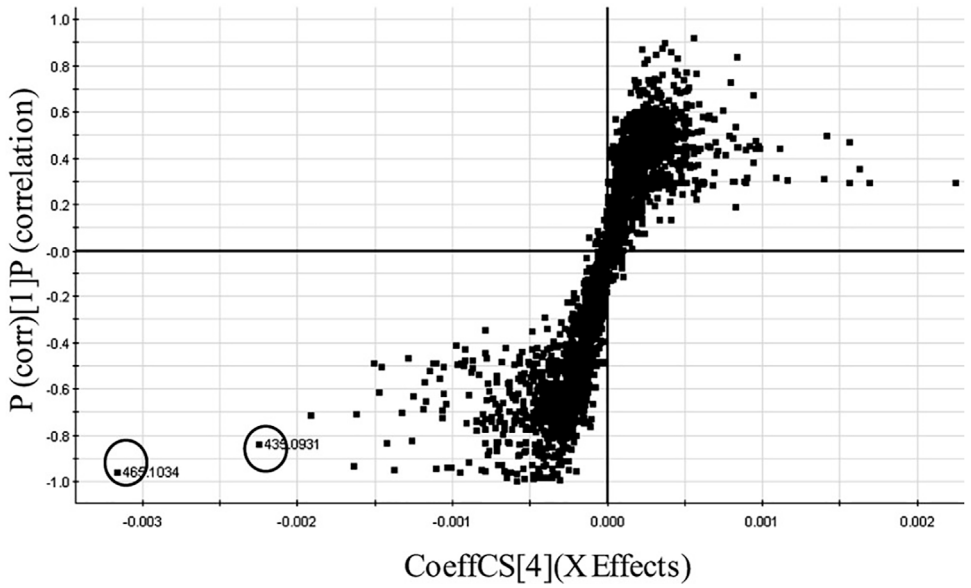

FIGURE 5 | S-plot of active versus inactive Cree plants leading of two significant biomarkers (circled) of inhibition of glucose uptake, quercetin 3-O-arabinoside and quercetin 3-O-galactoside. Figure appears as inset of Figure originally published in Shang et al. (2015). Novel approach to identify potential bioactive plant metabolites: pharmacological and metabolomics analyses of ethanol and hot water extracts of several Canadian medicinal plants of the Cree of Eeyou Istchee, PLoS One, 2015, 10(8), e0135721. Reproduced from Ref. 19, under the terms of a CC BY 4.0 license https://creativecommons.org/licenses/by/4.0/

compounds were isolated by preparative HPLC and identified by ^{1}H- and ^{13}C-NMR as the flavonoid sideroxylin (**Figure 3**) and its derivatives. Its mode of action was found to be the inhibition of the alkaloid efflux pump in the pathogenic bacteria.

Newer Methods in Identifying Bioactivity Markers

The disadvantage of classical BGF has been the need for large amounts of plant material (200–1500 g) and massive gravity columns to separate enough pure phytochemicals (2–3 mg) for structure elucidation by 1- and 2D-NMR spectroscopy and biotesting. A project like this often takes several months. Recent advances in technology now enable this process to be scaled down to 20 mg plant extract with rapid results achieved by integrating small scale bioassays with zebrafish. Bohni et al. (2013) developed a microscale bioassay guided platform for the study of the anti-angiogenic activity of a traditional medicine, *Rhynchosia viscosa* (Roth) DC (Fabaceae). They used rapid microfractionation of extracts, and microflow NMR methods allowing the identification of μg amounts of pure phytochemicals. They successfully screened these in zebrafish anti-angiogenic assays. The anti-angiogenic compounds identified were genistein and sophora isoflavone. Active principle identification can now be achieved rapidly using this and other microscale platforms.

Biochemometric analysis is an alternative method for the identification of bioactive compounds combining metabolomics, bioactivity studies and statistics and greatly reducing the need for assaying many column fractions. Nowadays, combination of bioassay and metabolomics guided isolation/fractionation are commonly used.

We undertook application of biochemometric analysis in a study of Echinacea phytochemicals active at cannabinoid targets relevant to a peripheral pain model (Liu et al., 2021a; Liu et al., 2021b). With a large number (40) of variable individual plant accessions of *Echinacea angustifolia* and *E. purpurea* available grown in a similar environment, linear regression of activity against concentration of phytochemical was feasible. Analyses of extracts were undertaken by HPLC DAD-MS for caffeic acid derivatives and alkamides and they were assayed for or CB1 and CB2 agonist activity or inhibition of fatty acid amide hydrolase (FAAH). Some of the results obtained with linear regression revealed CB2 agonist activity was positively and significantly (r^2 = 0.43 and p = 0.03) related with the major isomeric alkylamides, dodeca-2E, 4E, 8 Z, 10 E/Z tetraenoic acid isobutylamide in *E. angustifolia*. Caftaric acid, cichoric acid and one isobutyl amide are the strongest determinants of activity for FAAH inhibition in *E. pupurea* root. Results were confirmed with isolated compounds in the bioassays and in a rat model of inflammatory peripheral pain using a CB2 antagonist.

In another experiment, we used discriminant analysis to compare 17 Cree medicinal plant extracts that were very active in a antidiabetic assay for glucose uptake in C2C12 muscle cells, with species that displayed low activity (Shang et al., 2015). The metabolome of each extract was recorded using UPLC coupled to a quadrupole time of flight (QTOF)-MS. In this hyphenated technique, complex extracts were separated

into 400+ compounds through a small-bore reverse-phase column at very high pressure. Both the PCA and OPLSD plot showed separation of the high activity and low activity medicinal plants. Using an S-Plot analysis of the data to contrast the high activity and low activity species (**Figure 5**), two significant biomarkers for activity were discovered in the active plants and identified as quercetin-3-*O*-galactoside and quercetin 3-*O*-arabinoside (**Figure 3**) based on their accurate MS spectra. The compounds were tested in the antidiabetic assay and bioactivity was confirmed.

Discriminant methods can also be used with the fractions of one bioactive species (Kellogg et al., 2016), and comparisons of several methods were made to find the best statistical procedure. Fractions of the endophyte fungi *Alternaria* sp.(Deuteromycetes) and *Pyrenochaeta* sp. (Ascomycetes) were assayed for antimicrobial activity against the bacteria *Staphylococcus aureus* and analysed by LC-MS/MS. In the biochemometric analysis, significant antibacterial ions could be identified in fungal extracts using the S-plot analysis described above. However, they also evaluated a different statistic called the selectivity ratio which represents a quantitative measure of each variable's power to distinguish between different groups, and found it to be the best parameter for identifying bioactive ions from these extracts. In the study the method identified the antibacterial compounds altersetin (MIC 0.23 μg/ml) (**Figure 3**) and macrosphelide A (MIC 75 μg/ml).

This biochemometric approach using the selectivity ratio was also employed in a recent study of fractions of curled dock, *Rumex crispus* L. (Ranuculaceae), an indigenous remedy for diarrhea and skin infections studied here for antimicrobial activity (Pelzer et al., 2021). The selectivity ratio evaluated for fractions led to the identification of ten active antibacterial compounds including anthraquinones such as emodin and several of its derivatives, *iso*-ferulic acid, and scopoletin.

The biometric approach is also applicable to identifying synergists as revisited in goldenseal by Britton et al. (2017).

Dereplication

A challenge in ethnopharmacology is that it is important to find new active molecules in early stages of the chemical characterization or isolation, which can be achieved by a process known as dereplication. Conventionally this has been achieved in analytical methods combined with data bases of known compounds for comparison. Extracts with unidentified peaks are prioritized for isolation for pure compounds which are identified by conventional spectroscopy (1 and 2D NMR, IR and high-resolution MS). For example, El-Elimat et al. (2013) developed a method for dereplication of fungal metabolites. UPLC-PDA-HRMS-MS/MS was used for analysis of secondary metabolites in crude culture extracts and a database of 170 known fungal metabolites was constructed by recording HRMS and MS/MS spectra of fungal metabolites, utilizing both positive- and negative electrospray ionization modes. Cultures of 106 fungi were grown on a small scale extracted and tested for cytotoxicity to human cancer cell lines in culture, including MCF-7, H-460, and SF-268 cells. Active extracts were then analysed and only 55 containing unidentified peaks were prioritized for further isolation work.

With chemometrics and network pharmacology combined, powerful new methods are now available. An approach adopted for identification of antiviral compounds from *Euphorbia dendroides* L. (Euphorbiaceae) was developed by Nothias et al. (2018). After fractionation, each fraction was assessed by LC-MS and bioactivity scores were made using the relative abundance of a molecule in fractions and the bioactivity level of each fraction. Next, they assessed the potential bioactivity. First, they used a targeted approach, where prior knowledge was used, such as chemotaxonomic information and the sets of previously described bioactive molecules. Second, they used an untargeted approach by looking for consistent patterns of bioactive candidates in networks, such as clusters of phytochemicals with a high frequency of bioactive candidates. Cluster V in their study was identified as a priority and several deoxyphorbol ester derivatives were isolated by preparative HPLC in the study. Evaluation of the biological activity indicated two compounds that are selective inhibitors of Chikungunya virus replication in the submicromolar range.

An alternative approach to chemical dereplication is biological dereplication. It is well known that the distribution of bioactive phytochemicals in plants is specific to particular plant families. As a consequence, we undertook a phytochemical discovery program based on uninvestigated rare families are likely to be a source of novel phytochemicals. We applied this method to plants in the Sarracineaceae (Pitcher plant family) and the Lepidobotryaceae (tropical family with two genera, with few species). *Sarracinea purpurea* L. Moench (Sarracineaceae) , an antidiabetic plant used by Cree healers yielded over 13 phytochemicals including the novel 6′-O-caffeoyl goodyearoside (**Figure 3**) which was a new glucose uptake inhibitors (Muhammud et al., 2013). *Ruptiliocarpon caracolito* Hammel & N. Zamora (Lepidobotryaceae) (Asim et al., 2010) a plant used as a snuff by shaman in South America, yielded 17 novel spiro triterpenoids including spirocaracolitone A (**Figure 3**) with insecticidal and anxiolytic activity.

Recently, Wolfender's group has provided a review and synthesis of dereplication methods combining Liquid Chromatography–High Resolution Tandem Mass Spectrometry, NMR profiling, *In silico* studies, Spectral Databases, and Chemometrics analysis (Wolfender et al. (2018); Allard et al., 2016).

CONCLUSION

Consideration of some of the issues in this review by researchers can help them avoid defficiences leading to rejection of publications as well as lead to positive relationships and outcomes with First Peoples. The selected studies described in this review illustrate in part the rapid advances in technology and knowledge that is occurring in Phytochemistry and Ethnopharmacology today. The discipline has clearly moved from qualitative descriptive studies to quantitative, statistically rigorous science. There

are many uninvestigated plants to work on and we are truly at the beginning of a great age of drug discovery and scientific understanding of traditional knowledge.

AUTHOR CONTRIBUTIONS

All authors listed have made a substantial, direct, and intellectual contribution to the work,share first authorship and approved it for publication.

FUNDING

In Canada, JTA and CH received funding for projects reviewed here from Natural Sciences and Engineering Research Council (Harris (RGPIN-2015-05453) and to JTA (RGPIN-2015-06507)) and Mitacs Canada (IT04003). In Mexico, JAG acknowledges funding from Fondo Institucional de Fomento Regional para el Desarrollo Científico, Tecnológico y de Innovación (FORDECyT, grant number 292399) and Consejo Nacional de Ciencia y Tecnología (CONACyT, grant number 316998).

REFERENCES

Allard, P. M., Péresse, T., Bisson, J., Gindro, K., Marcourt, L., Pham, V. C., et al. (2016). Integration of Molecular Networking and In-Silico MS/MS Fragmentation for Natural Products Dereplication. *Anal. Chem.* 88 (6), 3317–3323. doi:10.1021/acs.analchem.5b04804

Arnason, J., Cal, V., Pesek, T., Awad, R., Bourbonnais-Spear, N., Collins, S., et al. (2022). A Review of Ethnobotany and Ethnopharmacology of Traditional Medicines Used by Q'eqchi' Maya Healers of Xna'ajeb' Aj Ralch'o'och', Belize. *Botany* 100 (2), 219–230. doi:10.1139/cjb-2021-0069

Asim, M., Hussien, H., Poveda, L., Arnason, J. T., and Durst, T. (2010). Triterpenoids from the Bark of *Ruptiliocarpon Caracolito*. *Phytochemistry* 71 (11-12), 1418–1422. doi:10.1016/j.phytochem.2010.04.020

Bauer, R., Remiger, P., and Wagner, H. (1988). Alkamides from the Roots of Echinacea Purpurea, *Phytochemistry*. 27, 2339–2342. doi:10.1211/0022357056127

Berger-Gonzalez, M., Scotti, F., Garcia, A. I., Hesketh, A., Hitziger, M., Thompson, I., et al. (2022). Green Health in Guatemala - How Can We Build up Mutualtrust and Partnerships for Developing Herbal Medicines'evidence-Base. *Botany*, 1–18. doi:10.1016/j.phytochem.2010.04.020

Bohni, N., Cordero-Maldonado, M. L., Maes, J., Siverio-Mota, D., Marcourt, L., Munck, S., et al. (2013). Integration of Microfractionation, qNMR and Zebrafish Screening for the *In Vivo* Bioassay-Guided Isolation and Quantitative Bioactivity Analysis of Natural Products. *PLoS ONE* 8 (5), e64006. doi:10.1371/journal.pone.0064006

Britton, E. R., Kellogg, J. J., Kvalheim, O. M., and Cech, N. B. (2017). Biochemometrics to Identify Synergists and Additives from Botanical Medicines: a Case Study with *Hydrastis canadensis* (Goldenseal). *J. Nat. Prod.* 81 (3), 484–493. doi:10.1021/acs.jnatprod.7b00654

Brown, P. N., Murch, S. J., and Shipley, P. (2012a). Phytochemical Diversity of cranberry (Vaccinium Macrocarpon Aiton) Cultivars by Anthocyanin Determination and Metabolomic Profiling with Chemometric Analysis. *J. Agric. Food Chem.* 60 (1), 261–271. doi:10.1021/jf2033335

Brown, P. N., Turi, C. E., Shipley, P. R., and Murch, S. J. (2012b). Comparisons of Large (Vaccinium Macrocarpon Ait.) and Small (*Vaccinium Oxycoccos* L., *Vaccinium Vitis-idaea* L.) cranberry in British Columbia by Phytochemical Determination, Antioxidant Potential, and Metabolomic Profiling with Chemometric Analysis. *Planta Med.* 78 (06), 630–640. doi:10.1055/s-0031-1298239

El-Elimat, T., Figueroa, M., Ehrmann, B. M., Cech, N. B., Pearce, C. J., and Oberlies, N. H. (2013). High-resolution MS, MS/MS, and UV Database of Fungal Secondary Metabolites as a Dereplication Protocol for Bioactive Natural Products. *J. Nat. Prod.* 76 (9), 1709–1716. doi:10.1021/np4004307

Ferrier, J. (2014) Ethnobotany, Pharmacology, and Metabolomics of Antidiabetic Plants Used by the Eeyou Istchee Cree, Lukomir Highlanders, and Q'eqchi' Maya. University of Ottawa. (Doctoral dissertation, Université d'Ottawa/University of Ottawa). Ottawa.

Gafner, S., Borchar, T., Bush, M., Sudberg, S., Feuillère, G., Justine, H., et al. (2021). Tales from the Elder: Adulteration Issues of Elderberry. *HerbalGram* 130, 24–31.

Geck, M. S., Cristians, S., Berger-González, M., Casu, L., Heinrich, M., and Leonti, M. (2020). Traditional Herbal Medicine in Mesoamerica: Toward its Evidence Base for Improving Universal Health Coverage. *Front. Pharmacol.* 11, 1160. doi:10.3389/fphar.2020.01160

Grand Council of the Crees (Eeyou Istchee) (2012). *Assembly of First Nations; Nunavut Tunngavik Inc.; First Nations Child and Family Caring Society of Canada; Native Women's Association of Canada; National Association of Friendship Centres; Canadian Friends Service Committee (Quakers); First Nations Summit; Union of British Columbia Indian Chiefs; BC Assembly of First Nations; Federation of Saskatchewan Indian Nations; Chiefs of Ontario; Nishnawbe Aski Nation; Assembly of First Nations of Québec and Labrador/Assemblée des Premières Nations du Québec et du Labrador Haudenosaunee of Kanehsatà:ke; Maritime Aboriginal Peoples Council; IKANAWTIKET; Indigenous World Association; First Peoples Human Rights Coalition 2012 Response to Canada's 19th and 20th Periodic Reports:Alternative Report on Canada's Actions on the Nagoya Protocol, Committee on the Elimination of Racial Discrimination 80th Session 13 February - 9 March 2012*. Geneva: International Indian Treaty Council; Innu Council of Nitassinan United Nations.

Guerrero-Analco, J. A., Martineau, L., Saleem, A., Madiraju, P., Muhammad, A., Durst, T., et al. (2010). Bioassay-guided Isolation of the Antidiabetic Principle from *Sorbus Decora* (Rosaceae) Used Traditionally by the Eeyou Istchee Cree First Nations. *J. Nat. Prod.* 73, 1519–1523. doi:10.1021/np1003005

Hall, B., Rapinski, M., Spoor, D., Eid, H. M., Saleem, A., Arnason, J. T., et al. (2022). A Meta-Analysis of the Anti-diabetes Ethnopharmacology of the Eeyou Istchee. *Front. Pharmacol.* 11, 450.doi:10.3389/fphar.2021.511078

Health Canda (2018). Health Canada Natural Health Product Black Cohosh. AvaliableAt: http://webprod.hc-sc.gc.ca/nhpid-bdipsn/atReq.do?atid=black.cohosh.actee.noire&lang=eng.

Hopkins, A. L. (2008). Network Pharmacology: the Next Paradigm in Drug Discovery. *Nat. Chem. Biol.* 4 (11), 682–690. doi:10.1038/nchembio.118

Junio, H. A., Sy-Cordero, A. A., Ettefagh, K. A., Burns, J. T., Micko, K. T., Graf, T. N., et al. (2011). Synergy-directed Fractionation of Botanical Medicines: a Case Study with Goldenseal (*Hydrastis canadensis*). *J. Nat. Prod.* 74 (7), 1621–1629. doi:10.1021/np200336g

Kellogg, J. J., Todd, D. A., Egan, J. M., Raja, H. A., Oberlies, N. H., Kvalheim, O. M., et al. (2016). Biochemometrics for Natural Products Research: Comparison of Data Analysis Approaches and Application to Identification of Bioactive Compounds. *J. Nat. Prod.* 79 (2), 376–386. doi:10.1021/acs.jnatprod.5b01014

Lai, X., Wang, X., Hu, Y., Su, S., Li, W., and Li, S. (2020). Editorial: Network Pharmacology and Traditional Medicine. *Front. Pharmacol.* 11, 1194. doi:10.3389/fphar.2020.01194

Liu, R., Burkett, K., Rapinski, M., Arnason, J. T., Johnson, F., Hintz, P., et al. (2021a). Biochemometric Analysis of Fatty Acid Amide Hydrolase Inhibition by Echinacea Root Extracts. *Planta Med.* 87 (04), 294–304. doi:10.1055/a-1289-9569

Liu, R., Salas, N. C., Li, W., Wang, L., Arnason, J. T., and Harris, C. S. (2021b). Interactions of Echinacea Spp. Root Extracts and Alkylamides with the Endocannabinoid System and Peripheral Inflammatory Pain. *Front. Pharmacol.* 12, 776. doi:10.3389/fphar.2021.651292

Mahady, G. B., Low Dog, T., Barrett, M. L., Chavez, M. L., Gardiner, P., Ko, R., et al. (2008). United States Pharmacopeia Review of the Black Cohosh Case Reports of Hepatotoxicity. *Menopause* 15 (4), 628–638. doi:10.1097/gme.0b013e31816054bf

Mamallapalli, J., Raju, K. S. R., Corral, P., Johnston, E., Zhuang, C., Mccurdy, C., et al. (2021). Characterization of Different Forms of Kava (*Piper methysticum*) Products by UPLC-MS/MS. *Planta Med*. doi:10.1055/a-1708-1994

Markus, M. A., Ferrier, J., Luchsinger, S. M., Yuk, J., Cuerrier, A., Balick, M. J., et al. (2014). Distinguishing *Vaccinium* Species by Chemical Fingerprinting Based on NMR Spectra, Validated with Spectra Collected in Different Laboratories. *Planta Med.* 80 (08/09), 732–739. doi:10.1055/s-0034-1368569

Mata, R., Contreras-Rosales, A. J., Gutiérrez-González, J. A., Villaseñor, J. L., and Pérez-Vásquez, A. (2022). *Calea ternifolia* Kunth, the Mexican "dream herb", a concise review. *Botany* 100 (2), 1–14. doi:10.1139/cjb-2021-0063

Moerman, D. E., Mudge, E. M., Murch, S. J., and Brown, P. N. (2018). *Native American Ethnobotany*, Portland ORChemometric Analysis of Cannabinoids: Chemotaxonomy and Domestication Syndrome. *Timber PressScientific Rep.* 8 (1), 1–9. 10.1038/s41598-018-31120-2.

Mudge, E. M., Brown, P. N., and Murch, S. J. (2019). The Terroir of Cannabis: Terpene Metabolomics as a Tool to Understand Cannabis Sativa Selections. *Planta Med.* 85 (09/10), 781–796. doi:10.1055/a-0915-2550

Muhammad, A., Haddad, P. S., Durst, T., and Arnason, J. T. (2013). Phytochemical Constituents of *Sarracenia Purpurea* L. (Pitcher Plant). *Phytochemistry* 94, 238–242. doi:10.1016/j.phytochem.2013.05.015

Murch, S. J., Simmons, C. B., and Saxena, P. K. (1997). Melatonin in Feverfew and Other Medicinal Plants. *Lancet* 350, 1598–1599. doi:10.1016/S0140-6736(05)64014-7

Nothias, L. F., Nothias-Esposito, M., da Silva, R., Wang, M., Protsyuk, I., Zhang, Z., et al. (2018). Bioactivity-based Molecular Networking for the Discovery of Drug Leads in Natural Product Bioassay-Guided Fractionation. *J. Nat. Prod.* 81 (4), 758–767. doi:10.1021/acs.jnatprod.7b00737

Pelzer, C. V., Houriet, J., Crandall, W. J., Todd, D. A., Cech, N. B., and Jones, D. D., Jr (2021). More Than Just a Weed: An Exploration of the Antimicrobial Activity of Rumex Crispus Using a Multivariate Data Analysis Approach. *Planta Med*. doi:10.1055/a-1652-1547

Ravaglia, L. M., Pizzotti, A. B. C., and Alcantara, G. B. (2019). NMR-based and Chemometric Approaches Applicable to Adulteration Studies for Assessment of the Botanical Origin of Edible Oils. *J. Food Sci. Technol.* 56 (1), 507–511. doi:10.1007/s13197-018-3485-3

Robinson, A. (2018) Turtle Island". The Canadian Encyclopedia, 06 November 2018, Historica Canada. AvaliableAt: www.thecanadianencyclopedia.ca/en/article/turtle-island (Accessed January 06, 2022).

Shang, N., Guerrero-Analco, J. A., Musallam, L., Saleem, A., Muhammad, A., Walshe-Roussel, B., et al. (2012). Adipogenic constituents from the bark of Larix laricina du roi (K. koch; Pinaceae), an important medicinal plant used traditionally by the Cree of Eeyou Istchee (Quebec, Canada) for the treatment of type 2 diabetes symptoms. *J. Ethnopharmacol.* 141, 1051–1057. doi:10.1016/j.jep.2012.04.002

Shang, N., Saleem, A., Musallam, L., Walshe-Roussel, B., Badawi, A., Cuerrier, A., et al. (2015). Novel Approach to Identify Potential Bioactive Plant Metabolites: Pharmacological and Metabolomics Analyses of Ethanol and Hot Water Extracts of Several Canadian Medicinal Plants of the Cree of Eeyou Istchee. *PLoS One* 10 (8), e0135721. doi:10.1371/journal.pone.0135721

Simmler, C., Graham, J. G., Chen, S. N., and Pauli, G. F. (2018). Integrated Analytical Assets Aid Botanical Authenticity and Adulteration Management. *Fitoterapia* 129, 401–414. doi:10.1016/j.fitote.2017.11.017

Stayawat/Joseph, L. (2022). Spéńem T'úyt – Plant Medicine: An Indigenous Perspective on the Role of Ethnobotany in Cultural Resurgence - Preface to Ethnobotany and Ethnopharmacology in the Americas. *Botany* vii. doi:10.1139/cjb-2021-0180

Türker-Kaya, S., and Huck, C. W. (2017). A Review of Mid-infrared and Near-Infrared Imaging: Principles, Concepts and Applications in Plant Tissue Analysis. *Molecules* 22 (1), 168. doi:10.3390/molecules22010168

Upton, R. (2004). *Echinacea Purpurea Root Echinacea Purpurea (L.) Moench. Standards of Analysis, Quality Control and Therapeutics*. Denver, CO: American Herbal Pharmacopoeia and Therapeutic Compendium. Inner Doorway LLC, 1–50.

Wallace, E. D., Todd, D. A., Harnly, J. M., Cech, N. B., and Kellogg, J. J. (2020). Identification of Adulteration in Botanical Samples with Untargeted Metabolomics. *Anal. Bioanal. Chem.* 412 (18), 4273–4286. doi:10.1007/s00216-020-02678-6

Wolfender, J. L., Nuzillard, J. M., Van Der Hooft, J. J. J., Renault, J. H., and Bertrand, S. (2019). Accelerating Metabolite Identification in Natural Product Research: Toward an Ideal Combination of Liquid Chromatography-High-Resolution Tandem Mass Spectrometry and NMR Profiling, In Silico Databases, and Chemometrics. *Anal. Chem.* 91 (1), 704–742. doi:10.1021/acs.analchem.8b05112

Conflict of Interest: The authors declare that the research was conducted in the absence of any commercial or financial relationships that could be construed as a potential conflict of interest.

frontiers | Frontiers in Pharmacology

REVIEW
published: 12 May 2022
doi: 10.3389/fphar.2022.823881

Role of Phytochemicals in Skin Photoprotection *via* Regulation of Nrf2

Anyamanee Chaiprasongsuk[1] *and Uraiwan Panich*[2]*

[1]*Princess Srisavangavadhana College of Medicine, Chulabhorn Royal Academy, Bangkok, Thailand,* [2]*Department of Pharmacology, Faculty of Medicine Siriraj Hospital, Mahidol University, Bangkok, Thailand*

Ethnopharmacological studies have become increasingly valuable in the development of botanical products and their bioactive phytochemicals as novel and effective preventive and therapeutic strategies for various diseases including skin photoaging and photodamage-related skin problems including abnormal pigmentation and inflammation. Exploring the roles of phytochemicals in mitigating ultraviolet radiation (UVR)-induced skin damage is thus of importance to offer insights into medicinal and ethnopharmacological potential for development of novel and effective photoprotective agents. UVR plays a role in the skin premature aging (or photoaging) or impaired skin integrity and function through triggering various biological responses of skin cells including apoptosis, oxidative stress, DNA damage and inflammation. In addition, melanin produced by epidermal melanocytes play a protective role against UVR-induced skin damage and therefore hyperpigmentation mediated by UV irradiation could reflect a sign of defensive response of the skin to stress. However, alteration in melanin synthesis may be implicated in skin damage, particularly in individuals with fair skin. Oxidative stress induced by UVR contributes to the process of skin aging and inflammation through the activation of related signaling pathways such as the mitogen-activated protein kinase (MAPK)/activator protein-1 (AP-1), the phosphatidylinositol 3-kinase (PI3K)/protein kinase B (Akt), the nuclear factor kappa B (NF-κB) and the signal transducer and activator of transcription (STAT) in epidermal keratinocytes and dermal fibroblasts. ROS formation induced by UVR also plays a role in regulation of melanogenesis in melanocytes *via* modulating MAPK, PI3K/Akt and the melanocortin 1 receptor (MC1R)-microphthalmia-associated transcription factor (MITF) signaling cascades. Additionally, nuclear factor erythroid 2-related factor 2 (Nrf2)-regulated antioxidant defenses can affect the major signaling pathways involved in regulation of photoaging, inflammation associated with skin barrier dysfunction and melanogenesis. This review thus highlights the roles of phytochemicals potentially acting as Nrf2 inducers in improving photoaging, inflammation and hyperpigmentation *via* regulation of cellular homeostasis involved in skin integrity and function. Taken together, understanding the role of phytochemicals targeting Nrf2 in photoprotection could provide an insight into potential development of natural products as a promising strategy to delay skin photoaging and improve skin conditions.

Keywords: phytochemicals, photoaging, Nrf2, inflammation, skin barrier dysfunction

OPEN ACCESS

Edited by:
Cheorl-Ho Kim, Sungkyunkwan University, South Korea

Reviewed by:
Wei Hsum Yap, Taylor's University, Malaysia
Maged El-Sayed Mohamed, King Faisal University, Saudi Arabia

***Correspondence:**
Uraiwan Panich
uraiwan.pan@mahidol.ac.th

Specialty section:
This article was submitted to Ethnopharmacology, a section of the journal Frontiers in Pharmacology

Received: *28 November 2021*
Accepted: *11 April 2022*
Published: *12 May 2022*

Citation:
Chaiprasongsuk A and Panich U (2022) Role of Phytochemicals in Skin Photoprotection via Regulation of Nrf2. Front. Pharmacol. 13:823881. doi: 10.3389/fphar.2022.823881

INTRODUCTION

The skin is the largest organ in the body, and one of its main functions is to protect the body from environmental stressors including ultraviolet radiation (UVR), which can result in dermatological disorders, such as skin premature aging, abnormal pigmentation and inflammatory reactions. UVR has been generally known to have both beneficial and detrimental effects on human health. While UVR plays a role in natural synthesis of vitamin D, melanin, and various peptides in the skin that have positive biological implications (Slominski et al., 2000; Lin et al., 2016), excessive exposure to UVR can lead to acute and chronic adverse effects on the health of skin and is involved in the pathogenesis of premature aging (or photoaging) and increased risk of photocarcinogenesis. In addition, UVR is accepted as human carcinogen through oxidative mechanisms accountable for increased risk of developing skin cancers including non-melanoma and melanoma skin cancers (Tran et al., 2008). The incidence of skin cancer has dramatically risen in particular among fair-skinned populations, primarily due to lifestyle changes and increased recreational exposure to UVR including outdoor activities and sunbathing for cosmetic purposes (Narayanan et al., 2010). Both male and female independent of age are affected by dermatological concerns and increasingly interested in rejuvenation and skin cancer prevention. While the use of sunscreens is recommended in order to minimize the risk of photoaging and other UV-related skin disorders, sunscreen alone does not provide sufficient protection against deleterious effects of UVR. Oxidative stress plays a crucial role in UVR-induced photodamage *via* mediating multiple biological responses including apoptosis, DNA damage, mitochondrial dysfunction, inflammation, abnormal pigmentation and upregulation of matrix metalloproteinases (MMPs) (such as MMP-1) in related skin cell types including keratinocytes, fibroblasts and melanocytes (Liebel et al., 2012; Denat et al., 2014; Silva et al., 2017; Lohakul et al., 2021b). Therefore, cellular and molecular regulation of antioxidant defenses to combat oxidative stress and promote redox balance could be a potential therapeutic and preventive strategies for photodamaged skin.

Nuclear factor erythroid 2-related factor 2 (Nrf2) is an important transcription factor controlling antioxidant responses in various tissues including the skin and plays a major role in cytoprotection against chemical and environmental insults including UVR (Ikehata and Yamamoto, 2018). Targeting Nrf2 could improve photoaging, wound repair and dyspigmentation as well as prevent photocarcinogenesis *via* regulation of cellular homeostasis involved in skin integrity and function (Saw et al., 2011; Gegotek and Skrzydlewska, 2015). Phytochemicals, which are ubiquitously present in plant-based diets and are active ingredients in several botanical drugs, have thus gained remarkable attention as promising candidates for effective photoprotective agents due to their abilities to activate Nrf2 signaling-regulated redox balance and subsequently maintain cellular homeostasis involved in skin integrity and function. Much attention has been focused on the role of dietary polyphenols in the repair of photodamaged skin and prevention of solar-induced skin diseases (Surh and Na, 2008; Saw et al., 2011; Dunaway et al., 2018). In this review, we provide an overview of the promising roles of phytochemicals in mitigating UVR-induced skin damage via regulation of Nrf2-mediated antioxidant response to offer an insight into ethnopharmacological potential for development of novel and effective anti-photodamaging agents.

The Role of UVR-Induced Oxidative Stress in Skin Photodamage

The skin is a primary target of oxidative stress because it is constantly exposed to environment including UVR, which induces reactive oxygen species (ROS) generation in the skin. It has been well accepted that both UVA and UVB rays play a significant role in the premature aging and photodamage of the skin through various mechanisms involving oxidative stress (Lephart, 2016; Gegotek et al., 2017). While UVB has biological impact on the skin primarily by causing direct damage to DNA and inflammation (Halliday and Lyons, 2008), UVA accounts for skin photodamage by generating various types of ROS, such as superoxide anion radical ($O_2^{\bullet-}$), singlet oxygen ($^1\Delta gO_2$) and hydrogen peroxide (H_2O_2). ROS can interact with biomolecules and interfere with cell signaling, affecting cell survival and function of the skin cells (Dunaway et al., 2018). Considerable studies have reported that UVA exposure significantly led to ROS accumulation responsible for oxidative damage to biomolecules including DNA (O'Donovan et al., 2005), lipid (Dissemond et al., 2003) and protein in the skin cells including fibroblasts, keratinocytes (Brem et al., 2017) and melanocytes. Oxidative damage mediated by both UVA and UVB is associated with apoptosis and necrosis of the skin cells associated with sunburn reaction and photoaging process (Didier et al., 2001; Suschek et al., 2001; Kawachi et al., 2008; Parrado et al., 2016).

Skin Photoaging

Photoaging is characterized by epidermal thickness, termed hyperkeratosis, due to increased keratinocyte hyperproliferation as well as degradation or degeneration and disorganization of collagen fibers caused by upregulation of MMPs (Quan et al., 2009; Pittayapruek et al., 2016). In addition, dysregulated proliferation of transformed neoplastic keratinocytes or actinic keratosis is the key event in the progression from photoaged skin to squamous cell carcinoma (Berman and Cockerell, 2013). UVR (both UVA and UVB) is well accepted to play a vital role in photoaging *via* several mechanisms including DNA damage, oxidative stress, apoptosis, senescence, inflammation, immunomodulation (Rijken and Bruijnzeel-Koomen, 2011; Brand et al., 2017) and degradation and/or remodeling of the extracellular matrix (ECM) (Bosch et al., 2015). Generally, the characteristic hallmarks of photoaged skin are alterations in the ECM including accumulation of disorganized elastin fibers and depletion of collagens, the main structural proteins of the dermal connective tissues. Both UVA and UVB radiation can induce hyperkeratosis and several types of MMPs (including MMP-1 or collagenase) in mouse models of photoaging (Chaiprasongsuk et al., 2017; Misawa et al., 2017). Several *in vitro*

and *in vivo* studies have reported that UV irradiation stimulates expression of MMP-1, MMP-3 and MMP-9, which are the major UV-inducible collagenolytic enzymes, regulated at the transcriptional level (Afaq et al., 2009; Quan et al., 2009; Pittayapruek et al., 2016). MMPs are co-expressed in response to various stimuli including oxidative insults, inflammatory cytokines and growth factors (Greenlee et al., 2007; Lee et al., 2021). MMPs are suggested to be downstream targets within signaling pathways of upstream response genes, which encode several signaling proteins that activate different transcription factors capable of binding the promoters of MMP genes. The key transcription-binding sites involved in the regulation of MMP genes include the activator protein-1 (AP-1) site, the nuclear factor kappa B (NF-κB) site and the signal transducer and activator of transcription (STAT) site (Fanjul-Fernandez et al., 2010). In addition, MMPs can be co-regulated because they share several transcription-binding sites in their promoter sequences. NF-κB and AP-1 are the transcription factors that can bind the promoters of MMP-1, 3 and 9 (Watanabe et al., 2004). The AP-1 transcription complex, a family of dimeric transcription factors composed of members of the Jun and Fos family proteins, is the main transcription factor regulating MMP-1 gene (Angel et al., 2001). In general, the c-Jun and c-Fos genes are activated rapidly and transiently in response to stimuli and are thus considered immediate-early response genes. Binding of heterodimer complexes of c-Jun with c-Fos to the AP-1 site, which is specific DNA sequences (5′-TGAG/CTCA-3′), termed TREs (TPA (tetradecanoylphorbol-12-Acetate)-response elements), is responsible for transactivation of AP-1 that regulates MMP-1, 3 and 9 expressions (Mackay et al., 1992; Watanabe et al., 2004). Both c-Jun and c-Fos are controlled by mitogen-activated protein kinase (MAPK) signaling pathways which are stimulated by extracellular stimuli including growth factors and cytokines as well as environmental stimuli including UVR. Three distinct types of MAPKs, ERK (extracellular signal-regulated kinase), JNK (c-Jun NH_2-terminal kinase) and p38 MAPK, differentially affect AP-1 activity in response to various stimuli (Karin, 1995). The ERKs generally are triggered by growth factors and hormones as well as JNK and p38 MAPK are activated by environmental stresses including UVR and pro-inflammatory mediators, such as tumor necrosis factor (Chang and Karin, 2001; Silvers et al., 2003; Whitmarsh, 2007). UVR is suggested to primarily cause the greatest increases in JNK activity. Upon exposure to some stimuli, phosphorylation of c-Fos in the AP-1 complex at two C-terminal sites (Ser362 and Ser374) by MAPKs, in particular ERK, is required for transactivation at the specific AP-1 site (McBride and Nemer, 1998). In addition, c-Jun is activated and stabilized by JNK- and p38-catalyzed phosphorylation at the NH_2-terminal sites (Ser63 and Ser73) located within transactivation domain of c-Jun. p38 MAPK indirectly activates AP-1 by phosphorylating other transcription factors such as AP-1 family proteins ATF2 (the activating transcription factor) forming a heterodimer with c-Jun, which then binds to the promoter elements in the c-Jun gene and regulates its transcription, leading to the subsequent upregulation of c-Jun expression and synthesis (Pramanik et al., 2003).

ROS participates in the photoaging process through several mechanisms including DNA damage, apoptosis, upstream modulation of MAPK/AP-1, NF-κB and JAK (janus kinase)-STAT signaling cascades, activation of cytokine and growth factor receptors and immune reaction of melanocytes and keratinocytes. Upregulation of MAPK/AP-1 signaling results in induction of transcription and production of MMPs (such as collagenase-1 (MMP-1), stromelysin-1 (MMP-3), and gelantinase A (MMP-2), that subsequently degrade ECM including collagen and elastin as well as suppress the collagen synthesis in the dermal fibroblasts. Furthermore, keratinocytes play an indirect role in photoaging through secreting paracrine factors, which stimulate the signaling cascades-mediated upregulation of MMPs in dermal fibroblasts. Several studies including ours suggested that ROS formation is involved in the molecular mechanisms of photoaging *via* activating MAPK/AP-1 signaling pathway, resulting in both upregulation of MMPs and downregulation of procollagen I production (Li et al., 2019). ROS induced by UVR is implicated in MAPKs-dependent activation of AP-1 signaling, leading to upregulation of various MMPs including MMP-1, MMP-3 and MMP-9 in both keratinocytes and fibroblasts (Rittie and Fisher, 2002; Pittayapruek et al., 2016). Our *in vitro* and *in vivo* studies demonstrated the role of ROS induced by UVA exposure in upregulation of MMP-1 through activation of MAPK/AP-1 signaling pathway in keratinocytes and mouse skin. In addition, UVB has been shown to trigger MMP-1 and MMP-3 expressions through ROS generation and MAPK/AP-1 activation in irradiated keratinocytes and fibroblasts (Kim et al., 2013; Kim et al., 2015; Lu et al., 2016). In addition, UVB radiation is suggested to induce ROS formation, leading to increased MMP-9 activity and expression in mouse embryonic fibroblasts and HaCaT keratinocytes (Chang et al., 2017; Ma et al., 2018). UVB-induced oxidative stress was observed to activate MAPK signaling in association with increased expression of MMP-9 in UVB-exposed dermal fibroblasts (Gunaseelan et al., 2017). Moreover, ROS was found to be involved in activation of p38 MAPK and induction of MMP-9 expression in UVB-exposed HaCaT keratinocytes (Li et al., 2017b) and mouse dermis (Li et al., 2017b). In addition to collagen and elastin degradation by MMPs, UVB plays a role in a reduction of procollagen type I synthesis through activating AP-1-mediated downregulation of transforming growth factor beta (TGF-β) signaling (Pittayapruek et al., 2016; Gao et al., 2018a).

It should also be taken into account that photoaging of the skin is a complex multifactorial process. Apart from ROS/MAPK/AP-1 signaling cascades, UVR which can activate various cell surface receptors can stimulate downstream signaling pathways that control other different transcription factors regulating expression of many genes involved in photoaging process. Eventually, it is important to inhibit ECM degradation that leads to solar scar, a process taking place with each exposure to UV even at low doses. Since ROS serve as important second messengers, which act upstream of MAPK/AP-1 signaling-mediated induction of MMPs and reduction of procollagen

implicated in pathogenesis of photoaging, controlling ROS homeostasis could represent promising pharmacological and molecular approaches to impede photoaging.

Skin Inflammation and Skin Barrier Dysfunction

The skin barrier dysfunction and oxidative stress are suggested to play a role in the development of chronic inflammatory skin conditions (e.g., dermatitis) and alteration of wound healing process (Wikramanayake et al., 2014). The accumulation and alteration of external stimuli exposures result in a compromised barrier function of the skin through cutaneous inflammation and the imbalance of skin homeostasis (Egawa and Kabashima, 2018). Previous studies have demonstrated that UVB irradiation has a negative impact on epidermal morphology and barrier function by increasing stratum corneum (SC) thickness, causing changes in SC lipids and stimulating transepidermal water loss (Biniek et al., 2012). ROS generation induced by UVR plays a role in epidermal barrier dysfunction through oxidative damage to proteins and lipids, leading to alteration of tissue structure (Rinnerthaler et al., 2015). Regulation of Nrf2 activity has also been proposed to offer a potential strategy to improve skin barrier integrity by mitigating UVR-induced damage of keratinocytes and modulating inflammatory responses of the skin. Downregulation of Nrf2 signaling was shown to be involved in UVB-induced upregulation of pro-inflammatory mediators such as tumor necrosis factor alpha (TNF-α), cyclooxygenase-2 (COX-2), interleukin-6 (IL-6), interleukin-1 beta (IL-1β), and interleukin-8 (IL-8) in keratinocyte HaCaT cells (Park et al., 2021). A previous study using a mouse model of UVB-induced photodamage revealed that basal activity of Nrf2 in keratinocytes of normal skin is vital for improvement of skin barrier integrity and for prevention of skin carcinogenesis. UVB-mediated apoptosis of epidermal cells was involved in impaired skin integrity and activation of Nrf2 was observed to protect against UVB-induced apoptosis of basal keratinocytes in a paracrine, glutathione (GSH)/cysteine-dependent manner. Furthermore, enhanced levels of Nrf2-dependent genes in all layers of epidermis in response to UVB exposure were involved in the suppression of apoptosis *in vivo* (Schafer et al., 2010). The connection between the Nrf2 and antioxidant response element (ARE) system proved the protective pathways of skin inflammation via the regulation of the inflammatory factors (Saha et al., 2020). The *NFE2L2* gene encoding for Nrf2 contains ARE-like sequences, providing a positive feedback mechanism to amplify antioxidant and anti-inflammatory signaling such as glutathione S-transferase (GST), NAD(P)H quinone oxidoreductase-1 (NQO-1), heme oxygenase-1 (HO-1) (Nguyen et al., 2009; Luo et al., 2018). Nrf2 has been suggested to play a role in modulating several signaling pathways involved in the inflammatory responses include NF-κB, MAPK, and JAK-STAT. Previous studies have reported the crosstalk between Nrf2 and NF-κB pathway. Nrf2 negatively regulated the NF-κB signaling pathway and proinflammatory cytokine production by inhibiting oxidative stress-induced NF-κB and preventing the IκB-α (NF-κB inhibitor) proteasomal degradation (Ma, 2013; Saha et al., 2020). In addition, several proinflammatory cytokines (e.g., IL-6, TNF-α and IL-1β), growth factors (e.g., epidermal growth factor (EGF), fibroblast growth factor, keratinocyte growth factor (KGF) and vascular endothelial growth factor (VEGF) and MMPs (e.g., MMP-2 and MMP-9) play a role in wound repair consisting of a series of multiple stages including inflammation, proliferation and remodeling (Shao et al., 2019; Suntar et al., 2021). Activation of Nrf2 in response to ROS production in inflamed tissues is thus suggested to play a role in promoting wound healing and regulating repair-related inflammation. Moreover, Nrf2 transcripts several genes encoding skin barrier structural and functional components including the keratins (KRT), the cornified envelope family members, small proline rich proteins, secretory leukocyte protease inhibitor, and the EGF family member epigen (Rojo de la Vega et al., 2017). In addition to Nrf2, STAT3 (in cell proliferation and differentiation), Smad proteins (in collagen production) and Forkhead box protein N1 (FOXN1) (in re-epithelization) are important transcriptional regulators involved in the process of wound repair. Furthermore, without involvement of inflammatory cells, upregulation of Nrf2 activity and its target antioxidant NQO-1 or HO-1 was demonstrated to promote the migration of corneal epithelial cells during wound repair *in vitro* and *in vivo* (Hayashi et al., 2013). In response to ROS produced in the early phase of wound repair, upregulation of Nrf2 as a target of KGF in keratinocytes is involved in the healing process in association with modulating proinflammatory cytokine IL-1, IL-6, and TNF-α and TGF-β1 and VEGF *in vitro* and *in vivo* (Braun et al., 2002). Nevertheless, the regulatory role of Nrf2 in epidermal homeostasis is complex and needs further clarification as prolonged activation of Nrf2 in keratinocytes could interfere skin homeostasis. Previous *in vitro* and *in vivo* studies demonstrated that increased activity of Nrf2 in keratinocytes resulted in epithelial abnormalities, altered epidermal barrier and development of hyperkeratosis (Kypriotou et al., 2012; Schafer et al., 2012).

Skin Hyperpigmentation

While melanin plays a crucial role in protecting the skin against harmful effects of UVR, excessive production of melanin could be detrimental because melanin precursors and intermediate metabolites produced during melanogenesis in response to UVR exert phototoxic properties (Schmitz et al., 1995). Whereas hyperpigmentation mediated by UV irradiation could reflect a sign of defensive response of the skin to stress, alteration in melanin synthesis may be implicated in skin damage, particularly in individuals with fair skin. UVR-dependent elevated melanogenesis has been suggested to be biologically harmful, genotoxic and contributed to development of melanoma skin cancer, especially in lightly pigmented individuals. The incidence of skin cancer has dramatically risen in particular among fair-skinned populations, primarily due to lifestyle changes and increased recreational exposure to UVR including outdoor activities and sunbathing for cosmetic purposes (Narayanan et al., 2010; D'Orazio et al., 2013; Watson et al., 2016). Furthermore, the growth of skin fairness products is dramatic particularly in Asia and Africa, although the use of skin

bleaching products is associated with adverse side effects (Shroff et al., 2017). Thus, there is a need to develop effective and safe strategies for improvement of skin dyspigmentation or uneven complexion. Melanogenesis in melanocytes is a complex biosynthetic process involving the tyrosinase-catalyzed oxidation of tyrosine. Two main types of melanin, pheomelanin and eumelanin, are found in human skin and hair. Eumelanin is the brown/black insoluble pigment, characterizing dark phenotypes, and pheomelanin is the red/yellow, sulfur-containing pigment, predominating in red-haired individuals (Slominski et al., 2004). Eumelanin functions as a UV absorbent and subsequently has photoprotective action. Pheomelanin is photolabile and can produce ROS as by-products that lead to further DNA damage and is thus suggested to be carcinogenic following UVR (Brenner and Hearing, 2008).

Tyrosinase, a copper-containing membrane-bound located in melanosomes, catalyzes hydroxylation of L-tyrosine to L-DOPA, which is the first and the rate-limiting step of melanogenesis for both eumelanin and pheomelanin. In addition to tyrosinase, crucial enzymes involved in eumelanin synthesis include tyrosinase related proteins (TRP-1) and dopachrome tautomerase (DCT or TRP-2). Pheomelanin is produced *via* benzothiazine intermediates deriving from the oxidative polymerization of cysteinyl dopa derivatives generated through the condensation of the cysteine or GSH with the dopaquinone (Lu et al., 2021). Environmental stimuli (e.g., UVR and drugs), endogenous factors (e.g., hormone and mediators) and genetic factors can influence melanogenesis regulated by tyrosinase *via* various signal pathways, primarily the melanocortin 1 receptor (MC1R)-microphthalmia-associated transcription factor (MITF) signaling. MC1R is a G protein-coupled receptor that controls the quantity and quality of melanin synthesized in melanocytes. Important agonists of MC1-R acting as the main intrinsic regulator of pigmentation are peptide hormones and neuropeptides including stimulating hormone (α-MSH), endothelin-1 (ET-1) and adrenocorticotropic hormone (ACTH), which are cleavage products of proopiomelanocortin (POMC) (Lin and Fisher, 2007). The major signal transduction pathways that mediate the regulation of melanogenesis involve the binding of agonists to MC1R that trigger events inside melanocytes through raising intracellular cyclic 3′-5′-cyclic adenosine monophosphate (cAMP) and activating the adenylate cyclase enzyme, protein kinase A (PKA), leading to phosphorylation of the cAMP responsive binding element (CREB), which promotes the activation of MITF, which is the master transcription factor that regulates expression of several melanogenic genes including tyrosinase, TYRP1 and TYRP2. Moreover, upon activation of MC1R, enhanced levels of cAMP and subsequent activation of PKA were observed to activate the MAPK signaling cascades including p38, leading to activation of MITF (Smalley and Eisen, 2000). However, inhibition of MC1R in normal melanocytes and melanoma cells was observed to trigger PI3K/Akt and MAPK/ERK pathways, leading to inhibition of MITF and subsequent suppression of melanogenesis (Chae et al., 2017; Wu et al., 2018). Mechanisms underlying the role of phytochemicals in regulating pigmentation involve the direct suppression of tyrosinase activity and/or gene expression, direct scavenging of ROS, promotion of Nrf2-regulated antioxidant defense and inhibition of signaling pathways involved in inflammatory responses (Vomund et al., 2017; Boo, 2019). Nrf2 is suggested to play a role in modulating crucial signaling pathways including MAPK, PI3K/Akt and MC1R-MITF signaling cascades involved in regulation of melanin synthesis (Shin et al., 2014; Chaiprasongsuk et al., 2016). Moreover, exposure of the skin to UVR can stimulate keratinocytes to secrete hormones including ACTH, ET-1, α-MSH that bind to MC1R, activating MITF and upregulating melanogenesis-related proteins. Activation of Nrf2 has been observed to suppress the paracrine factors (such as α-MSH) derived from keratinocytes that results in downregulation of signaling pathways (including the cAMP/CREB/MITF pathway) involved in melanogenesis in melanocytes (Hseu et al., 2020; Chen SJ. et al., 2021). Therefore, application of compounds having abilities to activate Nrf2 might represent a promising approach to prevent and treat hyperpigmentation disorders.

Moreover, in response to UVR, melanogenesis acts as a shield against the harmful effect of UVR on the skin and thus approaches promoting melanin production can mitigate UVR-induced melanocyte damage. We previously demonstrated the role of Nrf2 in regulating the release of paracrine factor α-MSH by keratinocytes that influenced UVB-mediated melanocyte responses including DNA damage, oxidative stress, apoptosis and inflammation (Jeayeng et al., 2017). Several natural compounds such as flavonoids and coumarins having abilities to induce melanogenesis and restore melanocyte viability might thus be useful in the prevention and treatment of hypopigmentation disorders such as vitiligo (Niu and Aisa, 2017). Therefore, phytochemicals have been proposed to exert beneficial effects against abnormal melanogenesis *via* improving hyperpigmentation or hypopigmentation caused by disruption of melanocyte homeostasis and/or loss of functional melanocytes. While this review highlights the studies demonstrating the roles of phytochemicals in improving UVR-induced hyperpigmentation *via* Nrf2-dependent mechanisms, it should be taken into account that melanocyte biology is complex and the role of phytochemicals in regulating melanogenesis involved in maintaining the skin homeostasis needs further clarification.

The Role of Nrf2-Regulated Antioxidant Defense Against Cutaneous Photodamage

The primary endogenous antioxidant defenses include antioxidant and detoxification enzymes such as catalase, glutamate cysteine ligase (GCL) (composed of a catalytic subunit GCLC and a modifier subunit GCLM), the rate-limiting enzyme in GSH synthesis, glutathione peroxidase (GPx), GST, HO-1, NQO-1 and superoxide dismutase (SOD) regulated by various transcription factors including Nrf2 (Surh, 2003; Hseu et al., 2012). Nrf2 is a master regulator of antioxidant and cytoprotective genes involved in the human skin adaption to the environmental insults including UVR and thus plays a beneficial role in maintenance of skin homeostasis. Activity of

Nrf2 is tightly regulated by proteins including Kelch-ECH associated protein 1 (Keap 1) and proteasome degradation system and thus regulation of Nrf2-mediated antioxidant response pathway is complicated. Under homeostatic conditions, two molecules of Keap1 bound to Nrf2 is responsible for the continuous ubiquitylation and degradation of Nrf2. In response to Nrf2 activating stimuli or oxidative stress, Keap1 is oxidized at critical cysteine residues, especially Cys151, leading to dissociation of Keap1-Nrf2 that allows Nrf2 to escape from Keap1-mediated ubiquitination. Nrf2 is then translocated into the nucleus and binds to the ARE promoter, a *cis*-acting enhancer sequence located in the 5′-flanking regions of genes encoding phase II and antioxidant cytoprotective enzymes including GST, NQO-1 and GCL (Schafer et al., 2010; Liu et al., 2016; Boo, 2020b).

Nrf2 plays a vital role in maintaining redox homeostasis and cellular metabolism in skin cells involved in the skin's structural integrity and function (Ikehata and Yamamoto, 2018). Oxidative insults, such as UVR and H_2O_2, and electrophilic chemicals, such as butylated hydroxyanisole and its active de-methylated metabolite *tert*-butyl hydroquinone (tBHQ); phenolic flavonoids [e.g., green tea polyphenols and epigallocatechin-3-gallate (EGCG)]; and the naturally occurring isothiocyanates including sulforaphane (SFN) and curcumin, can stimulate Nrf2 activity *via* modification of Keap1 cysteine residues, suggested as the stress sensors for Nrf2 activator (Baird and Yamamoto, 2020). The cysteine modifications result in a conformational change in the associated motif of Keap1–Nrf2 that facilitates the dissociation of Nrf2 from Keap1 and subsequently Nrf2 nuclear translocation (Kong et al., 2001). Generally, various environmental stressors including UVR lead to post-translational activation of Nrf2 through Keap1 inactivation. The upregulation of Nrf2-mediated antioxidant defense system was demonstrated *in vitro* and *in vivo* to protect the human skin from harmful effects of UVR. UVA-1-mediated lipid oxidation induces expression of antioxidant response genes, which is dependent on the redox-regulated transcription factor Nrf2 in dermal fibroblasts (Gruber et al., 2010). Exposure of keratinocytes (including primary human epidermal keratinocytes and HaCaT keratinocyte cell lines) to UVA (20 J/cm^2) increased Nrf2 activity *via* enhancing Keap1 expression. UVA exposure led to stimulation of Nrf2 activity and its target proteins (HO-1, NQO-1, GST) in HaCaT keratinocytes and dermal fibroblasts, although Nrf2 activity was minimally affected in UVA-irradiated primary keratinocytes (Rysava et al., 2020). In fact, the regulatory role of Nrf2 in skin cell survival and function affected by UVR is complex because UVR can either upregulate or downregulate Nrf2-mediated antioxidant defense in various skin cell types. Changes in the Nrf2 activity are dynamic and dependent on types of UV ray, UVR's intensity and time following the exposure (Chaiprasongsuk et al., 2016; Rysava et al., 2020; Rysava et al., 2021). Previous observations indicate that both UVA and UVB downregulate Nrf2 antioxidant signaling pathway in skin keratinocytes, fibroblasts and melanocytes *in vitro* and in skin tissues *in vivo*. UVB exposure led to reduced expressions of Nrf2 and its target antioxidant HO-1 proteins in HaCaT keratinocyte cells and mouse skin *in vivo*

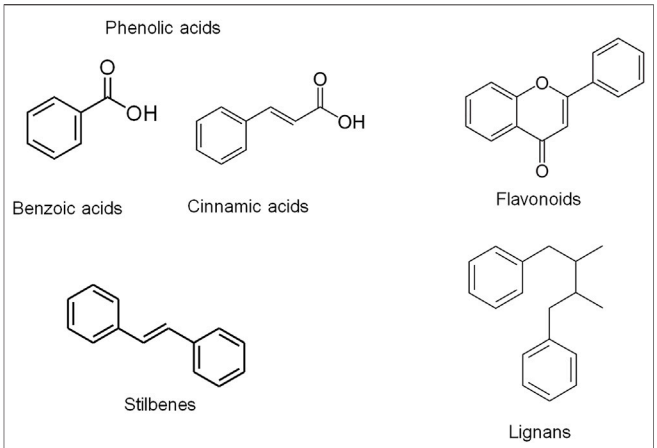

FIGURE 1 | Chemical structures of the different classes of phenolic compounds including phenolic acids, flavonoids, stilbenes and lignans. Phenolic compounds are classified into different groups on the basis of the number of phenolic rings they contain and of the structural elements binding the rings to one another. They are generally divided into four classes including phenolic acids, flavonoids, stilbenes and lignans. Phenolic acids are further classified as hydroxyl benzoic and hydroxyl cinnamic acid derivatives (Johnsson, 2004; Nishiumi et al., 2011).

(Rodriguez-Luna et al., 2018; Rodriguez-Luna et al., 2019). UVR was observed to downregulate antioxidant and detoxifying enzymes including GST, NQO-1 and γ-GCS (γ-glutamylcysteine synthetase) in the skin cells through modulating activity of Nrf2 (Kannan and Jaiswal, 2006; Lohakul et al., 2021b). The DNA damage or modulation of signaling cascades (including MAPKs) that take place rapidly in response to UVR exposure is suggested to mediate the downregulation of Nrf2 antioxidant response pathway (Lopez-Camarillo et al., 2012). The p38 was suggested to reduce Nrf2 nuclear translocation and its transcriptional activity (Boo, 2020b). In addition, activation of Nrf2 signaling has been suggested to protect against UVR-mediated skin damage *via* several mechanisms including promotion of antioxidant and cytoprotective defense, DNA repair, anti-inflammatory signaling. Upregulation of Nrf2/HO-1 signaling accompanied with increased activities and protein levels of catalase, GPx and SOD was observed to suppress apoptosis induced by UVR [UVA (3 J/cm^2)+UVB (90 mJ/cm^2)] *via* activating the PI3K/Akt signaling pathway in the 3D skin model (Xian et al., 2019). Thus, understanding the role of Nrf2 in the pathogenesis of skin photodamage could give an insight into development of potential compounds having Nrf2 inducing activity for prevention and treatment of skin photodamage.

Phytochemicals Targeting Nrf2 in Skin Photodamage: Development of Botanicals and Phytochemicals as Promising Photoprotective Agents

Several reports have highlighted the potential role of bioactive phytochemicals of plant-based diets and botanical drugs that have been used in ethnomedicine or reported in

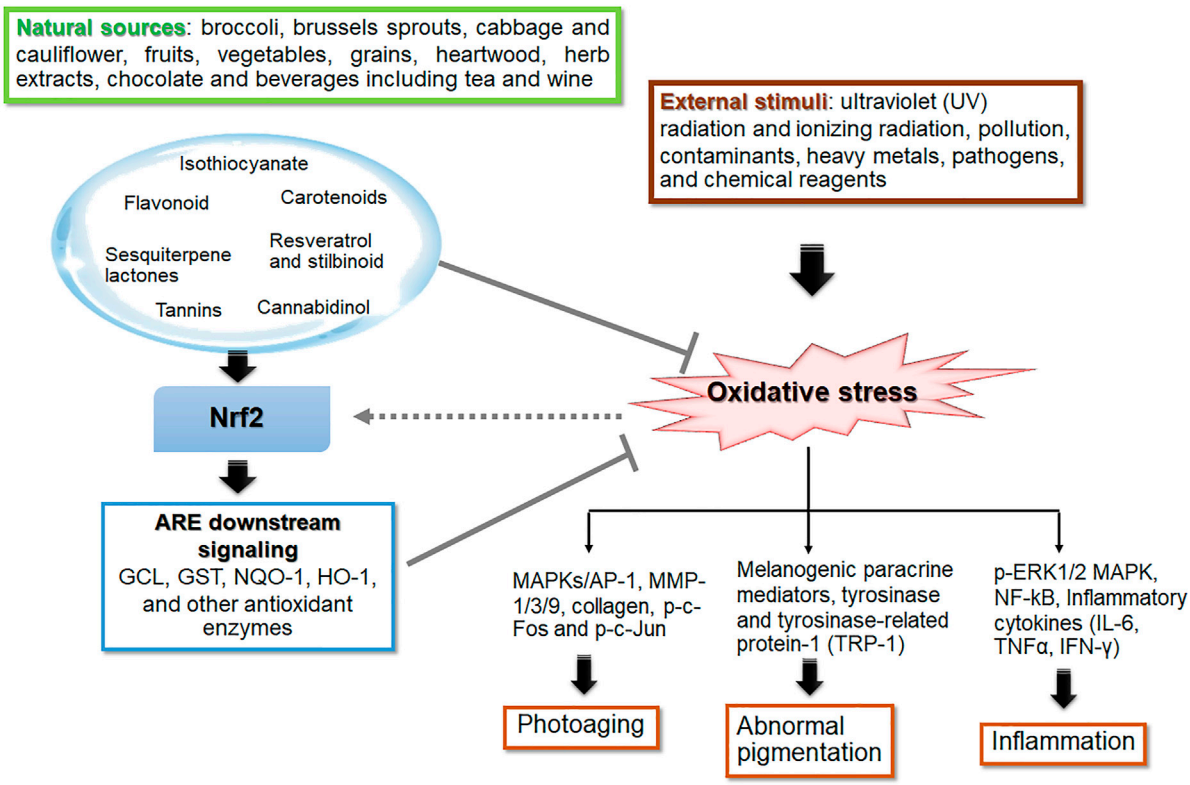

FIGURE 2 | The role of phytochemicals in skin photoprotection *via* regulation of Nrf2 signaling. Phytochemicals are naturally occurring compounds in botanical products which exert biological activities providing medical and nutritional benefit. Oxidative stress, an imbalance in the redox state of the cell, is the result of cellular response to various stimuli including UV and ionizing radiation, pollution, contaminants, heavy metal, pathogens, and chemical reagents. Most of the natural antioxidants are derived from plant materials such as fruits, vegetables, grains, legumes, botanical drugs, spices and plant-based beverages (including tea, coffee, wine and cocoa). The bioactive phytochemicals, e.g., isothiocyanates (in broccoli, brussels sprouts, cabbage and cauliflower), flavonoids, carotenoids, resveratrol and stilbinoid, exhibit a wide range of photoprotective effects, including anti-photoaging, anti-inflammation, and anti-melanogenesis. These protective effects involve activation of nuclear factor erythroid 2-related factor 2 related to the antioxidant response element (Nrf2-ARE) signaling pathway that regulates expression of its downstream target genes including glutamate cysteine ligase (GCL), glutathione S-transferase (GST), NAD(P)H quinone oxidoreductase-1 (NQO-1), heme oxygenase-1 (HO-1) and other antioxidant genes, to cope with various stressors including UVR. The thick arrows and bar-headed lines mean activation and inhibition of the pathway, respectively. The dash arrow means modulation of Nrf2 signaling by ROS levels.

ethnopharmacological studies. The bioactive phytochemicals are naturally occurring compounds in botanical products including plants and botanical drugs which exert biological activities providing medical and nutritional benefit. These compounds exert antioxidant effects by directly scavenging ROS or by promoting the antioxidant defense system through the Nrf2-dependent pathway (L Suraweera et al., 2020). Phytochemicals include polyphenols and the non-phenolic phytochemicals. Phenolic compounds are classified into different groups on the basis of the number of phenolic rings they contain and of the structural elements binding the rings to one another. They are generally divided into four classes including phenolic acids, flavonoids, stilbenes and lignans (**Figure 1**). Phenolic acids are further classified as hydroxyl benzoic and hydroxyl cinnamic acid derivatives (Pandey and Rizvi, 2009). The natural sources of polyphenols include fruits (e.g., apple, berries, cherries, grapes, strawberries and pomegranate), vegetables, soybeans, cereals, tea, cocoa, soy and *Phlebodium aureum* (L.) J.Sm. The common flavonoids include catechins, quercetin, genistein, epicatechin, catechin and anthocyanins (Bosch et al., 2015). The common phenolic acids are hydroxycinnamic acids including caffeic acid and ferulic acid as well as gallic acid (also known as 3,4,5-trihydroxybenzoic acid). Gallic acid is the most abundant phenolic acid found in plant-based diets (Hano and Tungmunnithum, 2020). For non-flavonoid phenolics, the most widely studied stilbene is resveratrol. The commonly studied non-phenolic phytochemicals include carotenoids, caffeine and sulforaphane (SFN) (Bosch et al., 2015).

Phytochemicals play a crucial role in photoprotection against UVR-induced skin photodamage *via* UV-absorbing, antioxidant, melanin-modulating, anti-inflammatory properties Antioxidant phytochemicals have been demonstrated to mitigate skin photodamage *in vitro* and *in vivo via* directly scavenging ROS, promoting antioxidant defense capacity, modulating various signaling pathways involved in inflammation, controlling DNA repair, cellular viability and function of the skin (Boo, 2020a; Garg et al., 2020). This review focuses the photoprotective role of phytochemicals in UVR-mediated photoaging,

hyperpigmentation and inflammation affecting skin barrier integrity *via* Nrf2-dependent pathway (**Figure 2**). The phytochemicals as electrophiles can promote cytoprotective proteins and antioxidant defenses *via* upregulating Nrf2 signaling. Keap1 and Cul3 comprise a unique ubiquitin E3 ligase responsible for degradation of Nrf2. Keap1 is a homodimeric protein belonging to the BTB (Broad complex, Tramtrack, Bric-á-brac)-Kelch family of proteins, which are named Kelch-like 1 to 42 (KLHL1–42). The BTB domain of Keap1 is necessary for Keap1 homodimerization and for mediating interactions with cul3/Rbx1 E3 ubiquitin ligase system. The BTB domain contains reactive cysteine residue responsible for interaction with electrophiles and thus plays a crucial role in sensing environmental electrophiles. Post-translational modifications of the highly reactive Cys 151 in Keap1 result in dimerization of Keap1, resulting in loss of Nrf2 ubiquitination, which stabilize the Nrf2 proteasomal degradation (Shin et al., 2020) and subsequent accumulation of Nrf2 and activation of the Nrf2-driven cytoprotective gene machinery (Cleasby et al., 2014). Phytochemicals, which are thiol-reactive electrophiles, covalently bind to the cysteine residue(s) in the dimerization domain of Keap1. Then, the activated ligase complex fails to degrade Nrf2, allowing the transcriptional activation of Nrf2 target genes (Yamamoto et al., 2008). Well-known Nrf2 activators including the isothiocyanate SFN, the alkylating agent iodoacetamide, tBHQ and diethylmaleate were demonstrated to modify C151 in Keap1, that mediates proteasomal degradation, leading to Nrf2 stabilization and enhancing its nuclear accumulation (Deshmukh et al., 2017; Dayalan Naidu et al., 2018; Dayalan Naidu and Dinkova-Kostova, 2020; Taguchi and Yamamoto, 2020).

In addition to the role of phytochemicals as indirect antioxidants by upregulating antioxidant genes, phytochemicals can act as direct antioxidants by their ROS scavenging activities (Dinkova-Kostova and Talalay, 2008). Direct antioxidants, such as (–)-epicatechin-3-gallate and carotenoids (i.e., β-carotene and lycopene) can protect skin cells from ROS-induced damage to the skin cells. Their protective effects are short-lived and involve their abilities to neutralize ROS. ROS is involved in regulating the activity of Nrf2 *via* several mechanisms. Keap1 is considered as a cysteine-based sensor for a variety of endogenous and exogenous stressors including electrophiles and oxidants. ROS is involved in modulate Nrf2 activity *via* Keap-1-dependent and independent mechanisms. For Keap1-dependent mechanism, ROS (e.g., H_2O_2) has been demonstrated to promote Nrf2 activity via oxidative modification of Keap1 cysteines, leading to the release of Nrf2 and allowing its nuclear translocation (Espinosa-Diez et al., 2015; Suzuki et al., 2019). For Keap1-independent regulation of Nrf2 activity, MAPKs and glycogen synthase kinase-3 (GSK-3) are suggested to play a role in posttranslational modifications of Nrf2 via phosphorylation accountable for the alterations in its binding to the proteins involved in controlling Nrf2 stability and subsequent transcriptional activity (He et al., 2020). For instance, GSK-3 activation can stimulate Nrf2 nuclear export as well as ubiquitination and degradation, leading to downregulation of the Nrf2/ARE signaling pathway of brain ischemia and reperfusion injury (Chen et al., 2016). In addition, suppression of GSK-3 by activation of upstream phosphoinositide 3-kinase-protein kinase B/Akt (PI3K-PKB/Akt) results in Nrf2 stabilization. Activation of ERK leads to Nrf2 downregulation in diabetic hearts in response to oxidative stress (Tan et al., 2011). Thus, it is possible that ROS which can act as second messengers in protein kinase cascades also have a regulatory role in Nrf2 activity *via* Keap1-independent manner. Phytochemical polyphenols that act as both pro-oxidants through autoxidation to generate ROS (Babich et al., 2011) and direct antioxidants that can increase and decrease cellar ROS levels can affect Nrf2 activity *via* both Keap1-dependent and -independent manners.

In fact, skin is the largest body organ that is continuously exposed to environmental stressors including UVR. Oxidative stress induced by UVR plays a role in the stress responses of keratinocytes, melanocytes and fibroblasts responsible for photodamaged skin. Hence, development of phytochemicals that can activate the Nrf2 transcription factor is considered a promising pharmacological strategy to prevent and treat UVR-induced skin damage. The phytochemical derivatives that are effective for these photoprotective strategies include polyphenols, flavonoids, non-flavonoids and non-phenolic derivatives. The phytochemicals having ROS scavenging properties could suppress UVB-induced MMP-1 expression in HaCaT cells and human dermal fibroblasts and promote type I procollagen production in human dermal fibroblasts via downregulation of MAPK/AP-1 signaling cascades in association with upregulation of Nrf2 signaling (Kim et al., 2015). Moreover, botanical extracts including extracts of sunflower (*Helianthus annuus* L.) (Hwang et al., 2019), cherry blossoms (Li et al., 2018) and Foeniculum vulgare Mill. (Sun et al., 2016), which are rich sources of antioxidant phytochemicals, were observed to exert the protective effect against UVB-induced ROS formation, MMPs (MMP-1 and MMP-3) production and procollagen type I depletion *via* downregulation of MAPK signaling in association with upregulation of Nrf2 activity in human dermal fibroblasts. The anti-photoaging actions of the sunflower extract were also related to suppression of UVB-induced inflammatory cytokines including IL-6, COX-2, iNOS (inducible nitric oxide synthase), and TNF-α production (Hwang et al., 2019). In addition, the phytochemicals acting as direct or indirect Nrf2 inducers were demonstrated to exert the anti-photoaging effects *via* downregulation of MMPs including MMP-1 *via* MAPK/AP-1 signaling pathways in mouse skin (Sun et al., 2016; Li et al., 2018). Thus, indirect or direct targeting of Nrf2-dependent antioxidant response could offer a promising pharmacological strategy for prevention and inhibition of skin photodamage. The crosstalk between Nrf2 and other signaling pathways (e.g., MAPK/AP-1 pathway) involved in the mechanisms underlying the protective effects of phytochemicals on photodamaged skin were shown in **Figure 3** (Kim et al., 2015; Sun et al., 2016; Li et al., 2018; Hwang et al., 2019; Garg et al., 2020). Several *in vitro*, *in vivo* and clinical studies showing the protective roles of botanicals and phytochemicals against photoaging, inflammation, skin barrier

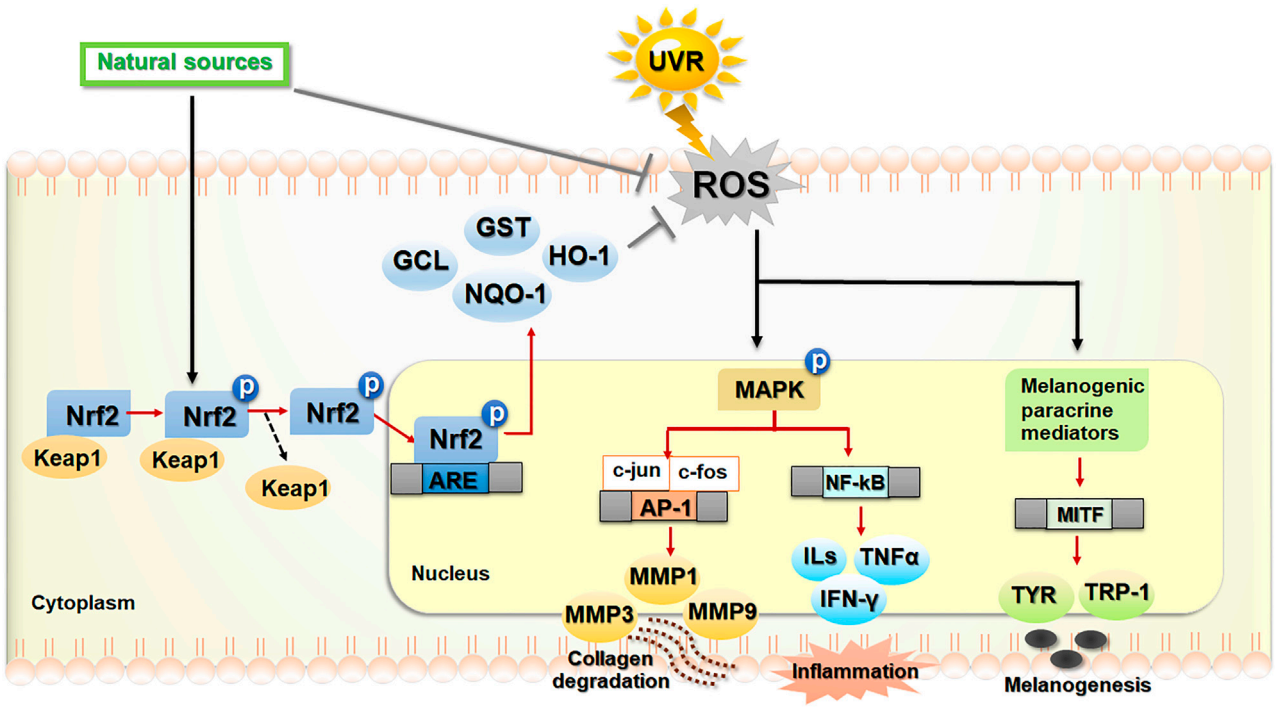

FIGURE 3 | The regulatory mechanism of Nrf2-dependent antioxidant and cytoprotective actions against photoaging, inflammation and hyperpigmentation. Phytochemicals play a photoprotective role against skin photodamage directly *via* scavenging reactive oxygen species (ROS) and indirectly via activation of nuclear factor erythroid 2-related factor 2 (Nrf2) signaling, leading to upregulation of antioxidant and cytoprotective genes. In response to ultraviolet ray (UVR)-induced oxidative stress, ROS, produced in keratinocytes, melanocytes and fibroblasts, can modulate several related signaling pathways involved in photoaging, inflammation and melanogenesis. Exposure of human skin to UVR causes cells to produce ROS, which can modulate the signaling pathways involved in upregulation of matrix metalloproteinases (MMPs) which includes MMP-1/3/9, leading to collagen degradation, inflammation (nuclear factor kappa B also known as NF-κB and its downstream signaling) and the upregulation of melanogenesis-related genes including the microphthalmia-associated transcription factor (MITF), tyrosinase (TYR), and tyrosinase related proteins (TRP-1). Dietary phytochemicals as natural sources of antioxidants play the protective roles against UVR-induced ROS by the inhibition of ROS formation and the activation of Nrf2 signaling. In response to oxidative insults, Nrf2 is activated by the phosphorylation and disassociation of Nrf2 from Kelch-ECH associated protein 1 (Keap1), a repressor protein in the cytoplasm. Then, Nrf2 translocated to the nucleus binds to the ARE in the promoter region of downstream genes encoding antioxidant and phase II detoxifying enzymes including glutamate cysteine ligase (GCL), glutathione S-transferase (GST), NAD(P)H quinone oxidoreductase-1 (NQO-1), heme oxygenase-1 (HO-1). The activation of Nrf2 improves oxidative status of the cells and promotes cytoprotection against skin oxidative damage and inflammation. The black/red arrows and bar-headed lines mean activation and inhibition of the pathway, respectively. The dash arrow means dissociation of the Keap1–Nrf2 complex.

dysfunction and hyperpigmentation *via* Nrf2-dependent mechanisms are described below and summarized in **Table 1**.

Isothiocyanates

Isothiocyanates are sulfur-containing compounds having the general formula R–N=C=S and are commonly found in cruciferous vegetables from the *Brassica* genus including broccoli, brussels sprouts, cabbage and cauliflower. Members of isothiocyanates widely known as Nrf2 activators including SFN and phenethyl isothiocyanate (PEITC) protected human *ex vivo* full skin against UVR-induced sunburn cells, apoptosis and the decreased activity of the antioxidant enzyme catalase in correlation to upregulation of Nrf2 activity and its target genes (γ-GCS, HO-1, NQO-1) in HaCaT keratinocytes (Kleszczynski et al., 2013). SFN (0.6 μM/cm^2) was observed to exert anti-photoaging effects on mouse skin via inhibition of MAPK/AP-1 signaling in UVA-irradiated mouse skin (Chaiprasongsuk et al., 2017). Treatment of keratinocyte cell line NCTC2544 with SFN (10 μM) combined with the Fernblock® XP (1 and 2 mg/ml), obtained from the tropical fern *Phlebodium aureum* (L.) J.Sm., substantially suppressed the production of MMP-1, MMP-3 and IL-1 in association with a decrease in ROS production. The SFN (5 and 10 μM) and Fernblock® XP (1 mg/ml) combination also showed inhibitory effects on melanoma cell growth and migration *in vitro* in association with the ability to inhibit the inflammatory microenvironment and neo-angiogenesis (Serini et al., 2020).

Benzyl isothiocyanate and 6-(Methylsulfinyl)hexyl isothiocyanate derived from Wasabi, have been reported to suppress a transcriptional levels of COX-2, an enzyme synthesizing the pro-inflammatory mediators (Lee et al., 2009; Uto et al., 2012). The disturbance of phosphorylated MAPKs signaling, ERK, p38 kinase, and JNK, was observed in the ITCs treatment, resulting in the downregulation of the transcription of inflammatory genes such as COX-2, iNOS, TNF-α, IL-1β, and IL-6 (Lee et al., 2009; Latronico et al., 2021). The effects of allyl-isothiocyanate and SFN on the Nrf2 nuclear translocation were associated with the downregulation of p65 protein, a subunit of

TABLE 1 | The protective roles of botanicals and phytochemicals against photoaging, inflammation, skin barrier dysfunction and hyperpigmentation *via* Nrf2 regulation.

Phytochemicals	Active compounds and sources	Effects	Treatment and study model	Mechanism of action	References
Isothiocyanates	Sulforaphane (SFN), broccoli, brussels sprouts, cabbage and cauliflower	Anti-photoaging	Topical administration of SFN (0.6 μM/cm^2) for 2 weeks *In vivo*: BALB/c mice	↓: MMP-1, 8-OHdG DNA damage, MAPKs signaling, c-Jun, and c-Fos ↑: Nrf2 translocation, Nrf2-target genes, collagen	Chaiprasongsuk et al. (2017)
	SFN, broccoli, brussels sprouts, wasabi	Anti-inflammation and improvement of skin barrier function	Topical administration of SFN (2.5–10 mg/kg) *In vivo*: BALB/c mice	↓: Janus kinase 1/STAT3 signaling, skin thickness and eosinophil accumulation in atopic dermatitis mouse skin lesions ↑: Nrf2 and Nrf2-dependent antioxidant enzymes (HO-1)	Wu et al. (2019)
	SFN	Hyper-pigmentation	B16F10 cells treated with 10 μM of SFN for 6 h	↓: Tyrosinase activity, melanin content, ROS and 8-OHdG ↑: Nrf2 and Nrf2-dependent antioxidant enzymes (GCL, GST, NQO-1)	Chaiprasongsuk et al. (2016)
Flavonoids	Flavanones (Hesperetin; HSP)	Anti-photoaging	Topical administration of HSP (0.3, 1, and 3 mg/cm^2) for 2 weeks *In vivo*: BALB/c mice	↓: MMP-1, 8-OHdG DNA damage, MAPKs signaling, c-Jun, and c-Fos ↑: Nrf2 translocation, Nrf2-target genes, collagen	Lohakul et al. (2021a)
	Fisetin	Anti-inflammation and improvement of skin barrier function	Topical administration of Fisetin (25–100 μM) for 10 weeks *In vivo*: BALB/c mice	↓: pro-inflammatory mediators (COX-2, IL-6, and NF-κB), aquaporin and filaggrin (the protein markers of skin barrier function) ↑: Nrf2	Wu et al. (2017)
	Caffeic acid, ferulic acid, quercetin and rutin	Hyper-pigmentation	Treatment of cells with of caffeic acid, ferulic acid, quercetin and rutin prior to UVA irradiation *In vitro*: B16F10 melanoma cells	↓: Melanogenesis ↑: Nrf2 and Nrf2 targeted genes	Chaiprasongsuk et al. (2016)
	Ellagic acid		Treatment with ellagic acid (20–80 μM) for 24–72 h *In vitro*: keratinocyte HaCaT cells	↓: protein levels of the paracrine factors, proopiomelanocortin (POMC), α-MSH, and AKT/JNK/ERK signaling ↑: Nrf2 nuclear protein	Yang et al. (2021)
Carotenoids	Rosemary extract (carnosic acid)	Anti-photoaging	Pre-treatment with rosemary extract containing carnosic acid (2.5–10 μM) for 6–9 h *In vitro*: HaCaT keratinocytes and KERTr keratinocytes	↓: matrix metalloproteinases (MMPs) ↑: Nrf2/ARE systems	Calniquer et al. (2021)
	Crystalline lycopene preparations purified from tomato extract (>97%), carotenoid-rich Tomato Nutrient Complex (TNC), rosemary extract	Anti-inflammation and improvement of skin barrier function	Pre-treatment with the different compounds at a concentration of 5 μM *In vitro*: HaCaT keratinocytes	↓: NF-κB activity and IL-6 ↑: ARE/Nrf2 activity	Calniquer et al. (2021)
	Fucoxanthin		topical application of cream containing the fucoxanthin (0.2% w/w) to mouse skin *In vivo*: Female Swiss CD-1 mice	↓: melanin index and skin edema, COX and IL-6 ↑: Nrf2-dependent antioxidant enzymes; heme oxygenase-1 (HO-1)	Rodriguez-Luna et al. (2018)

(Continued on following page)

TABLE 1 | (*Continued*) The protective roles of botanicals and phytochemicals against photoaging, inflammation, skin barrier dysfunction and hyperpigmentation *via* Nrf2 regulation.

Phytochemicals	Active compounds and sources	Effects	Treatment and study model	Mechanism of action	References
Resveratrol and stilbenoid	Grape peel extract, dried heartwood of *Pterocarpus marsupium* Roxb.	Anti-photoaging	Oral administration of either 2 g GPE or 2 mg resveratrol per kg body weight in mice *In vivo*: mice	↓: skin wrinkle formation ↑: Nrf2-dependent antioxidant enzymes; heme oxygenase-1 (HO-1)	Kim et al. (2019)
	Resveratrol	Hyper-pigmentation	Treatment of UVB-irradiated skin with resveratrol *In vivo*: Guinea Pig Skin	↓: MITF and its target proteins including TYR, TRP1, TRP2 ↑: Nrf2/HO-1 proteins	Lee et al. (2014)
	Pterostilbene extracted from the dried heartwood of *Pterocarpus marsupium* Roxb.		Treatment with pterostilbene *In vitro*: B16F10 mouse melanoma cells Keratinocyte HaCaT cells	↓: melanogenesis and tyrosinase activity ↑: Nrf2-mediated HO-1, γ-GCLC, and NQO-1 protein expressions	Li et al. (2017a), Majeed et al. (2020)
	Pterostilbene (Pter)	Anti-inflammation and improvement of skin barrier function	Pre-treatment with Pter (5 and 10 μM) for 24 h prior to UVB irradiation (300 mJ/cm^2) *In vitro*: HaCaT keratinocytes	↓: ROS generation ↑: Nuclear translocation and phosphorylation of Nrf2, expression of Nrf2-dependent antioxidant enzymes, DNA repair activity, phosphatidylinositol-3-kinase (PI3K) phosphorylated kinase, Akt	Li et al. (2017a)
Sesquiterpene lactones	Santamarine isolated from Asteraceae scoparia, artichoke (*Cynara scolymus* L.)	Anti-photoaging	Pre-treatment with Santamarine (1–10 μM) for 1 h *In vitro*: human dermal fibroblasts	↓: ROS levels, MAPKs/AP-1, and MMP-1/3/9, p-c-Fos and p-c-Jun ↑: collagen I, TGF-β/Smad signaling, Nrf2-dependent intracellular antioxidant mechanism (SOD and HO-1)	Oh et al. (2021)
	Cynaropicrin (Cyn)	Anti-inflammation and improvement of skin barrier function	Pre-treatment with Cyn (up to 100 μM) prior to UVB irradiation (50 mJ/cm^2) *In vitro*: Normal human epidermal keratinocyte (NHEKs)	↓: ROS generation, TNF-α, BaP ↑: Nrf2, Nrf2-dependent antioxidant enzymes (NQO-1)	Takei et al. (2015)
Tannins	Red raspberries (*Rubus idaeus* L.) extracts	Anti-photoaging	Pre-treatment with *Rubus idaeus* L. (1–100 μM) for 1 h *In vitro*: normal human dermal fibroblasts (NHDFs)	↓: MAPK/AP-1, NF-κβ and TGF-β/Smad ↑: type I procollagen and Nrf2 nuclear transfer	Gao et al. (2018b)
	Alchemilla mollis (Buser) Rothm. (AM) extract		Treatment with AM (1, 10 and 100 μg/ml) for 4 h after UVB irradiation (144 mJ/cm^2) *In vitro*: NHDFs *In vivo*: hairless mice	↓: ROS production, TGF-β1, MMP-1, IL-6, and nucleus NFATc1 dephosphorylation, wrinkle formation, skin thickening, water loss, and erythema ↑: type I procollagen and elastin expression, Nrf2-dependent antioxidant enzymes (NQO-1 and HO-1)	Hwang et al. (2018)
	Red raspberries extract (RBE)	Anti-inflammation and improvement of skin barrier function	Pre-treatment with RBE (62.5–1,000 μg/ml) for 48 h prior to UVB irradiation (100 mJ/cm^2) Topical treatment with RBE (750 μg/ml) *In vitro*: HaCaT cells *In vivo*: nude mice (ICR-Foxn/nu strain)	↓: Cell viability, epidermal thickness ↑: Nrf2, Nrf2-dependent antioxidant enzymes (catalase, SOD, NQO-1, and HO-1)	Wang et al. (2019)

(Continued on following page)

TABLE 1 | (*Continued*) The protective roles of botanicals and phytochemicals against photoaging, inflammation, skin barrier dysfunction and hyperpigmentation *via* Nrf2 regulation.

Phytochemicals	Active compounds and sources	Effects	Treatment and study model	Mechanism of action	References
Terpenoids: diterpene, triterpene and sesquiterpene	Ginsenosides compound Mx (C-Mx) from Notoginseng stem-leaf	Anti-photoaging	Pre-treatment with the Ginsenosides C-Mx (1–20 uM) for 3–72 h *In vitro*: NHDFs were obtained via skin biopsy from a healthy young male donor	↓: MMP-1 and 3 ↑: Nrf2, Nrf2-dependent antioxidant enzymes (NQO-1 and HO-1), procollagen	Liu et al. (2018)
	Ginsenoside Rg1	Anti-inflammation and improvement of skin barrier function	Pre-treatment with Rg1 (50 μM) for 1 h *In vitro*: HaCaT cells	↓: IL6 and 8 ↑: Nrf2, Nrf2-dependent antioxidant enzymes (GCLC, GCLM, and HO-1)	Li et al. (2016)
	Ginsenoside C-Y, a Ginsenoside Rb2 Metabolite from American Ginseng	Hyper-pigmentation	Pre-treatment with C-Y (10, 20, 30 IM) for 72 h *In vitro*: NHDFs	↓: melanin content and tyrosinase activity ↑: Nrf2, Nrf2-dependent antioxidant enzymes (NQO-1 and HO-1)	Liu et al. (2019)

the transcription factor NF-κB (Wagner et al., 2012). A previous study also suggested a connection between activation of Nrf2 and expression of keratin 16, a key intermediate cytoskeletal protein responsible for maintaining the skin barrier integrity in response to injury or inflammation. While genetic deletion of Nrf2 caused an early onset of hyperkeratotic lesions in *Krt16* null mice which developed palmoplantar keratoma, topical treatment with SFN prevented the development of the skin lesions in footpad skin in association with restoring redox balance (Kerns et al., 2016).

Isothiocyanates including SFN and 7-methylsulfonylheptyl isothiocyanate (7-MSI), the sulfur-rich phytochemicals found in cruciferous vegetables, have been observed to exert anti-melanogenic effects via downregulation of MAPKs, the main regulatory pathways of melanogenesis (Shirasugi et al., 2010). 7-MSI treatment significantly reduced melanogenesis in B16F1 melanoma cells *via* activation of ERK signaling, leading to activation of autophagy and downregulation of MITF, tyrosinase and TRP-1 (Kim et al., 2021). Additionally, SFN exerted protective effects on particulate matter-induced melanogenesis *via* decreasing the release of paracrine factors by keratinocytes (Ko et al., 2020). Our previous study also revealed that the mechanisms underlying the anti-melanogenic effects of SFN involved the activation of Nrf2-mediated antioxidant response (Chaiprasongsuk et al., 2016).

Flavonoids

Flavonoids are most abundant polyphenols found in fruits, vegetables, grains, chocolate and beverages including tea and wine. This group has a common basic structure consisting of two aromatic rings bound together by three carbon atoms forming an oxygenated heterocycle. The flavonoids include flavanols (e.g., catechin, epicatechin), flavonols (e.g., quercetin, kaempferol, rutin), flavanones (e.g., hesperetin), flavones (e.g., apigenin, luteolin, hispidulin), isoflavones (e.g., daidzein, genistein) and anthocyanins (e.g., cyanidin) (Panche et al., 2016).

Rutin (Q-3-*O*-rutinoside) is a flavonol glycoside abundantly found in plants such as tea, onions, wine, apples and berries. Previous studies reported the protective role of rutin in aging on human dermal fibroblasts (HDFs) *via* upregulation of collagen type 1 and downregulation of *MMP-1* mRNA in HDF. Application of the rutin-containing cream also improved skin elasticity as well as length and area of crow's feet (Choi et al., 2016). Furthermore, the analysis of proteome profiles revealed that rutin treatment caused an induction of proteins involved in the antioxidant defenses and a reduction of proteins involved in the degradation of Nrf2 in UVB-irradiated dermal fibroblasts (Gegotek et al., 2018). Hesperidin, (hesperetin-7-rutinoside), and its aglycone, hesperetin, mostly found in citrus fruits and botanical drugs, have been demonstrated to provide *in vitro* and *in vivo* anti-photoaging effects on the skin *via* stimulating collagen synthesis in association with the antioxidant properties (Lohakul et al., 2021a). Citrus sinensis peel extract containing hesperidin loaded lipid nanoparticles showed photoprotective effects on UVR-mediated induction of MMP-1 *via* JNK signaling, reduction of collagen accompanied by decreased SOD protein production as well as stimulated inflammatory markers (COX-2, prostaglandin E2) and lipid oxidation product, malondialdehyde (MDA), in mouse skin (Amer et al., 2021). It was also suggested that the protective effect of a mixture of methylated derivatives of hesperidin on UVB-induced skin damage might involve the abilities to promote Nrf2 nuclear translocation and mRNA levels of its target gene GCLC and HO-1 in keratinocytes (Kuwano et al., 2015). In addition, a clinical trial showed that a 12-week topical application of a serum containing 0.1% hesperetin significantly promoted skin hydration and elasticity *via* enhancing the synthesis of hyaluronic acid (Sheen et al., 2021). Moreover, hesperetin and polyherbal formula extracts containing hesperetin topically applied to mouse skin before UVA exposure three times per week for 2 weeks (a total dose of 60 J/cm^2) significantly attenuated MMP-1 upregulation and collagen depletion concomitant with promoting Nrf2 activity and the level of its target proteins

(GST and NQO-1) as well as reducing 8-hydroxy-2′-deoxyguanosine (8-OHdG), a product of oxidatively damaged DNA damage, in irradiated mouse skin (Lohakul et al., 2021a). Grape fruit stem extract from Muscat Bailey A containing catechin, epicatechin and trans-resveratrol showed protective effects on UVB-induced destruction of collagen fiber through reduction of MMP-1 expression in association with a decrease in lipid peroxidation and restoration of GSH levels in mouse skin (Cho et al., 2018).

Furthermore, flavonoids consequently affect immune mechanisms that are essential in the development of the inflammatory processes (Maleki et al., 2019). Treatment of human epidermal keratinocytes (HaCaT cells) with 6-shogaol, an active ingredient of ginger, resulted in suppressing the UVB (180 mJ/cm^2)-induced iNOS, COX-2 and TNF-α, which are the key mediators of inflammatory response, through modulating Nrf2 signaling (Wu et al., 2011; Du et al., 2018; Chen et al., 2019). In addition, the flavonoids have been suggested to exert anti-inflammatory actions in association with Nrf2 activation *in vitro* and *in vivo*. The mechanisms underlying the anti-inflammatory effects of flavonoids involved inhibition of production of pro-inflammatory cytokines including IL-33, TNF-α, IL-1β, IL-6 and downregulation of NF-κB activity (Staurengo-Ferrari et al., 2018). Gallocatechin-silver nanoparticle was observed to improve wound healing in diabetic rats via inhibiting TLR4/NF-κB inflammatory signaling pathway and modulating Nrf2/HO-1 pathway (Ni et al., 2015). The flavonol Galangin, obtained from *Alpinia officinarum* Hance and propolis extracts, was able to mitigate imiquimod-induced psoriasis-like skin inflammation in BALB/c mice *via* inhibiting pro-inflammatory mediators of COX-2, iNOS, NF-κB pathway and pro-inflammatory cytokines IL-17, IL-23, IL-1β in the skin as well as IL-6, TNF-α in both skin and serum. The anti-inflammatory effects of galangin were also associated with its ability to induce Nrf2 activity (Sangaraju et al., 2021). Recent evidence has revealed that the flavone luteolin improved impaired healing and promoted re-epithelization of skin wound in streptozotocin-induced diabetic rats *via* suppressing expressions of inflammatory proteins including MMP-9, TNF-α, IL-6, IL-1β and downregulating NF-κB in association with activation of Nrf2-dependent upregulation of antioxidant enzymes (Chen LY. et al., 2021). Topical application of a flavonoid fisetin (50 and 200 μM) for 10 weeks to mouse skin after UVB exposure was demonstrated to mitigate skin photodamage by inhibiting MMP-1 and MMP-2 protein expressions and collagen degradation as well as by improving skin barrier dysfunction. The fisetin treatment resulted in restoring skin hydration and barrier function in UVB-irradiated mouse skin through promoting contents of filaggrin, a structural protein in the stratum corneum, and aquaporins, integral epidermal cell membrane proteins, responsible for epidermal hydration and barrier function. The anti-photodamaging effects of fisetin are suggested to involve upregulation of Nrf2 and downregulation of pro-inflammatory mediators (COX-2, IL-6, and NF-κB) (Wu et al., 2017).

We previously observed that caffeic acid, ferulic acid, quercetin and rutin provided anti-melanogenic effects *via* enhancing Nrf2-mediated antioxidant defense responses in UVA-irradiated B16F10 cells (Chaiprasongsuk et al., 2016). Ellagic acid was shown to suppress α-MSH-induced melanin synthesis and tyrosinase activity by downregulating cAMP-mediated CREB and MITF signaling in B16F10 cells. Ellagic acid also had ability to suppress protein levels of the paracrine factors, POMC and α-MSH, through Nrf2 activation in keratinocyte HaCaT cells (Yang et al., 2021).

Licorice root extracts have traditionally been used for skin problems and are suggested as one the top cosmeceutical ingredients for hyperpigmentation (Searle et al., 2020). The root and rhizome extracts of licorice and several flavonoids identified as its bioactive ingredients have been suggested to provide beneficial effects on the skin through tyrosinase inhibitory activity, ROS scavenging activity, anti-inflammatory activity and Nrf2 inducing activity (Ciganovic et al., 2019). Glycyrrhiza flavonoids and licochalcone A, a major component of the licorice root extracts, showed the inhibitory effects on melanogenesis via activation of ERK and the subsequent downregulation of MITF/tyrosinase pathway in B16F10 cells. Isoliquiritigenin, a flavonoid component from the hydrolysis products of licorice root, was observed to exert anti-melanogenic effects on α-MSH-, ACTH- and UV-induced melanin synthesis and on melanocyte dendricity and melanosome transport through downregulation of melanogenic proteins including tyrosinase, TRP-1, DCT, Rab27a and Cdc42 in melanocytes (Lv et al., 2020).

Tannins

There are three major classes of tannins: condensed tannins (e.g., proanthocyanidins, flavonol-based compounds); hydrolyzable tannins (gallotannins and ellagitannins) and phlorotannins. Gallic acid, a chemical constituent of tannins, and its derivatives are found in almost all organ of a plant including bark, wood, leaf (in particular tea leaves), fruit, root and seed.

Red raspberries (*Rubus idaeus* L.) extracts containing high levels of anthocyanins and ellagitannins including Sanguiin H-6 and lambertianin C showed the protective effect on UVB-induced photoaging in normal human dermal fibroblasts (NHDFs). Treatment with the red raspberry extracts resulted in a significant reduction of MMPs secretion and production of pro-inflammatory mediator IL-6 possibly via downregulating MAPK, NF-κβ and AP-1 as well as increased procollagen type I production *via* activating the TGF-β/Smad pathway. The anti-photoaging effects of the tannin-rich botanical drugs involved promotion of Nrf2 activity and its target antioxidants including HO-1 and NQO-1 (Gao et al., 2018b). *Alchemilla mollis* (Buser) Rothm. ethanolic extract possessing gallic acid showed protective effects on UVB-induced photoaging in NHDFs and in mouse skin *in vivo*. Treatment with *Alchemilla mollis* (Buser) Rothm. ethanolic extract led to a substantial reduction in ROS formation as well as MMP-1 and IL-6 promotion through downregulating AP-1 activity in NHDFs exposed to UVB (144 mJ/cm^2) irradiation. Furthermore, treatment with *Alchemilla mollis* (Buser) Rothm. extract and gallic acid protected against UVB-induced a reduction of type I procollagen levels in association with promotion of TGF-β1 *in vitro* and *in vivo*. Oral administration of *Alchemilla mollis* (Buser) Rothm.

extract and gallic acid also improved UVB-induced wrinkle formation, skin dryness, epidermal thickening and collagen fiber density in hairless mice. The antioxidant mechanism underlying the anti-photoaging effects of *Alchemilla mollis* (Buser) Rothm. extract also involved the upregulation of Nrf2/HO-1 pathway (Hwang et al., 2018). Black tea (Fuzhuan-brick tea, rich in gallic acid and tea polyphenols) and gallic acid were also demonstrated to provide anti-photoaging effects *via* upregulation of Nrf2/HO-1 signaling in association with activation of MAPK signaling (p38 and ERK1/2 phosphorylation) in UVB-exposed keratinocyte HaCaT cells (Zhao et al., 2018). Cocoa phytochemicals including procyanidins and the flavanol catechin and epicatechin have been suggested to have several biological activities including antioxidant and anti-inflammatory activities possibly responsible for their beneficial effects on various age-related diseases including skin aging (Kim et al., 2014). Long term consumption of cocoa beverage for 12 weeks protected against UV-induced skin erythema and improved skin conditions (including erythema, skin roughness and scaling) in women (Heinrich et al., 2006). Procyanidins showed abilities to activate Nrf2 signaling in various *in vitro* and *in vivo* models (Truong et al., 2014). Therefore, it is possible that mechanisms underlying the anti-photoaging effects of procyanidins involve activation of Nrf2-regulated antioxidant defenses.

Phlorotannins (PTNs) are tannins found primarily in brown algae and play a role in protecting cells against UVR. PTNs applied topically attenuated radiation-induced inflammatory responses by downregulating NF-κB signaling and its downstream COX-2 and inflammasome activation in a mouse model of radiation dermatitis. PTNs also showed the abilities to promote wound healing process by enhancing aquaporin 3 involved in epidermal hydration and homeostasis. The mechanisms underlying the anti-inflammatory and wound healing-promoting effects of PTNs on irradiated mouse skin also involved upregulation of Nrf2/HO-1 signaling (Yang et al., 2020).

Gallic acid, gallotannin, valonia tannin and extracts of plants (e.g., Ceylon olive leaves and pomegranate peel) containing gallic acid exerted antimelanogenic effects directly by acting as a competitive inhibitor of tyrosinase and indirectly by inhibiting tyrosinase *via* antioxidant actions that affect melanogenesis pathway *in vitro* and *in vivo* (Chen et al., 2009; Panich et al., 2013; Su et al., 2013; Kanlayavattanakul et al., 2020; Huang et al., 2021; Liu et al., 2021). A randomized, double-blind, placebo-controlled clinical trial demonstrated that continuous administration of apple polyphenol rich in procyanidins for 12 weeks improved UV-induced skin pigmentation in heathy women (Shoji et al., 2020). Our previous study demonstrated that gallic acid protected against UVA (8 J/cm^2)-induced melanogenesis via modulation of Nrf2 signaling and promotion of antioxidant defenses (including GSH, catalase, GPx and GST) in B16F10 melanoma cells (Onkoksoong et al., 2018).

Resveratrol and its Derivatives

Resveratrol was observed to provide photoprotective effects in UVB-induced photoaging *via* the antioxidant, anti-inflammatory and antiapoptotic actions in human keratinocyte HaCaT cells and ICR mice *in vivo*. The mechanism underlying its antiphotoaging actions involves upregulation of Nrf2 signaling and the antioxidant defenses (including HO-1, NQO-1, SOD1, GPx-4) in association with suppression of aging markers (MMP-1 and MMP-9) and proinflammatory mediators (IL-6, TNF-α, VEGF-B) by inhibiting ROS-mediated MAPK and COX-2 signaling cascades (Cui et al., 2022). Oral administration of grape peel extract and resveratrol exerted the anti-photoaging effects on UVB-induced skin wrinkle formation *via* promotion of Nrf2/HO-1 signaling cascades (Kim et al., 2019). In addition, a formulation containing 0.4% pterostilbene, the resveratrol analog, extracted from the dried heartwood of *Pterocarpus marsupium* Roxb., showed substantial reduction of aging markers and improvement of wrinkles, skin hydration elasticity in healthy volunteers (Majeed et al., 2020).

Topical treatment with pterostilbene, the resveratrol analog, suppressed an acute UVB radiation-induced skin inflammation and prevented chronic UVB radiation-mediated carcinogenesis in mice. The mechanisms involved in the photoprotective effects of pterostilbene might be attributed its ability to absorb UVB, protect against oxidative damage to DNA, protein and lipid, promote activities of antioxidant enzymes including catalase, SOD and GPx as well as activate Nrf2-dependent antioxidant response (Pastore et al., 2012; Sirerol et al., 2015). Moreover, resveratrol was observed to promote wound healing by restoring cell proliferation and migration, along with increased Nrf2 activity and Mn-SOD expression in the diabetic rat model (Zhou et al., 2021).

Resveratrol acting as a direct antioxidant, Nrf2 activator and tyrosinase inhibitor has been suggested to suppress melanogenesis (Wang et al., 2018; Boo, 2019). Resveratrol treatment led to a substantial reduction of UVB-induced melanogenesis *via* downregulation of MITF and its target proteins including TYR, TRP1, TRP2 in correspondence to upregulation of Nrf2/HO-1 proteins in melanocytes (Jian et al., 2011). Topical administration of 0.4% resveratryl triacetate and 0.4% resveratryl triglycolate twice daily for up to 8 weeks after the artificial pigmentation was shown to provide whitening efficacy in human subjects (Ryu et al., 2015; Jo et al., 2018). Pterostilbene, a stilbinoid, found in blueberries and grapes was demonstrated to exert anti-melanogenic effects *via* promotion of autophagy in melanocytes and downregulation of CREB (cAMP response element-binding protein)-MITF-tyrosinase pathway in B16F10 cells treated with HaCaT conditioned medium. The protective effects of pterostilbene on melanogenesis involved suppression of UVA-induced α-MSH expression and upregulation of Nrf2-mediated HO-1, γ-GCLC, and NQO-1 protein expressions in HaCaT cells (Hseu et al., 2021). Additionally, the application of a 0.4% formulation of natural pterostilbene for 4 and 8 weeks showed the skin brightening and anti-aging effects, respectively, in healthy volunteers in an open-label, single-arm, monocentric efficacy study (Majeed et al., 2020).

Carotenoids

Carotenoids, which belong to the tetraterpenes family, are liposoluble pigments responsible for the yellow, orange or red

color of fruits, leaves and flowers. The carotenoids are divided into carotenes, xanthophylls and lycopene, and are abundantly present in tomato, carrots, pumpkin, seaweeds and algae (Milani et al., 2017). The main carotenoids including astaxanthin, canthaxanthin, β-carotene, lycopene and lutein have been suggested to exert photoprotective effects against UVR-induced skin photodamage *via* inhibition of inflammatory responses and photoaging biomarkers as well as promotion of antioxidant defense system in several *in vitro*, *in vivo* and clinical studies (Aust et al., 2005; Camera et al., 2009; Cavinato et al., 2017; Cooperstone et al., 2017; Kohandel et al., 2022). Previous reports have suggested that the carotenoids including astaxanthin and lycopene exert pharmacological activities including antioxidant, anti-inflammatory and chemopreventive activities against skin damage *via* activation of Nrf2 signaling (Wang et al., 2020; Ahn and Kim, 2021; Kohandel et al., 2021).

Dietary carotenoids combined with rosemary extract containing carnosic acid having abilities to activate Nrf2/ARE system exerted an inhibitory effect on UVB (20–60 mJ/cm^2)-induced TNF-α and MMP-1 secretion from dermal fibroblasts (Calniquer et al., 2021). The tomato extracts rich in lycopene also protected against H_2O_2-induced photodamage of fibroblasts via promotion of pro-collagen secretion and suppression of apoptotic cell death and ROS formation (Darawsha et al., 2021).

Lutein, a xanthophyll carotenoid obtained from green leafy vegetables and egg yolk, has been reported to exert the anti-inflammatory effects *via* modulation of oxidant-sensitive inflammatory signaling pathways including NF-κB and STAT3 pathways and suppression of inflammatory cytokines (such as IL-1β, IL-6, TNF-α, COX-2, iNOS) (Ahn and Kim, 2021). Astaxanthin was demonstrated to exert anti-inflammatory effects by suppressing the expression of pro-inflammatory cytokines, for example, COX-2, LOX-1, NF-κB p65, TNF, and IL-1 (Kishimoto et al., 2010). Additionally, combinations of tomato nutrient complex containing lycopene and carotenoids and rosemary extract containing carnosic acid were observed to protect against UVB-induced oxidative stress, photoaging and inflammatory responses by inhibition of NF-κB activity and IL-6 production, along with activation of the ARE/Nrf2 system using HaCaT and KERTr keratinocyte cell lines (Calniquer et al., 2021). Bixin, an apocarotenoid isolated from the Achiote (*Bixa Orellana* L.), is one of the most consumed food colorants and topical preparations of seed extracts of the achiote have been in ethno-pharmacological use for treatment of wound healing and the pathologies related to epithelial barrier disruption. The mechanisms underlying the pharmacological actions of bioxin in improving skin barrier function were suggested to involve activation of Nrf2-mediated antioxidant systems including thioredoxin (TRX)/thioredoxin reductase (TXNRD1), regulation of peroxisome proliferator-activated receptors (PPARs), responsible for skin homeostasis and epithelial repair and modulation of Toll-like receptor 4 (TLR4)/NF-κB inflammatory signaling pathway (Rojo de la Vega et al., 2017). The marine carotenoid fucoxanthin (found in brown seaweeds, the microalgae and diatoms) showed anti-inflammatory actions through inhibiting proinflammatory cytokines including TNF-α, IL-6 and IL-8 levels as well as suppressing UVB-mediated oxidative stress in keratinocyte HaCaT cells. Moreover, topical application of cream containing the fucoxanthin to mouse skin protected against UVB-induced skin inflammation and hyperplasia *via* downregulation of COX-2 and iNOS, along with upregulation of Nrf2 activity and its target protein HO-1 (Rodriguez-Luna et al., 2018).

Terpenoids: Diterpene, Triterpene and Sesquiterpene

Santamarine, a sesquiterpene lactone, isolated from sunflower family provided anti-photoaging effects via suppression of UVA (8 J/cm^2)-induced MAPK/AP-1 pathways involved in upregulation of MMPs and *via* promotion of TGF-β/Smad-mediated collagen production in HDFs. Furthermore, santamarine treatment led to a significant restoration of UVA-mediated downregulation of Nrf2-dependent antioxidant defenses including SOD-1 and HO-1 at the mRNA and protein levels (Oh et al., 2021). Zerumbone (ZER), a natural sesquiterpene, from *Zingiber zerumbet* (L.) Roscoe ex Sm. rhizomes was demonstrated to protect against UVA irradiation (3 J/cm^2)-induced ROS formation, MMP-1 activity and collagen III degradation in HDFs. ZER was suggested to exert the anti-photoaging effects *via* downregulation of AP-1 activity and promotion of Nrf2/ARE pathway (Hseu et al., 2019). Furthermore, treatment of dermal fibroblasts with rosemary extracts rich in the diterpene carnosic acid having abilities to induce ARE/Nrf2 reporter activity protected against TNF-α-induced MMP-1 secretion (Calniquer et al., 2021). Ginsenosides, triterpene saponins, are major bioactive compounds responsible for pharmacological activities of Panax (ginseng), which has traditionally been used to treat and prevent various conditions associated with aging including skin aging. Previous studies demonstrated that the rare minor ginsenosides (C-Mc and Mx), which may act as potential antiphotoaging compounds, suppressed MMP production *via* regulating MAPK/AP-1/NF-κB pathway and promoted collagen production via the TGF-β/Smad pathway in association with upregulation of Nrf2 signaling in UVB-irradiated human dermal fibroblasts (Liu et al., 2018; Liu et al., 2022).

Cynaropicrin, a sesquiterpene lactone, is the major bioactive phytochemical in the artichoke (*Cynara cardunculus* L.) that can activate aryl hydrocarbon receptor (AhR), resulting in nuclear translocation of Nrf2. Activation of AhR/Nrf2/NQO-1 pathway by cynaropicrin was involved in its inhibitory effects on UVB-mediated production of proinflammatory cytokines including IL-1 and TNF-α in keratinocytes (Takei et al., 2015). Hemistepsin A, a sesquiterpene lactone isolated from *Saussurea lyrata* (Bunge) Franch., has been demonstrated to exert pharmacological actions including anti-inflammatory and antioxidant activities. Treatment of keratinocyte HaCaT cells with hemistepsin A protected against H_2O_2-induced cytotoxicity, DNA damage and apoptosis-mediated by mitochondrial dysfunction via upregulation of Nrf2/HO-1 signaling pathway (Park et al., 2020). The ginseng leaf extract rich in ginsenosides (including ginsenoside Rg1) applied topically

to mouse skin protected against UVB-induced photoaging and skin barrier dysfunction through suppression of MMP-2, MMP-9 and MMP-13 protein expressions (Hong et al., 2017). Moreover, ginsenoside Rg1 showed anti-inflammatory effects against UVB-induced glucocorticoid resistance in keratinocyte HaCaT cells via promotion of Nrf2 activity (Li et al., 2016).

The sesquiterpene lactone eupalinolide A and B from *Eupatorium lindleyanum* DC. showed inhibitory effects against UVB-induced melanogenesis, skin damage and inflammatory responses *in vitro* and mouse skin *in vivo* (Yamashita et al., 2012). Previous evidence revealed that, apart from the anti-photoaging effect, a minor ginsenoside (C-Y) having ability to induce Nrf2 activity was observed to exert whitening effects by inhibiting melanin production, tyrosinase activity in Melan-a and zebrafish embryos (Liu et al., 2019).

Cannabidinol

Cannabidiol (CBD), the second most prevalent active ingredient in cannabis, is the non-psychoactive phytocannabinoid that has antioxidant and anti-inflammatory effects. CBD has been reported to provide photoprotective effects against UVA and UVB-induced damage to skin cells including NHDFs and keratinocyte HaCaT cells (Vacek et al., 2021). Treatment of 2D and 3D cultured fibroblasts with CBD caused a substantial attenuation in the levels of lipid peroxidation-derived aldehydes (4-hydroxynonenal (HNE), MDA and acrolein-protein adducts) in UVA (20 J/cm^2)- and UVB (200 mJ/cm^2)-irradiated cells (Gegotek et al., 2019). The formation of aldehyde-protein adducts induced by the highly reactive aldehydes could subsequently change the structure and/or function of several proteins including main ECM elastin in hairless mice exposed to UVA (Larroque-Cardoso et al., 2015). In addition, 4-HNE was suggested to play a role in UVA-induced fibroblast senescence in skin photoaging (Swiader et al., 2021). The compounds having abilities to neutralize aldehydes and inhibit the formation of protein adducts could thus have a beneficial role against skin photoaging.

Moreover, the analytical chemistry revealed that CBD compound could interact with the Nrf2/NF-κB transcriptional activity (Jastrzab et al., 2019). The biological effects of CBD have been found to maintain membrane integrity by preventing protein and phospholipid modifications (Atalay et al., 2020) and prevent the inflammatory responses (nuclear receptor coactivator-3 and paralemmin-3) (Atalay et al., 2021).

CONCLUSION AND FUTURE CHALLENGES: INSIGHT INTO ETHNOPHARMACOLOGY

Ethnopharmacology is defined as "the interdisciplinary exploration of biologically active agents traditionally employed or observed by man" (Bruhn and Rivier, 2019). Identifying the ingredients and exploring the effects of the ingredients are crucial in the study of traditional medicine. Phytochemicals are bioactive compounds in plant-based products that have been historically used to rejuvenate the skin and alleviate skin disorders. Bioactive compounds of plant origin have thus been considered as invaluable sources of potential preventive or therapeutic agents for dermatological indications due to their pharmacological activities including antioxidant, UV absorption and anti-inflammation. The phytochemicals exert antioxidant effects by directly scavenging ROS or by promoting the antioxidant defense system through activation of Nrf2 signaling. It should also be taken into consideration that while Nrf2 plays a crucial role in maintaining cellular homeostasis under stress and inflammatory conditions, several studies have discussed a detrimental aspect of Nrf2 defined as the "dark side of Nrf2" in the cancer biology as enhanced Nrf2 activity is involved in a pro-carcinogenic effect and therapeutic resistance of cancer cells (Sporn and Liby, 2012). Thus, dietary phytochemicals having the potential to provide either chemopreventive or cancer-promotive properties, depending on the stage of carcinogenesis (L Suraweera et al., 2020). This review discusses the protective role of Nrf2 against UVR-induced skin photodamage and thus application of phytochemicals acting as Nrf2 activators is regarded as a promising strategy to prevent and treat premature aging and photodamage-related skin problems. Targeting Nrf2-dependent antioxidant and cytoprotective response has been suggested to represent a promising pharmacological strategy for development of effective and safe anti-photoaging and photoprotective agents. Furthermore, the therapeutic potential of phytochemicals can be limited by their poor bioavailability and thus development of drug delivery systems (such as nano-engineered formulations) is needed to improve efficacy of promising bioactive compounds as effective photoprotective agents.

AUTHOR CONTRIBUTIONS

AC wrote the manuscript and created the graphical figure and tables; UP contributed to the design, the conception of the study and wrote the manuscript. All authors have read and approved the final manuscript.

FUNDING

This work was supported by the Thailand Research Fund (Grant Number: RSA6280101), the "Mahidol University" Grant; and the Chulabhorn Royal Academy. This work was financially supported by Office of the Permanent Secretary, Ministry of Higher Education, Science, Research and Innovation, "Research Grant for New Scholar (RGNS)", Grant No. RGNS 63-246.

REFERENCES

Afaq, F., Zaid, M. A., Khan, N., Dreher, M., and Mukhtar, H. (2009). Protective Effect of Pomegranate-Derived Products on UVB-Mediated Damage in Human Reconstituted Skin. *Exp. Dermatol.* 18 (6), 553–561. doi:10.1111/j.1600-0625.2008.00829.x

Ahn, Y. J., and Kim, H. (2021). Lutein as a Modulator of Oxidative Stress-Mediated Inflammatory Diseases. *Antioxidants (Basel)* 10 (9). doi:10.3390/antiox10091448

Amer, R. I., Ezzat, S. M., Aborehab, N. M., Ragab, M. F., Mohamed, D., Hashad, A., et al. (2021). Downregulation of MMP1 Expression Mediates the Anti-aging Activity of Citrus Sinensis Peel Extract Nanoformulation in UV Induced Photoaging in Mice. *Biomed. Pharmacother.* 138, 111537. doi:10.1016/j.biopha.2021.111537

Angel, P., Szabowski, A., and Schorpp-Kistner, M. (2001). Function and Regulation of AP-1 Subunits in Skin Physiology and Pathology. *Oncogene* 20 (19), 2413–2423. doi:10.1038/sj.onc.1204380

Atalay, S., Dobrzyńska, I., Gęgotek, A., and Skrzydlewska, E. (2020). Cannabidiol Protects Keratinocyte Cell Membranes Following Exposure to UVB and Hydrogen Peroxide. *Redox Biol.* 36, 101613. doi:10.1016/j.redox.2020.101613

Atalay, S., Gęgotek, A., Wroński, A., Domigues, P., and Skrzydlewska, E. (2021). Therapeutic Application of Cannabidiol on UVA and UVB Irradiated Rat Skin. A Proteomic Study. *J. Pharm. Biomed. Anal.* 192, 113656. doi:10.1016/j.jpba.2020.113656

Aust, O., Stahl, W., Sies, H., Tronnier, H., and Heinrich, U. (2005). Supplementation with Tomato-Based Products Increases Lycopene, Phytofluene, and Phytoene Levels in Human Serum and Protects against UV-Light-Induced Erythema. *Int. J. Vitam Nutr. Res.* 75 (1), 54–60. doi:10.1024/0300-9831.75.1.54

Babich, H., Schuck, A. G., Weisburg, J. H., and Zuckerbraun, H. L. (2011). Research Strategies in the Study of the Pro-oxidant Nature of Polyphenol Nutraceuticals. *J. Toxicol.* 2011, 467305. doi:10.1155/2011/467305

Baird, L., and Yamamoto, M. (2020). The Molecular Mechanisms Regulating the KEAP1-NRF2 Pathway. *Mol. Cell Biol* 40 (13). doi:10.1128/MCB.00099-20

Berman, B., and Cockerell, C. J. (2013). Pathobiology of Actinic Keratosis: Ultraviolet-dependent Keratinocyte Proliferation. *J. Am. Acad. Dermatol.* 68 (1 Suppl. 1), S10–S19. doi:10.1016/j.jaad.2012.09.053

Biniek, K., Levi, K., and Dauskardt, R. H. (2012). Solar UV Radiation Reduces the Barrier Function of Human Skin. *Proc. Natl. Acad. Sci. U S A.* 109 (42), 17111–17116. doi:10.1073/pnas.1206851109

Boo, Y. C. (2020a). Emerging Strategies to Protect the Skin from Ultraviolet Rays Using Plant-Derived Materials. *Antioxidants (Basel)* 9 (7). doi:10.3390/antiox9070637

Boo, Y. C. (2019). Human Skin Lightening Efficacy of Resveratrol and its Analogs: From *In Vitro* Studies to Cosmetic Applications. *Antioxidants (Basel)* 8 (9). doi:10.3390/antiox8090332

Boo, Y. C. (2020b). Natural Nrf2 Modulators for Skin Protection. *Antioxidants (Basel)* 9 (9). doi:10.3390/antiox9090812

Bosch, R., Philips, N., Suárez-Pérez, J. A., Juarranz, A., Devmurari, A., Chalensouk-Khaosaat, J., et al. (2015). Mechanisms of Photoaging and Cutaneous Photocarcinogenesis, and Photoprotective Strategies with Phytochemicals. *Antioxidants (Basel)* 4 (2), 248–268. doi:10.3390/antiox4020248

Brand, R. M., Epperly, M. W., Stottlemyer, J. M., Skoda, E. M., Gao, X., Li, S., et al. (2017). A Topical Mitochondria-Targeted Redox-Cycling Nitroxide Mitigates Oxidative Stress-Induced Skin Damage. *J. Invest. Dermatol.* 137 (3), 576–586. doi:10.1016/j.jid.2016.09.033

Braun, S., Hanselmann, C., Gassmann, M. G., auf dem Keller, U., Born-Berclaz, C., Chan, K., et al. (2002). auf dem Keller, UNrf2 transcription factor, a novel target of keratinocyte growth factor action which regulates gene expression and inflammation in the healing skin wound. *Mol. Cell Biol* 22 (15), 5492–5505. doi:10.1128/MCB.22.15.5492-5505.2002

Brem, R., Macpherson, P., Guven, M., and Karran, P. (2017). Oxidative Stress Induced by UVA Photoactivation of the Tryptophan UVB Photoproduct 6-Formylindolo[3,2-B]carbazole (FICZ) Inhibits Nucleotide Excision Repair in Human Cells. *Sci. Rep.* 7 (1), 4310. doi:10.1038/s41598-017-04614-8

Brenner, M., and Hearing, V. J. (2008). The Protective Role of Melanin against UV Damage in Human Skin. *Photochem. Photobiol.* 84 (3), 539–549. doi:10.1111/j.1751-1097.2007.00226.x

Bruhn, J. G., and Rivier, L. (2019). Ethnopharmacology - A Journal, a Definition and a Society. *J. Ethnopharmacol* 242, 112005. doi:10.1016/j.jep.2019.112005

Calniquer, G., Khanin, M., Ovadia, H., Linnewiel-Hermoni, K., Stepensky, D., Trachtenberg, A., et al. (2021). Combined Effects of Carotenoids and Polyphenols in Balancing the Response of Skin Cells to UV Irradiation. *Molecules* 26 (7). doi:10.3390/molecules26071931

Camera, E., Mastrofrancesco, A., Fabbri, C., Daubrawa, F., Picardo, M., Sies, H., et al. (2009). Astaxanthin, Canthaxanthin and Beta-Carotene Differently Affect UVA-Induced Oxidative Damage and Expression of Oxidative Stress-Responsive Enzymes. *Exp. Dermatol.* 18 (3), 222–231. doi:10.1111/j.1600-0625.2008.00790.x

Cavinato, M., Waltenberger, B., Baraldo, G., Grade, C. V. C., Stuppner, H., and Jansen-Dürr, P. (2017). Plant Extracts and Natural Compounds Used against UVB-Induced Photoaging. *Biogerontology* 18 (4), 499–516. doi:10.1007/s10522-017-9715-7

Chae, J. K., Subedi, L., Jeong, M., Park, Y. U., Kim, C. Y., Kim, H., et al. (2017). Gomisin N Inhibits Melanogenesis through Regulating the PI3K/Akt and MAPK/ERK Signaling Pathways in Melanocytes. *Int. J. Mol. Sci.* 18 (2). doi:10.3390/ijms18020471

Chaiprasongsuk, A., Lohakul, J., Soontrapa, K., Sampattavanich, S., Akarasereenont, P., and Panich, U. (2017). Activation of Nrf2 Reduces UVA-Mediated MMP-1 Upregulation via MAPK/AP-1 Signaling Cascades: The Photoprotective Effects of Sulforaphane and Hispidulin. *J. Pharmacol. Exp. Ther.* 360 (3), 388–398. doi:10.1124/jpet.116.238048

Chaiprasongsuk, A., Onkoksoong, T., Pluemsamran, T., Limsaengurai, S., and Panich, U. (2016). Photoprotection by Dietary Phenolics against Melanogenesis Induced by UVA through Nrf2-dependent Antioxidant Responses. *Redox Biol.* 8, 79–90. doi:10.1016/j.redox.2015.12.006

Chang, L., and Karin, M. (2001). Mammalian MAP Kinase Signalling Cascades. *Nature* 410 (6824), 37–40. doi:10.1038/35065000

Chang, T. M., Tsen, J. H., Yen, H., Yang, T. Y., and Huang, H. C. (2017). Extract from Periostracum Cicadae Inhibits Oxidative Stress and Inflammation Induced by Ultraviolet B Irradiation on HaCaT Keratinocytes. *Evid. Based Complement. Alternat Med.* 2017, 8325049. doi:10.1155/2017/8325049

Chen, F., Tang, Y., Sun, Y., Veeraraghavan, V. P., Mohan, S. K., and Cui, C. (2019). 6-shogaol, a Active Constiuents of Ginger Prevents UVB Radiation Mediated Inflammation and Oxidative Stress through Modulating NrF2 Signaling in Human Epidermal Keratinocytes (HaCaT Cells). *J. Photochem. Photobiol. B* 197, 111518. doi:10.1016/j.jphotobiol.2019.111518

Chen, L. G., Chang, W. L., Lee, C. J., Lee, L. T., Shih, C. M., and Wang, C. C. (2009). Melanogenesis Inhibition by Gallotannins from Chinese Galls in B16 Mouse Melanoma Cells. *Biol. Pharm. Bull.* 32 (8), 1447–1452. doi:10.1248/bpb.32.1447

Chen, L. Y., Cheng, H. L., Kuan, Y. H., Liang, T. J., Chao, Y. Y., and Lin, H. C. (2021a). Therapeutic Potential of Luteolin on Impaired Wound Healing in Streptozotocin-Induced Rats. *Biomedicines* 9 (7). doi:10.3390/biomedicines9070761

Chen, S. J., Hseu, Y. C., Gowrisankar, Y. V., Chung, Y. T., Zhang, Y. Z., Way, T. D., et al. (2021b). The Anti-melanogenic Effects of 3-O-Ethyl Ascorbic Acid via Nrf2-Mediated α-MSH Inhibition in UVA-Irradiated Keratinocytes and Autophagy Induction in Melanocytes. *Free Radic. Biol. Med.* 173, 151–169. doi:10.1016/j.freeradbiomed.2021.07.030

Chen, X., Liu, Y., Zhu, J., Lei, S., Dong, Y., Li, L., et al. (2016). GSK-3β Downregulates Nrf2 in Cultured Cortical Neurons and in a Rat Model of Cerebral Ischemia-Reperfusion. *Sci. Rep.* 6, 20196. doi:10.1038/srep20196

Cho, B. O., Che, D. N., Shin, J. Y., Kang, H. J., and Jang, S. I. (2018). Ameliorative Effects of Fruit Stem Extract from Muscat Bailey A against Chronic UV-Induced Skin Damage in BALB/c Mice. *Biomed. Pharmacother.* 97, 1680–1688. doi:10.1016/j.biopha.2017.12.003

Choi, S. J., Lee, S. N., Kim, K., Joo, da. H., Shin, S., Lee, J., et al. (2016). Biological Effects of Rutin on Skin Aging. *Int. J. Mol. Med.* 38 (1), 357–363. doi:10.3892/ijmm.2016.2604

Ciganović, P., Jakimiuk, K., Tomczyk, M., and Zovko Končić, M. (2019). Glycerolic Licorice Extracts as Active Cosmeceutical Ingredients: Extraction Optimization, Chemical Characterization, and Biological Activity. *Antioxidants* 8 (10), 445. doi:10.3390/antiox8100445

Cleasby, A., Yon, J., Day, P. J., Richardson, C., Tickle, I. J., Williams, P. A., et al. (2014). Structure of the BTB Domain of Keap1 and its Interaction with the Triterpenoid Antagonist CDDO. *PLoS One* 9 (6), e98896. doi:10.1371/journal.pone.0098896

Cooperstone, J. L., Tober, K. L., Riedl, K. M., Teegarden, M. D., Cichon, M. J., Francis, D. M., et al. (2017). Tomatoes Protect against Development of UV-Induced Keratinocyte Carcinoma via Metabolomic Alterations. *Sci. Rep.* 7 (1), 5106. doi:10.1038/s41598-017-05568-7

Cui, B., Wang, Y., Jin, J., Yang, Z., Guo, R., Li, X., et al. (2022). Resveratrol Treats UVB-Induced Photoaging by Anti-MMP Expression, through Anti-inflammatory, Antioxidant, and Antiapoptotic Properties, and Treats Photoaging by Upregulating VEGF-B Expression. *Oxid Med. Cell Longev* 2022, 6037303. doi:10.1155/2022/6037303

D'Orazio, J., Jarrett, S., Amaro-Ortiz, A., and Scott, T. (2013). UV Radiation and the Skin. *Int. J. Mol. Sci.* 14 (6), 12222–12248. doi:10.3390/ijms140612222

Darawsha, A., Trachtenberg, A., Levy, J., and Sharoni, Y. (2021). The Protective Effect of Carotenoids, Polyphenols, and Estradiol on Dermal Fibroblasts under Oxidative Stress. *Antioxidants (Basel)* 10 (12). doi:10.3390/antiox10122023

Dayalan Naidu, S., and Dinkova-Kostova, A. T. (2020). KEAP1, a Cysteine-Based Sensor and a Drug Target for the Prevention and Treatment of Chronic Disease. *Open Biol.* 10 (6), 200105. doi:10.1098/rsob.200105

Dayalan Naidu, S., Muramatsu, A., Saito, R., Asami, S., Honda, T., Hosoya, T., et al. (2018). C151 in KEAP1 Is the Main Cysteine Sensor for the Cyanoenone Class of NRF2 Activators, Irrespective of Molecular Size or Shape. *Sci. Rep.* 8 (1), 8037. doi:10.1038/s41598-018-26269-9

Denat, L., Kadekaro, A. L., Marrot, L., Leachman, S. A., and Abdel-Malek, Z. A. (2014). Melanocytes as Instigators and Victims of Oxidative Stress. *J. Invest. Dermatol.* 134 (6), 1512–1518. doi:10.1038/jid.2014.65

Deshmukh, P., Unni, S., Krishnappa, G., and Padmanabhan, B. (2017). The Keap1-Nrf2 Pathway: Promising Therapeutic Target to Counteract ROS-Mediated Damage in Cancers and Neurodegenerative Diseases. *Biophys. Rev.* 9 (1), 41–56. doi:10.1007/s12551-016-0244-4

Didier, C., Kerblat, I., Drouet, C., Favier, A., Béani, J. C., and Richard, M. J. (2001). Induction of Thioredoxin by Ultraviolet-A Radiation Prevents Oxidative-Mediated Cell Death in Human Skin Fibroblasts. *Free Radic. Biol. Med.* 31 (5), 585–598. doi:10.1016/s0891-5849(01)00617-7

Dinkova-Kostova, A. T., and Talalay, P. (2008). Direct and Indirect Antioxidant Properties of Inducers of Cytoprotective Proteins. *Mol. Nutr. Food Res.* 52 Suppl 1 (Suppl. 1), S128–S138. doi:10.1002/mnfr.200700195

Dissemond, J., Schneider, L. A., Brenneisen, P., Briviba, K., Wenk, J., Wlaschek, M., et al. (2003). Protective and Determining Factors for the Overall Lipid Peroxidation in Ultraviolet A1-Irradiated Fibroblasts: *In Vitro* and *In Vivo* Investigations. *Br. J. Dermatol.* 149 (2), 341–349. doi:10.1046/j.1365-2133.2003.05457.x

Du, D., Yao, L., Zhang, R., Shi, N., Shen, Y., Yang, X., et al. (2018). Protective Effects of Flavonoids from Coreopsis Tinctoria Nutt. On Experimental Acute Pancreatitis via Nrf-2/ARE-Mediated Antioxidant Pathways. *J. Ethnopharmacol* 224, 261–272. doi:10.1016/j.jep.2018.06.003

Dunaway, S., Odin, R., Zhou, L., Ji, L., Zhang, Y., and Kadekaro, A. L. (2018). Natural Antioxidants: Multiple Mechanisms to Protect Skin from Solar Radiation. *Front. Pharmacol.* 9, 392. doi:10.3389/fphar.2018.00392

Egawa, G., and Kabashima, K. (2018). Barrier Dysfunction in the Skin Allergy. *Allergol. Int.* 67 (1), 3–11. doi:10.1016/j.alit.2017.10.002

Espinosa-Diez, C., Miguel, V., Mennerich, D., Kietzmann, T., Sánchez-Pérez, P., Cadenas, S., et al. (2015). Antioxidant Responses and Cellular Adjustments to Oxidative Stress. *Redox Biol.* 6, 183–197. doi:10.1016/j.redox.2015.07.008

Fanjul-Fernández, M., Folgueras, A. R., Cabrera, S., and López-Otín, C. (2010). Matrix Metalloproteinases: Evolution, Gene Regulation and Functional Analysis in Mouse Models. *Biochim. Biophys. Acta* 1803 (1), 3–19. doi:10.1016/j.bbamcr.2009.07.004

Gao, W., Lin, P., Hwang, E., Wang, Y., Yan, Z., Ngo, H. T. T., et al. (2018a). Pterocarpus Santalinus L. Regulated Ultraviolet B Irradiation-Induced Procollagen Reduction and Matrix Metalloproteinases Expression through Activation of TGF-β/Smad and Inhibition of the MAPK/AP-1 Pathway in Normal Human Dermal Fibroblasts. *Photochem. Photobiol.* 94 (1), 139–149. doi:10.1111/php.12835

Gao, W., Wang, Y.-s., Hwang, E., Lin, P., Bae, J., Seo, S. A., et al. (2018b). Rubus Idaeus L. (Red Raspberry) Blocks UVB-Induced MMP Production and Promotes Type I Procollagen Synthesis via Inhibition of MAPK/AP-1, NF-Kβ and Stimulation of TGF-β/Smad, Nrf2 in normal Human Dermal Fibroblasts. *J. Photochem. Photobiol. B: Biol.* 185, 241–253. doi:10.1016/j.jphotobiol.2018.06.007

Garg, C., Sharma, H., and Garg, M. (2020). Skin Photo-protection with Phytochemicals against Photo-Oxidative Stress, Photo-Carcinogenesis, Signal Transduction Pathways and Extracellular Matrix Remodeling-An Overview. *Ageing Res. Rev.* 62, 101127. doi:10.1016/j.arr.2020.101127

Gęgotek, A., Atalay, S., Domingues, P., and Skrzydlewska, E. (2019). The Differences in the Proteome Profile of Cannabidiol-Treated Skin Fibroblasts Following UVA or UVB Irradiation in 2D and 3D Cell Cultures. *Cells* 8 (9). doi:10.3390/cells8090995

Gęgotek, A., Domingues, P., and Skrzydlewska, E. (2018). Proteins Involved in the Antioxidant and Inflammatory Response in Rutin-Treated Human Skin Fibroblasts Exposed to UVA or UVB Irradiation. *J. Dermatol. Sci.* 90 (3), 241–252. doi:10.1016/j.jdermsci.2018.02.002

Gęgotek, A., Rybałtowska-Kawałko, P., and Skrzydlewska, E. (2017). Rutin as a Mediator of Lipid Metabolism and Cellular Signaling Pathways Interactions in Fibroblasts Altered by UVA and UVB Radiation. *Oxidative Med. Cell Longevity* 2017, 1–20. doi:10.1155/2017/4721352

Gęgotek, A., and Skrzydlewska, E. (2015). The Role of Transcription Factor Nrf2 in Skin Cells Metabolism. *Arch. Dermatol. Res.* 307 (5), 385–396. doi:10.1007/s00403-015-1554-2

Greenlee, K. J., Werb, Z., and Kheradmand, F. (2007). Matrix Metalloproteinases in Lung: Multiple, Multifarious, and Multifaceted. *Physiol. Rev.* 87 (1), 69–98. doi:10.1152/physrev.00022.2006

Gruber, F., Mayer, H., Lengauer, B., Mlitz, V., Sanders, J. M., Kadl, A., et al. (2010). NF-E2-related Factor 2 Regulates the Stress Response to UVA-1-Oxidized Phospholipids in Skin Cells. *FASEB J.* 24 (1), 39–48. doi:10.1096/fj.09-133520

Gunaseelan, S., Balupillai, A., Govindasamy, K., Ramasamy, K., Muthusamy, G., Shanmugam, M., et al. (2017). Linalool Prevents Oxidative Stress Activated Protein Kinases in Single UVB-Exposed Human Skin Cells. *PLoS One* 12 (5), e0176699. doi:10.1371/journal.pone.0176699

Halliday, G. M., and Lyons, J. G. (2008). Inflammatory Doses of UV May Not Be Necessary for Skin Carcinogenesis. *Photochem. Photobiol.* 84 (2), 272–283. doi:10.1111/j.1751-1097.2007.00247.x

Hano, C., and Tungmunnithum, D. (2020). Plant Polyphenols, More Than Just Simple Natural Antioxidants: Oxidative Stress, Aging and Age-Related Diseases. *Medicines (Basel)* 7 (5). doi:10.3390/medicines7050026

Hayashi, R., Himori, N., Taguchi, K., Ishikawa, Y., Uesugi, K., Ito, M., et al. (2013). The Role of the Nrf2-Mediated Defense System in Corneal Epithelial Wound Healing. *Free Radic. Biol. Med.* 61, 333–342. doi:10.1016/j.freeradbiomed.2013.04.008

He, F., Ru, X., and Wen, T. (2020). NRF2, a Transcription Factor for Stress Response and beyond. *Int. J. Mol. Sci.* 21 (13). doi:10.3390/ijms21134777

Heinrich, U., Neukam, K., Tronnier, H., Sies, H., and Stahl, W. (2006). Long-term Ingestion of High Flavanol cocoa Provides Photoprotection against UV-Induced Erythema and Improves Skin Condition in Women. *J. Nutr.* 136 (6), 1565–1569. doi:10.1093/jn/136.6.1565

Hong, Y. H., Lee, H. S., Jung, E. Y., Han, S. H., Park, Y., and Suh, H. J. (2017). Photoprotective Effects of Topical Ginseng Leaf Extract Using Ultraflo L against UVB-Induced Skin Damage in Hairless Mice. *J. Ginseng Res.* 41 (4), 456–462. doi:10.1016/j.jgr.2016.07.007

Hseu, Y. C., Chang, C. T., Gowrisankar, Y. V., Chen, X. Z., Lin, H. C., Yen, H. R., et al. (2019). Zerumbone Exhibits Antiphotoaging and Dermatoprotective Properties in Ultraviolet A-Irradiated Human Skin Fibroblast Cells via the Activation of Nrf2/ARE Defensive Pathway. *Oxid Med. Cell Longev* 2019, 4098674. doi:10.1155/2019/4098674

Hseu, Y. C., Chen, X. Z., Vudhya Gowrisankar, Y., Yen, H. R., Chuang, J. Y., and Yang, H. L. (2020). The Skin-Whitening Effects of Ectoine via the Suppression of α-MSH-Stimulated Melanogenesis and the Activation of Antioxidant Nrf2 Pathways in UVA-Irradiated Keratinocytes. *Antioxidants (Basel)* 9 (1). doi:10.3390/antiox9010063

Hseu, Y. C., Chou, C. W., Senthil Kumar, K. J., Fu, K. T., Wang, H. M., Hsu, L. S., et al. (2012). Ellagic Acid Protects Human Keratinocyte (HaCaT) Cells against UVA-Induced Oxidative Stress and Apoptosis through the Upregulation of the HO-1 and Nrf-2 Antioxidant Genes. *Food Chem. Toxicol.* 50 (5), 1245–1255. doi:10.1016/j.fct.2012.02.020

Hseu, Y. C., Vudhya Gowrisankar, Y., Wang, L. W., Zhang, Y. Z., Chen, X. Z., Huang, P. J., et al. (2021). The *In Vitro* and *In Vivo* Depigmenting Activity of Pterostilbene through Induction of Autophagy in Melanocytes and Inhibition of UVA-Irradiated α-MSH in Keratinocytes via Nrf2-Mediated Antioxidant Pathways. *Redox Biol.* 44, 102007. doi:10.1016/j.redox.2021.102007

Huang, C.-Y., Liu, I.-H., Huang, X.-Z., Chen, H.-J., Chang, S.-T., Chang, M.-L., et al. (2021). Antimelanogenesis Effects of Leaf Extract and Phytochemicals from Ceylon Olive (Elaeocarpus Serratus) in Zebrafish Model. *Pharmaceutics* 13 (7), 1059. doi:10.3390/pharmaceutics13071059

Hwang, E., Gao, W., Xiao, Y. K., Ngo, H. T. T., and Yi, T. H. (2019). Helianthus Annuus L. Flower Prevents UVB-Induced Photodamage in Human Dermal Fibroblasts by Regulating the MAPK/AP-1, NFAT, and Nrf2 Signaling Pathways. *J. Cell Biochem* 120 (1), 601–612. doi:10.1002/jcb.27417

Hwang, E., Ngo, H. T. T., Seo, S. A., Park, B., Zhang, M., and Yi, T. H. (2018). Protective Effect of Dietary Alchemilla Mollis on UVB-Irradiated Premature Skin Aging through Regulation of Transcription Factor NFATc1 and Nrf2/ARE Pathways. *Phytomedicine* 39, 125–136. doi:10.1016/j.phymed.2017.12.025

Ikehata, H., and Yamamoto, M. (2018). Roles of the KEAP1-NRF2 System in Mammalian Skin Exposed to UV Radiation. *Toxicol. Appl. Pharmacol.* 360, 69–77. doi:10.1016/j.taap.2018.09.038

Jastrząb, A., Gęgotek, A., and Skrzydlewska, E. (2019). Cannabidiol Regulates the Expression of Keratinocyte Proteins Involved in the Inflammation Process through Transcriptional Regulation. *Cells* 8 (8), 827. doi:10.3390/cells8080827

Jeayeng, S., Wongkajornsilp, A., Slominski, A. T., Jirawatnotai, S., Sampattavanich, S., and Panich, U. (2017). Nrf2 in Keratinocytes Modulates UVB-Induced DNA Damage and Apoptosis in Melanocytes through MAPK Signaling. *Free Radic. Biol. Med.* 108, 918–928. doi:10.1016/j.freeradbiomed.2017.05.009

Jian, Z., Li, K., Liu, L., Zhang, Y., Zhou, Z., Li, C., et al. (2011). Heme Oxygenase-1 Protects Human Melanocytes from H2O2-Induced Oxidative Stress via the Nrf2-ARE Pathway. *J. Invest. Dermatol.* 131 (7), 1420–1427. doi:10.1038/jid.2011.56

Jo, D. J., Seok, J. K., Kim, S. Y., Park, W., Baek, J. H., Kim, Y. M., et al. (2018). Human Skin-Depigmenting Effects of Resveratryl Triglycolate, a Hybrid Compound of Resveratrol and Glycolic Acid. *Int. J. Cosmet. Sci.* 40, 256–262. doi:10.1111/ics.12458

Johnsson, P. (2004). *Phenolic Compounds in Flaxseed Chromatographic and Spectroscopic Analyses of Glucosidic Conjugates*. Uppsala, Sweden: Swedish University of Agricultural Sciences.

Kanlayavattanakul, M., Chongnativisit, W., Chaikul, P., and Lourith, N. (2020). Phenolic-rich Pomegranate Peel Extract: *In Vitro*, Cellular, and *In Vivo* Activities for Skin Hyperpigmentation Treatment. *Planta Med.* 86 (11), 749–759. doi:10.1055/a-1170-7785

Kannan, S., and Jaiswal, A. K. (2006). Low and High Dose UVB Regulation of Transcription Factor NF-E2-Related Factor 2. *Cancer Res.* 66 (17), 8421–8429. doi:10.1158/0008-5472.CAN-06-1181

Karin, M. (1995). The Regulation of AP-1 Activity by Mitogen-Activated Protein Kinases. *J. Biol. Chem.* 270 (28), 16483–16486. doi:10.1074/jbc.270.28.16483

Kawachi, Y., Xu, X., Taguchi, S., Sakurai, H., Nakamura, Y., Ishii, Y., et al. (2008). Attenuation of UVB-Induced Sunburn Reaction and Oxidative DNA Damage with No Alterations in UVB-Induced Skin Carcinogenesis in Nrf2 Gene-Deficient Mice. *J. Invest. Dermatol.* 128 (7), 1773–1779. doi:10.1038/sj.jid.5701245

Kerns, M. L., Hakim, J. M., Lu, R. G., Guo, Y., Berroth, A., Kaspar, R. L., et al. (2016). Oxidative Stress and Dysfunctional NRF2 Underlie Pachyonychia Congenita Phenotypes. *J. Clin. Invest.* 126 (6), 2356–2366. doi:10.1172/JCI84870

Kim, A. J., Park, J. E., Cho, Y. H., Lim, D. S., and Lee, J. S. (2021). Effect of 7-Methylsulfinylheptyl Isothiocyanate on the Inhibition of Melanogenesis in B16-F1 Cells. *Life (Basel)* 11 (2). doi:10.3390/life11020162

Kim, J., Kim, J., Shim, J., Lee, C. Y., Lee, K. W., and Lee, H. J. (2014). Cocoa Phytochemicals: Recent Advances in Molecular Mechanisms on Health. *Crit. Rev. Food Sci. Nutr.* 54 (11), 1458–1472. doi:10.1080/10408398.2011.641041

Kim, J., Oh, J., Averilla, J. N., Kim, H. J., Kim, J. S., and Kim, J. S. (2019). Grape Peel Extract and Resveratrol Inhibit Wrinkle Formation in Mice Model through Activation of Nrf2/HO-1 Signaling Pathway. *J. Food Sci.* 84 (6), 1600–1608. doi:10.1111/1750-3841.14643

Kim, J. M., Noh, E. M., Kwon, K. B., Hwang, B. M., Hwang, J. K., You, Y. O., et al. (2013). Dihydroavenanthramide D Prevents UV-Irradiated Generation of Reactive Oxygen Species and Expression of Matrix Metalloproteinase-1 and -3 in Human Dermal Fibroblasts. *Exp. Dermatol.* 22 (11), 759–761. doi:10.1111/exd.12243

Kim, M., Park, Y. G., Lee, H. J., Lim, S. J., and Nho, C. W. (2015). Youngiasides A and C Isolated from Youngia Denticulatum Inhibit UVB-Induced MMP Expression and Promote Type I Procollagen Production via Repression of MAPK/AP-1/NF-κB and Activation of AMPK/Nrf2 in HaCaT Cells and Human Dermal Fibroblasts. *J. Agric. Food Chem.* 63 (22), 5428–5438. doi:10.1021/acs.jafc.5b00467

Kishimoto, Y., Tani, M., Uto-Kondo, H., Iizuka, M., Saita, E., Sone, H., et al. (2010). Astaxanthin Suppresses Scavenger Receptor Expression and Matrix Metalloproteinase Activity in Macrophages. *Eur. J. Nutr.* 49 (2), 119–126. doi:10.1007/s00394-009-0056-4

Kleszczyński, K., Ernst, I. M., Wagner, A. E., Kruse, N., Zillikens, D., Rimbach, G., et al. (2013). Sulforaphane and Phenylethyl Isothiocyanate Protect Human Skin against UVR-Induced Oxidative Stress and Apoptosis: Role of Nrf2-dependent Gene Expression and Antioxidant Enzymes. *Pharmacol. Res.* 78, 28–40. doi:10.1016/j.phrs.2013.09.009

Ko, H. J., Kim, J. H., Lee, G. S., and Shin, T. (2020). Sulforaphane Controls the Release of Paracrine Factors by Keratinocytes and Thus Mitigates Particulate Matter-Induced Premature Skin Aging by Suppressing Melanogenesis and Maintaining Collagen Homeostasis. *Phytomedicine* 77, 153276. doi:10.1016/j.phymed.2020.153276

Kohandel, Z., Farkhondeh, T., Aschner, M., Pourbagher-Shahri, A. M., and Samarghandian, S. (2022). Anti-inflammatory Action of Astaxanthin and its Use in the Treatment of Various Diseases. *Biomed. Pharmacother.* 145, 112179. doi:10.1016/j.biopha.2021.112179

Kohandel, Z., Farkhondeh, T., Aschner, M., and Samarghandian, S. (2021). Nrf2 a Molecular Therapeutic Target for Astaxanthin. *Biomed. Pharmacother.* 137, 111374. doi:10.1016/j.biopha.2021.111374

Kong, A. N., Owuor, E., Yu, R., Hebbar, V., Chen, C., Hu, R., et al. (2001). Induction of Xenobiotic Enzymes by the MAP Kinase Pathway and the Antioxidant or Electrophile Response Element (ARE/EpRE). *Drug Metab. Rev.* 33 (3-4), 255–271. doi:10.1081/dmr-120000652

Kuwano, T., Watanabe, M., Kagawa, D., and Murase, T. (2015). Hydrolyzed Methylhesperidin Induces Antioxidant Enzyme Expression via the Nrf2-ARE Pathway in Normal Human Epidermal Keratinocytes. *J. Agric. Food Chem.* 63 (36), 7937–7944. doi:10.1021/acs.jafc.5b01992

Kypriotou, M., Huber, M., and Hohl, D. (2012). The Human Epidermal Differentiation Complex: Cornified Envelope Precursors, S100 Proteins and the 'fused Genes' Family. *Exp. Dermatol.* 21 (9), 643–649. doi:10.1111/j.1600-0625.2012.01472.x

L Suraweera, T., Rupasinghe, H. P. V., Dellaire, G., and Xu, Z. (2020). Regulation of Nrf2/ARE Pathway by Dietary Flavonoids: A Friend or Foe for Cancer Management? *Antioxidants (Basel)* 9 (10). doi:10.3390/antiox9100973

Larroque-Cardoso, P., Camaré, C., Nadal-Wollbold, F., Grazide, M. H., Pucelle, M., Garoby-Salom, S., et al. (2015). Elastin Modification by 4-Hydroxynonenal in Hairless Mice Exposed to UV-A. Role in Photoaging and Actinic Elastosis. *J. Invest. Dermatol.* 135 (7), 1873–1881. doi:10.1038/jid.2015.84

Latronico, T., Larocca, M., Milella, S., Fasano, A., Rossano, R., and Liuzzi, G. M. (2021). Neuroprotective Potential of Isothiocyanates in an *In Vitro* Model of Neuroinflammation. *Inflammopharmacology* 29 (2), 561–571. doi:10.1007/s10787-020-00772-w

Lee, E.-J., Zheng, M., Craft, C. M., and Jeong, S. (2021). Matrix Metalloproteinase-9 (MMP-9) and Tissue Inhibitor of Metalloproteinases 1 (TIMP-1) Are Localized in the Nucleus of Retinal Müller Glial Cells and Modulated by Cytokines and Oxidative Stress. *PLoS One* 16 (7), e0253915. doi:10.1371/journal.pone.0253915

Lee, T. H., Seo, J. O., Baek, S. H., and Kim, S. Y. (2014). Inhibitory Effects of Resveratrol on Melanin Synthesis in Ultraviolet B-Induced Pigmentation in Guinea Pig Skin. *Biomol. Ther. (Seoul)* 22 (1), 35–40. doi:10.4062/biomolther.2013.081

Lee, Y. M., Seon, M. R., Cho, H. J., Kim, J. S., and Park, J. H. (2009). Benzyl Isothiocyanate Exhibits Anti-inflammatory Effects in Murine Macrophages and in Mouse Skin. *J. Mol. Med. (Berl)* 87 (12), 1251–1261. doi:10.1007/s00109-009-0532-6

Lephart, E. D. (2016). Skin Aging and Oxidative Stress: Equol's Anti-aging Effects via Biochemical and Molecular Mechanisms. *Ageing Res. Rev.* 31, 36–54. doi:10.1016/j.arr.2016.08.001

Li, H., Jiang, N., Liang, B., Liu, Q., Zhang, E., Peng, L., et al. (2017a). Pterostilbene Protects against UVB-Induced Photo-Damage through a Phosphatidylinositol-3-kinase-dependent Nrf2/ARE Pathway in Human Keratinocytes. *Redox Rep.* 22 (6), 501–507. doi:10.1080/13510002.2017.1329917

Li, H., Li, Z., Peng, L., Jiang, N., Liu, Q., Zhang, E., et al. (2017b). Lycium Barbarum Polysaccharide Protects Human Keratinocytes against UVB-Induced Photo-Damage. *Free Radic. Res.* 51 (2), 200–210. doi:10.1080/10715762.2017.1294755

Li, J., Liu, D., Wu, J., Zhang, D., Cheng, B., Zhang, Y., et al. (2016). Ginsenoside Rg1 Attenuates Ultraviolet B-Induced Glucocortisides Resistance in Keratinocytes via Nrf2/HDAC2 Signalling. *Sci. Rep.* 6, 39336. doi:10.1038/srep39336

Li, L., Hwang, E., Ngo, H. T. T., Lin, P., Gao, W., Liu, Y., et al. (2018). Antiphotoaging Effect of Prunus Yeonesis Blossom Extract via Inhibition of

MAPK/AP-1 and Regulation of the TGF-βI/Smad and Nrf2/ARE Signaling Pathways. *Photochem. Photobiol.* 94 (4), 725–732. doi:10.1111/php.12894

Li, L., Ngo, H. T. T., Hwang, E., Wei, X., Liu, Y., Liu, J., et al. (2019). Conditioned Medium from Human Adipose-Derived Mesenchymal Stem Cell Culture Prevents UVB-Induced Skin Aging in Human Keratinocytes and Dermal Fibroblasts. *Int. J. Mol. Sci.* 21 (1). doi:10.3390/ijms21010049

Liebel, F., Kaur, S., Ruvolo, E., Kollias, N., and Southall, M. D. (2012). Irradiation of Skin with Visible Light Induces Reactive Oxygen Species and Matrix-Degrading Enzymes. *J. Invest. Dermatol.* 132 (7), 1901–1907. doi:10.1038/jid.2011.476

Lin, J. Y., and Fisher, D. E. (2007). Melanocyte Biology and Skin Pigmentation. *Nature* 445 (7130), 843–850. doi:10.1038/nature05660

Lin, Z., Marepally, S. R., Kim, T. K., Janjetovic, Z., Oak, A. S., Postlethwaite, A. E., et al. (2016). Design, Synthesis and Biological Activities of Novel Gemini 20S-Hydroxyvitamin D3 Analogs. *Anticancer Res.* 36 (3), 877–886.

Liu, C., Vojnovic, D., Kochevar, I. E., and Jurkunas, U. V. (2016). UV-A Irradiation Activates Nrf2-Regulated Antioxidant Defense and Induces p53/Caspase3-dependent Apoptosis in Corneal Endothelial Cells. *Invest. Ophthalmol. Vis. Sci.* 57 (4), 2319–2327. doi:10.1167/iovs.16-19097

Liu, J., Liu, Y., He, X., Teng, B., and McRae, J. M. (2021). Valonea Tannin: Tyrosinase Inhibition Activity, Structural Elucidation and Insights into the Inhibition Mechanism. *Molecules* 26 (9), 2747. doi:10.3390/molecules26092747

Liu, X. Y., Hwang, E., Park, B., Ngo, H. T. T., Xiao, Y. K., and Yi, T. H. (2018). Ginsenoside C-Mx Isolated from Notoginseng Stem-Leaf Ginsenosides Attenuates Ultraviolet B-Mediated Photoaging in Human Dermal Fibroblasts. *Photochem. Photobiol.* 94 (5), 1040–1048. doi:10.1111/php.12940

Liu, X. Y., Li, H., Hwang, E., Park, B., Xiao, Y. K., Liu, S., et al. (2022). Chemical Distance Measurement and System Pharmacology Approach Uncover the Novel Protective Effects of Biotransformed Ginsenoside C-Mc against UVB-Irradiated Photoaging. *Oxid Med. Cell Longev* 2022, 4691576. doi:10.1155/2022/4691576

Liu, X. Y., Xiao, Y. K., Hwang, E., Haeng, J. J., and Yi, T. H. (2019). Antiphotoaging and Antimelanogenesis Properties of Ginsenoside C-Y, a Ginsenoside Rb2 Metabolite from American Ginseng PDD-Ginsenoside. *Photochem. Photobiol.* 95 (6), 1412–1423. doi:10.1111/php.13116

Lohakul, J., Chaiprasongsuk, A., Jeayeng, S., Saelim, M., Muanjumpon, P., Thanachaiphiwat, S., et al. (2021a). The Protective Effect of Polyherbal Formulation, Harak Formula, on UVA-Induced Photoaging of Human Dermal Fibroblasts and Mouse Skin via Promoting Nrf2-Regulated Antioxidant Defense. *Front. Pharmacol.* 12, 649820. doi:10.3389/fphar.2021.649820

Lohakul, J., Jeayeng, S., Chaiprasongsuk, A., Torregrossa, R., Wood, M. E., Saelim, M., et al. (2021b). Mitochondria-Targeted Hydrogen Sulfide Delivery Molecules Protect against UVA-Induced Photoaging in Human Dermal Fibroblasts, and in Mouse Skin *In Vivo*. *Antioxid. Redox Signaling* 2021. doi:10.1089/ars.2020.8255

López-Camarillo, C., Ocampo, E. A., Casamichana, M. L., Pérez-Plasencia, C., Alvarez-Sánchez, E., and Marchat, L. A. (2012). Protein Kinases and Transcription Factors Activation in Response to UV-Radiation of Skin: Implications for Carcinogenesis. *Int. J. Mol. Sci.* 13 (1), 142–172. doi:10.3390/ijms13010142

Lü, J., Kundrát, M., and Shen, C. (2016). New Material of the Pterosaur Gladocephaloideus Lü et al., 2012 from the Early Cretaceous of Liaoning Province, China, with Comments on Its Systematic Position. *PLoS One* 11 (6), e0154888. doi:10.1371/journal.pone.0154888

Lu, Y., F. Tonissen, K., and Di Trapani, G. (2021). Modulating Skin Colour: Role of the Thioredoxin and Glutathione Systems in Regulating Melanogenesis. *Biosci. Rep.* 41 (5). doi:10.1042/BSR20210427

Luo, J. F., Shen, X. Y., Lio, C. K., Dai, Y., Cheng, C. S., Liu, J. X., et al. (2018). Activation of Nrf2/HO-1 Pathway by Nardochinoid C Inhibits Inflammation and Oxidative Stress in Lipopolysaccharide-Stimulated Macrophages. *Front. Pharmacol.* 9, 911. doi:10.3389/fphar.2018.00911

Lv, J., Fu, Y., Cao, Y., Jiang, S., Yang, Y., Song, G., et al. (2020). Isoliquiritigenin Inhibits Melanogenesis, Melanocyte Dendricity and Melanosome Transport by Regulating ERK-Mediated MITF Degradation. *Exp. Dermatol.* 29 (2), 149–157. doi:10.1111/exd.14066

Ma, Q., Liu, Q., Yuan, L., and Zhuang, Y. (2018). Protective Effects of LSGYGP from Fish Skin Gelatin Hydrolysates on UVB-Induced MEFs by Regulation of Oxidative Stress and Matrix Metalloproteinase Activity. *Nutrients* 10 (4). doi:10.3390/nu10040420

Ma, Q. (2013). Role of Nrf2 in Oxidative Stress and Toxicity. *Annu. Rev. Pharmacol. Toxicol.* 53, 401–426. doi:10.1146/annurev-pharmtox-011112-140320

Mackay, A. R., Ballin, M., Pelina, M. D., Farina, A. R., Nason, A. M., Hartzler, J. L., et al. (1992). Effect of Phorbol Ester and Cytokines on Matrix Metalloproteinase and Tissue Inhibitor of Metalloproteinase Expression in Tumor and normal Cell Lines. *Invasion Metastasis* 12 (3-4), 168–184.

Majeed, M., Majeed, S., Jain, R., Mundkur, L., Rajalakshmi, H. R., Lad, P. S., et al. (2020). An Open-Label Single-Arm, Monocentric Study Assessing the Efficacy and Safety of Natural Pterostilbene (Pterocarpus Marsupium) for Skin Brightening and Antiaging Effects. *Clin. Cosmet. Investig. Dermatol.* 13, 105–116. doi:10.2147/CCID.S238358

Maleki, S. J., Crespo, J. F., and Cabanillas, B. (2019). Anti-inflammatory Effects of Flavonoids. *Food Chem.* 299, 125124. doi:10.1016/j.foodchem.2019.125124

McBride, K., and Nemer, M. (1998). The C-Terminal Domain of C-Fos Is Required for Activation of an AP-1 Site Specific for Jun-Fos Heterodimers. *Mol. Cell Biol* 18 (9), 5073–5081. doi:10.1128/MCB.18.9.5073

Milani, A., Basirnejad, M., Shahbazi, S., and Bolhassani, A. (2017). Carotenoids: Biochemistry, Pharmacology and Treatment. *Br. J. Pharmacol.* 174 (11), 1290–1324. doi:10.1111/bph.13625

Misawa, E., Tanaka, M., Saito, M., Nabeshima, K., Yao, R., Yamauchi, K., et al. (2017). Protective Effects of Aloe Sterols against UVB-Induced Photoaging in Hairless Mice. *Photodermatol. Photoimmunol Photomed.* 33 (2), 101–111. doi:10.1111/phpp.12286

Narayanan, D. L., Saladi, R. N., and Fox, J. L. (2010). Ultraviolet Radiation and Skin Cancer. *Int. J. Dermatol.* 49 (9), 978–986. doi:10.1111/j.1365-4632.2010.04474.x

Nguyen, T., Nioi, P., and Pickett, C. B. (2009). The Nrf2-Antioxidant Response Element Signaling Pathway and its Activation by Oxidative Stress. *J. Biol. Chem.* 284 (20), 13291–13295. doi:10.1074/jbc.R900010200

Ni, H., Jin, W., Zhu, T., Wang, J., Yuan, B., Jiang, J., et al. (2015). Curcumin Modulates TLR4/NF-κB Inflammatory Signaling Pathway Following Traumatic Spinal Cord Injury in Rats. *J. Spinal Cord Med.* 38 (2), 199–206. doi:10.1179/2045772313Y.0000000179

Nishiumi, S., Miyamoto, S., Kawabata, K., Ohnishi, K., Mukai, R., Murakami, A., et al. (2011). Dietary Flavonoids as Cancer-Preventive and Therapeutic Biofactors. *Front. Biosci. (Schol Ed.* 3, 1332–1362. doi:10.2741/229

Niu, C., and Aisa, H. A. (2017). Upregulation of Melanogenesis and Tyrosinase Activity: Potential Agents for Vitiligo. *Molecules* 22 (8). doi:10.3390/molecules22081303

O'Donovan, P., Perrett, C. M., Zhang, X., Montaner, B., Xu, Y. Z., Harwood, C. A., et al. (2005). Azathioprine and UVA Light Generate Mutagenic Oxidative DNA Damage. *Science* 309 (5742), 1871–1874. doi:10.1126/science.1114233

Oh, J. H., Kim, J., Karadeniz, F., Kim, H. R., Park, S. Y., Seo, Y., et al. (2021). Santamarine Shows Anti-photoaging Properties via Inhibition of MAPK/AP-1 and Stimulation of TGF-β/Smad Signaling in UVA-Irradiated HDFs. *Molecules* 26 (12). doi:10.3390/molecules26123585

Onkoksoong, T., Jeayeng, S., Poungvarin, N., Limsaengurai, S., Thamsermsang, O., Tripatara, P., et al. (2018). Thai Herbal Antipyretic 22 Formula (APF22) Inhibits UVA-Mediated Melanogenesis through Activation of Nrf2-Regulated Antioxidant Defense. *Phytother Res.* 32 (8), 1546–1554. doi:10.1002/ptr.6083

Panche, A. N., Diwan, A. D., and Chandra, S. R. (2016). Flavonoids: an Overview. *J. Nutr. Sci.* 5, e47. doi:10.1017/jns.2016.41

Pandey, K. B., and Rizvi, S. I. (2009). Plant Polyphenols as Dietary Antioxidants in Human Health and Disease. *Oxid Med. Cell Longev* 2 (5), 270–278. doi:10.4161/oxim.2.5.9498

Panich, U., Pluemsamran, T., Tangsupa-a-nan, V., Wattanarangsan, J., Phadungrakwittaya, R., Akarasereenont, P., et al. (2013). Protective Effect of AVS073, a Polyherbal Formula, against UVA-Induced Melanogenesis through a Redox Mechanism Involving Glutathione-Related Antioxidant Defense. *BMC Complement. Altern. Med.* 13, 159. doi:10.1186/1472-6882-13-159

Park, C., Lee, H., Noh, J. S., Jin, C. Y., Kim, G. Y., Hyun, J. W., et al. (2020). Hemistepsin A Protects Human Keratinocytes against Hydrogen Peroxide-Induced Oxidative Stress through Activation of the Nrf2/HO-1 Signaling Pathway. *Arch. Biochem. Biophys.* 691, 108512. doi:10.1016/j.abb.2020.108512

Park, C., Park, J., Kim, W.-J., Kim, W., Cheong, H., and Kim, S.-J. (2021). Malonic Acid Isolated from Pinus Densiflora Inhibits UVB-Induced Oxidative Stress and Inflammation in HaCaT Keratinocytes. *Polymers* 13 (5), 816. doi:10.3390/polym13050816

Parrado, C., Mascaraque, M., Gilaberte, Y., Juarranz, A., and Gonzalez, S. (2016). Fernblock (Polypodium Leucotomos Extract): Molecular Mechanisms and

Pleiotropic Effects in Light-Related Skin Conditions, Photoaging and Skin Cancers, a Review. *Int. J. Mol. Sci.* 17 (7). doi:10.3390/ijms17071026

Pastore, S., Lulli, D., Pascarella, A., Maurelli, R., Dellambra, E., Potapovich, A., et al. (2012). Resveratrol Enhances Solar UV-Induced Responses in normal Human Epidermal Keratinocytes. *Photochem. Photobiol.* 88 (6), 1522–1530. doi:10.1111/j.1751-1097.2012.01195.x

Pittayapruek, P., Meephansan, J., Prapapan, O., Komine, M., and Ohtsuki, M. (2016). Role of Matrix Metalloproteinases in Photoaging and Photocarcinogenesis. *Int. J. Mol. Sci.* 17 (6). doi:10.3390/ijms17060868

Pramanik, R., Qi, X., Borowicz, S., Choubey, D., Schultz, R. M., Han, J., et al. (2003). p38 Isoforms Have Opposite Effects on AP-1-dependent Transcription through Regulation of C-Jun. The Determinant Roles of the Isoforms in the P38 MAPK Signal Specificity. *J. Biol. Chem.* 278 (7), 4831–4839. doi:10.1074/jbc.M207732200

Quan, T., Qin, Z., Xia, W., Shao, Y., Voorhees, J. J., and Fisher, G. J. (2009). Matrix-degrading Metalloproteinases in Photoaging. *J. Investig. Dermatol. Symp. Proc.* 14 (1), 20–24. doi:10.1038/jidsymp.2009.8

Rijken, F., and Bruijnzeel-Koomen, C. A. (2011). Photoaged Skin: the Role of Neutrophils, Preventive Measures, and Potential Pharmacological Targets. *Clin. Pharmacol. Ther.* 89 (1), 120–124. doi:10.1038/clpt.2010.221

Rinnerthaler, M., Bischof, J., Streubel, M. K., Trost, A., and Richter, K. (2015). Oxidative Stress in Aging Human Skin. *Biomolecules* 5 (2), 545–589. doi:10.3390/biom5020545

Rittié, L., and Fisher, G. J. (2002). UV-light-induced Signal Cascades and Skin Aging. *Ageing Res. Rev.* 1 (4), 705–720. doi:10.1016/s1568-1637(02)00024-7

Rodríguez-Luna, A., Ávila-Román, J., González-Rodríguez, M. L., Cózar, M. J., Rabasco, A. M., Motilva, V., et al. (2018). Fucoxanthin-Containing Cream Prevents Epidermal Hyperplasia and UVB-Induced Skin Erythema in Mice. *Mar. Drugs* 16 (10). doi:10.3390/md16100378

Rodríguez-Luna, A., Ávila-Román, J., Oliveira, H., Motilva, V., and Talero, E. (2019). Fucoxanthin and Rosmarinic Acid Combination Has Anti-inflammatory Effects through Regulation of NLRP3 Inflammasome in UVB-Exposed HaCaT Keratinocytes. *Mar. Drugs* 17 (8). doi:10.3390/md17080451

Rojo de la Vega, M., Krajisnik, A., Zhang, D. D., and Wondrak, G. T. (2017). Targeting NRF2 for Improved Skin Barrier Function and Photoprotection: Focus on the Achiote-Derived Apocarotenoid Bixin. *Nutrients* 9 (12). doi:10.3390/nu9121371

Ryšavá, A., Čížková, K., Franková, J., Roubalová, L., Ulrichová, J., Vostálová, J., et al. (2020). Effect of UVA Radiation on the Nrf2 Signalling Pathway in Human Skin Cells. *J. Photochem. Photobiol. B: Biol.* 209, 111948. doi:10.1016/j.jphotobiol.2020.111948

Ryšavá, A., Vostálová, J., and Rajnochová Svobodová, A. (2021). Effect of Ultraviolet Radiation on the Nrf2 Signaling Pathway in Skin Cells. *Int. J. Radiat. Biol.* 97 (10), 1383–1403. doi:10.1080/09553002.2021.1962566

Ryu, J. H., Seok, J. K., An, S. M., Baek, J. H., Koh, J. S., and Boo, Y. C. (2015). A Study of the Human Skin-Whitening Effects of Resveratryl Triacetate. *Arch. Dermatol. Res.* 307 (3), 239–247. doi:10.1007/s00403-015-1556-0

Saha, S., Buttari, B., Panieri, E., Profumo, E., and Saso, L. (2020). An Overview of Nrf2 Signaling Pathway and its Role in Inflammation. *Molecules* 25 (22). doi:10.3390/molecules25225474

Sangaraju, R., Alavala, S., Nalban, N., Jerald, M. K., and Sistla, R. (2021). Galangin Ameliorates Imiquimod-Induced Psoriasis-like Skin Inflammation in BALB/c Mice via Down Regulating NF-κB and Activation of Nrf2 Signaling Pathways. *Int. Immunopharmacol* 96, 107754. doi:10.1016/j.intimp.2021.107754

Saw, C. L., Huang, M. T., Liu, Y., Khor, T. O., Conney, A. H., and Kong, A. N. (2011). Impact of Nrf2 on UVB-Induced Skin Inflammation/photoprotection and Photoprotective Effect of Sulforaphane. *Mol. Carcinog* 50 (6), 479–486. doi:10.1002/mc.20725

Schäfer, M., Farwanah, H., Willrodt, A. H., Huebner, A. J., Sandhoff, K., Roop, D., et al. (2012). Nrf2 Links Epidermal Barrier Function with Antioxidant Defense. *EMBO Mol. Med.* 4 (5), 364–379. doi:10.1002/emmm.201200219

Schäfer, M., Dütsch, S., auf dem Keller, U., Navid, F., Schwarz, A., Johnson, D. A., et al. (2010). auf dem Keller, UNrf2 establishes a glutathione-mediated gradient of UVB cytoprotection in the epidermis. *Genes Dev.* 24 (10), 1045–1058. doi:10.1101/gad.568810

Schmitz, S., Thomas, P. D., Allen, T. M., Poznansky, M. J., and Jimbow, K. (1995). Dual Role of Melanins and Melanin Precursors as Photoprotective and Phototoxic Agents: Inhibition of Ultraviolet Radiation-Induced Lipid Peroxidation. *Photochem. Photobiol.* 61 (6), 650–655. doi:10.1111/j.1751-1097.1995.tb09883.x

Searle, T., Al-Niaimi, F., and Ali, F. R. (2020). The Top 10 Cosmeceuticals for Facial Hyperpigmentation. *Dermatol. Ther.* 33 (6), e14095. doi:10.1111/dth.14095

Serini, S., Guarino, R., Ottes Vasconcelos, R., Celleno, L., and Calviello, G. (2020). The Combination of Sulforaphane and Fernblock® XP Improves Individual Beneficial Effects in Normal and Neoplastic Human Skin Cell Lines. *Nutrients* 12 (6). doi:10.3390/nu12061608

Shao, Y., Dang, M., Lin, Y., and Xue, F. (2019). Evaluation of Wound Healing Activity of Plumbagin in Diabetic Rats. *Life Sci.* 231, 116422. doi:10.1016/j.lfs.2019.04.048

Sheen, Y. S., Huang, H. Y., and Liao, Y. H. (2021). The Efficacy and Safety of an Antiaging Topical Serum Containing Hesperetin and Sodium Cyclic Lysophosphatidic Acid: A Single-center Clinical Trial. *J. Cosmet. Dermatol.* 20, 3960–3967. doi:10.1111/jocd.14063

Shin, J. M., Kim, M. Y., Sohn, K. C., Jung, S. Y., Lee, H. E., Lim, J. W., et al. (2014). Nrf2 Negatively Regulates Melanogenesis by Modulating PI3K/Akt Signaling. *PLoS One* 9 (4), e96035. doi:10.1371/journal.pone.0096035

Shin, J. W., Chun, K. S., Kim, D. H., Kim, S. J., Kim, S. H., Cho, N. C., et al. (2020). Curcumin Induces Stabilization of Nrf2 Protein through Keap1 Cysteine Modification. *Biochem. Pharmacol.* 173, 113820. doi:10.1016/j.bcp.2020.113820

Shirasugi, I., Kamada, M., Matsui, T., Sakakibara, Y., Liu, M. C., and Suiko, M. (2010). Sulforaphane Inhibited Melanin Synthesis by Regulating Tyrosinase Gene Expression in B16 Mouse Melanoma Cells. *Biosci. Biotechnol. Biochem.* 74 (3), 579–582. doi:10.1271/bbb.90778

Shoji, T., Masumoto, S., Moriichi, N., Ohtake, Y., and Kanda, T. (2020). Administration of Apple Polyphenol Supplements for Skin Conditions in Healthy Women: A Randomized, Double-Blind, Placebo-Controlled Clinical Trial. *Nutrients* 12 (4). doi:10.3390/nu12041071

Shroff, H., Diedrichs, P. C., and Craddock, N. (2017). Skin Color, Cultural Capital, and Beauty Products: An Investigation of the Use of Skin Fairness Products in Mumbai, India. *Front. Public Health* 5, 365. doi:10.3389/fpubh.2017.00365

Silva, S. A. M. E., Michniak-Kohn, B., and Leonardi, G. R. (2017). An Overview about Oxidation in Clinical Practice of Skin Aging. *Bras Dermatol.* 92 (3), 367–374. doi:10.1590/abd1806-4841.20175481

Silvers, A. L., Bachelor, M. A., and Bowden, G. T. (2003). The Role of JNK and P38 MAPK Activities in UVA-Induced Signaling Pathways Leading to AP-1 Activation and C-Fos Expression. *Neoplasia* 5 (4), 319–329. doi:10.1016/S1476-5586(03)80025-8

Sirerol, J. A., Feddi, F., Mena, S., Rodriguez, M. L., Sirera, P., Aupí, M., et al. (2015). Topical Treatment with Pterostilbene, a Natural Phytoalexin, Effectively Protects Hairless Mice against UVB Radiation-Induced Skin Damage and Carcinogenesis. *Free Radic. Biol. Med.* 85, 1–11. doi:10.1016/j.freeradbiomed.2015.03.027

Slominski, A., Tobin, D. J., Shibahara, S., and Wortsman, J. (2004). Melanin Pigmentation in Mammalian Skin and its Hormonal Regulation. *Physiol. Rev.* 84 (4), 1155–1228. doi:10.1152/physrev.00044.2003

Slominski, A., Wortsman, J., Luger, T., Paus, R., and Solomon, S. (2000). Corticotropin Releasing Hormone and Proopiomelanocortin Involvement in the Cutaneous Response to Stress. *Physiol. Rev.* 80 (3), 979–1020. doi:10.1152/physrev.2000.80.3.979

Smalley, K., and Eisen, T. (2000). The Involvement of P38 Mitogen-Activated Protein Kinase in the Alpha-Melanocyte Stimulating Hormone (Alpha-MSH)-Induced Melanogenic and Anti-proliferative Effects in B16 Murine Melanoma Cells. *FEBS Lett.* 476 (3), 198–202. doi:10.1016/s0014-5793(00)01726-9

Sporn, M. B., and Liby, K. T. (2012). NRF2 and Cancer: the Good, the Bad and the Importance of Context. *Nat. Rev. Cancer* 12 (8), 564–571. doi:10.1038/nrc3278

Staurengo-Ferrari, L., Badaro-Garcia, S., Hohmann, M. S. N., Manchope, M. F., Zaninelli, T. H., Casagrande, R., et al. (2018). Contribution of Nrf2 Modulation to the Mechanism of Action of Analgesic and Anti-inflammatory Drugs in Pre-clinical and Clinical Stages. *Front. Pharmacol.* 9, 1536. doi:10.3389/fphar.2018.01536

Su, T. R., Lin, J. J., Tsai, C. C., Huang, T. K., Yang, Z. Y., Wu, M. O., et al. (2013). Inhibition of Melanogenesis by Gallic Acid: Possible Involvement of the PI3K/Akt, MEK/ERK and Wnt/β-Catenin Signaling Pathways in B16F10 Cells. *Int. J. Mol. Sci.* 14 (10), 20443–20458. doi:10.3390/ijms141020443

Sun, Z., Park, S. Y., Hwang, E., Park, B., Seo, S. A., Cho, J. G., et al. (2016). Dietary Foeniculum Vulgare Mill Extract Attenuated UVB Irradiation-Induced Skin

Photoaging by Activating of Nrf2 and Inhibiting MAPK Pathways. *Phytomedicine* 23 (12), 1273–1284. doi:10.1016/j.phymed.2016.06.008

Süntar, I., Çetinkaya, S., Panieri, E., Saha, S., Buttari, B., Profumo, E., et al. (2021). Regulatory Role of Nrf2 Signaling Pathway in Wound Healing Process. *Molecules* 26 (9). doi:10.3390/molecules26092424

Surh, Y. J. (2003). Cancer Chemoprevention with Dietary Phytochemicals. *Nat. Rev. Cancer* 3 (10), 768–780. doi:10.1038/nrc1189

Surh, Y. J., and Na, H. K. (2008). NF-kappaB and Nrf2 as Prime Molecular Targets for Chemoprevention and Cytoprotection with Anti-inflammatory and Antioxidant Phytochemicals. *Genes Nutr.* 2 (4), 313–317. doi:10.1007/s12263-007-0063-0

Suschek, C. V., Briviba, K., Bruch-Gerharz, D., Sies, H., Kröncke, K. D., and Kolb-Bachofen, V. (2001). Even after UVA-Exposure Will Nitric Oxide Protect Cells from Reactive Oxygen Intermediate-Mediated Apoptosis and Necrosis. *Cell Death Differ* 8 (5), 515–527. doi:10.1038/sj.cdd.4400839

Suzuki, T., Muramatsu, A., Saito, R., Iso, T., Shibata, T., Kuwata, K., et al. (2019). Molecular Mechanism of Cellular Oxidative Stress Sensing by Keap1. *Cell Rep* 28 (3), 746–e4. doi:10.1016/j.celrep.2019.06.047

Swiader, A., Camaré, C., Guerby, P., Salvayre, R., and Negre-Salvayre, A. (2021). 4-Hydroxynonenal Contributes to Fibroblast Senescence in Skin Photoaging Evoked by UV-A Radiation. *Antioxidants (Basel)* 10 (3). doi:10.3390/antiox10030365

Taguchi, K., and Yamamoto, M. (2020). The KEAP1-NRF2 System as a Molecular Target of Cancer Treatment. *Cancers (Basel)* 13 (1). doi:10.3390/cancers13010046

Takei, K., Hashimoto-Hachiya, A., Takahara, M., Tsuji, G., Nakahara, T., and Furue, M. (2015). Cynaropicrin Attenuates UVB-Induced Oxidative Stress via the AhR-Nrf2-Nqo1 Pathway. *Toxicol. Lett.* 234 (2), 74–80. doi:10.1016/j.toxlet.2015.02.007

Tan, Y., Ichikawa, T., Li, J., Si, Q., Yang, H., Chen, X., et al. (2011). Diabetic Downregulation of Nrf2 Activity via ERK Contributes to Oxidative Stress-Induced Insulin Resistance in Cardiac Cells *In Vitro* and *In Vivo*. *Diabetes* 60 (2), 625–633. doi:10.2337/db10-1164

Tran, T. T., Schulman, J., and Fisher, D. E. (2008). UV and Pigmentation: Molecular Mechanisms and Social Controversies. *Pigment Cell Melanoma Res* 21 (5), 509–516. doi:10.1111/j.1755-148X.2008.00498.x

Truong, V. L., Bak, M. J., Jun, M., Kong, A. N., Ho, C. T., and Jeong, W. S. (2014). Antioxidant Defense and Hepatoprotection by Procyanidins from almond (Prunus Amygdalus) Skins. *J. Agric. Food Chem.* 62 (34), 8668–8678. doi:10.1021/jf5027247

Uto, T., Hou, D. X., Morinaga, O., and Shoyama, Y. (2012). Molecular Mechanisms Underlying Anti-inflammatory Actions of 6-(Methylsulfinyl)hexyl Isothiocyanate Derived from Wasabi (Wasabia Japonica). *Adv. Pharmacol. Sci.* 2012, 614046. doi:10.1155/2012/614046

Vacek, J., Vostalova, J., Papouskova, B., Skarupova, D., Kos, M., Kabelac, M., et al. (2021). Antioxidant Function of Phytocannabinoids: Molecular Basis of Their Stability and Cytoprotective Properties under UV-Irradiation. *Free Radic. Biol. Med.* 164, 258–270. doi:10.1016/j.freeradbiomed.2021.01.012

Vomund, S., Schäfer, A., Parnham, M. J., Brüne, B., and von Knethen, A. (2017). Nrf2, the Master Regulator of Anti-Oxidative Responses. *Int. J. Mol. Sci.* 18 (12). doi:10.3390/ijms18122772

Wagner, A. E., Boesch-Saadatmandi, C., Dose, J., Schultheiss, G., and Rimbach, G. (2012). Anti-inflammatory Potential of Allyl-Isothiocyanate-Rrole of Nrf2, NF-(κ) B and microRNA-155. *J. Cell Mol Med* 16 (4), 836–843. doi:10.1111/j.1582-4934.2011.01367.x

Wang, P. W., Cheng, Y. C., Hung, Y. C., Lee, C. H., Fang, J. Y., Li, W. T., et al. (2019). Red Raspberry Extract Protects the Skin against UVB-Induced Damage with Antioxidative and Anti-inflammatory Properties. *Oxid Med. Cell Longev* 2019, 9529676. doi:10.1155/2019/9529676

Wang, S., Wu, Y. Y., Wang, X., Shen, P., Jia, Q., Yu, S., et al. (2020). Lycopene Prevents Carcinogen-Induced Cutaneous Tumor by Enhancing Activation of the Nrf2 Pathway through P62-Triggered Autophagic Keap1 Degradation. *Aging (Albany NY)* 12 (9), 8167–8190. doi:10.18632/aging.103132

Wang, Y., Hao, M. M., Sun, Y., Wang, L. F., Wang, H., Zhang, Y. J., et al. (2018). Synergistic Promotion on Tyrosinase Inhibition by Antioxidants. *Molecules* 23 (1). doi:10.3390/molecules23010106

Watanabe, H., Shimizu, T., Nishihira, J., Abe, R., Nakayama, T., Taniguchi, M., et al. (2004). Ultraviolet A-Induced Production of Matrix Metalloproteinase-1 Is Mediated by Macrophage Migration Inhibitory Factor (MIF) in Human Dermal Fibroblasts. *J. Biol. Chem.* 279 (3), 1676–1683. doi:10.1074/jbc.M303650200

Watson, M., Holman, D. M., and Maguire-Eisen, M. (2016). Ultraviolet Radiation Exposure and its Impact on Skin Cancer Risk. *Semin. Oncol. Nurs.* 32 (3), 241–254. doi:10.1016/j.soncn.2016.05.005

Whitmarsh, A. J. (2007). Regulation of Gene Transcription by Mitogen-Activated Protein Kinase Signaling Pathways. *Biochim. Biophys. Acta* 1773 (8), 1285–1298. doi:10.1016/j.bbamcr.2006.11.011

Wikramanayake, T. C., Stojadinovic, O., and Tomic-Canic, M. (2014). Epidermal Differentiation in Barrier Maintenance and Wound Healing. *Adv. Wound Care (New Rochelle)* 3 (3), 272–280. doi:10.1089/wound.2013.0503

Wu, M. Y., Hung, S. K., and Fu, S. L. (2011). Immunosuppressive Effects of Fisetin in Ovalbumin-Induced Asthma through Inhibition of NF-κB Activity. *J. Agric. Food Chem.* 59 (19), 10496–10504. doi:10.1021/jf202756f

Wu, P. Y., Lyu, J. L., Liu, Y. J., Chien, T. Y., Hsu, H. C., Wen, K. C., et al. (2017). Fisetin Regulates Nrf2 Expression and the Inflammation-Related Signaling Pathway to Prevent UVB-Induced Skin Damage in Hairless Mice. *Int. J. Mol. Sci.* 18 (10). doi:10.3390/ijms18102118

Wu, P. Y., You, Y. J., Liu, Y. J., Hou, C. W., Wu, C. S., Wen, K. C., et al. (2018). Sesamol Inhibited Melanogenesis by Regulating Melanin-Related Signal Transduction in B16F10 Cells. *Int. J. Mol. Sci.* 19 (4). doi:10.3390/ijms19041108

Wu, W., Peng, G., Yang, F., Zhang, Y., Mu, Z., and Han, X. (2019). Sulforaphane Has a Therapeutic Effect in an Atopic Dermatitis Murine Model and Activates the Nrf2/HO-1 axis. *Mol. Med. Rep.* 20 (2), 1761–1771. doi:10.3892/mmr.2019.10405

Xian, D., Xiong, X., Xu, J., Xian, L., Lei, Q., Song, J., et al. (2019). Nrf2 Overexpression for the Protective Effect of Skin-Derived Precursors against UV-Induced Damage: Evidence from a Three-Dimensional Skin Model. *Oxid Med. Cell Longev* 2019, 7021428. doi:10.1155/2019/7021428

Yamamoto, T., Suzuki, T., Kobayashi, A., Wakabayashi, J., Maher, J., Motohashi, H., et al. (2008). Physiological Significance of Reactive Cysteine Residues of Keap1 in Determining Nrf2 Activity. *Mol. Cell Biol* 28 (8), 2758–2770. doi:10.1128/MCB.01704-07

Yamashita, Y., Ikeda, T., Matsuda, M., Maji, D., Hoshino, T., and Mizushima, T. (2012). Purification and Characterization of HSP-Inducers from Eupatorium Lindleyanum. *Biochem. Pharmacol.* 83 (7), 909–922. doi:10.1016/j.bcp.2011.12.040

Yang, H. L., Lin, C. P., Vudhya Gowrisankar, Y., Huang, P. J., Chang, W. L., Shrestha, S., et al. (2021). The Anti-melanogenic Effects of Ellagic Acid through Induction of Autophagy in Melanocytes and Suppression of UVA-Activated α-MSH Pathways via Nrf2 Activation in Keratinocytes. *Biochem. Pharmacol.* 185, 114454. doi:10.1016/j.bcp.2021.114454

Yang, K., Kim, S. Y., Park, J. H., Ahn, W. G., Jung, S. H., Oh, D., et al. (2020). Topical Application of Phlorotannins from Brown Seaweed Mitigates Radiation Dermatitis in a Mouse Model. *Mar. Drugs* 18 (8). doi:10.3390/md18080377

Zhao, P., Alam, M. B., and Lee, S. H. (2018). Protection of UVB-Induced Photoaging by Fuzhuan-Brick Tea Aqueous Extract via MAPKs/Nrf2-Mediated Down-Regulation of MMP-1. *Nutrients* 11 (1). doi:10.3390/nu11010060

Zhou, X., Ruan, Q., Ye, Z., Chu, Z., Xi, M., Li, M., et al. (2021). Resveratrol Accelerates Wound Healing by Attenuating Oxidative Stress-Induced Impairment of Cell Proliferation and Migration. *Burns* 47 (1), 133–139. doi:10.1016/j.burns.2020.10.016

Conflict of Interest: The authors declare that the research was conducted in the absence of any commercial or financial relationships that could be construed as a potential conflict of interest.

Publisher's Note: All claims expressed in this article are solely those of the authors and do not necessarily represent those of their affiliated organizations, or those of the publisher, the editors and the reviewers. Any product that may be evaluated in this article, or claim that may be made by its manufacturer, is not guaranteed or endorsed by the publisher.

frontiers | Frontiers in Pharmacology

REVIEW
published: 05 August 2022
doi: 10.3389/fphar.2022.825842

Crocins for Ischemic Stroke: A Review of Current Evidence

Kiran Shahbaz[1]*, *Dennis Chang*[1], *Xian Zhou*[1], *Mitchell Low*[1], *Sai Wang Seto*[1,2,3] and *Chung Guang Li*[1]*

[1]NICM Health Research Institute, Western Sydney University, Penrith, NSW, Australia, [2]Reserach Centre for Chinese Medicine Innovation, The Hong Kong Polytechnic University, Kowloon, Hong Kong SAR, China, [3]Department of Applied Biology and Chemical Technology, The Hong Kong Polytechnic University, Kowloon, Hong Kong SAR, China

OPEN ACCESS

Edited by:
Aiping Lu,
Hong Kong Baptist University, Hong Kong SAR, China

Reviewed by:
Seyed Zachariah Moradi,
Kermanshah University of Medical Sciences, Iran
Neda Roshanravan,
Tabriz University of Medical Sciences, Iran

***Correspondence:**
Kiran Shahbaz
k.shahbaz@westernsydney.edu.au
Chung Guang Li
c.li@westernsydney.edu.au

Specialty section:
This article was submitted to Ethnopharmacology, a section of the journal Frontiers in Pharmacology

Received: 30 November 2021
Accepted: 28 April 2022
Published: 05 August 2022

Citation:
Shahbaz K, Chang D, Zhou X, Low M, Seto SW and Li CG (2022) Crocins for Ischemic Stroke: A Review of Current Evidence. Front. Pharmacol. 13:825842. doi: 10.3389/fphar.2022.825842

Crocins (CRs) and the related active constituents derived from *Crocus sativus* L. (Saffron) have demonstrated protective effects against cerebral ischemia and ischemic stroke, with various bioactivities including neuroprotection, anti-neuroinflammation, antioxidant, and cardiovascular protection. Among CRs, crocin (CR) has been shown to act on multiple mechanisms and signaling pathways involved in ischemic stroke, including mitochondrial apoptosis, nuclear factor kappa light chain enhancer of B cells pathway, S100 calcium-binding protein B, interleukin-6 and vascular endothelial growth factor-A. CR is generally safe and well-tolerated. Pharmacokinetic studies indicate that CR has poor bioavailability and needs to convert to crocetin (CC) in order to cross the blood-brain barrier. Clinical studies have shown the efficacy of saffron and CR in treating various conditions, including metabolic syndrome, depression, Alzheimer's disease, and coronary artery disease. There is evidence supporting CR as a treatment for ischemic stroke, although further studies are needed to confirm their efficacy and safety in clinical settings.

Keywords: ischemic stroke, Crocins, saffron, neuroinflammation, antioxidant, molecular targets, toxicity and safety, clinical trial

INTRODUCTION

Stroke (cerebral apoplexy) is a serious cerebrovascular disease and the second leading cause of death globally (WHO, 2020). There are three different categories of stroke, namely ischemic stroke (IS), hemorrhagic stroke (Waziry et al., 2020), and transient ischemic attack (Martinez et al., 2020). The prevalence of stroke varies in different countries, with a high incidence in Oceania, Asia, North Africa, and parts of America (Venketasubramanian, 2021; Zhou et al., 2021). Globally, 101.5 million people suffered from a stroke in 2019, causing 6.6 million deaths. Of these, 77.2 million were IS, resulting in 3.3 million deaths (AMA, 2021; Yang et al., 2021).

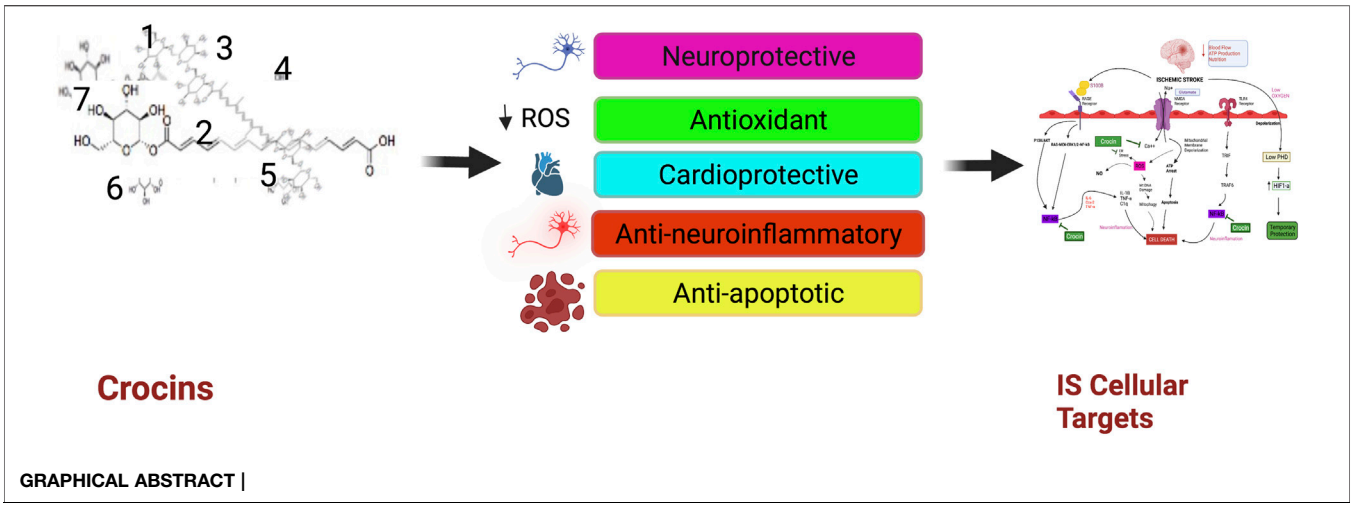

GRAPHICAL ABSTRACT |

IS is caused by a blood clot formed in the brain vasculature (thrombotic stroke) or in the peripheral system travelling to the brain through the bloodstream (embolic stroke) (Shiber et al., 2010; Khan et al., 2017; Ye et al., 2021). Currently, there are still limited therapies for IS, either by surgical intervention to remove the thrombus *via* thrombectomy (Yoo and Andersson, 2017) or pharmacological interventions using recombinant tissue plasminogen activator (rtPA) intravenous (IV) and lipid-lowering drugs such as statins (Fuentes et al., 2009; Kazley et al., 2013; Alakbarzade and Pereira, 2020; Barthels and Das, 2020; Wechsler, 2020; Orset et al., 2021). These therapies have limited efficacy (Singh and Singh, 2019), low prognosis, and are associated with adverse reactions and the risk of complications (Zheng et al., 2019; Cui et al., 2020; Pergolizzi Jr et al., 2020). In addition, IS patients often have limited access to rtPA (Barthels and Das, 2020) due to the narrow therapeutic window (which must be administered within 4.5 h of IS onset) (Fukuta et al., 2017; Barthels and Das, 2020). The adverse effects of rtPA, such as hemorrhagic transformation with increased matrix metalloprotein (MMP) (Orset et al., 2021), anaphylaxis and systemic bleeding (Chapman et al., 2014; Khandelwal et al., 2021) have restricted its clinical prescription (Cao et al., 2021).

Due to the limitations of the aforementioned therapies, there have been continuing efforts to discover, develop, research, and implement new therapies for IS (Marquez-Romero et al., 2020; Williams et al., 2020). A number of natural ingredients and traditional herbal medicines have been investigated as potential therapies for IS, including ginsenoside Rg1 and Rb1 (Gao, Bai et al., 2020), *Naoxinqing* (NXQ) (Bei et al., 2004), *Buyang Huanwu* Decoction (Hao et al., 2012), saffron (SF) (Sharma et al., 2020) and related formulas including *Naodesheng* (Sugawara and Chan, 2003; Hao et al., 2015), *Weinaokang* (Zhang et al., 2010), also known as *Sailoutong* (SLT) (Fan et al., 2021). SLT is a standardized combination of SF that has been shown to be effective for vascular dementia in Phase I and Phase II clinical trials and is currently under the phase III trial for vascular dementia (Chang et al., 2016; Jia et al., 2018; Steiner et al., 2018). NXQ and SLT have shown vigorous antioxidant activity that may play a role in their neuroprotective effects (Bei et al., 2004; Bei et al., 2009; Fan et al., 2021). Ginsenoside Rg1 was demonstrated with a protective effect in animal models against ischemia/reperfusion (I/R) induced injuries (Xie et al., 2015b; Chen et al., 2019; Gao et al., 2020) possibly *via* alleviating blood-brain barrier (BBB) disruption (Zhou et al., 2014), downregulating inflammatory mediators (Zheng et al., 2019) and ameliorating protease-activated receptor-1 expression (Xie et al., 2015a). Additionally, Gj-4, a CR enrichment extract from *Gardenia Jasminoides J. Ellis* improved neurovascular protection, mitigating endothelial cell damage (Yang, 2020) and protecting memory deficit in rodents focal cerebral ischemia (Li et al., 2014; Pang et al., 2020; Liu et al., 2021a).

C. sativus L. (Iridaceae) in the superorder of monocots and subdivision of spermatophytes (Crocus-sativus, 2010) yields saffron (SF—the dried stigma) which demonstrated various pharmacological effects, including aphrodisiac (Kashani et al., 2013), anticonvulsant (El Khoudri et al., 2021), antitussive, and antianxiety (Khazdair et al., 2019). SF has long been used as a folk medicine to treat a variety of diseases and conditions, including neurodegenerative diseases, memory disorders, atherosclerosis, hyperlipidaemia, diabetes, high blood pressure, ulcers, and fatty liver disease (Abe and Saito, 2000; Sheikhani et al., 2017; Awasthi and Kulkarni, 2020). *C. sativus* L. is known to be native to Greece and Iran, and has been extensively cultivated in other countries such as southern Europe, Tibet, and India (Jan et al., 2014). The global production of SF is expected to increase by 12.09% in 2020–2027 (Kothari et al., 2021b), with 90% from Iran (Dhar and Mir, 1997; Kothari et al., 2021a). Iran has been reported as a country with a highly sustainable cultivation source of *C. sativus* L. based on climatic and edaphic conditions, and production and processing practices (Ghorbani and Koocheki, 2017). CR compounds can also be obtained from other sustainable species. For example, an extraction containing 17% of CRs can be obtained from *Gardenia Jasminoides* (Sommano et al., 2020). In addition petals of *C. sativus* L. which are considered a waste product in saffron production, may also be a sustainable source

TABLE 1 | CR and related compounds of SF.

Compound	CAS reg no.	Structure	Synonym	M. W (g/Mol)	MF	Isomeric SMILE	Ref.
CR	42553-65-1	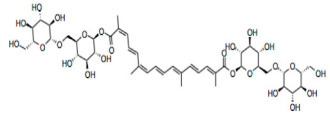	Crocin I; alpha-crocin; CR1, CR	977	$C_{44}H_{64}O_{24}$	C/C(=C\C=C\C=C(\C)/C=C/C=C(/C)\C(=O)O[C@H]1[C@@H]([C@H]([C@@H]([C@H](O1)CO[C@H]2[C@@H]([C@H]([C@@H]([C@H](O2)CO)O)O)O)O)O)O)/C=C/C=C(\C)/C(=O)O[C@H]3[C@@H]([C@H]([C@@H]([C@H](O3)CO[C@H]4[C@@H]([C@H]([C@@H]([C@H](O4)CO)O)O)O)O)O)O	(Hadizadeh et al., 2010; Alavizadeh and Hosseinzadeh, 2014a)
CR 2	55750-84-0	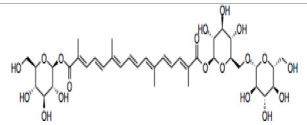	Crocin II; tricrocin, trans-crocin 3, crocin B, CR2	814.8	$C_{38}H_{54}O_{19}$	C/C(=C\C=C\C=C(/C)\C=C\C=C(/C)\C(=O)O[C@H]1[C@@H]([C@H]([C@@H]([C@H](O1)CO[C@H]2[C@@H]([C@H]([C@@H]([C@H](O2)CO)O)O)O)O)O)O)/C=C/C=C(\C)/C(=O)O[C@H]3[C@@H]([C@H]([C@@H]([C@H](O3)CO)O)O)O	(Pfister et al., 1996; Wang et al., 2009)
CR 3	55750-85-1	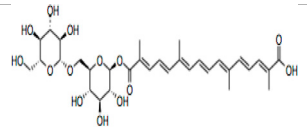	Beta-D-gentiobiosyl crocetin; crocin C, CR3	652.7	$C_{32}H_{44}O_{14}$	C/C(=C\C=C\C=C(/C)\C=C\C=C(/C)\C(=O)O[C@H]1[C@@H]([C@H]([C@@H]([C@H](O1)CO[C@H]2[C@@H]([C@H]([C@@H]([C@H](O2)CO)O)O)O)O)O)O)/C=C/C=C(\C)/C(=O)O	(Chen et al., 2008; Lech et al., 2009)
CR 4	55750-86-2	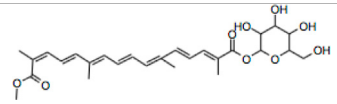	Crocin IV, CR4	504.6	$C_{27}H_{36}O_{9}$	C/C(=C\C=C\C=C(\C)/C=C/C=C(\C)/C(=O)OC1C(C(C(C(O1)CO)O)O)O)/C=C/C=C(/C)\C(=O)OC	(Zhang et al., 2001; Karkoula et al., 2018)
CR 5	174916-30-4		Trans crocin 5, CR5	434.4	$C_{22}H_{26}O_{9}$	C([C@@H]1[C@H]([C@@H]([C@H]([C@@H](O1)OC(=O)/C=C/C=C/C=C/C=C/C=C/C=C/C=C/C(=O)O)O)O)O)O	(Zhang et al., 2001; Hadizadeh et al., 2010)
CR 6	164455-25-8	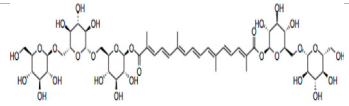	(13Z)-8,8'-Diapo-Psi, Psi-Carotene-8,8'-Dioic Acid 8-[6-O-(6-O-beta-D-glucopyranosyl-beta-D-glucopyranosyl)-beta-D-glucopyranosyl]8'-(6-O-beta-D-glucopyranosyl-beta-D-glucopyranosyl) ester, CR6	1139.1	$C_{50}H7_{4}O_{29}$	C/C(=C\C=C\C=C(/C)\C=C\C=C(/C)\C(=O)O[C@H]1[C@@H]([C@H]([C@@H]([C@H](O1)CO[C@H]2[C@@H]([C@H]([C@@H]([C@H](O2)CO[C@H]3[C@@H]([C@H]([C@@H]([C@H](O3)CO)O)O)O)O)O)O)O)O)O)/C=C/C=C(\C)/C(=O)O[C@H]4[C@@H]([C@H]([C@@H]([C@H](O4)CO[C@H]5[C@@H]([C@H]([C@@H]([C@H](O5)CO)O)O)O)O)O)O	(Carmona et al., 2006; Hadizadeh et al., 2010; Verma and Middha, 2010)
CR 7	864547-06-8 (Unspecified)	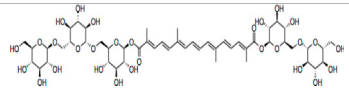	CR7	1301.2	$C_{56}H_{84}O_{34}$	C/C(=C\C=C\C=C(\C=C\C=C(\C(=O)O[C@@H]1O[C@@H]([C@H]([C@@H]([C@H]1O)O)O)CO[C@@H]2O[C@@H]([C@H]([C@@H]([C@H]2O)O)O)CO[C@@H]3O[C@@H]([C@H]([C@@H]([C@H]3O)O)O)CO)/C)/C)/C=C/C=C(/C(=O)O[C@@H]4O[C@@H]([C@H]([C@@H]([C@H]4O)O)O)CO[C@@H]5O[C@@H]([C@H]([C@@H]([C@H]5O)O)	(Zougagh et al., 2005; NCBI, 2021)

(Continued on following page)

TABLE 1 | (*Continued*) CR and related compounds of SF.

Compound	CAS reg no.	Structure	Synonym	M. W (g/Mol)	MF	Isomeric SMILE	Ref.
						O)CO[C@@H]6O[C@@H]([C@H]([C@@H]([C@H]6O)O)O)CO)\C	
	101124079 *(PubChem CID)						
CC	27876-94-4	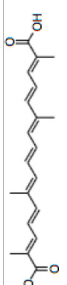	Transcrocetin; transcrocitinate, CC	328.4	$C_{20}H_{24}O_4$	C/C(=C\C=C\C=C(\C=C\C=C(\C(=O)O)/C)/C)/C=C/C=C(/C(=O)O)\C	(Giaccio, 2004; Jackson et al., 2021; Qin et al., 2021)
Dimethyl Crocetin	5892-54-6	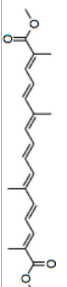	Crocetin dimethyl ester; gamma-crocetin, DMCC	356.5	$C_{22}H_{28}O_4$	C/C(=C\C=C\C=C(\C=C\C=C(\C(=O)OC)/C)/C)/C=C/C=C(/C(=O)OC)\C	(Frederico et al., 2003; SUN et al., 2012)
Dicrocin	57710-64-2		Crocetin diglucosyl ester; constitutional isomer of CR 3	652.7	$C_{32}H_{44}O_{14}$	C/C(=C\C=C\C=C(\C=C\C=C(\C(=O)O[C@@H]1O[C@@H]([C@@H]([C@@H]1O)O)OC)/C)/C=C/C=C/C(=O)O[C@@H]2O[C@@H]([C@H]([C@@H]([C@H]2O)O)O)CO)\C	(Girme et al., 2021; Moratalla-López et al., 2021)

of CR (Zeka et al., 2020) with an estimated 0.6% (w/w) of CR can be recovered from dried petals (Zeka et al., 2015).

More than 100 compounds have been identified from SF, mainly terpenes, flavonoids, and anthraquinones (Chang et al., 2013), including CRs and crocetin (CC), which are responsible for the color of SF (Akbari et al., 2018; Kermanshahi et al., 2020; Csupor et al., 2021; Pandita, 2021). Given that CR is the main active ingredient of SF and SF-containing products such as SLT, it is of prime interest to review the current evidence for CRs in IS and related conditions. The effect of SF on IS has recently been briefly reviewed, although CRs and related compounds were not covered in detail (Azami et al., 2021). Thus, the focus of this review is to evaluate the current evidence on CR and associated analogues for IS, including pre-clinical and clinical studies, molecular mechanisms, toxicity, and safety, as well as current gaps and future directions.

LITERATURE SEARCH STRATEGY

Electronic databases including PubMed, Cochrane Library, Medline, Embase, Scopus, China National Knowledge Infrastructure (CNKI), and Web of Science were searched for relevant studies from their inception to 16 February 2022. The search terms include "crocin and analogues," AND "Saffron" OR "*Crocus sativus* L." AND "stroke" OR "ischemic stroke" AND "clinical trials" AND "pharmacokinetics," "crocin" AND "neurons, astrocytes, microglial cells" OR "neuroprotection" OR "cytokines" OR "neuroinflammation" OR "neurotoxicity" OR "antioxidant" OR "apoptosis" OR "signaling pathways" OR "molecular targets" OR "mitochondria" OR "pharmacokinetics" OR "acute/chronic toxicity" OR "clinical trial," OR "nanoparticle formulation," "safranal," "picrocrocin," "crocetin" and their combinations. 287 research items including peer-reviewed papers, websites, and Chinese data-related research papers were considered suitable according to the review search criterion. Our inclusion criterion was all primary studies involving ischemic stroke, CR, and related compounds OR stroke OR ischemia OR hypoxia. All items identified were screened for relevant references excluding duplicates and non-peer-reviewed articles. Chemical structures of CR compounds were drawn using ChemDraw software (**Table 1**). Structural information of CRs such as isomeric SMILE was retrieved from PubChem and SciFinder Databases. Human metabolomics data were retrieved from the Human Metabolome Database v4 (HMDB) Canadian Database System (Wishart et al., 2018). All the diagrams (**Figure 1**) have been created with Adobe Illustrator (Adobe Inc., 2019), Preview MacOS v10.0 (944.5) and BioRender.com.

CROCIN AND RELATED COMPOUNDS

Crocins (CRs) are a group of carotenoid compounds isolated from SF that also contain other active compounds, including picrocrocin and safranal (Suchareau et al., 2021). Seven different natural CR analogues have been identified from SF, namely CR (crocin 1, CR, CR1), CR 2 (crocin 2, CR II), CR 3 (crocin 3), CR 4

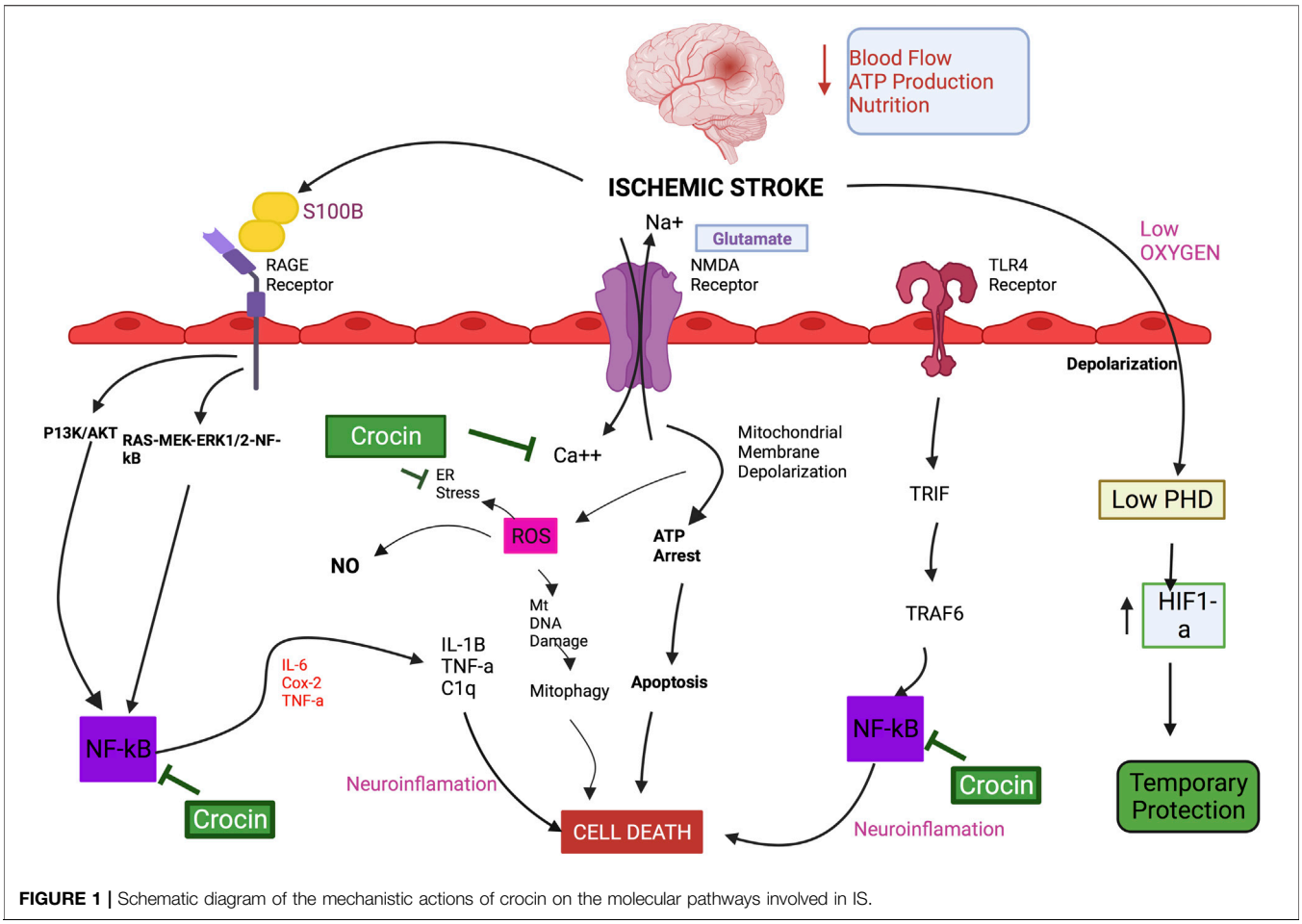

FIGURE 1 | Schematic diagram of the mechanistic actions of crocin on the molecular pathways involved in IS.

(crocin 4), CR 5 (crocin 5), CR 6 (crocin 6), and CR 7 (crocin 7) (Zhang et al., 2004; Mehrnia et al., 2017; Song et al., 2021b). All are mono or di glycosyl polyene esters of CC (Mohajeri et al., 2010a; Nam et al., 2010; Pang et al., 2020). CR and CR2 are the disaccharide analogues, whilst CR3 and CR4 are the monosaccharide analogues, which are more potent than CR and CR2 because of their structural orientations (Ulbricht et al., 2011). The biosynthesis of CRs is related to several enzymes such as cytochrome p450 (Gao et al., 2021), carotenoid cleavage dioxygenase (CCD), UDP-glycosyl transferase (UGT), and aldehyde dehydrogenase (Nagatoshi et al., 2012; Liu et al., 2020; Pu et al., 2020).

CR is one of the main bioactive ingredients in SF (Kothari et al., 2021b). The level of CRs in SF depends on their origin and quality. A high-quality SF contains about 30% of CRs (Azami et al., 2021). It was shown that Spanish SF contains more CRs, especially CR (9%), than that from other sources (Li et al., 1999). According to the Chinese Pharmacopeia, the total content of CR and CR2 in dried SF used in traditional Chinese medicine shall not be less than 10.0%, and the content of picrocrocin shall not be less than 5.0% (PPRC, 2020). On the other hand, dicrocin and CR3 are the isomers. Tricrocin, CR II or CR 2 are synonyms with the same molecular structure amidst isomeric structural orientation differentiations. To date, studies on CR3, CR4, CR5, CR6, and CR7 are still lacking. **Table 1** shows the chemical structures of CR and related compounds.

CR molecule embodies two D-gentiobiose moieties (Mohajeri et al., 2010b; Ebrahim-Habibi et al., 2010). Studies on its structural activity relationship (SAR) revealed that the sugar moieties of CR related to its antioxidant activity and water solubility (Akhtari et al., 2013; Rahaiee et al., 2015; Akbari et al., 2018). Gentiobiose terminus is known to be involved in the conversion of CR to CC in enterocytes (Singla and Giliyaru, 2011). On the other hand, some synthetic CR analogues have been developed. For example, a-glucosyl-(1-6)-trans CRs have been shown with improved water solubility, and antioxidant and neuroprotective activities in mouse neuronal cell line (HT22) neuronal cells (Mok et al., 2020).

CC is a carotenoid (lacking provitamin functionality) recognized by diterpenic and symmetrical structure along with seven double bonds, four methyl functional groups, and two carboxylic groups (Giaccio, 2004) (**Table 1**). Its sodium salt, trans-sodium crocetinate (TSC), has been developed as a potential drug candidate (Gainer, 2000; Xi and Qian, 2006; Gainer, 2008; Wang et al., 2014; Shah et al., 2021). CC and TSC have similar pharmacological activities as CR (see below). Some bioactive synthetic analogues of CC have also been synthesized such as the diamide derivative of CC (Gao et al., 2017).

TABLE 2 | Bioactivity of CRs *in vitro* and *in vivo*.

Compound	Animal/cell line	Type of study	Treatment	Effect	Mechanism	Reference
CR	Rat microglia	*In vitro*	10–50 μM	Antioxidant	Inhibited ROS production	(Mehri et al., 2011; Rao et al., 2019a)
	Mice brain slices	*In vitro*	10–20 μM	Anti-inflammation	Inhibited cytokines such as TNF-α, ROS, NO, and IL-1β	(Nam et al., 2010; Salama et al., 2020)
	Mice/rat brain	*In vitro*	0.5–2 μM/3 h	Anti-apoptosis	Inhibited Ca^{2+} overload inhibited ROS	(Mehri et al., 2011; Wang et al., 2019)
	Pheochromocytoma cell line-12 (PC-12 cells)/rats	*In vitro/ in vivo*	10 mg/kg		Inhibited mRNA expression of p38, CASP-3 lowers brain damage, ROS	(Nam et al., 2010; Huang and Jia, 2019a)
	Pheochromocytoma cell line-12 (PC-12 cells)	In vitro	10 μM/6 days		Inhibited peroxide lipids Regulated SOD level	(Ochiai et al., 2004a; Wang et al., 2019)
	Pheochromocytoma cell line-12 (PC-12 cells)	*In vitro*	10 μM		Inhibited TNF-α Inhibited caspase-3	(Soeda et al., 2001; Huang and Jia, 2019a)
	Mouse neuroblastoma neuro-2a (N2a)/ APP695swe cells.	*In vitro*	100–200 μM		Inhibited ROS Inhibited caspase-3 Inhibited cytochrome release, reduced apoptosis	(Ochiai et al., 2004a; Du et al., 2021)
	AMI rats	*In vivo*	15 and 30 mg/kg	Decreased mitochondrial stress	Increased viability of mitochondrial respiratory enzymes, Increased ATP, Increased Na + -K + -ATP enzyme and Increased Ca^{2+}-ATP enzyme and Inhibited mitochondrial Ca^{2+}	Leijiao Fan, (2021a)
	Adult albino mice (CFT-Swiss mice)	*In vivo*	25 mg/kg/day; i.p.	Reduced rotenone-induced neurotoxicity; improved performance of mice in behavioral tests.	Inhibition of ROS generation; an increase of antioxidant enzymes activities; modulation of mitochondrial function; restored levels of dopamine, α-synuclein, and AChE activity in the striatum	Rao et al. (2019a)
	Wistar rats	*In vivo*	30 mg/kg/day; i.p.	Improved behavioral tests, Increased dopamine level in striatum	Activation of PI3K/Akt/mTOR pathways and enhanced miRNA-7 and miRNA-	Salama et al. (2020)
	Diabetic rats	*In vivo*	10^{-9} –10^{-5} mol/L	Downregulated vasoconstriction	Increased endothelial nitric oxide synthase	Sai Li, (2017)
	Hemorrhagic shock rats	*In vivo*	60 mg/kg	Antioxidant properties	Increased MDA in the lungs, kidneys, and liver	Yang (2020)
	Rat	*In vivo*	50 mg/kg	Neuroprotection	Suppresses caspase-3	Chen et al. (2015)
	Rat	*In vivo*	15, 30, 60, 120 mg/kg, I.p	Neuroprotection; Lowered infarct size	Inhibited MDA and increased GPx and SOD	Vakili et al. (2014)
	Rat hippocampus	*In vivo*	12.5, 25, and 50 mg/kg/ 21 day, I.p	Antidepressant effect	Increased BDNF and CREB levels	Vahdati Hassani et al. (2014)
	Rat	*In vivo*	40 mg/kg/day orally for 10 day	Neuroprotection	Suppressed ROS, HIF-1a and caspase-3	Oruc et al. (2016)
	Rat	*In vivo*	50, 100, and 200 mg/kg Ip	Neuroprotection	Improved biochemical indices, and enzyme level	Hariri et al. (2010)
	Rat	*In vivo*	10, 20, and 40 mg/kg, i.p. once/day	Neuroprotection	Suppressed ROS, increased MDA, SOD, and CAT activities, and inhibited cytokines including TNF, IL-1β, and IL-6 and IFN-γ	Bin Wen et al. (2020)
	Bovine Aortic endothelial cells (EC)	*In vivo*	25, 50, 100 mg/kg/day	Antiatherosclerosis	Decreased LDL and EC apoptosis; lowers MDA, NO, and Intracellular Ca^{++}	He et al. (2005)
	Rat	*In vivo*	4.84, 9.69, and 19.38 mg/kg for 5 days	Antioxidant	Decreased total cholesterol, Triglycerides, SOD, CAT, GSH, MDA, and alkaline phosphatase	(Asdaq and Inamdar, 2010)
	Rats	*In vivo*	50 and 150 mg/kg	Antihyperglycemic	Lowers HbA1c, fasting blood glucose (FBS), and Upregulated blood insulin level	Kianbakht and Hajiaghaee, (2011)

(Continued on following page)

TABLE 2 | (*Continued*) Bioactivity of CRs *in vitro* and *in vivo*.

Compound	Animal/cell line	Type of study	Treatment	Effect	Mechanism	Reference
CR & CR 2	Rat I/R Injury Model	*In vivo*	50 mg/kg	Neuroprotection	ROS suppression, decreased Bcl2, Bax, caspase 3, P38, NFkB, and increased total SOD	Lv et al. (2019)

TNF-a, tumor necrosis factor-alpha; OGD, oxygen glucose deprivation; iSOD, intracellular superoxide dismutase; NO, nitric oxide; ROS, reactive oxygen species; AMI, acute myocardial infarction; CREB, cAMP response element-binding protein; BDNF, brain-derived neurotrophic factor; NFkB, nuclear factor kappa light chain enhancer of B cells; IL-6, interleukin-6; ATP, adenosine triphosphate; AChE, acetylhydrolase; HIF-1a, hypoxia inducible factor-1a.

PHARMACOLOGICAL ACTIONS OF CROCIN AND RELATED COMPOUNDS AGAINST ISCHEMIC STROKE

Effect on Experimental Ischemic Stroke

The injuries caused by cerebral ischemic and IS are mainly caused by oxidative and nitrosative stress, and are also related to inflammation, apoptosis, BBB dysfunction, and edema formation, which increases the intracranial pressure and decreases the cerebral blood perfusion of ischemic areas (Akbari et al., 2018). The commonly used animal models of cerebral ischemia and IS injuries include middle cerebral artery occlusion (MCAO) in rodents to mimic the I/R injuries in humans after stroke. A number of studies have demonstrated the protective effects of CRs *in vitro* and *in vivo* (**Table 2**). Similar findings were reported by a group showing the protective effects of CR (20 mg/kg) and *Weinaokang* (10 and 20 mg/kg, which contains CR), against cerebral microvessel injury induced by global ischemia (Zheng et al., 2010). Vakili et al. (2014) reported CR (30, 60, and 120 mg/kg, i.p., given at the start of ischemia) dose-dependently decreased the infarct volume of cerebral I/R injuries. They also found that CR (60 mg/kg, given 1 h before, at the start, or 1 h after ischemia) reduced brain edema by 48%, 52%, and 51%, respectively. Sarshoori et al. (2014) showed in MCAO rats that CR (50 and 80 mg/kg, p.o.) reduced the cortical infarct volume by 48%–60%, and decreased striatal infarct volume by 45%–75%, respectively, with improved neurological deficit scores and decreased number of eosinophilic (prenecrotic) neurons,fiber demyelination and axonal damage in ischemic regions. Similar findings were obtained by Oruc et al. (2016) who used a global cerebral I/R model in rats (bilateral occlusion for 30 min followed by 30 min of reperfusion) and demonstrated that CR (40 mg/kg/day, orally) reduced the histopathological changes and apoptosis, and improved tissues oxidative index (Oruc et al., 2016). CR (10, 20, and 40 mg/kg/day i.p., given 7 days before the operation) attenuated the brain injury compared to that of the model group, with improved symptom score, attenuated brain edema, and improved pathological morphological and structural changes (Finley et al., 2017). Furthermore, CR was also shown to protect the BBB function during cerebral hypoxia/ischemia (Zhang et al., 2017). Similarly, Huang et al. (2019) demonstrated that CR at 50 and 100 mg/kg (p.o. for 7 days) decreased infarct volume and neurological scores in MCAO rats. Bin Wen et al. (2020) found significant results, stating that CR protected brain tissue against cerebral I/R damage, and that this effect was linked to its anti-oxidant and anti-inflammatory properties.

In addition, the curative effect of CR has also been demonstrated. Zheng et al. (2007) used a transient global cerebral ischemia mice model and demonstrated that CR (5, 10, and 20 mg/kg, given intragastrically from day 0 to day 21 after ischemia) significantly improved the capillary integrity and reduced mitochondria damage caused by I/R. Ochiai et al. (2004) reported that CR (10 mg/kg, IV, administrated immediately and 3 h after MCAO) significantly reduced the infarct volume in mice. They also showed that CR was more effective than other CR analogues and SF compounds (tricrocin, dicrocin, and picrocrocin) in promoting the expression of γ-glutamylcysteinyl synthase (γ-GCS) mRNA. γ-GCS is involved in the *de novo* synthesis of glutathione (GSH) as a rate-limiting enzyme reaction and plays a crucial role in IS (Su et al., 2020; Wu et al., 2020). CR (10 mg/kg) has also been shown to reduce the brain edema and infarct areas induced by hypoxia-ischemia when given immediately or after hypoxia-ischemia in post-natal C57BL/6J mice (Huang et al., 2019). Furthermore, it has been reported recently that CR (30 mg/kg and 60 mg/kg, p.o. for 7 days, administrated after cerebral ischemia) improved the memory loss in a rat model of cerebral ischemia, which was linked to increased hippocampal acetylcholine (ACh) level and reduced apoptosis (Yuan et al., 2020), a finding similar to an earlier observation using CR (25 mg/kg, i.p.) and hydroalcoholic extract of SF (250 mg/kg, i.p.) in a rat model of vascular dementia after permanent bilateral ligation of the common carotid arteries (Hosseinzadeh et al., 2012).

A recent study reported that the cerebral-protective effects of CR against cerebral I/R injury may involve gut microbiota (Zhang et al., 2019). Using a rat transient MCAO model, the investigators showed that the oral administration of CR was more effective than IV injection in reducing infarct volume and improving neurological behaviour changes. Since CC was detected in plasma after oral administration of CR but not after IV injection of CR, and the orally administered CC showed similar protection to that of CR, it indicated the importance of gut microbiota in facilitating the transformation of CR into CC. This was confirmed by the finding that CR could be deglycosylated to CC in the gut content of normal rats, but not in pseudo-germ-free rats. Metabolomics studies also indicated that gut microbiota facilitated the transformation of CR into CC (Zhang et al., 2019).

CC has demonstrated similar pharmacological actions to CR, including neuroprotection, anti-oxidation, and anti-inflammation (Tseng et al., 1995; Li et al., 2018; Hashemi and Hosseinzadeh, 2019; Cerdá-Bernad et al., 2020) as well as protective against cardiac ischemic mitochondrial injury (Gao et al., 2017). Recently Liu et al. (2021) showed that CC (5–50 mg/L) protected hypoxia-induced cell injuries and inhibited apoptosis in cultured human U87 glioma cells, and CC (5,10, and 50 mg/kg) reduced the infarct size and apoptotic cell numbers in brain tissue and improved pathological status in rats. These effects were associated with modulation of miR145-5p, toll-like receptor 4 (TLR4) and nuclear factor kappa light chain enhancer of B cells (NFκB) (p65) (Liu et al., 2021b). CC and related oxygen diffusion-enhancing compounds have been recently reviewed (Shah et al., 2021). These compounds have been shown with properties that improve the diffusion of oxygen in plasma, thus increasing oxygenation in ischemic brain tissue (Manabe et al., 2010; Wang et al., 2014; Bahr-Hosseini et al., 2021; Shah et al., 2021). TSC has shown potential as a therapeutic drug for early stroke intervention reducing the infarct and hemorrhagic volume in rodent models of ischemic and hemorrhagic stroke (Lapchak, 2010; Wang et al., 2014; Shah et al., 2021). In obese MCAO mice, TSC (0.14 mg/kg) showed a significant improvement in neurological deficit and neuroprotective effects evidenced by lowered brain edema, MMP-2, MMP-9, and inflammatory cytokine markers in brain tissues (Deng et al., 2015).

Neuroprotection

One strategy for developing new therapies for IS to target neuroprotective signaling pathways (Rodriguez et al., 2021; Liu et al., 2012). CR has been extensively studied for its neuroprotective effects *in vitro* and *in vivo* (**Table 2**) (Yuan et al., 2020). Studies have shown that CR and related compounds protected CNS neurons in various conditions. For example, CR was demonstrated to protect against PC-12 cells injury in rats by increasing the synthesis of GSH (Ochiai et al., 2004b; Soeda et al., 2007), nitric oxide (NO), and decreasing MMP (Zheng et al., 2007). It induced the proliferation and migration of neural stem cells and inhibited the apoptosis of neural stem cells in cerebral I/R conditions, the effect involved Notch1 signaling and inhibition of inflammatory factors (An et al., 2020). CC also modulated the amyloidogenic pathway and tau misprocessing in neuronal cells (Shah et al., 2021). In the retinal ganglionic cells (RGC), CR prevented apoptosis induced by ischemic injury (Qi et al., 2013). In diabetic rats, CR was shown to act as a neuroprotective agent by lowering the malondialdehyde (MDA) and xanthine oxidase levels in the brain and cerebellum tissue (Altinzo et al., 2014). In addition, CR dose-dependently inhibited the ischemic cerebral neuronal apoptosis of proinflammatory cytokines in the ischemic tissue (Oruc et al., 2016). Huo et al. (2012) investigated the neuroprotective effect of CR in mice with traumatic brain injury. It was found that the intraperitoneal injection of CR (50–200 mg/kg) markedly reduced brain edema and motor functional deficits after the traumatic brain injury induced by physical damage from cortical impact injury. The traumatic brain injury restricted the supply of blood and oxygen in the area which led to the accumulation of reactive oxygen species and subsequent neuronal death.

Recently, CR was found to protect against hippocampal neuron damage in IS (Wu et al., 2020) and dopaminergic neuron damage in 1-methyl-4-phenyl-1,2,3,6-tetrahydropyridine (MPTP)-induced Parkinson's disease mouse models (Haeri et al., 2019). CR (25 mg/kg) has also been shown to protect neurons against neurotoxicity induced by rotenone, methamphetamine, and acrylamide in mice and Wistar rats (Rao et al., 2019b; Salama et al., 2020; Mehri et al., 2015; Shafahi et al., 2018), as well as improving neuronal survival in hypoxic ischemia related brain damage (Huang and Jia, 2019b). Another study showed that CR (30 mg/kg) alleviated apoptosis, neurodegeneration, and enhanced protection in rotenone-induced Parkinson's disease rats *via* mammalian target of rapamycin (mTOR) pathway activation (Salama et al., 2020). CR, *via* its metabolite crocetin monoglucuronide (CM), was also shown to inhibit ACh activity as predicted by docking studies (Zhu et al., 2019b). In addition, CR improved gut microbiota in stressed mice and decreased serum levels of interleukin (IL-6) and necrosis factor—α (TNF-α) (Wu et al., 2020).

Both CR and CR2 have been shown to enhance neuronal survival by downregulating caspase-3 (Casp3) and Nfkb1 mRNA expression after hypoxic ischemic CNS amelioration (Lv et al., 2019). In addition, CR has been shown to reduce the neurological deficit in a heme oxygenase-1 (HO-1) knockout mouse model of intracerebral hemorrhage (Duan et al., 2019) and reduce cytotoxicity induced by lethal agents. In glutamate-damaged HT22 cells, CR improved cell viability, suppressed reactive oxygen species (ROS) accumulation, calcium ion (Ca^{+2}) load, and apoptosis (Wang et al., 2019). In diazinon induced subacute toxicities, CR at 50, 100, or 200 mg/kg doses (i.p.) significantly ameliorated the adverse effect of diazinon on enzyme levels, and biochemical indices and downregulated the levels of S100 calcium-binding protein B (S100B) (Hariri et al., 2010). Interestingly, S100B is the prime secretary cytokine from astrocyte during metabolic stress and is related to astrocyte activation (Gerlach et al., 2006). Thus, CR may affect the function of astrocytes in its anti-IS action, although its exact effect is still not clear, it has been suggested that neuroprotection in the central nervous system (CNS) may involve astrocyte support (Teo and Bourne, 2018). Targeting astrocytic survival has been shown to lead to lowered neurodegeneration (Freitas-Andrade and Naus, 2016), especially in IS conditiosn (Becerra-Calixto and Cardona-Gómez, 2017).

Anti-Neuroinflammation

There is strong evidence for the involvement of CRs anti-neuroinflammatory effects in their neuroprotective actions (Deslauriers et al., 2011; Ahmed et al., 2020). Studies have shown that CR inhibited the production of certain inflammatory mediators such as TNF-α and interleukin-1B (IL-1B) in microglial cells (Nam et al., 2010; Bin Wen et al., 2020). CR at a dose of 40 mg/kg significantly lowered levels of IL-6 and TNF-α in chronic restraint stress mice (Xiao et al., 2020), as

well as inhibited IL-1B in depression-induced mice (Xiao et al., 2019). The anti-neuroinflammatory effect of CR was also shown in the methamphetamine-induced neurotoxicity model in rats (Shafahi et al., 2018), and inhibited inflammation-related microglial activation in mice (Fernández-Albarral et al., 2019), and also mitigated neuroinflammation in rat striatum (Eteghadi et al., 2021). CR (50 mg/kg and 100 mg/kg) inhibited lipopolysaccharide (LPS) induced neuroinflammation in rats, whilst the effect was not dose-dependent (Azmand and Rajaei, 2021). Furthermore, CR downregulated IL-1β, NO, IL-6, and TNF-α generation in rats with hemorrhagic shock (HS) and increased the level of IL-10 (Yang and Dong, 2017). IL-10 is an anti-neuroinflammatory cytokine expressed by immune cells (Saraiva and O'garra, 2010). The upregulation of IL-10 by CR is also supported by other studies (Bakshi et al., 2018; Badavi et al., 2020; Yousefi et al., 2021), although there is a contradictory finding that CR decreased IL-10 level (Dianat and Radan, 2014). The reason for this discrepancy is not clear. It may be related to experimental or disease conditions. CR (10 mg/kg) attenuated TNF-a, inducible nitric oxide synthase (iNOS), NFκB expressions during doxorubicin-induced nephrotoxicity in rats (Hussain et al., 2021). In addition, CR has also been shown to regulate cyclooxygenase-1 (COX-1) and COX-2 enzymes in LPS induced RAW264.7 cells (Xu et al., 2009). In 5XFAD (5X Familial AD) mice, CR (10 mg/kg/day) improved BBB integrity and lowered amyloid ß (Aß) associated neuroinflammation while this effect was accompanied by suppressing mitogen-activated protein kinase (MAPK) and NFκB but activating nuclear factor-erythroid factor 2 related factor 2 (Nrf2) pathways (Batarseh et al., 2017; Hashemzaei et al., 2020). The role of anti-inflammatory effect of CRs on neuronal pain has been recently reviewed, showing suppression of NFκB in turn downregulates the levels of IL-6, IL-10, IL-1β, and TNF-α (Hashemzaei et al., 2020). NFκB relates closely to IS involving inflammatory biosensors (Harari and Liao, 2010). Similarly, anti-neuroinflammatory activities of CC and TSC have also been demonstrated, including inhibiting the formation of proinflammatory mediators, such as NO and cytokines, and regulating NFκB pathway (Deng et al., 2015; Hashemi and Hosseinzadeh, 2019; Liu et al., 2021b; Shah et al., 2021).

Antioxidant Activity

Numerous studies have demonstrated that endogenous antioxidant levels were lowered after acute IS due to oxidative stress (Ullegaddi et al., 2006), and increased cellular ROS levels could ultimately lead to mitochondrial injury and cell death (Shahbaz, 2017a; Shahbaz, 2017b). Hence, antioxidants have long been investigated as a potential therapy for reducing IS injury (Shirley et al., 2014; Cichoń et al., 2017). The antioxidant activity of CR and related compounds have been well established, with increasing superoxide dismutase (SOD) and GSH synthesis and activities in brain tissue (Bandegi et al., 2014; Chen et al., 2015; Mehri et al., 2015; Zhang et al., 2017a; Krishnaswamy et al., 2020; Yousefi et al., 2021), decreasing oxidized lipids and oxidative stress in PC-12 cells (Ochiai et al., 2004b; Soeda et al., 2007), and reducing hypoxia-induced cell damage (Javandoost et al., 2017; Bukhari et al., 2018; Ghaffari and Roshanravan, 2019). In human myoblast cells, 0.3 μM CR inhibited hydrogen peroxide (H_2O_2) induced toxicity accompanied by decreased ROS and increased antioxidant enzyme activity (Nassar et al., 2020). In addition, CR was shown to upregulate MMP-2 and MMP-9 protein expression which contributes to neuroprotection and maintenance of BBB integrity (Yang and Rosenberg, 2015; Zhang et al., 2017a). In particular, Vakili et al. (2014) showed that the anti-IS effect of CR was associated with increased SOD and glutathione peroxidase (GPx) activity and reduced MDA content in the ischemic cortex. Oruc et al. (2016) reported that CR-induced protection of cerebral I/R is associated with improved tissues oxidative index. CR was also shown to curb ROS in depression-induced mice (Xiao et al., 2019). In addition, a study indicates that the antioxidant effect of CR may contribute to its protection against organ damage in HS (Yang and Dong, 2017). Similarly, the antioxidant activity of CC and TSC have been demonstrated, including inhibition of ROS formation, improving antioxidant enzyme activities, and suppression of related mitochondrial apoptosis, and Aβ mechanisms (Hashemi and Hosseinzadeh, 2019; Shah et al., 2021). It has been reported that the free radical quenching activity of CR is weaker than SF, indicating that SF may contain other antioxidant constituents or has a synergistic effect among its ingredients (Asdaq and Inamdar, 2010). It was found that trans-crocin-4 exhibited more potent antioxidant activity than CC in the human brain cells, indicating the sugar molecules in CR may be important for its antioxidant activity and Aß fibril formation inhibition (Papandreou et al., 2006). In addition, SLT, a CR-containing formula was shown to reduce H_2O_2 related injury in EA hy926 cells (Seto et al., 2017). However, it is not clear if this effect of SLT relates to CR.

Cardiovascular Protection

Cardiovascular function is important for blood supply to the brain, thus the effect of CRs on cardiovascular functions may affect or contribute to their effects against IS. CR has demonstrated anti-ischemia effects in cardiac and vascular tissue. For example, CR (20 mg/kg) was shown to exhibit cardioprotective activity in I/R-related myocardial injury and decreased infarct size in ischemia the rats' hearts by altering antioxidant status (Jahanbakhsh et al., 2012; Dianat et al., 2014). CR (100 mg/kg/day) attenuated cardiac inflammation and improved antioxidant capacity in female rats (Kocaman et al., 2021). Additionally, a study using cardiac ischemic rats showed CR at 20 mg/kg/day i.p. protected cardiac injury and increased SOD, MDA, and GSH antioxidant markers (Jahanbakhsh et al., 2012). Another study found that pre-treatment with CR followed by I/R (2 h hypoxia, 4 h reoxygenation) protected myocardial ischemic injury and regulated autophagy AMP-activated protein kinase (AMPK) mechanistic pathway (Zeng et al., 2016). Fan et al. (2021) showed CR protected myocardial mitochondria injury and acute myocardial infarction in rats (Leijiao Fan, 2021b). CR (15 and 30 mg/kg) significantly attenuated mitochondrial damage by increasing the membrane potential and reducing the

mitochondrial permeability transition pore openness. The mechanism was associated with increased viability of mitochondrial respiratory enzymes, adenosine triphosphate (ATP), Na^+-K^+-ATP enzyme and Ca^{2+}-ATP enzyme, and reduced mitochondrial Ca^{2+} concentration (Leijiao Fan, 2021b). Similar activities have been reported for CC and TCS, including cardioprotective effects against I/R injury, inhibiting myocardial infraction and cardiac hypertrophy, reducing blood pressure, and inhibiting platelet aggregation (Hashemi and Hosseinzadeh, 2019; Shah et al., 2021). For example, in a myocardial I/R rats model TSC (50 and 100 μg/kg) significantly alleviated I/R-induced cell injury *via* the SIRT3/FOXO3a/SOD2 signaling pathway (Chang et al., 2019). CR and related compounds have also been shown to possess vascular protective activity which may also contribute to their anti-IS actions. For example, CR improved vasodilation by acting on endogenous NO and endothelial NO synthase (Sai Li and ding, 2017) and reduced I/R injury in mice cerebral microvessels (Zheng et al., 2007). CC (25 and 50 mg/kg/day) was also shown to protect vascular function in stroke-prone spontaneously hypertensive rats (SHRSPs), with downregulated thrombogenesis, improved vasodilation, and endothelial function (elicits NO production), and antioxidant capacity (Higashino et al., 2014).

MECHANISM OF ACTIONS OF CROCIN AND RELATED COMPOUNDS

Potential Cellular Targets

CR has been shown to act on multiple brain cells including microglia, neurons, and astrocytes (Hosseinzadeh et al., 2014b; Zhu et al., 2019a). **Table 2** shows the effects of CR and related compounds on different cells including microglia, endothelial cells and neurons (**Table 2**). For example, in syncytin-1-expressed primary human foetal astrocytes, CR (100, 200, and 400 μM) inhibited endoplasmic reticulum (ER) stress and nitric oxide synthase 2 and interferon gamma (IFN-α) expressions (Deslauriers et al., 2011). Although CR mitigated TNF-a release in astrocytes, microglia, and neurons after LPS stimulation (Gullo et al., 2017), the effect of CRs on astrocytes involving IS microvessels is still not clear. Astrocytes may play a critical role in neuroprotection during IS through their specialized functional and structural properties in the CNS (Liu and Chopp, 2016; Sun et al., 2019) including regulation of metabolic and homeostasis (Liddelow et al., 2017; Escartin et al., 2021). It is also necessary to investigate the effect of CRs on different phenotypes of astrocytes such as A1 (neuroinflammatory), A2 (neuroprotective), and A0 (nascent astrocytes).

Potential Molecular Targets

As mentioned above, CRs have therapeutic action on multiple pathways, related to cell signalingsignaling, transportations, energy production, and redox homeostasis (Hosseinzadeh et al., 2014a), in particular neuroinflammation, antioxidation, and apoptosis mechanisms (**Table 2**). For example, CR inhibited hypoxia-inducible factor-1α which is an important molecular target in IS (Oruc et al., 2016) (**Table 2**). The action of CR on mitochondrial apoptosis is also important for their neuroprotective effects against IS (Li et al., 2021; Yousefsani et al., 2021), including casp 3, casp 8, casp 9, B-cell lymphoma-2 (Bcl-2), and Bcl-2 Associated X-protein (Bax) (**Table 2**). The key ROS-related enzymes targeted by CR and associated compounds or analogues include SOD, reduced nicotinamide adenine dinucleotide phosphate (NADPH) oxidase, and GPx (Bandegi et al., 2014; Chen et al., 2015; Zhang et al., 2017b). In addition, it has been suggested that matrix MMPs activation plays a role in IS (Yang and Rosenberg, 2015) and amelioration of MMP-2 and MMP-9 expressions by CR may provide neuroprotection and protection of BBB functions under cerebral ischemia (Zhang et al., 2017b). The key inflammatory signaling molecules influenced by CR and related compounds include TNF-α, IL-1β, IL-1α, IL-6, IL-1, and MMP-9, monocyte chemoattractant protein-1 (MCP-1), macrophage inflammatory proten-1α (MIP-1α), vascular adhesion molecule-1 (VCAM-1), E-selectin and fractalkine (CX3CL1) and related signaling pathways namely NFκB, MAPK, TLR4, c-Jun N-terminal kinase (JNK), and P38 (Che et al., 2001; Hussein et al., 2019; Barthels and Das, 2020). In addition, autophagy is another important cellular mechanism involved in various cellular functions (Shen et al., 2021), and is a significant adaptive mechanism in IS (Ajoolabady et al., 2021). It has been suggested that activation of autophagy is involved in the protective effect of CR against IS (Zeng et al., 2016) CR enhanced autophagy by downregulating the LC3-II/I and upregulating the p62 and mTOR expression in IS model of HT22 cells (Huang et al., 2019). CC and TSC have shown with similar activities affecting cellular redox signaling and inflammatory pathways, as well as regulating autophagy, which contribute to their anti-IS and neuroprotective pharmacological actions (Tseng et al., 1995; Hashemi and Hosseinzadeh, 2019; Cerdá-Bernad et al., 2020; Shah et al., 2021; Wani et al., 2021).

Table 3 shows the IS-related human proteins potentially regulated by CR, based on the human metabolomic data retrieved from the standard HMDB Canadian Database System. We identified 11 proteins as the possible targets of CRs, including S100β, vascular endothelial growth factor (VEGF), glial fibrillary acidic protein (GFAP) and compliment component 1q (C1q). Since S100B is elevated in patients after IS (Lasek-Bal et al., 2019) and higher S100B levels were observed in the hospitalized IS patients (Shotar et al., 2019), S100B may be a potential diagnostic and therapeutic biomarker of IS. Intracellularly S100B can act as a regulator of Ca^{++} homeostasis (Donato et al., 2009). Extracellularly, it can activate inflammatory and other signaling pathways, such as the mitogenic Ras-MEK-ERK1/2-NF-κB pathway. SF has also been shown to regulate glial GFAP, VEGF, and C1q in MCAO animals (Yang et al., 2019; Abdel-Rahman et al., 2020; Zhong et al., 2020), although the exact role of CR and related compounds in these actions is not clear. Further studies are mandatory to elucidate the mechanisms involved in the actions of CRs against IS and related conditions in human (Karkoula et al., 2020).

TABLE 3 | IS-related human proteins targeted by CR, based on the metabolomic data by CRs (retrieved from the HMDB Canadian Database System).

Protein	Effect of CR	HMBD protein Id	Cellular location	Chromosome location	Main function	Metabolites
S100B	Downregulate	HMDBP07977	Nucleus and cytoplasm	Chr. 2	Involved in Ca^{2+} ion binding	Ca^{2+}, Olopatadine
FIH-1	—	HMDBP01023	Nucleus (Potential),	Chr. 10	Oxygen sensing inhibits HIF1-a	Oxoglutaric acid, succinic acid, Fe^{2+}, and CO_2, O_2, D-tartaric acid
VEGFA	Downregulated	HMDBP02130	Membrane	Chr. 6	Growth factor activity in angiogenesis and endothelial cell proliferation	Atorvastatin, pyroglutamic acid, heparin, and simvastatin
C1q	—	HMDBP02512	Secreted	Chr. 3	Involved in cytokine activity	Cyclic AMP
S100A10	—	HMDBP07984	—	Chr. 1	Ca^{2+} ion binding	Ca^{2+}
Vimentin	Up-regulation	HMDBP01682	—	Chr. 1	Structural molecular activity	Carnosine
PHD1	Up-regulation	HMDBP09211	Nucleus and cytoplasm	Chr.19	Oxidoreductase activity	Ascorbic acid, L-proline, oxoglutaric acid, succinic acid, O_2, and 4-hydroxyproline
NSE	Downregulate	HMDBP01086	Cell membrane	Chr. 12	Neuroprotective	Water, Ca^{2+}, magnesium, 2-phospho-d-glyceric acid, phosphoenolpyrovic acid, and 3-dehydroquinic acid
MMP9	Downregulation	HMDBP02128	Secreted, extracellular matrix	Chr. 2	Metallopeptidase activity	Simvastatin, marimastat, $Ca^{2+,}$ minocycline, Zinc, and Captopril
IL-1B (catabolin)	Downregulation	HMDBP02072	Secreted	Chr. 2	IL-1 receptor binding, inflammatory response	Minocycline
TNF-a (cachectin)	Downregulation	HMDBP02070	Enzymatic protein secreted	Chr. 6	TNFR binding	Butyric acid, isopropyl alcohol, glucosamine, atorvastatin, simvastatin, cis,trans-5′ hydroxythalidomide, chloroquine, clenbuterol, pranlukast, amrinone, and ethyl pyruvate
IL-6	Downregulate	HMDBP02087	Enzymatic protein secreted	Chr. 7	Cytokine activity, IL-6 receptor binding	Simvastatin

Chr, chromosome number; "-", No data as per human metabolomic database; TNFR, tumor necrosis factor receptor.

PHARMACOKINETICS OF CROCINS

The pharmacokinetics of CR and related compounds have been reviewed (Xi and Qian, 2006; Khorasany and Hosseinzadeh, 2016; Hosseini et al., 2018; Hashemi and Hosseinzadeh, 2019; Veisi et al., 2020; Song et al., 2021a; Shah et al., 2021).

Asai et al. (2005) studied the absorption of CR and CC in mice and showed that neither CR nor CR2 were detectable in the plasma after the oral administration of a mixed micelle solution containing CC or CRs, whereas CC was rapidly absorbed into the blood and detected in plasma as free form and glucuronide conjugates, indicating the metabolism of CRs mainly involves glucuronidation in the intestine and liver. Another study confirmed that CM (CR metabolite) was detected in blood and brain after oral administration of CR (Zhang et al., 2012). Xi et al. (2007) studied the absorption of CR and CC in rats after single or repeated oral doses (40 mg/kg by oral gavage), and found that CR was not detectable, while CC was present in the plasma at low concentrations. They also demonstrated that CR was excreted through the intestinal tract following oral administration, indicating the intestinal tract may serve as a site for CR *via* hydrolysis. Another study in stroke-prone spontaneously hypertensive rats found a high level of CC in plasma and brain after oral administration of 100 mg/kg CC (Yoshino et al., 2011). The elimination half-life (t1/2k) after an oral dose of CR (1 mg/kg) was reported as 3.0 ± 0.6 h (Zhang et al., 2012). Studies in humans confirm that CC is rapidly absorbed after oral administration (Hosseini et al., 2018). In healthy adult volunteers, it was reported that the peak plasm (Cmax) level of CC after receiving 7.5, 15, and 22.5 mg doses was 100.9–279.7 ng/ml, and the mean time to reach maximum concentration (T_{max}) was 4–4.8 h, AUC0–24 h ranged from 556.5 to 1720.8 ng h/ml and the mean elimination half-life ($T_{1/2}$) was 6.1–7.5 h (Umigai et al., 2011). The pharmacokinetics of CC after oral and IV administrations is consistent with a two-compartment model (Xi and Qian, 2006).

There is evidence that CR could not penetrate Caco-2 monolayers, while trans-crocetin permeated the intestinal barrier (Lautenschläger et al., 2015). It has been suggested that CRs are hydrolyzed in the intestine by intestinal cells to the deglycosylated trans-crocetin, which is subsequently absorbed by passive transcellular diffusion (Lautenschläger et al., 2015; Karkoula et al., 2018; Shah et al., 2021), most likely *via* gut microbiota mediated biotransformation as mentioned above (Zhang et al., 2019). This mechanism may be important for CRs to exert their anti-IS and

neuroprotective actions in the brain, as CC has been shown to be able to permeate BBB and accumulate in the brain (Lautenschläger et al., 2015; Karkoula et al., 2018). On the other hand, some CRs such as trans-crocin 4 were shown to be able to across BBB in mice after ip administration despite its highly hydrophilic character (Lautenschläger et al., 2015; Karkoula et al., 2018). Studies showed that CC can be rapidly distributed into different tissues, including the liver and kidneys, partly due to its weak binding to plasma albumin (Xi and Qian, 2006; Hosseini et al., 2018; Christodoulou et al., 2019; Hashemi and Hosseinzadeh, 2019; Shah et al., 2021). A study on rats by Zhang et al., showed that $T_{1/2}$ was estimated as 2.5–2.9 h after oral administration of different doses of CC (Zhang et al., 2017a). CR is excreted primarily through the intestinal tract in feces after oral administration (40 mg/kg), with 59.507% ± 13.56% excreted (Asai et al., 2005), and *via* urine after IV administration with a cumulative excretion fraction of 67.17% ± 4.79% within 48 h (Zhang et al., 2019).

Nanoparticle Formulation and Green Synthesis

Nanoscale drug delivery is an important tool to improve the pharmacokinetics and bioavailability of drugs and natural drugs (Puglia et al., 2010). Nanoparticle (NP)-based drug delivery systems have shown advantages in improvised bioavailability, bioadhesion, and controlled drug release in the gastrointestinal (GI) tract (Kim et al., 2006; Dudhani and Kosaraju, 2010). For example, some chitosan-alginate biofilm forming agents have been used for pH-sensitive nanomolecular formulations to control drug movement across the GI tract (George and Abraham, 2006). Thus, NP-based formulations can be used to enhance the bioavailability and activity of CRs and CC (Shah et al., 2021). A nano-encapsulated formulation of chitosan alginate biofilm-forming agents has been shown with improved CR stability and bioavailability, and controlled release (Rahaiee et al., 2015) (Mirhadi et al., 2020). CR chitosan-alginate NPs also showed improved antioxidant and anticancer activities *in vivo*, suggesting potential therapeutic applications for these preparations (Rahaiee et al., 2017). Another recent study explored an NP-CR formulation with dextran/chitosan sulphate (DS/CH) coated NPs loaded with CR, and demonstrated its activity in downregulating VEGF and AB142 levels accompanied by a stronger antioxidant capacity in SHSY5Y cells (Song et al., 2022). In addition, a water-soluble crocetin-γ-cyclodextrin formulation significantly increased the bioavailability of CC and facilitated it crossing the BBB to enter the brain (Wong et al., 2020). Furthermore, CR-NPs have been formulated with polymeric carriers to improve the stability of CR (Mirhadi et al., 2020).

Green synthesis is an advanced method that uses natural reducing agents, plugs, and stabilizers surpassing the employment of toxic and expensive chemicals and high energy costs (Hussain et al., 2016). There is an increasing need for optimal eco-friendly and non-toxic methods of developing NPs such as gold NPs (AuNPs) preparation with CR (Hoshyar et al., 2016) and SF (Abootorabi et al., 2016). Solid lipid nanoparticles belong to the lipid nanotransporter family that can solubilize hydrophilic and lipophilic molecules in physiological environments. This is controlling their release and protects them from degradation (Tapeinos et al., 2017). CC and CR solid lipid nanoparticles can be prepared using Softisan 100 (hydrogenated coco glyceride) and Pluronic F68 (Poloxamer 188) with these lipid substrates commonly regarded as the best with low melting point (35°C), which is an important property related to the stability of NPs (Puglia et al., 2019). These nanoparticles have been tested in cancer cell lines and showed a prolonged antioxidant activity, and better antitumor cytotoxicity than free CR (Puglia et al., 2019).

Clinical Evidence

A number of clinical studies on SF and CR have been conducted, involving healthy subjects or patients with various conditions such as metabolic syndrome (Kermani et al., 2017), depression, and coronary artery disease (CAD) (Abedimanesh et al., 2017). **Table 4** summarizes the clinical studies on SF and CR. For example, a study with SF extract capsules (200 mg/day) showed that it was effective against IS with a long term (up to 3 months) neuroprotective effect, based on the National Institute of Health Stroke Scale (NIHSS), with improved Barthel index and brain-derived neurotrophic factor (BDNF) levels, and decreased stroke severity with lowered levels of serum neuron-specific enolase (NSE) and S100 (Asadollahi et al., 2019). A similar finding was obtained in an RCT involving 40 patients with acute IS, and revealed that SF at 400 mg/day decreased the severity of stroke as assessed by the NIHSS score, with an improved MDA level (Gudarzi et al., 2020). Other studies demonstrated the effectiveness of SF, in combination with Ritalin, for patients with attention deficit hyperactivity disorder (ADHD) (Pazoki et al., 2022), or CAD with a significant inhibition of circulating MCP-1 (Abedimanesh et al., 2020). In addition, a study showed that 30 mg of SF supplement for 16 weeks improved cognition function (change in both AD Scale-cognitive subscale (ADAS-cog) and clinical dementia ratings-scale sums of boxes (CDR-SB) in patients with mild to moderate Alzheimer's disease (Akhondzadeh et al., 2010). This is supported by a recent systematic review of five RCTs involving 325 subjects on AD and mild cognitive impairment, suggesting that SF may be as efficacious as common drugs against AD, although it should be taken with caution as there may be an unknown or high risk of bias due to the low quality of some of the studies included (Avgerinos et al., 2020). On the other hand, a recent trial involving 50 patients with type 2 diabetes (T2D) confirmed a significant improvement in glycaemic control and insulin resistance after administration of 15 mg CR twice daily for up to 12 weeks (Behrouz et al., 2020). Furthermore, a double-blind RCT involving 62 participants with mild erectile dysfunction (ED) showed that administering 15 mg SF twice a day improved erectile function without obvious side effects, indicating it may be effective against ED, especially in patients reluctant to accept the prescription of phosphodiesterase type 5 inhibitors (Najafabadi et al., 2022). A small trial (40 patients) on depression compared the effect of SF (30 mg/day) and fluoxetine (40 mg/day) and found no significant difference between the two groups in reduction of Hamilton depression rating scale, and the frequency of adverse events, indicating SF has similar antidepressant activity as fluoxetine, although further research with larger sample size is needed (Shahmansouri et al., 2014). Currently, there is no

TABLE 4 | Clinical studies on CR and SF.

Testing agent	Study design	Treatment	Key finding	Reference
SF	RCT on IS (*n* = 39)	SF extract (200 mg/kg) for 4 days and 3 months follow-up Placebo *n* = 20 SF treatment *n* = 19	Lowered stroke severity, higher Barthel index, short- and long-term protective effect	Asadollahi et al. (2019)
SF	RCT on IS	SF capsule 400 mg/day for 4 days Placebo (*n* = 20) Treatment (*n* = 40)	Lowered stroke severity on NIHSS score Oxidative stress markers decreased Decreased NSE	Gudarzi et al. (2020)
SF	Double-blind, RCT in healthy subjects (*n* = 60)	200–400 mg/day for a week Placebo (*n* = 20) SF (*n* = 20)	Not affecting coagulant or anti-coagulant system	Ayatollahi et al. (2014)
SF	Healthy subjects (*n* = 10)	200 mg/day		Modaghegh et al. (2008)
Safranal & CR (Affron)	RCT Placebo controlled trial on depression *n* = 128)	Placebo (*n* = 3) 22 mg/day (*n* = 41) 28 mg/day (*n* = 42)	Reduced anxiety and the doses were safe No side effects observed	Kell et al. (2017)
CR	Placebo controlled trial in patient with metabolic syndrome *n* = 30)	15 mg/twice per day for 8 weeks placebo *n* = 30 treatment *n* = 30	Decreased Serum PAB No side effect	Nikbakht-Jam et al. (2016)
CR	Placebo-RCT on diabetic maculopathy (*n* = 60); (*n* = 101 eyes)	5–15 mg/day tablet for 3 months third group as Placebo (*n* = 34) CR 5 mg/day *n* = 34 CR 15 mg/day *n* = 33	CR 5mg/day improves central macular thickness (CMT), HbA1c, and FBS levels Some side effects reported such as feet swelling and polyphagia	Sepahi et al. (2018)
CR	Placebo RCT of MMT (methadone maintenance treatment) patient	CR, 15 mg twice a day, CR *n* = 25 Placebo, 15 mg twice a day, *n* = 25	Improved mental health status	Khalatbari-mohseni et al. (2019)
CR	RCT Methadone maintenance treatment (MTT) patients	15 mg/day for 8 days CR (*n* = 26), placebo (*n* = 27)	Improved mental health and metabolic profile	Ghaderi et al. (2019)
SF	Alzheimer's disease	30 mg/day capsule for 16 days	Improved cognitive function	Akhondzadeh et al. (2010)
CR	Healthy volunteers	42 healthy volunteers CR tablet 20 mg/day for a month (*n* = 22) To check the safety profile	Lowered amylase and WBCs after 1-month treatment. No significant changes in kidney and liver functions. No major adverse events were observed	Mohamadpour et al. (2013)
CR	RCT Metabolic syndrome	100 mg/day tablet for 6 weeks *n* = 24 placebo *n* = 24 CR	Lowered cholesterol and TG	Kermani et al. (2017)
CR	RCT CAD depression	30 mg/8 weeks 45–55 years CAD patients	Reduced depression	Abedimanesh et al. (2017)
CR	RCT Metabolic Syndrome	30 mg/day for 8 weeks 44 patients *n* = 22 CR *n* = 22 placebo	Increased serum cholesteryl ester transfer protein, no effect on HDL, LDL, TG, FBG	Javandoost et al. (2017)

PAB, pro-oxidant–antioxidant balance; TG, triglyceride; LDL, low-density lipoprotein; HDL, high-density lipoprotein; FBG, fasting blood glucose; RCT, randomized controlled trial; CAD, coronary artery disease.

published RCT on CR or related compounds for treating IS. Zhu et al. (2010) described earlier a study using a CR injection (40 and 80 mg/day for 2 weeks) treating 60 patients with thrombotic cerebral infarction, and showed a significant improvement in symptoms, with an overall effective rate of 91% and 80%, respectively, and without obvious side effects. Given that CR has been demonstrated with efficacy in various conditions (**Table 4**), further clinical trials on the effect of CR on IS are mandatory. On the other hand, TSC has been studied as a synthetic carotenoid drug to enhance oxygenation of hypoxic tissue in addition to the standard of care, including Covid-19 and a Phase 2 trial on efficacy and safety for suspected stroke. However, the stroke trial was terminated due to the COVID-19 pandemic, according to the information posted on Clinicaltrials.gov (Zhu, 2010; Shah et al., 2021; Streinu-Cercel et al., 2021).

Toxicity and Safety of Saffron, Crocin, and Related Compounds

The toxicity of SF has been well studied (Alavizadeh and Hosseinzadeh, 2014b; Abu-Izneid et al., 2020) with a lethal dose (LD_{50}) ranging from 1 to 5 g/kg, indicating it is mildly toxic compared to nontoxic compounds (LD_{50} > 5 g/kg) (Abu-Izneid et al., 2020). A recent study on the acute toxicity of orally administrated SF showed its LD_{50} as 4.12 ± 0.55 g/kg in mice

(Gupta and Pandey, 2020). SF at the therapeutic doses (30–60 mg/day) has been shown with certain side effects including hypomania, sedation, nausea, mild headache and anxiety, dry mouth, dizziness, vomiting, and fatigue after 6 or 22 weeks (Akhondzadeh et al., 2005; Akhondzadeh et al., 2010). In general, SF at 1.5 g/day has been considered to be safe with no significant adverse drug effects (Ghaffari and Roshanravan, 2019). At a high dosage of 10 g/day in humans, SF manifested abortion or life-threatening complications (Mollazadeh et al., 2015), such as temporary paralysis after hallucination and abortion accompanied by maternal morbidity (Moghaddasi, 2010; Ghorbani and Koocheki, 2017). In comparison, the LD_{50} for CR could not be obtained as it did not cause mortality in mice after i.p. administration at 0.5–3 g/kg (Hosseinzadeh et al., 2010). An early study found that a high dose of CR (100 mg/kg for 2 weeks) caused liver injury and black pigmentation in rats (Wang et al., 1984). However, a recent comprehensive study on the acute and subacute toxicity of CR (up to 3 g/kg po and i.p.) in rodent found it did not cause damage to major organs (Hosseinzadeh et al., 2010). Another study found that CR at doses of 50,100, and 200 mg/kg (once a week for 4 weeks, i.p.) in rats did not cause significant changes in liver enzymatic profile and non-pathological tissue changes (Hariri et al., 2010). Rats fed with 1% CR for 4 months showed a reversible pigmentation (Wang et al., 1984; Imran et al., 2019). These findings indicate that CR is generally safe and well-tolerated. However, CR at 200 and 600 mg/kg i.p. was found to affect skeleton formation in pregnant mice indicating it may have developmental toxicity at very high doses (Moallem et al., 2016). On the other hand, CC was reported with a teratogenic effect at high concentration (200 μM) in frog (Xenopus) embryos (Martin et al., 2002), although no genotoxicity was observed for CC in V79 Chinese hamster cells (Ozaki et al., 2002), and no retinal toxicity was observed for CC in rabbit eyes (Wang et al., 2019). CR and CC have been well demonstrated for their cytotoxic activity against several cancer cells (Hoshyar and Mollaei, 2017; Hashemi and Hosseinzadeh, 2019; Veisi et al., 2020).

The clinical safety of CR has been demonstrated in several human trials (Ahmed et al., 2020). In a randomized double-blind placebo-controlled trial in healthy volunteers (n = 42), CR at 20 mg/day administrated for 1 month showed a safe profile of CR, with only minor adverse reactions in conjunction with decreased partial thromboplastin time, amylase, and mixed monocytes, basophils, and eosinophils (Mohamadpour et al., 2013). Another double-blind placebo-controlled study in schizophrenic patients (n = 22) found that CR tablet (15 mg/twice a day) caused no side effects or significant changes in liver, kidney, and thyroid markers and hepatological components (Mousavi et al., 2015). A randomized trial on diabetic maculopathy diagnosed 60 patients, and showed that CR tablets (5 or 15 mg/day for 3 months) caused some minor adverse reactions including polyphagia (4 patients), foot swelling (2 patients), burning of eyes (3 patient), red-eye (2 patients), subconjunctival hemorrhage (5 patients), eye swelling (3 patients) and stomach ache (1 patient) (Sepahi et al., 2018). Another clinical trial on CR as an adjunct therapy to methadone against opioid withdrawal in 50 patients found that CR at 15 mg twice a day for 8 weeks caused some minor side effects including headache, insomnia, nausea, and dyspnoea (Khalatbari-mohseni et al., 2019). Similarly, CC at 7.5 mg/day for 14 days in a randomized, double-blind, placebo-controlled, crossover trial on sleep quality was found to improve subjective sleep quality and no obvious adverse events linked to CC intake were observed, indicating that CC at this dose and treatment protocol is safe (Umigai et al., 2011). A 12-week RCT involving 32 healthy adult volunteers showed that CC (7.5 mg/day) had no significant adverse effects (Yamashita et al., 2018) while increased delta power and enhanced the refreshing feeling while waking up (Umigai et al., 2018). Overall, CR and CC at common therapeutic doses are generally safe in humans. Animal toxicology studies and phase I clinical trials had been conducted for TSC and showed it was well tolerated and safe in humans, although no published data are available (Gainer, 2008). Nevertheless, Mohler III et al. (2011) showed that TSC at a dose range (0.25 to 2.0 mg/kg, IV, once daily for 5 days) was safe and well-tolerated in patients with peripheral artery disease (PAD).

FURTHER REMARKS AND CONCLUSIONS

Significant progress has been made recently in understanding the actions of CR and related compounds on IS-related conditions and the mechanisms involved. The current pre-clinical and clinical evidence indicates a great potential of CR, CC, and TSC to treat IS and related conditions. However, these studies have some limitations and there are still gaps that curb the clinical translation of research findings. For example, although there is strong pre-clinical evidence for the beneficial actions of CR against IS, the current clinical trials on CR and related compounds are limited to other conditions, and specific clinical trials on IS are still lacking. In addition, many published studies are with small sample sizes and some are subject to potential bias, thus, high-quality clinical studies are needed to further confirm their efficacy and safety. It is also important to establish the proper treatment protocol and compare the effects of these compounds under short-term and long-term treatments. More research is needed to improve the bioavailability of CR, including developing formulations or delivery systems to maximize their efficacy and safety, with proper dosage regimen and route of administration. Further research is also needed to elucidate the mechanism(s) involved in the actions of CR and related compounds, including transformation and site of actions, molecular targets, and sensitive markers. Among these, the synergy of these compounds with other drugs or ingredients needs to be explored. For example, it has been shown that TSC, given in combination with rtPA either before or after embolization, improved the treatment outcomes in experimental acute IS (Lapchak, 2010). CR has also been shown with a synergistic effect with zinc sulfate to reduce hepatic I/R injury in Rats (Mard et al., 2017). Further research in this area will warrant the potential therapeutic value of these compounds not only as drug candidates by themselves but also as a complementary therapy with existing therapies and other drugs available. Finally, current studies have focused on CR and CC, more research on other forms of CRs is needed.

In conclusion CRs, most importantly CR, are key active compounds of *C. sativus* L. (SF). These compounds have been demonstrated with beneficial pharmacological actions in preventing or reducing IS-induced injury *via* multiple mechanisms including

neuroprotective, antioxidant, anti-inflammation, and other cerebral protective activities. CR can act on various cellular and molecular mechanisms related to IS in particular neuroinflammatory mitochondrial signaling pathways, HIF1a, VEGF, and cytokines. CR has low bioavailability and its conversion to CC by gut microbiota may be important in mediating its therapeutic effect. Toxicological and clinical studies indicate that CR is generally safe in humans. The current evidence indicates that CR and related products may have potential as stand-alone or adjuvant therapy for treating IS, although further confirming clinical studies are needed. The elucidation of CRs molecular targets and synergistic mechanisms with other drugs or ingredients may help translate preclinical findings into novel therapies for the intervention, management, and prognosis of IS and related conditions.

AUTHOR CONTRIBUTIONS

CL and KS conceptualised the review. KS and CL drafted and revised the manuscript. DC, XZ, ML, and SS contributed to the revision of the manuscript. KS, CL, and XZ contributed to reference collection. KS drew all chemical structures and figures. All authors approved the submitted version.

FUNDING

This work was supported by Western Sydney University (WSU) Research Training Scheme. KS was supported by a WSU Postgraduate Research Scholarship.

REFERENCES

Abdel-rahman, R. F., El awdan, S. A., Hegazy, R. R., Mansour, D. F., Ogaly, H. A., and Abdelbaset, M. (2020). Neuroprotective Effect of Crocus Sativus against Cerebral Ischemia in Rats. *Metab. Brain Dis.* 35, 427–439. doi:10.1007/s11011-019-00505-1

Abe, K., and Saito, H. (2000). Effects of Saffron Extract and its Constituent Crocin on Learning Behaviour and Long-Term Potentiation. *Phytother. Res.* 14, 149–152. doi:10.1002/(sici)1099-1573(200005)14:3<149::aid-ptr665>3.0.co;2-5

Abedimanesh, N., Motlagh, B., Abedimanesh, S., Bathaie, S. Z., Separham, A., and Ostadrahimi, A. (2020). Effects of Crocin and Saffron Aqueous Extract on Gene Expression of SIRT1, AMPK, LOX1, NF-Kb, and MCP-1 in Patients with Coronary Artery Disease: A Randomized Placebo-Controlled Clinical Trial. *Phytother. Res.* 34, 1114–1122. doi:10.1002/ptr.6580

Abedimanesh, N., Ostadrahimi, A., Bathaie, S. Z., Abedimanesh, S., Motlagh, B., Jafarabadi, M. A., et al. (2017). Effects of Saffron Aqueous Extract and its Main Constituent, Crocin, on Health-Related Quality of Life, Depression, and Sexual Desire in Coronary Artery Disease Patients: A Double-Blind, Placebo-Controlled, Randomized Clinical Trial. *Iran. Red Crescent Med. J.* 19. doi:10.5812/ircmj.13676

Abootorabi, Z., Poorgholami, M., Hanafi-Bojd, M. Y., and Hoshyar, R. (2016). Green Synthesis of Gold Nanoparticles Using Barberry and Saffron Extracts. *Mod. Care J.* 13, e13000. doi:10.5812/modernc.13000

Abu-Izneid, T., Rauf, A., Khalil, A. A., Olatunde, A., Khalid, A., Alhumaydhi, F. A., et al. (2020). Nutritional and Health Beneficial Properties of Saffron (Crocus Sativus L): A Comprehensive Review. *Crit. Rev. food Sci. Nutr.*, 1–24.

Adobe inc (2019). *Adobe Illustrator*. [Online]. Available at: https://adobe.com/products/illustrator. [accessed].

Ahmed, S., Hasan, M. M., Heydari, M., Rauf, A., Bawazeer, S., Abu-Izneid, T., et al. (2020). Therapeutic Potentials of Crocin in Medication of Neurological Disorders. *Food Chem. Toxicol.* 145, 111739. doi:10.1016/j.fct.2020.111739

Ajoolabady, A., Wang, S., Kroemer, G., Penninger, J. M., Uversky, V. N., Pratico, D., et al. (2021). Targeting Autophagy in Ischemic Stroke: from Molecular Mechanisms to Clinical Therapeutics. *Pharmacol. Ther.* 225, 107848. doi:10.1016/j.pharmthera.2021.107848

Akbari, G., Ali Mard, S., and Veisi, A. (2018). A Comprehensive Review on Regulatory Effects of Crocin on Ischemia/reperfusion Injury in Multiple Organs. *Biomed. Pharmacother.* 99, 664–670. doi:10.1016/j.biopha.2018.01.113

Akhondzadeh, S., Sabet, M. S., Harirchian, M. H., Togha, M., Cheraghmakani, H., Razeghi, S., et al. (2010). Saffron in the Treatment of Patients with Mild to Moderate Alzheimer's Disease: A 16-week, Randomized and Placebo-Controlled Trial. *J. Clin. Pharm. Ther.* 35, 581–588. doi:10.1111/j.1365-2710.2009.01133.x

Akhondzadeh, S., Tahmacebi-Pour, N., Noorbala, A. A., Amini, H., Fallah-Pour, H., Jamshidi, A. H., et al. (2005). Crocus Sativus L. In the Treatment of Mild to Moderate Depression: A Double-blind, Randomized and Placebo-controlled Trial. *Phytotherapy Res. Int. J. Devoted Pharmacol. Toxicol. Eval. Nat. Prod. Deriv.* 19, 148–151. doi:10.1002/ptr.1647

Akhtari, K., Hassanzadeh, K., Fakhraei, B., Fakhraei, N., Hassanzadeh, H., and Zarei, S. A. (2013). A Density Functional Theory Study of the Reactivity Descriptors and Antioxidant Behavior of Crocin. *Comput. Theor. Chem.* 1013, 123–129. doi:10.1016/j.comptc.2013.03.015

Alakbarzade, V., and Pereira, A. C. (2020). What Proportion of Patients Admitted with Stroke or Transient Ischemic Attack May Be Suitable for Newer Cholesterol-Lowering Treatment? *J. Stroke Cerebrovasc. Dis.* 29, 104457. doi:10.1016/j.jstrokecerebrovasdis.2019.104457

Alavizadeh, S. H., and Hosseinzadeh, H. (2014a). Bioactivity Assessment and Toxicity of Crocin: A Comprehensive Review. *Food Chem. Toxicol.* 64, 65–80. doi:10.1016/j.fct.2013.11.016

Alavizadeh, S. H., and Hosseinzadeh, H. (2014b). Bioactivity Assessment and Toxicity of Crocin: A Comprehensive Review. *Food Chem. Toxicol.* 64, 65–80. doi:10.1016/j.fct.2013.11.016

Altinzo, E., Oner, Z., Elbe, H., and Vardi, N. (2014). Neuro-Protective Effects of Crocin on Brain and Cerebellum Tissues in Diabetic Rats. *Afr. J. Traditional, Complementary Altern. Med.* 11, 33–39.

Ama (2021). *Global Burden of Disease-2021statistical Fact Sheet*. American Heart Association. [Online] (Accessed 08 11, 21).

An, B., Ma, Y., Xu, Y., Liu, X., Zhang, X., Zhang, J., et al. (2020). Crocin Regulates the Proliferation and Migration of Neural Stem Cells After Cerebral Ischemia by Activating the Notch1 Pathway. *Folia Neuropathol.* 58 (3), 201–212.

Asadollahi, M., Nikdokht, P., Hatef, B., Sadr, S. S., Sahraei, H., Assarzadegan, F., et al. (2019). Protective Properties of the Aqueous Extract of Saffron (Crocus Sativus l.) in Ischemic Stroke, Randomized Clinical Trial. *J. Ethnopharmacol.* 238, 111833. doi:10.1016/j.jep.2019.111833

Asai, A., Nakano, T., Takahashi, M., and Nagao, A. (2005). Orally Administered Crocetin and Crocins Are Absorbed into Blood Plasma as Crocetin and its Glucuronide Conjugates in Mice. *J. Agric. Food Chem.* 53, 7302–7306. doi:10.1021/jf0509355

Asdaq, S. M. B., and Inamdar, M. N. (2010). Potential of Crocus Sativus (Saffron) and its Constituent, Crocin, as Hypolipidemic and Antioxidant in Rats. *Appl. Biochem. Biotechnol.* 162, 358–372. doi:10.1007/s12010-009-8740-7

Avgerinos, K. I., Vrysis, C., Chaitidis, N., Kolotsiou, K., Myserlis, P. G., and Kapogiannis, D. (2020). Effects of Saffron (Crocus Sativus l.) on Cognitive Function. A Systematic Review of Rcts. *Neurol. Sci.* 41, 2747–2754. doi:10.1007/s10072-020-04427-0

Awasthi, R., and Kulkarni, G. (2020). Therapeutic Benefits of Saffron in Brain Diseases: New Lights on Possible Pharmacological Mechanisms. *Saffron Age-Old Panacea a New Light*, 117.

Ayatollahi, H., Javan, A. O., Khajedaluee, M., Shahroodian, M., and Hosseinzadeh, H. (2014). Effect of Crocus Sativus l. (Saffron) on Coagulation and Anticoagulation Systems in Healthy Volunteers. *Phytotherapy Res.* 28, 539–543. doi:10.1002/ptr.5021

Azami, S., Shahriari, Z., Asgharzade, S., Farkhondeh, T., Sadeghi, M., Ahmadi, F., et al. (2021). Therapeutic Potential of Saffron (Crocus Sativus l.) in Ischemia Stroke. In *Evidence-based Complementary and Alternative Medicine*. doi:10.1155/2021/6643950

Azmand, M. J., and Rajaei, Z. (2021). Effects of Crocin on Spatial or Aversive Learning and Memory Impairments Induced by Lipopolysaccharide in Rats. *Avicenna J. Phytomedicine* 11, 79.

Badavi, M., Mard, S. A., Dianat, M., and Dashtbozorgi, N. (2020). Crocin Attenuates Oxidative Stress and Inflammation in Myocardial Infarction Induced by Isoprenaline via Pparγ Activation in Diabetic Rats. *J. Diabetes & Metabolic Disord.* 19, 1517–1525. doi:10.1007/s40200-020-00686-y

Bahr-Hosseini, M., Bikson, M., Iacoboni, M., Liebeskind, D. S., Hinman, J. D., Carmichael, S. T., et al. (2021). Primed2 Preclinical Evidence Scoring Tool to Assess Readiness for Translation of Neuroprotection Therapies. *Transl. Stroke Res.*, 1–6. doi:10.1007/s12975-021-00922-4

Bakshi, H. A., Hakkim, F. L., Sam, S., Javid, F., and Rashan, L. (2018). Dietary Crocin Reverses Melanoma Metastasis. *J. Biomed. Res.* 32, 39.

Bandegi, A. R., Rashidy-Pour, A., Vafaei, A. A., and Ghadrdoost, B. (2014). Protective Effects of Crocus Sativus L. Extract and Crocin against Chronic-Stress Induced Oxidative Damage of Brain, Liver and Kidneys in Rats. *Adv. Pharm. Bull.* 4, 493. doi:10.5681/apb.2014.073

Barthels, D., and Das, H. (2020). Current Advances in Ischemic Stroke Research and Therapies. *Biochimica Biophysica Acta (bba)-Molecular Basis Dis.* 1866, 165260. doi:10.1016/j.bbadis.2018.09.012

Batarseh, Y. S., Bharate, S. S., Kumar, V., Kumar, A., Vishwakarma, R. A., Bharate, S. B., et al. (2017). Crocus Sativus Extract Tightens the Blood-Brain Barrier, Reduces Amyloid β Load and Related Toxicity in 5xfad Mice. *Acs Chem. Neurosci.* 8, 1756–1766. doi:10.1021/acschemneuro.7b00101

Becerra-Calixto, A., and Cardona-Gómez, G. P. (2017). The Role of Astrocytes in Neuroprotection after Brain Stroke: Potential in Cell Therapy. *Front. Mol. Neurosci.* 10, 88. doi:10.3389/fnmol.2017.00088

Behrouz, V., Dastkhosh, A., Hedayati, M., Sedaghat, M., Sharafkhah, M., and Sohrab, G. (2020). The Effect of Crocin Supplementation on Glycemic Control, Insulin Resistance and Active Ampk Levels in Patients with Type 2 Diabetes: A Pilot Study. *Diabetology Metabolic Syndrome* 12, 1–9. doi:10.1186/s13098-020-00568-6

Bei, W., Peng, W., Ma, Y., and Xu, A. (2004). Naoxinqing, an Anti-stroke Herbal Medicine, Reduces Hydrogen Peroxide-Induced Injury in Ng108-15 Cells. *Neurosci. Lett.* 363, 262–265. doi:10.1016/j.neulet.2004.04.031

Bei, W., Zang, L., Guo, J., Peng, W., Xu, A., Good, D. A., et al. (2009). Neuroprotective Effects of a Standardized Flavonoid Extract from Diospyros Kaki Leaves. *J. Ethnopharmacol.* 126, 134–142. doi:10.1016/j.jep.2009.07.034

Bin Wen, Q. Z., Jin, L., Kang, L., and Yang, Y. (2020). Protective Effect of Crocin Pretreatment on Global Cerebral Ischemia Reperfusion Injury in Rats. *Drug Eval. Res.* 43, 429–435.

Bukhari, S. I., Manzoor, M., and Dhar, M. (2018). A Comprehensive Review of the Pharmacological Potential of Crocus Sativus and its Bioactive Apocarotenoids. *Biomed. Pharmacother.* 98, 733–745. doi:10.1016/j.biopha.2017.12.090

Cao, H., Seto, S. W., Bhuyan, D. J., Chan, H. H., and Song, W. (2021). Effects of Thrombin on the Neurovascular Unit in Cerebral Ischemia. *Cell. Mol. Neurobiol.* doi:10.1007/s10571-020-01019-6

Carmona, M., Zalacain, A., Sánchez, A. M., Novella, J. L., and Alonso, G. L. (2006). Crocetin Esters, Picrocrocin and its Related Compounds Present in Crocus Sativus Stigmas and Gardenia Jasminoides Fruits. Tentative Identification of Seven New Compounds by Lc-Esi-Ms. *J. Agric. Food Chem.* 54, 973–979. doi:10.1021/jf052297w

Cerdá-Bernad, D., Valero-Cases, E., Pastor, J.-J., and Frutos, M. J. (2020). Saffron Bioactives Crocin, Crocetin and Safranal: Effect on Oxidative Stress and Mechanisms of Action. *Crit. Rev. Food Sci. Nutr.*, 1–18.

Chang, D., Colagiuri, B., and Luo, R. (2013). 10 Chinese Medicine Used. In *Advances in Natural Medicines*. Boca Raton, Fla: Nutraceuticals and Neurocognition, 205.

Chang, D., Liu, J., Bilinski, K., Xu, L., Steiner, G. Z., Seto, S. W., et al. (2016). *Herbal Medicine for the Treatment of Vascular Dementia: An Overview of Scientific Evidence-Based Complementary and Alternative Medicine*, 2016.

Chang, G., Chen, Y., Zhang, H., and Zhou, W. (2019). Trans Sodium Crocetinate Alleviates Ischemia/reperfusion-Induced Myocardial Oxidative Stress and Apoptosis via the Sirt3/foxo3a/sod2 Signaling Pathway. *Int. Immunopharmacol.* 71, 361–371. doi:10.1016/j.intimp.2019.03.056

Chapman, S. N., Mehndiratta, P., Johansen, M. C., Mcmurry, T. L., Johnston, K. C., and Southerland, A. M. (2014). Current Perspectives on the Use of Intravenous Recombinant Tissue Plasminogen Activator (Tpa) for Treatment of Acute Ischemic Stroke. *Vasc. Health Risk Manag.* 10, 75. doi:10.2147/VHRM.S39213

Che, X., Ye, W., Panga, L., Wu, D.-C., and Yang, G.-Y. (2001). Monocyte Chemoattractant Protein-1 Expressed in Neurons and Astrocytes during Focal Ischemia in Mice. *Brain Res.* 902, 171–177. doi:10.1016/s0006-8993(01)02328-9

Chen, J., Zhang, X., Liu, X., Zhang, C., Shang, W., Xue, J., et al. (2019). Ginsenoside Rg1 Promotes Cerebral Angiogenesis via the Pi3k/akt/mtor Signaling Pathway in Ischemic Mice. *Eur. J. Pharmacol.* 856, 172418. doi:10.1016/j.ejphar.2019.172418

Chen, L., Qi, Y., and Yang, X. (2015). Neuroprotective Effects of Crocin against Oxidative Stress Induced by Ischemia/reperfusion Injury in Rat Retina. *Ophthalmic Res.* 54, 157–168. doi:10.1159/000439026

Chen, Y., Zhang, H., Tian, X., Zhao, C., Cai, L., Liu, Y., et al. (2008). Antioxidant Potential of Crocins and Ethanol Extracts of Gardenia Jasminoides Ellis and Crocus Sativus l.: A Relationship Investigation between Antioxidant Activity and Crocin Contents. *Food Chem.* 109, 484–492. doi:10.1016/j.foodchem.2007.09.080

Christodoulou, E., Grafakou, M.-E., Skaltsa, E., Kadoglou, N., Kostomitsopoulos, N., and Valsami, G. (2019). Preparation, Chemical Characterization and Determination of Crocetin's Pharmacokinetics after Oral and Intravenous Administration of Saffron (Crocus Sativus l.) Aqueous Extract to C57/bl6j Mice. *J. Pharm. Pharmacol.* 71, 753–764. doi:10.1111/jphp.13055

Cichoń, N., Bijak, M., Miller, E., and Saluk, J. (2017). Extremely Low Frequency Electromagnetic Field (Elf-emf) Reduces Oxidative Stress and Improves Functional and Psychological Status in Ischemic Stroke Patients. *Bioelectromagnetics* 38, 386–396. doi:10.1002/bem.22055

Crocus-sativus (2010). *Iridaceae of North America Update*. Database (Version 2010), Updated for Itis by the Fora of North America Expertise Network, in Connection with an Update for Usda Plants (2007-2010) *itis.gov*.

Csupor, D., Tóth, B., Mottaghipisheh, J., Zangara, A., and Al-Dujaili, E. A. S. (2021). "Chapter 15 - The Psychopharmacology of Saffron, a Plant with Putative Antidepressant and Neuroprotective Properties," in *Nutraceuticals in Brain Health and Beyond*. Editor d. ghosh (Academic Press).

Cui, C., Dong, S., Chen, N., Bao, J., and He, L. (2020). Low-Dose Statin Pretreatment Improves Function and Prognosis of Recurrent Ischemic Stroke Patients. *Ther. Adv. Neurological Disord.* 13, 1756286420920078. doi:10.1177/1756286420920078

Deng, J., Xiong, L., and Zuo, Z. (2015). Trans-Sodium Crocetinate Provides Neuroprotection Against Cerebral Ischemia and Reperfusion in Obese Mice. *J. Neurosci. Res.* 93, 615–622. doi:10.1002/jnr.23522

Deslauriers, A. M., Afkhami-Goli, A., Paul, A. M., Bhat, R. K., Acharjee, S., Ellestad, K. K., et al. (2011). Neuroinflammation and Endoplasmic Reticulum Stress Are Coregulated by Crocin to Prevent Demyelination and Neurodegeneration. *J. Immunol.* 187, 4788–4799. doi:10.4049/jimmunol.1004111

Dhar, A., and Mir, G. (1997). Saffron in Kashmir-Vi: A Review of Distribution and Production. *J. Herbs, Spices Med. Plants* 4, 83–90. doi:10.1300/j044v04n04_09

Dianat, M., Esmaeilizadeh, M., Badavi, M., Samarbafzadeh, A., and Naghizadeh, B. (2014). Protective Effects of Crocin on Hemodynamic Parameters and Infarct Size in Comparison with Vitamin e After Ischemia Reperfusion in Isolated Rat Hearts. *Planta Medica*. 80, 393–398. doi:10.1055/s-0033-1360383

Dianat, M., and Radan, M. (2014). *A Review on the Effective Properties of Crocin in the Management of Cardiopulmonary Dysfunction*.

Donato, R., Sorci, G., Riuzzi, F., Arcuri, C., Bianchi, R., Brozzi, F., et al. (2009). S100b's Double Life: Intracellular Regulator and Extracellular Signal. *Biochimica Biophysica Acta (bba) - Mol. Cell. Res.* 1793, 1008–1022. doi:10.1016/j.bbamcr.2008.11.009

Du, J., Li, y., Song, d., Liu, j., Huang, q., Li, J., et al. (2021). *Protective Effects of Crocin Against Endogenous Aβ-Induced Neurotoxicity in N2a/app695swe Cells*. Berl: Psychopharmacology.

Duan, Z., Li, H., Qi, X., Wei, Y., Guo, X., Li, Y., et al. (2019). Crocin Attenuation of Neurological Deficits in a Mouse Model of Intracerebral Hemorrhage. *Brain Res. Bull.* 150, 186–195. doi:10.1016/j.brainresbull.2019.05.023

Dudhani, A. R., and Kosaraju, S. L. (2010). Bioadhesive Chitosan Nanoparticles: Preparation and Characterization. *Carbohydr. Polym.* 81, 243–251. doi:10.1016/j.carbpol.2010.02.026

Ebrahim-Habibi, M. B., Amininasab, M., Ebrahim-Habibi, A., Sabbaghian, M., and Nemat-Gorgani, M. (2010). Fibrillation of α-lactalbumin: Effect of Crocin and Safranal, Two Natural Small Molecules from Crocus Sativus. *Biopolymers* 93, 854–865.

El Khoudri, M., Ouahhoud, S., Lahmass, M., Khoulati, A., Benyoussef, S., Mamri, S., et al. (2021). Biological Effects and Pharmacological Activities of Saffron of Crocus Sativus. *Arabian J. Med. Aromatic Plants* 7, 254–268.

Escartin, C., Galea, E., Lakatos, A., O'callaghan, J. P., Petzold, G. C., Serrano-Pozo, A., et al. (2021). Reactive Astrocyte Nomenclature, Definitions, and Future Directions. *Nat. Neurosci.* 24, 312–325. doi:10.1038/s41593-020-00783-4

Eteghadi, M.-R., Nasehi, M., Vaseghi, S., and Hesami-Tackallou, S. (2021). The Effect of Crocin on Tfam and Pgc-1α Expression and Catalase and Superoxide Dismutase Activities Following Cholestasis-Induced Neuroinflammation in the Striatum of Male Wistar Rats. *Metab. Brain Dis.*, 1–11. doi:10.1007/s11011-021-00748-x

Fan, X.-D., Yao, M.-J., Yang, B., Han, X., Wang, G.-R., Li, P., et al. (2021). *Chinese Herbal Preparation Sailuotong Alleviates Brain Ischemia via Nrf2 Antioxidation Pathway Dependent Cerebral Microvascular Protection*.

Fernández-Albarral, J. A., Ramírez, A. I., De Hoz, R., López-Villarín, N., Salobrar-García, E., López-Cuenca, I., et al. (2019). Neuroprotective and Antiinflammatory Effects of a Hydrophilic Saffron Extract in a Model of Glaucoma. *Int. J. Mol. Sci.* 20, 4110.

Finley, J. W., Gao, S. J. J. O. A., and Chemistry, F. 2017. A Perspective on Crocus Sativus l.(Saffron) Constituent Crocin: A Potent Water-Soluble Antioxidant and Potential Therapy for Alzheimer's Disease. 65**,** 1005–1020. doi:10.1021/acs.jafc.6b04398

Frederico, D., Donate, P. M., Constantino, M. G., Bronze, E. S., and Sairre, M. I. (2003). A Short and Efficient Synthesis of Crocetin-Dimethylester and Crocetindial. *J. Org. Chem.* 68, 9126–9128. doi:10.1021/jo034545y

Freitas-Andrade, M., and Naus, C. (2016). Astrocytes in Neuroprotection and Neurodegeneration: The Role of Connexin43 and Pannexin1. *Neuroscience* 323, 207–221. doi:10.1016/j.neuroscience.2015.04.035

Fuentes, B., Martínez-Sánchez, P., and Díez-Tejedor, E. (2009). Lipid-lowering Drugs in Ischemic Stroke Prevention and Their Influence on Acute Stroke Outcome. *Cerebrovasc. Dis.* 27, 126–133. doi:10.1159/000200450

Fukuta, T., Asai, T., Yanagida, Y., Namba, M., Koide, H., Shimizu, K., et al. (2017). Combination Therapy with Liposomal Neuroprotectants and Tissue Plasminogen Activator for Treatment of Ischemic Stroke. *faseb J.* 31, 1879–1890. doi:10.1096/fj.201601209R

Gainer, J. L. (2008). Trans-sodium Crocetinate for Treating Hypoxia/ischemia. *Expert Opin. Investigational Drugs* 17, 917–924. doi:10.1517/13543784.17.6.917

Gainer, J. L. (2000). *Trans-Sodium Crocetinate, Methods of Making and Methods of Use Thereof*. Alexandria, United States: Google Patents.

Gao, G., Wu, J., Li, B., Jiang, Q., Wang, P., and Li, J. (2021). Transcriptomic Analysis of Saffron at Different Flowering Stages Using Rna Sequencing Uncovers Cytochrome P450 Genes Involved in Crocin Biosynthesis. *Mol. Biol. Rep.* 48, 3451–3461. doi:10.1007/s11033-021-06374-1

Gao, J., Bai, P., Li, Y., Li, J., Jia, C., Wang, T., et al. (2020). Metabolomic Profiling of the Synergistic Effects of Ginsenoside Rg1 in Combination with Neural Stem Cell Transplantation in Ischemic Stroke Rats. *J. Proteome Res.* 19, 2676–2688. doi:10.1021/acs.jproteome.9b00639

Gao, J., Chen, M., Ren, X.-C., Zhou, X.-B., Shang, Q., Lu, W.-Q., et al. (2017). Synthesis and Cardiomyocyte Protection Activity of Crocetin Diamide Derivatives. *Fitoterapia* 121, 106–111. doi:10.1016/j.fitote.2017.06.014

George, M., and Abraham, T. E. (2006). Polyionic Hydrocolloids for the Intestinal Delivery of Protein Drugs: Alginate and Chitosan—A Review. *J. Control. Release* 114, 1–14. doi:10.1016/j.jconrel.2006.04.017

Gerlach, R., Demel, G., König, H.-G., Gross, U., Prehn, J., Raabe, A., et al. (2006). Active Secretion of S100b from Astrocytes During Metabolic Stress. *Neuroscience* 141, 1697–1701. doi:10.1016/j.neuroscience.2006.05.008

Ghaderi, A., Rasouli-Azad, M., Vahed, N., Banafshe, H. R., Soleimani, A., Omidi, A., et al. (2019). Clinical and Metabolic Responses to Crocin in Patients under Methadone Maintenance Treatment: A Randomized Clinical Trial. *Phytotherapy Res.* 33, 2714–2725. doi:10.1002/ptr.6445

Ghaffari, S., and Roshanravan, N. (2019). Saffron; An Updated Review on Biological Properties with Special Focus on Cardiovascular Effects. *Biomed. Pharmacother.* 109, 21–27. doi:10.1016/j.biopha.2018.10.031

Ghorbani, R., and Koocheki, A. (2017). *Sustainable Cultivation of Saffron in Iran. Sustainable Agriculture Reviews*. Springer. doi:10.1007/978-3-319-58679-3_6

Giaccio, M. (2004). Crocetin from Saffron: An Active Component of an Ancient Spice. *Crit. Rev. Food Sci. Nutr.* 44, 155–172. doi:10.1080/10408690490441433

Girme, A., Pawar, S., Ghule, C., Shengule, S., Saste, G., Balasubramaniam, A. K., et al. (2021). Bioanalytical Method Development and Validation Study of Neuroprotective Extract of Kashmiri Saffron Using Ultra-fast Liquid Chromatography-Tandem Mass Spectrometry (Uflc-ms/ms): *In Vivo* Pharmacokinetics of Apocarotenoids and Carotenoids. *Molecules* 26, 1815. doi:10.3390/molecules26061815

Gudarzi, S., Jafari, M., Pirzad Jahromi, G., Eshrati, R., Asadollahi, M., and Nikdokht, P. (2020). Evaluation of Modulatory Effects of Saffron (Crocus Sativus l.) Aqueous Extract on Oxidative Stress in Ischemic Stroke Patients: A Randomized Clinical Trial. *Nutr. Neurosci.*, 1–10. doi:10.1080/1028415X.2020.1840118

Gullo, F., Ceriani, M., D'aloia, A., Wanke, E., Constanti, A., Costa, B., et al. (2017). Plant Polyphenols and Exendin-4 Prevent Hyperactivity and Tnf-α Release in Lps-Treated *In Vitro* Neuron/astrocyte/microglial Networks. *Front. Neurosci.* 11, 500. doi:10.3389/fnins.2017.00500

Gupta, A., and Pandey, A. K. (2020). *Saffron and its Active Ingredients: A Natural Product with Potent Anticancer Property. Drug Development for Cancer and Diabetes*. Apple Academic Press. doi:10.1201/9780429330490-17

Hadizadeh, F., Mohajeri, S., and Seifi, M. (2010). Extraction and Purification of Crocin from Saffron Stigmas Employing a Simple and Efficient Crystallization Method. *Pak. J. Biol. Sci.* 13, 691–698. doi:10.3923/pjbs.2010.691.698

Haeri, P., Mohammadipour, A., Heidari, Z., and Ebrahimzadeh-Bideskan, A. (2019). Neuroprotective Effect of Crocin on Substantia Nigra in Mptp-Induced Parkinson's Disease Model of Mice. *Anatomical Sci. Int.* 94, 119–127. doi:10.1007/s12565-018-0457-7

Hao, C.-H., Xi, W.-G., Zheng, H.-J., Wang, W.-T., and Zhao, Z.-Y. (2015). Effect of Chinese Patent Medicine Naodesheng against Repeated Transient Global Cerebral Ischemia in Mice. *Chin. Herb. Med.* 7, 339–343. doi:10.1016/s1674-6384(15)60062-4

Hao, C.-Z., Wu, f., Shen, j., Lu, l., Fu, D.-L., Liao, W.-J., et al. (2012). *Clinical Efficacy and Safety of Buyang Huanwu Decoction for Acute Ischemic Stroke: A Systematic Review and Meta-Analysis of 19 Randomized Controlled Trials Evidence-Based Complementary and Alternative Medicine*.

Harari, O. A., and Liao, J. K. (2010). Nf-κb and Innate Immunity in Ischemic Stroke. *Ann. N. Y. Acad. Sci.* 1207, 32–40. doi:10.1111/j.1749-6632.2010.05735.x

Hariri, A. T., Moallem, S. A., Mahmoudi, M., Memar, B., and Hosseinzadeh, H. (2010). Sub-acute Effects of Diazinon on Biochemical Indices and Specific Biomarkers in Rats: Protective Effects of Crocin and Safranal. *Food Chem. Toxicol.* 48, 2803–2808. doi:10.1016/j.fct.2010.07.010

Hashemi, M., and Hosseinzadeh, H. (2019). A Comprehensive Review on Biological Activities and Toxicology of Crocetin. *Food Chem. Toxicol.* 130, 44–60. doi:10.1016/j.fct.2019.05.017

Hashemzaei, M., Mamoulakis, C., Tsarouhas, K., Georgiadis, G., Lazopoulos, G., Tsatsakis, A., et al. (2020). Crocin: A Fighter against Inflammation and Pain. *Food Chem. Toxicol.* 143, 111521. doi:10.1016/j.fct.2020.111521

He, S.-Y., Qian, Z.-Y., Tang, F.-T., Wen, N., Xu, G.-L., and Sheng, L. (2005). Effect of Crocin on Experimental Atherosclerosis in Quails and its Mechanisms. *Life Sci.* 77, 907–921. doi:10.1016/j.lfs.2005.02.006

Higashino, S., Sasaki, Y., Giddings, J. C., Hyodo, K., Fujimoto Sakata, S., Matsuda, K., et al. (2014). Crocetin, a Carotenoid from Gardenia Jasminoides Ellis, Protects against Hypertension and Cerebral Thrombogenesis in Stroke-prone Spontaneously Hypertensive Rats. *Phytotherapy Res.* 28, 1315–1319. doi:10.1002/ptr.5130

Hoshyar, R., Khayati, G. R., Poorgholami, M., and Kaykhaii, M. (2016). A Novel Green One-step Synthesis of Gold Nanoparticles Using Crocin and Their Anti-cancer Activities. *J. Photochem. Photobiol. B Biol.* 159, 237–242. doi:10.1016/j.jphotobiol.2016.03.056

Hoshyar, R., and Mollaei, H. (2017). A Comprehensive Review on Anticancer Mechanisms of the Main Carotenoid of Saffron, Crocin. *J. Pharm. Pharmacol.* 69, 1419–1427. doi:10.1111/jphp.12776

Hosseini, A., Razavi, B. M., and Hosseinzadeh, H. (2018). Pharmacokinetic Properties of Saffron and its Active Components. *Eur. J. Drug Metabolism Pharmacokinet.* 43, 383–390. doi:10.1007/s13318-017-0449-3

Hosseinzadeh, H., Mehri, S., Heshmati, A., Ramezani, M., Sahebkar, A., and Abnous, K. (2014a). Proteomic Screening of Molecular Targets of Crocin. *Daru J. Pharm. Sci.* 22, 5. doi:10.1186/2008-2231-22-5

Hosseinzadeh, H., Mehri, S., Heshmati, A., Ramezani, M., Sahebkar, A., and Abnous, K. (2014b). Screening of Molecular Targets of Crocin. *Daru J. Fac. Pharm.* Berlin/Heidelberg, Germany: Springer: Google Patents. 22, 5. doi:10.1186/2008-2231-22-5

Hosseinzadeh, H., Sadeghnia, H. R., Ghaeni, F. A., Motamedshariaty, V. S., and Mohajeri, S. A. (2012). Effects of Saffron (Crocus Sativus l.) and its Active Constituent, Crocin, on Recognition and Spatial Memory after Chronic Cerebral Hypoperfusion in Rats. *Phytotherapy Res.* 26, 381–386. doi:10.1002/ptr.3566

Hosseinzadeh, H., Sharíaty, V. M., Sameni, A. K., and Vahabzadeh, M. (2010). Acute and Sub-acute Toxicity of Crocin, a Constituent of Crocus Sativus l. (Saffron), in Mice and Rats. *Pharmacologyonline* 2, 943–951.

Huang, A., and Jia, L. (2019a). Crocin Enhances Hypothermia Therapy in Hypoxic Ischemia-Induced Brain Injury in Mice. *Acta Neurol. Belg.* doi:10.1007/s13760-019-01198-0

Huang, A., and Jia, L. (2019b). Crocin Enhances Hypothermia Therapy in Hypoxic Ischemia-Induced Brain Injury in Mice. *Acta Neurol. Belg.*, 1–8. doi:10.1007/s13760-019-01198-0

Huang, Z., Xu, J., Huang, X., Sun, G., Jiang, R., Wu, H., et al. (2019). Crocin Induces Anti-ischemia in Middle Cerebral Artery Occlusion Rats and Inhibits Autophagy by Regulating the Mammalian Target of Rapamycin. *Eur. J. Pharmacol.* 857, 172424. doi:10.1016/j.ejphar.2019.172424

Hussain, I., Singh, N. B., Singh, A., Singh, H., and Singh, S. C. (2016). Green Synthesis of Nanoparticles and its Potential Application. *Biotechnol. Lett.* 38, 545–560. doi:10.1007/s10529-015-2026-7

Hussain, M. A., Abogresha, N. M., Abdelkader, G., Hassan, R., Abdelaziz, E. Z., and Greish, S. M. (2021). Antioxidant and Antiinflammatory Effects of Crocin Ameliorate Doxorubicin-Induced Nephrotoxicity in Rats. *Oxidative Med. Cell. Longev.* 2021, 8841726. doi:10.1155/2021/8841726

Hussein, S. A., Ahmed, T. E., Amin, A., and Ali, A. H. (2019). The Antiinflammatory and Anti-apoptotic Role of Crocin against Expression of Mmp-9, Timp-1, Mcp-1, Caspase-3, Pparα in Heart Tissue, and Metamorphoses of Microrna 188 in Hyperhomocysteinemic Rats. *Recent Adv. Biol. Med.* 5, 10601. doi:10.18639/rabm.2019.883878

Imran, M., Imran, A., Arshad, M. U., and Suleria, H. A. R. (2019). *Crocin: A Mechanistic Treatise. Bioactive Compounds from Plant Origin*. Apple Academic Press. doi:10.1201/9780429029288-5

Jackson, P. A., Forster, J., Khan, J., Pouchieu, C., Dubreuil, S., Gaudout, D., et al. (2021). Effects of Saffron Extract Supplementation on Mood, Well-Being, and Response to a Psychosocial Stressor in Healthy Adults: A Randomized, Double-Blind, Parallel Group, Clinical Trial. *Front. Nutr.*, 365. doi:10.3389/fnut.2020.606124

Jahanbakhsh, Z., Rasoulian, B., Jafari, M., Shekarforoush, S., Esmailidehaj, M., Taghi Mohammadi, M., et al. (2012). Protective Effect of Crocin against Reperfusion-Induced Cardiac Arrhythmias in Anaesthetized Rats. *Excli J.* 11, 20.

Jan, S., Wani, A. A., Kamili, A. N., and Kashtwari, M. (2014). Distribution, Chemical Composition and Medicinal Importance of Saffron (Crocus Sativus l.). *Afr. J. plant Sci.* 8, 537–545.

Javandoost, A., Afshari, A., Nikbakht-Jam, I., Khademi, M., Eslami, S., Nosrati, M., et al. (2017). Effect of Crocin, a Carotenoid from Saffron, on Plasma Cholesteryl Ester Transfer Protein and Lipid Profile in Subjects with Metabolic Syndrome: A Double Blind Randomized Clinical Trial. *Arya Atheroscler.* 13, 245–252.

Jia, J., Wei, C., Chen, S., Li, F., Tang, Y., Qin, W., et al. (2018). Efficacy and Safety of the Compound Chinese Medicine Sailuotong in Vascular Dementia: A Randomized Clinical Trial. *Alzheimer's Dementia Transl. Res. Clin. Interventions* 4, 108–117. doi:10.1016/j.trci.2018.02.004

Karkoula, E., Dagla, I.-V., Baira, E., Kokras, N., Dalla, C., Skaltsounis, A.-L., et al. (2020). A Novel Uhplc-Hrms-Based Metabolomics Strategy Enables the Discovery of Potential Neuroactive Metabolites in Mice Plasma, Following I.P. Administration of the Main Crocus Sativus L. Bioactive Component. *J. Pharm. Biomed. Analysis* 177, 112878. doi:10.1016/j.jpba.2019.112878

Karkoula, E., Lemonakis, N., Kokras, N., Dalla, C., Gikas, E., Skaltsounis, A.-L., et al. (2018). Trans-crocin 4 Is Not Hydrolyzed to Crocetin Following Ip Administration in Mice, While it Shows Penetration through the Blood Brain Barrier. *Fitoterapia* 129, 62–72. doi:10.1016/j.fitote.2018.06.012

Kashani, L., Raisi, F., Saroukhani, S., Sohrabi, H., Modabbernia, A., Nasehi, A. A., et al. (2013). Saffron for Treatment of Fluoxetine-induced Sexual Dysfunction in Women: Randomized Double-blind Placebo-controlled Study. *Hum. Psychopharmacol. Clin. Exp.* 28, 54–60. doi:10.1002/hup.2282

Kazley, A. S., Simpson, K. N., Simpson, A., Jauch, E., and Adams, R. J. (2013). Optimizing the Economic Impact of Rtpa Use in a Stroke Belt State: the Case of South Carolina. *Am. Health & Drug Benefits* 6, 155.

Kell, G., Rao, A., Beccaria, G., Clayton, P., Inarejos-García, A. M., and Prodanov, M. (2017). Affron® a Novel Saffron Extract (Crocus Sativus l.) Improves Mood in Healthy Adults over 4 Weeks in a Double-Blind, Parallel, Randomized, Placebo-Controlled Clinical Trial. *Complementary Ther. Med.* 33, 58–64. doi:10.1016/j.ctim.2017.06.001

Kermani, T., Kazemi, T., Molki, S., Ilkhani, K., Sharifzadeh, G., and Rajabi, O. (2017). The Efficacy of Crocin of Saffron (Crocus Sativus l.) on the Components of Metabolic Syndrome: A Randomized Controlled Clinical Trial. *J. Res. Pharm. Pract.* 6, 228. doi:10.4103/jrpp.JRPP_17_26

Kermanshahi, S., Ghanavati, G., Abbasi-Mesrabadi, M., Gholami, M., Ulloa, L., Motaghinejad, M., et al. (2020). Novel Neuroprotective Potential of Crocin in Neurodegenerative Disorders: an Illustrated Mechanistic Review. *Neurochem. Res.* 45, 2573–2585. doi:10.1007/s11064-020-03134-8

Khalatbari-Mohseni, A., Banafshe, H. R., Mirhosseini, N., Asemi, Z., Ghaderi, A., and Omidi, A. (2019). The Effects of Crocin on Psychological Parameters in Patients under Methadone Maintenance Treatment: A Randomized Clinical Trial. *Subst. Abuse Treat. Prev. Policy* 14, 9. doi:10.1186/s13011-019-0198-1

Khan, M. T., Ikram, A., Saeed, O., Afridi, T., Sila, C. A., Smith, M. S., et al. (2017). Deep Vein Thrombosis in Acute Stroke-A Systemic Review of the Literature. *Cureus* 9. doi:10.7759/cureus.1982

Khandelwal, P., Martínez-Pías, E., Bach, I., Prakash, T., Hillen, M. E., Martínez-Galdámez, M., et al. (2021). Severe Epistaxis after Tissue Plasminogen Activator Administration for Acute Ischemic Stroke in Sars-Cov-2 Infection. *Brain Circ.* 7, 135. doi:10.4103/bc.bc_17_21

Khazdair, M. R., Anaeigoudari, A., Hashemzehi, M., and Mohebbati, R. (2019). Neuroprotective Potency of Some Spice Herbs, a Literature Review. *J. Traditional Complementary Med.* 9, 98–105. doi:10.1016/j.jtcme.2018.01.002

Khorasany, A. R., and Hosseinzadeh, H. (2016). Therapeutic Effects of Saffron (Crocus Sativus l.) in Digestive Disorders: A Review. *Iran. J. Basic Med. Sci.* 19, 455.

Kianbakht, S., and Hajiaghaee, R. (2011). Anti-Hyperglycemic Effects of Saffron and its Active Constituents, Crocin and Safranal, in Alloxan-Induced Diabetic Rats. *Jmpir* 10, 82–89.

Kim, D.-G., Jeong, Y.-I., Choi, C., Roh, S.-H., Kang, S.-K., Jang, M.-K., et al. (2006). Retinol-encapsulated Low Molecular Water-Soluble Chitosan Nanoparticles. *Int. J. Pharm.* 319, 130–138. doi:10.1016/j.ijpharm.2006.03.040

Kocaman, G., Altinoz, E., Erdemli, M. E., Gul, M., Erdemli, Z., Zayman, E., et al. (2021). Crocin Attenuates Oxidative and Inflammatory Stress-Related Periodontitis in Cardiac Tissues in Rats. *Adv. Clin. Exp. Med.* 30, 517–524. doi:10.17219/acem/133753

Kothari, D., Thakur, R., and Kumar, R. (2021a). Saffron (Crocus Sativus l.): Gold of the Spices—A Comprehensive Review. *Hortic. Environ. Biotechnol.* 62, 661–677. doi:10.1007/s13580-021-00349-8

Kothari, D., Thakur, R., and Kumar, R. (2021b). Saffron (Crocus Sativus l.): Gold of the Spices—A Comprehensive Review. *Hortic. Environ. Biotechnol.*, 1–17.

Krishnaswamy, V., Alugoju, P., and Periyasamy, L. (2020). Effect of Short-Term Oral Supplementation of Crocin on Age-Related Oxidative Stress, Cholinergic, and Mitochondrial Dysfunction in Rat Cerebral Cortex. *Life Sci.* 263, 118545. doi:10.1016/j.lfs.2020.118545

Lapchak, P. A. (2010). Efficacy and Safety Profile of the Carotenoid Trans Sodium Crocetinate Administered to Rabbits Following Multiple Infarct Ischemic Strokes: A Combination Therapy Study with Tissue Plasminogen Activator. *Brain Res.* 1309, 136–145. doi:10.1016/j.brainres.2009.10.067

Lasek-Bal, A., Jedrzejowska-Szypulka, H., Student, S., Warsz-Wianecka, A., Zareba, K., Puz, P., et al. (2019). The Importance of Selected Markers of Inflammation and Blood-Brain Barrier Damage for Short-Term Ischemic Stroke Prognosis. *J. Physiology Pharmacol.* 70, 209–217. doi:10.26402/jpp.2019.2.04

Lautenschläger, M., Sendker, J., Hüwel, S., Galla, H., Brandt, S., Düfer, M., et al. (2015). Intestinal Formation of Trans-crocetin from Saffron Extract (Crocus

Sativus l.) and *In Vitro* Permeation through Intestinal and Blood Brain Barrier. *Phytomedicine* 22, 36–44.

Lech, K., Witowska-Jarosz, J., and Jarosz, M. (2009). Saffron Yellow: Characterization of Carotenoids by High Performance Liquid Chromatography with Electrospray Mass Spectrometric Detection. *J. Mass Spectrom.* 44, 1661–1667. doi:10.1002/jms.1631

Leijiao Fan, G. H. (2021a). Protective Effect of Crocin on Myocardial Mitochondria in Rats with Acute Myocardial Infaction. *Chin. J. Arterioscler.* 29, 383–388.

Leijiao Fan, G. H. (2021b). Protective Effect of Crocin on Myocardial Mitochondria in Rats with Acute Myocardial Infaction. *Chin. J. Arterioscler.* 29, 383–388.

Li, N., Lin, G., Kwan, Y.-W., and Min, Z.-D. (1999). Simultaneous Quantification of Five Major Biologically Active Ingredients of Saffron by High-Performance Liquid Chromatography. *J. Chromatogr. A* 849, 349–355. doi:10.1016/s0021-9673(99)00600-7

LI, W., Li, X., Du, Q., Li, F., Zhu, Y., Liu, Y., et al. (2014). Effect of Tongluojiunao Injection Made from Sanqi (Radix Notoginseng) and Zhizi (Fructus Gardeniae) on Brain Microvascular Endothelial Cells and Astrocytes in an *In Vitro* Ischemic Model. *J. Traditional Chin. Med.* 34, 725–732. doi:10.1016/s0254-6272(15)30088-1

Li, X., Liu, Y., Cao, A., Li, C., Wang, L., Wu, Q., et al. (2021). Crocin Improves Endothelial Mitochondrial Dysfunction via gpx1/ros/kca3.1 Signal Axis in Diabetes. *Front. Cell. Dev. Biol.* 9, 651434. doi:10.3389/fcell.2021.651434

Li, Y., Kakkar, R., and Wang, J. (2018). *In Vivo* and *In Vitro* Approach to Anti-arthritic and Anti-inflammatory Effect of Crocetin by Alteration of Nuclear Factor-E2-Related Factor 2/hem Oxygenase (Ho)-1 and Nf-Kb Expression. *Front. Pharmacol.* 9, 1341. doi:10.3389/fphar.2018.01341

Liddelow, S. A., Guttenplan, K. A., Clarke, L. E., Bennett, F. C., Bohlen, C. J., Schirmer, L., et al. (2017). Neurotoxic Reactive Astrocytes Are Induced by Activated Microglia. *Nature* 541, 481–487. doi:10.1038/nature21029

Liu, H., Zhang, Z., Zang, C., Wang, L., Yang, H., Sheng, C., et al. (2021a). Gj-4 Ameliorates Memory Impairment in Focal Cerebral Ischemia/reperfusion of Rats via Inhibiting Jak2/stat1-Mediated Neuroinflammation. *J. Ethnopharmacol.* 267, 113491. doi:10.1016/j.jep.2020.113491

Liu, J., Ye, C., Lv, G., Li, G., Gao, Y., and Ji, X. (2021b). *Crocetin Improves Ischaemic Stroke* in Vitro *and Vivo*. Berlin/Heidelberg, Germany: Springer.

Liu, R., Yuan, H., Yuan, F., and Yang, S.-H. (2012). Neuroprotection Targeting Ischemic Penumbra and Beyond for the Treatment of Ischemic Stroke. *Neurological Res.* 34, 331–337. doi:10.1179/1743132812Y.0000000020

Liu, T., Yu, S., Xu, Z., Tan, J., Wang, B., Liu, Y.-G., et al. (2020). Prospects and Progress on Crocin Biosynthetic Pathway and Metabolic Engineering. *Comput. Struct. Biotechnol. J.* 18, 3278–3286. doi:10.1016/j.csbj.2020.10.019

Liu, Z., and Chopp, M. (2016). Astrocytes, Therapeutic Targets for Neuroprotection and Neurorestoration in Ischemic Stroke. *Prog. Neurobiol.* 144, 103–120. doi:10.1016/j.pneurobio.2015.09.008

Lv, B., Yin, J., Feng, C., and Li, Y. (2019). *Neuroprotective Effects of Crocin I and Ii in an Ischemia-Reperfusion Injury Model*. New York, United States: Biorxiv, 757971.

Manabe, H., Okonkwo, D. O., Gainer, J. L., Clarke, R. H., and Lee, K. S. (2010). Protection against Focal Ischemic Injury to the Brain by Trans-sodium Crocetinate. *J. Neurosurg.* 113, 802–809. doi:10.3171/2009.10.JNS09562

Mard, S. A., Akbari, G., Dianat, M., and Mansouri, E. (2017). Protective Effects of Crocin and Zinc Sulfate on Hepatic Ischemia-Reperfusion Injury in Rats: A Comparative Experimental Model Study. *Biomed. Pharmacother.* 96, 48–55.

Marquez-Romero, J. M., Góngora-Rivera, F., Hernández-Curiel, B. C., Aburto-Murrieta, Y., García-Cazares, R., Delgado-Garzón, P., et al. (2020). Endovascular Treatment of Ischemic Stroke in a Developing Country. *Vasc. Endovascular Surg.* 54, 305–312. doi:10.1177/1538574420906941

Martin, G., Goh, E., and Neff, A. (2002). Evaluation of the Developmental Toxicity of Crocetin on Xenopus. *Food Chem. Toxicol.* 40, 959–964. doi:10.1016/s0278-6915(02)00040-6

Martinez, C., Wallenhorst, C., Rietbrock, S., and Freedman, B. (2020). Ischemic Stroke and Transient Ischemic Attack Risk Following Vitamin K Antagonist Cessation in Newly Diagnosed Atrial Fibrillation: a Cohort Study. *J. Am. Heart Assoc.* 9, e014376. doi:10.1161/JAHA.119.014376

Mehri, S., Abnous, K., Khooei, A., Mousavi, S. H., Shariaty, V. M., and Hosseinzadeh, H. (2015). Crocin Reduced Acrylamide-Induced Neurotoxicity in Wistar Rat through Inhibition of Oxidative Stress. *Iran. J. basic Med. Sci.* 18, 902.

Mehri, S., Abnous, K., Mousavi, S. H., Shariaty, V., and Hosseinzadeh, H. (2011). Neuroprotective Effect of Crocin on Acrylamide-Induced Cytotoxicity in Pc12 Cells. *Cell. Mol. Neurobiol.* 32, 227–235. doi:10.1007/s10571-011-9752-8

Mehrnia, M.-A., Jafari, S.-M., Makhmal-Zadeh, B. S., and Maghsoudlou, Y. J. F. H. (2017). Rheological and Release Properties of Double Nano-Emulsions Containing Crocin Prepared with Angum Gum. *Arabic Gum Whey Protein* 66, 259–267. doi:10.1016/j.foodhyd.2016.11.033

Mirhadi, E., Nassirli, H., and Malaekeh-Nikouei, B. (2020). An Updated Review on Therapeutic Effects of Nanoparticle-Based Formulations of Saffron Components (Safranal, Crocin, and Crocetin). *J. Pharm. Investigation* 50, 47–58. doi:10.1007/s40005-019-00435-1

Moallem, S. A., Afshar, M., Etemad, L., Razavi, B. M., and Hosseinzadeh, H. (2016). Evaluation of Teratogenic Effects of Crocin and Safranal, Active Ingredients of Saffron, in Mice. *Toxicol. Industrial Health* 32, 285–291. doi:10.1177/0748233713500818

Modaghegh, M.-H., Shahabian, M., Esmaeili, H.-A., Rajbai, O., and Hosseinzadeh, H. (2008). Safety Evaluation of Saffron (Crocus Sativus) Tablets in Healthy Volunteers. *Phytomedicine* 15, 1032–1037. doi:10.1016/j.phymed.2008.06.003

Moghaddasi, M. S. (2010). Saffron Chemicals and Medicine Usage. *J. Med. Plants Res.* 4, 427–430.

Mohajeri, S. A., Hosseinzadeh, H., Keyhanfar, F., and Aghamohammadian, J. (2010a). Extraction of Crocin from Saffron (Crocus Sativus) Using Molecularly Imprinted Polymer Solid-Phase Extraction. *J. Sep. Sci.* 33, 2302–2309. doi:10.1002/jssc.201000183

Mohajeri, S. A., Hosseinzadeh, H., Keyhanfar, F., and Aghamohammadian, J. (2010b). Extraction of Crocin from Saffron (Crocus Sativus) Using Molecularly Imprinted Polymer Solid-Phase Extraction. *J. Sep. Sci.* 33, 2302–2309. doi:10.1002/jssc.201000183

Mohamadpour, A. H., Ayati, Z., Parizadeh, M. R., Rajbai, O., and Hosseinzadeh, H. (2013). Safety Evaluation of Crocin (A Constituent of Saffron) Tablets in Healthy Volunteers. *Iran. J. Basic Med. Sci.* 16, 39.

Mohler, E. R., iii, Gainer, J. L., Whitten, K., Eraso, L. H., Thanaporn, P. K., and Bauer, T. (2011). Evaluation of Trans Sodium Crocetinate on Safety and Exercise Performance in Patients with Peripheral Artery Disease and Intermittent Claudication. *Vasc. Med.* 16, 346–353. doi:10.1177/1358863X11422742

Mok, I.-K., Nguyen, T. T. H., Kim, D. H., Lee, J. W., Lim, S., Jung, H.-Y., et al. (2020). Enhancement of Neuroprotection, Antioxidant Capacity, and Water-Solubility of Crocins by Transglucosylation Using Dextransucrase under High Hydrostatic Pressure. *Enzyme Microb. Technol.* 140, 109630. doi:10.1016/j.enzmictec.2020.109630

Mollazadeh, H., Emami, S. A., and Hosseinzadeh, H. (2015). Razi's Al-Hawi and Saffron (Crocus Sativus): A Review. *Iran. J. basic Med. Sci.* 18, 1153.

Moratalla-López, N., Parizad, S., Habibi, M. K., Winter, S., Kalantari, S., Bera, S., et al. (2021). Impact of Two Different Dehydration Methods on Saffron Quality, Concerning the Prevalence of Saffron Latent Virus (Salv) in Iran. *Food Chem.* 337, 127786. doi:10.1016/j.foodchem.2020.127786

Mousavi, B., Bathaie, S. Z., Fadai, F., Ashtari, Z., Ali Beigi, N., Farhang, S., et al. (2015). Safety Evaluation of Saffron Stigma (Crocus Sativus l.) Aqueous Extract and Crocin in Patients with Schizophrenia. *Avicenna J. Phytomedicine* 5, 413–419.

Nagatoshi, M., Terasaka, K., Owaki, M., Sota, M., Inukai, T., Nagatsu, A., et al. (2012). Ugt75l6 and ugt94e5 Mediate Sequential Glucosylation of Crocetin to Crocin in Gardenia Jasminoides. *Febs Lett.* 586, 1055–1061. doi:10.1016/j.febslet.2012.03.003

Najafabadi, B. T., Farsinejad, M., Shokraee, K., Momtazmanesh, S., Violette, P. D., Esalatmanesh, S., et al. (2022). Possible Effects of Saffron (Crocus Sativus) in the Treatment of Erectile Dysfunction: A Randomized, Double-Blind, Placebo-Controlled Trial. *J. Herb. Med.*, 100551. doi:10.1016/j.hermed.2022.100551

Nam, K. N., Park, Y.-M., Jung, H.-J., Lee, J. Y., Min, B. D., Park, S.-U., et al. (2010). Antiinflammatory Effects of Crocin and Crocetin in Rat Brain Microglial Cells. *Eur. J. Pharmacol.* 648, 110–116. doi:10.1016/j.ejphar.2010.09.003

Nassar, R., Eid, S., Chahine, R., Chabi, B., Bonnieu, A., Sabban, M. E., et al. (2020). Antioxidant Effects of Lebanese Crocus Sativus L. And its Main Components, Crocin and Safranal, on Human Skeletal Muscle Cells. *Eur. J. Integr. Med.* 40, 101250. doi:10.1016/j.eujim.2020.101250

Ncbi, P. (2021). Crocin 7. [Online]. Pubchem.ncbi.nih. Available: https://pubchem.ncbi.nlm.nih.gov/compound/101124079 (Accessed 11 08, 2021).

Nikbakht-Jam, I., Khademi, M., Nosrati, M., Eslami, S., Foroutan-Tanha, M., Sahebkar, A., et al. (2016). Effect of Crocin Extracted from Saffron on Pro-oxidant–anti-oxidant Balance in Subjects with Metabolic Syndrome: A Randomized, Placebo-Controlled Clinical Trial. *Eur. J. Integr. Med.* 8, 307–312. doi:10.1016/j.eujim.2015.12.008

Ochiai, T., Ohno, S., Soeda, S., Tanaka, H., Shoyama, Y., and Shimeno, H. (2004a). Crocin Prevents the Death of Rat Pheochromyctoma (Pc-12) Cells by its Antioxidant Effects Stronger Than Those of α-tocopherol. *Neurosci. Lett.* 362, 61–64. doi:10.1016/j.neulet.2004.02.067

Ochiai, T., Soeda, S., Ohno, S., Tanaka, H., Shoyama, Y., and Shimeno, H. (2004b). Crocin Prevents the Death of Pc-12 Cells through Sphingomyelinase-Ceramide Signaling by Increasing Glutathione Synthesis. *Neurochem. Int.* 44, 321–330. doi:10.1016/s0197-0186(03)00174-8

Orset, C., Arkelius, K., Anfray, A., Warfvinge, K., Vivien, D., and Ansar, S. (2021). Combination Treatment with U0126 and Rt-Pa Prevents Adverse Effects of the Delayed Rt-Pa Treatment after Acute Ischemic Stroke. *Sci. Rep.* 11, 1–10. doi:10.1038/s41598-021-91469-9

Oruc, S., Gönül, Y., Tunay, K., Oruc, O. A., Bozkurt, M. F., Karavelioğlu, E., et al. (2016). The Antioxidant and Antiapoptotic Effects of Crocin Pretreatment on Global Cerebral Ischemia Reperfusion Injury Induced by Four Vessels Occlusion in Rats. *Life Sci.* 154, 79–86. doi:10.1016/j.lfs.2016.04.028

Ozaki, A., Kitano, M., Furusawa, N., Yamaguchi, H., Kuroda, K., and Endo, G. (2002). Genotoxicity of Gardenia Yellow and its Components. *Food Chem. Toxicol.* 40, 1603–1610. doi:10.1016/s0278-6915(02)00118-7

Pandita, D. (2021). *Saffron (Crocus Sativus l.): Phytochemistry, Therapeutic Significance and Omics-Based Biology*. Medicinal and Aromatic Plants. Elsevier.

Pang, Q., Zhang, W., Li, C., Li, H., Zhang, Y., Li, L., et al. (2020). Antidementia Effects, Metabolic Profiles and Pharmacokinetics of Gj-4, a Crocin-Rich Botanical Candidate from Gardeniae Fructus. *Food & Funct.* 11, 8825–8836. doi:10.1039/d0fo01678k

Papandreou, M. A., Kanakis, C. D., Polissiou, M. G., Efthimiopoulos, S., Cordopatis, P., Margarity, M., et al. (2006). Inhibitory Activity on Amyloid-β Aggregation and Antioxidant Properties of Crocus Sativus Stigmas Extract and its Crocin Constituents. *J. Agric. Food Chem.* 54, 8762–8768. doi:10.1021/jf061932a

Pazoki, B., Zandi, N., Assaf, Z., Moghaddam, H. S., Zeinoddini, A., Mohammadi, M. R., et al. (2022). Efficacy and Safety of Saffron as Adjunctive Therapy in Adults with Attention-Deficit/hyperactivity Disorder: A Randomized, Double-Blind, Placebo-Controlled Clinical Trial. In *Advances in Integrative Medicine*. doi:10.1016/j.aimed.2022.01.002

Pergolizzi, J. V., jr, Coluzzi, F., Colucci, R. D., Olsson, H., Lequang, J. A., Al-Saadi, J., et al. (2020). *Expert Review of Clinical Pharmacology*. doi:10.1080/17512433.2020.1734451 Statins and Muscle Pain.

Pfister, S., Meyer, P., Steck, A., and Pfander, H. (1996). Isolation and Structure Elucidation of Carotenoid–Glycosyl Esters in Gardenia Fruits (Gardenia Jasminoides Ellis) and Saffron (Crocus Sativus Linne). *J. Agric. Food Chem.* 44, 2612–2615. doi:10.1021/jf950713e

Pprc, C. P. C. (2020). *Pharmacopoeia of the People's Republic of China*. Beijing, China: China Medical Science Press. (Chinese Edition).

Pu, X., He, C., Yang, Y., Wang, W., Hu, K., Xu, Z., et al. (2020). *In Vivo* Production of Five Crocins in the Engineered Escherichia Coli. *Acs Synth. Biol.* 9, 1160–1168. doi:10.1021/acssynbio.0c00039

Puglia, C., Rizza, L., Drechsler, M., and Bonina, F. (2010). Nanoemulsions as Vehicles for Topical Administration of Glycyrrhetic Acid: Characterization and *In Vitro* and *In Vivo* Evaluation. *Drug Deliv.* 17, 123–129. doi:10.3109/10717540903581679

Puglia, C., Santonocito, D., Musumeci, T., Cardile, V., Graziano, A. C. E., Salerno, L., et al. (2019). Nanotechnological Approach to Increase the Antioxidant and Cytotoxic Efficacy of Crocin and Crocetin. *Planta Medica.* 85, 258–265. doi:10.1055/a-0732-5757

QI, Y., Chen, L., Zhang, L., Liu, W.-B., Chen, X.-Y., and Yang, X.-G. (2013). Crocin Prevents Retinal Ischaemia/reperfusion Injury-Induced Apoptosis in Retinal Ganglion Cells through the Pi3k/akt Signaling Pathway. *Exp. Eye Res.* 107, 44–51. doi:10.1016/j.exer.2012.11.011

Qin, L., Liu, H., Wang, J., Wang, W., and Zhang, L. (2021). Crocetin Exerts a Cardio-Protective Effect on Mice with Coxsackievirus B3-Induced Acute Viral Myocarditis. *J. Oleo Sci.* 70, 1115–1124. doi:10.5650/jos.ess21100

Rahaiee, S., Hashemi, M., Shojaosadati, S. A., Moini, S., and Razavi, S. H. (2017). Nanoparticles Based on Crocin Loaded Chitosan-Alginate Biopolymers: Antioxidant Activities, Bioavailability and Anticancer Properties. *Int. J. Biol. Macromol.* 99, 401–408. doi:10.1016/j.ijbiomac.2017.02.095

Rahaiee, S., Shojaosadati, S. A., Hashemi, M., Moini, S., and Razavi, S. H. (2015). Improvement of Crocin Stability by Biodegradeble Nanoparticles of Chitosan-Alginate. *Int. J. Biol. Macromol.* 79, 423–432. doi:10.1016/j.ijbiomac.2015.04.041

Rao, S. V., Hemalatha, P., Yetish, S., Muralidhara, M., and Rajini, P. S. (2019a). Prophylactic Neuroprotective Propensity of Crocin, a Carotenoid against Rotenone Induced Neurotoxicity in Mice: Behavioural and Biochemical Evidence. *Metab. Brain Dis.*, 1–13. doi:10.1007/s11011-019-00451-y

Rao, S. V., Hemalatha, P., Yetish, S., Muralidhara, M., and Rajini, P. S. (2019b). Prophylactic Neuroprotective Propensity of Crocin, a Carotenoid against Rotenone Induced Neurotoxicity in Mice: Behavioural and Biochemical Evidence. *Metab. Brain Dis.* 34, 1341–1353. doi:10.1007/s11011-019-00451-y

Rodriguez, C., Agulla, J., and Delgado-Esteban, M. (2021). *Refocusing the Brain: New Approaches in Neuroprotection against Ischemic Injury*, 46. Berlin/Heidelberg, Germany: Springer. doi:10.1007/s11064-020-03016-z

Sai Li, H. Y., and Xuansheng, D. (2017). The Effect of Crocin on Thoracic Aorta Artery Systolic and Diastolic Function on Diabetic Rats. *Pharm. Clin. Res.* 25, 183–186.

Salama, R. M., Abdel-Latif, G. A., Abbas, S. S., Hekmat, M., and Schaalan, M. F. (2020). Neuroprotective Effect of Crocin against Rotenone-Induced Parkinson's Disease in Rats: Interplay between Pi3k/akt/mtor Signaling Pathway and Enhanced Expression of Mirna-7 and Mirna-221. *Neuropharmacology* 164, 107900. doi:10.1016/j.neuropharm.2019.107900

Saraiva, M., and O'garra, A. (2010). The Regulation of Il-10 Production by Immune Cells. *Nat. Rev. Immunol.* 10, 170–181. doi:10.1038/nri2711

Sarshoori, J. R., Asadi, M. H., and Mohammadi, M. T. (2014). Neuroprotective Effects of Crocin on the Histopathological Alterations Following Brain Ischemia-Reperfusion Injury in Rat. *Iran. J. Basic Med. Sci.* 17, 895.

Sepahi, S., Mohajeri, S. A., Hosseini, S. M., Khodaverdi, E., Shoeibi, N., Namdari, M., et al. (2018). Effects of Crocin on Diabetic Maculopathy: A Placebo-Controlled Randomized Clinical Trial. *Am. J. Ophthalmol.* 190, 89–98. doi:10.1016/j.ajo.2018.03.007

Seto, S., Chang, D., Ko, W., Zhou, X., Kiat, H., Bensoussan, A., et al. (2017). Sailuotong Prevents Hydrogen Peroxide (H2o2)-induced Injury in Ea. Hy926 Cells. *Int. J. Mol. Sci.* 18, 95. doi:10.3390/ijms18010095

Shafahi, M., Vaezi, G., Shajiee, H., Sharafi, S., and Khaksari, M. (2018). Crocin Inhibits Apoptosis and Astrogliosis of hippocampus Neurons against Methamphetamine Neurotoxicity via Antioxidant and Antiinflammatory Mechanisms. *Neurochem. Res.* 43, 2252–2259. doi:10.1007/s11064-018-2644-2

Shah, H. M., Jain, A. S., Joshi, S. V., and Kharkar, P. S. (2021). *Crocetin and Related Oxygen Diffusion-enhancing Compounds: Review of Chemical Synthesis, Pharmacology, Clinical Development, and Novel Therapeutic Applications*. Hoboken, New Jersey, United States: Wiley.

Shahbaz, K. (2017a). Oxidative Stress Causes Aging: Genetics and Epigenetics. *Merit Res. J. Med. Med. Sci.* 5, 604–610.

Shahbaz, K. (2017b). Tamoxifen: Pharmacokinetics and Pharmacodynamics. *Pharm. Res.* 1, 000143.

Shahmansouri, N., Farokhnia, M., Abbasi, S.-H., Kassaian, S. E., Tafti, A.-A. N., Gougol, A., et al. (2014). A Randomized, Double-Blind, Clinical Trial Comparing the Efficacy and Safety of Crocus Sativus L. With Fluoxetine for Improving Mild to Moderate Depression in Post Percutaneous Coronary Intervention Patients. *J. Affect. Disord.* 155, 216–222. doi:10.1016/j.jad.2013.11.003

Sharma, B., Kumar, H., Kaushik, P., Mirza, R., Awasthi, R., and Kulkarni, G. (2020). *Therapeutic Benefits of Saffron in Brain Diseases: New Lights on Possible Pharmacological Mechanisms*. Saffron. Elsevier.

Sheikhani, A., Kholdi, N., and Mokhtari, M. (2017). An Overview of the Most Effective Tranquilizer Herbs. *J. Basic Clin. Pathophysiol.* 5, 27–34. doi:10.22342/jims.23.1.257.27-42

Shen, J. Z., Wu, G., and Guo, S. (2021). *Amino Acids in Autophagy: Regulation and Function Amino Acids in Nutrition and Health*. Springer.

Shiber, J. R., Fontane, E., and Adewale, A. (2010). Stroke Registry: Hemorrhagic vs Ischemic Strokes. *Am. J. Emerg. Med.* 28, 331–333. doi:10.1016/j.ajem.2008.10.026

Shirley, R., Ord, E. N., and Work, L. M. (2014). Oxidative Stress and the Use of Antioxidants in Stroke. *Antioxidants* 3, 472–501. doi:10.3390/antiox3030472

Shotar, E., Amouyal, C., Jacquens, A., Mathon, B., Boulouis, G., Monneret, D., et al. (2019). S100b Serum Elevation Predicts In-Hospital Mortality after Brain Arteriovenous Malformation Rupture. *Stroke* 50, 1250–1253. doi:10.1161/STROKEAHA.119.025033

Singh, P., and Singh, R. K. (2019). The Advantage of Higher Statin Concentrations to Improve Outlook after Ischemic Stroke.

Singla, R. K., and Giliyaru, V. (2011). Crocin: An Overview. *Indo Glob. J. Pharm. Sci.* 1, 281–286.

Soeda, S., Ochiai, T., Paopong, L., Tanaka, H., Shoyama, Y., and Shimeno, H. (2001). Crocin Suppresses Tumor Necrosis Factor-α-Induced Cell Death of Neuronally Differentiated Pc-12 Cells. *Life Sci.* 69, 2887–2898. doi:10.1016/s0024-3205(01)01357-1

Soeda, S., Ochiai, T., Shimeno, H., Saito, H., Abe, K., Tanaka, H., et al. (2007). Pharmacological Activities of Crocin in Saffron. *J. Nat. Med.* 61, 102–111. doi:10.1007/s11418-006-0120-9

Sommano, S. R., Suppakittpaisarn, P., Sringarm, K., Junmahasathien, T., and Ruksiriwanich, W. (2020). Recovery of Crocins from Floral Tissue of Gardenia Jasminoides Ellis. *Front. Nutr.* 7, 106. doi:10.3389/fnut.2020.00106

Song, G., Liu, J., Wang, Q., Wang, D., Chu, B., Li, L., et al. (2022). Layer-by-layer Self-Assembly of Hollow Dextran Sulfate/chitosan-Coated Zein Nanoparticles Loaded with Crocin: Fabrication, Structural Characterization and Potential Biological Fate. *Food Hydrocoll.* 125, 107420. doi:10.1016/j.foodhyd.2021.107420

Song, Y.-N., Wang, Y., Zheng, Y.-H., Liu, T.-L., and Zhang, C. (2021a). *Crocins: A Comprehensive Review of Structural Characteristics, Pharmacokinetics and Therapeutic Effects*. Amsterdam, Netherlands: Elsevier. 104969. doi:10.1016/j.fitote.2021.104969

Song, Y.-N., Wang, Y., Zheng, Y.-H., Liu, T.-L., and Zhang, C. (2021b). Crocins: A Comprehensive Review of Structural Characteristics, Pharmacokinetics and Therapeutic Effects. *Fitoterapia* 153, 104969. doi:10.1016/j.fitote.2021.104969

Steiner, G. Z., Bensoussan, A., Liu, J., Hohenberg, M. I., and Chang, D. H. (2018). Study Protocol for a Randomised, Double-Blind, Placebo-Controlled 12-week Pilot Phase Ii Trial of Sailuotong (Slt) for Cognitive Function in Older Adults with Mild Cognitive Impairment. *Trials* 19, 1–10. doi:10.1186/s13063-018-2912-0

Streinu-Cercel, A., Sandulescu, O., Miron, V. D., Oana, A.-A., Motoi, M. M., and Galloway, C. D. (2021). *Trans Sodium Crocetinate (Tsc) to Improve Oxygenation in Covid-19*. London: Cold Spring Harbor Laboratory.

SU, X.-T., Wang, L., Ma, S.-M., Cao, Y., Yang, N.-N., Lin, L.-L., et al. (2020). Mechanisms of Acupuncture in the Regulation of Oxidative Stress in Treating Ischemic Stroke. *Oxidative Med. Cell. Longev.* doi:10.1155/2020/7875396

Suchareau, M., Bordes, A., and Lemée, L. (2021). Improved Quantification Method of Crocins in Saffron Extract Using Hplc-Dad after Qualification by Hplc-Dad-Ms. *Food Chem.*, 130199. doi:10.1016/j.foodchem.2021.130199

Sugawara, T., and Chan, P. H. (2003). Reactive Oxygen Radicals and Pathogenesis of Neuronal Death after Cerebral Ischemia. *Antioxidants Redox Signal.* 5, 597–607. doi:10.1089/152308603770310266

Sun, L., Zhang, Y., Liu, E., Ma, Q., Anatol, M., Han, H., et al. (2019). The Roles of Astrocyte in the Brain Pathologies Following Ischemic Stroke. *Brain Inj.* 33, 712–716. doi:10.1080/02699052.2018.1531311

Sun, P.-D., Wang, J.-X., Fang, Z.-K., and Tang, D.-D. (2012). *Synthesis of Crocetin Dimethyl Ester with Wittig and Wittig-Horner Reaction*. Beijing, China: Chemical World, 06.

TAPEINOS, C., Battaglini, M., and Ciofani, G. (2017). Advances in the Design of Solid Lipid Nanoparticles and Nanostructured Lipid Carriers for Targeting Brain Diseases. *J. Control. Release* 264, 306–332. doi:10.1016/j.jconrel.2017.08.033

Teo, L., and Bourne, J. A. (2018). Current Opinion on a Role of the Astrocytes in Neuroprotection. *Neural Regen. Res.* 13, 797. doi:10.4103/1673-5374.232466

Tseng, T.-H., Chu, C.-Y., Huang, J.-M., Shiow, S.-J., and Wang, C.-J. (1995). Crocetin Protects against Oxidative Damage in Rat Primary Hepatocytes. *Cancer Lett.* 97, 61–67. doi:10.1016/0304-3835(95)03964-x

Ulbricht, C., Conquer, J., Costa, D., Hollands, W., Iannuzzi, C., Isaac, R., et al. 2011. An Evidence-Based Systematic Review of Saffron (Crocus Sativus) by the Natural Standard Research Collaboration. 8, 58–114. doi:10.3109/19390211.2011.547666

Ullegaddi, R., Powers, H. J., and Gariballa, S. E. (2006). Antioxidant Supplementation with or without B-group Vitamins after Acute Ischemic Stroke: A Randomized Controlled Trial. *J. Parenter. Enter. Nutr.* 30, 108–114. doi:10.1177/0148607106030002108

Umigai, N., Murakami, K., Ulit, M., Antonio, L., Shirotori, M., Morikawa, H., et al. (2011). The Pharmacokinetic Profile of Crocetin in Healthy Adult Human Volunteers after a Single Oral Administration. *Phytomedicine* 18, 575–578. doi:10.1016/j.phymed.2010.10.019

Umigai, N., Takeda, R., and Mori, A. (2018). Effect of Crocetin on Quality of Sleep: a Randomized, Double-Blind, Placebo-Controlled, Crossover Study. *Complementary Ther. Med.* 41, 47–51. doi:10.1016/j.ctim.2018.09.003

Vahdati Hassani, F., Naseri, V., Razavi, B. M., Mehri, S., Abnous, K., and Hosseinzadeh, H. (2014). Antidepressant Effects of Crocin and its Effects on Transcript and Protein Levels of Creb, Bdnf, and Vgf in Rat hippocampus. *Daru J. Fac. Pharm. Tehran Univ. Med. Sci.* 22, 16. doi:10.1186/2008-2231-22-16

Vakili, A., Einali, M. R., and Bandegi, A. R. (2014). Protective Effect of Crocin against Cerebral Ischemia in a Dose-dependent Manner in a Rat Model of Ischemic Stroke. *J. Stroke Cerebrovasc. Dis.* 23, 106–113. doi:10.1016/j.jstrokecerebrovasdis.2012.10.008

Veisi, A., Akbari, G., Mard, S. A., Badfar, G., Zarezade, V., and Mirshekar, M. A. (2020). Role of Crocin in Several Cancer Cell Lines: An Updated Review. *Iran. J. Basic Med. Sci.* 23, 3. doi:10.22038/IJBMS.2019.37821.8995

Venketasubramanian, N. (2021). Stroke Epidemiology in Oceania: A Review. *Neuroepidemiology*, 1–10. doi:10.1159/000512972

Verma, R. S., and Middha, D. (2010). Analysis of Saffron (Crocus Sativus L. Stigma) Components by Lc–Ms–Ms. *Chromatographia* 71, 117–123. doi:10.1365/s10337-009-1398-z

Wang, C., Cai, X., Hu, W., Li, Z., Kong, F., Chen, X., et al. (2019). Investigation of the Neuroprotective Effects of Crocin via Antioxidant Activities in Ht22 Cells and in Mice with Alzheimer's Disease. *Int. J. Mol. Med.* 43, 956–966. doi:10.3892/ijmm.2018.4032

Wang, C., Hwang, L. S., and Lin, J. (1984). Reversible Hepatic Black Pigmentation and Enzyme Alteration Induced by Prolonged Feeding of High Dose of Crocin Dyes in Rats. *Proc. Natl. Sci. Counc. Repub. China. Part B, Life Sci.* 8, 246–253.

Wang, Y., Han, T., Zhu, Y., Zheng, C.-J., Ming, Q.-L., Rahman, K., et al. (2009). Antidepressant Properties of Bioactive Fractions from the Extract of Crocus Sativus L. *J. Nat. Med.* 64, 24. doi:10.1007/s11418-009-0360-6

Wang, Y., Yoshimura, R., Manabe, H., Schretter, C., Clarke, R., Cai, Y., et al. (2014). Trans-sodium Crocetinate Improves Outcomes in Rodent Models of Occlusive and Hemorrhagic Stroke. *Brain Res.* 1583, 245–254. doi:10.1016/j.brainres.2014.08.013

Wani, A., Al Rihani, S. B., Sharma, A., Weadick, B., Govindarajan, R., Khan, S. U., et al. (2021). Crocetin Promotes Clearance of Amyloid-β by Inducing Autophagy via the Stk11/lkb1-Mediated Ampk Pathway. *Autophagy*, 1–20. doi:10.1080/15548627.2021.1872187

Waziry, R., Chibnik, L. B., Bos, D., Ikram, M. K., and Hofman, A. (2020). Risk of Hemorrhagic and Ischemic Stroke in Patients with Alzheimer Disease: A Synthesis of the Literature. *Neurology* 94, 265–272. doi:10.1212/WNL.0000000000008924

Wechsler, L. R. (2020). *Statins and Stroke—It's Complicated*. England, United Kingdom: Mass Medical Soc.

Who (2020). *The Top 10 Causes of Death [Online]. Who* (Accessed July 19, 2021 2020).

Williams, E. I., Betterton, R. D., Davis, T. P., and Ronaldson, P. T. (2020). Transporter-mediated Delivery of Small Molecule Drugs to the Brain: A Critical Mechanism that Can Advance Therapeutic Development for Ischemic Stroke. *Pharmaceutics* 12, 154. doi:10.3390/pharmaceutics12020154

Wishart, D. S., Feunang, Y. D., Marcu, A., Guo, A. C., Liang, K., Vázquez-Fresno, R., et al. (2018). Hmdb 4.0: The Human Metabolome Database for 2018. *Nucleic Acids Res.* 46, d608–d617. doi:10.1093/nar/gkx1089

Wong, K. H., Xie, Y., Huang, X., Kadota, K., Yao, X.-S., Yu, Y., et al. (2020). Delivering Crocetin across the Blood-Brain Barrier by Using γ-cyclodextrin to Treat Alzheimer's Disease. *Sci. Rep.* 10, 1–12. doi:10.1038/s41598-020-60293-y

Wu, L., Xiong, X., Wu, X., Ye, Y., Jian, Z., Zhi, Z., et al. (2020). Targeting Oxidative Stress and Inflammation to Prevent Ischemia-Reperfusion Injury. *Front. Mol. Neurosci.* 13, 28. doi:10.3389/fnmol.2020.00028

Xi, L., Qian, Z., Du, P., and Fu, J. (2007). Pharmacokinetic Properties of Crocin (Crocetin Digentiobiose Ester) Following Oral Administration in Rats. *Phytomedicine* 14, 633–636. doi:10.1016/j.phymed.2006.11.028

Xi, L., and Qian, Z. (2006). Pharmacological Properties of Crocetin and Crocin (Digentiobiosyl Ester of Crocetin) from Saffron. *Nat. Product. Commun.* 1, 1934578x0600100112. doi:10.1177/1934578x0600100112

Xiao, Q., Shu, R., Wu, C., Tong, Y., Xiong, Z., Zhou, J., et al. (2020). Crocin-i Alleviates the Depression-like Behaviors Probably via Modulating "Microbiota-gut-brain" Axis in Mice Exposed to Chronic Restraint Stress. *J. Affect. Disord.* 276, 476–486. doi:10.1016/j.jad.2020.07.041

Xiao, Q., Xiong, Z., Yu, C., Zhou, J., Shen, Q., Wang, L., et al. (2019). Antidepressant Activity of Crocin-I Is Associated with Amelioration of Neuroinflammation and Attenuates Oxidative Damage Induced by Corticosterone in Mice. *Physiology Behav.* 212, 112699. doi:10.1016/j.physbeh.2019.112699

Xie, C.-L., Li, J.-H., Wang, W.-W., Zheng, G.-Q., and Wang, L.-X. (2015a). Neuroprotective Effect of Ginsenoside-Rg1 on Cerebral Ischemia/reperfusion Injury in Rats by Downregulating Protease-Activated Receptor-1 Expression. *Life Sci.* 121, 145–151. doi:10.1016/j.lfs.2014.12.002

Xie, C.-L., Wang, W.-W., Xue, X.-D., Zhang, S.-F., Gan, J., and Liu, Z.-G. (2015b). A Systematic Review and Meta-Analysis of Ginsenoside-Rg1 (G-rg1) in Experimental Ischemic Stroke. *Sci. Rep.* 5, 7790. doi:10.1038/srep07790

Xu, G.-L., Li, G., Ma, H.-P., Zhong, H., Liu, F., and Ao, G.-Z. (2009). Preventive Effect of Crocin in Inflamed Animals and in Lps-Challenged Raw 264.7 Cells. *J. Agric. Food Chem.* 57, 8325–8330. doi:10.1021/jf901752f

Yamashita, S. I., Umigai, N., Kakinuma, T., and Takara, T. (2018). Safety Evaluation of Excessive Intake of Crocetin in Healthy Adult Volunteers-A Randomized, Double-Blind, Placebo-Controlled, Parallel-Group Comparison Trial. *Pharmacol. Treat.* 46, 393–401.

Yang, C., Fan, F., Sawmiller, D., Tan, J., Wang, Q., and Xiang, Y. (2019). C1q/tnf-related Protein 9: A Novel Therapeutic Target in Ischemic Stroke? *J. Neurosci. Res.* 97, 128–136. doi:10.1002/jnr.24353

Yang, L., and Dong, X. (2017). Inhibition of Inflammatory Response by Crocin Attenuates Hemorrhagic Shock-Induced Organ Damages in Rats. *J. Interferon & Cytokine Res.* 37, 295–302. doi:10.1089/jir.2016.0137

Yang, W. Z. A. L. (2020). Study on the Protective Effect of Saffron on Organ Damage Caused by Hemorrhagic Shock in Rats. Modern Journal of Integrated. *Tradit. Chin. West. Med.* 29, 1742–1746.

Yang, Y., Han, K., Park, S. H., Kim, M. K., Yoon, K.-H., and Lee, S.-H. (2021). High-density Lipoprotein Cholesterol and the Risk of Myocardial Infarction, Stroke, and Cause-Specific Mortality: A Nationwide Cohort Study in Korea. *J. Lipid Atheroscler.* 10, 74. doi:10.12997/jla.2021.10.1.74

Yang, Y., and Rosenberg, G. A. (2015). Matrix Metalloproteinases as Therapeutic Targets for Stroke. *Brain Res.* 1623, 30–38. doi:10.1016/j.brainres.2015.04.024

YE, F., Garton, H. J., Hua, Y., Keep, R. F., and Xi, G. (2021). The Role of Thrombin in Brain Injury after Hemorrhagic and Ischemic Stroke. *Transl. Stroke Res.* 12, 496–511. doi:10.1007/s12975-020-00855-4

Yoo, A. J., and Andersson, T. (2017). Thrombectomy in Acute Ischemic Stroke: Challenges to Procedural Success. *J. Stroke* 19, 121. doi:10.5853/jos.2017.00752

Yoshino, F., Yoshida, A., Umigai, N., Kubo, K., and Masaichi, C.-I. L. (2011). Crocetin Reduces the Oxidative Stress Induced Reactive Oxygen Species in the Stroke-Prone Spontaneously Hypertensive Rats (Shrsps) Brain. *J. Clin. Biochem. Nutr.* 49, 182–187. doi:10.3164/jcbn.11-01

Yousefi, F., Arab, F. L., Rastin, M., Tabasi, N. S., Nikkhah, K., and Mahmoudi, M. (2021). Comparative Assessment of Immunomodulatory, Proliferative, and Antioxidant Activities of Crocin and Crocetin on Mesenchymal Stem Cells. *J. Cell. Biochem.* 122, 29–42. doi:10.1002/jcb.29826

Yousefsani, B. S., Mehri, S., Pourahmad, J., and Hosseinzadeh, H. (2021). Protective Effect of Crocin against Mitochondrial Damage and Memory Deficit Induced by Beta-Amyloid in the Hippocampus of Rats. *Iran. J. Pharm. Res.* 20, 79–94. doi:10.22037/ijpr.2020.112206.13604

Yuan, Y., Shan, X., Men, W., Zhai, H., Qiao, X., Geng, L., et al. (2020). The Effect of Crocin on Memory, Hippocampal Acetylcholine Level, and Apoptosis in a Rat Model of Cerebral Ischemia. *Biomed. Pharmacother.* 130, 110543. doi:10.1016/j.biopha.2020.110543

Zeka, K., Marrazzo, P., Micucci, M., Ruparelia, K. C., Arroo, R. R., Macchiarelli, G., et al. (2020). Activity of Antioxidants from Crocus Sativus L. Petals: Potential Preventive Effects Towards Cardiovascular System. *Antioxidants* 9, 1102. doi:10.3390/antiox9111102

Zeka, K., Ruparelia, K. C., Continenza, M. A., Stagos, D., Vegliò, F., and Arroo, R. R. (2015). Petals of Crocus Sativus L. As a Potential Source of the Antioxidants Crocin and Kaempferol. *Fitoterapia* 107, 128–134. doi:10.1016/j.fitote.2015.05.014

Zeng, C., Li, H., Fan, Z., Zhong, L., Guo, Z., Guo, Y., et al. (2016). Crocin-elicited Autophagy Rescues Myocardial Ischemia/reperfusion Injury via Paradoxical Mechanisms. *Am. J. Chin. Med.* 44, 515–530. doi:10.1142/S0192415X16500282

Zhang, H., Zeng, Y., Yan, F., Chen, F., Zhang, X., Liu, M., et al. (2004). Semi-preparative Isolation of Crocins from Saffron (Crocus Sativus l.). *Chromatographia* 59, 691–696. doi:10.1365/s10337-004-0311-z

Zhang, H., Zhang, X., Yan, F., Zeng, Y., and Chen, F. (2001). Separation and Preparation of Crocins in Saffron by Low-Pressure Liquid Chromatography. *Chin. J. Anal. Chem.*

Zhang, X., Fan, Z., and Jin, T. (2017a). Crocin Protects against Cerebral-Ischemia-Induced Damage in Aged Rats through Maintaining the Integrity of Blood-Brain Barrier. *Restor. Neurology Neurosci.* 35, 65–75. doi:10.3233/RNN-160696

Zhang, X., Fan, Z., and Ting, J. (2017b). Crocin Protects against Cerebral- Ischemia-Induced Damage in Aged Rats through Maintaining the Integrity of Blood-Brain Barrier. *Restor. Neurology Neurosci.* 35, 65–75. doi:10.3233/RNN-160696

Zhang, Y., Geng, J., Hong, Y., Jiao, L., Li, S., Sun, R., et al. (2019). Orally Administered Crocin Protects against Cerebral Ischemia/reperfusion Injury through the Metabolic Transformation of Crocetin by Gut Microbiota. *Front. Pharmacol.* 10, 440. doi:10.3389/fphar.2019.00440

Zhang, Y., Liu, J., Lin, L., and Li, L. (2012). Pharmacokinetics of Crocin-1 after Oral Administration in Rats. *Chin. Pharm. J.* 47, 136–140.

Zheng, T., Jiang, H., Jin, R., Zhao, Y., Bai, Y., Xu, H., et al. (2019). Ginsenoside Rg1 Attenuates Protein Aggregation and Inflammatory Response Following Cerebral Ischemia and Reperfusion Injury. *Eur. J. Pharmacol.* 853, 65–73. doi:10.1016/j.ejphar.2019.02.018

Zheng, Y.-Q., Liu, J.-X., Li, X.-Z., and Xu, L. (2010). Effects and Mechanism of Weinaokang (维脑康) on Reperfusioninduced Vascular Injury to Cerebral Microvessels after Global Cerebral Ischemia. *Chin. J. Integr. Med.* 16, 145–150. doi:10.1007/s11655-010-0145-5

Zheng, Y.-Q., Liu, J.-X., Wang, J.-N., and Xu, L. (2007). Effects of Crocin on Reperfusion-Induced Oxidative/nitrative Injury to Cerebral Microvessels after Global Cerebral Ischemia. *Brain Res.* 1138, 86–94. doi:10.1016/j.brainres.2006.12.064

Zhong, K., Wang, R.-X., Qian, X.-D., Yu, P., Zhu, X.-Y., Zhang, Q., et al. (2020). Neuroprotective Effects of Saffron on the Late Cerebral Ischemia Injury through Inhibiting Astrogliosis and Glial Scar Formation in Rats. *Biomed. Pharmacother.* 126, 110041. doi:10.1016/j.biopha.2020.110041

Zhou, B., Perel, P., Mensah, G. A., and Ezzati, M. (2021). Global Epidemiology, Health Burden and Effective Interventions for Elevated Blood Pressure and Hypertension. *Nat. Rev. Cardiol.*, 1–18. doi:10.1038/s41569-021-00559-8

Zhou, Y., Li, H.-Q., Lu, L., Fu, D.-L., Liu, A.-J., Li, J.-H., et al. (2014). Ginsenoside Rg1 Provides Neuroprotection against Blood Brain Barrier Disruption and Neurological Injury in a Rat Model of Cerebral Ischemia/reperfusion through Downregulation of Aquaporin 4 Expression. *Phytomedicine* 21, 998–1003. doi:10.1016/j.phymed.2013.12.005

Zhu, A., Lao, C., Wang, Z., Chen, Y., and Bai, C. (2019a). Characterization of Crocetin-Monoglucuronide as a Neuron-Protective Metabolite of Crocin-1. *Mol. Nutr. Food Res.* 63, 1900024. doi:10.1002/mnfr.201900024

Zhu, A., Lao, C., Wang, Z., Chen, Y., and Bai, C. (2019b). Characterization of Crocetin-monoglucuronide as a Neuron-protective Metabolite of Crocin-1. *Mol. Nutr. Food Res.* 63, 1900024. doi:10.1002/mnfr.201900024

Zhu, Y. (2010). *Clinical Study on Crocin Injection in the Treatment of Arteriosclerotic Thrombotic Cerebral Infarction (Stroke Recovery Period-Blood Stasis Blocking Collaterals Syndrome)*. Jilin, China: Changchun University of Traditional Chinese Medicine. Master Thesis (in chinese).

Zougagh, M., Simonet, B. M., Ríos, A., and Valcárcel, M. (2005). Use of Non-aqueous Capillary Electrophoresis for the Quality Control of Commercial Saffron Samples. *J. Chromatogr. A* 1085, 293–298. doi:10.1016/j.chroma.2005.06.041

Conflict of Interest: The authors declare that the research was conducted in the absence of any commercial or financial relationships that could be construed as a potential conflict of interest.

Publisher's Note: All claims expressed in this article are solely those of the authors and do not necessarily represent those of their affiliated organizations, or those of the publisher, the editors, and the reviewers. Any product that may be evaluated in this article, or claim that may be made by its manufacturer, is not guaranteed or endorsed by the publisher.

Advantages of publishing in Frontiers

OPEN ACCESS
Articles are free to read for greatest visibility and readership

FAST PUBLICATION
Around 90 days from submission to decision

HIGH QUALITY PEER-REVIEW
Rigorous, collaborative, and constructive peer-review

TRANSPARENT PEER-REVIEW
Editors and reviewers acknowledged by name on published articles

Frontiers
Avenue du Tribunal-Fédéral 34
1005 Lausanne | Switzerland

Visit us: www.frontiersin.org
Contact us: frontiersin.org/about/contact

REPRODUCIBILITY OF RESEARCH
Support open data and methods to enhance research reproducibility

DIGITAL PUBLISHING
Articles designed for optimal readership across devices

FOLLOW US
@frontiersin

IMPACT METRICS
Advanced article metrics track visibility across digital media

EXTENSIVE PROMOTION
Marketing and promotion of impactful research

LOOP RESEARCH NETWORK
Our network increases your article's readership